HIGH VOLUME UTILIZATION OF WASTE GLASS POWDER AS A CEMENT REPLACEMENT IN THE COMPOSITION OF SELF-COMPACTING CONCRETE

A thesis submitted in partial fulfilment of the requirements for the degree of

Doctor of Philosophy in Civil Engineering

By

SAMIA TARIQ

Supervised by

Dr. Allan N. Scott

Dr. James R. Mackechnie

DEPARTMENT OF CIVIL AND NATURAL RESOURCES ENGINEERING

UNIVERSITY OF CANTERBURY

CHRISTCHURCH, NEW ZEALAND

SEPTEMBER 2016

Dedicated to the bright memory of my deceased father,

Tariq Masood,

for his continuous love and support throughout my life

TABLE OF CONTENTS

CHAPTER 3: MATERIAL CHARACTERIZATION, MIX DESIGN, TEST METHODS AND PRELIMINARY TRIALS

LIST OF FIGURES

LIST OF TABLES

ACRONYMS USED

10G30%	Mix containing 10 microns washed glass powder replaced by 30% of GP cement
20G20%	Mix containing 20 microns washed glass powder replaced by 20% of GP cement
20G30%	Mix containing 20 microns washed glass powder replaced by 30% of GP cement
20G40%	Mix containing 20 microns washed glass powder replaced by 30% of GP cement
20UG30%	Mix containing 20 microns unwashed glass powder replaced by 30% of GP cement
40G30%	Mix containing 20 microns washed glass powder replaced by 30% of GP cement
CTR	All materials class: GP, class F and C fly ashes and glass powder/Control materials class: GP, class F and C fly ashes
FA	Concrete containing 30% class F Fly Ash and cured under standard conditions
FAC30%	Mix containing class C fly ash replaced by 30% of GP cement
FAE-D	Concrete containing 30% class F Fly Ash, kept at elevated temperature ($50^{o}C$) for 18 hours and subsequently dry-cured until testing
FAE-W	Concrete containing 30% class F Fly Ash, kept at elevated temperature ($50^{o}C$) for 18 hours and subsequently water-cured until testing
FAF30%	Mix containing class F fly ash replaced by 30% of GP cement
GL-CN	Washed glass powder classified according to content: added at 20%, 30% and 40%; having fineness of 20 µm
GL-FN	Washed glass powder classified according to fineness: having fineness of 10 µm, 20 µm and 40 µm; added at 30%
GP	GP cement control mix cured under standard conditions
GPE-D	GP cement control concrete kept at elevated temperature ($50^{o}C$) for 18 hours and subsequently dry-cured until testing
GPE-W	GP cement control concrete kept at elevated temperature ($50^{o}C$) for 18 hours and subsequently water-cured until testing
LP30%	Mix containing limestone powder replaced by 30% of GP cement

SF1	SCC mixes having flow below 500 mm
SF2	SCC mixes having flow within the range of 660-750 mm
SF3	SCC mixes having flow above 790 mm
UG	Concrete containing 30% unwashed glass and cured under standard conditions
UGE-D	Concrete containing 30% unwashed glass, kept at elevated temperature (50^{o}C) for 18 hours and subsequently dry-cured until testing
UGE-W	Concrete containing 30% unwashed glass, kept at elevated temperature (50^{o}C) for 18 hours and subsequently water-cured until testing
WG	Concrete containing 30% washed glass and cured under standard conditions
WGE-D	Concrete containing 30% washed glass, kept at elevated temperature (50^{o}C) for 18 hours and subsequently dry-cured until testing
WGE-W	Concrete containing 30% washed glass, kept at elevated temperature (50^{o}C) for 18 hours and subsequently water-cured until testing

ACKNOWLEDGEMENTS

Creating a Ph.D. thesis is not an individual experience; rather it takes place in a social context and includes several people whom I would like to thank sincerely. First of all, I wish to express my gratitude to my Ph.D. supervisor, Dr. Allan Scott, for his guidance, encouragement, and advice he provided during my time as his student. Dr. Scott is a great thinker and a man who never gets tired of his passion for looking for new insights. Pursuing an experiment-based research is similar to diving in a sea where you expect to face open-mouthed crocodiles and whirlpool in every tide. Misfortunes in the form of unanticipated results keep befalling on the sea water droplets until they become pearls when you finally achieve your objectives. The simple yet valuable words, “wrong results are after all some results”, spoken by Dr. Scott at the time of my experimental failures have been a great motivation throughout this challenging phase.

I wish to sincerely thank my co-supervisor, Dr. James Mackechnie, who always responded to my enquiries promptly, asked inspiring questions and assisted me with his great skills related to concrete industry. In addition, he believed in me and provided me references in order to obtain research funding. I have been an admirer of his writing skills since I read his first research paper and wish to learn his simple and direct yet effective expression of writing in coming years of my professional development. I would also like to acknowledge all the technicians of civil engineering laboratories at the university who helped me in pursuing the experimental work. I have been aided for years by Mr. Tim Perigo, a fine technician who always directed me using his own skills and experience in the concrete laboratory. I would like to give special thanks to BRANZ and Glass Packaging Forum for financial support, Allied Concrete for technical support and Golden Bay Cement for material delivery.

Ph.D. is an exhausting and emotional struggle, where you are forced to confront all of your fears, insecurities and doubts you have about yourself and somehow overcome them. It is a terrifying journey and a lot of bravery is required, which is only possible with the encouragement of your loved ones. My three and a half years of Ph.D. were not only a step towards obtaining a prestigious degree, these years have also been of assistance for me to mature as a person. I have had my moments of low self-assurance when I only foresaw catastrophes and almost admitted my defeat. Overcoming the demise of the closest relation in the midst of Ph.D., followed by many other traumas made me emotionally fragile and many times I also lost all expectations from my academic progress. This destination could never be possible without the support of Dr. Rabia Nazir, who was always ‘present’ through

holding my hand when I was having a painful moment, listening with her whole mind, giving all her attention, acknowledging my internal experience, sitting with equally intense emotions, summarizing her own feelings about my situation and giving her valuable opinions and suggestions. Being an emotionally delicate person living far from my family, she has been my counsellor, psychologist, listener and advisor apart from being second family and a high-quality friend. In short, I wish to express my heartfelt gratitude for her help in making me a stronger and less sensitive person as I am today, with a note that I can write pages and pages describing how special she is to me.

I am forever indebted to my father for providing me the opportunities and experiences that have made me who I am today. He always selflessly encouraged me to explore new directions in life and seek my own destiny. I would like to thank my mother for raising me as a person who can fight with all the battles of life, be it academic, personal or social. My deep and earnest gratitude to my brother in law, Mr. Syed Anzar Hassan, for his inspiring conversations; my sister, Mrs. Nashia Anzar, for her prayers and my younger siblings for their continuous interruption during my work time that made me feel their presence close to me. I am filled with gratitude for Mr. Amir Malek, Ms. Zeinab Chegini, Mr. Kaveh Andisheh and Mr. Karim Tarbali for their suggestions, guidance, and helpful discussions. I also wish to express my deepest appreciation to Andrew Bradfield, and Hayden Whyte for their assistance in performing some experiments. Last but not the least, I would like to thank God, who helped me to survive even after all the storms I have been through during the last few years of my Ph.D. study.

Samia Tariq

ABSTRACT

The principle objective of this research was to assess the capability of self-compacting concrete utilizing waste glass as partial replacement for GP cement and as an alternate to class F and class C fly ashes and limestone filler. The viability of using this self-compacting concrete was assessed by conducting various tests. The incorporation of glass powder, whether finer/coarser or in less/more proportions, influenced rheology of self-compacting concrete. A better rheological performance was achieved by the mixes containing glass powders of finer sizes and added at lower contents. However, excessive use of superplasticizer beyond a certain limit resulted in strength loss due to microstructural damage and increase in pore areas. The use of finer glass powder at lower replacement levels in self-compacting concrete resulted in higher compressive strength, splitting tensile strength and elastic modulus than coarser glass powder used at higher contents. The durability was also improved particularly with the addition of smaller sizes of glass powder and lower glass powder contents. Glass powder improved concrete properties by reactive filler effect and pozzolanic action that led to reduction in pore sizes and well packed concrete mix. The improved particle distribution of glass powder also resulted in reduction of the thickness of transition zone leading to densely packed stronger concrete. On the other hand, the mechanical properties of concrete containing unwashed glass powder worsened compared to washed glass incorporated mixes. In addition, the replacement of cement with unwashed glass powder resulted in concrete with inadequate durability properties. Accelerated cured mix incorporating washed glass powder achieved its target strength and improved the microstructure, irrespective of the following curing regime. Conversely, elevated cured self-compacting concrete containing unwashed glass powder could not reach its design strength even with subsequent water-curing. Hence, GP cement, class F and C fly ashes and limestone filler can successfully be replaced by glass powder of fineness 10 µm added up to 30% and 20 µm added up to 20%-30%, in a self-compacting concrete mix, particularly where both strength and durability are essential requirements. Moreover, limestone filler can be replaced by glass powder of fineness 20 µm added up to 40% and 40 µm added up to 30% in a self-compacting concrete mix, where durability is of a greater concern and strength can be compromised. The present research will benefit concrete producers and consumers and will increase economic and environmental advantages for concrete industry by limiting the production of cement and utilizing waste glass resources in New Zealand and around the globe.

Deputy Vice-Chancellor's Office
Postgraduate Office

UNIVERSITY OF CANTERBURY
Te Whare Wānanga o Waitaha
CHRISTCHURCH NEW ZEALAND

CO-AUTHORSHIP FORM

This form is to accompany the submission of any thesis that contains research reported in co-authored work that has been published, accepted for publication, or submitted for publication. A copy of this form should be included for each co-authored work that is included in the thesis. Completed forms should be included at the front (after the thesis abstract) of each copy of the thesis submitted for examination and library deposit.

Please indicate the chapter/section/pages of this thesis that are extracted from co-authored work and provide details of the publication or submission from the extract comes:

1. Chapter 4:

Tariq, S. A., Scott, A. N., Mackechnie, J. R. (2016). "Controlling fresh properties of self-compacting concrete containing waste glass powder and its influence on strength and permeability." *Proc., Fourth International Conference on Sustainable Construction Materials and Technologies (SCMT4),* Las Vegas, United States.

2. Chapter 6:

Ali, S., Scott, A. N., Mackechnie, J. R. (2015). "Effects of waste glass on strength and durability characteristics of self-compacting concrete." *Proc., The New Zealand Concrete Industry Conference 2015,* Rotorua, New Zealand.

3. Chapter 7:

Scott, A., Mackechnie, J., Matthews, J., Bull, D., Cook, D., and Ali, S. (2014). "Preliminary assessment of the influence of accelerated curing on concrete quality." *Proc., The New Zealand Concrete Industry Conference 2014,* Taupo, New Zealand, 111-120.

Please detail the nature and extent (%) of contribution by the candidate:

The candidate did all the work (100%) under supervision for 1 and 2.

The candidate did 30% of the work under supervision for 3. The paper presented preliminary trial word on elevated curing of GP Cement which was then subsequently developed and expanded considerably by the candidate in Chapter 7 of her thesis.

Certification by Co-authors:

If there is more than one co-author then a single co-author can sign on behalf of all
The undersigned certifies that:

- The above statement correctly reflects the nature and extent of the PhD candidate's contribution to this co-authored work
- In cases where the candidate was the lead author of the co-authored work he or she wrote the text

Name: *Allan N. Scott* Signature: 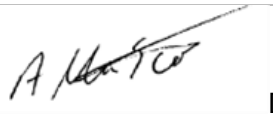 Date: *27th Sep, 2016.*

LIST OF PUBLICATIONS

The following papers have been published based on the work reported in this thesis.

Tariq, S. A., Scott, A. N., Mackechnie, J. R. (2016). “Controlling fresh properties of self-compacting concrete containing waste glass powder and its influence on strength and permeability.” *Proc., Fourth International Conference on Sustainable Construction Materials and Technologies (SCMT4),* Las Vegas, United States.

Ali, S., Scott, A. N., Mackechnie, J. R. (2015). “Effects of waste glass on strength and durability characteristics of self-compacting concrete.” *Proc., The New Zealand Concrete Industry Conference 2015,* Rotorua, New Zealand.

Scott, A., Mackechnie, J., Matthews, J., Bull, D., Cook, D., and Ali, S. (2014). “Preliminary assessment of the influence of accelerated curing on concrete quality.” *Proc., The New Zealand Concrete Industry Conference 2014,* Taupo, New Zealand, 111-120.

CHAPTER 1

INTRODUCTION

HIGHLIGHTS

- Introduction to the utilization of supplementary cementing materials in concrete production.
- Significance of this research for concrete industry and the motivation behind this research.
- Identification of the research scope and objectives to produce effective information for the concrete industry.
- Planning of the experimental program and expected key outputs from this research.
- Thesis outline to clarify the sequence of information provided in the next chapters.

1.1 Introduction

In the past few decades, major changes regarding the conservation of resources and recycling of wastes through proper management have taken place. The utilization of recycled materials in construction is one of the most interesting options because of the large available quantities of waste materials and widespread sites of construction (Shi and Zheng, 2007). The conception of utilizing recycled waste materials for construction works has a continuous and successful history, which includes materials such as fly ash, slag, silica fume, rubber tyres, expanded polystyrene, ceramic and plastics (Figure 1.1). These land filled waste materials have been questioned in the past but are now considered precious substitutions for improving significant properties of concrete. Another waste material, which continues to face challenges as a component of concrete is glass (Federico and Chidiac, 2009). Since glass is one of the commonly used materials in man's day to day life, large quantities of glass are being produced every year in various forms, the most common being soda-lime silica glass. This large-scale production results in increased recycling needs of the significant volumes of glass. Due to this, several research efforts have been carried out in the construction industry so that glass wastes can be used in the composition of concrete.

Figure 1.1: Commonly used supplementary cementitious materials. From left to right: fly ash (class C), metakaolin (calcined clay), fly ash (class F), silica fume, slag, and calcined shale (Portland Cement Association, 2015)

Glass can be considered as a good pozzolanic material, provided that the material is fine enough, therefore the beneficial utilization of glass in concrete is anticipated. The size of glass particles plays a significant role in estimating the range of expansion in concrete. The expansion in concrete is the worst for coarser glass particles; however, negligible expansion is produced with finer glass sizes. A significant effect of glass pessimum size is the internal micro-cracking of glass structure during the crushing process, which encourages durability problems (Mackechnie and Munn, 2012). In addition, there are few more risks associated with waste glass that may become an obstacle against its effective utilization in concrete and need to be addressed (Sullivan and Horwitz-Bennett, 2012). These issues will be discussed in the succeeding chapters.

In the last few decades, considerable research works have aimed attention at the issues associated with the use of waste glass in concrete (Meyer and Baxter, 1996, 1998; Pollery and Cramer, 1998; Bazant et al., 2000; Dyer and Dhir, 2001; Byars et al., 2004; Dhir et al., 2004; Shi et al., 2004; Shayan and Xu, 2004, 2005; Mackechnie and Munn, 2012). These include the harmful effects of coarse glass on concrete properties, such as workability, air content, strength, and especially alkali-silica reaction. Although glass as an aggregate replacement has already been the focus of many investigations, there has been limited study on the partial substitution of cement with glass. Consequently, glass has been used as an aggregate replacement around the globe but due to the lack of evidence available on the effectiveness of glass powder as a cement replacement, the partial substitution of cement with glass is uncommon. Hence, there is a considerable interest in investigating the addition of glass as a cement replacement in concrete. The addition of glass in concrete as a cement substitute is expected to enhance its overall behaviour due to relatively large quantities of silicon and calcium resulting in cementitious properties when finely grounded.

1.2 Research Significance and Motivations

The increased utilization of existing resources, associated with the construction industry of New Zealand, is reducing their availability for future generations. One possible solution to this problem is to collect and reuse the abundant wastes and produce alternate materials for construction (Figure 1.2). This indicates that the use of readily available recycled waste materials in construction is an attractive option because of their availability in large quantities. However, minimization of any costs incurred for additional processing is also essential; otherwise, the resulting product containing waste materials becomes too expensive to be used. Moreover, utilization of wastes in construction materials is a better option than transporting natural materials to construction sites located at longer distances. The current challenge for the concrete industry is to ensure that concrete made from recycled wastes is of a suitable quality appropriate for its application. In addition to providing a source of material for the concrete industry, the use of wastes also provides a potentially chargeable benefit to other industries through the disposal of their waste products.

Glass consumption has increased significantly over the past decade and has continued to trend upwards in terms of utilization. New Zealand consumes an estimated 250,000 tonnes of glass each year. Out of this, about 185,000 tonnes is container glass i.e. bottles and jars (Arnold et al., 2008). In the South Island, the estimate of total glass consumption is between 33,300 tonnes and 44,400 tonnes per year (Thomas, 2005). Glass is typically recovered for recycling through council funded kerbside collections and drop-off centres, commercial recycling collections, and transfer stations or recovery centres in New Zealand. The only glass that can be collected through household collections is in the form of bottles and jars. Glass collected through the recycling and recovery systems is approximately 16,000 tonnes,

Figure 1.2: Waste collection for recycling (Shi et al., 2004)

out of which 7,000 tonnes of glass is recovered in Christchurch alone. According to Christchurch City Council, the overall average kilograms of glass collected at the kerbside by Council's contractor is 5-7 kilograms per person living in Christchurch per month (Christchurch City Council, 2013). Although the recycling process has been improved as well as in practice since the past few years, New Zealanders dispose of an estimated 2.46 million tonnes of waste to landfills each year, out of which glass waste represents an estimated 4% by weight of landfill. This means approximately 100,000 tonnes of glass ends up in the landfills each year (New Zealand's Industry Association, 2016).

The cement and concrete industry annually produces and uses about 1 million tonnes of cement in New Zealand, which equates to around 3 million cubic meters of concrete for new residential, non-residential and commercial construction (Gaimster, 2014). Considering the large available quantities of glass going to landfills, utilizing this glass waste in the production of concrete seems to be an economical alternative. This research should result in the potential utilization of higher volumes of glass in construction. Even if a low percentage of 10% cement is replaced by glass in concrete, the construction industry could utilize approximately 100,000 tonnes of glass per year.

Presently, Allied Concrete in New Zealand is utilizing glass in the production of concrete and has also been recognized through an Excellence in Concrete Innovation Award for its Recycled Glass Sand Initiative. Three of its plants have been converted to be able to use crushed glass as a sand replacement in a number of low strength concrete mixes. Allied Concrete is also carrying out investigations on using recycled glass material in its own region of generation. It is currently collecting glass from the Kapiti District and transporting it to Wellington for processing and utilizing at their Kiwi Point plant. In addition, glass collected in the Southland region is processed and utilized in both Invercargill and Wanaka. Allied Concrete is pre-blending glass sand and natural sand at Nelson plant and then running it through their satellite plant as a standalone operation.

Although utilization of glass as sand replacement in concrete has already been in practice in New Zealand, additional research on its potential benefits is still required for its utilization in other forms and at different replacement levels. The current scenario has developed motivation for the researchers in New Zealand to assess the possible effects of using waste glass as cement replacements on the performance of concrete, which would ultimately benefit the concrete producers. Self Compacting Concrete (SCC) is one of the most widely used concrete types mainly because of its self compacting characteristics and additional benefits. SCC offers various advantages in the construction process due to its improved quality, productivity, and working conditions. Due to differences in mixture design,

placement and consolidation techniques, SCC technology improves the performance in terms of hardened concrete properties like surface quality, strength and durability. Considering the benefits associated with the production and utilization of SCC, this research has investigated the potential use of recycled glass wastes in the production of SCC.

There is currently inadequate information available in the literature regarding the use of glass powder in the composition of SCC. The limited available information is related to the addition of glass as coarse or fine aggregates in conventional concrete; however, glass aggregate is susceptible to harmful reactions resulting from coarse glass particles. Hence, efforts have been made in the present study to investigate the performance of fine glass powder as cement substitute for concrete, which is a novel direction for investigation. There is also insufficient data on concrete containing fine glass powder having comparable fineness as cement and added at various contents to estimate the optimum glass content for reasonable performance of glass modified concrete. The fine glass powder used as cement replacement is likely to improve concrete properties due to its pozzolanic reactivity resulting from its smaller size. Glass also has the potential to demonstrate better durability performance in an SCC mix due to its impermeable nature and particle morphology by achieving denser microstructure. Therefore, the present research investigates the effects of high volumes of finely ground glass in SCC on long-term strength and durability characteristics. The study of alkali silica reaction was not included in the scope of this study although the potential for increased alkali aggregate reactivity is generally considered a main concern for concrete containing glass particles. ASR needs multi-year study as significant amount of work can be done on ASR alone, which was not possible with extensive scope of current research. Moreover, there have been many researches done in the past on ASR for concrete containing glass particles that recommended using very fine glass to minimize its effects. This recommendation was used in the present study.

1.3 Research Questions

The gaps in the existing literature have resulted in the possibility of further investigations for effective utilization of glass as any other construction material. In the light of the scenario discussed in the preceding section, following research questions emerge:

1. Can fine waste glass be used as cement replacements in the composition of SCC in order to achieve target performance of SCC?
2. What is the contribution of fine waste glass to the improvement of long-term strength and durability as well as overall performance of SCC?

1.4 Research Objectives and Scope

The following research key objectives have been identified for investigations in order to effectively utilize glass wastes in SSC:

- **i.** Comprehensive investigations on the potential use of the waste glass, as either a fine filler or a pozzolan, to produce SSC.
- **ii.** Determination of the rheological properties of SSC containing glass powder as a partial substitution of cement.
- **iii.** Assessment of the long-term mechanical properties of SSC incorporating glass of various sizes and replacement rates.
- **iv.** Evaluation of the effects of multiple sizes and replacement levels of glass as cement replacements on the long-term durability performance of SSC.
- **v.** Investigation of the behaviour of SSC containing glass powder, under different curing conditions, in terms of the long-term strength and durability.
- **vi.** Comparison of the performance of glass powder with traditionally used binder GP cement and other supplementary cementing materials such as fly ash and limestone powder.

The scope of research is explained below:

- **i.** Material characterization:
  - **a.** Determination of the physical and chemical properties of glass wastes in terms of their type (washed or unwashed), chemical composition, organic content, and structural characteristics.
  - **b.** Consideration of different parameters and combinations of parameters, such as glass size fractions (i.e.; 10, 20 and 40 microns) and particle size distributions, governing their effects on the behaviour and engineering properties of SCC.
- **ii.** Optimization of the content or replacement levels of waste glass, such as 20%, 30% and 40%, based on both fresh and hardened properties of SCC prepared in preliminary trials.
- **iii.** Examination of the effects of different superplasticizer dosages on rheology, strength and durability characteristics of SCC.
- **iv.** Evaluation of the fresh properties of SCC containing glass powder, such as slump flow, flow time, and visual stability index.
- **v.** Assessment of the basic long-term mechanical properties of SCC considering parameters such as compressive strength, splitting tensile strength and elastic modulus.

vi. Conduct studies on the long-term durability characteristics of SCC, such as permeability, porosity, electrical resistivity, chloride resistance, and drying shrinkage.

1.5 Thesis Outline

This Ph.D. thesis is a combination of detailed literature review and experimental research data obtained as part of this investigation that has already been published, together with the results and interpretation not currently available in the literature. The thesis has been organized in the following eight chapters.

Chapter 2 contains the detailed history of the utilization of glass in the composition of conventional concrete and SCC as a fine aggregate replacement and as a partial substitute for cement. The addition of glass having various size ranges has also been discussed with regards to the previous applications in conventional concrete and SCC. An overview of the literature has been presented, the available historical data has been compiled and demonstrated in graphics. The use of glass in concrete previously investigated has been put up as a meta-analysis in the end of the literature review.

Chapter 3 gives an introduction to the physical and chemical properties of the materials used in the production of mortar and SCC for the present study. It also discusses the particle size analysis of different types of binders, including GP cement, fly ashes, limestone powder, and different size ranges of glass powder. In addition, it involves the discussion of the methods used to find these basic properties of the materials and the tests to measure the effects of these properties on mortar and SCC. Finally, it contains the findings of the preliminary trials that became the foundation for the large-scale tests.

Chapter 4 presents the findings from fresh concrete testing, including rheology of all types of SCC. The effects of glass particle sizes and contents on fresh properties of SCC are outlined, along with the variable requirements of superplasticizer dosages according to these changing parameters. The study of the plastic viscosity and yield stress of SCC, incorporating GP cement, fly ashes, and different sizes and replacement rates of glass powder has also been included. It also reports the effects of different superplasticizer levels on early-age strength and durability properties of SCC.

Chapter 5 reports the data obtained from the long-term compressive strength, splitting tensile strength and elastic modulus tests undertaken on SCC samples. Waste glass powder of different parameters was tested in SCC to discover its effects on these properties. The results have been presented in the form of graphs and have been discussed in detail. Additionally, the correlations between different properties have been included. A section including strength activity index of mortar cubes has also been presented in this chapter.

Chapter 6 details investigations on the long-term durability characteristics of all types of SCC; including oxygen permeability, porosity, electrical resistivity and chloride diffusion. The effects of glass finenesses and contents on the durability of SCC have been presented and discussed in this chapter. The correlations between different properties have also been included. In addition, it presents the findings from drying shrinkage tests performed on SCC specimens up to a specified age.

Chapter 7 contains sets of data based on the effects of curing on the long-term mechanical properties and durability characteristics of SCC. Compressive strength, elastic modulus, oxygen permeability, porosity, electrical resistivity and chloride diffusion of SCC with glass powder were tested, after being treated with different curing regimes. Overall, it presents the results obtained from the testing of SCC samples, containing different glass sizes and replacement rates, kept at elevated temperature for 18 hours after casting and subsequently wet and dry-cured.

Chapter 8 presents a comprehensive summary of the main conclusions of the research, including the suitability of glass powder as filler or pozzolan, the appropriate glass replacement rates and sizes to achieve long-term strength and durability properties, and the proper curing regime for glass modified SCC for an effective performance. It also includes the comparison of glass powder with conventionally used binder and other supplementary cementing materials for potential utilization in concrete. Finally, this chapter provides recommendations for future research in the direction of glass utilization in SCC.

Appendices including the complete data obtained from this extensive research study. To elaborate, appendix A, B, C, D, E and F contain the information and/or data related to the findings discussed in Chapters 2, 3, 4, 5, 6, and 7 respectively.

References

Arnold, G., Werkmeister, S., and Alabaster, D. (2008). *The effect of adding recycled glass on the performance of basecourse aggregate,* NZ Transport Agency Research Report 351. Wellington, New Zealand.

Bazant, Z. P., Zi, G., and Meyer, C. (2000). "Fracture mechanics of ASR in concrete with waste glass particles of different sizes." *Journal of Engineering Mechanics,* 126(3), 226-232.

Byars, E.A., Morales-Hernandez B., and Zhu H. Y. (2004). "Waste glass as concrete aggregate and pozzolan." *Concrete, Elsevier,* 38(1), 41–44.

Cement and Concrete Association of New Zealand. (2011). *TR 14 Best Practice Guide for the use of Recycled Aggregates in New Concrete,* Wellington, New Zealand.

Christchurch City Council. (2013). *Waste Management and Minimization Plan 2013.*Christchurch City Council, <http://www.ccc.govt.nz> (Feb. 21, 2016).

Dhir, R., Dyer, T., Tang, A., and Cui, Y. (2004). "Towards maximizing the value and sustainable use of glass." *The Concrete Society, Elsevier,* 38(1), 38–40.

Dyer, D., and Dhir, K. (2001). "Chemical Reactions of glass cullet used as cement component." *Journal of materials in Civil Engineering,* 13(6), 412-417.

Federico, L. M., and Chidiac, S. E. (2009). "Waste glass as a supplementary cementitious material in concrete – Critical review of treatment methods." *Cement and Concrete Composites, Elsevier,* 31(8), 606–610.

Gaimster, R. (2014). "Changes to Acceptable Solutions and Verification Method for Protection from Fire and Backcountry Huts." *Cement and Concrete Association of New Zealand,*<http://www.ccanz.org.nz/files/documents/546a51f7-3b8a-413b-bfb7-89cb0b282812/SU%2074%20-%20Submission%20%20Changes%20to%20AS%20and%20VM%20for%20Protection%20from%20Fire%20etc.pdf> (Feb. 21, 2016)

Mackechnie, J., and Munn, C. (2012). "Characterizing recycled aggregates for use in New Zealand ready-mix concrete production." Allied Concrete, New Zealand.

Meyer, C., and Xi, Y. (1998). "Use of recycled glass and fly ash for precast concrete". *Journal of Materials and Civil Engineering,* 11(2), 89-90.

Meyer, C., Baxter, S., and Jin, W. (1996). “Alkali-aggregate reaction in concrete with waste glass as aggregate.” *Proc., 4th Materials Engineering Conference: Materials for the New Millennium,* ASCE, Va., 1388–1397.

Plastic NZ - New Zealand’s Industry Association. (2016). “Waste Reduction.” http://www.plastics.org.nz/environmental/manufacturingmoreefficiently/wastereduction/(July. 22, 2016).

Pollery, C., Cramer, S. M., and Cruz R. V. (1998). “Potential for using waste glass in Portland cement concrete.” *Journal of Materials and Civil Engineering,* 10(4), 210–219.

Portland Cement Association. (2015). “Supplementary Cementing Materials.” <http://www.cement.org/cement-concrete-basics/concrete-materials/supplementary-cementing-materials> (Feb. 21, 2016).

Shayan, A., and Xu, A. (2004). “Value-added utilization of waste glass in concrete.” *Cement and Concrete Research, Pergamon,* 34, 81–89.

Shayan, A., and Xu, A. (2005). “Performance of glass powder as a pozzolanic material in concrete: A field trial on concrete.” *Cement and Concrete Research, Elsevier,* 36(3), 457–468.

Shi, C., and Zheng, K. (2007). “A review on the use of waste glasses in the production of cement and concrete.” *Resources, Conservation and Recycling, Elsevier,* 52(2), 234–247.

Shi, C., Wu, Y., Shao, Y., Riefler, C. (2004). “Alkali-aggregate reaction of concrete containing ground glass powder.” *Proc., 12th International Conference on AAR in Concrete,* 789–795.

Sullivan, C. C., and Horwitz-Bennett, B. (2012). “AIA Course: New Developments in Concrete Construction.” <http://www.bdcnetwork.com/aia-course-new-developments-concrete-construction> (Feb. 21, 2016).

Thomas, C. (2005). *Market Study for Recycled Glass in the South Island*, Zero Waste New Zealand Trust, Auckland, New Zealand.

CHAPTER 2

BACKGROUND AND PAST RESEARCH

HIGHLIGHTS

- The classification of glass, its chemical characteristics and physical appearance.
- Detailed literature review on the fresh, mechanical and durability properties of concrete containing waste glass as sand and cement replacements.
- Past research efforts with the spotlight on the application of waste glass in self-compacting concrete investigating the fresh, mechanical and durability performance.
- Literature analysis to recognize the focus of previous investigations on coarse glass and the requirement to research more on the use of fine glass as a replacement for cement in SCC.

2.1. Introduction

Glass is a versatile inert material that can be completely recycled. Glass-made objects can be collected, washed and re-utilized in various forms. Recycled waste glass can be melted with raw materials to produce glass containers without changing the chemical properties of glass (Byars et al., 2004; Shayan and Xu, 2004). Usually, waste glass is found in combination with ceramics, plastics, and metals, in a mixture of different colours and contaminated with organic matters such as sugars, liquids, and mercury (Meyer et al., 2001; Shao et al., 2000). However, it is not always practical to clean glass through chemical processing. Since glass is usually found in a combination of different colours, its re-production in one colour is somewhat challenging. Sorting and cleaning glass is extremely expensive and results in glass recycling of only small quantities (Meyer et al., 2001). Therefore, the surplus amounts of glass are either utilized for other purposes or are discarded to landfills.

2.1.1 Classification of glass

Glass can be classified into the following categories, on the basis of its composition: vitreous silica, alkali silicates, soda-lime glasses, borosilicate glasses, lead glasses, barium glasses, and alumina silicate glasses. Out of these types, soda-lime glasses are mostly used to

produce containers or sheets and account for approximately 80% of the total. Soda-lime glass consists of approximately 73% SiO_2, 13% Na_2O and 10% CaO. Therefore, this glass is likely to be pozzolanic and cementitious in nature according to its chemical composition. Another major kind of glass is lead glass, which is generally obtained from electronic parts. However, it has a large amount of lead that can be potentially dangerous for the environment and hence, it may not be utilized in cement and concrete. Borosilicate glasses are usually not considered for utilization. When waste glass is classified according to colour, it is found that 63% is clear, 25% is amber, 10% is green and 2% is blue or other colours. The basic constituents of these glasses are identical, except for small amounts of additives that are added to achieve different colour ranges (Shi and Zheng, 2007). Some specific characteristics of glass can also be enhanced through the addition of tiny amounts of additives during its production phase.

2.1.2 Chemical characteristics

Figure 2.1 represents silica glass, which is an amorphous and a very orderly crystalline material. Since glass is an amorphous material in nature that contains an enormous amount of silica, both of these characteristics are good indicators for any material to be pozzolanic (Shi and Zheng, 2007). Pozzolanic materials produce cementitious products when they react with calcium hydroxide and hence, they can be mixed with Portland cement to produce concrete. These pozzolanic materials are often found in concrete mixes as they assist in the formation of cement hydration products. The potential of glass being used as a pozzolanic material was first considered in 1973 (Pattengill and Shutt, 1973) and since then its pozzolanacity has been further demonstrated (Dyer and Dhir, 2001). Because the inclusion of other pozzolanic materials, such as silica fume, ground blast furnace slag and fly ash, has resulted in the lowering of cracks arising from alkali-silica reaction (ASR), this reduction of cracking has allowed for further investigation on the waste glass as a material for concrete.

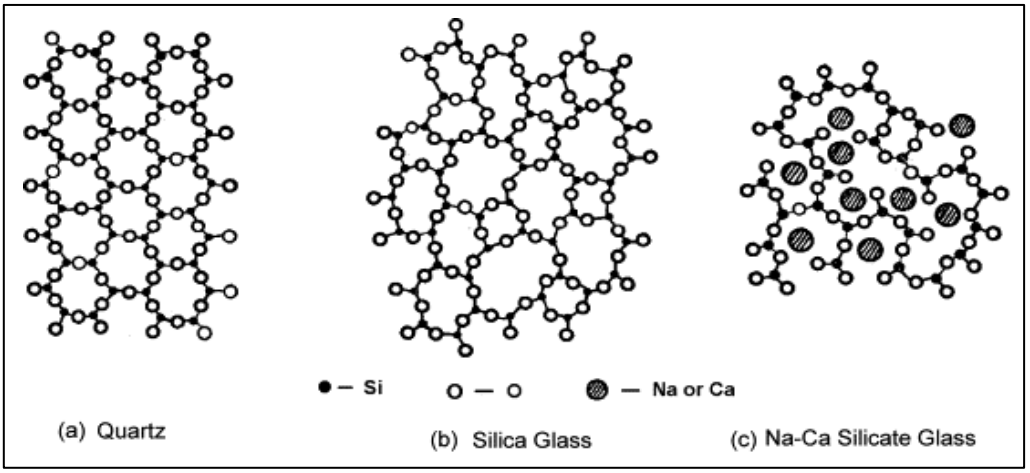

Figure 2.1: Structure of quartz, silica glass, and Na^+– Ca^+ silicate glass (Din, 1979)

It is apparent that glass has the potential to undergo ASR in concrete. ASR is mostly caused by the reaction between the hydroxyl ions within the concrete and the silica that is contained in glass material in the form of chert, quartzite or opal (Shamy et al., 1972). This reaction produces a gel type substance, which increases in volume as it absorbs water, leading to swelling. This expansion creates an addition of pressure within the hardened concrete, which if left without reinforcement, results in failure of that particular concrete sample. The ASR can also cause serious cracking in concrete, resulting in critical structural problems that can even force the demolition of a particular structure.

Glass particle size and colour are important parameters for ASR; therefore, their impact on ASR expansion has been studied in the past. The glass grain size of 1.18–0.60 mm has been recognized as a pessimum size at which maximum expansion is observed (Jin at al., 2000). However, several studies have mentioned that a fine glass powder, ground to a particle size smaller than 75 µm, acts as a pozzolanic material, which can also help to reduce the tendency of reactive glass to initiate ASR by lowering the ASR susceptibility. In addition, it has been established that clear glass shows the maximum expansion, followed by amber, and then green. One explanation for the variation in results is linked to the different chromium contents in different colours of glass (Meyer et al., 2000). However, there are contradictions to this explanation, suggesting that there may be a component other than chromium responsible for expansion (Byars et al., 2004).

Due to the destructive nature of ASR, it has been very complicated for the construction industry to accommodate the usage of recycled glass in their concrete applications. Until recently, there was no technique to restrict the amount of cracking produced by ASR; however, some precautionary methods have been developed for suppressing ASR as well as providing stability to new concrete mixes that use silica-based glasses as aggregates. For instance, the efficiency of lithium admixtures, in order to lessen the cracking, has been broadly proposed in the literature. In addition, another well-established method to reduce ASR is to use a fine pozzolan as a partial replacement for the cement.

2.1.3 Appearance of glass

Crushed glass has an angular shape, sharp corners, a smooth surface texture and a higher aspect ratio, potentially due to the brittle nature of glass, as shown in Figure 2.2. However, previous research work (Du and Tan, 2013) revealed that grinding process of glass involves significant crushing processing due to which some micro-cracks appear in clear glass particles, as illustrated in optical microscopic (OM) and scanning electron microscopic (SEM) images in Figure 2.3 (a) and (b) respectively. Conversely, minor micro-cracks are observed in green glass particles, demonstrated in Figure 2.3 (c), and almost no micro-cracks exist in

Figure 2.2: Appearance of natural and glass sand (Du and Tan, 2013)

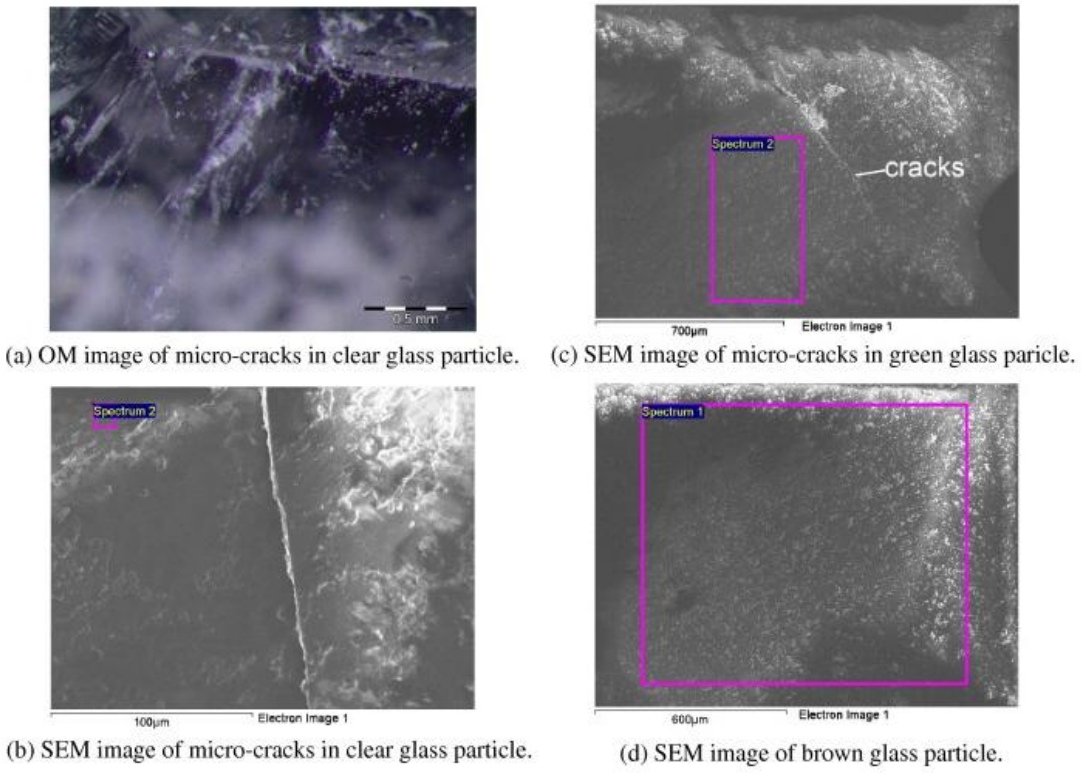

(a) OM image of micro-cracks in clear glass particle.

(c) SEM image of micro-cracks in green glass paricle.

(b) SEM image of micro-cracks in clear glass particle.

(d) SEM image of brown glass particle.

Figure 2.3: Appearance of glass sand after crushing (Du and Tan, 2013)

brown glass particles, shown in Figure 2.3 (d). The dissimilarity in the manufacturing processes of various glass bottles has been recognized as the reason for these different extents of micro-cracking (Dhir et al, 2009). Detailed microstructure of composite materials containing glass will be discussed in the following sections.

2.2. Utilization of waste glass in construction materials

Research studies on the utilization of recycled waste glass in construction materials started a few decades ago. These have been undertaken to investigate the possibility of utilizing waste glass in numerous civil engineering applications (Schmidt and Saia 1963; Chanbane et al., 1999; Rindl, 1998; Shayan et al., 1999). Schmidt and Saia (1963) reported the usage

of crushed glass in architectural concrete panels. The possibility of utilizing waste glass as coarse aggregate in concrete was first stated in a report by Johnson (1974) (Rajabipour, 2010). Later, Rindl (1998) stated that there can be multiple uses of waste glass in construction including road construction aggregate, asphalt paving, and concrete aggregate. Shayan (1999) further studied the use of waste glass as a pozzolanic material in the production of concrete. However, there are concerns about the use of glass in concrete (e.g. susceptibility to ASR) that have been indicated by the literature cited above. Therefore, it is essential to recognize that the performance of glass depends on its type, chemical composition and physical features, such as the presence of pores and particle size (Figg, 1981). The reactivity of glass also depends on whether the glass is replacing cement, fine aggregate or coarse aggregate and the percentage at which the glass is being replaced. These variations in material properties and mix design give considerably varying results related to the characteristics of concrete incorporating waste glass (Almesfer, 2013).

2.3. Effects of waste glass as sand replacements

2.3.1 Fresh Properties

Attempts have been made in the construction industry to study the effects of glass wastes on the flow properties of mortar and concrete. Du and Tan (2013) studied the effects of mixed coloured glass particles on the characteristics of mortar replaced with fine aggregates at 0%, 25%, 50%, 75% and 100%. The authors reported that the flows for brown, green, clear and mixed coloured glass sand mortars were 75%, 90%, 60% and 82% of normal sand mortar respectively, as shown in Figure 2.4. The flowability of mortar was reduced with an increase in glass content for all glass colours because the sharper edges, more angular shape and higher aspect ratio of glass restricted the movement of cement paste and glass particles.

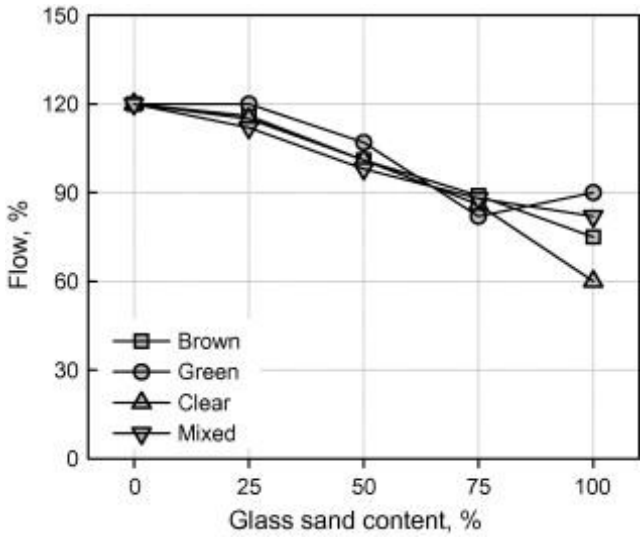

Figure 2.4: Flow of glass sand mortar (Du and Tan, 2013)

In an experimental investigation on the behaviour of concrete containing waste glass as a partial substitute for sand at 10%, 15%, and 20% undertaken by Ismail and Al-Hashimi (2009), the slump values were found to be 57.5 mm, 52.5 mm, and 50.0 mm for specimens made of 10%, 15%, and 20% waste glass, respectively. These findings exhibit the inclination of the slump to decline as the glass replacement ratio rises, possibly due to the poor glass geometry, which results in the lesser fluidity of the mixes and reduction in the fineness modulus. This pattern of decreasing ratios in slump has been illustrated in Figure 2.5.

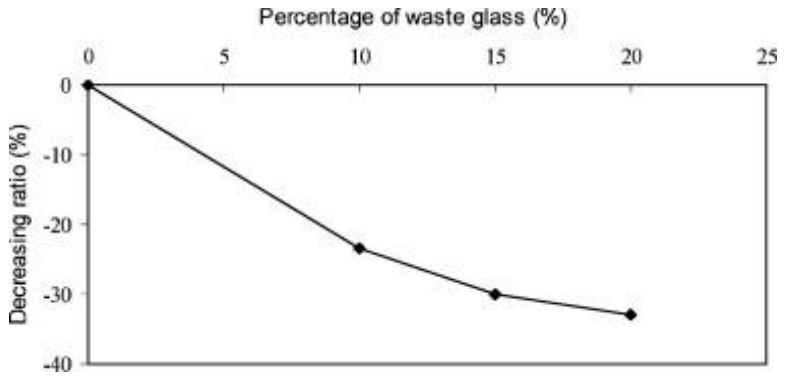

Figure 2.5: Decreasing ratios in the slump (Ismail and Al-Hashimi, 2009)

Park et al. (2004) carried out an experimental research to study the impact of different coloured soda-lime glasses as fine aggregates in concrete at input levels of 30%, 50%, and 70%, together with the inclusion of styrene-butadiene rubber (SBR) latex. It was informed that mixing ratio of waste glass at 30%, 50%, and 70% reduced the slump of concrete by 19.6%-26.9%, 30.1%-34.6%, and 38.5%-44.3%, respectively. Topcu and Canbaz (2004) confirmed that using a high proportion of waste glass decreases the slump value of concrete. Maier and Durham (2012) investigated the effects of recycled glass, added in increments of 0%, 25%, 50%, 75% and 100% as fine aggregates, on concrete properties coupled with recycled coarse aggregate and slag cement. The authors endorsed the aforementioned findings that the replacement of natural virgin aggregates with recycled coarse aggregates and crushed waste glass has a detrimental effect on the workability of a concrete mixture. The significantly high absorption capacity of the recycled aggregate in combination with the harshness of the waste glass decreases concrete workability.

Contrary to these findings, Batayneh et al. (2007) found that the presence of crushed glass in concrete mixes does not affect the flow behaviour of concrete significantly. The authors evaluated fresh and hardened properties of concrete, utilizing ground glass to replace up to 20% of fine aggregates in concrete mixes, along with crushed concrete up to 20% of coarse aggregates. Shayan and Xu (2006), who investigated the performance of crushed glass at different proportions of 40%, 50%, and 75% as a sand replacement in a field trial using a 40 MPa concrete mixture, also demonstrated that the replacement of sand with crushed glass

does not have an effect on the slump of concrete. However, Mackechnie and Munn (2012) conducted research using waste glass as sand replacements at 5%, 10%, and 15% by weight to produce 20 MPa concrete and reported different results that waste glass concrete generally exhibits higher slump as compared to control concrete, potentially due to higher air content of these mixes. The authors further reported that the presence of contamination from glass bottles and differences in angularity of glass results in continuous entrainment of air in concrete. The variations in air content with the addition of waste glass, in turn, affect slump of concrete, making it difficult to analyse the change in workability due to the addition of waste glass. Bleed of concrete increases with the increase in glass input, which was linked to variations in slump and air content values. Details for these concrete mixes and their fresh properties are shown in Table 2.1.

Table 2.1: Waste glass concrete mix details and fresh concrete properties (Mackechnie and Munn, 2012)

Glass	0%	0%	5%	5%	10%	10%	15%	15%
Location	CH	IV	CH	IV	CH	IV	CH	IV
Slump (mm)	100	120	110	140	120	130	120	120
Density (kg/m^3)	2403	2380	2396	2378	2358	2367	2350	2360
Air (%)	2.5	3.6	2.8	2.9	3.7	3.2	3.8	3.4
Bleed (L/m^3)	9.4	9.7	9.1	10.8	9.3	13.0	10.5	12.3

Few more researchers have attempted to determine the influence of glass waste on air content of mortar and concrete. Park et al. (2004) recorded 12.2%-21.6%, 23.7%-30.4%, and 30.6%-41.4% increase in air content for the glass replacement ratios of 30%, 50%, and 70% respectively, owing to the irregular shape of the glass grains and a larger relative surface area that maintained more air in comparison to the natural concrete aggregate. The

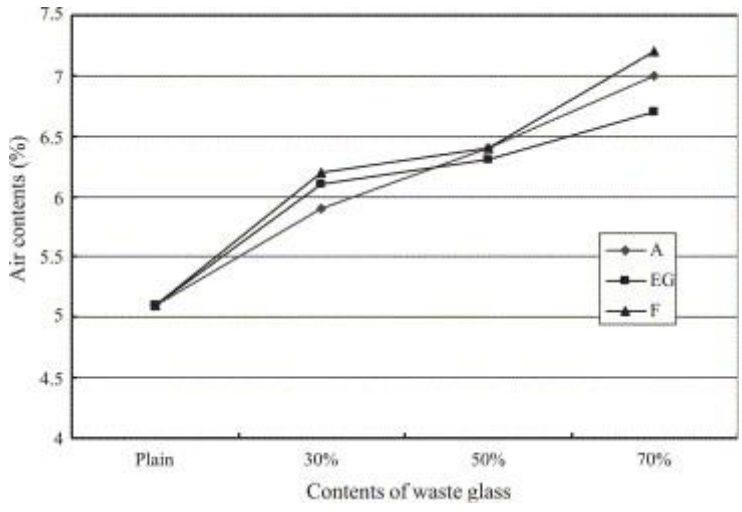

Figure 2.6: Results of air content (where A, EG, and F stand for amber, emerald green and flint coloured glass) (Park et al., 2004)

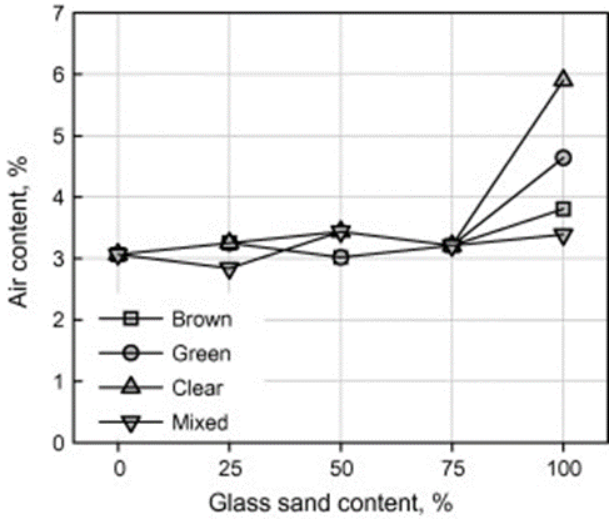

Figure 2.7: Air content of glass sand mortar (Du and Tan, 2013)

air content test results of that study are represented in Figure 2.6. Similarly, Du and Tan (2013) found that the air content of glass sand mortar was within 3% and 3.5%, showing a minor increase with higher glass sand content up to 75%. At 100% glass replacement, clear glass exhibited the highest air content of 5.9% that was almost two times more than the normal sand mortar (Figure 2.7). This was attributed to the sharper edge and higher aspect ratio of glass sand, which allowed more retained air at the glass particle surface.

Ismail and Al-Hashimi (2009) recorded the decreasing ratios (in reference to control concrete) of 1.28%, 1.96%, and 2.26% while testing fresh densities of specimens made of 10%, 15%, and 20% waste glass respectively, as shown in Figure 2.8. The reduction in the fresh density of the glass concrete mixes was related to the specific gravity of glass material that was around 14.8% lower than that of the natural sand. In spite of the decrease in the fresh density values of the glass concrete mixes, they were still comparable to the control mixes. Figure 2.9 shows the decreasing ratios in the dry densities of waste glass concrete mixes. Identical results were reported by Topcu and Canbaz (2004), which confirmed that unit weight of concrete with waste glass is lower than that without waste glass.

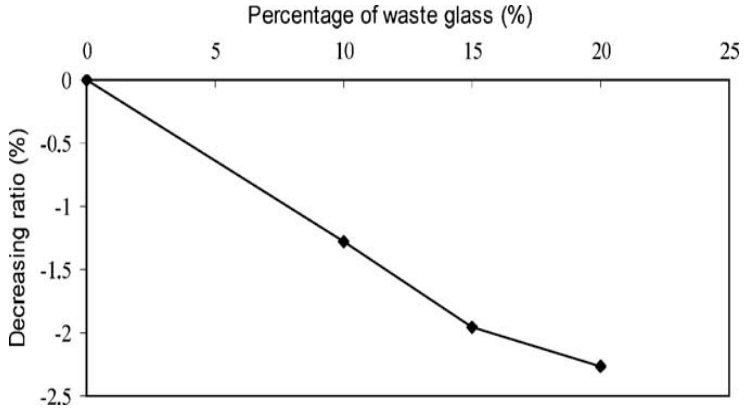

Figure 2.8: Decreasing ratios in fresh density (Ismail and Al-Hashimi, 2009)

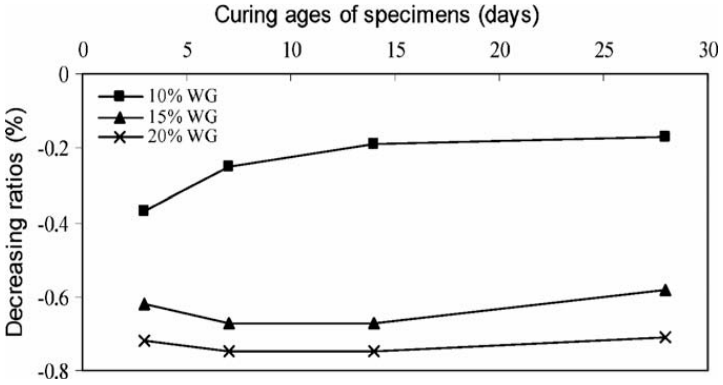

Figure 2.9: Decreasing ratios in dry densities (Ismail and Al-Hashimi, 2009)

2.3.2 Mechanical Properties

Many studies have been conducted to examine the mechanical properties of mortar and concrete containing glass waste as a sand substitute. Du and Tan (2013) reported that the addition of glass waste in concrete results in the reduction of compressive strength, owing to the smooth surface and sharper edges of glass particles, which leads to weaker bond strength at the Interfacial Transition Zone (ITZ) between glass particles and cement paste matrix. In that study, the glass sand up to the replacement rate of 25% did not considerably affect the compressive strength. Mortars with 100% brown, green, clear and mixed glass demonstrated 72%, 75%, 60%, and 70% respectively, of compressive strength shown by the

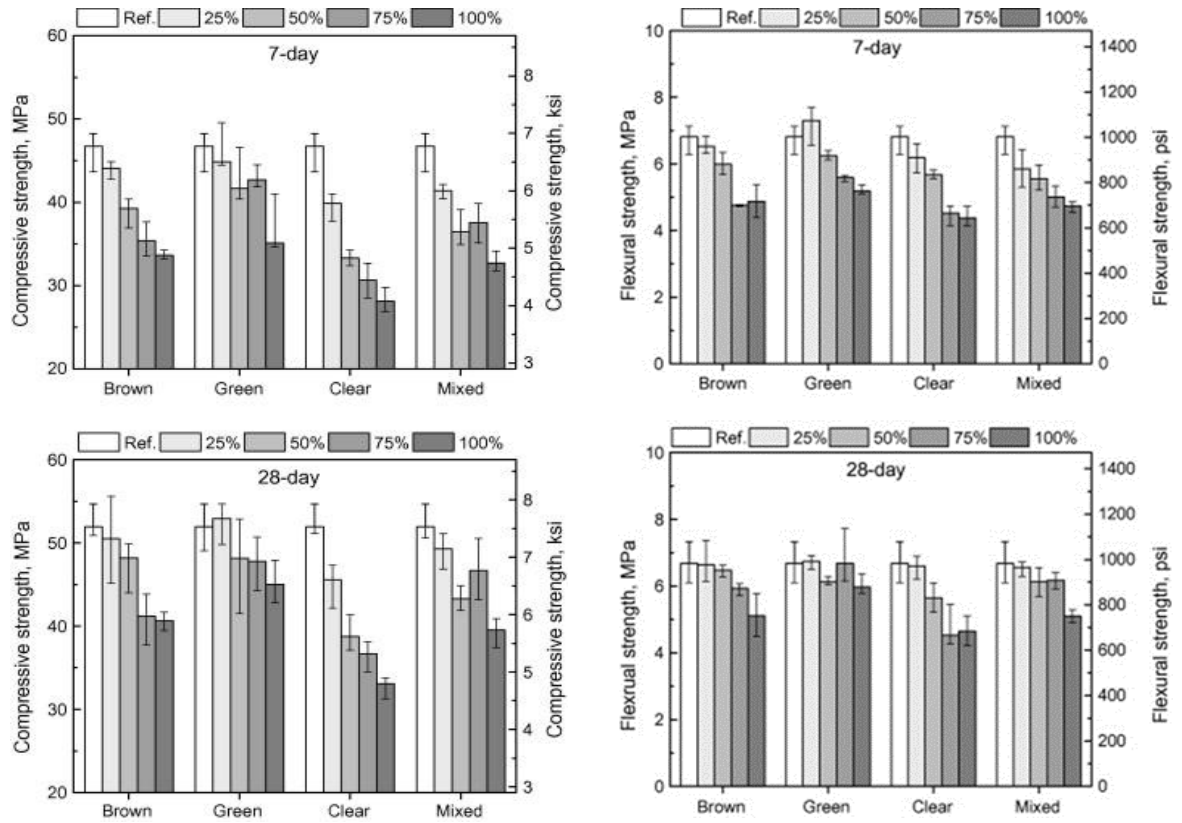

Figure 2.10: Compressive strength and flexural strength of glass sand mortar at 7 and 28-days (Du and Tan, 2013)

normal sand mortar at 7-days. At 28-days, this ratio rose to 78%, 87%, 64%, and 76%. The pozzolanic properties of fine glass particles might be the reason behind this as reported by Shayan and Xu (2004), Shao et al. (2000), Shi et al. (2005) and Federico and Chidiac (2009). Similarly, flexural strength reduced in concrete containing glass in excess to 25%, particularly in the case of clear glass. For the other types of glasses, the decline in 28-days strength was less than 10% when glass dosage was lower than 75%. The flexural strengths of mortar with 100% brown, green, clear and mixed glass sand were 76%, 90%, 70%, 76% respectively, compared to normal sand mortar, at 28-days. Figure 2.10 shows 7 and 28 days compressive and flexural strengths of glass sand mortar, as reported by Du and Tan (2013).

In another study conducted by Mackechnie and Munn (2012), it was reported that the addition of waste glass by up to 10% as a partial substitution for sand has minor deleterious impacts on hardened characteristics of the concrete. In that study, the compressive strength was found to marginally decrease with increasing quantity of waste glass, which was related to increasing air contents. The study concluded that glass has an increased risk of air-entrainment but this risk can be reduced by decreasing quantities of air-entraining agents used in lower strength concrete mixes. It was suggested that in order to reduce the threat of ASR- induced expansion, fine glass powder of less than 600 µm can be blended with coarser sand and/or relatively lower addition levels up to 5% glass waste can be added.

In contrast to the aforementioned results, Batayneh et al. (2006), reported that addition of crushed glass as a partial substitute of fine aggregates improves the strength characteristics of concrete; however, the alkali content of glass would have an impact on its long-term durability and strength, both of which need long-term investigation. The influence of various glass percentages on strength of concrete observed in that study is shown in Figure 2.11. It shows that compressive, flexural and splitting tensile strengths for up to 20% glass aggregate replacements are greater than those of normal concrete. This increase in strength was related to the surface texture and strength of glass particles compared to that of sand.

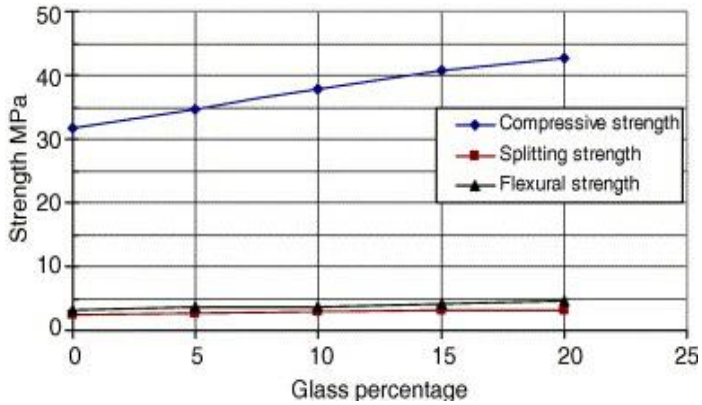

Figure 2.11: Relationship between the compressive strength and percentage of crushed glass content (Batayneh et al., 2006)

Lam et al. (2007) determined the mechanical properties of concrete paving blocks produced with 25%, 50% and 75% recycled glass sand, as a blend of three different colours (30% colourless, 40% green and 30% brown), along with pulverized fuel ash (PFA). It was noticed that the strength gain from 28-days to 90-days of the concrete mixtures at the different glass and PFA contents becomes more significant when the PFA content is increased, as demonstrated in Figure 2.12. The result was linked to the pozzolanic reaction of the PFA particles and recycled glass at late test ages. However, for the mixes other than those prepared with 0% PFA, the compressive strength gain escalated with an increase in glass content. This was attributed to the coarser particle size of the glass used, having fineness modulus of 4.25. Another study by Lam (2006) validated that an aggregate having fineness modulus ratio ranging from 3.5 to 4.5 would be most appropriate to produce concrete paving blocks, for a given aggregate to cement ratio.

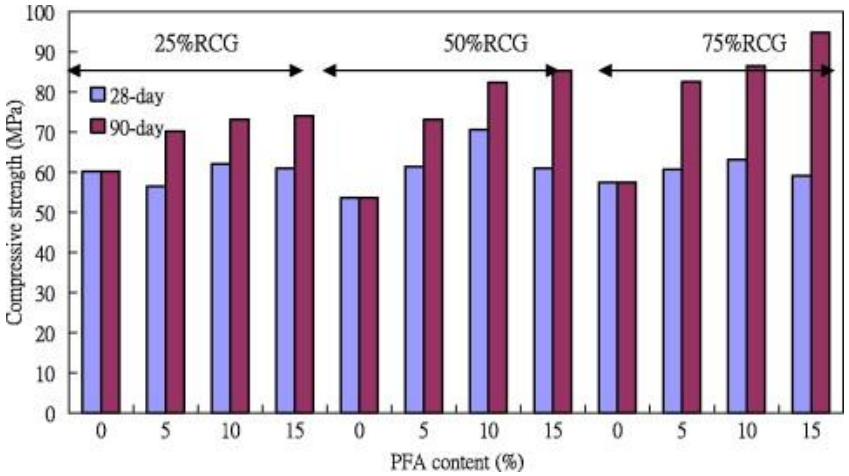

Figure 2.12: Results of 28-day and 90-day compressive strengths of concrete paving blocks prepared with different glass (RCG) and pulverized fuel ash (PFA) contents (Lam et al., 2007)

2.3.3 Durability Properties

Few studies have investigated the durability properties of mortar and concrete incorporating glass sand. Lam et al. (2007) showed that water absorption of paving concrete blocks is greatly connected to water absorbability of aggregate particles. Since glass particles have a relatively lower water absorption, it was already expected that the water absorption of paving blocks would decrease with the increase in recycled glass content. Figure 2.13 shows that the effect of PFA on water absorption of the concrete paving blocks is lower in comparison to that of the recycled crushed glass (RCG). Du and Tan (2013) reported that the replacement of natural sand by waste glass particles leads to a higher resistance to chloride ion penetration. The total charges passed in 50% brown, green, clear and mixed glass sand mortar were 93%, 69%, 71%, and 64% respectively, in comparison to the sand mortar. The Rapid Chloride Permeability Test (RCPT) results at 28-days are illustrated in Figure 2.14.

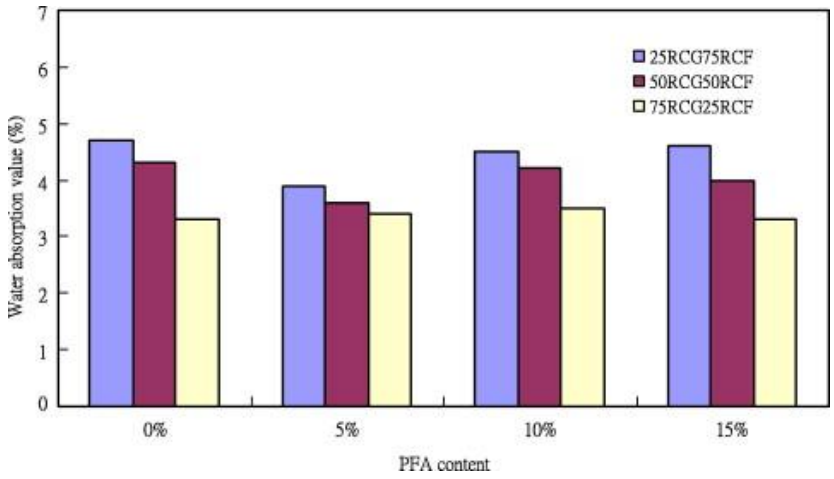

Figure 2.13: Results of water absorption of concrete paving blocks prepared with different glass and pulverized fuel ash (PFA) contents (Lam et al., 2007)

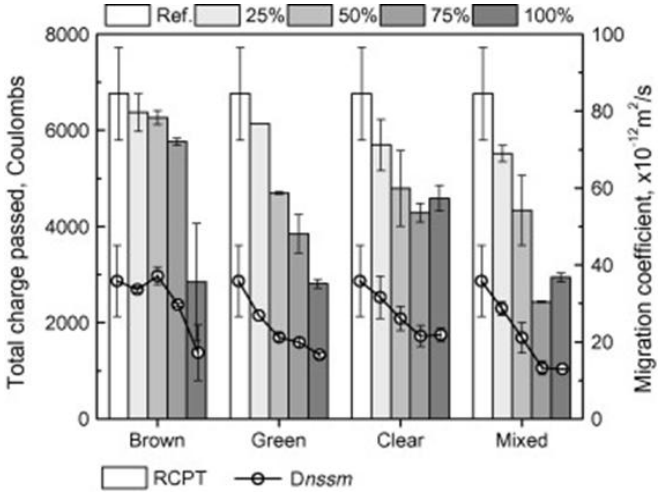

Figure 2.14: Rapid Chloride Permeability Test (RCPT) of glass mortar (Du and Tan, 2013)

These findings are persistent with a former study undertaken by Kou and Poon (2009), who reported a reduction of 60% in the charge passed for concrete containing 45% of the sand replaced by glass. Du and Tan (2013) also tested mortar cubes for sulphate attack through immersion of cubes in saturated $MgSO_4$ solution for 24 hours. Through visual investigation, it was observed that the cement pastes at the external sides of the mortar cubes were diffused, hence, revealing only the glass sand. There was a comparable loss in weights of all glass sand mortar cubes, irrespective of glass colour and glass content, as shown in Figure 2.15 (a). The outcomes of the research also revealed that all mortars cubes exhibited a rise in mechanical strength after the sulphate attack, specifically in terms of flexural strength, as demonstrated in Figure 2.15 (b). Chen et al. (2006) similarly reported that there is a lower decrease in strength with a higher replacement rate of glass sand, likely because only the external parts of mortar specimens are attacked by sulphate whereas central part remains unreacted. The rise in strength properties was associated with the pozzolanic reaction of fine glass grains at higher temperature levels during the test.

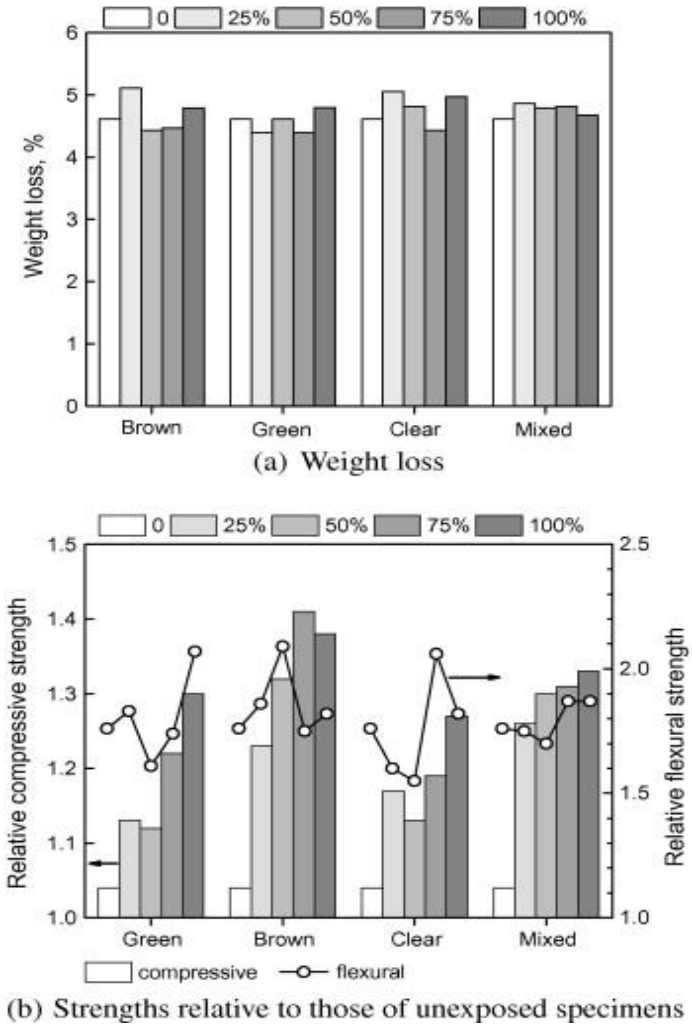

Figure 2.15: Sulphate attack test results of glass sand mortars (Du and Tan, 2013)

2.3.4 Alkali-Silica Reaction Investigations

Rajabipour et al. (2010) presented a comprehensive investigation of glass size effects on the properties of mortars containing various sized glass grains (SEM1: 1.18–2.36 mm; SEM2: 0.3–0.6 mm; SEM3: 0.075–0.15 mm) through SEM. Based on the imaging results, it was revealed that ASR took place only within internal cracks of glass particles. Moreover, glass sand smaller than 0.6 mm did not undergo damaging ASR expansions but coarser glass particles had larger and more permeable cracks that contributed towards higher alkali-silica reactivity. It was observed that SEM1 mortar bars started to expand and ASR gel was created within cracks inside glass particles at 7-days, as shown in Figure 2.16 (a). The gel-filled cracks seemed to be wider and swelling of the ASR gel was observed at 14-days, as demonstrated in Figure 2.16 (b). ASR gel became wider at 30-days, even more than 100 µm in width, partly due to the swelling of this gel, as exhibited in Figure 2.16 (c) and (d). An absence of major cracking in pastes was observed in SEM2 and SEM3 mortar specimens after 14 and 30 days of exposure, as evident in Figure 2.16 (e) and (f) respectively.

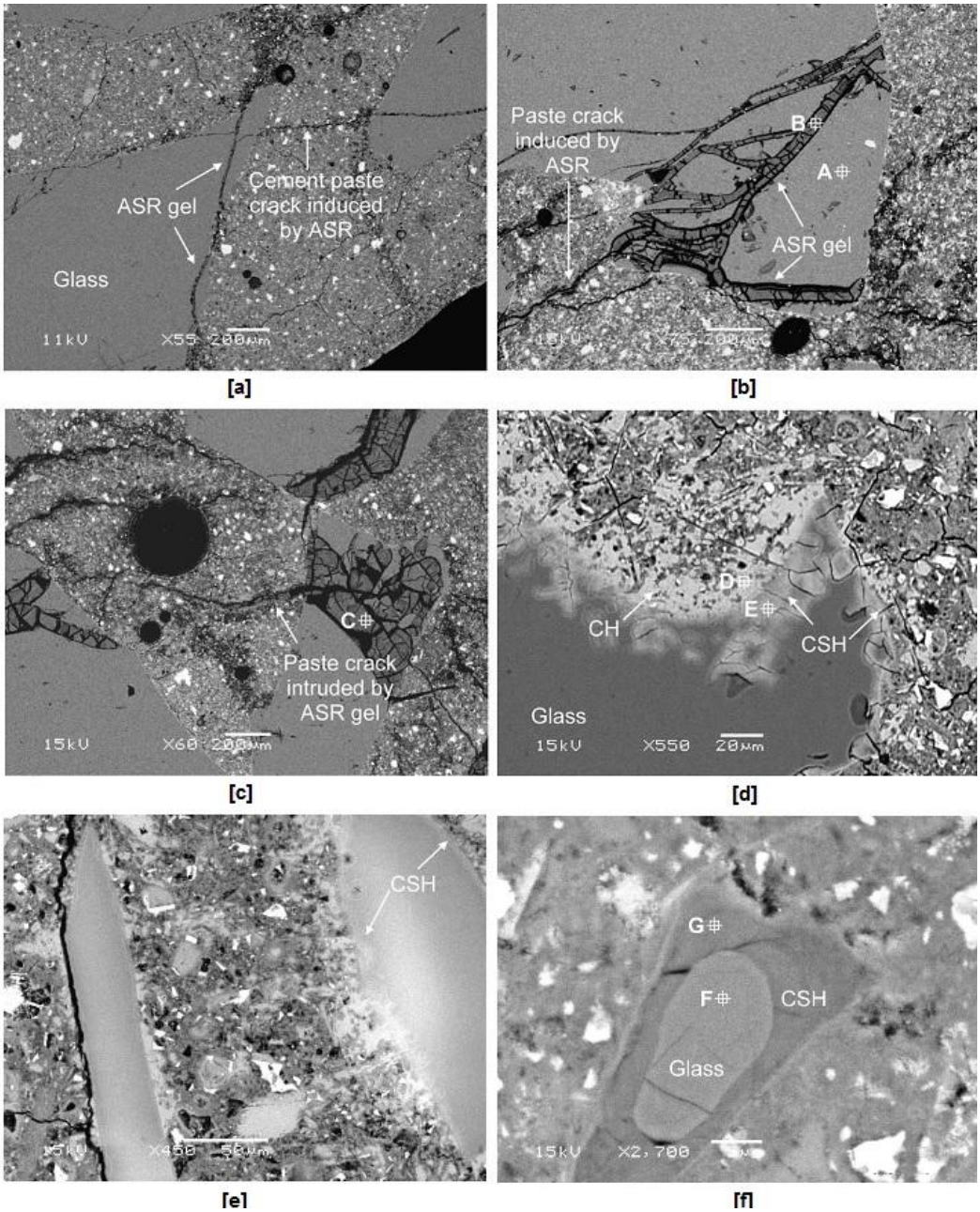

Figure 2.16: SEM micrographs of mortar: (a) SEM1 at 7 days; (b) SEM1 at 14 days; (c) and (d) SEM1 at 30 days; (e) SEM2 at 14 days and (f) SEM3 at 30 days of exposure to the NaOH bath (Rajabipour et al., 2010)

Du and Tan (2013) revealed that clear glass sand mortars show entirely different behaviour from green and brown glass sand mortars. According to the visual analysis of the specimens, cracks appeared on the surface of clear glass sand mortar at the curing age of 28-days. The increase in glass content led to an increase in width, length, and density of these cracks. However, no such cracks were seen in the case of brown and green glass. Owing to this, different colours of glass behaved differently to ASR reactivity. This implies that the existence of micro-cracks in clear glass particles would result in significant ASR expansion, as exhibited in Figure 2.17 (a) and (b). In comparison to this, green and brown coloured glasses resulted in minor ASR expansion, as demonstrated in Figure 2.17 (c).

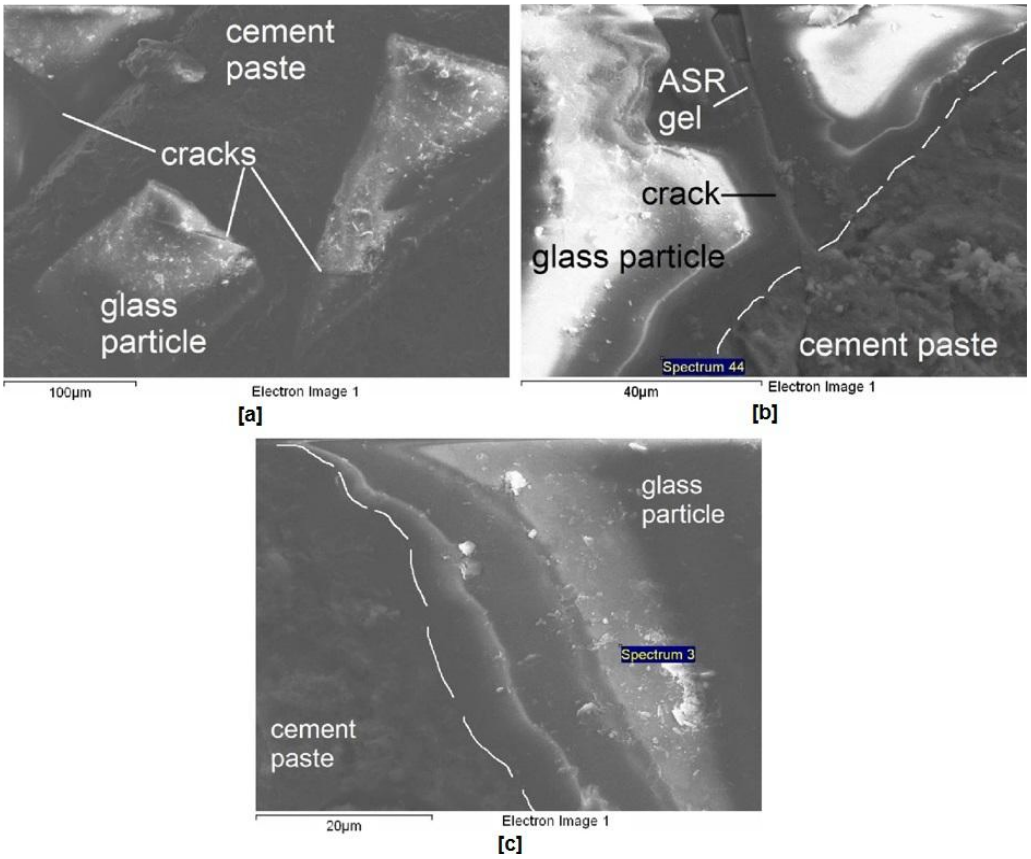

Figure 2.17: SEM micrographs of glass particles: (a) Clear glass particle in mortar before ASR test and (b) Clear glass particle in mortar after 14 days of ASR test (c) Brown glass particle in mortar after 14-days of ASR test (Du and Tan, 2013)

2.4. Effects of waste glass as partial substitution of cement

2.4.1 Fresh Properties

Several studies have been conducted on the fresh properties of mortar and concrete incorporating glass as a cement substitute. Matos and Sousa-Coutinho (2012) examined mortar samples containing waste glass powder of approximately 15 µm at 0%, 10%, and 20% cement replacements and reported that workability increases with the increase in waste glass powder content. However, initial setting times were 10 min and 20 min shorter for pastes with 10% and 20% glass powder respectively, compared to the control paste. On the other hand, final setting time was identical for all types of mortars. Similarly, Nassar and Soroushian (2012), who utilized milled glass waste of 13 µm as a supplementary cementing material in concrete, observed the slump to marginally increase with the inclusion of milled waste glass, possibly due to the low water absorption of glass. The density of fresh concrete somewhat reduced resulting from the addition of milled glass as a partial cement substitute, which was related to lower specific gravity of milled waste glass as that of Portland cement. Nevertheless, there was no significant impact of waste glass powder on air content of the mixes, as mentioned in Table 2.2. It is important to recognize that only M3, M5, M8 and M10

Table 2.2: Fresh concrete properties of low and high w/cm mix with and without glass (Nassar and Soroushian, 2012)

Mix Design	Slump (mm)	Density (kg/m3)	Air content (%)
M1	70	2299	4.5
M2	83	2219	5.0
M3	92	2209	5.0
M4	95	2213	6.0
M5	97	2193	6.0
M6	178	2208	7.0
M7	190	2121	8.0
M8	204	2118	7.0
M9	196	2084	8.0
M10	206	2096	7.5

contained 20% glass powder by weight of cement whereas all other mixes were produced with GP cement as a binder only and different types and proportions of coarse aggregates. Taha and Nounu (2008) studied the feasibility, plastic properties and mechanical characteristics of glass powder of size 45 µm replacing 20% cement in concrete and confirmed that plastic properties of concrete are improved, referring to the improved consistency and workability as well as reduced bleeding and segregation with glass powder addition. The results of this study have been illustrated in Figure 2.18. These findings were related to the improvement characteristics in the texture and shape of glass particles having fineness below 45 µm. Nevertheless, wet density of concrete incorporating glass was slightly lower than the control concrete, due to the decreased density of glass powder as compared to cement, which is consistent with findings reported by Nassar and Soroushian (2012).

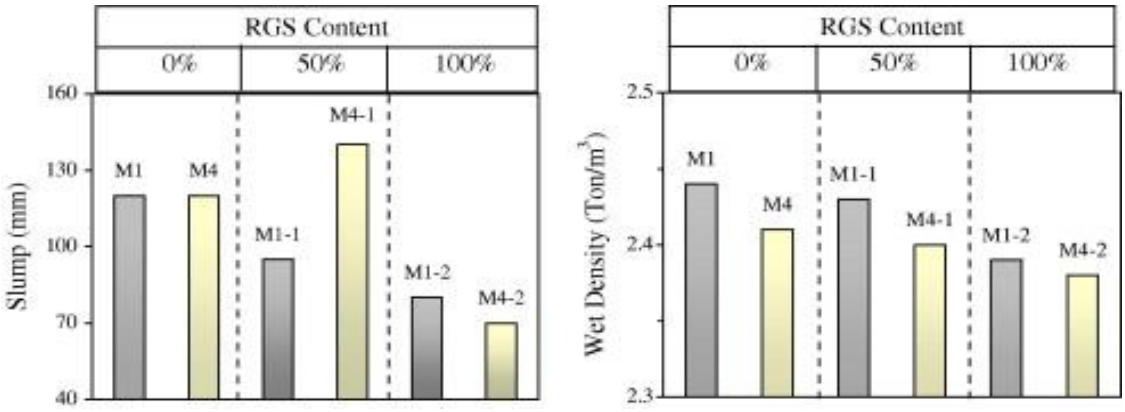

Figure 2.18: The effect of PGP on slump and wet density (Taha and Nounu, 2008)

Shayan and Xu (2006) conducted a field trial, using a 40 MPa concrete mix, subsuming different proportions of glass powder i.e. 0%, 20% and 30%, replaced by cement. Contrary to aforementioned findings, the authors noticed that the mixes which contained glass powder demonstrated a slight decrease in slump as compared to control mix, due to which a water reducer at dosage rate of 0.3 L per 100 kg cement was used to bring the slump to specified

range, though it did not work for some mixes. Likewise, Metwally (2007) also reported that increased proportion of glass powder causes workability loss and decrease in slump up to 45% for 20% cement replacement with glass powder, although Metwally (2007) utilized finer glass in comparison to the glass used by Taha and Nounu (2008), resulting in a higher surface area, which required more water to reach the same level of workability.

2.4.2 Mechanical Properties

Many researchers have studied the effect of glass powder on mechanical properties of mortar and concrete. Shao et al. (2000) investigated the pozzolanic activity, compressive strength and potential expansion of concrete, containing waste glass of sizes 150 µm, 75 µm and 38 µm as partial cement replacement at 30%, in mortar and concrete. The researchers stated that all types of glass concrete had lower strengths in comparison to the control concrete at the ages of 3, 7, 28 and 90 days, other than 38 µm glass concrete that surpassed control concrete by 8%, at the curing age of 90-days. The comparison of concrete containing ground waste glass with control concrete is shown in Figure 2.19. In general, it was observed that the smaller the particles size of the glass, the higher the strength of the glass concrete. For instance, the concrete containing 38 µm glass achieved 120% rise in strength from the age of 3 to 90 days. In addition, the strength activity index of 150 µm glass did not correspond to the ASTM criteria of being pozzolanic. However, 75 µm and 38 µm glass concrete samples were considered pozzolanic and showed comparable results to fly ash concrete at all ages. The strength activity indexes of concrete containing 30% mineral additives, including all glass sizes, are presented in Figure 2.20. It can be seen that the strength activity indexes of concrete, with 30% cement replaced by 38 µm glass, were 91%, 84%, 96%, and 108% at 3, 7, 28, and 90 days, respectively.

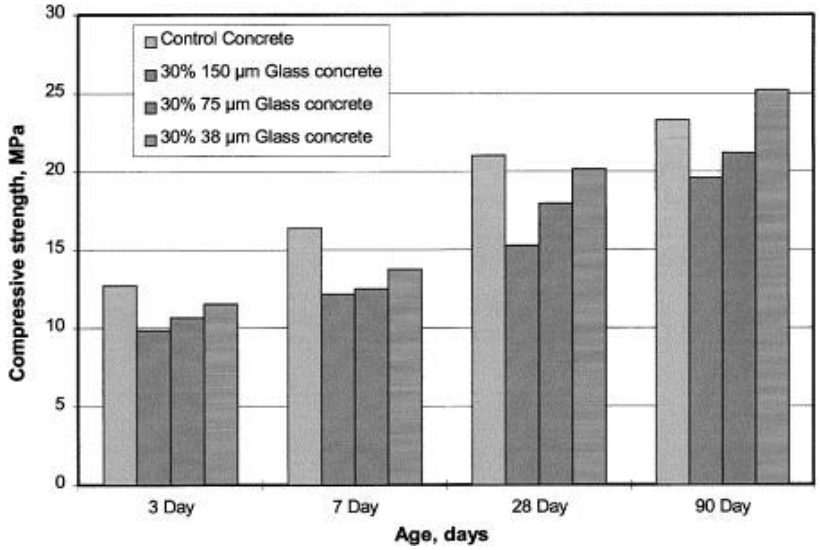

Figure 2.19: Compressive strength of concrete containing 30% ground glass (Shao et al., 2000)

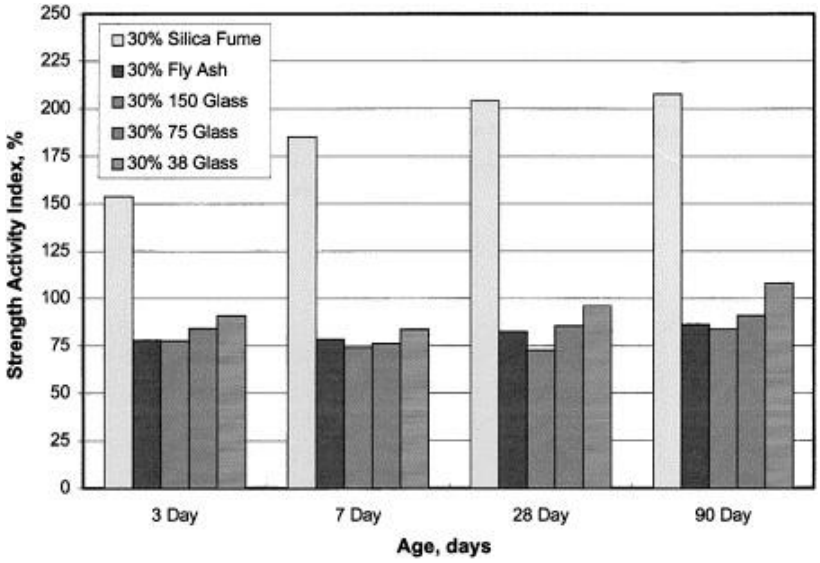

Figure 2.20: Strength activity index of concretes containing 30% mineral additives (Shao et al., 2000)

Matos and Sousa-Coutinho (2012) reported that the strength of glass mortar is lower compared to control mortar at 7 and 28 days. In that study, strength decreased with the replacement dosage and generally reached the strength of control by 90-days, as presented in Figure 2.21. Glass mortar at 20% replacement dosage (WGP20) gained significant strength between 28 and 90 days, showing pozzolanic reaction taking place during this time period. Additionally, Sobolev et al. (2007) examined the effects of various colours and types of waste glass particles on the microstructure to examine the interface between the cement matrix and glass particles as well as 7 and 28 days compressive and flexural strengths. The authors mentioned that the window glass showed the best 28-days compressive strength value of 50.1 MPa when added to the cement. The monitor glass, brown and green bottle glass based cement mortars approached compressive strength within the range of 44.5-46.0

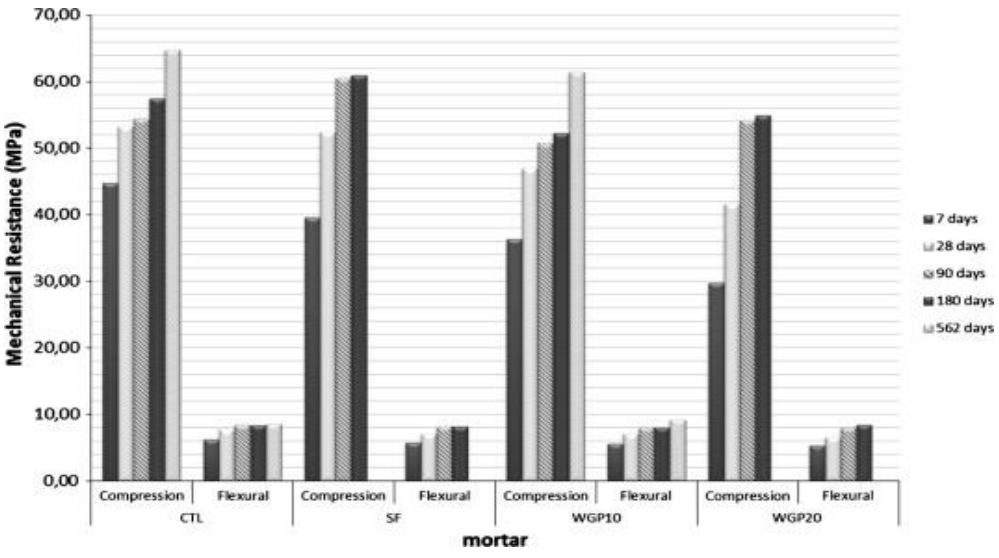

Figure 2.21: Compressive and flexural strength (Matos and Sousa-Coutinho, 2012)

MPa at 28-days, which was close to the strength of normal strength reference mix at 45.4 MPa. Nevertheless, all cements with waste glass exhibited considerably lower strength values compared to the high-performance control mix (72.3 MPa). In addition, 28-days flexural strengths of the glass cement mortars were within a small range of 6.9-7.3 MPa. These values were slightly higher than the 28-days flexural strength of normal strength reference mix at 6.7 MPa. This difference was related to the reduction of w/c ratio that was selected to meet the designated flow range. Similarly, high-performance control samples showed the highest flexural strength of 8.5 MPa at 28-days.

Shayan and Xu (2006) reported that among the mixes that utilized glass powder (GLP), only one containing 20% GLP satisfied the strength requirement of a 40 MPa concrete, according to 28-days strength results. All mix designations and research findings have been summarized in Figure 2.22. The authors reported that Mix 8 remained under-strength at the curing age of 90-days and Mix 6 just surpassed 40 MPa value. Mix 8 had the lowest strength, apparently because it contained 75% crushed glass as a sand substitute (CGS) in addition to 30% GLP as cement input. It was observed that Mix 4, having 30% GLP and without CGS, achieved major strength between the ages of 28 and 90 days, i.e. from 34 to 50.6 MPa, meaning 16.6 MPa additional strength. The control mix (Mix 1) gained only 6 MPa and Mix 2 with 10% silica fume 8 MPa over the same period. This shows that considerable pozzolanic reaction took place in this time frame in the presence of 30% GLP. Constant curing up to the age of 404-days generally resulted in considerable additional strength gain of up to 60 MPa, for Mixes 3, 6, 7, 8 and 10, which contained GLP. The 404-days strengths were considered good, considering the fact that the mixes having GLP, had only 70–80% of the cement content compared to the control mix.

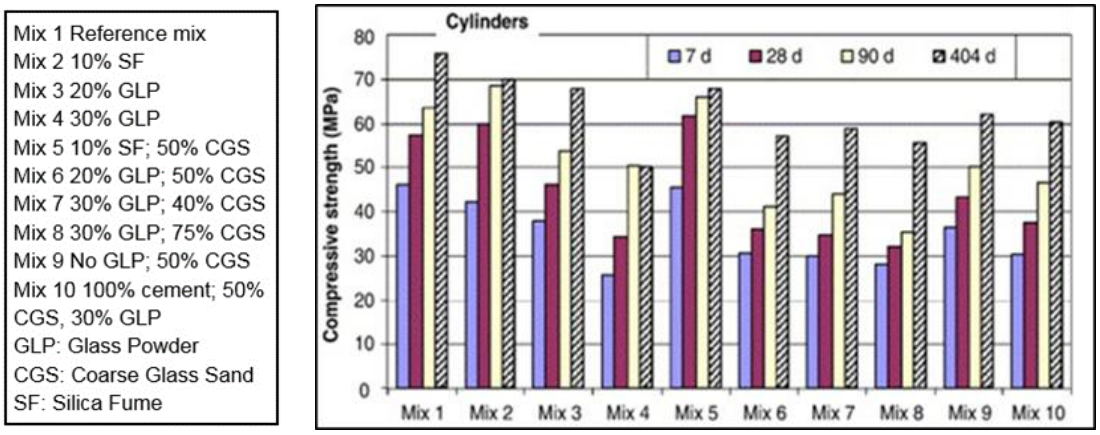

Figure 2.22: Compressive strength development in concrete cylinders (Shayan and Xu, 2006)

Shayan and Xu (2006) further stated that flexural strength adhered to the same trend as compressive strength. The mix containing 30% glass powder and the mix with 30% glass powder and 75% crushed glass sand, demonstrated the lowest flexural strengths. However,

small variations were observed among other mixes that were linked to normal sample variability. The flexural strength results, tested on concrete prisms at the age of 130-days have been graphically represented in Figure 2.23. The relative flexural strength of the mixes was identical to that of the splitting tensile strength as shown in Figure 2.24. The comparison between the flexural strengths of concrete prisms and the splitting tensile strengths tested on cylinders at 28-days showed that they were linearly related over the strength range achieved. The flexural strength of age 130-days was about 50% higher than the split tensile strength of age 28-days, due to older specimens used in the flexural strength tests.

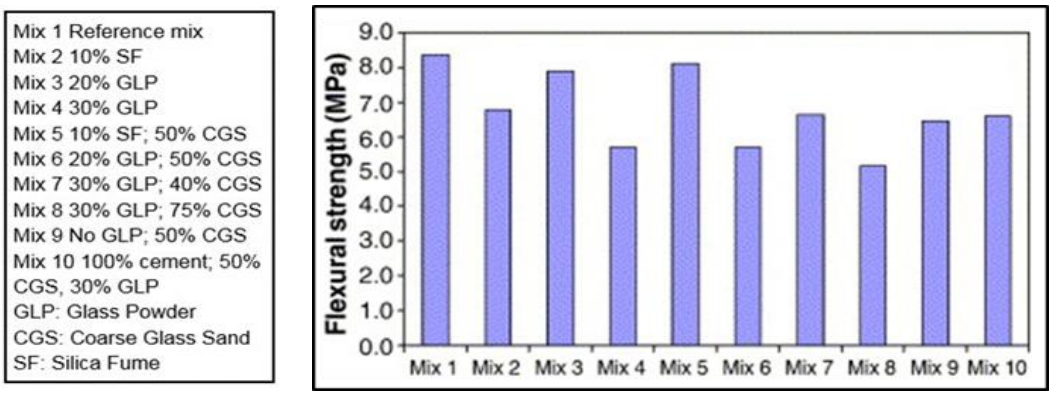

Figure 2.23: Flexural strength of concrete prisms at 130-days (Shayan and Xu, 2006)

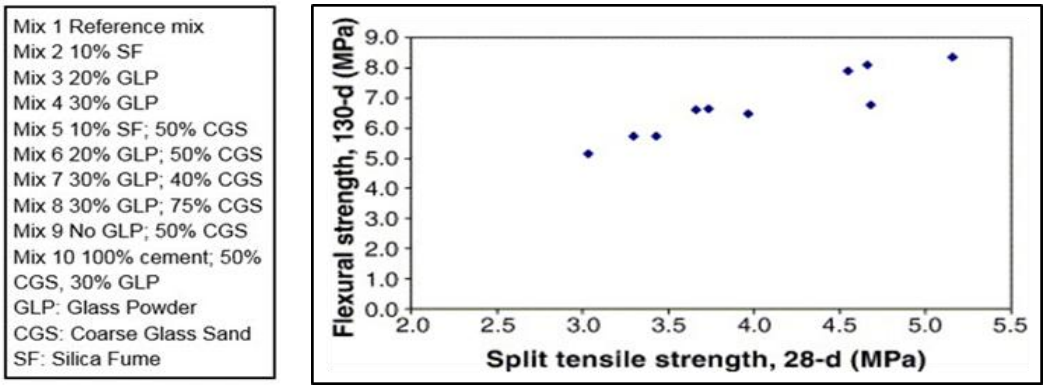

Figure 2.24: Relationship of 28-days splitting tensile strength and 130-days flexural strength (Shayan and Xu, 2006)

Nassar and Soroushian (2012) mentioned that flexural strength test results of the low and high w/c ratio concrete mix followed decreasing trends, identical to the pattern for compressive strength test results. Figure 2.25 (a) and (b) represent the corresponding test results for the low w/cm ratio and high w/c ratio concrete mixes, respectively. For low w/cm ratio concrete mixes, the 14-days flexural strengths with milled waste glass were lower than those without milled waste glass. Nevertheless, the addition of milled waste glass as a partial substitute for cement increased the flexural strength of concrete by 56-days of concrete age. The increase of 11% from M2 (no glass) to M3 (20% glass) and 14% from M4 (no glass) to M5 (20% glass) at 56-days tests was observed. Similarly, the flexural strengths

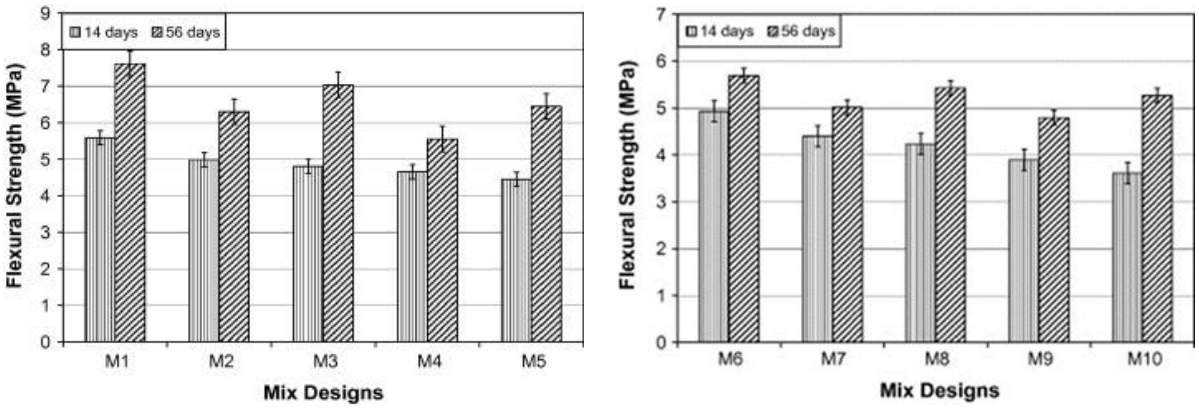

Figure 2.25: Flexural strength of (a) low w/cm (b) high w/cm concrete mixes (means and standard errors) (Nassar and Soroushian, 2012)

of high w/c ratio concrete mixes containing milled waste glass were less than those of the corresponding concrete materials without milled waste glass at 14-days of age. At 56-days of age, high w/c ratio concrete mixes with milled waste glass (M8 and M10) showed 8% and 10% higher flexural strengths than the corresponding concrete mixes without milled waste glass (M7 and M9), respectively.

2.4.3 Durability Properties

There have been few research efforts to determine the durability properties of concrete containing glass waste as a cement replacement. Ozkan and Yuksel (2008) tested the durability of mortar containing glass powder and observed decrease in the compressive strengths of mortar specimens exposed to NaCl (sodium chloride) and $MgSO_4$ (magnesium sulphate) solutions, as the glass replacement ratio increased. Incorporation of waste glass also increased the durability of mortar exposed to Na_2SO_4 (sodium sulphate) solution. Furthermore, there was no significant effect of the color of the glass on both sodium sulphate and magnesium sulfate resistances.

Shayan and Xu (2006) discovered that the chloride penetrability of Mixes 3, 4, 6, 7, 8 and 10, containing GLP, was significantly lower than that of the reference Mix 1, and comparable to or lower than that of Mixes 2 and 5, containing SF, as illustrated in Figure 2.26. Furthermore, the moist-cured cylinders showed lower chloride permeability as compared to the cores kept at external exposure, mentioning that GLP might be very beneficial under marine exposure conditions against chloride-induced corrosion of reinforcement in concrete. The relation between the volume of permeable voids and the chloride penetrability was poor, which was related to the fact that the latter was majorly affected by the concrete composition and pore solution chemistry instead by relatively small differences in the values of the volume of permeable voids. According to the authors, all mixes developed satisfactory drying

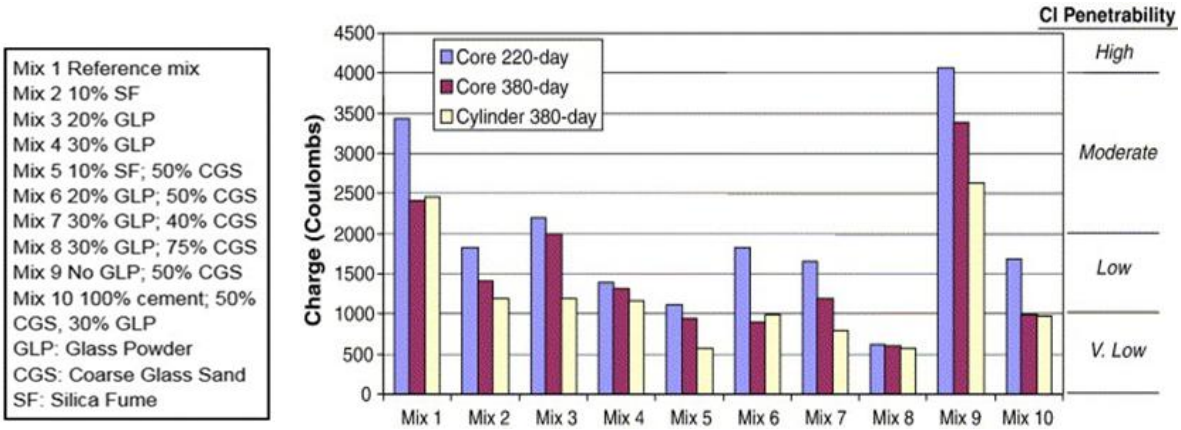

Figure 2.26: Results of the rapid chloride penetration test (Shayan and Xu, 2006)

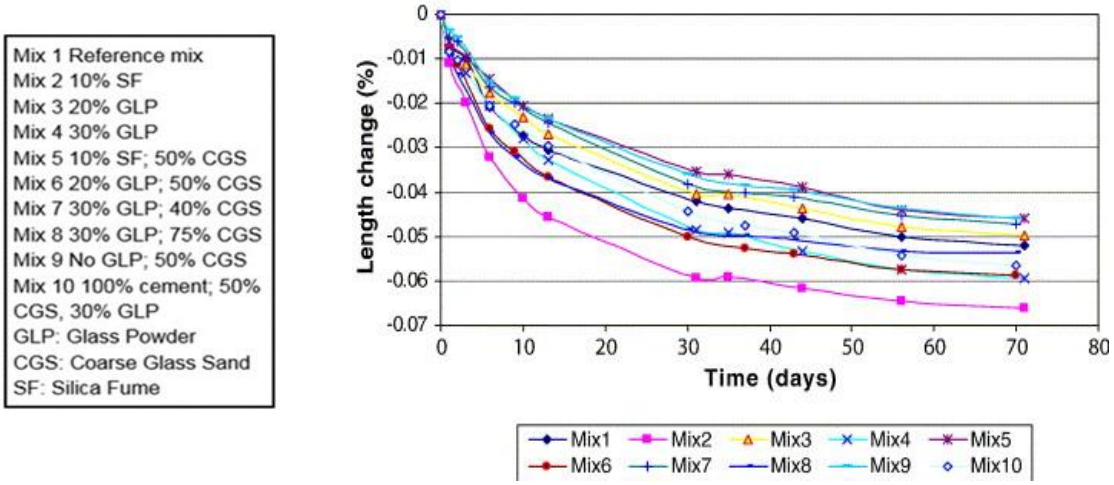

Figure 2.27: Drying shrinkage of concrete prisms (Shayan and Xu, 2006)

shrinkage values below 0.075% at 56-days, conforming to the Australian Standard AS 3600. Mix 2, containing 10% SF, showed shrinkage values larger than those of any of the other mixes. The drying shrinkage measurements found in that study are presented in Figure 2.27.

Conforming to the aforementioned findings, Nassar and Soroushian (2012) reported that the recycled aggregate concrete mix containing milled waste glass had the number of coulombs passed marginally over 2000. The addition of milled waste glass resulted in 54% reduction of the number of coulombs passed through concrete specimens, having 100% recycled aggregate, as compared to concrete specimens without milled waste glass. Concrete mixes with high w/c ratio followed the trend of low w/c mixes as a result of the inclusion of milled waste glass, where 46% and 53% reductions in a number of coulombs passed were observed in concrete mixes with 100% and 50% recycled aggregate concrete respectively. This increased resistance to chloride ion permeation was related to the pore refinement and pore blocking. Figure 2.28 shows the corresponding chloride permeability test results for concrete materials of low and high w/c ratio with and without milled waste glass.

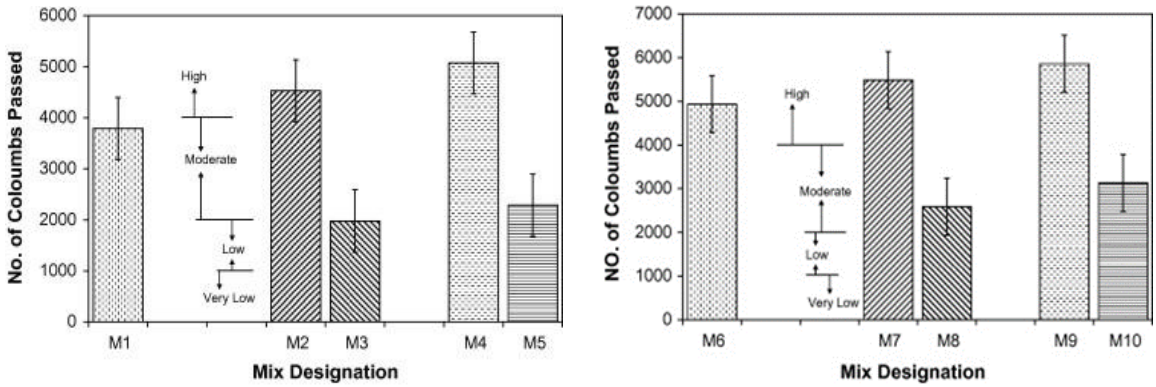

(a) **(b)**

Figure 2.28: Rapid chloride permeability test results for (a) low w/c ratio (b) high w/c ratio concrete materials with and without milled waste glass (Nassar and Soroushian, 2012)

Nassar and Soroushian (2012) also observed that the partial replacement of cement with milled waste glass increased the bulk density of concrete. This was related to the conversion of CH to C-S-H by the pozzolanic reaction of milled waste glass in concrete. Moreover, the filling effect of very fine glass particles resulted in improved particle packing and hence, less permeable microstructure. Utilization of milled waste glass as a partial substitute for cement also resulted in the reduction of the volume of voids in the concrete. The authors stated that water absorption of concrete decreased with milled waste glass input as a partial replacement for cement in both low and high w/c ratio mixes. Contrary to these results, Taha and Nounu (2008) noticed that the presence of glass powder as a cement replacement in concrete increased the water absorption of concrete. This was related to the variations in the nature of the microstructure of concrete mix and hydration product due to the presence of glass powder in concrete.

2.4.4 Microstructure Investigations

Efforts have been made in the construction industry to study the microstructure of waste recycled glass as a cement replacement for mortar and concrete. Sobolev et al. (2007) observed that glass grains were well-distributed in the cement paste, which resulted in a dense structure having reduced porosity, as displayed in Figures 2.29-2.31. There was a clear densification around the glass particles because of their partial hydration, which resulted in the formation of an additional C-S-H layer. At 7-days for window glass cement (Figure 2.29), the glass particles were enclosed by C-S-H layer made of hydration products. By 28-days, the glass particles were perfectly bonded with the matrix together and were covered with the thin C-S-H layer. The cement pastes, using brown and green bottle glass, had the microstructure composed of the gelatinous membrane around the glass grains at 7-days of hardening. By 28-days, further encapsulation of glass grains into hydration products was observed, as demonstrated in Figures 2.30 and 2.31 (right).

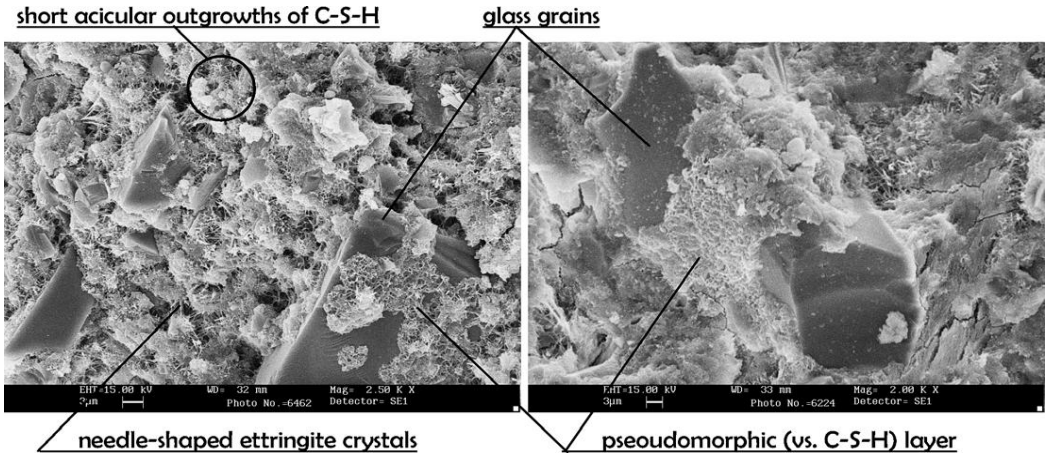

Figure 2.29: Microstructure of window glass cement at 7-days (left) and 28-days (right) (Sobolev et al., 2007)

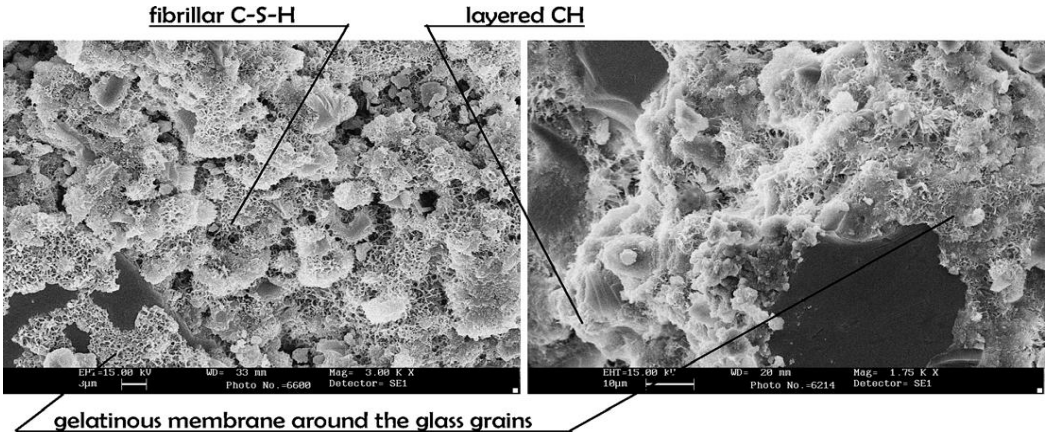

Figure 2.30: Microstructure of brown bottle glass cement at 7-days (left) and 28-days (right) (Sobolev et al., 2007)

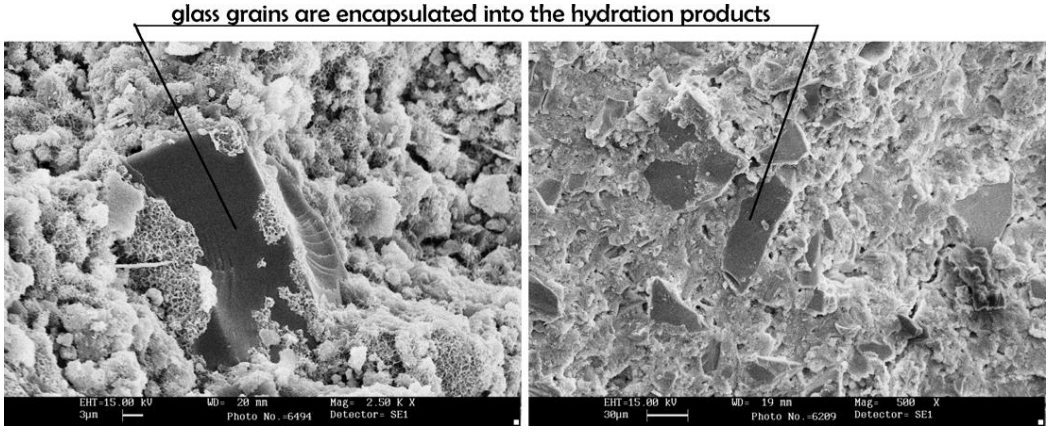

Figure 2.31: Microstructure of green bottle glass cement at 7-days (left) and 28-days (right) (Sobolev et al., 2007)

Figure 2.32 (a) and (b) show the typical SEM view of cement paste near a glass particle in reference mix and a reacted glass shard containing 20% glass, examined by Shayan and Xu (2006). The composition of the paste in Mix 3, containing 20% glass powder (GLP), showed abundance in silica and assimilation of fine glass reactive particles. The similar characteristic

was also observed in Mix 4, having 30% GLP (Figure 2.33) and in both cases, the reaction sites exhibited high Na amount. Some of the round particles of about 20 μm diameter in Mix 4 seemed to have reacted in the concrete but the reaction product had little contents of Na^+ and large contents of Ca^+, as shown in Figure 2.33 (b).

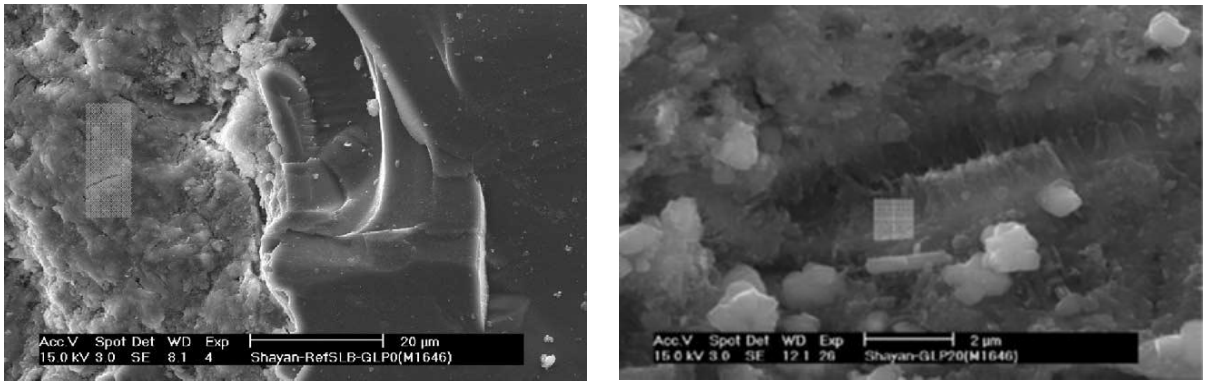

(a) **(b)**

Figure 2.32: (a) SEM view of cement paste near a glass particle in Mix 1 (reference) (b) SEM view of a reacted glass shard assimilated into Mix 3 (20% GLP) (Shayan and Xu. 2006)

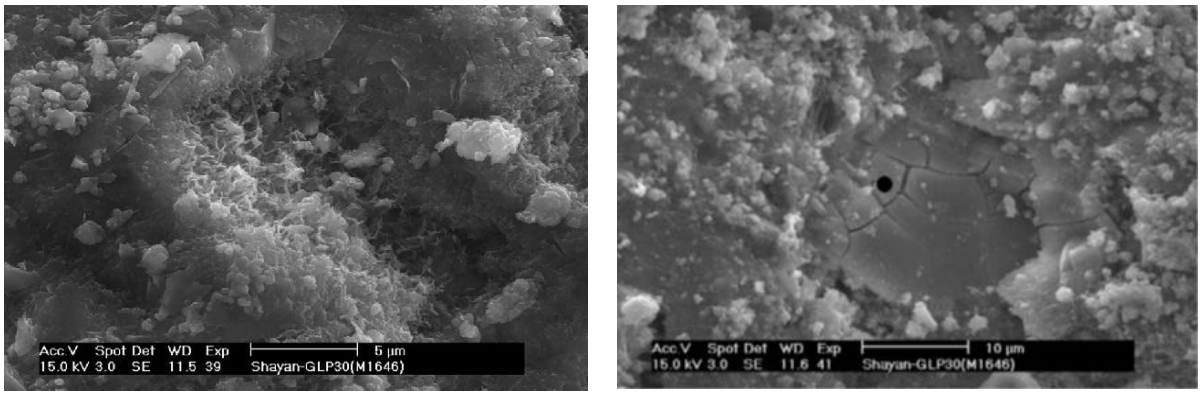

(a) **(b)**

Figure 2.33: (a) SEM view of paste near a reacted glass particle in Mix 4 (30% GLP) (b) SEM view of reacted glass forming a Ca-rich gel in Mix 4 (30% GLP) (Shayan and Xu, 2006)

According to Matos and Sousa-Coutinho (2012), glass particles appeared to be completely encapsulated and dispersed into the hydrated products of a dense and mature layer with needle-shaped crystals (refer to WGP10 10,000 and 20,000 times enlarged in Figure 2.34). CH layered crystals were noticed in the control mortar (refer to CTL 5000 times enlarged in Figure 2.34) and CSH gel filling the hydrated structure. CSH gel in glass replaced at 10% was observed to hold more calcium and alkalis than control mortar. These results are consistent with Sobolev et al. (2007), who informed that the major dissimilarity between mortar consuming glass and control Portland cement is linked to the reduction in size and the amount of CH, resulting from the consumption of CH due to the pozzolanic reaction involving glass grains. Shayan and Xu (2006) also stated that more alkalis were found in the

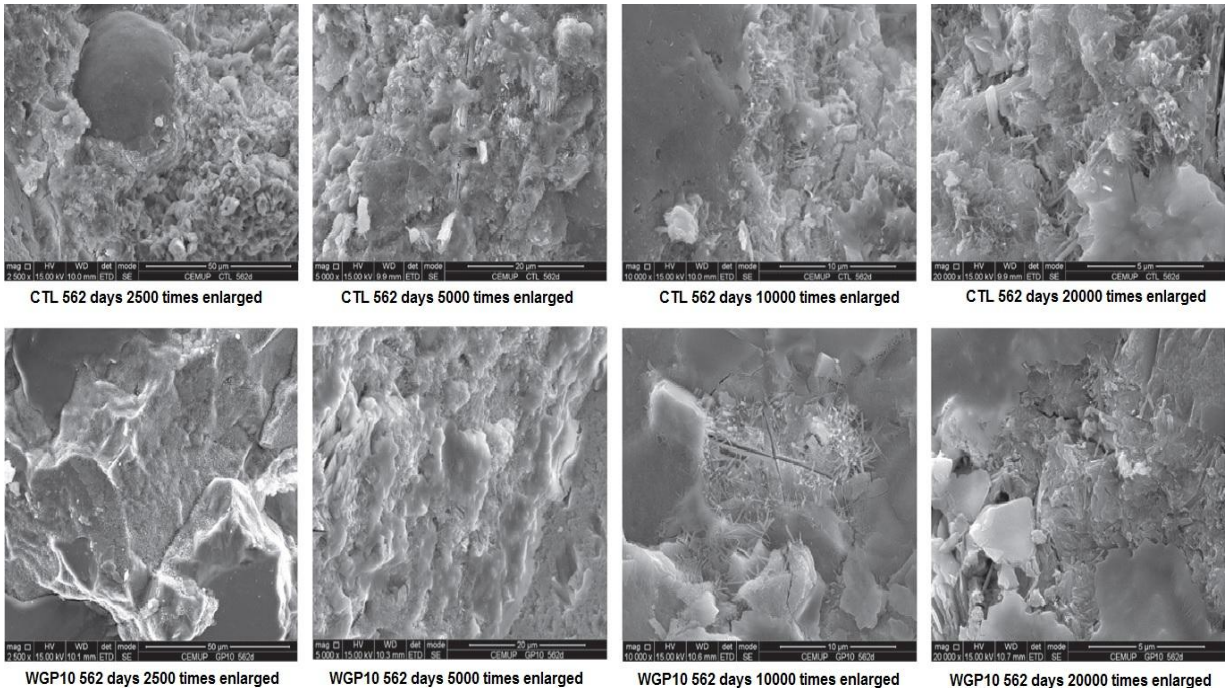

Figure 2.34: SEM on 562 days old mortar (Matos and Sousa-Coutinho, 2012)

gel of 10% glass powder as cement substitute compared to control due to the pozzolanic reaction of glass powder with cement, which initiates the binding of alkalis in the paste, making it unavailable for ASR.

2.5. Application of glass in self-compacting concrete

2.5.1 Fresh Properties

Few investigations have been conducted to evaluate the fresh properties of self-compacting concrete (SCC) with an addition of recycled glass waste as a sand replacement. Huang and Wang (2010) investigated the possibility of using recycled waste LCD glasses in SCC by replacement of four types of sand with glass particles (having maximum diameter of 11.8 mm) at the replacement levels of 0%, 10%, 20% & 30% and w/b ratios of 0.28, 0.32, and 0.36. The authors reported that the workability of high flow SCC increased with the increasing quantities of glass at all w/b ratios, as shown in Figures 2.35 and 2.36. SCC incorporating glass showed slump flows over 570 mm. At w/b of 0.28 and a glass replacement level of 10-30%, the slump flow increased from 20 to 100 mm; whereas, at w/b of 0.32-0.36, the slump flow reduced insignificantly. The lower slump flow at w/b of 0.32-0.36 was attributed to the lower paste volume of the mix. The higher slump flow at higher glass replacement dosages was related to the higher compactness of concrete granular skeleton. Because the glass sand was finer than the natural sand, it could fill the porosity of the coarse aggregates better. The findings were also linked to the fact that glass has a low water absorption and smooth surface.

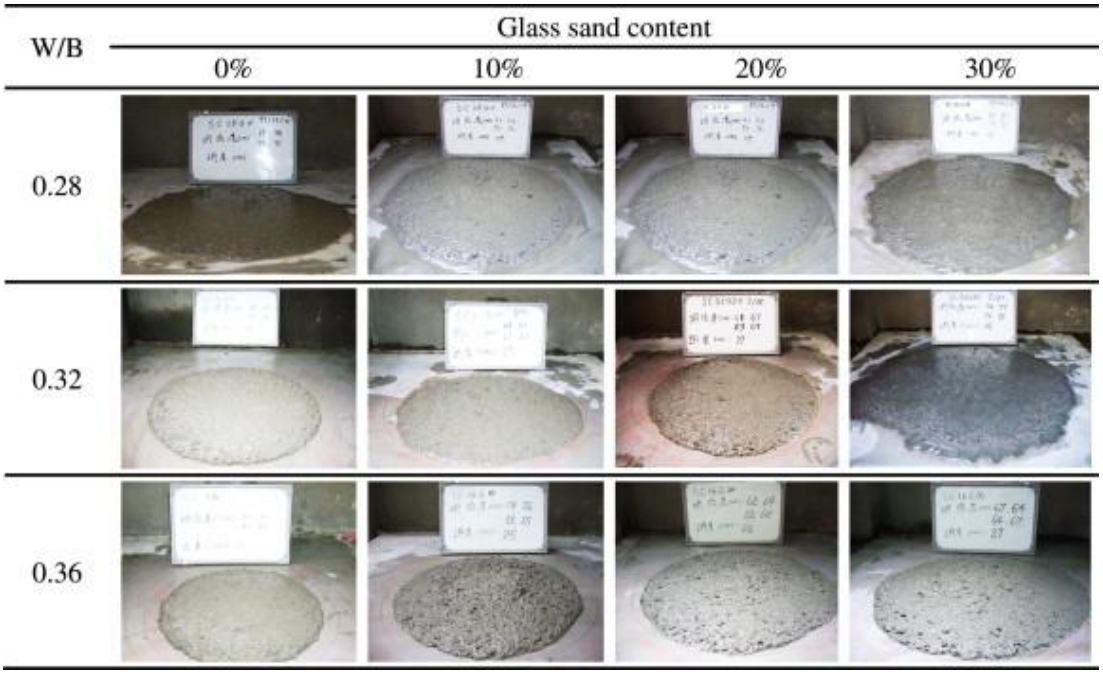

Figure 2.35: The appearance of slump flows for SCC containing glass (Huang and Wang, 2010)

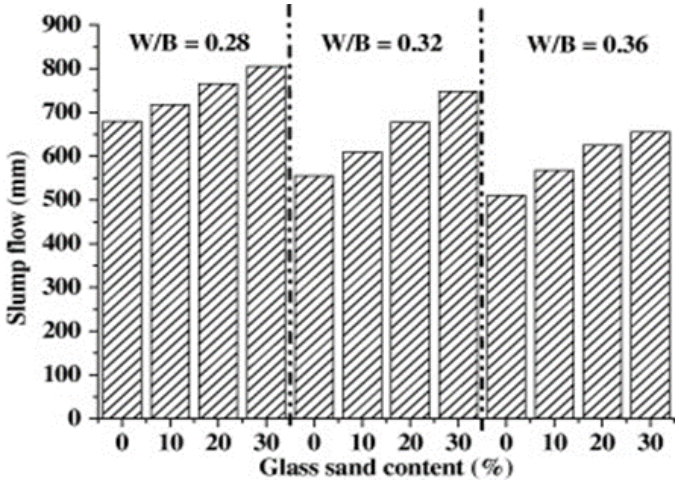

Figure 2.36: Slump flows of SCC incorporating glass (Huang and Wang, 2010)

Ali and Al-Tersawy (2012) studied the effects of utilizing recycled glass waste, as partial substitute of sand in proportions of 0%, 10%, 20%, 30%, 40% and 50%, on fresh and hardened properties of SCC. The researchers observed that the initial slump flow of recycled glass SCC mixes was identical to control mixes, though superplasticizer level was reduced. This was related to the weaker attachment between glass aggregates and cement paste due to their smooth surfaces. The results were found to be identical to the findings by Kou and Poon (2009) that there is no difference in slump values of control concrete and recycled glass waste concrete. Higher slump flows were observed at higher glass replacements, which was linked to the higher compactness of concrete granular skeleton. All the mixes had slump flows more than 650 mm and did not show segregation except mixes that contained 40% and 50% glass, at cement content of 350 kg/m^3, as shown in Figure 2.37.

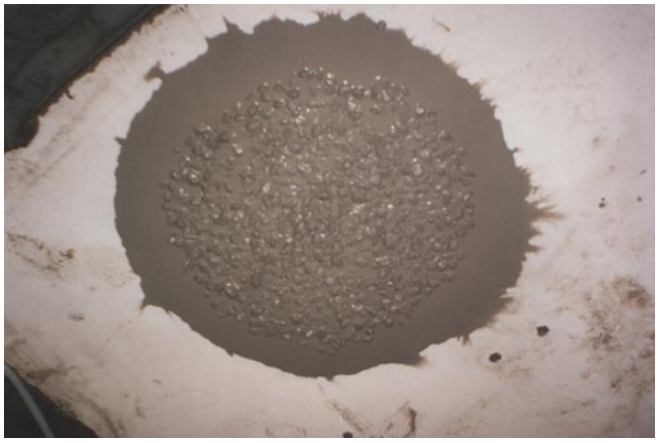

Figure 2.37: Typical segregation on slump flow (Ali and Al-Tersawy, 2012)

The flow ratios ranged from 0.83 to 0.89, indicating that the recycled glass SCC mixes achieve adequate passing ability, which agrees with Kou and Poon (2009) who also reported that the flow ratios varied from 0.84 to 0.87 for recycled glass SCC mixes. Likewise, Sharifi et al. (2013), who analyzed the impact of waste glass replaced as fine aggregate in ratios ranging from 0% to 50%, confirmed that the flowability of fresh concrete increases with an increase in waste glass replacement. In their study, slump flow was found to be more than 650 mm for all types of glass mixes. This trend was related to lower water absorption of glass sand and its smooth surface, which indicated good deformability.

As mentioned by Huang and Wang (2010), V-funnel test time was 6-10 sec longer for SCC containing glass (SCGC) as compared to the control group of mixtures, though the results still conformed to the standard flowability time. Figure 2.38 demonstrates that the passing time was prolonged with the increase in glass sand at the initial stage of mixing. This was linked to the fact that the unit weight of SCC containing waste liquid crystal glass was less compared to SCC containing normal sand. These results are similar to those observed by Ali and Al-Tersawy (2012), who also stated that the V-funnel test time was 6–10 sec longer than

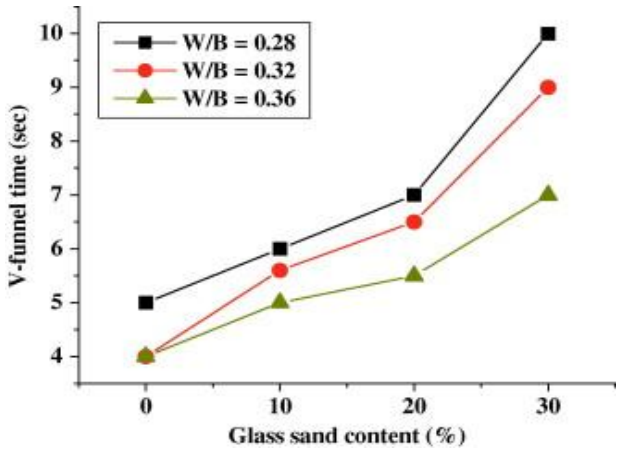

Figure 2.38: V-funnel test of SCGC (Huang and Wang, 2010)

that of the control group. Sharifi et al. (2013) conversely informed that V-funnel times were decreased with increase in the quantity of waste glass. The authors also mentioned that L-box ratio varied from 0.82 to 0.94, indicating that the waste glass mixes achieved satisfactory passing ability and maintained acceptable resistance to segregation around clogged reinforcement area. In addition, L box ratio was decreased with an increase in replacement of sand by glass, which was related to the sharp glass particles that created problems for concrete to pass through reinforcement.

Huang and Wang (2010) stated that SCC containing glass, at different w/b ratios, approached the maximum value of the JCES SCC R2 U-test, which is 340 mm, as shown in Figure 2.39 (a). The authors indicated that an increase in waste glass dosage did not affect SCC. However, the redundant water in the mix of 30% replacement level, at different w/b ratios, resulted in segregation. It was noted that when the glass sand replacement amount was raised at different w/b ratios, the concrete unit weight was reduced because the glass sand unit weight was lower than that of general sand, thus, it resulted in decreasing the concrete unit weight, as illustrated in Figure 2.39 (b). Since glass has a lower density than natural sand, the inclusion of glass sand with the same weight as natural sand in concrete also led to a reduction in air content, as demonstrated in Figure 2.40 (a).

Lastly, Huang and Wang (2010) observed that setting time increased with the increase in glass sand replacement, at various w/b ratios. This finding is consistent with the results observed by Terro (2006). At w/b of 0.32, initial setting and final setting time were observed to be 490–600 min and 970–1065 min, respectively. At w/b of 0.36, initial and final setting times were found to be 615–750 min and 1200–1340 min, respectively. Since glass sand is hydrophobic; hence, by increasing glass replacement and w/b, the efficient water content of concrete escalated and concrete setting time increased, as shown in Figure 2.40 (b).

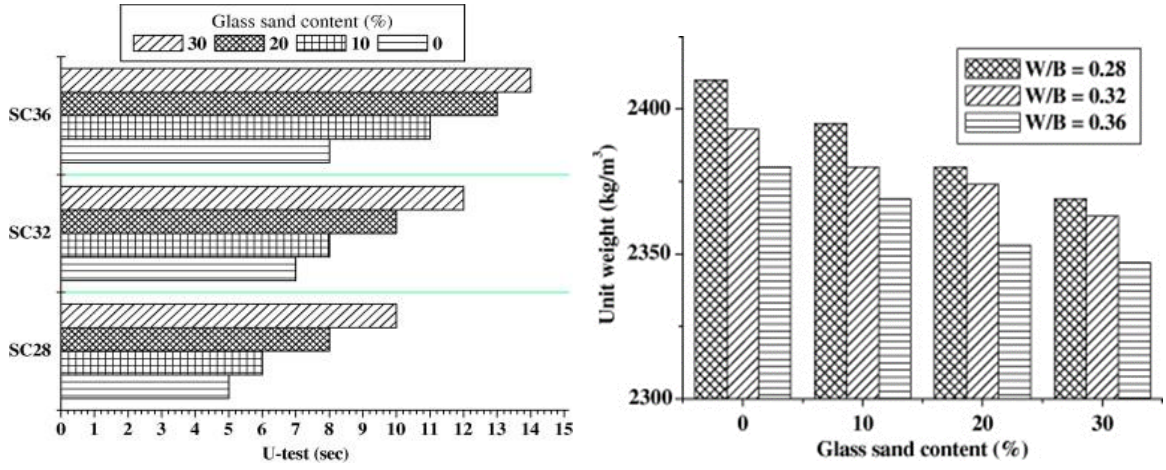

(a) **(b)**

Figure 2.39: (a) U-test of SCGC (b) Unit weight of SCGC (Huang and Wang, 2010)

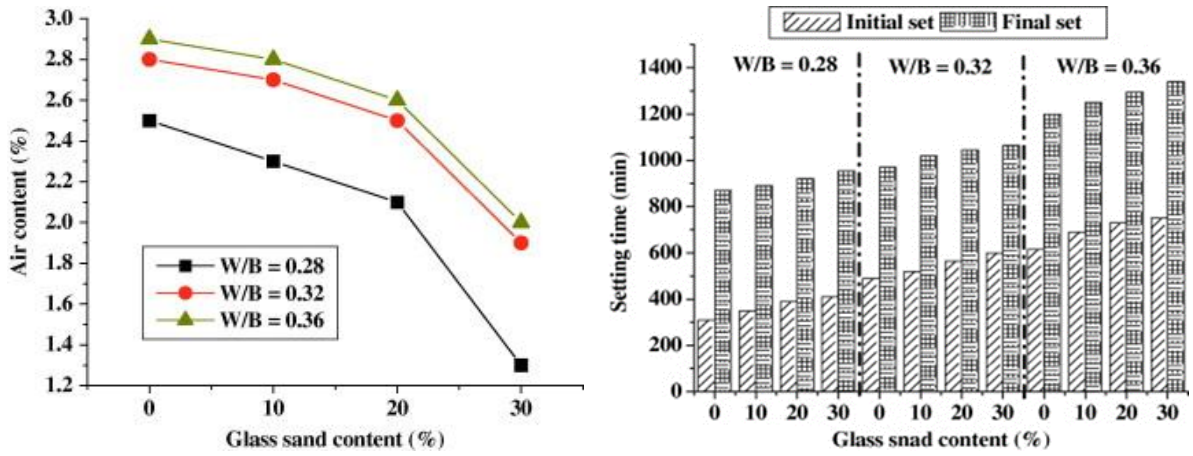

(a) **(b)**

Figure 2.40: (a) Air content of SCGC (b) Setting time of SCGC (Huang and Wang, 2010)

In contrast to the aforesaid investigations, limited studies have been done on the utilization of glass as a cement replacement in SCC. Vanjare and Mahure (2012) aimed to focus on the feasibility of using waste glass powder, in different percentages of 5%, 10% and 15% as a cement substitute, for the production of SCC. The authors noticed that the addition of glass powder in SCC mixes decreased the flow value by an average of 1.30%, 2.50%, and 5.36%, for glass powder replacements of 5%, 10%, and 15% respectively, which suggests the reduction in the deformability of the mix. This tendency of decrease in slump flow with the addition of glass powder has similarly been reported by Liu (2011), who examined the feasibility of using SCC, incorporating waste glass of sizes less than 120 µm as a partial substitute for 10% cement. Furthermore, Vanjare and Mahure (2012) reported that V-funnel time was enhanced by an average of 6.2%, 15.0% and 22.5% for glass powder contents of 5%, 10%, and 15% respectively. The increase in V-funnel time was connected to the higher viscosity of the mixes. The authors also observed that L box ratios followed a decreasing pattern with an average variation of 1.5%, 3.20% and 5% for glass powder replacements of 5%, 10%, and 15% respectively.

2.5.2 Mechanical Properties

Attempts have been made by researchers to determine the mechanical characteristics of SCC using recycled glass powder as a substitute to sand. Ali and Al-Tersawy (2012) reported that the usage of recycled glass in the ratios of 0%, 10%, 20%, 30%, 40%, and 50% as sand substitute led to the reduction in 28-days compressive strengths of recycled glass SCC mixes by [6%, 10.4%, 12.7%, 17.5%, 23.2%], [4.5%, 14.4%, 17.2%, 22.2%, 23.6%] and [3.7%, 10.5%, 13.5%, 17.5%, 21%] at cement contents of 350, 400, and 450 kg/m^3, respectively. The compressive strengths achieved by recycled glass SCC mixes at 28-days are illustrated in Figure 2.41. Park et al. (2004) found that the addition of 30% waste

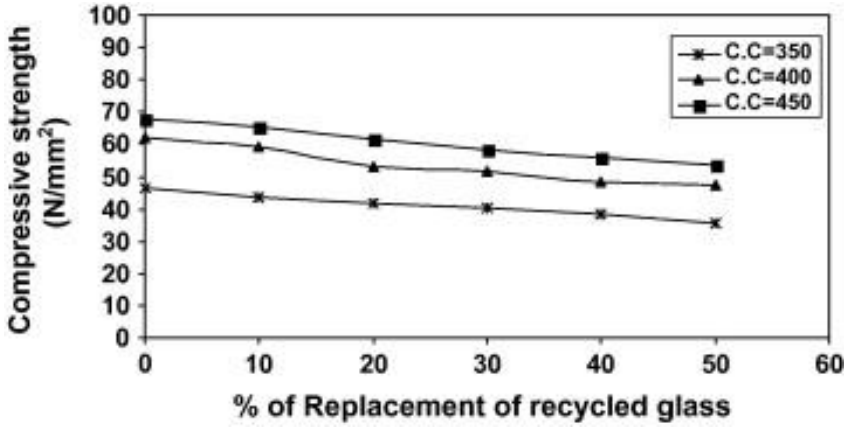

Figure 2.41: Relationship between compressive strength and% of replacement of recycled glass for w/c = 0.4 at 28 days (Ali and Al-Tersawy, 2012)

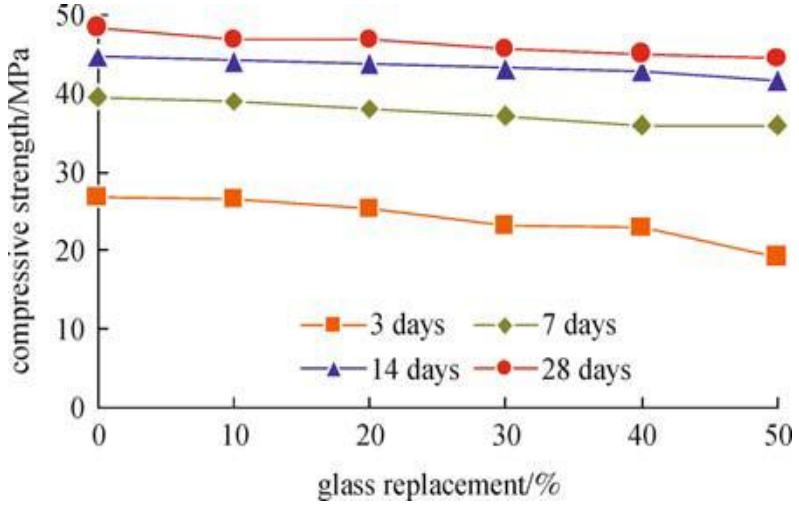

Figure 2.42: Compressive strength versus glass replacement (Sharifi et al., 2013)

glass to concrete reduced the compressive strength by 4% when compared with its control. However, Sharifi et al. (2013) revealed that using recycled glass as a sand substitute in SCC resulted in compressive strengths similar to the control mix. The experimental test results of the compressive strengths at 3, 7, 14 and 28 days are exhibited in Figure 2.42. The reduction in compressive strengths of 28-days was found to be 2.93%, 0.36%, 2.735%, 1.3% and 3.17% at the glass replacement of 10%, 20%, 30%, 40% and 50% respectively.

According to another result reported by Ali and Al-Tersawy (2012), the 28-days splitting tensile strengths were found to decrease by [10.6%, 10.6%, 12.7%, 17%, 23.4%], [8.8%, 14.7%, 16.2%, 23.5%, 27.9%] and [4.2%, 8.5%, 9.9%, 12.7%, 22.5%] at cement contents of 350, 400 and 450 kg/m^3 for replacement ratios of 10%, 20%, 30%, 40%, and 50%, respectively. Figure 2.43 shows the splitting tensile strength results at different replacement levels of recycled glass. These findings are similar to those, informed by Park et al. (2004) who reported that the 28-days splitting tensile strength of recycled glass concrete decreased by 5% at 28-days for 60% glass replacement.

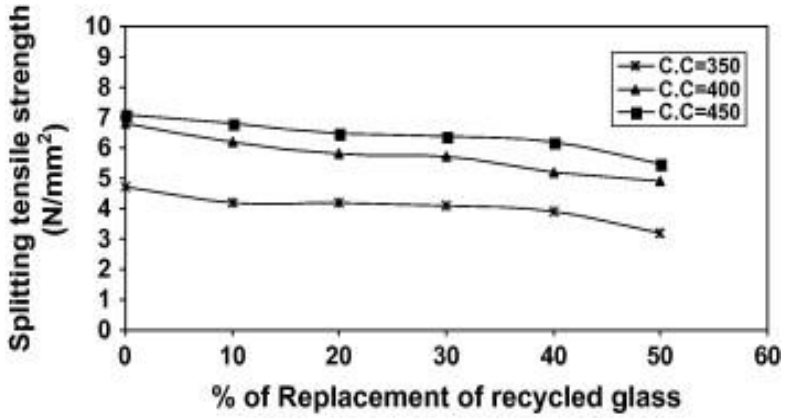

Figure 2.43: Relationship between splitting tensile strength and% of replacement of recycled glass for w/c = 0.4 at 28 days (Ali and Al-Tersawy, 2012)

Sharifi et al. (2013) confirmed these findings that the 28-days splitting tensile strength of SCC reduced by 5% with 50% replacement of sand by the recycled waste glass, as compared with its control mixture. This was attributed to the variations in densities of the recycled glass and natural sand. The relationship between glass replacement dosage and splitting tensile strength is illustrated in Figure 2.44. It should be noted that the labelling on the y-axis of this graph is wrong as published by the researchers.

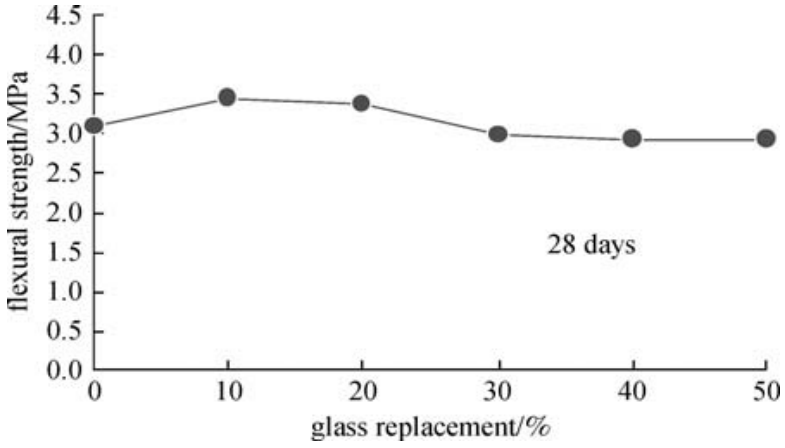

Figure 2.44: Splitting tensile strength versus glass replacement (Sharifi et al., 2013)

Sharifi et al. (2013) further explained that the flexural strengths decreased with the increase of the percentage of waste glass replacement as that of control, other than the mix that contained 10% glass replacement. The replacement of 50% of sand with recycled glass in SCC resulted in a decrease of 15% in flexural strength in comparison to its control mix. The results of the flexural strength after 28-days curing are presented in Figure 2.45. It should be noted that the labelling on the y-axis of this graph is wrong as published by the researchers. Likewise, Ali and Al-Tersawy (2012) noticed that the flexural strength showed a decreasing trend, with the increase in the percentage of recycled waste glass replacement, as compared to the control mix. These results have been demonstrated in Figure 2.46.

According to the test findings, the 28-days flexural strength values were found to decrease by [8.8%, 14.7%, 16.2%, 23.5%, 27.9%] and [4.2%, 8.5%, 9.9%, 12.7%, 22.5%] at cement contents of 350, 400, and 450 kg/m^3 for replacement ratios of 10%, 20%, 30%, 40%, and 50%, respectively. These results are in consistence with Topcu and Canbaz (2004) who reported that the flexural strength of recycled glass concrete decreased by 8% at 28-days.

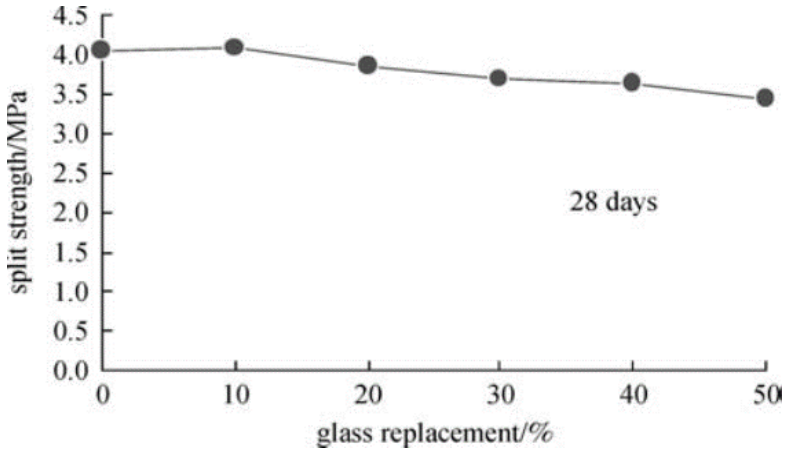

Figure 2.45: Flexural strength versus glass replacement (Sharifi et al., 2013)

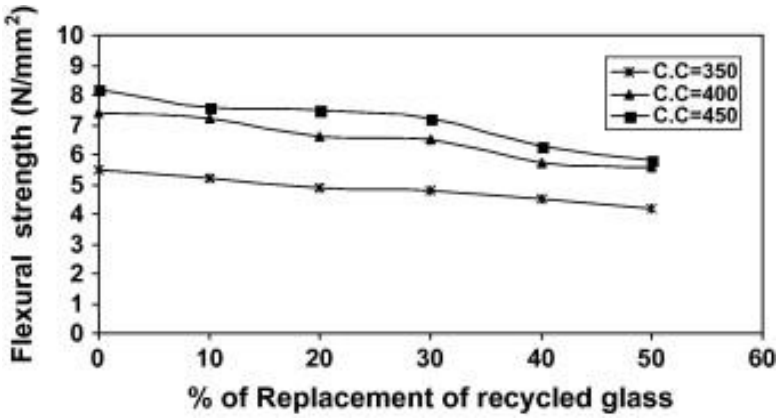

Figure 2.46: Relationship between flexural strength and% of replacement of recycled glass for w/c = 0.4 at 28 days (Ali and Al-Tersawy, 2012)

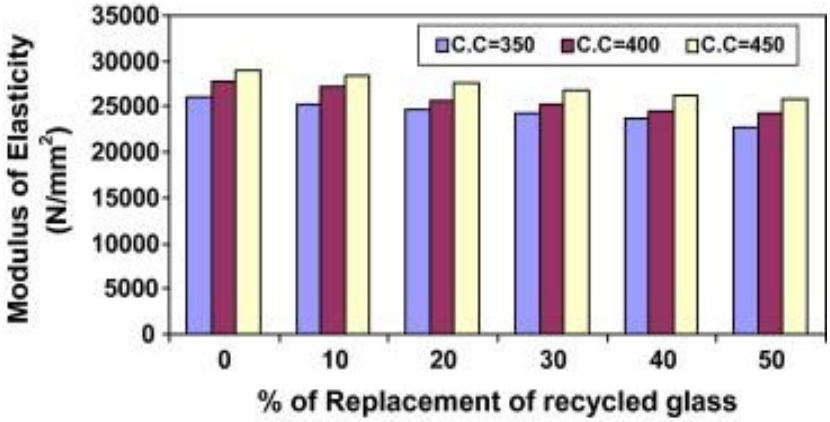

Figure 2.47: Relationship between modulus of elasticity and percentage of replacement for different cement contents (Ali and Al-Tersawy, 2012)

The results achieved by Ali and Al-Tersawy (2012) at 28-days revealed that static modulus of elasticity values were decreased by [3%, 5.3%, 6.6%, 9.2%, 12.3%], [2.2%, 7.5%, 8.9%, 11.8%, 12.6%] and [1.8%, 4.6%, 7%, 9.2%, 11%] at cement contents of 350, 400, and 450 kg/m^3 for replacement ratios of 10%, 20%, 30%, 40%, and 50%, respectively. These results are similar to those given by Kou and Poon (2009) who also stated that the static modulus of elasticity decreases with the increase of the recycled glass content. Figure 2.47 shows the static modulus of elasticity observed by Ali and Al-Tersawy (2012).

Studies concerning the utilization of glass powder as a cement replacement in SCC also presented its effects on mechanical properties. Vanjare and Mahure (2012) stated that there was a decrease in compressive strength for glass powder added to SCC compared to control SCC. The average reduction in compressive strength was around 6%, 15% and 20% for glass powder contents of 5%, 10%, and 15% respectively. It was observed that although glass powder distribution was homogeneous within the SCC composite but the compressive strength varied inversely with the addition of glass powder content. In addition, the authors stated that the flexural strengths of the mixes were found to reduce with increase in glass powder contents. The average reduction in flexural strengths was approximately 2%, 3.7% and 6.75% for glass powder contents of 5%, 10%, and 15% respectively.

Similarly, Liu (2011) reported that 28-days compressive strength varied from 58 to 75 MPa; splitting strength from 3.8 to 4.7 MPa, and elastic modulus from 45 to 49 GPa for target mixes depending on the w/b ratio, glass types, and replacement dosage. In that research, green glass mixes showed higher reduction in strength with an increase in the glass content in comparison to those containing white glass. This was related to the lower w/b ratio used in the mixes with green glass. The researchers also observed that the effect of 53-104 kg/m^3 white glass on elastic modulus was more significant than that of 51-100 kg/m^3 green glass.

2.5.3 Durability Properties

Very limited information is available in the literature regarding the influence of glass powder on the durability properties of SCC. Liu (2011) reported that the sorptivities of mixes with glass were greater than control mix, due to the combined effects of the increase in the w/b ratio, the decrease in the superplasticizer dosage and the increase in the glass content. The authors reported that curing from 7 to 90 days led to the reductions in sorptivity because the hydration products densified the concretes containing glass powder. From the sorptivity results, it was also discovered that the utilization of up to 4.3% volume ratio of ground glass in SCC did not affect the durability more than cement. Hence, the study concluded that the use of glass in SCC might not incur severe durability problems and could be utilized in the production of SCC as a supplementary cementing material.

2.6. Literature Analysis

It is essential to clarify the significance of a research in order to rationalize a large-scale investigation as the present study. In this research, this has been achieved by summarizing the available research data and identifying the missing information in the literature. A number of research studies, undertaken at the global level in the past few decades regarding glass utilization in concrete, have been thoroughly studied and compiled graphically in Figure 2.48. It is evident that the research interests on the addition of glass as coarse aggregates have been reduced to a large extent in recent times. This is potentially due to the concerns related to its susceptibility to deleterious reactions resulting from very coarse glass particles, as discussed in the preceding sections. However, there is still some ongoing research work investigating the effects of glass sand in concrete, to overcome the limitations of recycled glass as coarse aggregates. It can be seen from the literature analysis that the research efforts have recently been inclined towards using glass in concrete as a cement substitute. This inclination reinforces its suitability as a constituent for concrete, establishes its global research significance and motivates to put more research efforts in this direction.

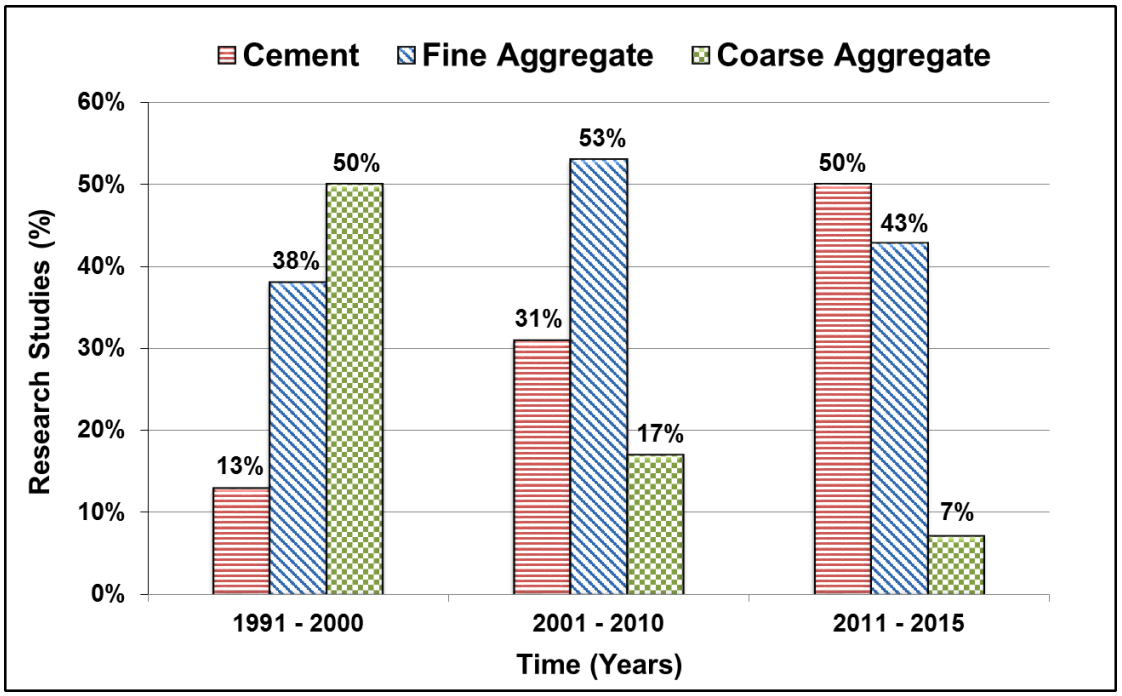

Figure 2.48: Research studies on the utilization of glass in concrete

Table 2.3 provides a compiled set of information regarding some of the past studies and their findings to determine the real picture of which problems have already been researched and which issues still need detailed investigation.

Table 2.3: Past Research Findings

STATE OF THE ART				
No.	**Author (Year)**	**Glass Size**	**Tests Performed**	**Research Findings and/or Recommendations**
1.	Shao et al. (2000)	38 µm 75 µm	Compressive Strength Strength Activity Index Mortar Bar Tests Lime Glass Tests XRD Analysis	The compressive strength of glass modified concrete, when added as a cement replacement, is higher than the threshold limit of 4.1 MPa. Compared to fly ash concrete, glass concrete has a higher early strength as well as a higher late-strength. Waste glass shows a pozzolanic behaviour when ground finer than 38 µm. The high alkali content in the mixture does not undermine the strength of the concrete at a late age. Instead, a gradual increase in strength is observed. A smaller particle size of the ground glass results in higher activity of glass with lime, a higher compressive strength in concrete as well as lower expansion. The optimal particle size distribution of glass needs to be determined to trade off the cost and performance in glass concrete.
2.	Dyer and Dhir (2001)	45 µm - 600 µm	Compressive Strength Rate of heat evolution Alkali-Silica Reaction XRD Analysis	The presence of ground glass has a minor effect on the kinetics of cement hydration. CSH levels are found to be higher in pastes containing glass as a cement substitute, with highest levels corresponding to enhanced strength development properties. The ASR expansion is found to be less in glass incorporated mortar. This might be the result

				of fine particles, promoting expansion that is found to be less in mortar specimens containing ground glass.
3.	Park and Lee (2004)	4.75 mm - 300 µm	ASR Analysis Compressive Strength Flexural Strength	The expansion rate by ASR shows an increasing tendency with an increase in glass sand content, irrespective of its type. The compressive and flexural strengths of mortar decrease with an increase in brown glass content. With the content of waste glass being 20%, the expansion rate of the mortar bars decreases by about 13–40%. The addition of reinforcing fibres to the mortar bars is effective in suppressing the expansion and strength reduction, caused by ASR when waste glasses are mixed into it.
4.	Shayan and Xu (2004)	<10 µm 0.15 mm - 4.75 mm 4.75 mm - 12 mm	Slump Air Content ASR Compressive Strength Drying Shrinkage SEM Analysis	There is a great potential for the utilization of waste glass in concrete. Glass powder provides a dense matrix and improves the durability properties of concrete. 30% glass powder can be replaced as cement or aggregate in concrete, without any long-term harmful effects. Up to 50% of both fine and coarse aggregates can also be replaced in 32 MPa strength grade concrete with satisfactory strength development characteristics.
5.	Shayan and Xu (2006)	< 10 µm 0.60 mm – 2.36 mm 0.15 mm - 0.30 mm	Slump Density Compressive Strength Splitting Tensile Strength	Natural sand, up to 40–50%, can be replaced by crushed glass sand. The strength of cores drilled from the slab is lower than that of the cast cylinder due to less efficient curing under field conditions. The drying shrinkage values of all the mixes are below 0.075% and meet the

			Flexural Strength Drying Shrinkage ASR Expansion Ultrasonic Pulse Velocity Volume of Permeable Voids Chloride Permeability SEM Observations	requirements of the Australian Standard AS 3600. Glass powder reduces the chloride ion penetrability of the concrete, thereby reducing the risk of chloride-induced corrosion of the steel reinforcement in concrete. However, this issue needs further electrochemical investigation. While performing concrete prism test, no harmful ASR expansion is observed in the presence of glass powder. These results indicate that both glass powder and glass aggregate can be used together in 40 MPa concrete without any unfavourable reaction.
6.	Sobolev et al. (2007)	4 mm max	Flexural Strength Compressive Strength SEM Observations	The developed eco-cement containing 50% of waste glass has almost identical flexural and compressive strength properties to normal cement. A visible densification around the glass grains is observed, due to partial hydrations of glass grains and formation of an additional CSH. Further research is required to investigate the resistance of cement to destructive factors.
7.	Taha and Nounu (2008)	45 µm < 5 mm	ASR Expansion X-Ray Fluorescent X-Ray Diffraction	The main reason behind mitigating risk of ASR expansion in concrete is the presence of pozzolanic glass powder as cement substitute as it changes concentration of hydroxide ions (OH-) in the pore solution. Lithium Nitrate can contribute towards total alkali content of concrete. This research approves the fact that lithium nitrate added as a chemical admixture can decrease ASR expansion.

8.	Liu (2011)	> 120 µm < 120 µm	Slump Flow V-Funnel Time J-Ring Step Sieve Stability Test Compressive Strength Splitting Tensile Strength Non-Destructive Test Dynamic Elastic Modulus Sorptivity ASR Tests	SCC having acceptable fresh properties can be produced by adding up to 104 kg/m^3 ground glass, replacing about 10% cement and 10% sand. The strength ratios show that glass is a promising addition in SCC. The sorptivities of glass mixes are all higher than those of the control mixes due to the overall impacts of an increase in glass content and w/b ratio and a reduction in superplasticizer dosage. The expansions in the ASR mortar bar tests of the mixes with and without glass are similar to those of the control mix and thus, can be considered harmless. There is an insignificant difference between mixes with green and white glass.
9.	Mackechnie and Munn (2012)	< 5 mm	Slump Fresh Density Air Entrainment Bleed Hardened Density Compressive Strength Drying Shrinkage Porosity	The addition of waste glass, as a sand replacement, has minor deleterious effects on fresh and hardened properties of concrete, for addition levels of up to 10%. Glass does appear to increase the risk of air-entrainment but this is controllable by reducing inputs of air entraining agents used in lower strength concrete mixes. The possibility of using glass as a fine aggregate depends on an effective ASR mitigation and specified methods that measure the risk of ASR expansion in concrete structures.
10.	Matos and Coutinho (2012)	0.1 µm - 100 µm	SEM Observations	Glass mortar shows an increase in strength activity index, significantly between 28-days and 90-days, which means

			Sorptivity Carbonation Depth Sulphate resistivity Chloride diffusion Alkali-Silica Reaction Activity Index Compressive Strength Flexural Strength Workability Soundness Setting Time Pozzolanacity Test	that pozzolanic activity occurred. Despite high alkali content in glass powder, ASR expansion is extremely reduced. There is higher resistance to chloride penetration for glass containing mortar, increasing with dosage replacement. Sorptivity of glass mixes is similar to control due to the effect of identical particle size distribution. Carbonation depth for all blended cement mixtures is greater than for the Portland cement mixture, increasing with replacement dosage in trend for pozzolanic materials. 10% glass modified mortar shows a remarkable resistance to sulphate attack, even better than silica fume.
11.	Ali and Al-Tersawy (2012)	0.075 mm - 5 mm	Slump Flow L. Box ratio V-funnel values Compressive Strength Flexural Strength Splitting Tensile Strength Static Modulus of Elasticity SEM Observations	The slump flow, flow ratio, and V-funnel of recycled glass SCC mixes increase directly with the increase of recycled glass content. The compressive strength, splitting tensile strength, flexural strength, and static modulus of elasticity of recycled glass SCC mixes decrease with the increase of recycled glass content. From the SEM micrograph, it is evident that there is poor contact between the cement matrix and recycled glass being a partial replacement of fine aggregate due to decrease in bond strength between the cement paste and the recycled glass.

12.	Nassar and Soroushian (2012)	13 µm	Slump Fresh Density Air Content Compressive Strength Flexural strength Hardened Density Sorption Chloride permeability Freeze–thaw resistance Alkali-silica reaction Water Absorption & Porosity SEM Observations	It is expected that glass particles of size (13 µm), as cement substitute in concrete, undergoes a pozzolanic reaction that enhances the microstructure of recycled aggregate concrete. This is due to the fact that the quality of paste is enhanced through the formation of an interface between recycled aggregate and new mortar in recycled aggregate concrete. This addition of glass powder also improves durability characteristics including sorption, chloride permeability and freeze-thaw resistance by improvement in pore characteristics and filling effect of glass particles. The remarkable increase in the later-age strength is achieved through the formation of denser and less permeable microstructure. The grinding of waste glass to much finer size is an essential element to benefit from its pozzolanic reaction.
13.	Cassar and Camilleri (2012)	100 µm - 600 µm	XRD Analysis Slump Fresh Density Compressive Strength Flexural Strength Ultrasonic Pulse Velocity Chloride Ion Penetration	The density of control concrete is higher than that of concrete replaced with 50% imploded glass. The concrete containing 40% glass replaced by cement shows satisfactory properties. An advantage of using imploded glass is that the particles are sharp free and easily separable from the contaminants present with waste glass. Concrete containing 10-20% glass powder shows higher resistance to chloride ion penetration, making this an ideal concrete for structures close to the shore.

The literature has been carefully reviewed and meta-analysis of the previous research results has been done. A number of graphs have been prepared for normalized strengths in order to comprehend the trends with respect to glass proportions, w/b ratios, and glass sizes. Figure 2.49 to Figure 2.52 illustrate the effects of glass proportions on strength characteristics, depending on the w/b ratios and size of glass particles, used in the studies from where the data has been obtained. In all graphs, the strength of each glass incorporated mix has been divided by the strength of control GP mix. This has been done in the expectation of identifying patterns among study results and other interesting relationships that may come to light in the context of multiple studies. A general formula used for normalization is defined in the following equation.

$$\text{Normalized Strength Factor} = \frac{\text{Strength achieved by the mix containing glass}}{\text{Strength of the control GP mix}}$$

However, the specific formula used to evaluate the normalization factor, illustrated in each figure, is described under each graph. It is essential to recognize that normalized strength factor is a unitless number. Some additional figures prepared for the literature analysis have been provided in Appendix A.

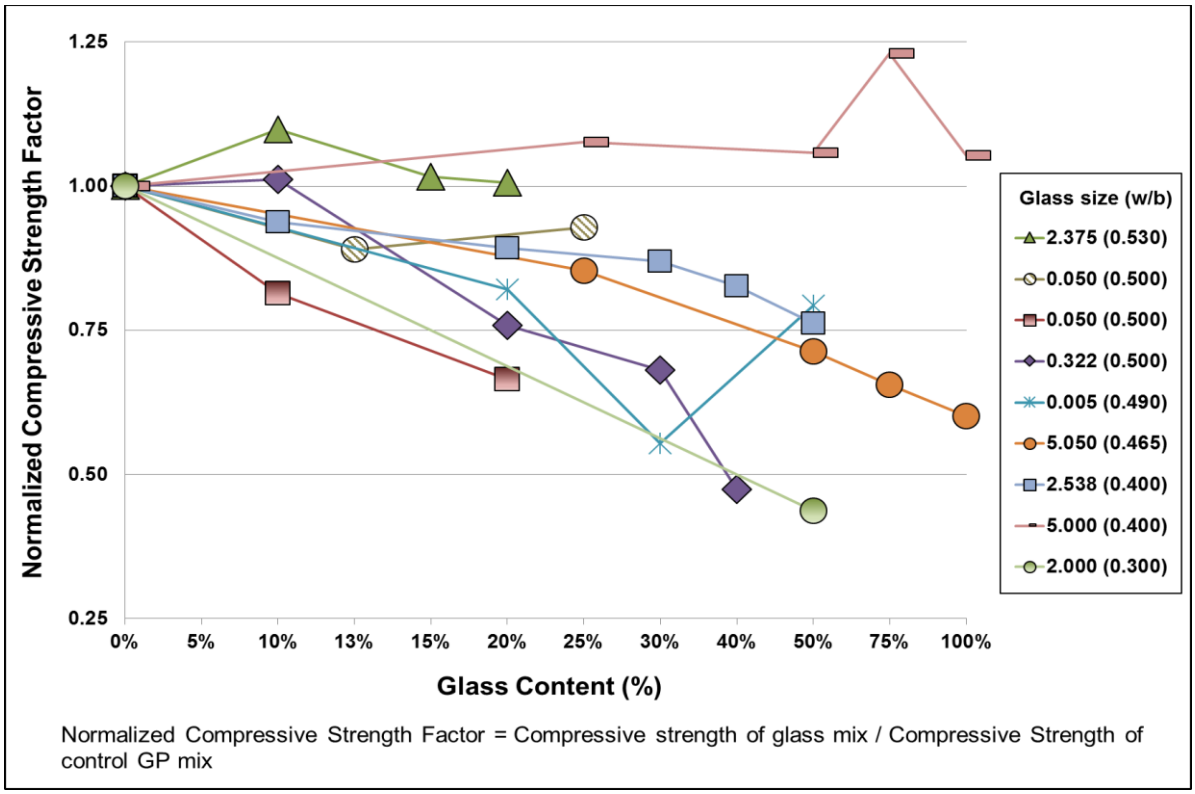

Figure 2.49: Graph between glass proportions and normalized 7-days compressive strengths

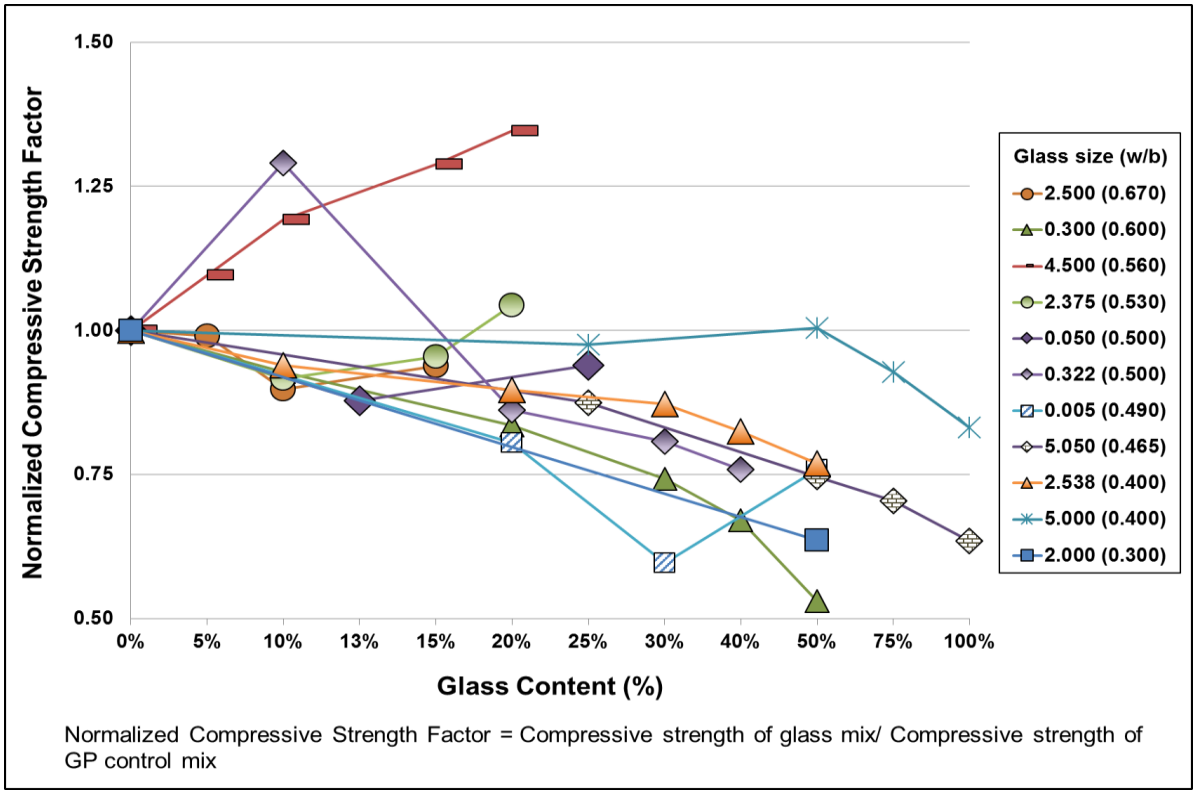

Figure 2.50: Graph between glass proportions and normalized 28-days compressive strengths

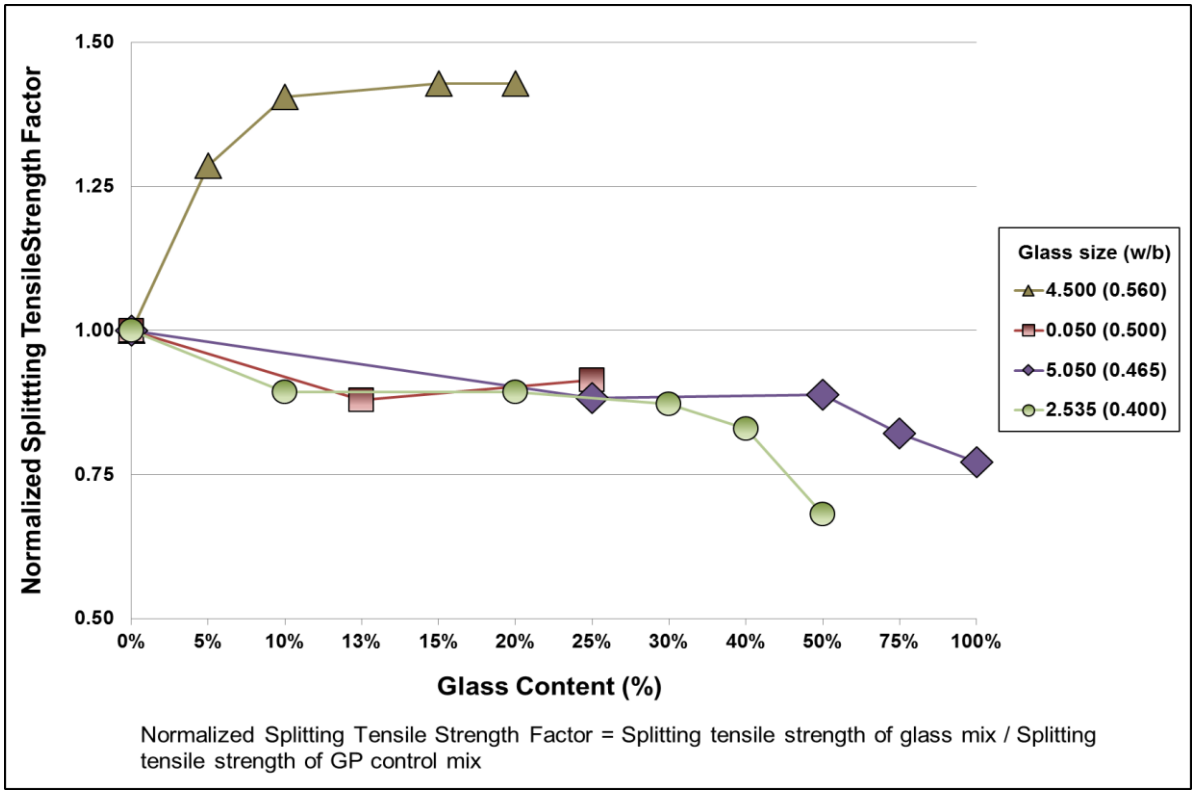

Figure 2.51: Graph between glass proportions and normalized 28-days splitting tensile strengths

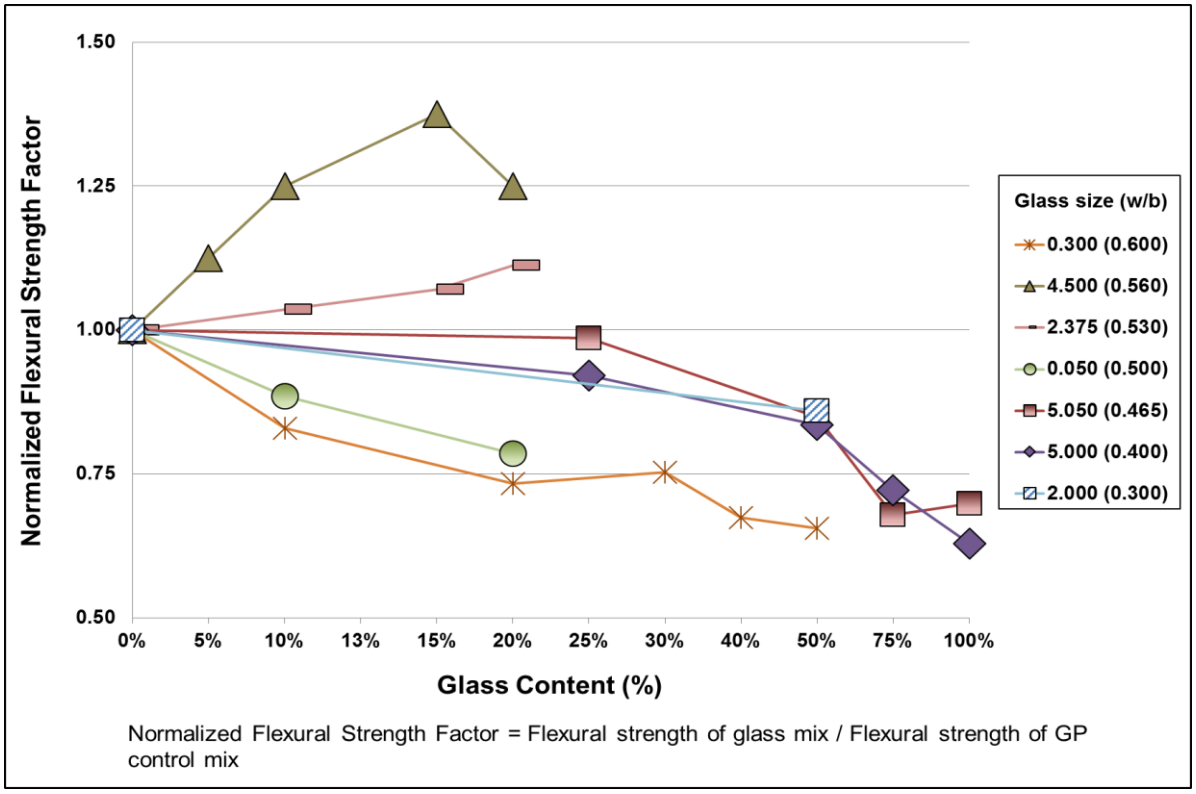

Figure 2.52: Graph between glass proportions and normalized 28-days flexural strengths

The comprehensive and interconnected coverage of previous studies has established that there are a lot of variations in the trial outcomes. These deviations are largely dependent on the glass particle size, its replacement level in concrete and w/b ratio of the concrete mix. The lower the glass size, the better the performance of glass incorporated concrete achieved, which is potentially due to the higher pozzolanicity of fine glass powder as discussed in the preceding sections. In the case where w/b ratio is same and glass size is considerably reduced, the variation in the compressive strength results is very significant [Refer to Figure 2.49; 2.538(0.400) and 5.000(0.400)]. Conversely, in an instance where glass size is approximately same and w/b ratio is decreased, there is not a substantial difference in compressive strengths [Refer to Figure 2.50; 2.375(0.530) and 2.538 (0.400)]. This suggests that the detrimental effects of coarser glass size, when combined with higher w/b ratio, can be better controlled with reducing glass size and w/b ratio, rather than reducing w/b ratio only. Additionally, there seems to be an uncertainty on the most effective replacement level of glass in concrete since this parameter also depends on the glass fineness and water added to the concrete mix. In general, it appears that glass size is the most significant parameter on which the potential behaviour of glass in concrete depends. However, there is an inadequate information on the utilization of fine glass powder that is comparable to the fineness of cement and added at various contents as a binder substitute, which restricts to reach a definite conclusion regarding the performance of glass powder.

2.7. Conclusion

Glass is an unconventional material for SCC but is certainly a promising material, considering its potential ecological and economical advantages. An extensive literature review has been presented on the use of waste glass in concrete. The ambiguity in the previous results and the lack of sufficient trials have assisted in recognizing the research gaps in the literature.

The performance of SCC utilizing waste glass mainly depends on whether the glass is replacing cement, fine aggregate or coarse aggregate, the level of replacement, and the properties of glass, such as particle size and chemical composition. It has been observed that the mechanism and effects of ASR on the performance of concrete containing glass have been thoroughly studied in the past through experimental testing. However, previous investigations were mostly aimed at the performance of concrete containing coarse glass particles, more than the pessimum size of 1.5 mm, which carries a higher risk of ASR. This leads us to consider the limitations of past research efforts and increases our interest to investigate the behaviour of concrete containing waste glass if the glass size is reduced further.

The glass has the potential of demonstrating improved characteristics compared to cement only in an SCC mix due to its impermeable nature and particle morphology. The idea of utilizing glass as a cement replacement is expected to improve concrete properties due to its pozzolanic reactivity resulting from its smaller size. It can be postulated that using fine glass powder as a partial binder, and hence, achieving denser microstructure of the modified concrete will have a significant effect on the mechanical properties of concrete. Moreover, the literature analysis suggests that the mechanical properties of concrete will change as the percent of glass substitution increases, depending on the fineness of glass powder. However, previously published results on the use of waste glass powder as cement substitute in concrete vary considerably and hence, detailed investigation is needed in this regard. The most important information, which appears to be insufficient in the literature, is the influence of very fine glass powder, possibly less than 50 µm, on the performance of SCC.

At present, the rate of waste glass utilization in the construction industry is not at the desired level due to the lack of knowledge on possible concrete applications utilizing waste glass. More specifically, this is also due to the limited evidence available on the performance characteristics, such as long-term strength and durability. There is also inadequate information on the rheological behaviour of SCC incorporating glass powder, which is an important parameter to assess its performance. The present research, therefore,

investigates the effects of high volumes of finely ground glass in SCC, produced with acceptable fresh properties, on the long-term strength and durability characteristics, thus expanding the quantities and types of additions available to SCC producers and consumers.

References

Ali, E., and Tersawy, H. (2012). “Recycled glass as a partial replacement for fine aggregate in self-compacting concrete.” *Construction and Building Materials, Elsevier,* 35, 785-791.

Allied Concrete, New Zealand. (2010). *Recycling: Recycled Glass.* <http://www.alliedconcrete.co.nz/why-allied/recycling/353-recycled-glass> (Sept. 30, 2013).

Almesfer, N. H. (2013). *Utilizing waste paint and waste glass in concrete,* Ph.D. thesis, The University of Auckland, New Zealand.

Balogh, A. (n.d.). *Green Ideas for Exterior Concrete.* <http://www.concretenetwork.com> (Sept. 30, 2013).

Batayneh, M., Marie, I., and Asi, I. (2007). “Use of selected waste materials in concrete mixes.” *Waste Management, Elsevier,* 27, 1870-1876.

Byars, E. A., Morales-Hernandez, B., Zhu, H. Y. (2004). “Waste glass as concrete aggregate and pozzolan.” *Concrete,* 38(1), 41-44.

Byars, E. A., Zhu, H. Y., and Morales, B. (2004). *ConGlassCrete 1 Project Final Report,* The Waste & Resources Action Programme, University of Sheffield, UK.

Cassar, J., and Camilleri, J. (2012). “Utilization of imploded glass in structural concrete”. *Construction and Building Materials, Elsevier,* 29, 299-307.

Cement and Concrete Association. (2011). *Best Practice Guide for the use of Recycled Aggregates in New Concrete (CCANZ TR 14),* Wellington, New Zealand.

Chanbane, B., Sholar, G. A., Musselman, J. A., and Page, G. C. (1999). *Ten-year performance evaluation of asphalt–rubber surface mixes.* Transportation Research Record No. 1681, Washington, USA, 10–18.

Chen, C. H., Huang, R., Wu, J. K., and Yang, C. C. (2006). “Waste E-glass particles used in cementitious mixtures." *Cement and Concrete Research, Elsevier,* 36(3), 449-456.

Dhir, R. K., Dyer, T. D., and Tang, M. C. (2003). “Expansion due to alkali-silica reaction (ASR) of glass cullet used in concrete.” *Proc., International Symposium on Recycling and Re-Use of Waste Materials,* University of Dundee, Scotland, UK, 751-760.

Dhir, R. K., Dyer, T. D., and Tang, M. C. (2009). “Alkali–silica reaction in concrete containing glass.” *Materials and Structures,* 42, 1451–62.

Dyer, D., and Dhir, K. (2001). “Chemical Reactions of glass cullet used as cement component.” *Journal of materials in Civil Engineering*, 13, 412-417.

El-Shamy, T. M., Lewins, J., and Douglas, R. W. (1972). “The dependence on the pH of the decomposition of glasses by aqueous solutions.” *Glass Technology,* 13(3), 81-87.

Federico, L. M., and Chidiac, S. E. (2009). “Waste glass as a supplementary cementitious material in concrete – critical review of treatment methods.” *Cement and Concrete Composites, Elsevier,* 31(8), 606–610.

Figg, J. W. (1981). “Reaction between cement and artificial glass in concrete.” *Proc., 5th International Conference on Alkali-Aggregate Reaction in Concrete*, Cape Town, South Africa, paper S252/7.

Flaherty, F. J., Mangat, P. S. (1999). “Influence of constituents on the properties of self-compacting repair materials.” *Proc., 1st International RILEM symposium on self-compacting concrete. RILEM proceedings, 7 (PRO 7),* 263-274.

Grzeszczyk, S., and Lipowski, G. (1997). “Effect of content and particle size distribution of high-calcium fly ash on the rheological properties of cement pastes.” *Cement Concrete Research. Elsevier*, 27(6), 907-916.

Idir, R., Cyr, M., and Hamou, T. A. (2010). “Use of fine glass as ASR inhibitor in glass aggregate mortars.” *Construction and Building Materials, Elsevier,* 24(7), 1309-1312.

Ismail, Z. Z., and Al-Hashmi, E. A. (2009). “Recycling of waste glass as a partial replacement for fine aggregate in concrete.” *Waste Management, Elsevier,* 29(2), 655-659.

Jin, W., Meyer, C., and Baxter, S. (2000). "Glasscrete - Concrete with glass aggregate.” *ACI Materials Journal*, 97(2), 208-213.

Johnson, C. D. (1974). “Waste glass as coarse aggregate for concrete.” *Journal of Testing and Evaluation,* 2(5), 344 350.

Kou, S. C., and Poon, C. S. (2009). “Properties of self-compacting concrete prepared with recycled glass aggregate.” *Cement and Concrete Composites, Elsevier,* 31(2):107-113.

Kozlova, S., Millrath, K., Meyer, C., and Shimanovich, S. (2003). “A suggested screening test for ASR in cement-bound composites containing glass aggregate based on autoclaving.” *Cement and Concrete Composites, Elsevier,* 2003: 26(7), 827-835.

Lam, C. S, Poon, C. S., and Chan, D. (2007). “Enhancing the performance of pre-cast concrete blocks by incorporating waste glass – ASR consideration.” *Cement and Concrete Composites, Elsevier,* 29(8), 616-625.

Lam, C. S. (2006). *Use of recycled construction and demolition wastes as aggregates in pre-cast block works.* M.Phil. thesis, The Hong Kong Polytechnic University, Hong Kong.

Lane, D. S., and Ozyildirim, C. (1998). “Preventive measures for alkali-silica reactions (binary and ternary systems).” *Cement and Concrete Research, Elsevier,* 29(8), 1281-1288.

Liu, M. (2009). *Wider Application of Additions in Self-compacting Concrete*. Ph.D. thesis, University College London, London, United Kingdom.

Liu, M. (2011). “Incorporating ground glass in self-compacting concrete.” *Construction and Building Materials, Elsevier,* 2011: 25(2), 919-925.

Mackechnie, J. R., and Munn, C. (2012). "Characterizing recycled aggregates for use in New Zealand ready-mix concrete production." *Allied Concrete, New Zealand*.

Maier, P. L., and Durham, A. S. (2012). “Beneficial use of recycled materials in concrete mixtures.” *Construction and Building Materials, Elsevier,* 29, 428-437.

Matos, A., and Coutinho, J. (2012). "Durability of mortar using waste glass powder as cement replacement.” *Construction and Building Materials, Elsevier,* 36, 205-215.

Metwally, I. M. (2007). “Investigations on the performance of concrete made with blended finely milled waste glass.” *Advances in Structural Engineering,* 10(1), 47-53.

Meyer, C., and Xi, Y. (1999). “Use of Recycled Glass and Fly Ash for Precast Concrete.” *Journal of Materials in Civil Engineering (ASCE),* 11(2), 89-90.

Meyer, C., Egosi, N., Andela, C. (2001). “Concrete with Waste Glass as Aggregate.” *Proc., International Symposium on Recycling and Re-use of Glass Cullet,* (Ed. Dhir, Dyer, and Limbachiya), Concrete Technology Unit of ASCE and University of Dundee, UK, 9 pages.

Nassar, R. D., and Soroushian, P. (2012). “Strength and durability of recycled aggregate concrete containing milled glass as a partial replacement for cement.” *Construction and Building Materials, Elsevier,* 29, 368-377.

Ozkan, O., and Yuksel, I. (2008). “Studies on mortars containing waste bottle glass and industrial by-products.” *Construction and Building Materials, Elsevier,* 22(6), 1288-1298.

Park, S. B., and Lee, B. C. (2004). “Studies on expansion properties in mortar containing waste glass and fibres.” *Cement and Concrete Research, Elsevier,* 34(7), 1145-1152.

Park, S. B., Lee, B. C., and Kim, J. H. (2004). “Studies on mechanical properties of concrete containing waste glass aggregate.” *Cement and Concrete Research, Elsevier,* 34(12), 2181-2189.

Pattengill, M., and Shutt, T. C. (1973). “Use of ground glass as a pozzolan.” *Proc., Symposium on Utilization of Waste Glass in Secondary Products,* Albuquerque, New Mexico.

Rajabipour, F., Maraghechi, H., and Fischer, G. (2010). “Investigating the alkali-silica reaction of recycled glass aggregates in concrete materials.” *ASCE Journal of Materials in Civil Engineering.* 22, 1201-1208.

Ravindra, K. D., Dyer, T. D. and Tang, M. C. (2009). “Alkali-silica reaction in concrete containing glass.” *Materials and Structures, RILEM,* 42, 1451-1462.

Rindl, J. (1998). *Recycling Manager, report by Recycling manager*, Dane Country, Department of Public Works, Madison, USA.

Safiuddin, Md., Jumaat, M. Z., Salam, M. A., Islam, M. S. and Hashim, R. (2010). "Utilization of solid wastes in construction materials." *International Journal of the Physical Sciences,* 5(13), 1952-1963.

Schmidt, A., and Saia, W. H. F. (1963). “Alkaline aggregate reaction tests on glass used for exposed aggregate wall panel work.” *ACI Materials Journal,* 60, 1235–1236.

Scholze, H., (1982). “Chemical durability of glasses.” *Journal of Non-Crystalline Solids,* 52, 91-103.

Scott. R. M. (2007). *Research and applications of concrete modified with waste glass and waste latex paint: Progress Report Stage 1*. Department of Civil Engineering, University of Canterbury, Christchurch, New Zealand.

Sekar, T, N., Ganesan, N., and Nampoothiri, N. V. N. (2011). "Studies on strength characteristics on utilization of waste materials as coarse aggregates in concrete." *Journal of Engineering Science and Technology, IJEST,* 3(7), 5436-5440.

Shao, Y., Lifort, T., Moras, S., and Rodriguez, D. (2000). “Studies on concrete containing ground waste glass.” *Cement and Concrete Research, Elsevier,* 30, 91-100.

Sharifi, Y., Hoshiar, M., and Aghebati, B. (2013). “Recycled glass replacement as fine aggregate in self-compacting concrete.” *Frontiers of Structural and Civil Engineering, 7*(4), 419-428.

Shayan, A., and Xu, A. (1999). *Utilization of glass as a pozzolanic material in concrete,* ARRB TR Internal Report RC91132, Australia.

Shayan, A., and Xu, A. (2004). “Value-added utilization of waste glass in concrete.” *Cement and Concrete Research, Elsevier,* 34(1), 81–89.

Shayan, A., and Xu, A. (2006). “Performance of glass powder as a pozzolanic material in concrete: A field trial on concrete slabs.” *Cement and Concrete Research, Elsevier,* 36(3), 457-468.

Shi, C., and Zheng, K. (2007). “A review on the use of waste glasses in the production of cement and concrete.” *Resources, Conservation and Recycling, Elsevier*, 52(2), 234-247.

Shi, C., Wu, Y., Riefler C., and Wang, H. (2005). “Characteristics and pozzolanic reactivity of glass powders.” *Cement and Concrete Research, Elsevier*, 35(5), 987-993.

Sobolev, K., Turker, P., Soboleva, S., and Iscioglu, G. (2007). “Utilization of waste glass in ECO-cement: Strength properties and microstructural observations”. *Waste Management, Elsevier,* 27(7), 971-976.

Taha, B., and Nounu, G. (2008). “Using lithium nitrate and pozzolanic glass powder in concrete as ASR suppressors.” *Cement and Concrete Composites, Elsevier,* 30(6), 497-505.

Tan, K. H., and Du, H. (2013). “Use of waste glass as sand in mortar: Part I – Fresh, mechanical and durability properties.” *Cement and Concrete Composites, Elsevier,* 35(1), 109-117.

Tan, K. H., and Du. H. (2013). “Use of waste glass as sand in mortar: Part II – Alkali–silica reaction and mitigation methods.” *Cement and Concrete Composites, Elsevier,* 35(1), 118-126.

Terro, M. J. (2006). “Properties of concrete made with recycled crushed glass at elevated temperatures.” *Build and Environment, Elsevier,* 41(5), 633–639.

Thomas, D., and Ravindra, K. (2001). “Chemical reactions of glass cullet used as cement component.” *Journal of Materials in Civil Engineering, American Society of Civil Engineers (ASCE),* 13(6), 412-417.

Topcu, I. B., and Canbaz, M. (2004). "Properties of concrete containing waste glass.” *Cement and Concrete Research, Elsevier,* 34(2), 267–274.

Wakim, N. (2009). *Recycled Materials in Civil Works and Energy Efficient Street Lighting: A Review of Waikato Territorial Authorities Procurement Practices.* Environment Waikato, New Zealand.

Wang, H. Y., and Huang, W. L. (2010). “A study on the properties of fresh self-consolidating glass concrete (SCGC).” *Construction and Building Materials, Elsevier*, 24(4), 619-624

Zachariasen, W. H. (1932). “The atomic arrangement in glass.” *Journal of the American Chemical Society,* 54(10), 3841-3851.

Zhu, H., and Byars, E. A. (2004). “Alkali-silica reaction of recycled glass in concrete, alkali-aggregate reaction in concrete.” *Proc., 12th International Conference on Alkali-Aggregate Reaction in Concrete,* 811–20.

CHAPTER 3

MATERIAL CHARACTERIZATION, MIX DESIGN, TEST METHODS AND PRELIMINARY TRIALS

HIGHLIGHTS

- Discussion on physical and chemical properties of constituent materials and tests undertaken to evaluate these properties.
- Explanation of the mix designs and mixing procedures for casting fresh mortar and self-compacting concrete.
- Description of the test methods carried out to evaluate fresh and hardened properties of mortar and self-compacting concrete and equipment used to perform these tests.
- Evaluation of small-scale preliminary trials undertaken on glass material as well as glass incorporated mortar to plan a framework for large-scale investigations.

3.1 Introduction

In order to obtain accurate results, it is essential that material properties, mixing process and testing procedures are as similar as possible, throughout the experimental program. In general, it means the use of similar equipment, test methods, laboratory environment and constituent materials. Due to this, all mixing and casting were done in Civil Engineering Laboratories at the campus of University of Canterbury, New Zealand, excluding some of the drying shrinkage tests that were done at Allied Concrete, Christchurch Plant, New Zealand. Prior to use, all materials were stored in the laboratory at ambient temperature. Mixing and testing were carried out at room temperature, normally between 18°C and 23°C.

3.2 Tests on constituent materials

Tests that were done on the constituent materials of mortar and SCC are discussed in the following section.

3.2.1 Binders

3.2.1.1 Particle Size Distribution

The particle size distributions (PSD) of cement (GP), class F and C fly ashes (FAF and FAC), limestone powder (LP) and all types of glass powders (GL) were measured by Laser Scattering Particle Size Distribution Analyzer LA-950, Horiba Ltd, as demonstrated in Figure 3.1. The instrument detects the correlation between intensity and angle of light scattered from a particle to measure the particle size of a material with laser scattering method and then calculates the particle size based on Mie-scattering theory (Wriedt, 2012). The equipment detects particle sizes as well as mixed-size samples. In order to measure the particle size, analysis conditions are first selected on the software, in a sequence proceeding from one item to the next. The sample is then added and the speed of the circulation pump is controlled. Following this; blank measurement, sampling, and measurement are controlled by the software. The final step of the measurement process is saving results as a file of the required format.

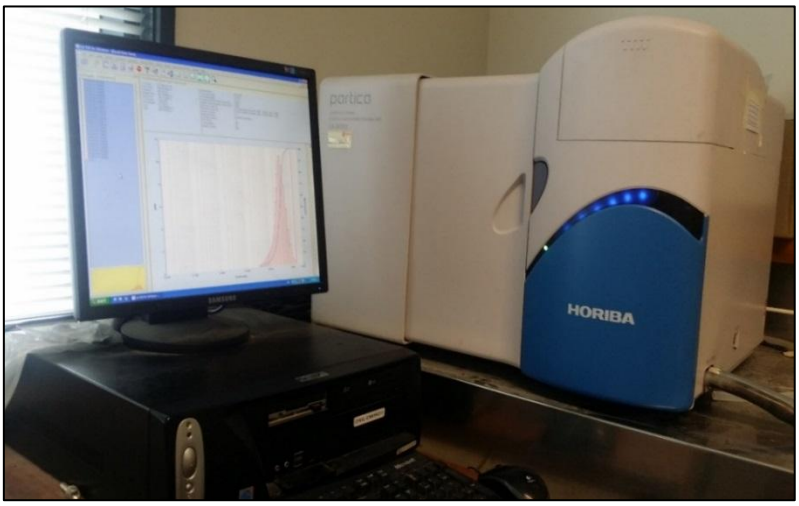

Figure 3.1: Equipment used for particle size distribution (PSD)

3.2.1.2 Scanning Electron Microscopic Imaging

The scanning electron microscopic imaging (SEM) of GP, FAF, FAC, LP and all GL types was accomplished by using the JEOL JSM 7000F Scanning Electron Microscope, as shown in Figure 3.2. Scanning electron microscope uses a focused beam of high-energy electrons to generate a variety of signals at the surface of solid specimens. The signals that derive from electron-sample interactions reveal information about the sample including external morphology, chemical composition (using energy dispersive system, EDS), crystalline structure and orientation of materials making up the sample. In addition, it examines the microstructural characteristics of the materials and helps to identify the nature of

deterioration or defects, to determine the degree of damage. To prepare materials before the examination, thin sections are cut from the concrete cores using a sawing equipment and are saturated with resin. The sections are then polished to remove the damage imparted by sawing and are later coated with a thin layer of conducting material, commonly carbon, gold, or some other metal or alloy.

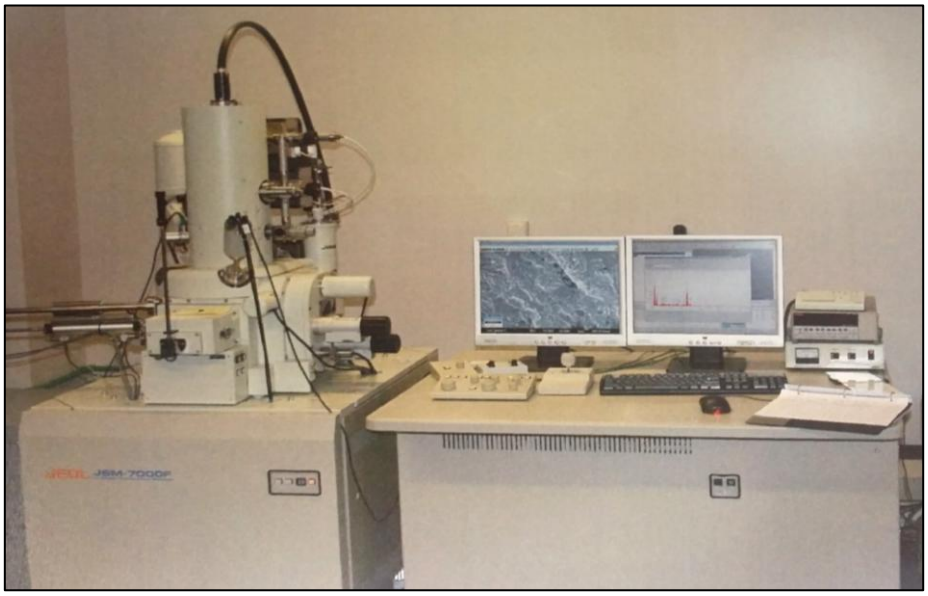

Figure 3.2: Equipment used for scanning electron microscopic imaging (SEM)

3.2.1.3 X-ray Powder Diffraction Analysis

Powder analysis consists of physical properties, such as crystallinity, dissolution rate and stability. The crystalline form of the particles has a large impact on the behaviour regarding solubility and stability. Hence, the x-ray powder diffraction (XRD) analysis of GP, FAF, FAC, LP and all GL types was also carried out in this study. XRD analysis is based on constructive interference of monochromatic X-rays and a crystalline sample. The X-rays are generated by a cathode ray tube, filtered to produce monochromatic radiation, assembled to concentrate, and directed towards the sample. The interaction of the incident rays with the sample produces constructive interference and a diffracted ray when conditions satisfy Bragg's Law ($n\lambda=2d \sin \theta$). In addition to the identification of crystalline material, the presence of X-ray amorphous material is also determined. The quantitative interpretive software 'Siroquant' is used to determine the relative abundance of major crystalline phases and to some extent, amorphous phases within the sample (Brady and Boardman, 1995).

3.2.2 Aggregates

The tests carried out on aggregates include sieve analysis, water absorption, moisture content and particle density.

3.2.2.1 Sieve analysis test

Sieve analysis of both coarse aggregates (CAG) and fine aggregates (FAG) was undertaken according to New Zealand standard NZS3111-1986, using the equipment illustrated in Figure 3.3. Initially, the aggregates were dried in an oven for 24 hours. Then, they were weighed (4 kg in case of CAG and 0.2 kg in case of FAG) and put in the sieves. The sieves were agitated by a mechanical shaker for a sufficient period of time in such a manner that upon completion, the amount passing any individual sieve during a further minute of mechanical shaking was not more than 0.1% of the test sample mass. The residue on each sieve was measured and the cumulative percent passing was calculated. Additionally, the fineness modulus (FM) of FAG was calculated by dividing the sum of cumulative percentages retained on all sieves by 100.

Figure 3.3: Equipment used for sieve analysis test

3.2.2.2 Density and water absorption test

The density and water absorption of both CAG and FAG fractions were obtained according to NZS3111-1986. The equipment used for density and water absorption tests of CAG and FAG have been illustrated in Figures 3.4 and 3.5 respectively. For CAG; an empty wire basket was suspended from the balance while immersed in water at 21+/-5°C and the balance reading was recorded as D. The test sample was then brought to a saturated surface-dry (SSD) condition, by rolling it in a large absorbent cloth, until all visible water film was removed and the weighed mass was recorded as B. Immediately, the test sample was placed in the wire basket and was suspended from the balance while immersed in water at 21+/-5°C. CAG was weighed and recorded as C. Then, the test sample was dried by stirring

periodically during drying to increase evaporation. When the sample was considered to be dry, it was weighed and recorded as the mass A. The density was calculated by the following formulas:

$$SSD\ basis = \frac{B}{B-(C-D)}\ x\ 1000\ kg/m^3 \qquad \text{Equation 3.1}$$

$$Oven-dry\ basis = \frac{A}{B-(C-D)}\ x\ 1000\ kg/m^3 \qquad \text{Equation 3.2}$$

In addition, the absorption was calculated as a percentage of the SSD mass by the following formula:

$$Absorption, \% = \frac{B-A}{B}\ x\ 100 \qquad \text{Equation 3.3}$$

Figure 3.4: Equipment used for density and water absorption of coarse aggregate

For FAG; SSD sand was divided into two almost equal parts and from each of these, a sample of 700+/-0.5 gm (mass, W) was collected. One of these samples was dried with the help of periodic stirring to accelerate the evaporation. When this sample was dried, its weight was recorded as A. The pycnometer was calibrated by filling with water at a temperature of 21+/-5^{o}C. The filled pycnometer was weighed and this weight was recorded as $M_{e.}$ With the pycnometer about half full of water, the second 700 gm sample was added. Then, it was vigorously shaken to release the entrapped air. The pycnometer and its contents were weighed and this mass was recorded as M. The density was calculated by the following formulas:

$$SSD\ basis = \frac{700}{Me+\ 700-M}\ x\ 1000\ kg/m^3 \qquad \text{Equation 3.4}$$

$$Oven - dry\ basis = \frac{A}{Me+700-M}\ x\ 1000\ kg/m^3$$ Equation 3.5

Furthermore, the absorption was calculated as a percentage of SSD mass by the following formula:

$$Absorption, \% = \frac{700-A}{700} x\ 100$$ Equation 3.6

Figure 3.5: Equipment used for density and water absorption of fine aggregate

3.2.2.3 Moisture content test

Accurate control of the water content of a mix is very important to avoid changes in the consistency of mortar or concrete. The aggregates were always kept in a condition greater than SSD. Moisture contents of aggregates were measured every time before casting a mix and were adjusted in the mix design to achieve same consistency of the mix according to the requirement. Moisture contents of both CAG and FAG were also tested by using standard NZS3111-1986. Each sample was weighed and recorded as the mass W. It was then dried in the container through periodic stirring to accelerate the evaporation. When the sample was considered dry, its weighed mass was noted as D. The moisture content was then calculated by the following formula:

$$M = \frac{W-D}{D}\ x\ 100$$ Equation 3.7

where; M = total moisture content of sample, % of dry mass

W = mass of original sample in kg

D = mass of dried sample in kg

3.2.2.4 Unit mass and void content test – coarse aggregate

The unit mass and void content of CAG were determined in compliance with the standard NZS3111-1986. The measure, shown in Figure 3.6, was filled about one-third full and the layer of CAG was rodded with 25 blows, the blows being evenly distributed over the surface. This step was repeated two more times and in the end, the surface of CAG was levelled. Finally, the net mass of CAG in the measure was determined. The unit mass of the CAG was calculated as:

$$Unit\ mass = \frac{net\ mass\ of\ aggregate\ in\ kilograms\ x\ 1000}{volume\ of\ measure\ in\ litres}$$ Equation 3.8

The void content in CAG was determined as:

$$Voids\ content = \frac{A-B}{A}\ x\ 100$$ Equation 3.9

where; A = density of the aggregate

B = unit mass of the aggregate

Figure 3.6: Equipment used for void content test of coarse aggregate

3.2.2.5 Void content and flow time test – fine aggregate

The standard NZS3111-1986 was used to test the void content and flow time of FAG. The equipment used to carry out this test is shown in Figure 3.7. A sufficient quantity of FAG was dried to a constant mass in an oven at 110+/-5^{o}C so as to get a sample mass of about 2500 gm after cooling at room temperature. From the material smaller than 4.75 mm, a sample weighing, to the nearest 1 gm, 0.38 times its dry density in kg/m^{3} was collected. The sample was then placed in the clean sealed glass container and shook vigorously for about 30 sec.

The mass of water, at 21+/-2°C, required to fill the receiving can was determined and recorded as A. The sand flow cone was mounted with its top rim horizontal on the stand, with the overflow can and the receiving can situated centrally below. The test sample was placed in the cone, the finger was placed over the orifice of the cone and was quickly removed, simultaneously starting the stopwatch. The time taken for FAG to run out of the cone was measured and recorded to the nearest 0.1 sec. The FAG collected in the receiving can was screed to a flat surface with short horizontal strokes. The mass of FAG in the receiving can was determined and recorded to the nearest 0.1 gm and then re-blended with the remaining sample in the overflow can. This procedure was repeated three times to get an average of three measurements of flow time.

Figure 3.7: Equipment used for void content and flow time test of fine aggregate

The void content in FAG was determined as:

$$Voids\ content = \left(1 - \frac{1000\,B}{AD}\right) x\ 100 \qquad \text{Equation 3.10}$$

where; A = mass in gm of water required to fill the can at 21+/-2°C

B = mass in gm of sand contained in the can and is the average of three runs

D = density of the sand (dry basis)

3.3 Physical and chemical properties of constituent materials

The constituent dry materials of mortar and/or SCC including GP, FAF, FAC, LP, GL, CAG, and FAG used throughout this study were obtained from the same source and batch. The FAs of two classifications were obtained from two different plants and were used separately for casting different mixes. Because it is difficult to anticipate the interaction between

cement, mineral additions, and chemical admixtures with assurance on results, the same superplasticizer (SP) and stabilizer (SB) for SCC were chosen for the complete research program. All the materials for this study were chosen to ensure both the quality of the SCC product as well as to meet the workability requirements of the fresh concrete. As this research included the challenges of large-scale mixing and potential utilization at the commercial level, it was important to choose materials that could be easily sourced locally and materials that the concrete manufacturers are familiar with. The materials outlined in this section were found to be the most appropriate in terms of production quality, cost-effectiveness, and commercial acceptance for practical application of this research. It is essential to mention here that the physical and chemical properties of admixtures recorded in Table 3.3 were the only data provided by the supplier. The remaining data mentioned in the current section were measured from the tests performed as part of this study.

3.3.1 Binders

Generally, binders make up the matrix within the mortar or concrete that holds the aggregates together and also provides strength. GP cement, which is the most common type of cement in New Zealand, was obtained from Golden Bay Cement. The GP cement, complying with ASTM Type II, was used as the principal cementitious material in this study. The mechanical properties of GP cement are listed in Table 3.1. The XRD and XRF data is included in Appendix B. With an increase in technical and environmental demands, using GP cement as the only binder has become less economically and environmentally feasible. Supplementary cementitious materials (SCM), when used individually with GP and/or in different combinations, contribute to the properties of hardened concrete. Hence, a number of SCMs, such as FAF, FAC, and LP, were also employed as control (CTR) cementitious materials for comparison with GL incorporated mixes. Gladstone FAF was obtained from Cement Australia, FAC from Golden Bay and LP from the quarry of McDonald located at Oparure, New Zealand. Crushed glass was obtained from a New Zealand glass recycling plant. The crushed glass was thoroughly washed with tap water to remove any impurities prior to milling. It should be noted that some preliminary trials were performed using as received finely ground glass powder, which was found to contain appreciable concentrations

Table 3.1: Mechanical properties of cement

Property	Measured values
Soundness (Le Chatelier) (mm)	1
Initial setting time (hrs:min)	1:59
Final setting time (hrs:min)	3:16
Compressive strength (MPa) (28d)	64.7

Table 3.2: Properties of GP, FAC, FAF and GL

Property	GP	FAF	FAC	GL
Colour	Fine white	Dark grey	Light brown	Light brown
Mean diameter (µm)	24.0	20.9	23.3	18.4
Loss on ignition (%)	4.54	3.31	4.02	0.90
SiO_2	20.76	49.87	39.77	70.35
Al_2O_3	3.54	21.88	16.96	2.01
Fe_2O_3T	2.06	7.78	7.29	1.59
CaO	62.46	8.91	23.06	10.95
MgO	0.88	2.54	2.80	0.56
SO_3	4.00	1.50	2.50	-
K_2O	0.49	1.20	0.49	0.58
Na_2O	0.24	0.50	1.91	12.88
TiO_2	0.19	1.04	1.21	0.09
P_2O_5	0.16	0.20	0.29	0.03
MnO	0.07	0.06	0.05	0.02

of sugars and other contaminants. The two major classes of pulverized FA used in this study, i.e. F and C, have been specified in ASTM C 618 on the basis of their chemical composition. FAF carries pozzolanic properties whereas, FAC has some cementitious properties as well as pozzolanic properties. The detailed composition and physical properties of the binders used in this study are presented in Table 3.2.

Figure 3.8 shows the PSDs of all binders used in this research. The precision of the PSD techniques was confirmed by scanning the identical sample three times and keeping average relative deviation less than 2%. Three GL finenesses were selected in this study for utilization in mortar and SCC to investigate their particle size effect on fresh and hardened properties of mortar and SCC. The finest glass had the size of 10 µm, the mid-range sized glass had 20 µm size and the coarsest glass had 40 µm size approximately. The PSDs were characterized using D_{50}, which is 50% passing size in the cumulative distribution. However, D_{10} and D_{90} were also observed from the PSD analysis for comparisons. The PSD of GP showed a quite narrow range of size distribution. The investigation on GP sample demonstrated that around 70% of particles were less than 30 µm. D_{50} for GP was found to be 24 µm. The percentage of GP particles below 9 µm was 10%, whereas the amount of particles below 46 µm was 90%. The PSDs of both FA types (FAC and FAF) showed an almost similar range of size distribution and both were slightly coarser than the GP, especially in the portion of particles smaller than 80 µm and larger than 20 µm. Specifically, 50% of FAC particles lied above and below 23.3 µm, whereas in case of FAF, D_{50} was found

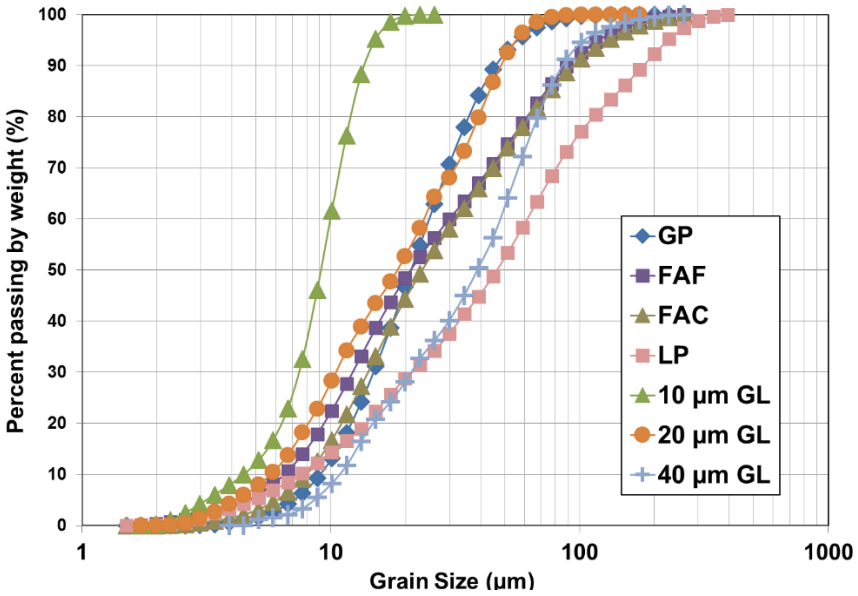

Figure 3.8: PSDs of GP, FAC, FAF, LP and GL of finenesses 10 µm, 20 µm, and 40 µm

to be 20.9 µm. Additionally, D_{10} and D_{90} obtained for FAC were 7.9 µm and 94.7 µm, respectively and for FAF were 6.5 µm and 89.4 µm, respectively. PSD analysis of LP demonstrated that this material was the coarsest of all other binders as well as the size range of particles was the widest, covering from 1.7 µm to 300 µm. D_{50} for LP was found to be 46.5 µm, D_{10} as 4.4 µm and D_{90} as 181 µm.

The equipment (Sala Laboratory Mill D300 x 450) used for the purpose of grinding glass powder is shown in Figure 3.9. The rod mill was used to grind the glass sample in a 10 L chamber, with a grinding media filling ratio of approximately 45%, the rotational speed of the mill was 80 rpm. The comparison between the energy consumptions while grinding cement and glass is complicated because of the high-efficiency motors and different grinding processes used in the cement industry for milling. Grinding time was the most important consideration while grinding glass powder. Figure 3.10 demonstrates that the particle size reduced efficiently at the beginning of the grinding process. When grinding proceeded to 5 hrs or 6 hrs, particle size reduction slowed down. After 5 hrs of grinding, a mean particle size of 29 µm was achieved. Different grinding times of milling were used: 3.5 hrs, 6.5 hrs, and 15 hrs, to achieve the preselected particle size ranges. The GL powder used in this study presents a wide range of particle sizes, with mean values ranging from approximately 9.9 µm to 40.7 µm, for 3.5 hrs to 15 hrs of grinding time. While reduction in particle size with the increase in grinding time is evident; however, shapes of the particles might be complex and will be discussed later. By analyzing the PSD measurements taken after specific time intervals of grinding, it was observed that mode and average size of the coarser population of particles, predominantly formed by those larger than about 10 µm, clearly became finer as grinding time was increased. On the other hand, the mode of the finer population of particles

Figure 3.9: Equipment used for grinding glass

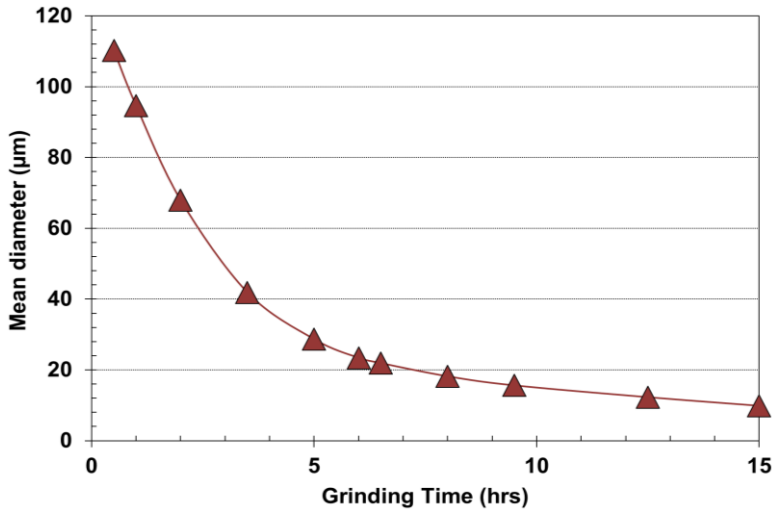

Figure 3.10: Effects of grinding time on mean diameter of glass powder

remained relatively constant at about 2.3 µm; however, the proportion of this population kept increasing with grinding time. The distinction between these two populations started to appear at longer grinding times, as they tended to separate.

Specifically, 50% of 10 µm GL particles lied above and below 9.4 µm, whereas D_{10} and D_{90} obtained for 10 µm GL were 4.5 µm and 13.6 µm respectively. There were approximately 76% particles in 10 µm GL below 11.5 µm. PSD analysis of 20 µm GL demonstrated that this material covered the size range from 4.3 µm to 88 µm. D_{50} for 20 µm GL was found to be 18.4 µm, D_{10} as 4.9 µm and D_{90} as 48.5 µm. Similarly, PSD analysis undertaken on 40 µm GL exhibited that D_{50} of 40 µm GL was 38.4 µm, D_{10} was 10.5 µm and D_{90} was 82.5 µm. Approximately 60% particles of 40 µm GL were less than 45 µm. It can be clearly seen from Figure 3.8 that 10 µm GL is much finer than all CTR binders, whereas 40 µm GL is much finer than LP in the coarser range of particles and slightly coarser than LP in the finer size range. GP, FAC, FAF, LP, 10 µm GL, 20 µm GL and 40 µm GL contained approximately 89%, 70%, 71%, 49%, 100%, 87%, and 60% respectively of particles smaller than 45 µm.

It is worthwhile to mention here that the properties of glass powder used for different experiments were consistent in the present research. Large amounts of crushed waste glass were washed and dried at a time. Subsequently, the washed and dried crushed glass sample was ground in the ball mill for an appropriate period of time required to achieve the desired fineness. A 6 kgs crushed glass sample was ground at a time in the ball mill and in the end, all batches of ground glass were collectively mixed in the mixer and stored in one container. All small-scale and large-scale experiments were undertaken using glass powder from that container, which ensured the consistency of glass powder used in all mixes.

All binder types were also viewed under the optical scanning electron microscope and SEM images were captured at various magnifications. The images obtained at 800 magnification of the samples have been demonstrated in Figure 3.11 (a) to (h). It can be seen from the figures that both FAs contain significant amounts of fine spherical particles, which are much rounder compared to the GP particles. The surface of LP seem to be very smooth compared to FA particles and are more or less rectangular. SEM observations also indicate that GL particles are more angular, denser and more pragmatically shaped compared to GP and naturally larger than spherical FA particles. The coarser glass (40 μm) has very rough surfaces, acute angles, and pointed edges. On the other hand, the finer glass ranges have much smoother surfaces (10 μm and 20 μm) as compared to the coarser glass (40 μm).

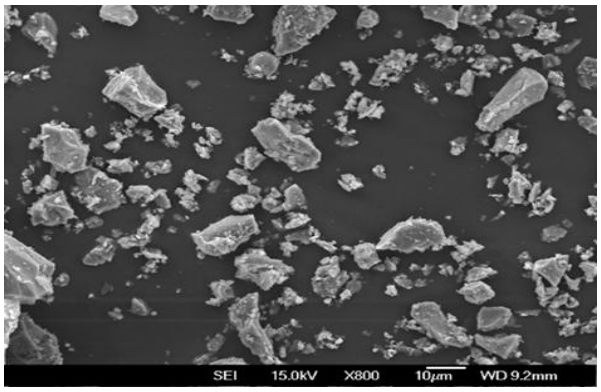

(a)

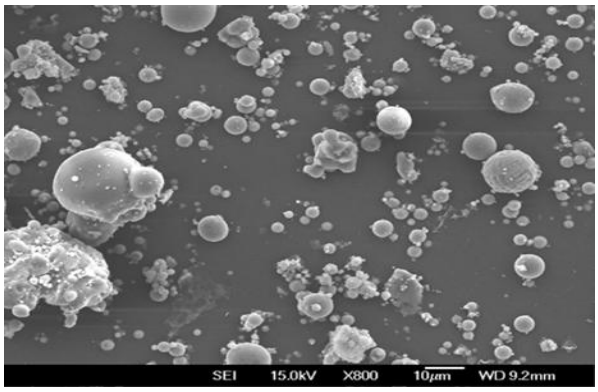

(b)

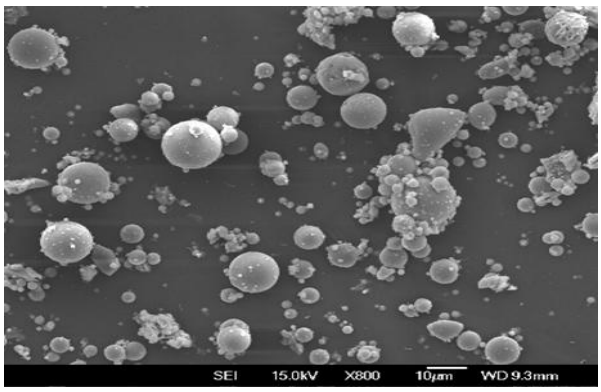

(c)

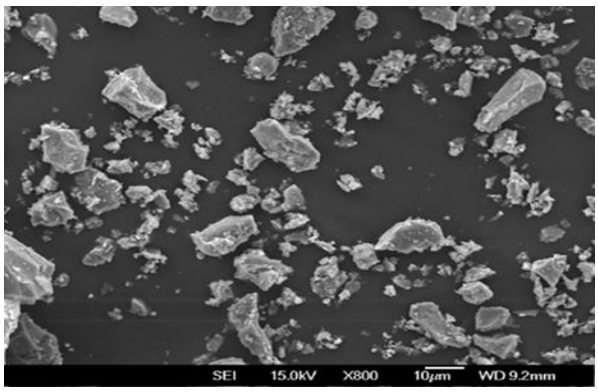

(d)

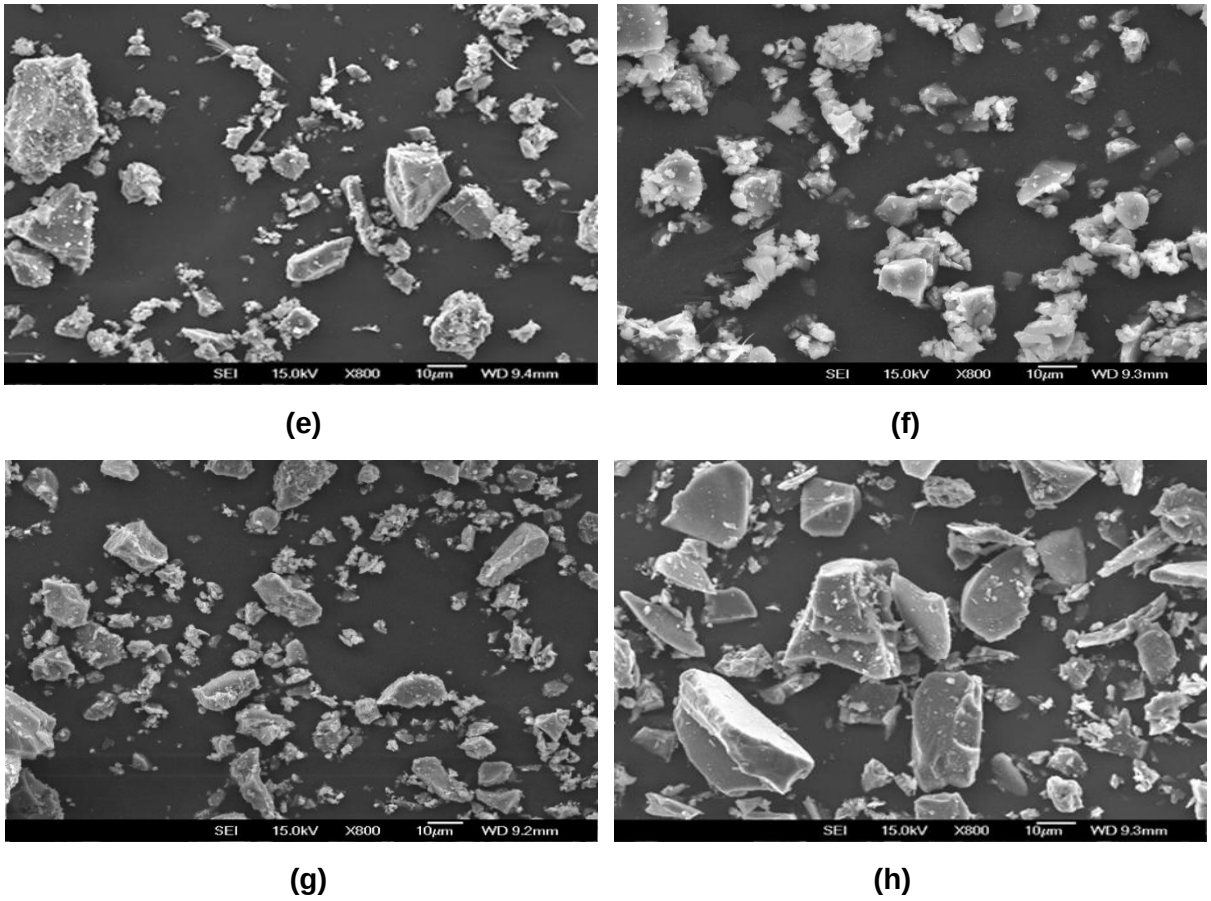

Figure 3.11: SEM of (a) GP (b) FAF (c) FAC (d) LP (e) 20 UGL (f) 10 GL (g) 20 GL (h) 40 GL

3.3.2 Superplasticizer

SP is used to improve the dispersion of the binder particles and consistency of the mortar or concrete but without the harmful side effects, such as reduced strength and segregation. Also known as high range water reducers, these polymers are used as dispersants to avoid particle segregation and improve flow characteristics by the use of polarity. This means that cement particles will be well-distributed throughout the mix when SP will be added to the mix. In this research, Sika Viscocrete 5-555 was used in all SCC mixes, which is an ideal SP type where water reduction, excellent flowability, and optimal cohesion are required. It is basically a third generation polymer-based ultra-high range SP and is an aqueous solution of modified polycarboxylate by form. Sika Viscocrete 5-555 satisfies the requirements for SPs in accordance with ASTM C494 Types A and F. The physical and chemical properties of SP are listed in Table 3.3.

3.3.3 Stabilizer

Sika Stabilizer 4R was used in all SCC mixes produced in the present study to fulfil the requirement of an SB. It is specially developed for SCC or standard concrete where improved stability is required during the transportation and placement. It is used to increase

Table 3.3: Physical and chemical properties of superplasticizer and stabilizer

Property	Superplasticizer	Stabilizer
Physical state	Hazy liquid	Hazy liquid
Colour	Light Blue	Blue
Odour	Pleasant	Odourless
Boiling Point	Not Available	>101^{o}C (>213.8^{o}F)
Vapour Pressure	Not Available	3.1 kPa (23 mm Hg)
Density	1.1 g/cm^{3} [20^{o}C (68^{o}F)]	1.025 g/cm^{3} [20^{o}C (68^{o}F)]
pH	5	7
Solubility	Easily soluble in cold water	Easily soluble in cold water

the cohesiveness of concrete, enable SCC to flow easily through confined spaces without segregation or bleeding and maintain workability. Sika Stabilizer 4R meets the requirements for ASTM C494, Type S admixture. It is classified as a liquid by its form. The physical and chemical properties of SB are also listed in Table 3.3.

3.3.4 Aggregates

The choice of aggregates is dependent on the availability and it is cheaper to use locally available aggregates. The performance of any given type of aggregate is a function of its size, shape, texture and strength; all of which contribute to the overall dimensional stability of the concrete. In this study, locally available semi-crushed coarse aggregate of the maximum size 13 mm (natural Waimakariri river stone) and fine aggregate (natural greywacke river sand) were used in mixes. In general, greywacke is a dull grey stone, which consists of alternating layers of hard muddy grey, slightly metamorphosed sandstone and darker mudstone (argillite). This means that it is mostly available in thick or thin beds with slates and limestone. New Zealand greywacke was formed in crumbled, folded layers as marine sediments were scraped off the ocean floor by the toe of an overriding plate (Thornton, 2003). Hence, it can be found in most places around New Zealand including on mountains, in rivers and on beaches. Since it forms a large percentage of the basement rock for the country, it has been subjected to considerable tectonic movements within the last 300 million years, though most of them are less than 250 million years old. It is a hard rock with grain sizes of 0.06–2 mm, typically with angular class visible to the naked eye (Smith, 2005). The particle size grading of aggregates used in the present research is provided in Table 3.4 and their physical properties are provided in Table 3.5. All the characteristics of fine and coarse aggregates were tested using the methods described in section 3.1. Large amounts of fine and coarse aggregates were mixed and stored in containers before initiating the experiments to ensure uniformity of the materials used in all trial mixes.

Table 3.4: Particle size grading of aggregates

Sieve size (mm)	19.0	13.2	9.5	4.75	2.36	1.18	0.6	0.3	0.15	0.075	Pan
FAG (% passing)	-	-	-	96	75	60	51	33	8	2	0
CAG (% passing)	100	93	48	1	-	-	-	-	-	-	0

Table 3.5: Physical properties of aggregates

Property	FAG	CAG
Colour	Grey	Grey
Specific gravity (g/cm^3)	2.61	2.63
Bulk density (kg/m3)	1550	1530
Void ratio (%)	0.54	0.72
Water absorption (%)	0.80	0.79

3.3.5 Water

Ordinary Christchurch tap water was used as the mixing water, throughout the research program.

3.4 Mix design, mixing procedure and curing

The purpose of mix design system is to enable the materials to be proportioned in such a way so as to produce good fit for purpose concrete of the desired strength. It involves the selection of suitable aggregates and determines their optimum relative proportions and cement requirement to produce a given strength at a given slump. The first important consideration is that the most advantageous selection of aggregates be made and the second is that the concrete should have the desired properties in the fresh state. The selection of available materials and their proportioning should be done in such a way that the most economical concrete is produced, which is suitable for the desired purpose.

The design of concrete mixes has become more complex due to the availability of many different cementitious materials (such as normal, high strength, sulphate resisting and low heat Portland cements and SCMs such as fly ash, limestone powder, and silica fume) as well as admixtures to reduce water demand, entail air, accelerate or retard setting, and reduce permeability or shrinkage. Understanding the requirement of the concrete industry of New Zealand, it was decided to choose a mix design that is representation of that which is already employed in the concrete industry. This was done to determine the potential influence of GL on an established SCC mixture, in comparison to other SCC. However, initial

preliminary trials on mortar cubes were undertaken using the mix design specified in ASTM standard. These tests were carried out to assess the effects of GL content and fineness on the behaviour of mortar, in order to arrive at the most effective GL replacement rate and size range, for effective results compared with GP and other SCMs.

Table 3.6 lists the details of mortar mix design for preliminary testing, which is in accordance with a standard method ASTM C 109/109M. This standard was also used for the preparation of mortar. For these mixes, 2 L batches were mixed in an electronically driven mechanical mixer of the type equipped with a paddle and mixing bowl. Water was put in the bowl first, the cement was added to the water and then mixer was turned on to mix at the slow speed of 140 +/- 5 r/min for 30 sec for the absorption of water. The entire quantity of sand was slowly added over this 30 sec period while mixing at slow speed. The mixer was then stopped, the speed was changed to medium speed (285 +/- 10 r/min) and mixed again for 30 sec. Then, the mixer was stopped and the mortar was allowed to stand for 90 sec. During the first 15 sec of this interval, any mortar collected on the side of the bowl was quickly scarped down into the batch and then for the remaining time, the mixer enclosure was closed. The mixing was then finished by mixing for 60 sec more, at the medium speed of 285 +/- 10 r/min. Finally, a representative sample from each mix was poured into moulds for setting, after which they were demoulded and kept in standard curing conditions, in accordance with ASTM C192/C192M, until the time of testing.

The same ASTM standard (ASTM C109/C109M) for casting mortar cubes was used in the main research program to perform strength activity index texts. The similar ten types of mortar mixes were prepared as listed in Table 3.6. All the quantities of the materials for making twelve test specimens were used, in compliance to ASTM C109. However, in contrast to the preliminary trials, water to cement ratios (w/c) for mixes other than GP mix were adjusted in that part of the study. Hence, w/c for standard mortar (GP) was kept at 0.485, as specified in ASTM C109, but w/c ratios for other mortars incorporating FAF, FAC, LP and all GL types were maintained to obtain a constant flow value 110 +/-5 mm, as that of standard GP mortar. The flow values of mortars were determined in conformity with ASTM C230 standard. All batches were prepared by using a mechanical mixer according to the requirements of ASTM C305. Mortars were cast in 50 x 50 x 50 mm standard moulds, removed from the moulds after 24 hrs of casting and then kept under standard curing conditions in accordance with ASTM C192/C192M.

It has been established that mixing procedure has a considerable effect on fresh properties of the SCC. Based on Jin's work (2002), a fixed mixing procedure was adopted and carried out throughout this research program for mixing SCC in order to achieve maximum efficiency

Table 3.6: Mixture proportions for preliminary trials of mortars

Mix Type	GP (%)	FA (%)	LP (%)	GL (%)	Sand/ Binder	Water/ Binder
Mortar with GP Cement only (GP)	100	-	-	-	2.75	0.485
Mortar with class F fly ash at 30% (FAF30%)	70	30	-	-	2.75	0.485
Mortar with class C fly ash at 30% (FAC30%)	70	30	-	-	2.75	0.485
Mortar with limestone powder at 30% (LM30%)	70	-	30	-	2.75	0.485
Mortar with unwashed glass at 30% (20UG30%)	70	-	-	30	2.75	0.485
Mortar with 10 µm glass at 30% (10G30%)	70	-	-	30	2.75	0.485
Mortar with 20 µm glass at 20% (20G20%)	80	-	-	20	2.75	0.485
Mortar with 20 µm glass at 30% (20G30%)	70	-	-	30	2.75	0.485
Mortar with 20 µm glass at 40% (20G40%)	60	-	-	40	2.75	0.485
Mortar with 40 µm glass at 30% (40G30%)	70	-	-	30	2.75	0.485

Table 3.7: Mixture proportions for standard cured SCC mixes

Mix Type	GP (kg/m^3)	FA (kg/m^3)	LP (kg/m^3)	GL (kg/m^3)	FAG (kg/m^3)	CAG (kg/m^3)	Water (kg/m^3)
SCC with GP Cement only (GP)	450	-	-	-	900	850	180
SCC with class F fly ash at 30% (FAF30%)	315	135	-	-			
SCC with class C fly ash at 30% (FAC30%)	315	135	-	-			
SCC with limestone powder at 30% (LM30%)	315	-	135	-			
SCC with unwashed glass at 30% (20UG30%)	315	-	-	135			
SCC with 10 µm glass at 30% (10G30%)	315	-	-	135			
SCC with 20 µm glass at 20% (20G20%)	360	-	-	90			
SCC with 20 µm glass at 30% (20G30%)	315	-	-	135			
SCC with 20 µm glass at 40% (20G40%)	270	-	-	180			
SCC with 40 µm glass at 30% (40G30%)	315	-	-	135			

Table 3.8: Mixture proportions for accelerated cured SCC mixes

Mix Type	GP (kg/m^3)	FA (kg/m^3)	GL (kg/m^3)	FAG (kg/m^3)	CAG (kg/m^3)	Water (kg/m^3)
SCC with GP Cement only (GPE)	450	-	-	900	850	180
SCC with class F fly ash at 30% (FAE)	315	135	-			
SCC with unwashed glass at 30% (UGE)	315	-	135			
SCC with 20 µm glass at 30% (WG)	315	-	135			

and full dispersion of the powder. The details of SCC mix design are presented in Tables 3.7 and 3.8 for standard and accelerated cured mixes respectively. For preliminary and small scale SCC trials, a 20 L pan mixer was used to cast mixes. However, 90 L capacity drum mixer was used for large scale mixes. The mixing procedure was same for all SCC mix types, irrespective of the batch sizes and constituent materials used in the mix.

Firstly, all the constituents were batched out into buckets in the required quantities. All dry materials were mixed for about 1 min in the mixer before introducing water, SP and SB to the mix. The 80% of required water was added in several stages while mixing, followed by an additional 1 min of mixing. The remaining 20% of water, which was premixed with required dosage of SP, was introduced to the mixer and another min of mixing was continued. At this stage, SCC was left for about a min in the mixer without mixing; after which, the entire mixing procedure was finished with a final min of mixing. SB was also added according to the requirement. Frequent visual checks were done during mixing to avoid over saturating the mix leading to an early and uncontrolled segregation. When the mix seemed to be of appropriate consistency, a slump flow test was carried out that will be explained later. This process was repeated until the flow of the mix was considered satisfactory. The final admixture dosages were noted at the end of mixing. The mix was then distributed into 44 test cylinders (100 mm x 200 mm) for curing under standard conditions as outlined in ASTM C192/C192M.

SCC mixes that were to be tested for the effects of elevated temperature curing condition were also produced according to the normal procedures, which was adopted for standard cured SCC mixes. However, representative samples of these mixes were poured in 44 cylindrical moulds (100 mm x 200 mm) after casting, the cylinders were covered and were placed in an oven, whose temperature was increased to 50°C for approximately 18 hrs. Prior to de-moulding, the specimens were allowed to cool for another 4 hrs. Subsequently, after the specimens were removed from the moulds, half of the specimens were placed in a

standard curing tank at approximately 21^{o}C and the other half were kept under ambient laboratory conditions with no further curing until testing.

3.5 Tests on mortar and self-compacting concrete

This section covers the tests undertaken on mortar and SCC mix types. Tests on mortar include slump flow and strength activity index. Tests on fresh SCC mixes include rheological investigation, slump flow, T_{500} and visual stability index. Tests on hardened SCC specimens include compressive strength, splitting tensile strength, elastic modulus, coefficient of permeability, porosity, electrical resistivity, bulk diffusion, and drying shrinkage. The order of testing after mixing SCC was slump flow test, T_{500}, visual stability index values, which were then followed by rheological testing. There was always an additional mixing round between T_{500} and rheological tests to achieve homogeneity again. SCC was dropped back into the mixer to simulate the mix after the first test and was remixed for 1 min before next test was done. SCC was inspected to ensure the homogeneity during handling and testing. The halo of cement paste and unevenly, distributed or clustered aggregates were also recorded. The same SCC mix was used for hardened tests to minimize concrete production in the laboratory.

3.5.1 Workability tests

Workability controls the ease and homogeneity with which concrete is placed. The mixes that that do not meet workability criteria may create voids and concrete may be inconsistent throughout the placement. Consistency is usually measured with the slump test for conventional concrete mixes or the spread test for SCC mixes; both using Abrams cone (Neville, 1995). To determine the flow of mortar mixes, a standard flow test procedure was undertaken in conformity with ASTM C1437, as demonstrated in Figure 3.12. A layer of mortar of about 25 mm in thickness was placed in the mould and was tamped 20 times with the tamper. Tamping was ensured to be uniformly distributed over the cross-section of each layer. Then, the mould was filled again with mortar and tamped as specified for the first layer. The mortar was cut off to a plane surface by drawing the straightedge or the edge of the trowel with a sawing motion across the top of the mould. The mould was lifted away from the mortar 1 min after completing the mixing procedure. Immediately after this, the table was dropped 25 times in 15 sec. The calliper, as specified in ASTM C230/C230M, was used to measure the diameter of the mortar along the four lines marked on the table top, recording each diameter as the number of calliper divisions, estimated to one tenth of a division. Finally, the flow was recorded, which was the resulting increase in average base diameter of the mortar mass, expressed as a percentage of the original base diameter.

(a) (b) (c)

Figure 3.12: (a) Apparatus used for the flow test (b) Placing mortar in the mould (c) Slump flow test for mortar workability (CAER, 2016)

The consistency of SCC mixes was determined using the slump flow test (ASTM C1611/C1611M). This test was undertaken with a standard cone of height 300 mm (major diameter of 200 mm and minor diameter of 100 mm), a flat, smooth-surfaced, non-absorbent 800 x 800 mm level tray as the base, and a measuring tape. With the cone placed upside down on the tray, concrete was poured into the cone until levelled at the top. Then, the cone was lifted up without tilting to about 50 mm above the tray over a two sec interval allowing concrete to flow outwards. Once SCC mix stopped flowing, two perpendicular diameter measurements were taken. The average of these two measurements, to the nearest 10 mm, was considered to be the spread (ASTM C1611/C1611M). The target for the main SCC mixes was the flow measurement of 680-750 mm, test results of which are discussed in Chapters 5 to 7. Figure 3.13 demonstrates how slump flow tests were carried out for this study.

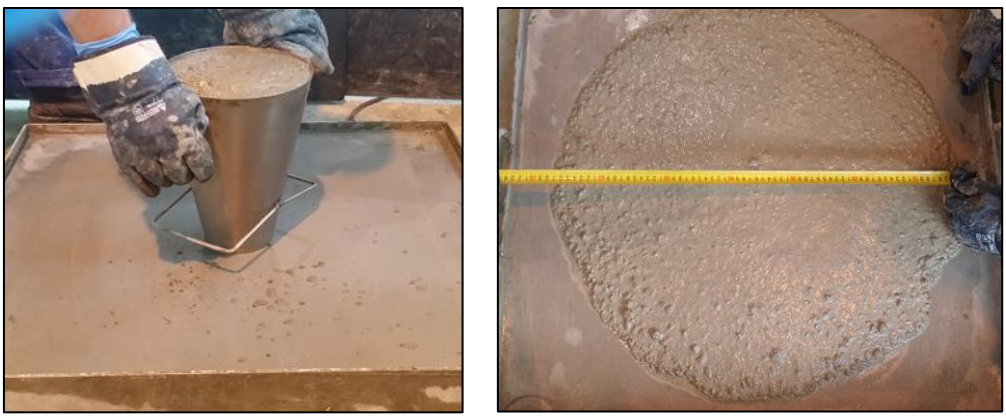

Figure 3.13: Slump flow test for SCC

Although this research is mainly focussed on SCC, the influence of different SP dosages on SCC was also investigated in one part of this research, for which slump test was carried out

at lower SP levels (Refer to Chapter 4). The method to perform slump test is shown in Figure 3.14. The standard ASTM C143/C143M was used for determination of slump. For this test, the cone was placed on a hard non-absorbent surface and was filled with fresh concrete in three layers. Each layer was tamped 25 times with a rod of standard dimensions. At the end of the third stage, concrete was levelled off to the top of the mould. The mould was carefully lifted vertically upwards with twisting motion, so as not to disturb the concrete cone. Finally, the slump was measured with a measuring device.

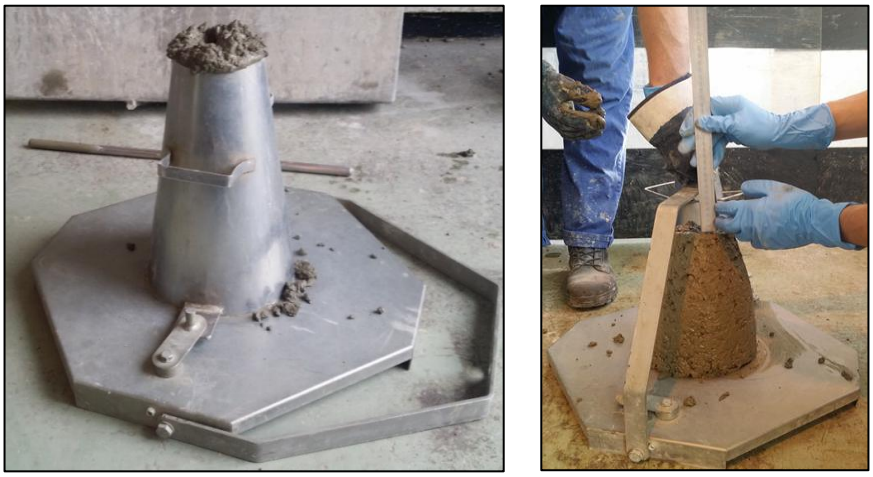

Figure 3.14: Slump test for workability of standard concrete

3.5.2 Rheological test

According to Koehler (2009), rheology is typically used to describe workability. It is the property that describes the ease with which concrete can be mixed, placed, consolidated, and finished to a homogenous condition. More specifically, rheology is a measure of yield shear stress, plastic viscosity, and shear rate. In this study, rheology was tested using the BML-Viscometer, as demonstrated in Figure 3.15, which is a coaxial cylinder viscometer for

Figure 3.15: Apparatus used for rheological measurements

coarse particle suspensions. The BML process is fully automated to minimise the influence of operator. To carry out this test, the bucket was filled with SCC mix up to approximately 30 mm from the top, then the coaxial cylinders were lowered into the mix. The standard test was used that starts at the highest speed and is slowly reduced to the lowest required speed for the mix. For a usual testing time of 3-4 min, the mix was only subjected to the movement for about 75 sec. As the outer cylinder rotated, the torque was applied to the stationary inner cylinder. During this process, a torque-speed diagram was plotted, which was used to calculate shear stress and plastic viscosity through linear regression.

3.5.3 Compressive strength tests of mortar cubes

The mortar cubes were tested in compression, according to ASTM C109/C109M, to determine indicative values of the compressive strength in each of the mortar types. This quantity is useful as it is the most universally understood property and concrete is often described in terms of its compressive strength. This value also provides extra evidence for the likely structural performance of a material. During this test, the cubes are compressed to ultimate failure using a loading cell with a loading capacity of 400 kN and the loading rate of 2 kN/s. An example of the cube in compression is shown in Figure 3.16.

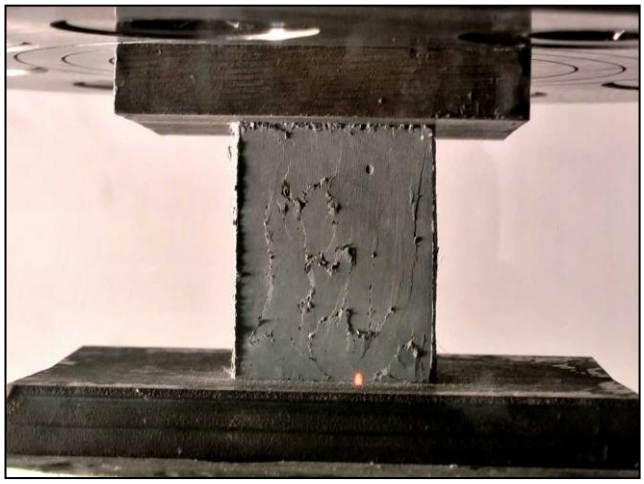

Figure 3.16: Compressive strength of mortar cube

3.5.4 Compressive strength test of SCC

The concrete structure design rules are often based on the compressive strength of the concrete. Various other mechanical properties (e.g. tensile strength, modulus of elasticity) and physical properties (e.g. related to durability) of concrete are expressed as a function of this parameter (CEB FIB Model Code 90). Some parameters which are known to affect the compressive strength of concrete including w/c, cement compressive strength, properties of the aggregates (shape, grading, surface texture mineralogy, strength, stiffness, and maximum grain size), air-entrainment, curing conditions, testing parameters, specimen

parameters, loading conditions, and test age (Vandegrift and Schindler, 2006; Elwell and Fu, 1995). This suggests the importance of accuracy in material characterization tests as well as mixing and curing concrete. In this study, the compression tests were performed in accordance with ASTM C39/C39M at the ages of 1, 3, 7, 28, 90, 180, 365 and 545 days using the MATEST Automated Concrete Compression Machine of 3000 kN capacity and the loading rate of 2 kN/s. Before undertaking tests, the specimens were prepared by grinding and levelling their uneven top surface. For each set of data, two specimens were tested and the average value was reported. In the case of variability in results, the third specimen was also tested and the average value was recorded. An example from compressive strength testing is shown in Figure 3.17.

Figure 3.17: Compressive strength test of SCC specimen

3.5.5 Splitting tensile strength test

Tensile strength tests are used to assess the cracking resistance of concrete and bond strength to reinforcing bars. However, direct tests on the tensile strength of concrete are difficult to conduct. The most commonly adopted tests for determining the indirect tensile strength are the flexural strength and the splitting test. In this study, splitting tensile strength was measured according to the standard ASTM C496/C496M, at the ages of 7, 28, 90, 180, 365 and 545 days, with the same automated equipment used for compressive strength tests. Before undertaking tests, the specimens were prepared by grinding and levelling their uneven top surface. For each set of data, two specimens were tested and the average value was reported. In the case of variability in results, the third specimen was also tested and the average value was recorded. An example of tensile strength testing is shown in Figure 3.18.

Figure 3.18: Splitting tensile strength test of SCC specimen

3.5.6 Modulus of elasticity test

In the present research program, the elastic modulus was measured in accordance with the standard ASTM C469/C469M, at the ages of 7, 28, 90, 180, 365 and 545 days. Before undertaking first set of tests, the specimens were prepared by grinding and levelling their uneven top surface. For each set of data, three specimens were tested and the average value was reported. The specimens were loaded to approximately 1/3 of the ultimate compressive strength to minimize any micro-cracking or substantially non-linear behaviour. The specimens were then returned to the same curing environment and were re-used on the next scheduled test day. An example from static elastic modulus testing is shown in Figure 3.19.

Figure 3.19: Elastic modulus test of SCC specimen

3.5.7 Oxygen permeability test

The flow of fluid through a permeable body is modelled by using Darcy's law. This law can also be used for gas flow through a permeable medium. The movement of fluids through a porous structure under an externally applied pressure can be determined from the permeability test. The oxygen permeability is presented as a permeability coefficient obtained from the measured flow of oxygen at different pressures through the specimen. Ballim (1991) developed a falling-head permeameter that allows simple measurement of oven-dried concrete exposed to oxygen under pressure. The oxygen permeability test in this study was carried out by a method described by Alexander et al. (1999a). This test method measures the pressure decay of oxygen passed through a core of concrete placed in a falling head permeameter, shown in Figure 3.20.

Two SCC cylinders were cut to obtain four 25 mm thick cores of SCC (two from each cylinder). These slices were kept in an oven at 50°C for drying until their weight became constant, as suggested in ASTM C642. The oven-dried specimens were subjected initially to oxygen at a pressure of 100 kPa and the pressure decay with time was monitored. The test was automated by using pressure transducers attached to the data logger and was continued until 8 hrs of complete testing or the drop of pressure up to 50 kPa, whichever approached first. The coefficient of permeability was calculated by conducting a linear regression analysis on the best-fit line achieved by plotting values of $\ln(P_o/P_t)$ against t, where P_o is initial pressure reading at the start of the test, and P_t are subsequent pressure readings at times 't' measured from the time of reading of initial pressure. The coefficients of

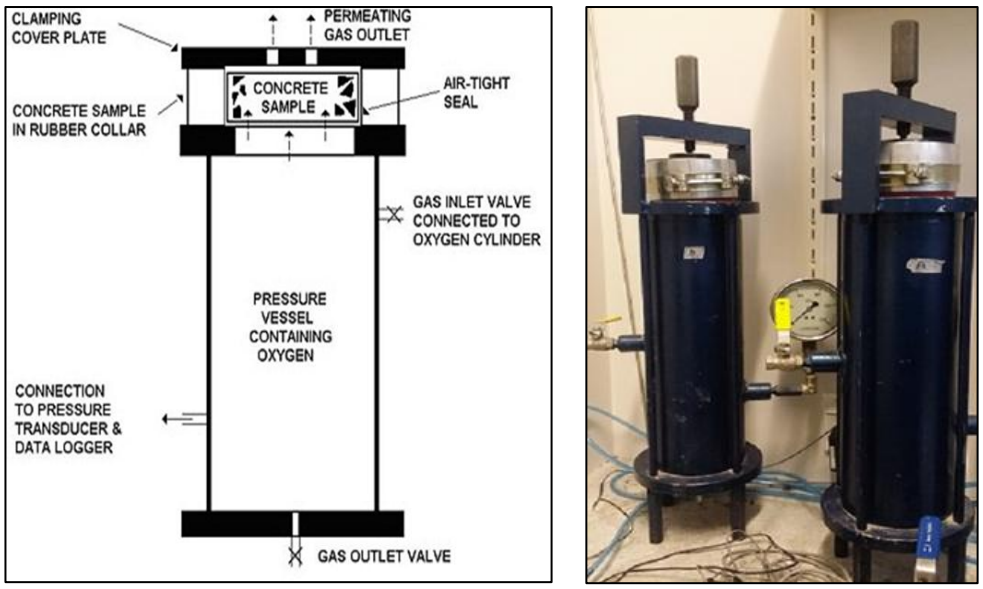

(a) **(b)**

Figure 3.20: (a) Schematic diagram (The Concrete Portal, n.d.) (b) Test set-up for the oxygen permeability test

permeability were calculated by using the formula given in Equation 3.11. Four specimens were used to measure coefficients of oxygen permeability at the curing ages of 3, 7, 28, 90, 180, 365 and 545 days and an average value for each curing age was reported.

$$K = \frac{\omega V g dz}{RA\vartheta} \qquad \text{Equation 3.11}$$

where; K = coefficient of permeability of a test sample (m/s)

ω = molecular mass of oxygen (O_2) = 32 kg/mol

V = the volume of oxygen under pressure in the permeameter (m^3)

g = acceleration due to gravity (m/s^2)

R = universal gas constant = 8.313 (Nm/K.mol)

A = superficial cross-sectional area of the sample (m^2)

D = sample thickness (m)

Θ = Absolute temperature (K)

Z = slope of line determined from the regression analysis

3.5.8 Porosity test

A porosity test has been used to estimate the density, percent absorption, and percent voids in hardened concrete specimen. In this test, oven-dried concrete samples are immersed in water and the total mass absorbed is used as a measure of the water absorption. In this study, same specimens tested for oxygen permeability were later vacuum saturated in tap water and the volume of permeable voids was found according to the standard ASTM C642. The test setup used for porosity test is demonstrated in Figure 3.21.

The specimens were dried in an oven at 50°C until their weight became constant. This dry weight was designated as ‘A’. The specimens were then vacuum-saturated for 12 hrs, were surface-dried and another mass ‘B’ was determined. Finally, the specimens were suspended and the apparent mass ‘C’ in suspension was measured. Four specimens were used to measure porosities at the curing ages of 3, 7, 28, 90, 180, 365 and 545 days and an average value for each curing age was reported. The porosity was calculated by using the formula provided in Equation 3.12.

$$P = \frac{(\mathrm{B} - \mathrm{A})}{(\mathrm{B} - \mathrm{C})}\, x\, 100 \qquad \text{Equation 3.12}$$

where; A = mass of oven-dried sample in air (g)

C = mass of surface-dry sample in air after immersion and boiling (g)

D = apparent mass of sample in water after immersion and boiling (g)

Figure 3.21: Test set-up for the porosity test

3.5.9 Electrical resistivity test

The electrical resistivity can be determined by a simple technique and is appropriate as a control test even during construction since it can be done quickly and relatively cheaply. This test provides a rapid indication of the likely resistance of concrete to the penetration of chloride ions and the likely subsequent rate of corrosion. This test method consists of measuring the electrical current passed through 25 mm thick slices extracted from concrete cylinders. The same disk specimens that were previously used for oxygen permeability and porosity tests were used again to perform electrical resistivity tests. The circuit was arranged, as shown in Figure 3.22.

AC resistivity testing was conducted whereby disks were placed between two parallel stainless steel plates. The sponges saturated with 5M NaCl (sodium chloride) were used to make electrical contact between concrete disks and steel plates. An alternating current was

Figure 3.22: Test set-up for electrical resistivity test

applied across the specimen and the voltage was measured. The specimen dimensions, alternating current, and voltage were used to calculate the electrical resistivity of the concrete using Equation 3.13. Four specimens were used to measure the electrical resistivities at the curing ages of 3, 7, 28, 90, 180, 365 and 545 days and an average value for each curing age was reported.

$$\rho = \frac{V}{I} x \frac{A}{t}$$ Equation 3.13

where; ρ = resistivity of sample (kΩ.cm)

I = electrical current (μA)

V = voltage (mV)

t = thickness of sample (cm)

A = cross sectional area of sample (cm^2)

3.5.10 Bulk diffusion test

Diffusion is the process when fluids or ions move through a porous material under the action of a concentration gradient. Diffusion occurs in partially saturated or fully saturated concrete and is the major internal transport mechanism for marine concrete. The apparent chloride diffusion coeffıcient, Da, is a chloride transport parameter, which is calculated from acid-soluble chloride profile data obtained from saturated specimens exposed to chloride solutions, using Fick's second law of diffusion. This test provides an indication of the ease with which chloride can penetrate into concrete. In this research, the apparent chloride diffusion coefficient of SCC was determined by bulk diffusion conforming to ASTM C1556. The test set-up to measure the apparent chloride concentration is shown in Figure 3.23.

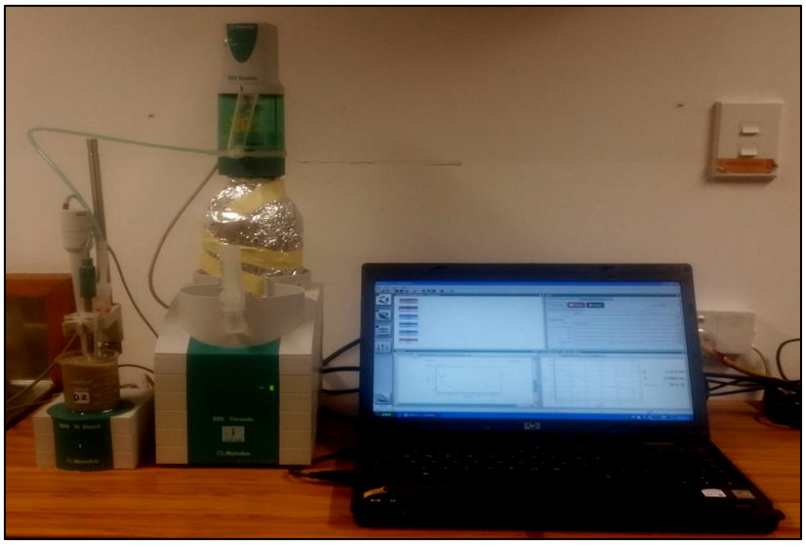

Figure 3.23: Test set-up for bulk diffusion test

To carry out bulk diffusion test, two samples having 75 mm depth from each SCC type were obtained at the curing ages of 28, 90, 180, 365 and 545 days. All sides of the test specimens were sealed with an epoxy coating except the finished surface. The sealed specimens were then vacuum-saturated in a calcium hydroxide solution, rinsed with tap water, and then placed in a sodium chloride solution for at least 35-days. When this exposure time was over, the test specimens were removed from the sodium chloride solution and ten thin layers from 0 mm to 20 mm (2 mm each) were ground off parallel to the exposed face of the specimens. Then, the acid-soluble chloride content of 4 gm sample obtained from each layer was determined. The apparent chloride diffusion coefficients were calculated using the initial chloride-ion contents and nine other related values for chloride-ion contents through regression analysis using Equation 3.14 and Equation 3.15, as outlined in the standard ASTM C1556.

$$C(x,t) = C_s - (C_s - C_i) \,.\, erf\left[\frac{x}{\sqrt{(4.D_a.t)}}\right] \qquad \text{Equation 3.14}$$

where; C (x, t) = chloride concentration, measured at depth x and exposure time t, mass (%)

Cs = projected chloride concentration at the interface between the exposure liquid and test specimen that is determined by the regression analysis, mass (%)

Ci = initial chloride-ion concentration of the cementitious mixture prior to submersion in the exposure solution, mass (%)

x = depth below the exposed surface (to the middle of a layer) (m)

D_a = apparent chloride diffusion coefficient (m^2/s)

t = the exposure time (sec)

erf = the error function described in Equation 3.15.

$$erf(z) = \frac{2}{\sqrt{\pi}} . \int_0^z exp(-u^2)\, du \qquad \text{Equation 3.15}$$

3.5.11 Drying shrinkage test

Drying shrinkage of concrete was determined in accordance to the standard AS 1012.13, which consists of measuring the drying shrinkage of prismatic specimens, having dimensions of 75 mm x 75 mm x 280 mm, in the controlled drying environment. The mould used for these tests is demonstrated in Figure 3.24. To perform these tests, SCC specimens were removed from the curing room at the age of 7-days after casting. Immediately after removing the specimens and wiping their surfaces dry, they were placed in the comparator in a way that their axes were aligned with the measuring anvil and their top surfaces did not bear on the locating supports of the comparator. At least five micrometer readings were recorded to obtain a precise measurement. Afterwards, all the specimens were placed in the

Figure 3.24: Mould used for drying shrinkage test (Controls Group, 2016)

drying room with suitably controlled temperature (23°C) and relative humidity (50%) conforming to the standard AS 1012.13. The specimens were placed in such a way there was a clearance of at least 50 mm on all sides, except for the necessary support. The subsequent measurements of three specimens were taken at 7, 14, 28, 56, 90 and 180 days of air drying and an average value of drying shrinkage in microstrain was reported for each drying age.

3.6 Preliminary trials undertaken on mortar cubes

In this section, the results of small-scale preliminary trials on glass powder and glass modified mortars are presented and discussed. The glass powders used in these preliminary trials had PSDs as shown in Figures 3.25 and 3.27. These glass powders were different than that reported in Figure 3.8, which showed the PSDs of glass powders used in main large-scale mixes and referred as 10G30%, 20G30% etc. The only glass powder that was used in both the preliminary trials and main large-scale mixes was the unwashed glass powder (UWG or WG2 or 20UG30%). The preliminary tests were carried out to assess the influence of glass size, substitution level and quality on the performance of mortar in order to select the most appropriate glass fineness and content for large-scale SCC mixes.

3.6.1 Stage One

Initially, waste glass (WG1) was obtained from a recycling plant and mortar cubes were produced using up to 50% WG1 to assess its performance in comparison to GP cement. Same GP and fine aggregate were used to prepare these mortar mixes, as described in Section 3.3. Similar mix design and mixing procedure were adopted as discussed in Section 3.4. However, PSD of WG1 used in this preliminary trial is presented in Figure 3.25.

The mortar mixes containing coarse glass particles having approximate mean size of 335 µm and replaced at 30%-50% by cement could not achieve the target spread and demonstrated reduced workability compared to GP. The results obtained from the flow measurements and compressive strength tests are shown in Figure 3.26. It can be observed

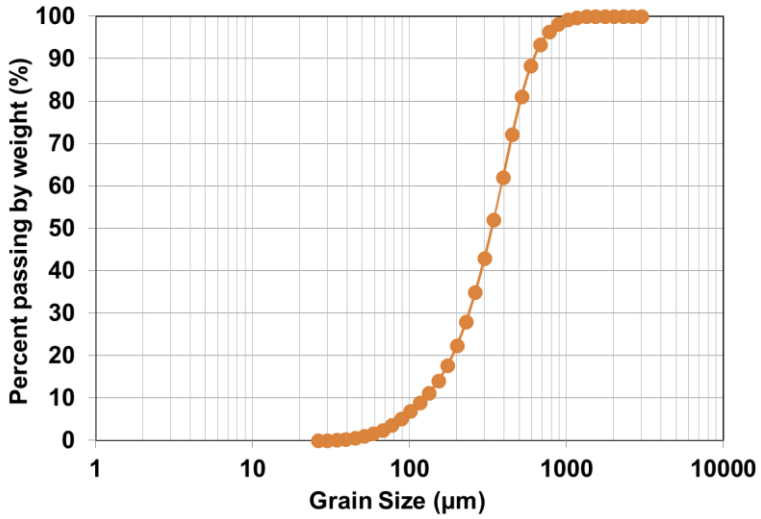

Figure 3.25: Particle size distribution of WG1

that all glass incorporated mortars, irrespective of glass replacement level, exhibited unsatisfactory strength results. However, the lower content of glass showed better workability and higher compressive strength compared to the higher glass levels in the mortar. There was a decrease of 66%-80% in 7-days compressive strengths of glass incorporated mortars in comparison to GP mortar. The strength declined by 47% and 62% at 28-days in the case of 30% and 40% replaced WG1 mortars when compared with GP mortar. Higher replacement rate (50%) of WG1 exhibited substantial decrease of 77% than GP cement at 28-days. These findings led to consider addition of glass powder at lower contents for the next trial. In addition, use of waste glass as cement replacement necessitated further reduction in particle size to achieve better strength.

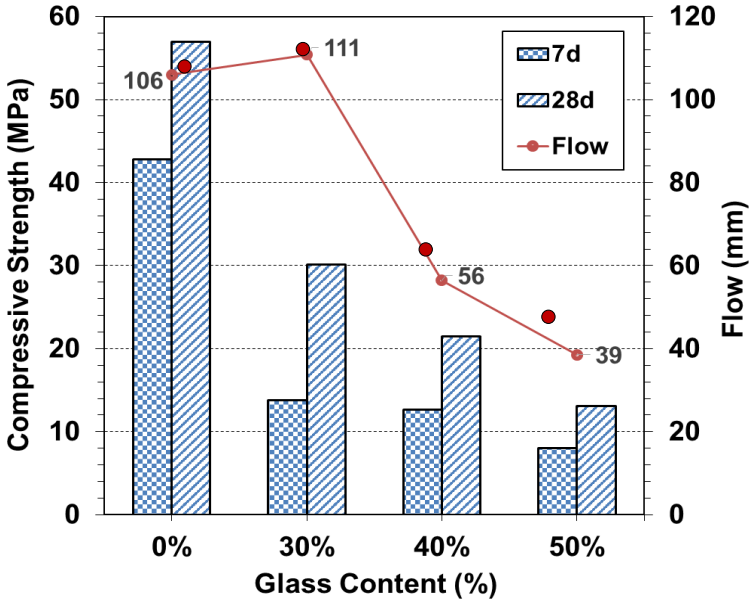

Figure 3.26: Compressive strength development of WG1 added at various replacement levels

3.6.2 Stage Two

A glass powder (WG2), for which the PSD is shown in Figure 3.27, was then utilized in this stage of trial program. Mortar cubes composed of up to 30%-50% WG2 were cast and tested for 7-days compressive strengths. All other materials and mixing procedure were consistent to that were described in Sections 3.3 and 3.4 respectively. The results completed from this early-age compressive strength testing revealed that compressive strength was much lower than GP especially at higher glass contents, though the glass particle size was considerably finer in these mortar mixes (Figure 3.28). The test results achieved in this trial motivated the researchers to assess the presence of impurities in WG2. It was postulated that the possible existence of impurities in WG2 could be the cause of decrease in compressive strength, which was later evaluated in Stage Three.

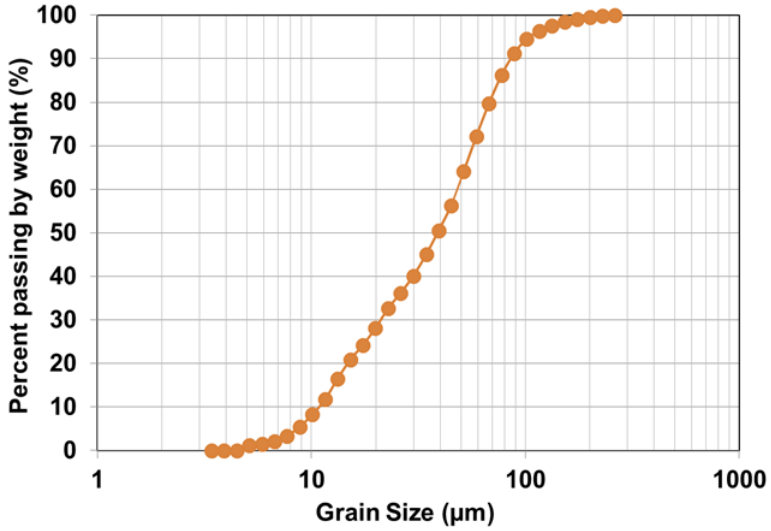

Figure 3.27: Particle size distribution of WG2

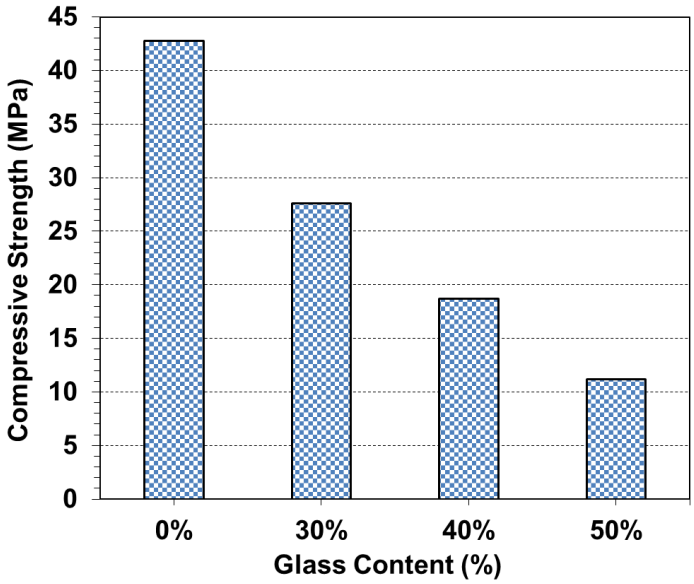

Figure 3.28: 7-days compressive strength in mortar containing WG2

3.6.3 Stage Three

The sample WG2 was tested for the presence and amount of impurities in this trial of preliminary study. AS 2758.1 specifies a maximum limit on the sugar content of aggregate of one part in 10,000 determined in accordance with AS 1141 (Section 35). The impurities can be detected by the test set out in NZS 3111 (Section 17) but it only gives an indication of their presence and not the actual amount of impurities. Hence, the chemical oxygen demand (COD) analysis of WG2 (2 gm sample dissolved in 10 ml of water) was determined, using the apparatus shown in Figure 3.29. COD is a measurement of the oxygen required to oxidize soluble and particulate organic matter. The method involves using a strong oxidizing chemical, potassium dichromate $Cr_2O_7^{2-}$, to oxidize the organic matter in solution to carbon dioxide and water under acidic conditions. The sample is digested for approximately 2 hours at 150°C. The amount of oxygen required is calculated from the quantity of chemical oxidant consumed, which is expressed as milligrams per litre (mg/L) of water. Higher COD levels mean a greater amount of oxidizable organic material in the sample, which will reduce dissolved oxygen (DO) levels (Realtech, 2015). The test undertaken on glass powder revealed that WG2 had a very high COD level of 1570 mg/L. The results obtained from this test are shown in Table 3.9.

Figure 3.29: Set-up to determine chemical oxygen demand

3.6.4 Stage Four

Since a good concrete cannot be produced with bad ingredients, the requirement for cleaning the glass to achieve best performance was evident. Hence, the presence of impurities in WG2 necessitated washing the material before utilization in mixes. To achieve this, elimination of organic impurities was undertaken through the use of chemicals and hence, the chemically cleaned glass (CWG) was obtained. However, since the focus of this research program was to utilize high volume of glass powder to produce cost-effective and sustainable concrete, it was unlikely to achieve this objective if glass had to be chemically washed before utilization. Considering this, the glass was also washed manually to evaluate the difference between the effectiveness of both cleaning procedures. Small quantities of

glass powder (MWG) were cleaned at a time, using tap water coming at high pressure, after sufficient number of washes. A considerably thick layer of impurities was observed on the top of MWG while washing, which reduced with the increasing number of washes. Some material from this top layer (SWG) was stored for further investigations. The MWG was dried in oven at 50°C after satisfactory number of washes and then retested for the presence of impurities. The COD test revealed that there was not a considerable difference in COD levels, listed in Table 3.9, after chemically and manually washing of glass powder. The COD level shown by CWG was 180 mg/L, whereas MWG had COD level of 178 mg/L. This result suggested utilizing MWG in next stage of study, instead of cleaning the glass with chemicals.

Table 3.9: COD levels of different types of glass powder

Glass Type	COD (mg/L)
WG2	1570
CWG	180
MWG	178

3.6.5 Stage Five

Another set of mortar cubes was prepared, using unwashed glass powder (WG2 or UWG), manually washed glass powder (MWG) and with the impurities left over from washing the glass powder (SWG) at a 30% replacement level in all three cases. The results obtained from compressive strength tests showed that SWG incorporated specimens reduced the performance of mortar mix considerably. The SWG mortar cubes crushed soon after any load was applied for compressive strength testing and hence, no data could be recorded. Additionally, 30% UWG showed approximately 22%-28% lower compressive strength compared to 30% MWG at 7-days and 28-days. The results also revealed satisfactory compressive strength development in MWG in comparison to GP. All these results will be discussed in Chapter 5, in detail.

3.7 Conclusion

It is essential to evaluate the characteristics of the constituent materials before casting a mortar or concrete mix. The purpose of mix design is to proportion the materials in such a way that the fresh and hardened properties of the concrete satisfy the engineering design and construction requirements. These materials should preferably be locally available in order to avoid unnecessary transportation costs. The sequence of performing tests on fresh SCC is designed to complete tests quickly; thus, minimizing any change in the properties of the SCC with time before casting. Hardened tests on SCC, such as strength tests and non-destructive tests, are applied to SCC in order to establish the relationships between strength and non-destructive test results for SCC's practical use. All such parameters were

considered in the present study prior to performing material characterization and small scale trial mix tests from which various lessons were learnt.

The lessons learnt from the material characterization and small scale tests suggested that a proper control on accuracy of tests is necessary and therefore, the selection of acceptance range of variation in results should be according to the standards. Furthermore, a single measurement in an experimental test is not reliable. Therefore, multiple readings were taken to reach the final numerical value or a definite conclusion. Small-scale trials give a valuable indication of the potential performance of the mixes when they will be used in large-scale trials and practical applications. In the present study, the preliminary trials gave an accurate evidence of the influence of particle size, replacement level and quality of glass powder on the performance of mortar mixes. It was found that larger glass particle size and higher glass replacement level were detrimental to the compressive strength of the mortar mixes. The necessity of using clean glass powder was also learnt since the strength largely reduced due to the use of glass powder containing impurities.

The decisions regarding the large-scale mix design were made according to the learning from the material characterization and small-scale trials. As a consequence, glass powder of finer size was utilized at lower replacement levels in the large-scale SCC mixes to reduce the strength loss arising due to higher glass fineness and substitution levels. However, unwashed glass was used in addition to washed glass in the large scale SCC trials to determine the likely impact of impurities, which may be present if the glass is not washed or prepared properly prior to grinding, on the rheological, mechanical and durability properties of the concrete.

References

Alexander, M. G., Mackechnie, J.R., Ballim, Y. (1999a). *Guide to the use of durability indexes for achieving durability in concrete structures*, Research Monograph No. 2: Department of Civil Engineering, University of Cape Town and University of the Witwatersrand.

AS 1012.13: Determination of the drying shrinkage of concrete for samples prepared in the field or in the laboratory.

AS 1141: Methods for sampling and testing aggregates Standards Australia.

AS 2758.1: Australian Standard - Aggregates and rock for engineering purposes.

ASTM C109: Standard Test Method for Compressive Strength of Hydraulic Cement Mortars (Using 2-in. or [50-mm] Cube Specimens).

ASTM C1362: Standard Test Method for Flow of Freshly Mixed Hydraulic-Cement Concrete.

ASTM C143: Standard Test Method for Slump of Hydraulic-Cement Concrete.

ASTM C1437: Standard Test Method for Flow of Hydraulic Cement Mortar.

ASTM C1556: Standard Test Method for Determining the Apparent Chloride Diffusion Coefficient of Cementitious Mixtures by Bulk Diffusion.

ASTM C1611: Standard Test Method for Slump Flow of Self-Consolidating Concrete.

ASTM C1749: Measurement of the Rheological Properties of Hydraulic Cementious Paste Using a Rotational Rheometer.

ASTM C1758: Standard Practice for Fabricating Test Specimens with Self-Consolidating Concrete.

ASTM C192: Standard Practice for Making and Curing Concrete Test Specimens in the Laboratory.

ASTM C230: Standard Specification for Flow Table for Use in Tests of Hydraulic Cement.

ASTM C39: Standard Test Method for Compressive Strength of Cylindrical Concrete Specimens.

ASTM C469: Standard Test Method for Static Modulus of Elasticity and Poisson's Ratio of Concrete in Compression Static Modulus of Elasticity.

ASTM C494: Standard Specification for Chemical Admixtures of Concrete.

ASTM C496: Standard Test Method for Splitting Tensile Strength of Cylindrical Concrete Specimens.

ASTM C642: Standard Test Method for Density, Absorption, and Voids in Hardened Concrete.

Ballim, Y. (1991). “A low cost falling head permeameter for measuring concrete gas permeability.” *Concrete Beton*, 61, 13-18.

Brady, J. B., and Boardman, S. J. (1995). “Introducing Mineralogy Students to X-ray Diffraction through Optical Diffraction Experiments Using Lasers.” *Jour. Geol. Education,* 43(5), 471-476.

Center for Applied Energy Research (CAER). (2016). “Evaluating Fly Ash for Mortar.” <http://www.caer.uky.edu/kyasheducation/index.html> (May 26, 2016).

ConTec 2003. The ConTec BML Viscometer, Viscometer 4&5, Operating Manual. In: LTD, C. (Ed. Laugarvegi, and Reykjavik), Iceland.

Controls Group. (2016). “Drying shrinkage prism mould (50x50x200 mm).” <http://www.controls-group.com/eng/aggregates-testing-equipment/drying-shrinkage-prism-mould-50x50x200-mm.php> (May 26, 2016).

Elwell, D. J., and Fu, G. (1995). *Compression testing of concrete: cylinders vs. cubes*. Report FHWA/ NY/SR-95/119, Special Report 119. Transportation Research and Development Bureau New York State Department of Transportation.

FIB Model Code for Concrete Structures. (1990). CEB Bulletin No. 213/214. Switzerland.

Jin, J. (2002). *Properties of mortar for self-compacting concrete.* University College London.

Khayat, K., and Mitchell, D. (2009). *Self-Consolidating Concrete for Precast, Prestressed Concrete Bridge Elements,* NCHRP Report 628, National Cooperative Highway Research Program, 99.

Koehler, E. P. (2009). “Use of Rheology to Specify, Design and Manage Self-Consolidating Concrete.” *Proc., Tenth ACI International Symposium on Recent Advances in Concrete Technology and Sustainability Issues,* Spain.

NZS3111:1986. New Zealand standard. Methods of test for water and aggregate for concrete.

RealTech. (2015). “Chemical Oxygen Demand (COD)” <http://realtechwater.com/chemical-oxygen-demand/> (May 26, 2016).

Smith, I. (2005). “Geology, Rocks and Minerals.” <flexiblelearning.auckland.ac.nz/rocks_minerals/rocks/greywacks.html> (May 26, 2016).

The Concrete Portal. (n.d.) “Performance based design for durability.” <http://www.theconcreteportal.com/perf_spec.html> (May 26, 2016).

Thornton, J. (2003). *Field Guide to New Zealand Geology*, Reed Publishing, Auckland.

Vandegrift, J. D., and Schindler, A. K. (2006). *The effect of test cylinder size on the compressive strength of sulphur capped concrete specimens.* Highway Research Center and Department of Civil Engineering at Auburn University, 83.

Wriedt, T. (2012). *The Mie Theory, Chapter 2, Mie Theory: A Review*, (Ed. Hergert, W., and Wriedt, T.), Springer, Germany, 53-71.

CHAPTER 4

INFLUENCE OF SUPERPLASTICIZER DOSAGES ON RHEOLOGY, AND EARLY AGE STRENGTH AND DURABILITY OF SELF-COMPACTING CONCRETE CONTAINING GLASS POWDER

Tariq, S. A., Scott, A. N., Mackechnie, J. R. (2016). “Controlling fresh properties of self-compacting concrete containing waste glass powder and its influence on strength and permeability.” *Proc., Fourth International Conference on Sustainable Construction Materials and Technologies (SCMT4)*, Las Vegas, United States.

ACRONYMS USED

GP	GP cement control mix
FAF30%	Mix containing class F fly ash replaced by 30% of GP cement
FAC30%	Mix containing class C fly ash replaced by 30% of GP cement
20UG30%	Mix containing 20 microns unwashed glass powder replaced by 30% of GP cement
10G30%	Mix containing 10 microns glass powder replaced by 30% of GP cement
20G20%	Mix containing 20 microns glass powder replaced by 20% of GP cement
20G30%	Mix containing 20 microns glass powder replaced by 30% of GP cement
20G40%	Mix containing 20 microns glass powder replaced by 30% of GP cement
40G30%	Mix containing 20 microns glass powder replaced by 30% of GP cement
SF1	SCC mixes having flow below 500 mm
SF2	SCC mixes having flow within the range of 660-750 mm
SF3	SCC mixes having flow above 790 mm
CTR	All materials class: GP, class F and C fly ashes and glass powder/Control materials class: GP, class F and C fly ashes
GL-FN	Glass powder classified according to fineness: having fineness of 10 µm, 20 µm and 40 µm; added at 30%
GL-CN	Glass powder classified according to content: added at 20%, 30% and 40%; having fineness of 20 µm

HIGHLIGHTS

- Discussion on the influence of superplasticizer dosage on flowability and flow rate of SCC containing different glass sizes and contents.
- Analysis of the effects of superplasticizer dosage, glass particle size and replacement level on plastic viscosity and yield stress of SCC.
- Investigation of the influence on compressive strength of SCC produced with different superplasticizer dosages and glass powder of various finenesses and replacement levels.
- Assessment of the effects of superplasticizer dosage on oxygen permeability, porosity and electrical resistivity of SCC incorporating glass powder of various sizes and contents.
- Evaluation of the performance of various glass sizes and contents included in SCC compared to the behaviour demonstrated by GP cement and fly ashes.

4.1 Introduction

Self-compacting concrete (SCC) has the ability to consolidate itself under the action of gravity and fill the formwork to a uniform level without segregation (Ashtiani et al., 2013). It is represented by a low yield stress, high deformability, and moderate viscosity, which are essential to ensure uniform suspension of solid particles during transportation and placement without vibration, and continue afterwards until the concrete sets (Aghabaglou et al., 2013). Segregation resistance has an essential role in SCC performance because weak segregation resistance would result in poor deformability, blockage around congested reinforcement and non-homogeneous characteristics of the hardened concrete. The improved cohesion in SCC compared to conventional concrete provides a better suspension of solid particles in fresh concrete and therefore, better deformability and filling capability during the spreading of fresh concrete (Esfahani et al., 2008; Okamura and Ozawa, 1995; Ozawa et al., 1995).

Properties of SCC depend on type and amount of additives, which are used for its production (Ali and Al-Tersawy, 2012). It is generally essential for SCC to use superplasticizer (SP) so as to achieve high mobility (Liu, 2011). The inclusion of high volumes of cement powder, along with supplementary cementitious materials (SCMs), binder and/or filler, increases the volume of the paste, which possibly leads to an increase in deformability, cohesiveness of the paste and stability of the SCC (Girish et al., 2010; Ioannis et al., 2014). In addition, the gradations of individual binding materials within the grading curve also influence the characteristics of SCC. Therefore, high flowability and mix stability

of SCC are determined primarily by the interactions between the powder, water, and SP as they influence both fresh and hardened properties of SCC mixtures (Kordts and Dusseldorf, 2003; Sahmaran et al., 2006; Felekoglu and Sarıkahya, 2008).

The key to obtaining higher workability in concrete is increasing the cement content, which also increases the water content thus improving the fluidity of concrete. However, this creates difficulties in the field for the given set of conditions because extra water is used, which in turn affects the strength and durability of concrete. In such cases, SP is an effective solution for reducing the water requirement, while still producing concrete of higher workability. According to Yamakawa et al. (1990), the use of SP improves both fresh and hardened characteristics of concrete. Provided that the water cement ratio (w/c) is maintained, an appropriate dosage of SP normally reduces the tendency of bleeding and prolongs the setting time of concrete. Although SP works to impart a higher level of flowability and deformability when compared to regular concrete, it can lead to a high degree of segregation at higher dosage levels in SCC. However, when only an SP is used, SCC tends to segregate due to the loss in plastic viscosity of the concrete and the fact that materials having different specific gravities reside within the mixture (Okamura and Ouchi, 2003).

Measuring rheology is an ideal way of determining concrete behaviour as it permits comprehensive analysis of the elastic and viscous properties of freshly made concrete (Plog, 2015). In order to determine the fresh behaviour of SCC, two elements, yield stress and plastic viscosity, have to be investigated as they present both the initial and ongoing resistance of the mix to flow (Ferraris, 2000). Generally, the increase in fine-ground material content in cement creates changes in the rheological properties of pastes and hence, influences the workability of concrete. These modifications may or may not be beneficial depending on many factors influencing the rheology of pastes (Grzeszczyk and Lipowski, 1997). Good correlations between rheological properties and filling ability of concrete can be established by performing rheological tests with a viscometer to determine the powder composition and estimate the SP dosage (Petersson et al., 1996) before utilizing concrete for construction works. However, it is usually necessary to provide a very large number of individual mixes with substantially the same workability properties on the building site for a cast-in-place concrete component. An influencing factor, apart from the sharply fluctuating weather conditions, is the fact that the concrete already present in the component may not have the same workability properties as the newly delivered concrete. Discrepancies in the supply can have worse consequences and can ultimately affect the hardened properties of concrete due to the variations in workability of individual mixes, poor productivity, and other problems. This means that overdosing or underdosing of admixtures, leading to variations in

workability, in real concrete construction can be a big problem in the long term that needs to be addressed. Hence, the investigations of the effects of SP dosages on rheology, strength and durability of concrete were selected in the present study.

The literature indicates that either the effects of the SP variations on rheological behaviour and hardened properties have not been completely investigated or have not been sufficiently reported. The researchers have generally focussed only on the workability tests and negligible attention has been given to the rheological measurements. In addition, some researchers have reported the improvement in workability and strength (Batayneh et al., 2006; Sobolev et al., 2007; Matos and Sousa-Coutinho, 2012; Nassar and Soroushian, 2012) and others have demonstrated the contradictory results (Shao et al., 2000; Park et al., 2004; Metwally, 2007; Du and Tan, 2013). There is not sufficient information on the rheology, strength, and durability of SCC incorporating glass powder with the variability in SP dosages, which may occur at the production site. This lack of information led the researchers to investigate the influence of SP on the rheology, strength, and durability of glass modified SCC, in the scope of the research program.

The main objective of this study was to investigate the influence of small deviations in the SP dosages on the flow characteristics, viscosity, shear behaviour, strength and durability of SCC utilizing glass contents of 20%, 30% and 40% and glass finenesses of 10 µm, 20 µm and 40 µm as partial replacements for cement. All the findings from these tests, depending on the replacement levels and finenesses of glass powder and their comparison with other binding materials, are presented and discussed in this chapter. As outlined in Chapter 3, glass size ranges of 10-40 µm and replacement levels of 20%-40% of cement by weight were selected, while the aggregate proportions, water to binder ratio (w/b) and stabilizer (SB) were maintained as constants. The types of SP and SB were also kept the same in all SCC mixes. However, the amount of SP was varied to achieve different slump flows for each type of SCC mix. Based on the slump flow, each SCC mix type was further categorized into three classes: SF1 (SCC mixes having flow below 500 mm), SF2 (SCC mixes having flow within the range of 660-750 mm) and SF3 (SCC mixes having flow above 790 mm). Figure 4.1 illustrates the examples of these pre-specified flow categories targeted in this study.

To start with, materials were dry mixed for about a minute before water and SB were introduced. Another couple of minutes were allowed for mixing. SP was incrementally added in different dosages to achieve the desired range of flows. Mixing time was accurately monitored because initial mixing time is more critical for polycarboxylate-based admixtures due to their dispersing mechanism and in order to sustain equilibrium viscosity, longer mixing times are required. Optimum mixing time and order were examined during pre-tests,

(a) SF1 **(b) SF2** **(c) SF3**

Figure 4.1: Flow range categories according to flow measurement (a) SF1 (b) SF2 (c) SF3

which showed that the total mixing time of 5 minutes was sufficient. Hence, the concrete was mixed for at least 5 minutes before undertaking flow tests. The slump flow, slump flow time, visual stability index and rheology measurements were taken within 2 minutes after mixing was completed. Once the rheological behaviour was assessed, representative samples from each mix were poured into cylinders and kept in the curing room for compressive strength, coefficient of permeability, porosity and electrical resistivity tests at the ages of 7, 28 and 90 days. All mixing and casting were done in Civil Engineering Laboratories on the campus of University of Canterbury, New Zealand. The mixing and testing were carried out at room temperature, normally between 18°C and 23°C. All materials, tests, mixing and experimental procedure have already been described in Chapter 3. However, the complete set of performed tests and references for their results in this chapter, are summarized in Table 4.1.

Table 4.1: Tests on SCC and references to their results

TESTS	AIMS	AM/CTR [1]	GL-FN [2]	GL-CN[3]
Slump flow and flow time (T_{500}) on fresh SCC	To assess the influence of superplasticizer dosage and binders on the flowability and flow rate of SCC	Figs. 4.1, 4.2, 4.3 Tab. 4.2	Fig. 4.4	Figs. 4.5. 4.6
Rheology measurements on fresh SCC	To assess the influence of superplasticizer dosage and binders on plastic viscosity and yield stress of SCC	Figs. 4.8, 4.18, 4.19	Figs. 4.9, 4.10, 4.11, 4.12	Figs. 4.13, 4.14, 4.15, 4.16, 4.17
Compressive strength tests on hardened SCC	To assess the influence of superplasticizer dosage and binders on compressive strength of SCC	Fig. 4.20 Tab. 4.3	Fig. 4.21	Fig. 4.22
Durability tests on hardened SCC	To assess the influence of superplasticizer dosage and binders on oxygen permeability, porosity and resistivity of SCC	Figs. 4.23, 4.24, 4.25, 4.32, 4.33, 4.34, 4.41, 4.42, 4.43	Tab. 4.4, Figs. 4.26, 4.28, 4.30, 4.35, 4.37, 4.39	Tab. 4.5 Figs. 4.27, 4.29, 4.31, 4.36, 4.38, 4.40

[1] All materials class: GP, class F and C fly ashes and glass powder/Control materials class: GP, class F and C fly ashes
[2] Glass powder classified according to fineness: having fineness of 10 µm, 20 µm and 40 µm; added at 30%
[3] Glass powder classified according to content: added at 20%, 30% and 40%; having fineness of 20 µm

4.2 Influence of superplasticizer dosage on Slump Flow, Flow Time and Visual Stability Index

The slump flow and flow time (T_{500}) are the tests to analyze the flowability and flow rate of SCC in the absence of hindrances. Slump flow provides an indication of the filling ability of SCC and T_{500} is a measure of the speed of flow to reach 500 mm indicating the viscosity of SCC mix. The visual stability index is a visual evaluation of the segregation of the SCC during the slump flow test. Visual stability index gives an evidence of the stability of the mix based on the presence of segregation, mortar halo, aggregate pile, and/or bleeding. Visual stability index values range from 0 (highly stable) to 3 (unacceptable stability). As described in the previous section, the amount of SP was adjusted to achieve different slump flows for each type of SCC mix and each SCC mix type was further categorized into three classes depending on the slump flows including SF1 (having slump flow below 500 mm), SF2 (having slump flow within the range of 660-750 mm) and SF3 (having slump flow above 790 mm). Figure 4.2 illustrates the comparison between the fresh behaviour of control (CTR) mixes and glass mixes categorized in GL-FN and GL-CN classes in terms of SP dosages (calculated as a percentage of binders) and T_{500}. Figure 4.3 shows the variation of flow time with increasing SP dosages for each mix. Table 4.2 lists the visual stability index rating of each SCC type based on the visual observation. It can be seen that for GP mix without any addition of mineral admixture, the SP dosage of 0.62% successfully produced the target SF2 mix whereas, there was an additional SP requirement of approximately 29% to achieve SF3 mix.

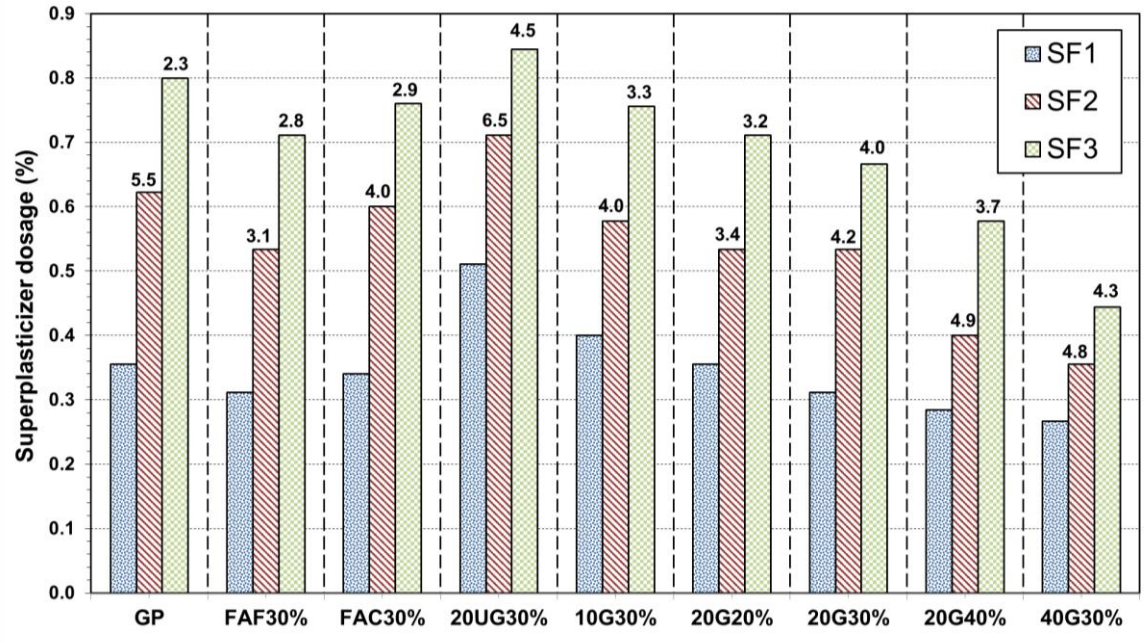

Figure 4.2: Superplasticizer demand of all SCC mixes to achieve different flows and T_{500} labelled above SF2 and SF3 bars

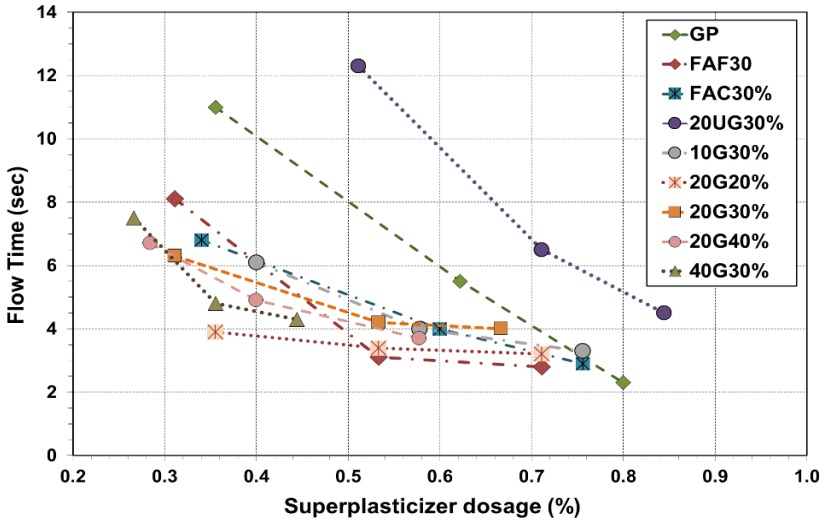

Figure 4.3: Relationship between superplasticizer dosage and flow time for all SCC mixes

Table 4.2: Visual stability indexes of all SCC types

VISUAL STABILITY INDEX			
MIX TYPE	**SF1**	**SF2**	**SF3**
GP	0	0	3
FAF30%	0	0	2
FAC30%	0	1	3
20UG30%	0	1	3
10G30%	0	0	2
20G20%	0	0	2
20G30%	0	0	2
20G40%	0	0-1	2
40G30%	0	0-1	2

In general, the spherical shape of fly ash (FA) particles increases the workability of concrete, while reducing water demand. At any given slump flow, FA concrete flows and consolidates better than GP cement concrete thus improving cohesiveness and filling ability (The Concrete Society and BRE, 2005) and reducing segregation of concrete. Moreover, Thomas (2007) indicated that FA with high levels of carbon generally produces a smaller reduction in water demand. Similar behaviour was noticed in this study as the SP requirement to produce SF2 mixes incorporating FAs was reduced by 4%-14% in comparison to SF2 mix of GP concrete. The reduction in SP demand of mixes incorporating FA has been similarly mentioned by Dumne (2014). In addition, FAF30% showed the least requirement of SP to achieve same flow range as compared to other CTR mixes. This might be attributed to the fact that class F FA holds better workability characteristics in comparison to GP and class C FA. Hence, FAF30% exhibited the reductions of 12%, 14% and 11% in SP demand for SF1, SF2 and SF3 mixes respectively, in contrast to GP mix. This result confirms a gross approximation reported by Thomas (2007) that each 10% of FA replaced by GP cement should allow a water reduction of at least 3%.

While undertaking the experimental tests, some preliminary effects of SP addition related to slump flow losses were also noticed. In an initial trial, SF3 mix of FAC30% showed a different trend as the mix reached the state of being overflow at a lower SP dosage than the amount it required to reach the optimum flow range (SF2). This unexpected behaviour was attributed to the sudden addition of SP in the mix instead of incremental dosages. By adding all the required SP quite in the start of mixing did not give SF3 mix (FAC30%) the chance to lose slump with time as compared to SF2 mix (FAC30%) where SP was added slowly with time, which also indicates the significance of incremental dosage inputs. It was also observed that after adding SP in the mix, T_{500} increased and the slump flow diameter decreased with the passage of time. This validates previously published theory that there is a chance of slump loss with time after SP is incorporated in the mix because the setting of concrete reduces its fluidity and hence, slump flow decreases (Alsadey, 2015).

Figure 4.4 demonstrates the effects of glass finenesses on SP dosages added to achieve different flow ranges. In this study, various types of SCC mixes were produced with coarser to finer range of glass powders to investigate the changes in their SP demands with variations in particle sizes. It was found that glass performance was more related to the fineness than the other factors, such as particle shape and composition (Byars et al., 2004). The SP demand of SCC incorporating glass dropped as the glass particle size became coarser. It has already been established that when mineral admixtures are used in SCC, they can reduce the amount of high-range admixture, which is essential to achieve the fluidity, but its requirements depend on their particle size, shape and surface characteristics

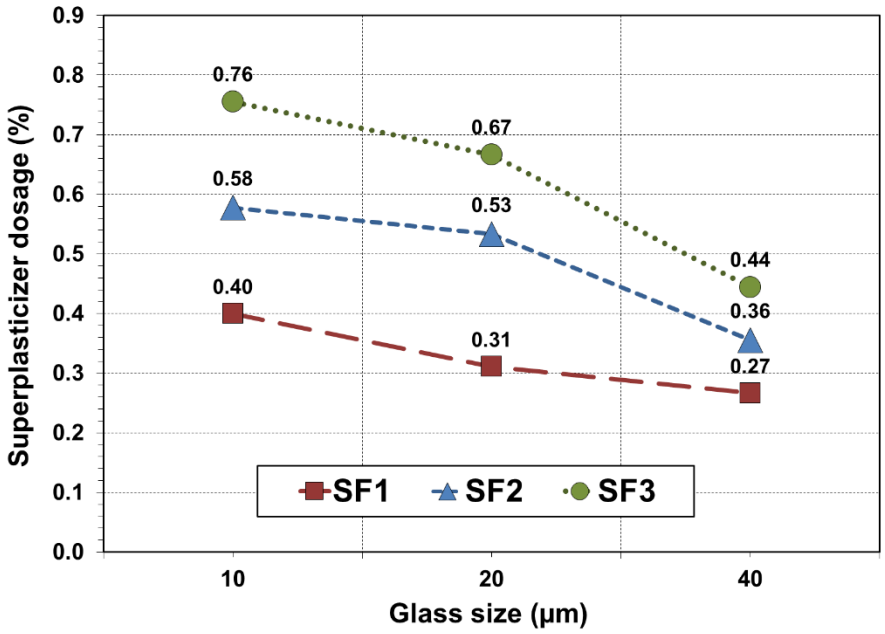

Figure 4.4: Effects of glass fineness added at 30% replacement rate on superplasticizer demand

(Ramanathan et al., 2013). It was also observed that the finer glass incorporated SCC mix required a larger dosage of SP to achieve each level of slump flow in order to compensate for its increased water demand. This implies that since these glass grains were the finest, they had higher surface area, which in turn required more water to achieve the same flowability than the coarser glass powders. Another observation during mixing was that 10G30% was unable to be properly mixed in the mixer until a small dosage of SP was added to achieve uniform mixing. In addition, the slump test could not be done even at 0.2% addition of SP in 10G30%, which indicates higher SP demand of 10G30% to be sufficiently workable. Felekoglu (2008) similarly mentioned that the coagulation of very fine particles less than 20 µm requires high SP dosage to disperse them. There was a reduction of 22% from 10G30% to 20G30% and 14% from 20G30% to 40G30% in SP dosages of SF1 mixes due to variations between fineness of glass particles, which can be related to the same reason mentioned before. These results are consistent to Habeeb and Fayyadh (2009) and Khan et al. (2014) that the finer mineral admixture requires increased SP content to maintain the desired workability. In addition, SF2 mixes demonstrated reduction of 8%-39% in SP requirements for 20 and 40 µm glass sizes than 10 µm glass. As anticipated, SF3 mixes demanded maximum amount of SP in comparison to SF1 and SF2 mixes, ranging from 0.4% to 0.8%, with the lower value required by 40G30%. Compared to GP, 10G30% required 6%-8% lower SP to achieve the flow ranges SF2 and SF3 whereas, for SF1, the situation was found to be reversed. Furthermore, a significant decrease of 33%, 75% and 80% in SP requirement was noticed in SF1, SF2, and SF3 of 40G30% respectively, compared to GP. From GL-FN class, 40G30% took the longest time of 4.3 sec to reach 500 mm target for SF3, which reflects its higher viscosity due to the lower quantities of SP as compared to other glass mixes. However, mix containing the finest glass (10G30%) exhibited the least amount of time to satisfy the requirement of T_{500} in all flow types. The time required to reach 500 mm was 20% shorter in 10G30% compared to 40G30% to achieve SF2 flow class.

Figure 4.5 shows the influence of glass content on the requirement of SP dosage to produce SCCs of different flow ranges. Various replacement levels of glass powders were utilized in SCC so as to study the variations in the fresh behavior of glass powder with differences in glass contents and SP levels. It was observed that the requirement of SP varied inversely with the percentage of glass powder content. The requirement of lower SP level at higher glass replacement ratios could also be due to the higher compactness of concrete granular skeleton. In addition, slump flow was found to slightly increase at the same SP level but with more glass powder, which can be ascribed to lower water absorption of glass as well as reduction in deformability of the mix. There were reductions of 14% and 9% in SP demand of

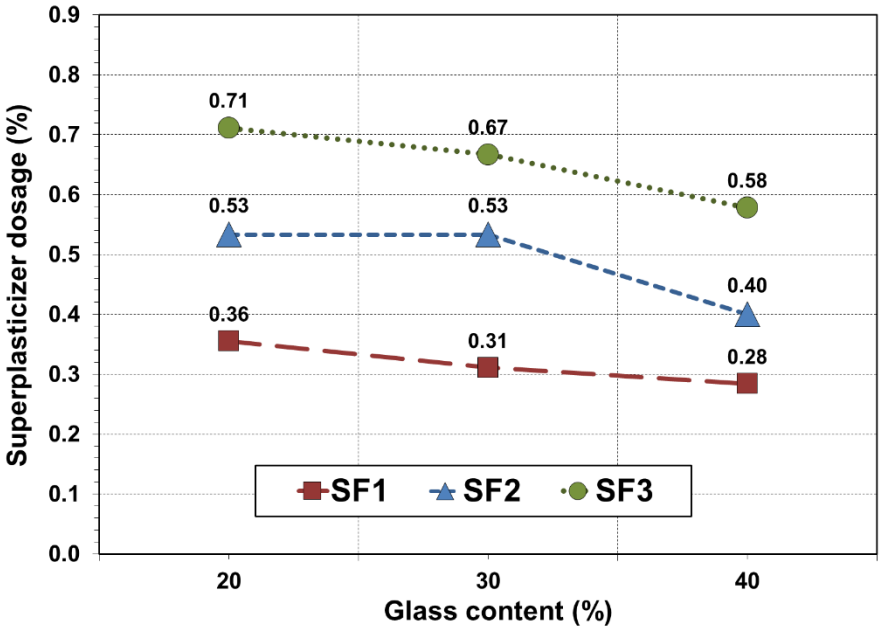

Figure 4.5: Effects of glass content having fineness of 20 µm on superplasticizer demand

SF1, from 20% to 30% and 30% to 40% glass replacements, respectively. Similarly, compared to 20% replacement, the SP dosage in SF3 was found to decrease by an average of 7% and 23% for glass powder replacements of 30% and 40% respectively. These results are consistent to those reported by Ali and Al-Tersawy (2012) that the slump flow of recycled glass SCC mixes increases directly with the recycled glass content, which implies that there is lesser SP requirement for higher glass ratios. Moreover, SP reduction of 13%- 56% was noticed in SF2 mix types of GL-CN class compared to SF2 mixes of GP and FAC30%. The T_{500} was observed to mostly increase with the increase in glass replacement level. This suggests that 20G20% was the most flowable mix as compared to 20G30% and 20G40%. It was observed that 20G40% exhibited the maximum variation in T_{500} values between different flow range classes.

An aspect to notice is that the rate of slump loss in 20G20% and 20G30% mixes was slower within some time after mixing but the reverse was observed in 20G40%, possibly due to the lower water absorption of the glass present in a larger proportion in that mix. Ravindrarajah et al. (2004) also concluded that an appropriate dosage of SP is capable of maintaining workability of a mix. In their study, the slump flow losses were found to be 60 mm and 180 mm after 15 minutes for lower and higher SP dosages respectively and from 15 to 60 minutes, respective flow losses were 140 mm and 120 mm respectively. Generally, T_{500} decreases with an increase in SP dosage until it reaches a certain point called the saturation point, after which it remains nearly constant or shows a slight increase. However, this study was limited to a specific SP amount at which mix could become overflow and saturation points of all the mixes were not observed. From the limited data available, it can be

postulated that 10G30% would demonstrate its saturation point at higher SP dosage in comparison to 20G30% and 40G30%. However, the saturation points for 20G20% and 20G30% could be at approximately similar SP dosages.

Figure 4.6 demonstrates the influence of unwashed glass powder on the requirement of SP dosage to produce SCCs of different flow ranges in comparison to the effect of washed glass powder of the similar fineness and content in SCC. 20UG30% mix was found to be too stiff at zero SP level and hence, slump test could not be undertaken for the mix containing no SP. This implies that unwashed glass powder has significantly higher SP demand than GP, FAs, and other glass mixes to wet the paste that is required to coat and lubricate the mix. The requirement of SP to achieve three target mixes in 20UG30% was approximately 31%-44%, 25%-44% and 16%-32% higher than SF1, SF2 and SF3 mixes of GL-CN class respectively. This can be related to the presence of impurities and organic content in the unwashed glass that increased its SP demand to achieve these flow ranges. Organic compounds in unwashed glass might also have influenced the performance and efficiency of the admixture. Hence, the dosage of SP had to be increased when used with unwashed glass powder containing high concentrations of organic compounds.

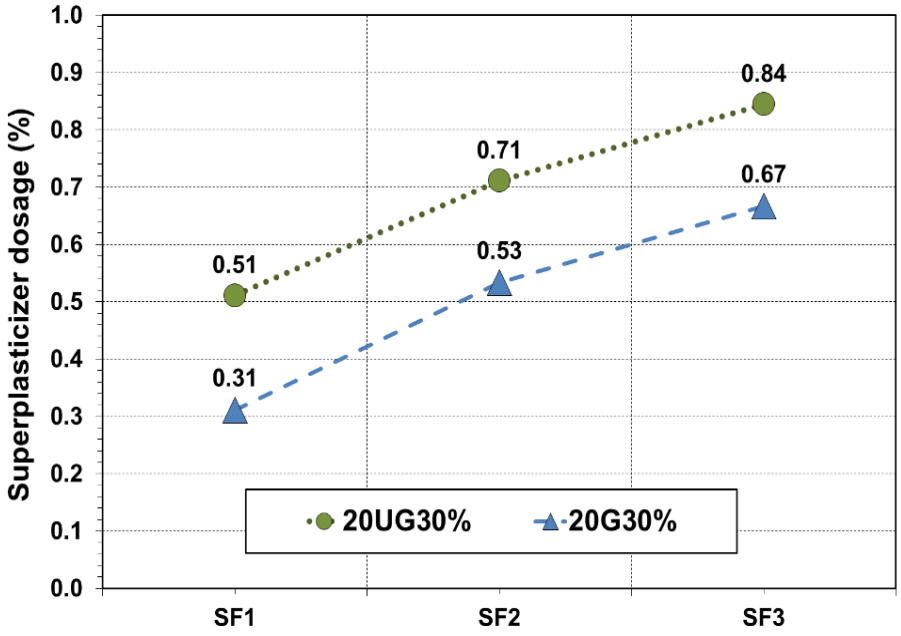

Figure 4.6: Effects of unwashed glass powder (having fineness of 20 µm and replaced by 30%) on superplasticizer demand compared to washed glass powder (having fineness of 20 µm and replaced by 30%)

All the results that have been discussed in the present section have been summarized in Table 4.3. The mix description has also been added in the table to easily correlate the properties of the mix containing different sizes and replacement levels of glass powder with the requirement of SP dosage and T_{500}.

Table 4.3: The requirement of SP dosage and flow time achieved by each SCC mix type

Mix Type	Mix Description	SP dosage (%)			T_{500} (sec)	
		SF1	SF2	SF3	SF2	SF3
GP	Mix containing 100% GP cement / control mix	0.36	0.62	0.80	5.5	2.3
FAF30%	Mix containing class F fly ash replaced by 30% of GP cement	0.31	0.53	0.71	3.1	2.8
FAC30%	Mix containing class C fly ash replaced by 30% of GP cement	0.34	0.60	0.76	4.0	2.9
20UG30%	Mix containing unwashed glass powder replaced by 30% of GP cement	0.51	0.71	0.84	6.5	4.5
10G30%	Mix containing 10 micron glass powder replaced by 30% of GP cement	0.40	0.58	0.76	4.0	3.3
20G20%	Mix containing 20 micron glass powder replaced by 20% of GP cement	0.36	0.53	0.71	3.4	3.2
20G30%	Mix containing 20 micron glass powder replaced by 30% of GP cement	0.31	0.53	0.67	4.2	4.0
20G40%	Mix containing 20 micron glass powder replaced by 40% of GP cement	0.28	0.40	0.58	4.9	3.7
40G30%	Mix containing 40 micron glass powder replaced by 30% of GP cement	0.27	0.36	0.44	4.8	4.3

4.3 Influence of superplasticizer dosage on rheology

As the rheology of cementitious materials is closely related to the developing performance of concrete, it is considered one of the most important factors for good performance of concrete. From the viewpoint of rheology, a good quality SCC is represented by low yield stress, which is necessary for high capacity of deformation, and moderate viscosity, required to ensure uniform suspension of solid particles during casting. In general, cohesion and viscosity can be enhanced by reducing the free water content and increasing the concentration of fine particles, which also improves the stability of SCC. This approach of minimizing free water content to improve stability can lead to the production of SCC mix with a low yield stress and moderate-to-high viscosity levels. However, the case where water content is kept constant/lower, a relatively higher dosage of high-range water reducer is required to achieve required deformability, particularly with lower fine contents (Khayat et al., 1999). SCC generally has low yield stress, usually lesser than 60 Pa, to ensure satisfactory

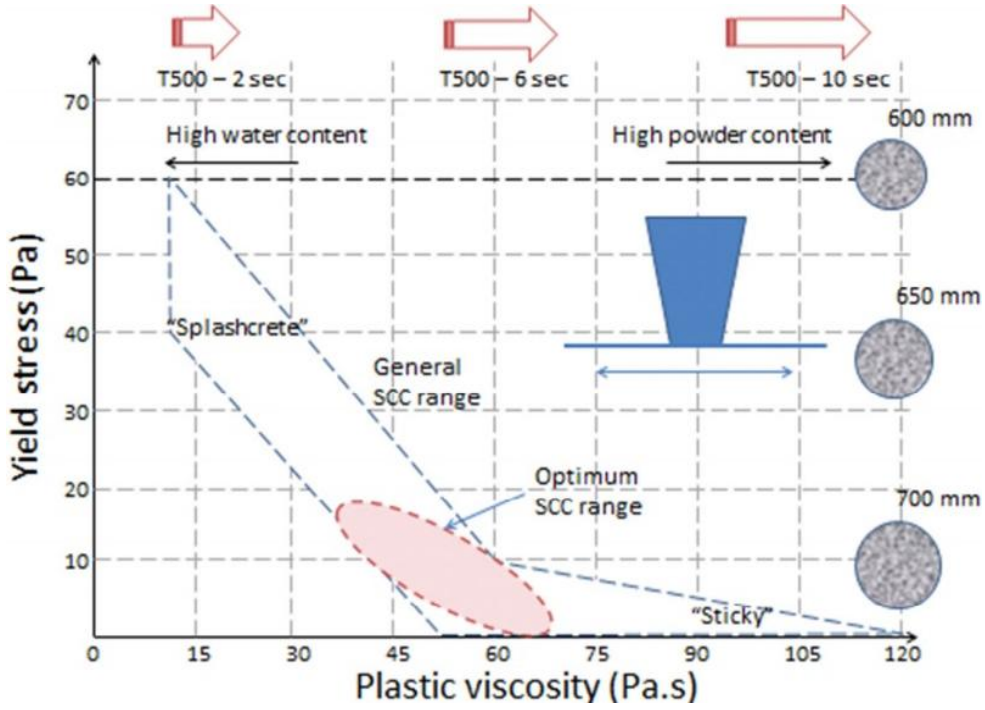

Figure 4.7: General and optimum rheological range for SCC (Mackechnie, 2013)

flowability. Plastic viscosity varies depending on the water and powder contents and yield stress varies depending on the slump flow and state of the mix structure, as shown in Figure 4.7. Low viscosity SCCs tend to have high yield stress and high viscosity SCCs are likely to have lower yield stress to provide the required flowability.

The yield stresses and plastic viscosities as function of GP cement and 30% replaced amounts of FAF and FAC for SF1 mixes (shown in Figure 4.8) and SF2 mixes were measured for comparison to the glass incorporated mixes. The rheological measurements of most of the SF3 mixes could not be done as the equipment did not support the mix and stopped working. Since overflow mixes were generally segregated, the aggregates settled at the bottom of the bucket and the paste separated from the mix making it difficult for the rheometer blades to move through the mix. This condition assisted in finding a disadvantage associated with using this equipment for rheological measurements that it might have been designed for relatively stiff concrete, which makes it impossible to obtain shear or velocity profiles for mixes with large slump flows. A similar observation has been described by Bartos et al. (2002) in a compendium report of tests on workability and rheology of fresh concrete.

GP concrete mix (SF1) showed the highest plastic viscosity value, which implies that this mix could be sticky and difficult to pump. SCC containing FA was found to be more cohesive, having improved pumpability and reduced bleeding. The mixes with class F FA showed lower plastic viscosities than the CTR mixes without class F FA. Compared to GP concrete, FAF30% showed 62% decrease in plastic viscosity but 26% increase in yield stress for SF1

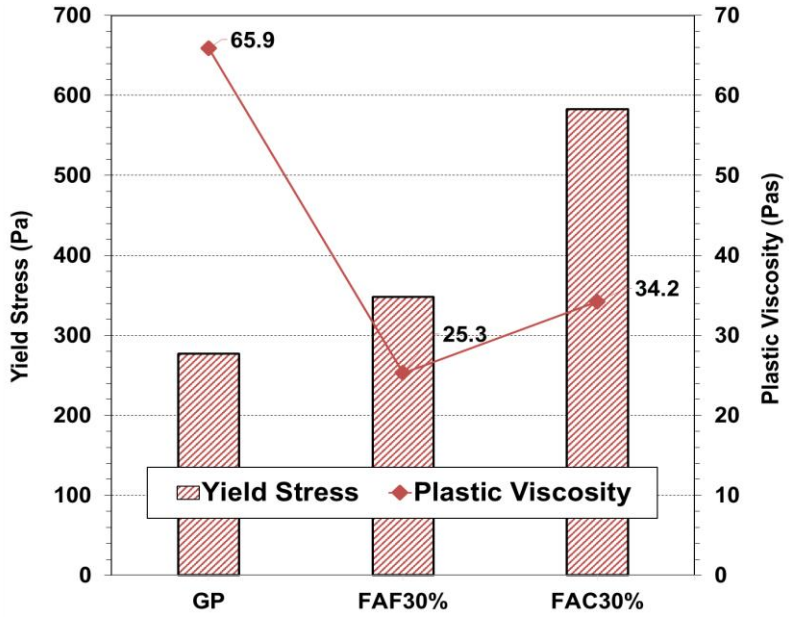

Figure 4.8: Rheological behaviour of SF1 mixes of CTR types

mix. Conversely, FAC30% showed slightly more than two-fold increase in yield stress in comparison to GP at underflow state (SF1). The higher yield stresses achieved in SF1 mixes of FAs implies that these mixes had higher resistances to initiate flows at lower SP dosages compared to GP. In SF2 mixes, however, both FA modified mixes exhibited better rheological performance. A reduction of 60% in plastic viscosity of FAF30% was found compared to GP, which can be related to its higher ball bearing effect to reduce inter-particle friction decreasing the plastic viscosity. In contrast, class C FA reduced some of these benefits, similarly mentioned by Ahari et al. (2015) and hence, there was not a significant variation in rheology behaviour of FAC30% (SF2) compared to GP. An increase of 8% in plastic viscosity was noticed in SF2 mix of FAC30%, while its plastic viscosity was found to be close to zero similar to GP. Park et al. (2004) also reported that FA incorporating mix shows higher plastic viscosity than the mix containing no FA. Additionally, it was observed that there were some variations in rheological behaviour of both FAs. Class C FA showed higher admixture demand than class F FA and increased plastic viscosity of mix whereas, class F FA reduced admixture demand compared to both GP and class C FA and decreased plastic viscosity of the mix at an optimum SP dosage. These results are consistent to those indicated by Ahari et al. (2015) and Manawadu et al. (2015). The workability enhancement in SF2 mixes incorporating FAs at an optimum SP dosage can be explained by the spherical shape of FA, which causes the particle to easily roll over one another reducing the interparticle friction, also described by Ramachandran (1995). Similar explanation has been presented by Sonebi and Bartos (1999) and Kim et al. (1996) that the spherical shape of FA minimizes the particle's surface-to-volume ratio resulting in low fluid demands thus its use provides greater cohesiveness by improving the grain-size distribution and particle packing.

It has been established that the incorporation of SCMs in concrete provides greater cohesiveness by improving the physical action, which relates to the grain-size distribution and particle packing. Moreover, their high pozzolanic activity leads to a densification of the pore structure that is achieved by the chemical action (pozzolanic products), which acts complementary to the physical action (Badogiannis et al., 2004; Cyr et al., 2006). Literature also indicates that the rheological properties of cementitious materials are governed by the interfaces between solid and water and in terms of the surface area of contact. In this study, the influence of the variations in glass particle size on the rheological behaviour of SCC was investigated. Figure 4.9 and Figure 4.10 illustrate the effects of glass size on the yield stress and plastic viscosity of SF1 and SF2 mixes, respectively. It can be noticed that the yield stress and the plastic viscosity of SCC decreased as the glass powder became finer, which suggests the influence of water-binder interface, SP dosage and particle size in this system. Evidently, the influence of particle size was a surface area effect in the fine-grained mixes and a simple volume effect in the coarser-grained mixes. For SF1 types, 10G30% demonstrated 8% and 26% lower plastic viscosities in comparison to 20G30% and 40G30% respectively. The reduction in the yield stress was found to be 87-109% in 10G30% compared to 20G30% and 40G30%. According to Banfill (2006), the yield stress of SCC ranges within 50-200 Pa and plastic viscosity lies between 20-100 Pas. The results obtained for yield stresses of SF1 mixes fall outside these ranges and hence, it can be inferred that SF1 mixes did not perform like an SCC mix in terms of rheology, potentially due to the insufficient SP dosages. The visual inspection of these mixes also led to the similar conclusion since these mixes were not sufficiently flowable as a traditional SCC mix. In SF2

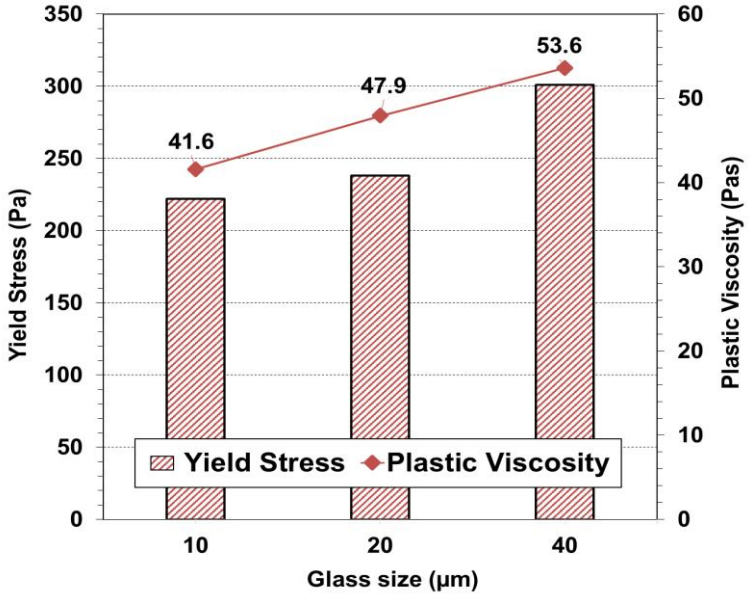

Figure 4.9: Rheological behaviour of SF1 mixes of GL-FN added at 30% replacement rate

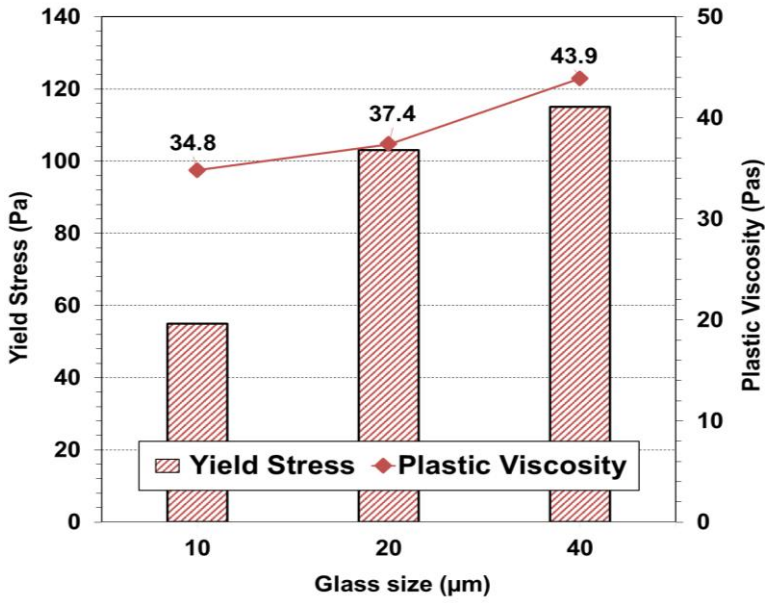

Figure 4.10: Rheological behaviour of SF2 mixes of GL-FN added at 30% replacement rate

mixes, however, the plastic viscosity drop in 10G30% increased to 15% and 29% in comparison to 20G30% and 40G30% respectively. In terms of the yield stress of SF2 mixes, 10G30% showed 25% -36% reduction compared to 20G30% and 40G30%. It is evident from the results that each SCC mix was a complex system with two variables that were varying: SP level and glass fineness. As a consequence, SP dosage was also found to affect the rheological behaviour of each mix, parallel to the fineness of the glass particles. Therefore, the lower plastic viscosity and yield stress in finer glass incorporated mix could be the combined result of higher SP level within the mix and the smaller glass particle size.

Generally, until the point where the surface area of the powder material is completely coated, the greater the dosage of SP, the greater the flowing ability of the concrete. However, there is always an upper limit of the SP, which if exceeds, there is excessive free water within the mix that can be removed from the material by normal forces, as informed by Ozawa et al. (1990) and Schober et.al. (2005). This results in a high degree of interparticle friction among the solid elements of the mix and ultimately leads to severe segregations. Similar observations were noticed in this study as very high SP dosages in SF3 glass mixes led to a considerable segregation and the rheological measurements could not be taken for those mixes. The rheological measurements before these upper limits were, therefore, studied in detail in order to completely comprehend the effects of variable glass finenesses in the SCC system at similar SP dosages, demonstrated in Figure 4.11 and Figure 4.12. It can be seen that the finer the added glass powder, the higher both measured yield stress and plastic viscosity at a constant SP dosage. This can be attributed to the fact the specific surface area of the materials increases by increasing the particle fineness for a similar mass.

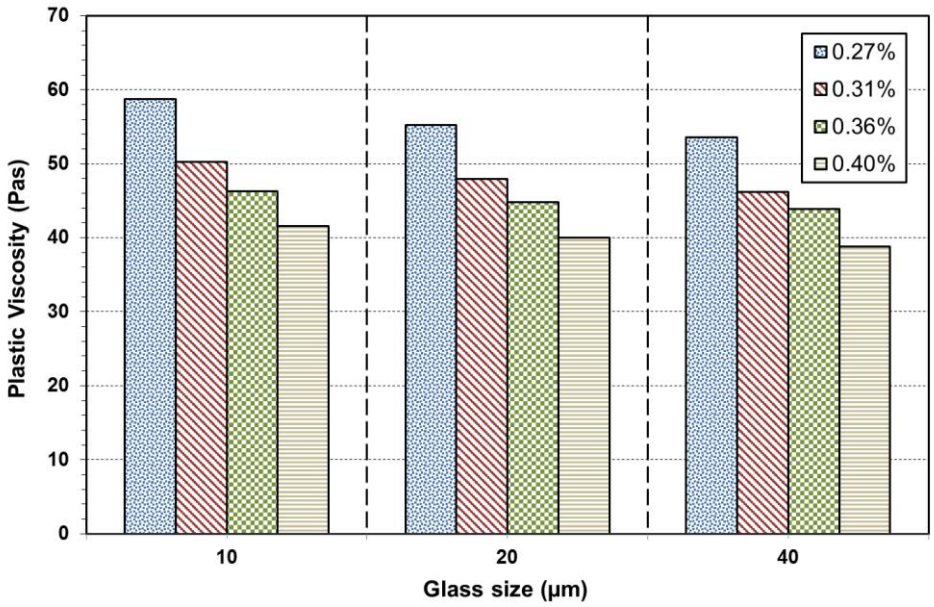

Figure 4.11: Effects of glass fineness (added at 30% rate) on plastic viscosity at various SP dosages

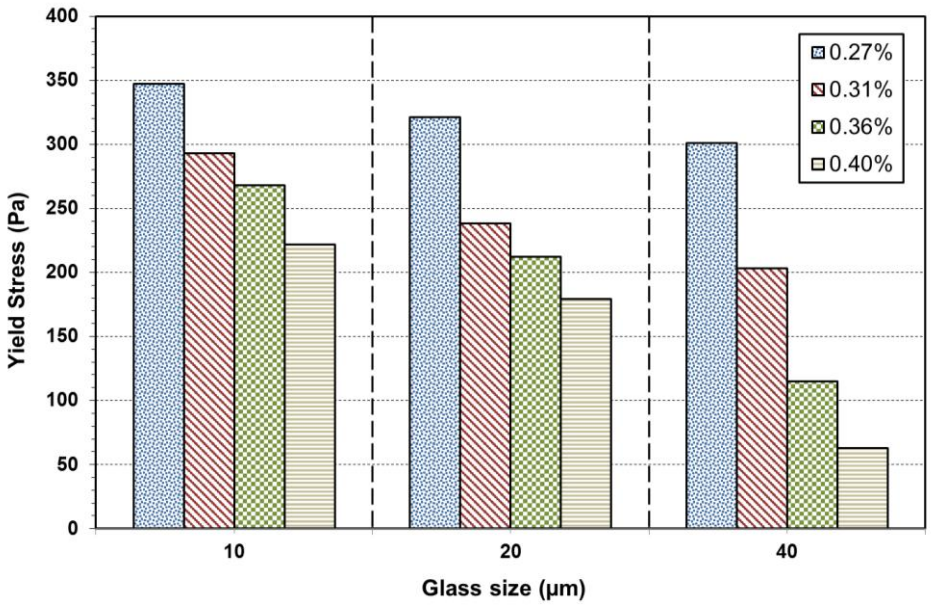

Figure 4.12: Effects of glass fineness (added at 30% rate) on yield stress at various SP dosages

The greater the surface area, the more SP is needed to enclose the total particle surface and at constant SP levels, there is less moveable water in the water-cement matrix system, which subsequently leads to higher resistance when the system is sheared. Moreover, on changing the particle size and surface geometry, the number of contacts between particles and their frictions also change, resulting in the reduction of plastic viscosity and yield stress as the particles in the complex SCC system become coarser. Zhang et al. (2000) and Christensen et al. (2005) presented consistent results and concluded that both yield stress and plastic viscosity are dependent on particle fineness of filler.

Experimental investigations were also made with the variations in replacement levels of glass powder to determine their influence on the rheological behaviour of SCC. Figure 4.13 and Figure 4.14 illustrate the effects of glass contents on the yield stress and plastic viscosity of SF1 and SF2 mixes respectively. The reduction in yield stress and plastic viscosity of GL-CN mixes at lower glass contents might be linked to the effect of water-binder interface and SP dosage in the mixes. For SF1 mixes, 20G20% demonstrated 7% and 11% lower plastic viscosities in comparison to 20G30% and 20G40% respectively, which can be due to the water absorption capacity of glass particles present in variable amounts in the mixes. The reduction in yield stress of 20G20% (SF1) was found to be 11%-

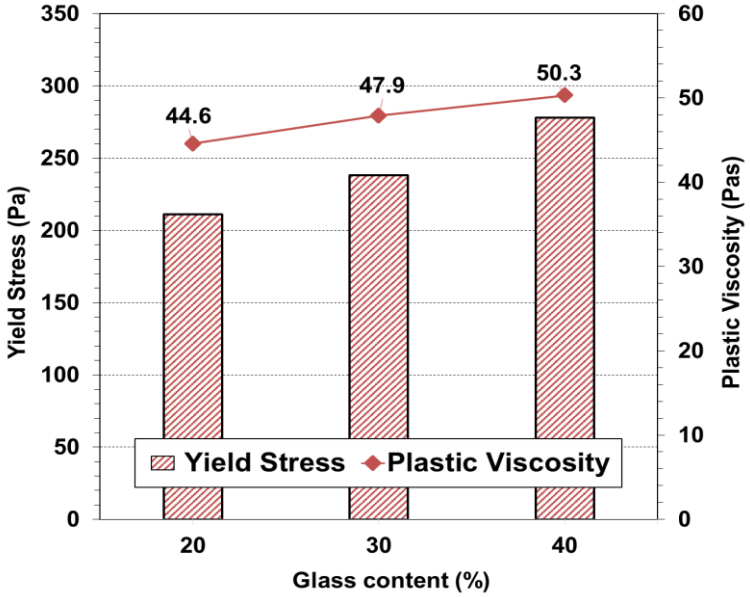

Figure 4.13: Rheological behaviour of SF1 mixes of GL-CN having particle fineness of 20 µm

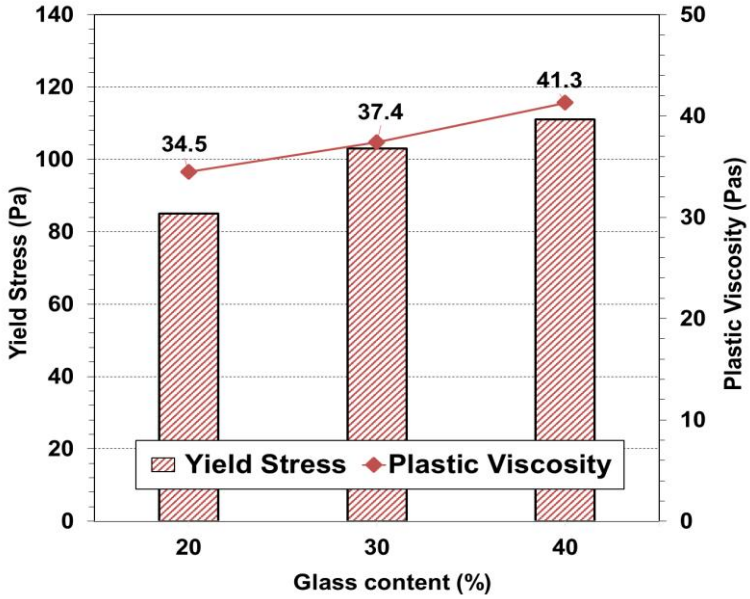

Figure 4.14: Rheological behaviour of SF2 mixes of GL-CN having particle fineness of 20 µm

24% compared to 20G30% and 20G40%. This finding can be linked to the fact that in fresh concrete, two opposing effects are present, one is the inter-particle friction effect, which dominates when fines are less and the other is the specific surface effect, when the fines are more. These effects are responsible for the variations in the rheology of concrete containing different contents of mineral admixtures, consistently mentioned by Zsigovics (2005) and Koehler and Fowler (2007). In terms of the yield stress of SF2 mixes, 20G20% showed 17% -23% reduction than 20G30% and 20G40%. The reduction in plastic viscosity in SF2 mix of 20G20% was found to be 8% and 16% than 20G30% and 20G40% respectively. Cyr et al. (2000), Aitcin et al. (1994), Banfill, (2003) and Nehdi and Mindess (1998) mentioned that in the self-compacting concretes, low plastic viscosity in the fresh mix indicates greater vulnerability to segregation. However, a different observation was noticed in this study as 20G40%, having a higher plastic viscosity, was found to slightly segregate within the duration of taking rheological measurements and pouring into cylinders for further testing. The mixes containing lower glass content showed lower plastic viscosity and yield stress due to the same reason mentioned before.

The rheological measurements were also studied to completely understand the effects of variable glass contents in the SCC system at similar SP dosages, demonstrated in Figure 4.15 and Figure 4.16. It can be noticed that plastic viscosity and yield stress values decreased with the increase of SP dosages. This might be related to the fact that SP improves the fluidity of pastes by the dispersion of binder particles. The adsorption of SP molecules on the binder particles restricts their flocculation due to the electrostatic repulsion forces and through steric hindrance. As a result, the particles are homogeneously distributed

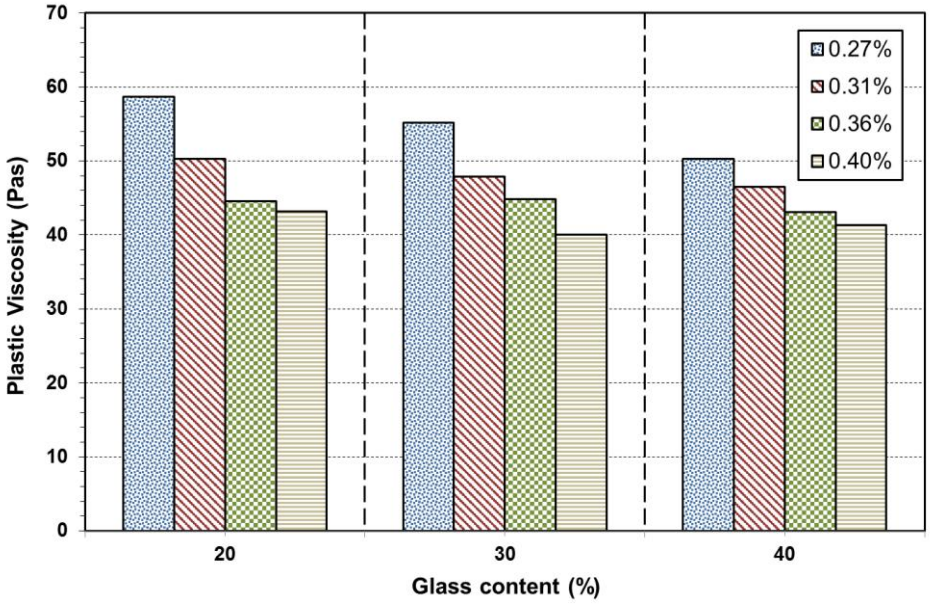

Figure 4.15: Effects of glass content (having fineness of 20 µm) on plastic viscosity at various SP dosages

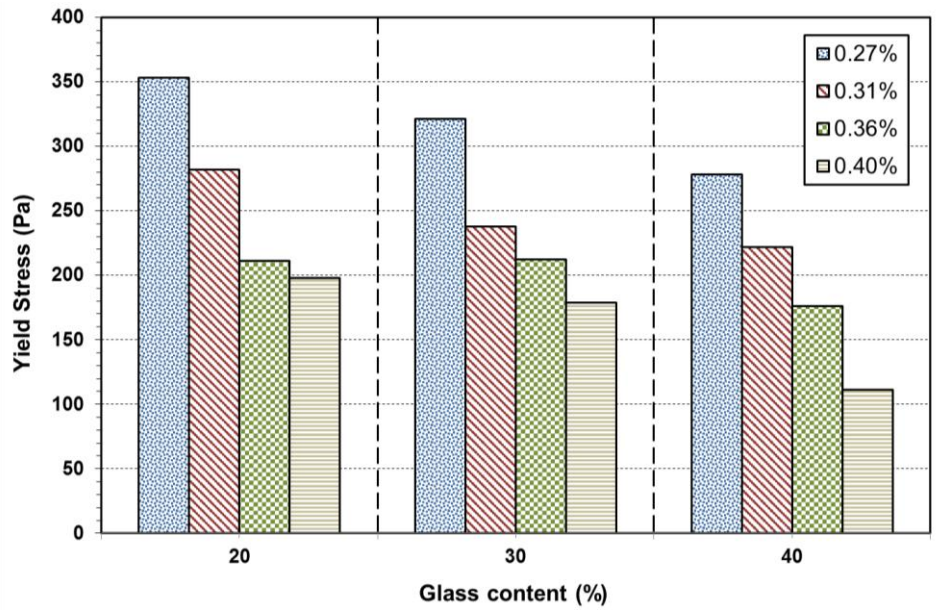

Figure 4.16: Effects of glass content (having fineness of 20 µm) on yield stress at various SP dosages

in the aqueous solution, decreasing the amount of water required for them to be dispersed leading to higher fluidity of pastes. Similar explanation has been given by Uchikawa et al. (1997) and Jolicoeur et al. (1994). Additionally, it was observed that the higher the glass content, the lower both measured yield stress and plastic viscosity at a constant SP dosage. This can be related to the fact that glass powder has a high specific surface area. Hence, glass particles fill the spaces by larger particles of cement (Zhang and Han, 2000; Ferraris et al., 1998) and decrease frictional forces within these SCC mixes, resulting in high flowability of the system (Park et al., 2005). These findings also mention the importance of SP dosage in an SCC system that it is unlikely for a mix to show the anticipated or target rheological performance, if SP dosage in that mix is lower than its optimum requirement.

The surface roughness and angularity of the particles, as well as their reactivity in the matrix system, are other important parameters that affect rheological properties. In addition, the incorporation of organic content in SCC can also deteriorate the rheological behaviour of the system. Figure 4.17 exhibits the influence of glass quality on the yield stress and plastic viscosity of SF1 and SF2 mixes. It was noticed that the irregular-shaped particles and organic content present in the unwashed glass powder modified mix (20UG30%) led to a significant increase in yield strength and plastic viscosity by 33%- 80% in comparison to other glass mixes. Consistent results were found in the literature (Cyr et al., 2000; Gallias et al, 2000) that particles with irregular shapes tend to show a shear thickening behaviour more easily and hence, an increase in viscosity is observed. Another observation was that SCC incorporated with irregular-shaped unwashed glass powder required very high dosage of SP, still, it could not manage to have similar yield stress as other glass mixes at any target flow.

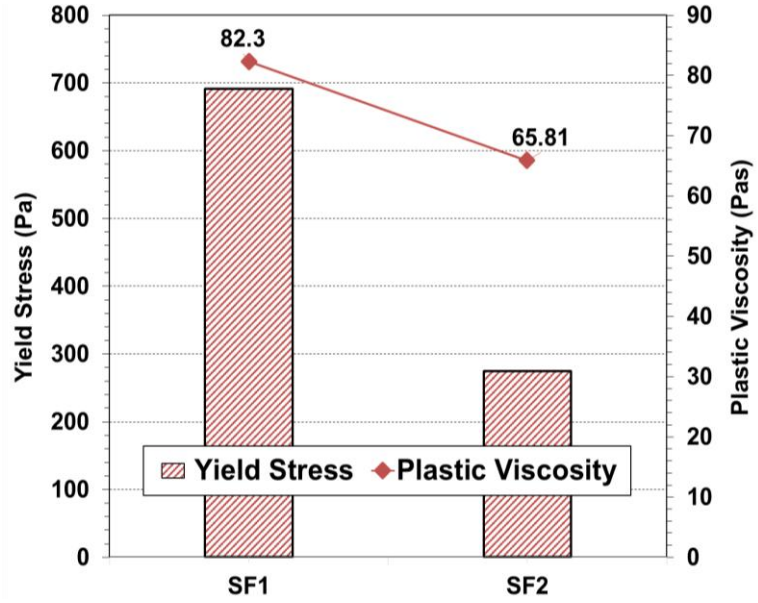

Figure 4.17: Rheological behaviour of 20UG30% having fineness of 20 µm replaced at 30%

The slump flow test and flow time test have been proposed by many researchers as suitable tests for assessing deformability and viscosity respectively. Slump flow is usually related to the yield stress of the fresh concrete and T_{500} is linked to the plastic viscosity of the fresh mix. Koehler (2012) found a good relationship between slump flow and yield stress and between T_{500} and plastic viscosity. However, that study concluded that empirical workability tests might be a function of rheology but rheology provides greater insight into workability. This implies that although the rheology of SCC can be roughly understood from the empirical tests, they do not provide a definitive guidance for all SCC mixes. Utsi et al. (2003) consistently mentioned that slump flow is not a very good indicator of yield stress and is not enough to characterize the fresh behaviour of concrete exactly. In that study, it was concluded that the relationship between workability and rheological parameters are strongly dependent on the properties that concrete exhibits; for a stiffer concrete, the correlation is acceptable but for a flowable concrete (slump flow more than 650 mm), some relation is almost impossible to observe. Hence, this relationship is dependent on the stiffness of the mix, which in turn relies on the SP content and mix ingredients.

In the present study, it was obvious that SCC mixes having similar flow ranges would not represent identical rheological characteristics due to the presence of different binders in the systems. Hence, some typical examples of the insufficiency of slump flow tests to characterize the rheology of the mix were noticed. The mixes, having nearly the same slump flow and flow time measurements, had somewhat different rheological behaviour in the fresh state. In order to illustrate the interactions between slump flow and yield stress and between T_{500} and plastic viscosity, the relationships were developed as shown in Figures 4.18 and 4.19 respectively. The findings indicate that at many instances, empirical consistence tests

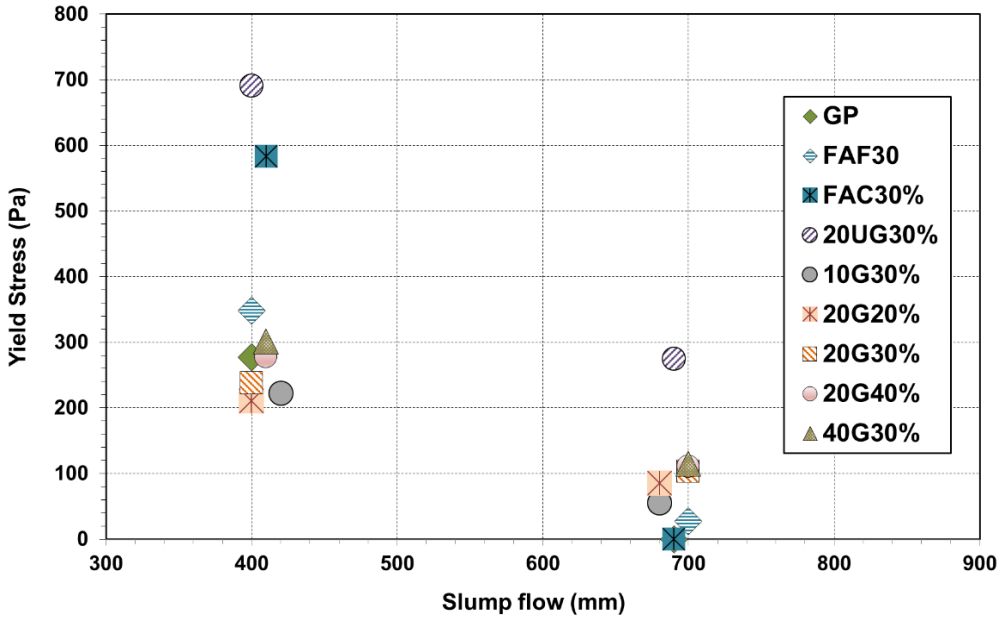

Figure 4.18: Relationship between slump flow and yield stress of all SCC mixes

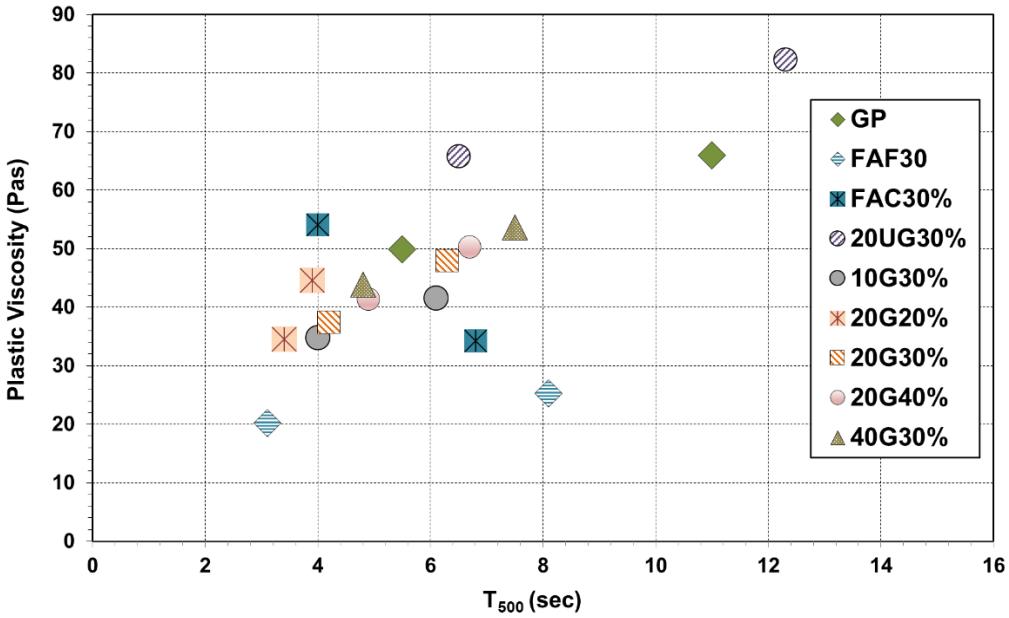

Figure 4.19: Relationship between flow time and plastic viscosity of all SCC mixes

could not provide a definite indication of the actual rheological behaviour of the SCC system. Despite being satisfactory in its standard slump flow targets, the empirical tests only evaluated an 'apparent' rheology and thereby, SCC flowability still lacked the transparency in physical meaningfulness largely due to the complexity of SCC mixtures. In the past, some work has been done towards correlating the yield stress of SCC to the mixture proportions (Wallevik, 2006; Petit et al., 2007) instead of the slump flow; however, some improvement is still required since they do not include the characteristics of the constituent materials. In addition, the proposed models integrate a certain number of assumptions and empirical factors, which strictly relate to specific mixtures observed. Therefore, it is not certain whether

such analytical approaches can be easily generalised for all SCC mixes containing different binder types. Some previous research studies, in compliance with the present study, have also shown that there is not always a correlation between Bingham parameters and slump flow test, highlighting the requirement for alternate test methods (Roussel, 2006; 2007) or the modifications in the presently used tests that can incorporate all contributing factors.

The results discussed in this section have been summarized in Tables 4.4 to 4.8.

Table 4.4: Yield stress and plastic viscosity of all SCC mixes for SF1 and SF3 flow types

Mix Type	Mix Description	Flow Type	Yield Stress (Pa)	Plastic Viscosity (Pas)
GP	Mix containing 100% GP cement / control mix	SF1	277	65.9
		SF2	0	49.9
FAF30%	Mix containing class F fly ash replaced by 30% of GP cement	SF1	348	25.3
		SF2	27	20.2
FAC30%	Mix containing class C fly ash replaced by 30% of GP cement	SF1	583	34.2
		SF2	0	54.1
20UG30%	Mix containing unwashed glass powder replaced by 30% of GP cement	SF1	691	82.3
		SF2	275	65.8
10G30%	Mix containing 10 micron glass powder replaced by 30% of GP cement	SF1	222	41.6
		SF2	55	34.8
20G20%	Mix containing 20 micron glass powder replaced by 20% of GP cement	SF1	211	44.6
		SF2	85	34.5
20G30%	Mix containing 20 micron glass powder replaced by 30% of GP cement	SF1	238	47.9
		SF2	103	37.4
20G40%	Mix containing 20 micron glass powder replaced by 40% of GP cement	SF1	278	50.3
		SF2	111	41.3
40G30%	Mix containing 40 micron glass powder replaced by 30% of GP cement	SF1	301	53.6
		SF2	115	43.9

Table 4.5: Yield stress of GL-FN at different SP levels

Yield Stress (Pa)				
	SP (%)			
Glass Size (µm)	0.27%	0.31%	0.36%	0.40%
10	347	293	268	222
20	321	238	212	179
40	301	203	115	63

Table 4.6: Yield stress of GL-CN at different SP levels

Yield Stress (Pa)				
	SP (%)			
Glass Content (%)	0.27%	0.31%	0.36%	0.40%
20	353	282	211	198
30	321	238	212	179
40	278	222	176	111

Table 4.7: Plastic viscosity of GL-FN at different SP levels

Plastic Viscosity (Pas)				
	SP (%)			
Glass Size (µm)	0.27%	0.31%	0.36%	0.40%
10	58.7	50.2	46.3	41.6
20	55.2	47.9	44.8	40.0
40	53.6	46.2	43.9	38.8

Table 4.8: Plastic viscosity of GL-CN at different SP levels

Plastic Viscosity (Pas)				
	SP (%)			
Glass Content (%)	0.27%	0.31%	0.36%	0.40%
20	58.7	50.3	44.6	43.2
30	55.2	47.9	44.8	40.0
40	50.3	46.5	43.1	41.3

4.4 Influence of superplasticizer dosage on compressive strength

The findings for the compressive strengths of all GP cement, class F and C fly ashes and glass powder incorporated SCC mixes have been discussed in this section. The compressive strength measurements of all SF1, SF2 and SF3 mixes were recorded at 7, 28 and 90 days. The test procedures, curing conditions and preparation of concrete specimens prior to testing have already been explained in Chapter 3. All the results discussed here are the average of three measurements. Complete data are shown in Appendix C. The compressive strength development in all CTR mixes and the glass mixes categorized in GL-FN and GL-CN classes, produced with pre-defined target slump flow of 660-750 mm (SF2), are illustrated in Figure 4.20.

At the age of 7-days, the compressive strength achieved by SF2 control GP mix was 62.1 MPa. The reductions of 36% and 18% were observed in the case of FAF30% and FAC30% concrete samples in comparison to GP. None of the glass samples could reach the strength

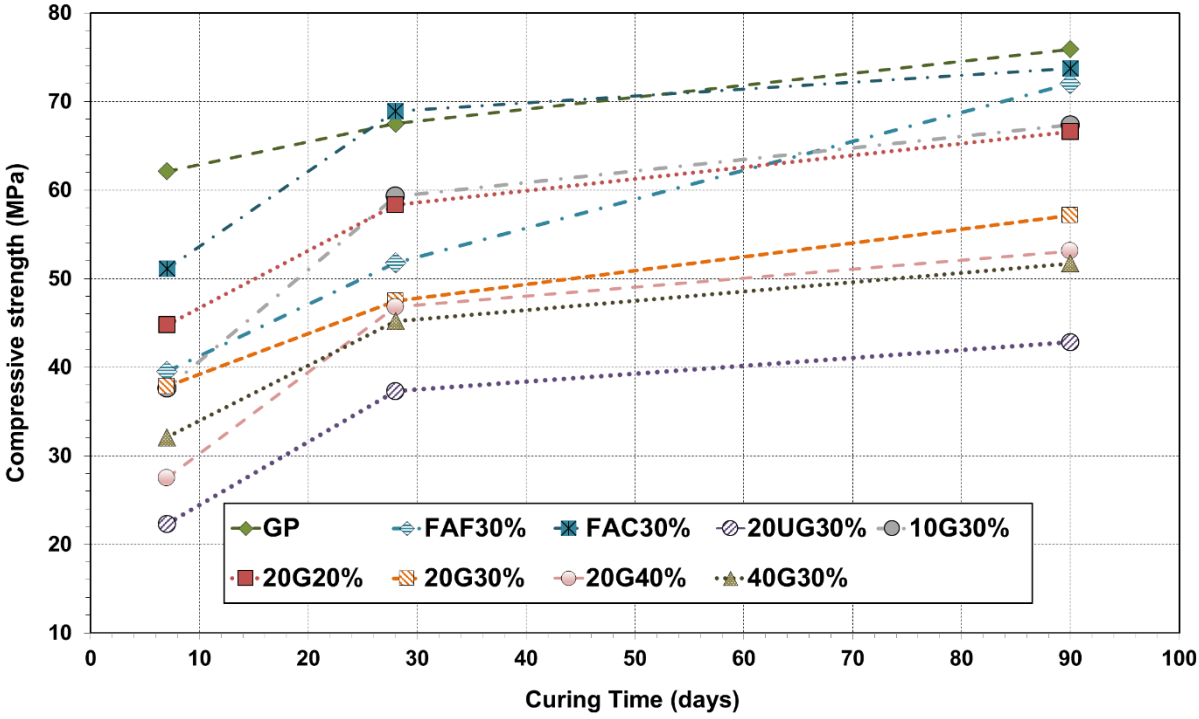

Figure 4.20: Compressive strength development in all SF2 mixes with curing age up to 90-days

target set by GP up to 7-days of curing age. The results from compressive strength testing indicated a strong inverse relationship between pozzolan grading and compressive strength development. There was a decrease of 40%, 39% and 48% in compressive strengths of 10G30%, 20G30% and 40G30% in comparison to the strength demonstrated by GP concrete respectively. These results can be correlated to Idir et al. (2011) who worked on a range of glass sizes and similarly found that the compressive strength of the mix containing glass depends on the glass powder fineness, with higher strengths obtained in a mix containing smaller glass particles (7.8 µm) compared to those containing coarser glass (23.5 µm). Furthermore, 10G30% demonstrated comparable performance to FAF30% as an insignificant reduction of 5% in compressive strength was observed in 10G30% compared to FAF30%. In terms of glass replacements, 20G20%, and 20G40% showed 28% and 56% strength reductions respectively, when compared with GP. The increase in glass content from 20% to 30% and 30% to 40% showed strength losses of 16% and 27% respectively. Ozkan and Yuksel (2008) also reported that compressive strength generally decreases as the replacement value of cement with glass powder increases. In addition, there was a 12%-13% strength loss in 20G20% mix in comparison to FAF30% and FAC30%. 20UG30%, however, showed poor compressive strength development at 7-days and achieved 178% lower compressive strength than GP, possibly due to presence of organic matter.

Out of all SF2 mixes, FAC30% surpassed GP at 28-days and showed the highest compressive strength of 68.9 MPa that was a little higher than GP by 1.4 MPa. It is

interesting to note that compressive strength shown by FAF30% was closer to most of the glass SCC samples at 28-days. In addition, the pozzolanic reaction seemed to kick in for finer glass incorporated SCC samples by 28-days and demonstrated a high increase of 37% and 20% in 10G30% and 20G30% from 7-days to 28-days. On the other hand, the rate of strength gain from 7-days to 28-days was found to be only 8% in GP. These findings are consistent to Dyer and Dhir (2001) that the rate of strength gain in mortars containing finely ground glass cullet is noticeably higher between 7 and 28 days compared to the control. Moreover, the finest glass SCC mix exhibited higher compressive strength in comparison to the coarsest glass SCC type. The 28-days compressive strength achieved by 10G30% was approximately 2%-20% higher than 20G30% and 40G30%. Reductions of 12%, 30% and 33% were observed in 10G30%, 20G30% and 40G30% specimens corresponding to GP mix. This phenomenon of strength decrease with increasing glass particle size has similarly been reported by Shao et al. (2000) who also revealed that 38 µm glass incorporating concrete showed lower strengths than GP within 28-days of the curing period. Similarly, SCC mixes 20G20% and 20G40% demonstrated 14% and 31% reductions in compressive strength at 28-days when compared with GP mix. Taha and Nounu (2008) also observed almost similar results that the 28-days compressive strength is decreased by up to 16% in concrete that utilizes 20% glass powder replacing cement, simply due to a change in the nature of hydration products.

The compressive strength measurements taken at 90-days demonstrated that GP exceeded all other specimens in compressive strength development and achieved approximately 76 MPa. FAF30% and FAC30% showed an increase of 7%-28% in strength between 28-days and 90-days, though they still remained lower than GP. Furthermore, 10G30% exhibited the highest compressive strength of about 67 MPa among glass modified specimens, which is about 15% and 23% higher than 20G30% and 40G30% respectively. The rate of strength gain in 10G30% was found to be slightly higher by 1% than the strength gain in GP from 28-days to 90-days. However, the rate of strength gain in FAF30% was found to be 2.3 times higher compared to 10G30%. Conversely, FAC30% demonstrated half rate of strength development than 10G30% between 28-days and 90-days. GL-CN class of mixes also exhibited substantial improvement in strength at 90-days. 20G20% showed about 14% and 20% higher strength compared to 20G30% and 20G40% respectively. Though obtaining the highest strength among GL-CN class, 20G20% still showed 8%-14% lower compressive strength in comparison to all CTR mixes. There was a reduction of 39%-43% in compressive strength development of 20G40% than GP, FAF30%, and FAC30%. Finally, 20UG30% achieved the lowest compressive strength than all other mixes, possibly due to the same reason mentioned before.

For using an admixture, there is always an optimum limit up to which the behaviour of concrete remains within satisfactory range. The suggested normal dosage of SP to increase the workability of the mix should be between 0.3% – 0.8% by weight of the binder, with the liquid SP containing only about 40% of active material (Neville, 1995). Although increment in the dosage of SP increases the compressive strength of concrete but if the dosage exceeds this specific limit reaching over-dosage state, it reduces the compressive strength instead of contributing towards strength gain. This phenomenon occurs due to the fact that excessive use of SP causes bleeding and segregation, which in turn affects the cohesiveness and uniformity of the concrete. The results listed in Table 4.9 suggest the same approach of SP dosage effects on the compressive strength development of underflow, optimum flow, and overflow mixes, mentioned as SF1, SF2, and SF3 respectively.

Table 4.9: Effects of superplasticizer dosage on compressive strength development of all mixes

Mix Type	Curing Age (days)	SF1		SF2		SF3	
		SP (%)	C.S. (MPa)	SP (%)	C.S. (MPa)	SP (%)	C.S. (MPa)
GP	7 d	0.36	39.3	0.62	62.1	0.80	35.1
	28 d		45.7		67.5		40.2
	90 d		65.1		75.9		48.3
FAF30%	7 d	0.31	37.9	0.53	39.5	0.71	24.0
	28 d		53.4		51.8		39.1
	90 d		59.8		72.0		42.7
FAC30%	7 d	0.34	37.3	0.60	51.1	0.76	35.0
	28 d		41.2		68.9		55.3
	90 d		67.6		73.7		60.9
20UG30%	7 d	0.51	18.8	0.71	22.3	0.84	14.1
	28 d		26.8		37.3		21.5
	90 d		33.2		42.8		26.9
10G30%	7 d	0.40	29.5	0.58	37.6	0.76	27.4
	28 d		48.5		59.3		43.7
	90 d		55.5		67.3		48.1
20G20%	7 d	0.36	40.4	0.53	44.8	0.71	29.8
	28 d		55.5		58.3		43.5
	90 d		57.1		66.6		56.7
20G30%	7 d	0.31	35.4	0.53	37.8	0.67	30.9
	28 d		44.0		47.5		42.0
	90 d		54.4		57.1		55.3
20G40%	7 d	0.28	26.5	0.40	27.5	0.58	19.6
	28 d		41.0		46.8		37.1
	90 d		51.4		53.1		51.1
40G30%	7 d	0.27	32.4	0.36	32.1	0.44	30.6
	28 d		40.9		45.2		38.3
	90 d		50.6		51.7		50.3

The results indicate that there was an increase in 7-days compressive strengths from SF1 to SF2 mixes and decrease in compressive strengths from SF2 to SF3, for most of the SCC mixes. It has been accepted that when the paste is not well-dispersed due to less SP dosage, the amount of interfacial transaction zone (ITZ) is reduced and can increase the compressive strength of the mix. On the other hand, good dispersion of a mix due to high SP dosage can increase the amount of ITZ, decreasing the compressive strength. This implies that dispersion and compressive strength are two parallel terms (Scrivener and Gariner, 1988). The mechanism of compressive strength reduction at very high SP dosage can also be explained by the phenomenon of segregation. The particles in the freshly-mixed concrete no longer remain in uniform positions due to the occurrence of segregation. Consequently, some particles are separated from the cement paste and lead to strength loss. The occurrence of segregation due to very high content of SP dosage was also reported by Lowke et al. (2010). It can also be noticed that the influence of SP addition on 10G30% was much more significant than on 40G30%. Similarly, this influence was more prominent in 20G20% compared to 20G40%. This can be attributed to lower demand of SP in SCC mixes incorporating higher amounts and coarser grains of glass, to achieve same flow range. From Table 4.9, it can be seen that compressive strength of GP concrete increased at 0.62% SP addition but there was a retardation effect of SP at higher dosage of 0.8%. Comparable results have been reported by Ahmed et al. (2005) that compressive strength of GP concrete with up to 0.7% SP increased, followed by a reduction with 0.8% SP addition.

Figure 4.21 and Figure 4.22 illustrate the influence of increasing glass fineness and content respectively on 28-days compressive strengths of all slump flow categories. At 28-days, there was increase in compressive strengths from all SF1 to SF2 SCC types. These results are supported by the findings of Puertas et al. (2001, 2005) and Xu and Beaudoin (2000) that a very low dosage addition of SP is not able to increase the strength of concrete and the highest strength is obtained in case of optimum SP dosage. The addition of SP optimizes the use of mixing water through deflocculation of the cement particles. Hence, increase in dosage to a certain extent increases the entrapped water and promotes hydration of cement, similarly mentioned by Alsadey (2015). Conversely, reductions in 28-days strengths were noticed from SF2 to SF3 mixes. Dumne (2014) noticed similar trend of increase in strength with SP dosage and reported that 28-days strength of SCC containing 90% GP + 10% FA increased by 10%, from 0.25% to 0.35% dosage of SP addition. However, that study was limited to the use of a pre-defined range of SP and the effect of further SP inclusion was not investigated. Finally, compressive strength achieved by SF2 mix of unwashed glass incorporated SCC (20UG30%) was observed to be about 28% higher than SF1 mix; however, reduction of about 42% was found in compressive strength from SF2 to SF3 mix.

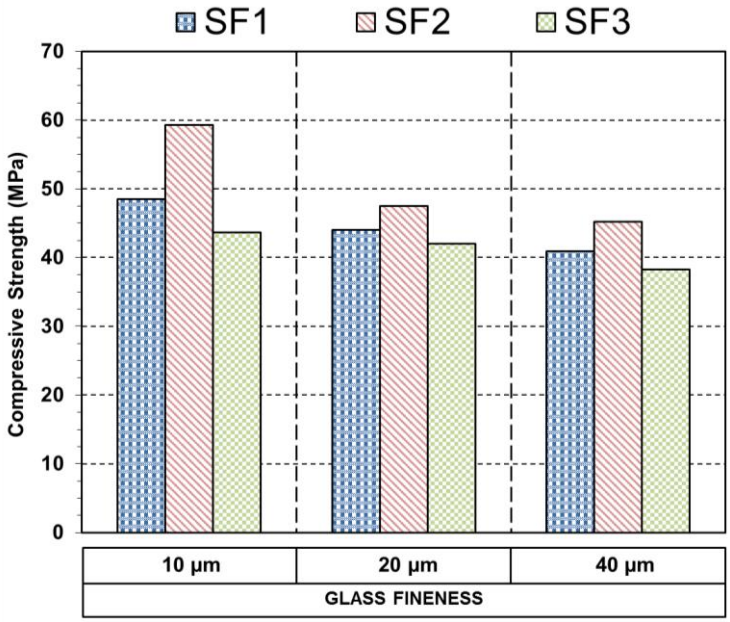

Figure 4.21: Compressive strength development in GL-FN class (added at 30% replacement rate) at 28-days

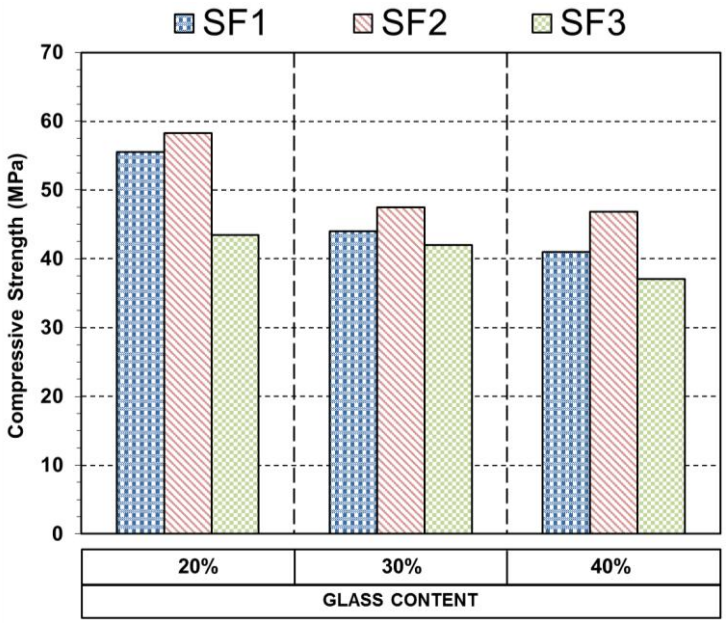

Figure 4.22: Compressive strength development in GL-CN class (having fineness of 20 µm) at 28-days

The 90-days compressive strength measurements indicated the similar relationships between the compressive strength development and SP dosages as that of 7 and 28 days. The overall results at 90-days agree with the findings reported by Chen and Struble (2009) that dispersing effect, which has a significant effect on compressive strength, is not apparent at low admixture dosage because the cement-admixture interaction depends on the level of added admixture. Additionally, any entrapped air resulting from inadequate compaction of the concrete leads to reduction in strength, which will be discussed in the next section. An

increase of 2%-18% in 90-days compressive strengths of glass incorporated mixes was noticed, from SF1 to SF2 SCC mixes. The lower compressive strengths achieved by SF1 mixes at 90-days can be related to the fact that in a condition of low SP to binder content, the unhydrated particles still remain and behave as filler among the hydrated binder particles resulting in strength reductions. The improvement of compressive strength due to higher content of SP dosage in SF2 compared to SF1, as found in this research, is also supported by the research results of Puertas et al. (2001, 2005), Jun-ichi and Hiromichi (2007) and Chen and Struble (2009), which concluded that more content of SP dosage produces good workability and high performance and hence, improves the compressive strength. The findings of this study confirmed the efficiency of SP in dispersing the binder particles and in reducing the amount of unhydrated particles. Furthermore, the reductions of 3%-29% in 90-days compressive strengths were observed in glass modified mixes from SF2 to SF3 SCC types. The difference in compressive strength of 20UG30% was found to be 22% from SF1 to SF2 mix and 37% from SF2 to SF3 mix, with SF2 being higher in both cases.

4.5 Influence of superplasticizer dosage on oxygen permeability

Permeability is used as an assessment of the overall movement of fluids into and through the concrete. In hydrated cement pastes, the size and continuity of the pores at any stage during the hydration process controls the permeability coefficient. SP reduces the macro-porosity by making concrete more flowable; however, insufficient SP dosage makes compaction difficult and lead to a higher level of permeability. It has been reported by Tam et al. (2012) that there is an optimum level of SP that results in the lowest permeability. Excessive amounts of SP are likely to result in the issues related to chemical incompatibility and segregation, leading to higher permeability. Literature indicates that the addition of mineral admixtures does not only change the inflow and filling ability properties and rheology of the cementitious materials in the fresh state but also modify the properties of hardened concrete, such as durability (Ramanathan et al., 2013). Generally, ultra-durable concretes with very high strengths are closely associated with densified microstructures, which are strongly controlled by rheology properties in the fresh state of concrete. However, since these additive materials have their particular properties, rheology of concrete can be controlled by mix design of chemical admixtures (Nehdi and Mendess, 1998; Cyr et al., 2000), which also has an influence on durability as mentioned before. The present section includes the findings from oxygen permeability tests undertaken on all CTR mixes and glass powder incorporated mixes. The coefficient of permeability measurements (K-values) were taken at 7, 28 and 90 days. The test procedures, curing conditions and preparation of specimens prior to testing have already been explained in Chapter 3. The average K-values

were obtained from four replicate specimens, taken out from two identical concrete cylinders. Complete data are shown in Appendix C. The K-values achieved by all CTR mixes and the glass mixes categorized in GL-FN and GL-CN classes, produced with pre-defined target slump flow of 660-750 mm (SF2), are shown in Figure 4.23.

At the curing age of 7-days, K-value achieved by SF2 control GP mix was 10% higher than FAF30% and 2% lower than FAC30%. The results from 7-days tests indicated that there was an irregular relationship between glass grading and K-values; however, glass mixes showed better oxygen permeation resistance than CTR in general. It has already been established that finely ground glass powder as a replacement for cement in concrete exhibits very high pozzolanic activity. The addition of fine glass powder also results in a denser structure and in the disconnection of existing pores forming an impermeable medium, limiting the transfer of gases inside concrete (Chaid et al., 2015). Hence, decrease of 1.6%, 47% and an increase of 78% in 7-days K-values of 10G30%, 20G30%, and 40G30% were found respectively, in comparison to GP. 10G30% was found to be comparable to FAs as an insignificant reduction of 4% in K-value was observed in 10G30% compared to FAC30%, whereas an increase of 10% was observed compared to FAF30%. In terms of glass replacements, 20G20%, and 20G40% showed a reduction of 38% and an increase of 22% respectively, than GP mix. The increase in glass content from 20% to 30% replacement rate demonstrated a reduction of 14% in K-value. There was a 22% decrease in 40G30% mix in comparison to FAC30%. Additionally, a substantial increase of 181% in K-value was found in 20UG30% compared to GP at 7-days.

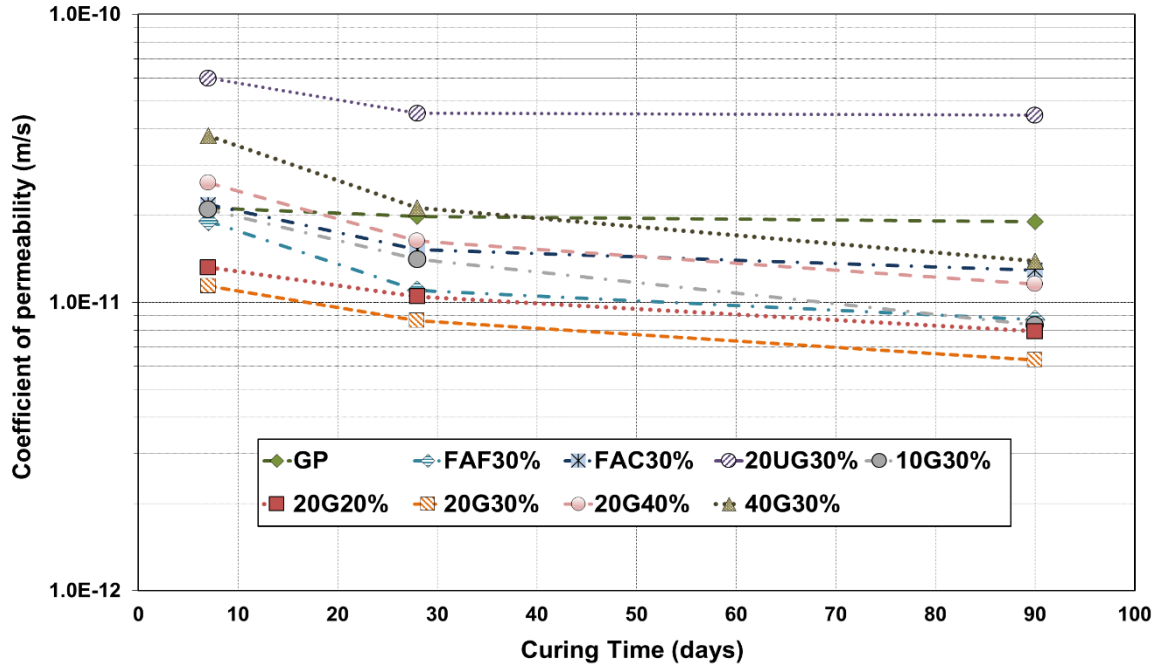

Figure 4.23: Coefficient of oxygen permeability in all SF2 mixes with curing age up to 90-days

Among SF2 mixes, FAF30% and FAC30% performed better than GP at 28-days and showed lower 30%-81% K-values than GP. It is interesting to note that the results shown by FAF30% were comparable to 20G20% at 28-days whereas, the performance demonstrated by FAC30% was closer to 20G40%. Additionally, decrease of 48% in K-value was observed in 20G40% than FAF30% at 28-days. There was 127% decrease in 28-days K-value of 20UG30% in comparison to GP. Furthermore, a decrease of 18% and an increase of 89% was found in SCC mixes, when glass substitution was increased from 20% to 30% and 30% to 40%. These findings can be related to the fact that glass by nature is an impermeable material and hence, the presence of glass particles in concrete reduces the permeability of the concrete mix and restricts the migration of gas inside the concrete (Pacheco-Torgal et al., 2013). This characteristic of glass powder improves the gas permeation resistance of concrete; however, the degree of improvement depends on its replacement level in the mix.

The oxygen permeability measurements taken at 90-days demonstrated that GP recorded the highest K-value among CTR mixes at 1.9E-11 m/s. FAF30% and FAC30% revealed the reduction of 18%-27% in K-values during 28 and 90 days and remained lower than GP. Moreover, 10G30% exhibited the lowest K-value of 8.3E-12 m/s among glass modified specimens, which is about 24% and 67% lower than 20G30% and 40G30% respectively. The rate of K-value reduction in 10G30% was found to be 16 times higher than the K-value reduction in GP from 28 to 90 days. However, the rate of K-value reduction in FAF30% was found to be 2.6 times lower compared to 10G30% during the same curing period. Nevertheless, GL-CN series of mixes exhibited substantial improvement in oxygen permeability at 90-days, possibly due to the same reason mentioned before. Hence, 20G20% showed approximately 46% lower K-value compared to 20G40%. 20G40% exhibited 64% lower K-value in comparison to GP cement mix. Finally, 20UG30% achieved the highest K-value of 4.5E-11 m/s at 90-days, which can be related to the presence of impurities and organic content in the unwashed glass powder.

The results listed in Table 4.10 and Table 4.11 show the effect of increasing glass fineness and content respectively, on 7-days and 28-days K-values of all slump flow classes. It is evident from the results that there was decrease in K-values from SF1 to SF2 mixes and increase in K-values from SF2 to SF3 for all SCC mix types. At the age of 28-days, there was increase of 32%, 24% and 5% in K-values for 10G30% and 40G30% respectively, from SF1 to SF2 SCC types. The lower K-values of SF2 in comparison to SF1 mixes might be explained by small and discontinuous pores that presented very homogenous, compacted and dense pastes. With the progress in hydration, the capillary network became more complicated as the interconnected pores were blocked by formation of CSH, which led to a continuous decrease in permeability. Similar observations have been reported by Tam et al.

Table 4.10: Coefficients of oxygen permeability of GL-FN series at 7 and 28 days

Glass Fineness (µm)	Curing Age (days)	SF1	SF2	SF3
		C.P. (m/s)	C.P. (m/s)	C.P. (m/s)
10 µm	7 d	1.4E-11	2.10E-11	9.9E-11
	28 d	9.2E-12	1.41E-11	2.7E-10
20 µm	7 d	2.0E-11	1.14E-11	1.6E-10
	28 d	1.3E-11	8.63E-12	3.3E-10
40 µm	7 d	2.2E-11	3.79E-11	6.9E-10
	28 d	1.7E-11	2.13E-11	2.9E-10

Table 4.11: Coefficients of oxygen permeability of GL-CN series at 7 and 28 days

Glass Content (%)	Curing Age (days)	SF1	SF2	SF3
		C.P. (m/s)	C.P. (m/s)	C.P. (m/s)
20%	7 d	1.9E-11	1.32E-11	4.8E-11
	28 d	1.1E-11	1.05E-11	7.9E-11
30%	7 d	2.0E-11	1.14E-11	1.6E-10
	28 d	1.3E-11	8.63E-12	3.3E-10
40%	7 d	3.1E-11	2.60E-11	1.6E-10
	28 d	1.7E-11	1.63E-11	6.9E-10

(2012). Moreover, the reduction of 80%-92% in 7-days K-values was observed for GL-CN mixes, from SF3 to SF2 SCC types. At 28-days, the reductions of 97% and 98% in K-values for 10G30% and 40G30% respectively were observed, from SF3 to SF2 SCC types. The 90-days tests of oxygen permeability reveled the similar behaviour of K-value reductions. These findings can be related to the evidence that increasing the SP dosage results in the decrease of viscosity, which leads to an increased air percentage due to the entrapped air bubbles that could not rise and escape from the surface due to high viscosity. Furthermore, SP causes the air trapping during mixing as a side effect. Due to this, the mixes having higher plastic viscosities (20G40% and 40G30%) also had higher oxygen permeability coefficients as they entrapped more air due to the high viscosity compared to other glass specimens.

It has been recognized that both strength and transport characteristics are linked to the pore structure of concrete. Comparing the compressive strength with the oxygen permeability, it was revealed that although GP showed the highest compressive strength, its resistance to oxygen permeation was lower than most of the other mixes. The resistance of washed glass mixes to oxygen penetration was better than GP possibly due to the pore-blocking effect through continuous hydration. The results of oxygen permeability versus compressive strength for mixes made from glass powder, having different finenesses and added at various replacement levels, are shown in Figure 4.24 for SF1 and SF3 mixes.

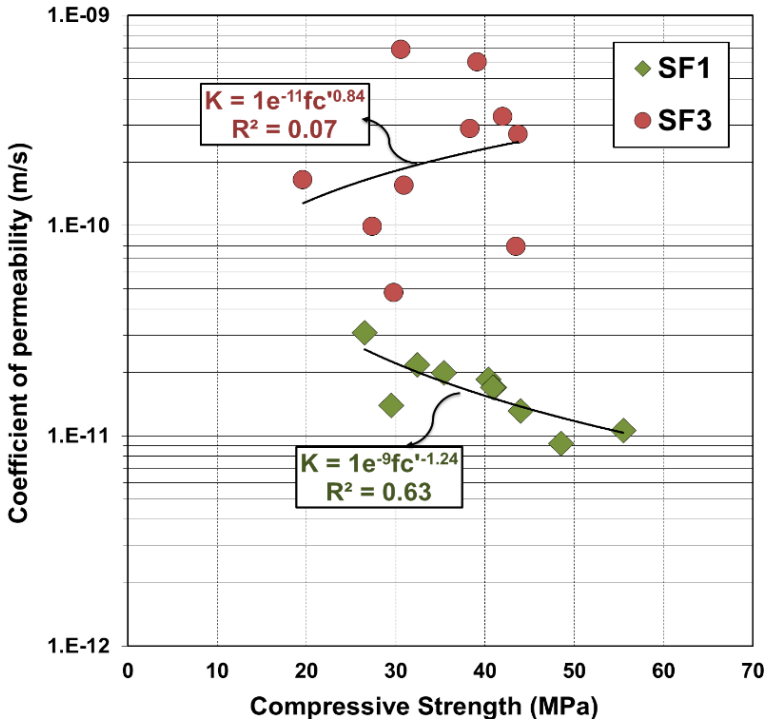

Figure 4.24: Relationship between compressive strength and coefficient of permeability of glass incorporating SF1 and SF3 mixes

For SF1: $K = 1 \times 10^{-9} fc'^{-1.24}$; $R^2 = 0.63$ Equation 4.1

For SF3: $K = 1 \times 10^{-11} fc'^{0.84}$; $R^2 = 0.07$ Equation 4.2

It can be seen that there is little correlation between compressive strength and oxygen permeability particularly for the SF3 mixes. This can be explained by the evidence that lack of compaction in SF1 mixes led to the formation of large voids, which reduced both compressive strength and gas permeation resistance of SF1 specimens. On the other hand, most of the SF3 mixes segregated either at the time of casting or by the time of pouring and therefore, aggregates settled to the bottom of the moulds. The disks cut from these cylinders for oxygen permeability tests might have had non-uniform distribution of the materials, which significantly affected their gas permeation resistance. This suggests that oxygen permeability test might be very sensitive to the overflow condition of mixes and hence, compressive strength of the overflow concrete is not a good indicator for the oxygen permeation resistance.

All the results that have been discussed in the present section have been summarized in Table 4.12. The mix description has also been added in the table to easily correlate the properties of the mix containing different sizes and replacement levels of glass powder with the requirement of SP dosage and T_{500}.

Table 4.12: Coefficient of oxygen permeability of all SCC mix types produced with different SP dosages

Mix Type	Mix Description	Days	Coefficient of Oxygen Permeability (m/s)		
			SF1	SF2	SF3
GP	Mix containing 100% GP cement / control mix	7	2.64E-11	2.13E-11	8.04E-11
		28	2.41E-11	1.99E-11	1.46E-10
		90	-	1.90E-11	-
FAF30%	Mix containing class F fly ash replaced by 30% of GP cement	7	3.60E-11	1.91E-11	1.17E-10
		28	5.63E-11	1.10E-11	7.67E-11
		90	-	8.70E-12	
FAC30%	Mix containing class C fly ash replaced by 30% of GP cement	7	1.76E-11	2.18E-11	9.19E-12
		28	9.02E-12	1.53E-11	1.27E-11
		90	-	1.29E-11	-
20UG30%	Mix containing unwashed glass powder replaced by 30% of GP cement	7	3.77E-11	6.00E-11	4.78E-10
		28	3.40E-11	4.53E-11	4.39E-10
		90	3.16E-11	4.46E-11	3.78E-10
10G30%	Mix containing 10 micron glass powder replaced by 30% of GP cement	7	1.4E-11	2.10E-11	9.9E-11
		28	9.2E-12	1.41E-11	2.7E-10
		90	7.6E-12	8.34E-12	-
20G20%	Mix containing 20 micron glass powder replaced by 20% of GP cement	7	1.9E-11	1.32E-11	4.8E-11
		28	1.1E-11	1.05E-11	7.9E-11
		90	-	7.94E-12	-
20G30%	Mix containing 20 micron glass powder replaced by 30% of GP cement	7	2.0E-11	1.14E-11	1.6E-10
		28	1.3E-11	8.63E-12	3.3E-10
		90	-	6.32E-12	-
20G40%	Mix containing 20 micron glass powder replaced by 40% of GP cement	7	3.1E-11	2.60E-11	1.6E-10
		28	1.7E-11	1.63E-11	6.0E-10
		90	-	1.16E-11	-
40G30%	Mix containing 40 micron glass powder replaced by 30% of GP cement	7	2.2E-11	3.79E-11	6.9E-10
		28	1.7E-11	2.13E-11	2.9E-10
		90	9.2E-12	1.39E-11	2.2E-10

4.6 Influence of superplasticizer dosage on porosity

The influence of SP on the pore structure of hardened concrete mainly depends on its chemical nature. When an SP is added to the concrete, the amount of pores greater than 0.1 µm diameter decrease, while the amount of those less than 0.1 µm increase (Sakai et al., 2006). It has been commonly believed that capillary pores of diameters greater than 0.1 µm adversely affect the concrete tightness and permeability (Deja, 2002). At normal dosages, the use of SP does not generally seem to create any special problems. However, if the dosage is increased, stability problems can occur (Plante et al., 1989a). SP can affect the

air-void system in two ways. Firstly, they increase the paste fluidity, which encourages air-void coalescence. Secondly, they increase the repulsive forces between the cement grains and can thus weaken the shell of cement paste that protects the air voids from coalescence. The influence of SP on the air-void system has been studied by a large number of researchers in the past (Mielenz and Sprouse, 1978; Tognon and Cangiano, 1982; MacInnis and Racic, 1986; Plante et al., 1989b; Saucier et al., 1990). However, very limited information is available in the literature on the influence of varying SP dosages on concrete porosity. Hence, this section includes the information on the porosity measurements of all CTR and glass powder incorporated SCC mixes. The porosity measurements were taken at 7, 28 and 90 days. The test procedures, curing conditions and preparation of concrete samples prior to testing have already been explained in Chapter 3. All the results discussed here are the average of four measurements. Complete data are shown in Appendix C. The percentage of porosities in all CTR mixes and the glass mixes categorized in GL-FN and GL-CN classes, produced with pre-defined target slump flow of 660-750 mm (SF2), have been shown in Figure 4.25.

The porosity demonstrated by SF2 control GP mix was about 11% at 7-days. A reduction of 4% and 2% was observed in the case of FAF30% and FAC30% as compared to GP. The results from porosity testing recorded an inverse relationship between pozzolan grading and porosity. There was a decrease of 5% and 4% and an increase of 2% in porosities of 10G30%, 20G30%, and 40G30% respectively, compared to GP concrete. 10G30% showed comparable performance to FAF30% as an insignificant reduction of almost 2% in porosity

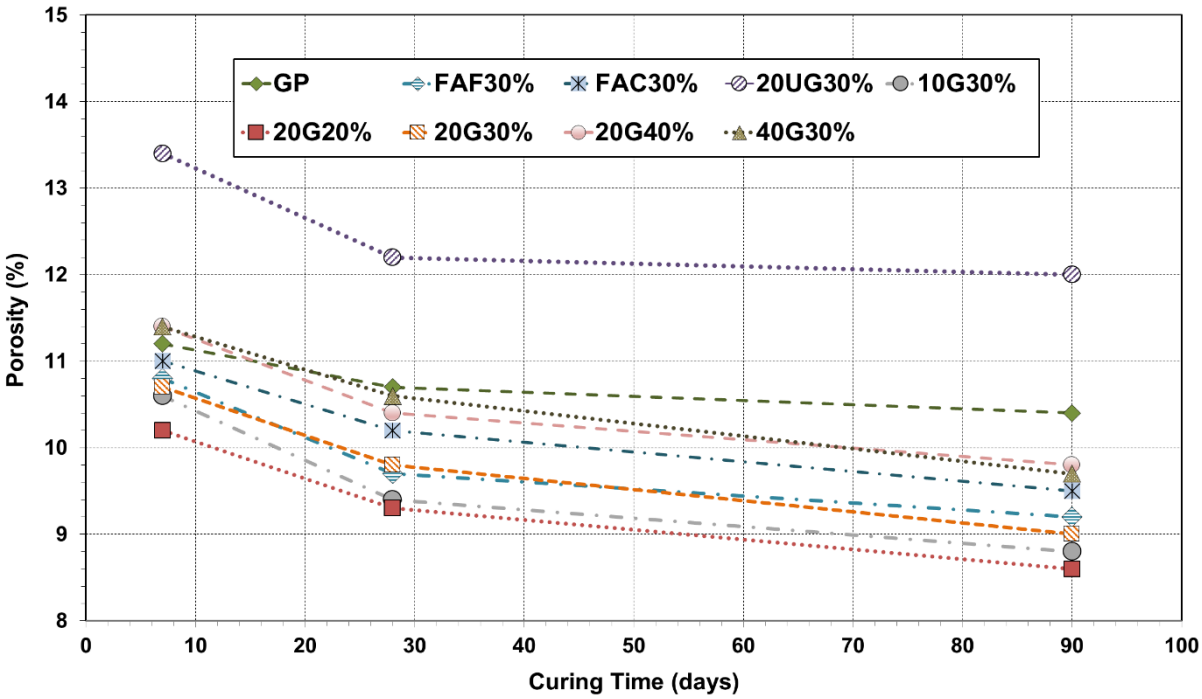

Figure 4.25: Porosity of all SF2 mixes with curing age up to 90-days

was found in 10G30% compared to FAF30%. In terms of glass replacements, 20G20%, and 20G40% showed 9% reduction and 2% increase respectively, when compared with GP. The increase in glass content from 20% to 30% and 30% to 40% demonstrated increase in porosity value by 5% and 6% respectively. In addition, there was 6%-7% porosity reduction in 20G20% mix in comparison to FAF30% and FAC30%. 20UG30%, however, showed poor porosity value at 7-days and achieved 20% higher porosity than GP.

Among SF2 control mixes, FAF30% outweighed GP at 28-days and showed the lowest porosity value of 9.7%. An interesting observation is that many glass specimens demonstrated lower porosity than CTR specimens at 28-days. The pozzolanic reaction, leading to pore structure refinement, was observed to start working for finer glass incorporated SCC samples by 28-days and demonstrated a high reduction of 8%-11% in 10G30% and 20G30% from 7-days to 28-days. Conversely, the rate of porosity reduction was found to be only 5% in GP from 7 to 28 days. Furthermore, the finest glass SCC mix exhibited the lowest porosity in comparison to the coarsest glass SCC type. A reduction of 12%, 8% and 1% was observed in 10G30%, 20G30% and 40G30% mix samples compared to GP mix. The increase in glass content from 20% to 30% and 30% to 40% demonstrated an increase in porosity value by 5% and 6% respectively. However, SCC mixes 20G20% and 20G40% demonstrated 13% and 3% reduction in porosity measurements at 28-days respectively, when compared with GP mix.

The porosity measurements taken at 90-days revealed that GP had the second highest porosity among all SCC mixes at 10.4%. FAF30% and FAC30% showed the reduction in porosity value by 5%-7% between 28 and 90 days. Moreover, 10G30% exhibited the lowest porosity of approximately 9%, which is about 2%-9% lower than 20G30% and 40G30%. The rate of porosity decrease in 10G30% was found to be more than double compared to the porosity loss in GP from 28 to 90 days. However, FAC30% demonstrated a higher rate of porosity reduction than 10G30% between 28 and 90-days. The higher the glass content in the mix, the higher the porosity measurement was recorded. Hence, 20G20% showed about 4% and 12% lower porosity compared to 20G30% and 20G40% respectively. However, there was a reduction of 6% in the porosity of 20G40% than GP and 3%-7% increase than FAF30% and FAC30% at 90-days. 20UG30% achieved the highest porosity value of 12% at 90-days, which can be related to the presence of impurities in the mix that affected the proper structure formation of concrete and left more voids within the microstructure.

Results indicate that a reduction in porosity was observed from SF1 to SF2 mixes and increase in porosity from SF2 to SF3 for most of the SCC mix types. Figure 4.26 and Figure 4.27 demonstrate the effect of increasing glass fineness and content respectively, on 7-days

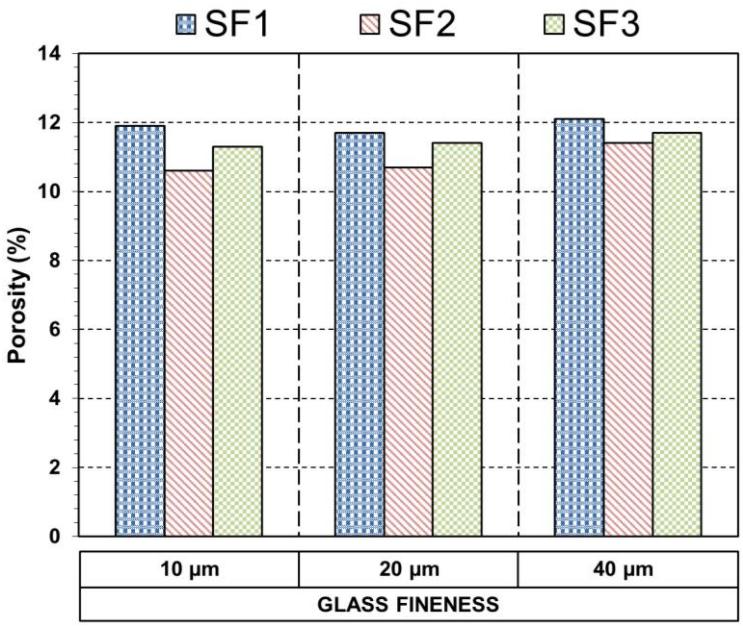

Figure 4.26: Porosity of GL-FN class at 7-days

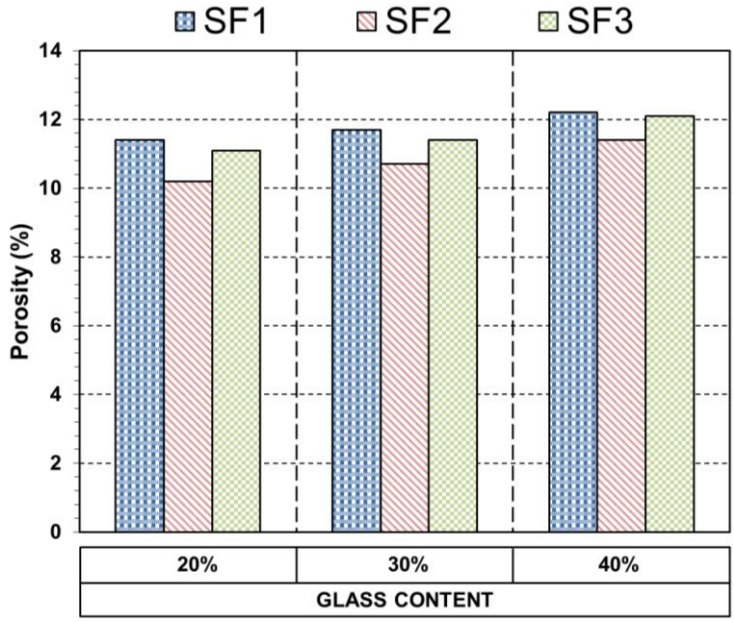

Figure 4.27: Porosity of GL-CN class at 7-days

porosities of all slump flow categories. There was a reduction of 6%-12% in 7-days porosity values of all washed glass mixes from SF1 to SF2 SCC mixes. It can be noticed that the influence of SP addition on 10G30% was much more significant than on 40G30%. Similarly, this influence was more prominent in 20G20% as compared to 20G40%. Likewise, an increase of 3%-8% in 7-days porosity values was observed for all washed glass mixes, from SF2 to SF3 SCC types. The variation in porosity values of 20UG30% was found to be 17% from SF1 to SF2 mix and 12% from SF2 to SF3 mix, with SF2 being lower in both cases. An interesting observation was that GP was highly sensitive to the addition of SP. The variations in SP dosages created the influence of 10%-15% in porosity for all GP mix categories, which

is higher than the effect noticed in most of the other SCC mixes. The results obtained in this study can be related to the evidence that SP induced microstructural modifications in SCC specimens, which in turn reduced porosity and induced refinement in pore size, the effect of which is that the mix was less liable to water absorption. However, variation in SP dosages above or below the optimum limits demonstrated deteriorating effects on the behaviour of SCC specimens. Roncero et al. (2001) similarly observed a decrease in porosity in cement pastes, which contained different SPs at optimum levels and reported identical results.

Figure 4.28 and Figure 4.29 illustrate the influence of increasing glass fineness and content respectively, on 28-days porosities of all slump flow classes. At 28-days, there was a reduction of 10%-12% in porosity of all washed glass mixes from SF1 to SF2 SCC types. Conversely, an increase of 5%-9% in 28-days porosities was noticed for all washed glass mixes from SF2 to SF3 SCC types. The reduction in porosities of SF2 mixes can be related to the fact that admixtures, when added at optimum levels, cause more regular and less porous microstructure. This microstructure-property relationship has an important effect on physical and mechanical properties, such as porosity, similarly mentioned by Ozturk and Baradan (2011). It can also be noticed from the results that there is a constant relationship between the rate of variation in porosities from 7 to 28 days, corresponding to glass size and replacement level. The porosity achieved by SF2 mix of 20UG30% was observed to be about 14% lower than SF1; however, an increase of about 10% was found in porosity from SF2 to SF3 mix. In general, these results are consistent to those reported by Baroninsh et al. (2011) that the porosity of concrete when SP is added at high amount is higher than the porosity of concrete with considerably lower/optimum SP addition by weight of cement.

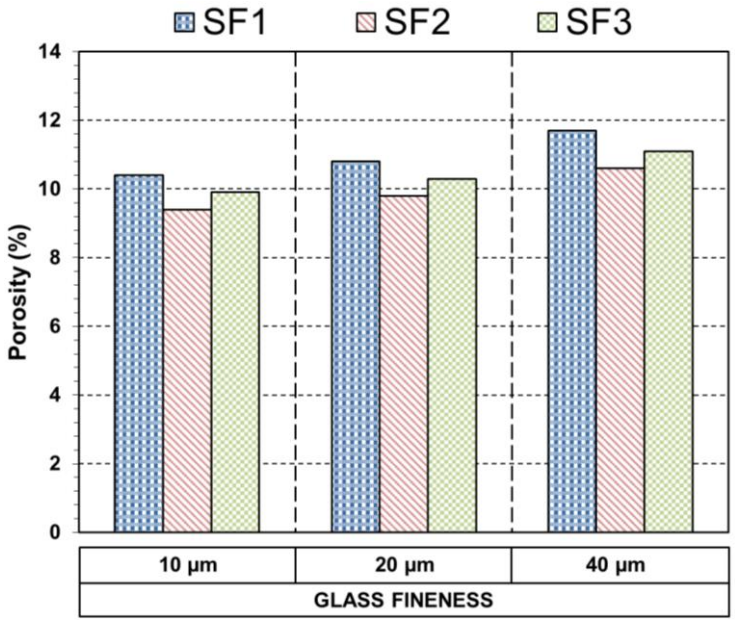

Figure 4.28: Porosity of GL-FN class at 28-days

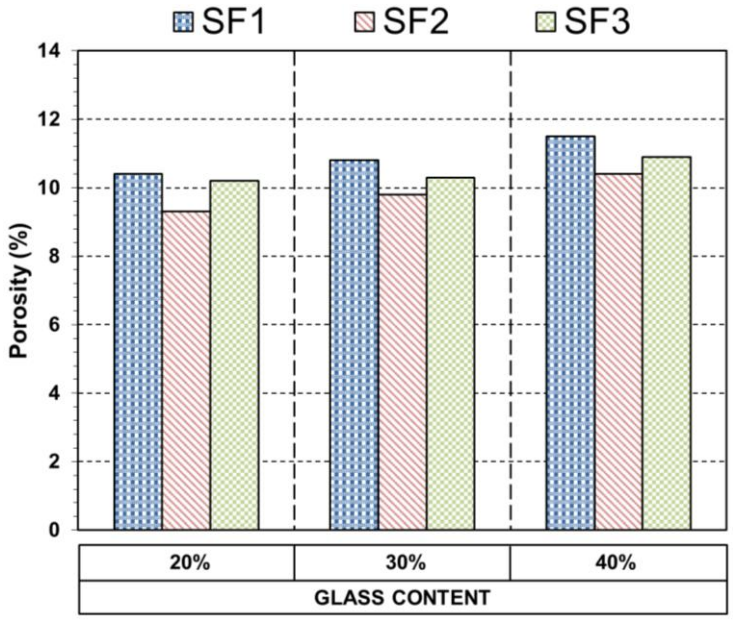

Figure 4.29: Porosity of GL-CN class at 28-days

Figure 4.30 and Figure 4.31 demonstrate the effects of glass fineness and content respectively, on 90-days porosities of all slump flow categories. A reduction of 8%-13% in 90-days porosities of washed glass modified mixes was noticed from SF1 to SF2 mixes. It can be seen that the effect of SP addition on 10G30% and 20G20% was much more significant than on 40G30% and 20G40% at 90-days also. The increase of 3%-9% in 90-days porosities was observed in all glass modified specimens from SF2 to SF3 SCC types. The difference in the porosities of 20UG30% was found to be 13% from SF1 to SF2 and 10% from SF2 to SF3, with SF2 being lower in both cases. Consistent findings have been

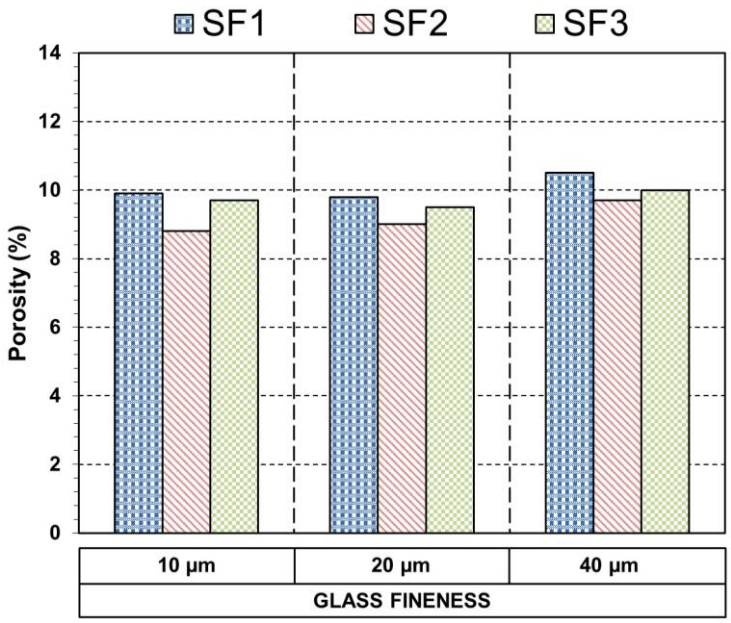

Figure 4.30: Porosity of GL-FN class at 90-days

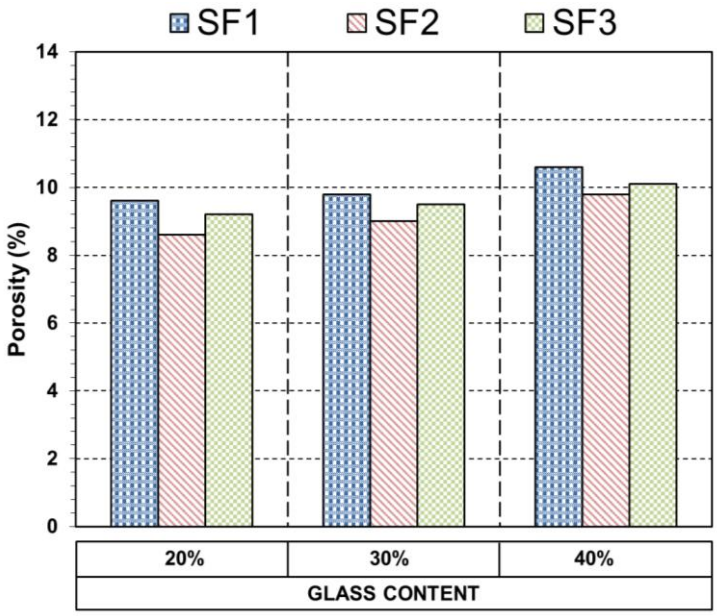

Figure 4.31: Porosity of GL-CN class at 90-days

reported by Ozturk and Baradan (2011) that although the pore area ratio increase as dosage of chemical admixture increases, pore area ratios become lower due to extra pozzolanic reactions at later-ages, leading to lower porosities at later-ages.

The results of porosity versus compressive strength for glass modified mixes are shown in Figure 4.32. The exponential regression analysis gave the following correlation equations for glass incorporating SF1 and SF3 mixes.

For SF1: $fc' = 772.1e^{-0.26p}$; $R^2 = 0.89$ Equation 4.3

For SF3: $fc' = 1201.4e^{-0.33p}$; $R^2 = 0.88$ Equation 4.4

It can be seen that both higher compressive strengths and porosities were achieved for SF1 mixes compared to SF3 mixes. Despite the large compaction voids found in SF1 mixes, the effects of segregation observed in SF3 mixes resulted in higher w/c ratio and non-uniform distribution of the materials, which led to lower overall compressive strengths.

The results of porosity versus coefficient of oxygen permeability for all mixes made from glass powder are illustrated in Figure 4.33. The power regression analysis gave the following correlation equations for glass incorporating SF1 and SF3 mixes.

For SF1: $K = 4e^{-17}p^{5.27}$; $R^2 = 0.77$ Equation 4.5

For SF3: $K = 8e^{-11}p^{0.41}$; $R^2 = 0.01$ Equation 4.6

A reasonable correlation was observed between porosity and permeability in SF1 mixes with some discrepancies in early-age relationships that can be related to the fact that pozzolanic

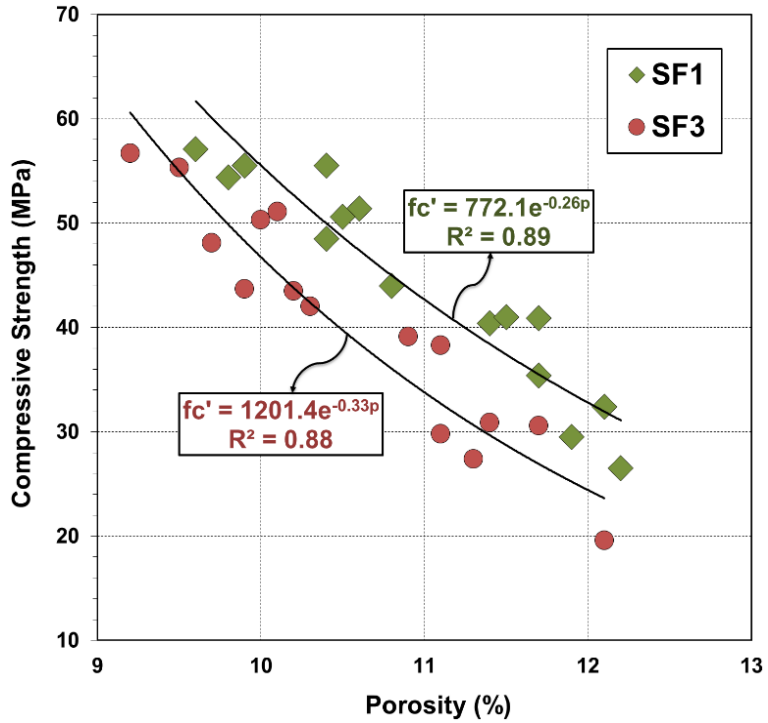

Figure 4.32: Relationship between compressive strength and porosity of glass incorporating SF1 and SF3 mixes

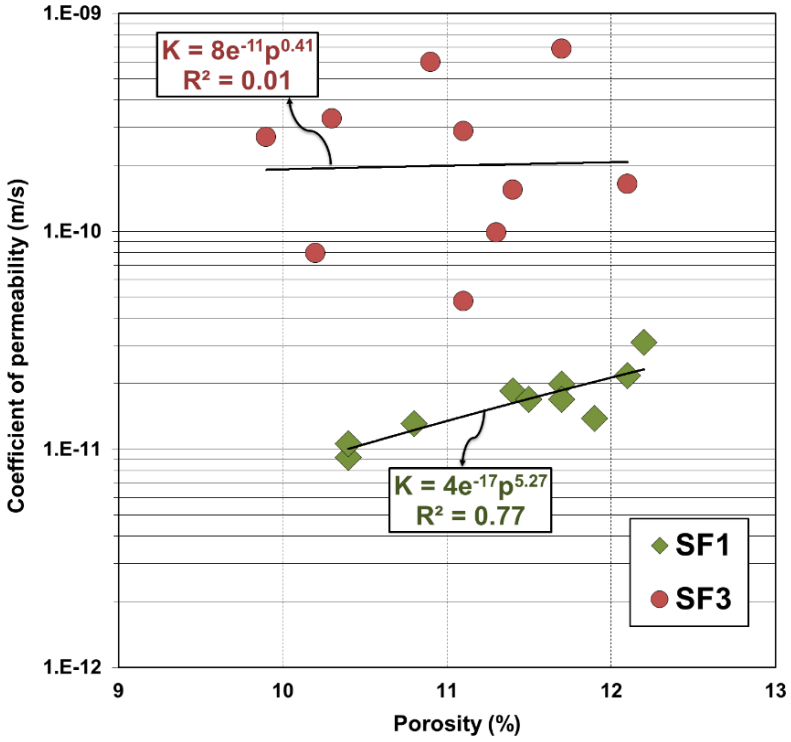

Figure 4.33: Relationship between coefficient of permeability and porosity of glass incorporating SF1 and SF3 mixes

materials require time to demonstrate their properties. There was no correlation between porosity and coefficient of oxygen permeability of SF3 mixes, which could only be related to the inconsistencies in their coefficient of oxygen permeability results as discussed before.

The combined results of the present section have been summarized in Table 4.13.

Table 4.13: Porosity of all SCC mix types produced with different SP dosages

Mix Type	Mix Description	Days	Porosity (%)		
			SF1	SF2	SF3
GP	Mix containing 100% GP cement / control mix	7	12.8	11.2	12.7
		28	12.3	10.7	11.9
		90	11.9	10.4	11.6
FAF30%	Mix containing class F fly ash replaced by 30% of GP cement	7	11.8	10.8	11.7
		28	10.4	9.7	10.6
		90	8.6	9.2	10.1
FAC30%	Mix containing class C fly ash replaced by 30% of GP cement	7	11.9	11.0	12.0
		28	11.2	10.2	10.9
		90	10.4	9.5	10.1
20UG30%	Mix containing unwashed glass powder replaced by 30% of GP cement	7	15.7	13.4	15.2
		28	13.9	12.2	13.6
		90	13.5	12.0	13.3
10G30%	Mix containing 10 micron glass powder replaced by 30% of GP cement	7	11.9	10.6	11.3
		28	10.4	9.4	9.9
		90	9.9	8.8	9.7
20G20%	Mix containing 20 micron glass powder replaced by 20% of GP cement	7	11.4	10.2	11.1
		28	10.4	9.3	10.2
		90	9.6	8.6	9.2
20G30%	Mix containing 20 micron glass powder replaced by 30% of GP cement	7	11.7	10.7	11.4
		28	10.8	9.8	10.3
		90	9.8	9.0	9.5
20G40%	Mix containing 20 micron glass powder replaced by 40% of GP cement	7	12.2	11.4	12.1
		28	11.5	10.4	10.9
		90	10.6	9.8	10.1
40G30%	Mix containing 40 micron glass powder replaced by 30% of GP cement	7	12.1	11.4	11.7
		28	11.7	10.6	11.1
		90	10.5	9.7	10.0

4.7 Influence of superplasticizer dosage on electrical resistivity

Electrical resistivity is an important physical property of concrete, which is directly related to chloride induced corrosion process that partially relies on concrete's microstructure. The increase of electrical resistivity is a fingerprint of the pore decrease process. According to Khatib and Mangat (1999), the addition of SP decreases the total pore volume of paste and leads to refinement of the pore structure. The microstructure, especially the pore structure, shows a great change in the setting process. This response leads to a variation in the rate of change of electrical resistivity, which is another important indicator of concrete durability.

The information included in this section consists of the findings on electrical resistivity measurements of all CTR and glass powder incorporated SCC mixes, produced with various target flows. The electrical resistivity measurements were taken at 7, 28 and 90 days. The test procedures, curing conditions and preparation of concrete specimens prior to testing have already been explained in Chapter 3. All the results discussed here are the average of four measurements. Complete data are shown in Appendix C. The electrical resistivity in all CTR mixes and the glass mixes categorized in GL-FN and GL-CN classes, produced with pre-defined target slump flow of 660-750 mm (SF2), have been illustrated in Figure 4.34.

At 7-days, the electrical resistivity achieved by SF2 control GP mix was 13 kohm.cm. The increase of 5%-10% was noticed in FAF30% and FAC30% compared to GP. Furthermore, the smaller the glass size, the higher the electrical resistivity was noticed. There was increase of 21% and 15% and decrease of 10% in electrical resistivity of 10G30%, 20G30% and 40G30% in comparison to the resistivity demonstrated by GP respectively. 10G30% demonstrated better performance than FAF30% as a significant increase of 10% was observed in 10G30% compared to FAF30%. The results from electrical resistivity testing indicated a strong inverse relationship between increasing glass content and electrical resistivity. The increase in glass content from 20% to 30% and 30% to 40% revealed the resistivity loss of 9% and 17% respectively. 20UG30%, however, exhibited poor resistivity performance at 7-days and achieved 26% lower electrical resistivity than GP.

Out of all SF2 control mixes, FAF30% surpassed in performance at 28-days and showed the highest electrical resistivity of almost 8 kohm.cm that was higher than GP by 2.7 kohm.cm.

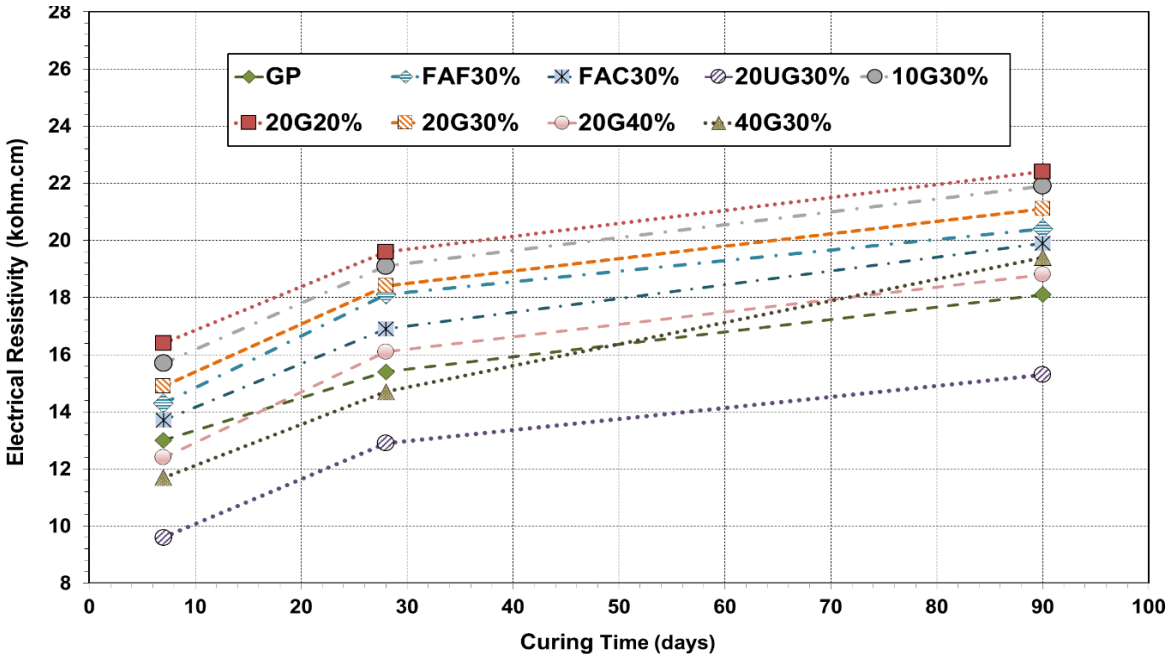

Figure 4.34: Electrical resistivity of all SF2 mixes with curing age up to 90-days

The rate of electrical resistivity increase from 7 to 28 days was found to be 23%-27% in FA modified mixes. It is interesting to note that electrical resistivity shown by FAF30% was lower than many of the glass incorporating SCC samples at 28-days. Glass incorporated specimens demonstrated an increase of 22% and 24% in 10G30% and 20G30% from 7 to 28 days. The finest glass SCC mix exhibited the higher electrical resistivity in comparison to the coarsest glass SCC type. An increase of 24%, 19% and a reduction of 5% was observed in 10G30%, 20G30%, and 40G30% mix samples respectively, corresponding to GP mix. Similarly, SCC mixes 20G20% and 20G40% demonstrated 27% and 5% increase in electrical resistivity at 28-days when compared with GP mix.

The electrical resistivity measurements taken at 90-days demonstrated that GP achieved 18.1 kohm.cm. FAF30% and FAC30% showed the increase in electrical resistivity between 28 and 90 days by 13%-18% and remained superior to GP. Furthermore, 10G30% exhibited the highest electrical resistivity, which is about 4% and 13% higher than 20G30% and 40G30% respectively. Similarly, GL-CN series exhibited substantial improvement in electrical resistivity at 90-days. The higher the glass content in the SCC mix, the lower the electrical resistivity was achieved. However, there was an increase of 4% in 20G40% than GP but the reduction of 8% and 6% in FAF30% and FAC30%. 20UG30% achieved the lowest electrical resistivity of about 15 kohm.cm at 90-days, which can be related to the presence of impurities in the unwashed glass powder utilized in 20UG30%.

It is evident from the results that increase in electrical resistivity was observed from SF1 to SF2 mixes and decrease in electrical resistivity from SF2 to SF3, for most of the SCC mix types. Figure 4.35 and Figure 4.36 illustrate the influence of increasing glass fineness and

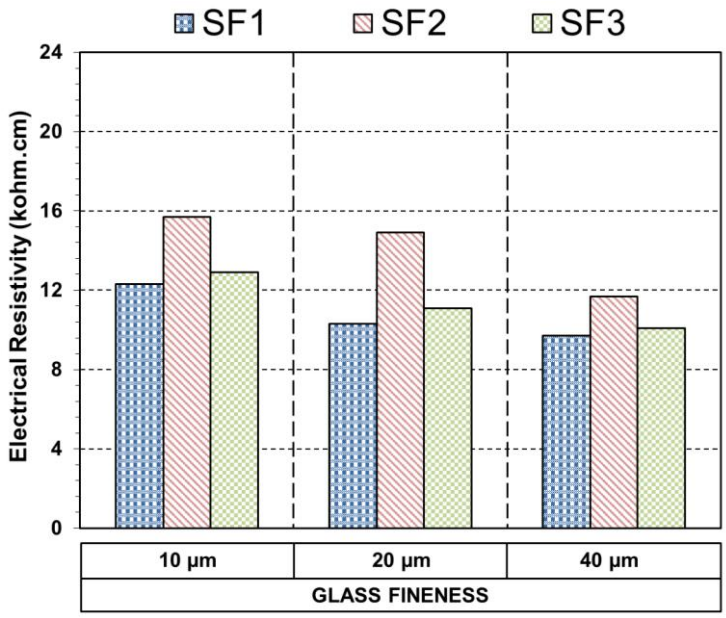

Figure 4.35: Electrical resistivity of GL-FN class at 7-days

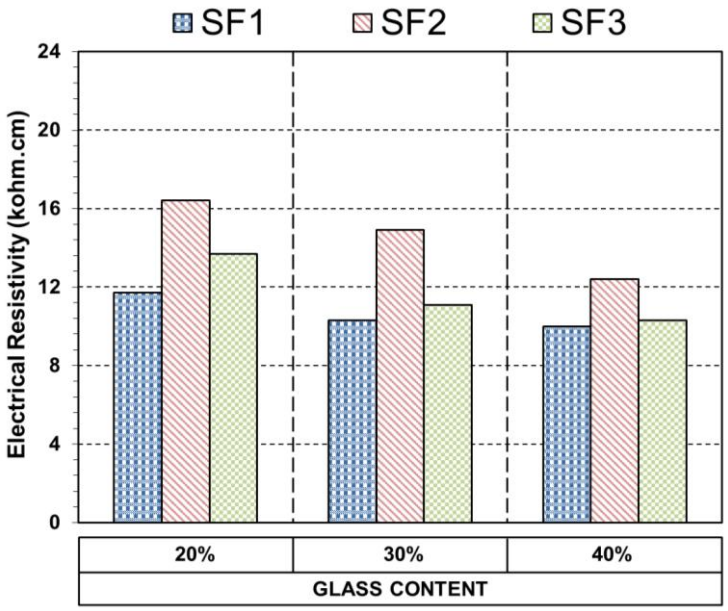

Figure 4.36: Electrical resistivity in GL-CN class at 7-days

content respectively, on the 7-days electrical resistivity of all slump flow categories. There was an increase of 15%-31% in 7-days electrical resistivity of GL-FN and GL-CN series from SF1 to SF2 SCC mixes. Likewise, reduction of 16%-34% in 7-days electrical resistivity was observed in GL-FN and GL-CN series from SF2 to SF3 SCC types. The difference in electrical resistivity of 20UG30% was found to be 15% from SF1 to SF2 mix and 12% from SF2 to SF3 mix, with SF2 being higher in both cases.

Figure 4.37 and Figure 4.38 demonstrate the influence of increasing glass fineness and content respectively on 28-days electrical resistivity of all slump flow classes. At the age of 28-days, there was an increase of 16%-27% in the electrical resistivity of GL-FN and GL-CN

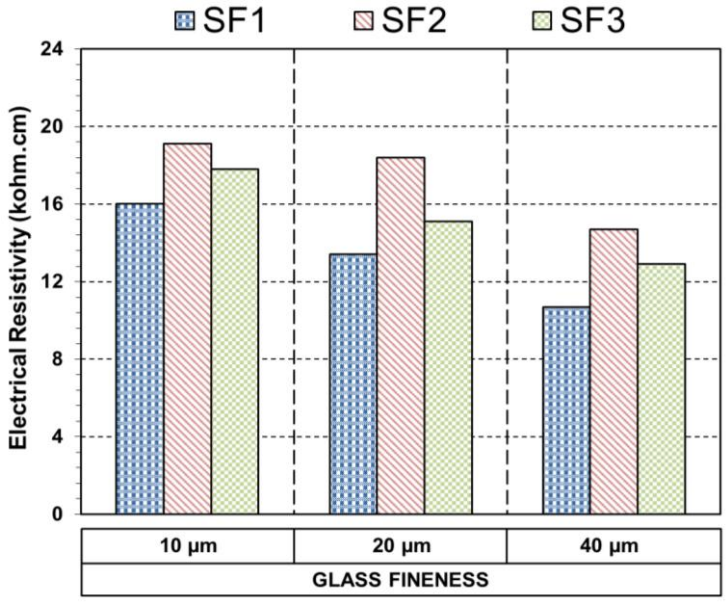

Figure 4.37: Electrical resistivity in GL-FN class at 28-days

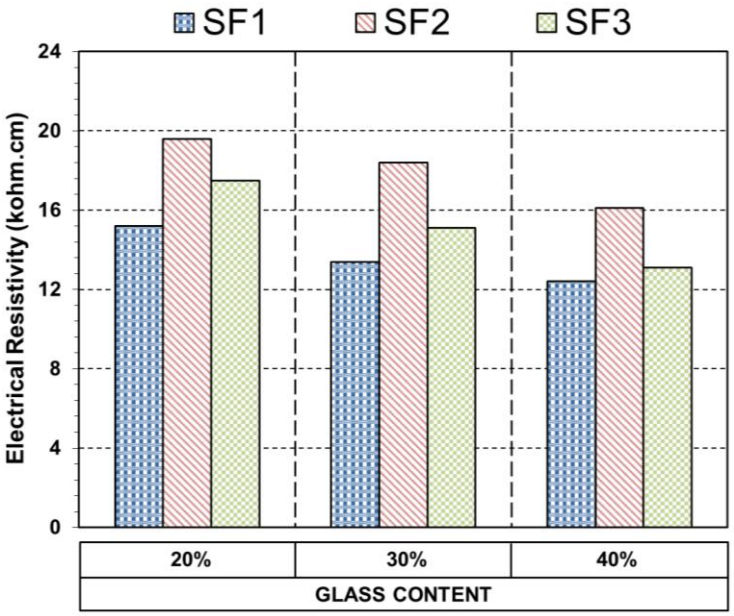

Figure 4.38: Electrical resistivity in GL-CN class at 28-days

series of mixes from SF1 to SF2 SCC types. Conversely, the reduction of 7%-23% in 28-days electrical resistivity was noticed in GL-FN and GL-CN series from SF2 to SF3 SCC types. The electrical resistivity achieved by SF2 mix of unwashed glass incorporating mix, 20UG30%, was found to be approximately 19% higher than SF1 mix, however, a reduction of about 5% was found in electrical resistivity from SF2 to SF3 mix.

Figures 4.39 and 4.40 demonstrate the influence of increasing glass fineness and content respectively on 90-days electrical resistivity of all slump flow mix categories. The 90-days measurements showed the similar relationships between the electrical resistivity and SP dosages as that of 7 and 28 days. An increase of 13%-34% in 90-days electrical resistivity of

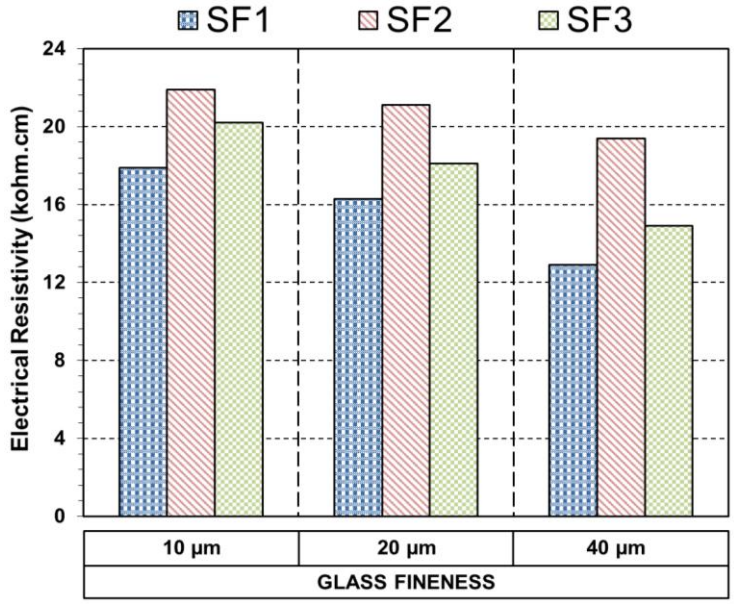

Figure 4.39: Electrical resistivity in GL-FN class at 90-days

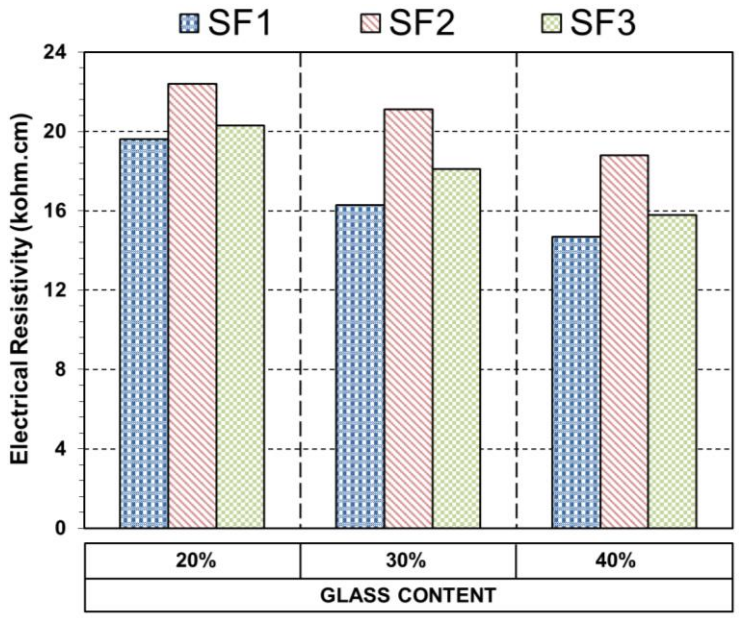

Figure 4.40: Electrical resistivity in GL-CN class at 90-days

GL-FN and GL-CN series was noticed from SF1 to SF2 SCC mixes. The reduction of 7%-30% in 90-days resistivity was observed for GL-FN and GL-CN class of mixes from SF2 to SF3 SCC types. The difference in the electrical resistivity of 20UG30% was found to be 19% from SF1 to SF2 mix and 4% from SF2 to SF3 mix, with SF2 being higher in both cases.

The relationship between electrical resistivity and porosity for all SF1 and SF3 mixtures produced from waste glass powder are illustrated in Figure 4.41. The exponential regression

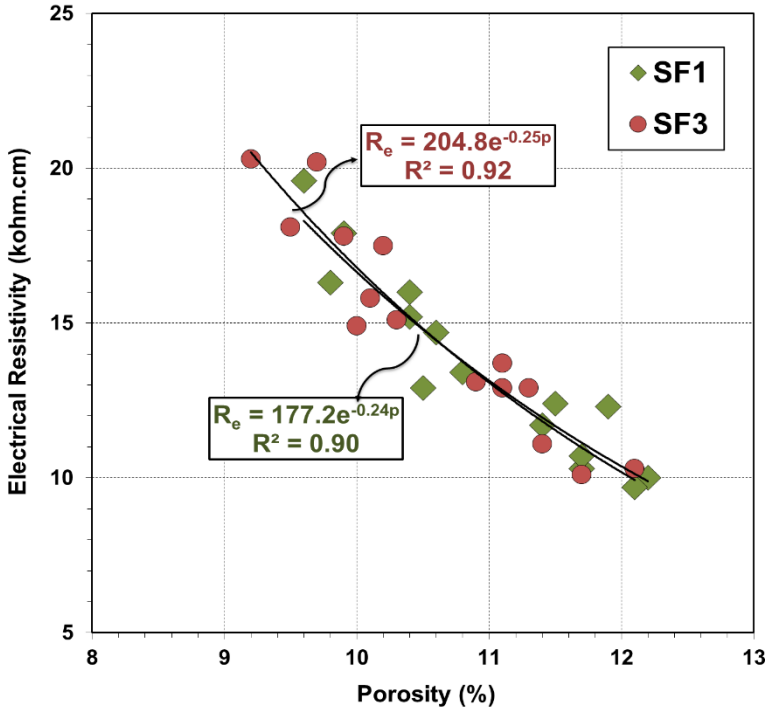

Figure 4.41: Relationship between electrical resistivity and porosity of glass incorporating SF1 and SF3 mixes

analysis gave the following correlation equation for glass incorporated SF1 and SF3 mixes.

For SF1: $R_e = 177.2e^{-0.24p}$; $R^2 = 0.90$ Equation 4.7

For SF3: $R_e = 204.8e^{-0.25p}$; $R^2 = 0.92$ Equation 4.8

The regression coefficients of 0.90 and 0.92 achieved in this study represent a very strong relationship between these two parameters. However, it can be noticed that all mixes, either underflow or overflow, demonstrated similar relationship trend between electrical resistivity and porosity. This indicates that amount of SP does not affect the correlation between electrical resistivity and porosity unlike the distinct relationship observed for oxygen permeability versus porosity and strength versus porosity for SF1 and SF3 mixes. The results discussed in this section have been summarized in Table 4.14.

Table 4.14: Electrical resistivity of all SCC mix types produced with different SP dosages

Mix Type	Mix Description	Days	Electrical Resistivity (kohm.cm)		
			SF1	SF2	SF3
GP	Mix containing 100% GP cement / control mix	7	11.1	13.0	12.1
		28	13.3	15.4	15.8
		90	15.1	18.1	18.1
FAF30%	Mix containing class F fly ash replaced by 30% of GP cement	7	10.5	14.3	11.1
		28	13.6	18.1	15.1
		90	15.7	20.4	16.8
FAC30%	Mix containing class C fly ash replaced by 30% of GP cement	7	16.0	13.7	17.2
		28	18.7	16.9	19.3
		90	20.6	19.9	21.8
20UG30%	Mix containing unwashed glass powder replaced by 30% of GP cement	7	8.2	9.6	10.9
		28	10.4	12.9	13.6
		90	12.4	15.3	16.0
10G30%	Mix containing 10 micron glass powder replaced by 30% of GP cement	7	12.3	15.7	12.9
		28	16.0	19.1	17.8
		90	17.9	21.9	20.2
20G20%	Mix containing 20 micron glass powder replaced by 20% of GP cement	7	11.7	16.4	13.7
		28	15.2	19.6	17.5
		90	19.6	22.4	20.3
20G30%	Mix containing 20 micron glass powder replaced by 30% of GP cement	7	10.3	14.9	11.1
		28	13.4	18.4	15.1
		90	16.3	21.1	18.1
20G40%	Mix containing 20 micron glass powder replaced by 40% of GP cement	7	10.0	12.4	10.3
		28	12.4	16.1	13.1
		90	14.7	18.8	15.8
40G30%	Mix containing 40 micron glass powder replaced by 30% of GP cement	7	9.7	11.7	10.1
		28	10.7	14.7	12.9
		90	12.9	19.4	14.9

4.8 Sensitivity Analysis

The detailed analysis of data revealed significant information related to the effects of the level of compaction or the slump flow on the performance of an SCC mix. Figure 4.42 and Figure 4.43 represent the consolidated summary of 90-days porosity and electrical resistivity data achieved for glass incorporating SF1, SF2 and SF3 mixes. In general, the consolidated results indicate that there was a large influence of compaction on durability of concrete and

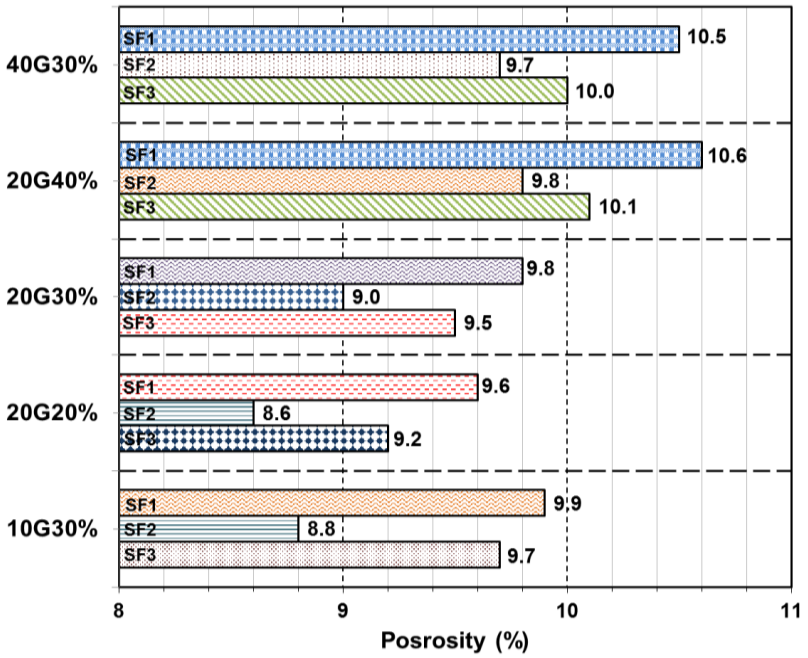

Figure 4.42: Consolidated summary of porosity data

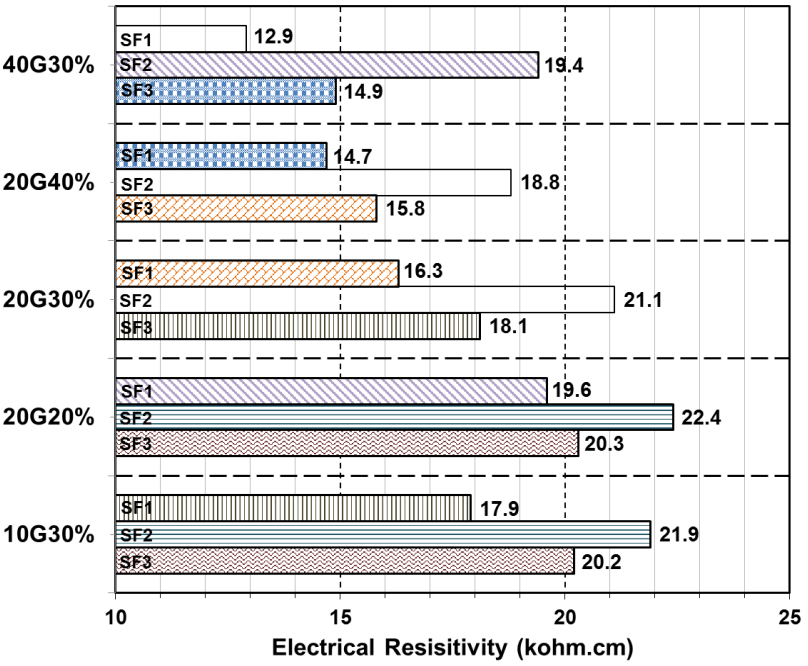

Figure 4.43: Consolidated summary of electrical resistivity data

hence, in many instances, an SCC mix type performed similar to another mix type only due to the variation of the level of compaction. This means that in the case where a mix design with 10 µm glass powder is specified but less attention is given to fresh properties of the mix, it might behave as a 40 µm glass mix, eliminating the performance advantages associated with using more costly material. Some of such examples, where different mixes containing different glass finenesses, contents and SP dosages showed approximately comparable porosity and electrical resistivity, have been provided in the following figures. It is apparent from the results of SF1 and SF3 that an under dosage of SP in the mix results in improved durability and strength characteristics compared with a mix which has been overdosed in SP. This comparison, however, does not take into account the effects of passing ability and surface finish, which would be severely compromised if the mix is too stiff.

4.9 Conclusions

Project specifications have requirements to achieve the intended hardened properties but often do not make suitable allowance for fresh properties of concrete. The optimization of the fresh properties of SCC requires an understanding of the effects of materials and mix designs before actual production. Not only does the understanding of rheological properties initially allow for better optimization of materials that influence workability, it also provides a valuable indicator for the potential strength and durability. The findings presented in this chapter have been used to draw these conclusions:

- Rheology of SCC is roughly understood from its paste fraction and/or by using consistence tests, such as slump flow and flow time tests, but these do not provide definite information for all SCC mixes. The characterization of rheology gives an accurate guidance on the rheological behaviour of SCC before production on site. Hence, there may be a need to optimize the mix proportions of SCC during actual production.

- For a typical SCC mix, as the dosage of SP increases, the yield stress, and the plastic viscosity decrease. However, the decrease in yield stress due to increased dosage of SP is more significant than the decrease in viscosity. There is an optimal limit of SP at which an SCC mix demonstrates good performance. At very low SP dosages, the performance of an SCC is nowhere close to an optimal SCC mix. When the amount of SP dosage exceeds the optimum dosage, segregation is likely to occur. This effect is more apparent in glass incorporated mixes, possibly due to the sharp edges and angular glass particles at the micro-level.

- The inclusion of glass powder into SCC, whether finer/coarser or in less/more proportions, affect the rheology of SCC and allowance may need to be made in SCC mix designs depending on the target properties of SCC. As the glass replacement rate increases and the glass grain size becomes coarser, a lower dosage of SP is required to achieve the same flow range. For instance, SP dosage of 0.58% was required in this study to achieve the same range of optimum flow for concrete with 10 µm glass in comparison to 0.36% for concrete with 40 µm glass.

- The finer the glass in size and lesser in content, the better performance of glass incorporated SCC in terms of rheology is observed. In the present study, the yield stress of 55-85 Pa and plastic viscosity of 34-35 Pas were observed in 10G30% and 20G20% mixes in comparison to yield stress of 111-115 Pa and plastic viscosity of 41-44 Pas observed in 20G40% and 40G30% mixes. In addition, the lower the SP dosage, the higher the yield stress and plastic viscosity were observed in glass modified mixes. However, these variations were more apparent in 10G30% and 20G20% than in 20G40% and 40G30%.

- The excessive use of SP beyond a certain limit results in segregation of the mix, which further leads to compressive strength loss due to microstructural damage and increase in pore volume ratios. The finer glass has more tendency to be affected by SP dosage compared to the coarser glass. The difference in compressive strengths of coarser glass, being introduced with variable amounts of SP, is found to be insignificant. For instance, the 90-days compressive strength of 40G30% lied between 49-51 MPa for all slump flow classes.

- SCCs with 10 µm and 20 µm glass added at 30% and 20% replacement level respectively, demonstrate the best performance in terms of compressive strength and durability compared with mixes incorporating coarser glass and at higher amounts. This means that higher strength and better durability are achieved by the finer glass incorporated mixes. The similar behaviour becomes more apparent with the curing time. In the present study, 90-days compressive strength of 66-68 MPa and porosity of 8-9% were shown by 10G30% and 20G20% in comparison to 90-days compressive strength of 51-54 MPa and porosity of 9-10% shown by 20G40% and 40G30%.

- Considering that glass powder mixes have better durability characteristics compared to GP cement and fly ash mixes, it is recommended that glass powder, depending on its

fineness and replacement level, can be used in the structural applications where durability is the major concern but strength can be compromized. However, the dosage of SP is a crucial factor for improving or worsening the durability properties of glass modified SCC. Therefore, the knowledge of the usage limits, limiting the effects and improving their ability, are important for using SP in SCC incorporating glass powder. Especially over-dosage effects of SP on glass powder are very important factors to assign the ultimate performance, such as strength and durability.

References

Ahari, R. S., Erdem, T. K., and Ramyar, K. (2015). “Effect of various supplementary cementitious materials on rheological properties of self-consolidating concrete.” *Construction and Building Materials, Elsevier,* 75, 89-98.

Ahmed, S., Nawaz, M., Elahi, A. (2005). “Effect of Superplasticizers on workability and strength of concrete.” *Proc., 30th Conference on Our World in Concrete and Structures,* Singapore. 12 pages.

Aitcin, P. C., Jolicoeur, C., and MacGregor, J. G. (1994). “Superplasticizers: how they work and why they occasionally don’t.” *Concrete International,* 5, 45-52.

Ali, E. E., and Al-Tersaway, S. H. (2012). “Recycled glass as a partial replacement for fine aggregate in self-compacting concrete.” *Construction and Building Materials, Elsevier,* 35, 785-791.

Alsadey, S. (2015). “Effect of Superplasticizer on Fresh and Hardened Properties of Concrete.” *Journal of Agricultural Science and Engineering,* 1(2), 70-74.

Ashtiani, M. S., Scott, A. N., and Dhakal, R. P. (2013). “Mechanical and fresh properties of high-strength self-compacting concrete containing class C fly ash.” *Construction and Building Materials*, *Elsevier,* 27, 1217-1224.

Badogiannis, E., Papadakis, V. G., Chaniotakis, E., and Tsivilis, S. (2004). “Exploitation of poor Greek kaolins: strength development of metakaolin concrete and evaluation by means of k-value.” *Cement and Concrete Research*, *Elsevier,* 34(6), 1035-1041.

Banfill, B. F. G. (2006). “Rheology of fresh cement and concrete.” *Rheology Reviews 2006, The British Society of Rheology, School of the Built Environment,* Heriot-Watt University Edinburgh, United Kingdom, 61-130.

Banfill, B. F. G. (2003). “The rheology of fresh cement and concrete – A review.” Proc., *11th International Cement Chemistry Congress,* Durban, 13 pages.

Baroninsh, J., Lagzdina, S., Krage, L., Shahmenko, G. (2011). “Influence of the dosage of super plasticizer on properties of high performance concrete.” *Proc., 5th Baltic Conference on Silicate Materials, IOP Conf. Series: Materials Science and Engineering,* 25, 1-6.

Bartos, P. J. M., Sonebi, M., and Tamini, A. K. (2002). “Workability and Rheology of Fresh Concrete: Compendium of Tests. Report of RILEM Technical Committee TC 145-WSM Workability of Special Concrete Mixes.” RILEM Publications, SARL, France.

Batayneh, M., Marie, I., and Asi, I. (2007). “Use of selected waste materials in concrete mixes.” *Jordan Waste Management, Elsevier,* 27, 1870-1876.

Billberg, P., Petersson, O. (1996). “Self-compacting concrete.” *Proc., Nordic Concrete Research Meeting,* Espoo, Finland, 75-76.

Byars, E. A., Morales-Hernandez, B., and HuiYing Z. (2004). “Waste glass as concrete aggregate and pozzolan.” Concrete, 38(1), 41-44.

Chaid, R., Kenai, K., Zeroub, H., and Raoul Jauberthie, R. (2015). “Microstructure and permeability of concrete with glass powder addition conserved in the sulphatic environment.” *European Journal of Environmental and Civil Engineering,* 19(2), 219-237.

Chen, C. T., and Struble, L. J. (2009). “Influence of mixing sequence on cement-admixture interaction.” *ACI Materials Journal,* 106(6), 503-508.

Christensen, B. J., Ong, F. S. (2005). “The performance of high-volume fly ash self-compacting concrete, (SCC)”, *Proc., Fourth International RILEM Symposium on Self-Compacting Concrete*, RILEM, USA, 139-144.

Cyr, M., Lawrence, P., and Ringot, E. (2006). “Efficiency of mineral admixtures in mortars: quantification of the physical and chemical effects of fine admixtures in relation with compressive strength.” *Cement and Concrete Research, Elsevier,* 36(2), 264–277.

Cyr, M., Legrand, C. and Mouret, M. (2000). “Study of the shear thickening effect of superplasticizers on the rheological behaviour of cement pastes containing or not mineral additives.” *Cement and Concrete Research, Elsevier,* 30(9), 1477-1483.

Du, H., and Tan, K. H. (2014). “Waste glass powder as cement replacement in concrete.” *Journal of Advanced Concrete Technology*, Japan Concrete Institute, 11(12), 468-477.

Dumne, S. M. (2014). “Effect of superplasticizer on fresh and hardened properties of self-compacting concrete containing fly ash.” *American Journal of Engineering Research (AJER),* 3(3), 205-211.

Dyer, T. D., and Dhir, R. K. (2011). “Chemical reactions of glass cullet used as cement component.” *Journal of Materials in Civil Engineering,* 13(6), 412-417.

Esfahani, M. R., Lachemi, M., and Kianoush, M. R. (2008). “Top-bar effect of steel bars in self-consolidating concrete (SCC).” *Cement and Concrete Composites, Elsevier,* 30(1), 52–60.

Felekoglu, B. (2007). “Utilisation of high volumes of limestone quarry wastes in concrete industry (self-compacting concrete case).” *Resources Conservation and Recycling, Elsevier,* 51(4), 770-791.

Felekoglu, B., and Sarıkahya, H. (2008). “Effect of chemical structure of polycarboxylate-based superplasticizers on workability retention of self-compacting concrete.” *Construction and Building Materials*, *Elsevier,* 22(9), 1972-1980.

Ferraris, C., F. and Larrard, F. D. (1998). *Testing and modelling of fresh concrete rheology.* Building and Fire Research Laboratory, National Institute of Standards and Technology, France.

Ferraris, C. F., Brower, L., Ozyildirim, C., Daczko, J. (2000). “Workability of self-compacting concrete.” *Proc., PCI/FHWA/FIB International Symposium on High Performance Concrete. The Economical Solution for Durable Bridges and Transportation Structures,* Orlando, United States. 398-407.

Ferraris, C., Larrard, F. D., Martys, N. (n.d.). “Fresh concrete rheology – Recent developments.” <http://ciks.cbt.nist.gov/~garbocz/materialscience2000/node2.htm> (Nov. 21, 2015).

Gallias, J. L., Kara-Ali, R., and Bigas, J. P. (2000). “The effect of fine mineral admixtures on water requirement of cement pastes.” *Cement and Concrete Research, Elsevier,* 30(10), 1543–1549.

Girish, S., Ranganath, R. V., and Vengala, J. (2010). “Influence of powder and paste on flow properties of SCC.” *Construction and Building Materials, Elsevier,* 24(12), 2481-2488.

Grzeszczyk, S., and Lipowski, G. (1997). “Effect of content and particle size distribution of high-calcium fly ash on the rheological properties of cement pastes.” *Cement and Concrete Research*, *Elsevier,* 27(6), 907-916.

Habeeb, G. A., and Fayyadh, M. M. (2009). “Rice Husk Ash concrete: the effect of RHA average particle size on mechanical properties and drying shrinkage.” *Australian Journal of Basic and Applied Sciences,* 3(3), 1616–1622.

Idir, R., Cyr, M., and Tagnit-Hamou, A. (2011). “Pozzolanic properties of fine and coarse color-mixed glass cullet.” *Cement and Concrete Composites, Elsevier,* 33(1), 19-29.

Jolicoeur, C., Nkinamubanzi, P. C., Simard, M. A., Piotte, M. (1994). “Progress in understanding the functional properties of superplasticizers in fresh concrete.” *Proc., 4th*

CANMET/ACI International Conference on Superplasticizers and Other Chemical Admixtures, American Concrete Institute, Detroit, USA, 63-87.

Jun-ichi, M., and Hiromichi, M. (2007). "Evaluation method for consistencies of mortars with varies mixture properties." *Journal of Advanced Concrete Technology,* 5(1), 87-97.

Khan, S. U., Nuruddin, M. F., Ayub, T., and Shafiq, N. (2014). "Effects of different mineral admixtures on the properties of fresh concrete." *The Scientific World Journal.* 2014, 11 pages.

Khatib, J. M., and Mangat, P. S. (1999). "Influence of superplasticizer and curing on porosity and pore structure of cement paste." *Cement and Concrete Composites, Elsevier,* 21(5–6), 431–437.

Khayat, K. H., Hu, C., Monty, H. (1999). "Stability of self-consolidating concrete, advantages, and potential applications." *Proc., First international RILEM symposium on self-compacting concrete,* Rilem Publications S.A.R.L., 143-152.

Kim, J. K., Han, S. H., Park, Y. D., Noh, J. H., Park, C. L., Kwon, Y. H., and Lee, S. G. (1996). "Experimental research on the material properties of super flowing concrete." *Proc., Production Methods and Workability of Concrete,* (Ed. Bartos, P. J. M., Marrs, D. L. and Cleland, D. J.), E&FN Spon, 271-284.

Koehler, E. (2012). "Use of rheology to design, specify and manage self-consolidating concrete." *Proc., 10th International Conference on Recent Advances in Concrete Technology and Sustainability Issues*.

Koehler, E. P., and Fowler, D. W. (2007). *Aggregates in self-consolidating concrete. Final Report,* International Center for Aggregate Research (ICAR), Project 108, Austin, University of Texas, USA.

Kordts, S., Dusseldorf, H. G. (2003). "Controlling the workability properties of self-compacting concrete used as ready-mixed concrete." *Proc., 3rd International Symposium on Self-Compacting Concrete*, Reykjavik, Iceland, 103-112.

Liu, M. (2011). "Incorporating ground glass in self-compacting concrete." *Construction and Building Materials, Elsevier,* 25(2), 919-925.

Lowke, D., Kränkel, T., Gehlen, C., and Schießl, P. (2010). "Effect of cement on superplasticizer adsorption, yield Stress, thixotropy and segregation resistance." *Design, Production and Placement of Self-Compacting Concrete,* RILEM State of the Art Reports, 1(3), 91-101.

MacInnis, C. and Racic, D. C. (1986). “The effect of Superplastizer on the entrained air-void system in concrete.” *Cement and Concrete Research, Elsevier,* 16(3), 345-352.

Mackechnie, J. R. (2013). “Optimising the fresh properties of concrete by understanding rheology.” *Proc., Concrete Institute of Australia Conference*, Gold Coast, Australia.

Manawadu, A. K., Wijesinghe, W. M. K. B., Abeyruwan, H. (2015). “Rheological Behaviour of Cement Paste with Fly Ash in the Formulation of Self-Compacting Concrete (SCC).” *Proc., 6th International Conference on Structural Engineering and Construction Management,* Kandy, Sri Lanka, 192-199.

Mardani-Aghabaglou, A., Tuyan, M., Yılmaz, G., Arıöz, O., and Ramyar, K. (2013). “Effect of different types of superplasticizer on fresh, rheological and strength properties of self-consolidating concrete.” *Construction and Building Materials, Elsevier,* 47, 1020–1025.

Matos, A. M., and Coutinho, J. S. (2012). “Durability of mortar using glass powder as cement replacement.” *Construction and Building Materials, Elsevier,* 35, 785-791.

Mehta. P. K., and Monterio, P. J. M. (2006). *Concrete: Microstructure, Properties and Materials,* 3rd Ed. McGraw Hill Professional.

Metwally, I. M. (2007). “Investigations on the performance of concrete made with blended finely milled waste glass.” *Advances in Structural Engineering,* 10(1), 47-53.

Mielenz, R. C., Sprouse, J. H. (1978). “High-Range Water Reducing Admixtures: Effect on the Air-Void System in Air-Entrained and Non-Air Entrained Concretes.” *Proc., First International Symposium on Superplasticizers in Concrete, ACI Special Publication SP-62,* (Ed. V.M. Malhotra), American Concrete Institute, Detroit, MI, 167-192.

Nassar, R. U. D., and Soroushian, P. (2012). “Strength and durability of recycled aggregate concrete containing milled glass as partial replacement for cement.” *Construction and Building Materials, Elsevier,* 29, 368-377.

Nehdi, M., Mindess, S., and Aitcin, P. C. (1998). “Rheology of high-performance concrete: effect of ultrafine particles.” *Cement and Concrete Research, Elsevier,* 28(5), 687-697.

Neville, A. M. (1995). *Properties of concrete,* 4th Ed. Wiley, New York.

Okamura, H., and Ouchi, M. (2003). “Self-Compacting Concrete.” *Journal of Advanced Concrete Technology, Japan Concrete Institute,* 1(1), 5-15.

Okamura, H., Ozawa, K. (1995). “Mix design for self-compacting concrete”. *Concrete Library of Japanese Society of Civil Engineers,* 25(6), 107-120.

Ozawa, K., Maekawa, K., and Okamura, H. (1990). “High-performance concrete with high filling capacity.” *Proc., RILEM International Symposium on Admixtures for Concrete: Improvement of properties,* Chapman and Hall Limited, Barcelona, 51-62.

Ozawa, K., Sakata, H., Okamura, H. (1995), “Evaluation of self-compatibility of fresh concrete using the funnel test”. *Proc., Japanese Society of Civil Engineers,* 25(6), 59-75.

Ozkan, O., and Yuksel, I. (2008). “Studies on mortars containing waste bottle glass and industrial by-products.” *Construction and Building Materials, Elsevier,* 22(6): 1288-1298.

Ozturk, A. U., and Baradan, B. (2011). “Effects of admixture type and dosage on microstructural and mechanical properties of cement mortars.” *KSCE Journal of Civil Engineering*, 15(7), 1237-1243.

Pacheco-Torgal, F., Jalali, S., Labrincha, J., and John, V. M. (2013). *Eco-efficient Concrete,* 1st Ed., Woodhead Publishing Limited.

Park, C. K., Noh, M. H., and Park, T. H. (2005). “Rheological properties of cementitious materials containing mineral admixtures.” *Cement and Concrete Research, Elsevier,* 35(5), 842-849.

Park, S. B., Lee, B. C., and Kim, J. H. (2004). “Studies on mechanical properties of concrete containing waste glass aggregate.” *Cement and Concrete Research, Elsevier,* 34(12), 2181-2189.

Petit, J. Y., Wirquin, E., Vanhove, Y., and Khayat, K. (2007). “Yield stress and viscosity equations for mortars and self-consolidating concrete.” *Cement and Concrete Research, Elsevier,* 37(5), 655-670.

Plante, P., Pigeon, M., and Foy, C. (1989b). “The influence of water-reducers on the production and stability of the air-void system in concrete.” *Cement and Concrete Research*, *Elsevier,* 19(4), 621-633.

Plante, P., Pigeon, M., and Saucier, F. (1989a). “Air Void Stability, Part II: Influence of superplasticizers and cement.” *ACI Materials Journal,* 86(6), 581-589.

Plog, J. P. (2015). “Rheology: The measure of successful concrete construction.” *ThermoFisher Scientific,* <http://acceleratingscience.com/mining/rheology-the-measure-of-successful-concrete-construction/> (Nov. 21, 2015).

Puertas, F., and Vazquez, T. (2001). “Early hydration cement: Effect of admixtures and superplasticizers.” Materiales de Construcción, 51(262), 53-61.

Puertas, F., Santos, H., Palacios, M., and Martinez-Ramirez, S. (2005). “Polycarboxylate superplasticizer admixtures: effect on hydration, microstructure and rheological behaviour in cement pastes.” *Advances in Cement Research,* 17(2), 77-89.

Ramachandran, V. S. (1995). *Concrete Admixtures Handbook: Properties, Science and Technology,* 2nd Ed, William Andrew Applied Sciences Publishers, Elsevier.

Ramanathan, P., Baskar, I., Muthupriya, P., and Venkatasubramani, R. (2013). “Performance of self-compacting concrete containing different mineral admixtures.” *KSCE Journal of Civil Engineering,* 17(2), 465- 472.

Ravindrarajah, R. S., Farrokhzadi, F., and Lahoud, A. “Properties of lowing concrete and self-compacting concrete with high-performance superplasticizer.” *Centre for Built Infrastructure Research, University of Technology,* Sydney, Australia.

Roncero, J., Gettu, R. and Martın, M. A. (2001). “Influencia de los superplastificantes y aditivos reductores de retraccio´n en el comportamiento diferido del hormigo´n structural.” *Proc., V Symposium of Asociacio´n Nacional de Fabricantes de Hormigo´n y Mortero*.

Roussel, N. (2006). “Correlation between yield stress and slump: Comparison between numerical simulations and concrete rheometers results.” *Materials and Structures,* 39, 501-509.

Russell, N. (2007). “The LCPC BOX: A cheap and simple technique for yield stress measurements of SCC.” *Materials and Structures,* 40(9), 889-896.

Sahmaran, M., Christianto, H. A., and Yaman, I. O. (2006). “The effect of chemical admixtures and mineral additives on the properties of self-compacting mortars.” *Cement and Concrete Composites*, *Elsevier,* 28(5), 432-440.

Sakai, E., Kasuga, T., Sugiyama, T., Asaga, K., and Daimon, M. (2006). “Influence of superplasticizers on the hydration of cement and the pore structure of hardened cement.” *Cement and Concrete Research, Elsevier,* 36(11), 2049-2053.

Saucier, F., Pigeon, M., and Plante, P. (1990). “Air-Void Stability, Part IV: Retempering.” *ACI Materials Journal,* 87(3), 252-259.

Schober, I., and Flatt, R. J. (2006). “Optimizing carboxylate polymers.” *Proc., 8th CAN/MET/ACI International Conference on Superplasticizers and other Chemical Admixtures in Concrete,* American Concrete Institute, Sorrento, 239, 169-184.

Scrivener, K. L., Gariner, E. M. (1988). “Microstructural gradients in cement paste around aggregate particles.” *Proc., Material Research Symposium Proceedings,* 114, 77-85.

Sfikas, I. P., Badogiannis, E. G., and Trezos, K. G. (2014). “Rheology and mechanical characteristics of self-compacting concrete mixtures containing metakaolin.” *Construction and Building Materials, Elsevier,* 64, 121–129.

Shao, Y., Lefort, T., Moras, S., and Rodriguez, D. (2000). “Studies on concrete containing ground waste glass.” *Cement and Concrete Research, Elsevier,* 30(1), 91-100.

Sobolev, K., Türker, P., Soboleva S, and Iscioglu G. (2006). “Utilization of waste glass in ECO cement, strength properties and microstructural observations.” *Waste Management, Elsevier,* 27(7), 971-976.

Sonebi, M., Bartos, P. J. M. (1999). “Hardened SCC and its bond with reinforcement.” *Proc., First International RILEM Symposium on Self-Compacting Concrete,* Stockholm, Sweden, 275–289.

Taha, B., and Nounu, G. (2008). “Properties of concrete contains mixed colour waste recycled glass as sand and cement replacement.” *Construction and Building Materials, Elsevier,* 22(5), 713-720.

Tam, C. M., Tam, V. W. Y., and Ng, K. M. (2012). “Assessing drying shrinkage and water permeability of reactive powder concrete produced in Hong Kong.” *Construction and Building Materials, Elsevier,* 26(1), 79-89.

The Concrete Society, BRE. (2005). “Self-compacting concrete: a review (Technical report No. 62),” Concrete Society, Surrey, UK.

Thomas, M. (2007). *Optimizing the Use of Fly Ash in Concrete.* University of New Brunswick. Portland Cement Association, Illinois, USA.

Tognon, G., and Cangiano, S. (1982). “Air Contained in Superplasticized Concretes.” *Journal of the American Concrete Institute,* 79(5), 350-354.

Uchikawa, H., Hanehara, S., and Sawaki, D. (1997). “The role of steric repulsive force in the dispersion of cement particles in fresh paste prepared with organic admixture.” *Cement and Concrete Research, Elsevier,* 27(1), 37–50.

Utsi, S., Emborg, M., Carlsward, J. (2003). “Relation between workability and rheological parameters.” *Proc., Third International RILEM Symposium on Self-Compacting Concrete,* (Ed: Wallevik, O. and Nielsson, I), Rilem Publications S.A.R.L., 154-164.

Wallevik, J. E. (2006). “Relationship between the Bingham parameters and slump.” *Cement and Concrete Research, Elsevier,* 36(7), 1214-1221.

Xu, G., and Beaudoin, J. J. (2000). “Effect of Polycarboxylate superplasticizer on contribution of interfacial transition zone to electrical conductivity of Portland cement mortars.” *ACI Materials Journal,* 97(4), 418-424.

Yamakawa, I., Kishtiani, K., Fukushi, I., Kuroha, K. (1990). “Slump Control and Properties of Concrete with a New Superplasticizer. II. High strength in situ concrete work at Hicariga-Oka Housing project.” *Proc., International RILEM Symposium on "Admixtures for Concrete: Improvement of Properties"*, (Ed: Vasquez, E.), Chapman & Hall, London, 94-105.

Zakka, Z. A., and Carrasquillo, R. L. (1989). “Effects of high-range water reducers on the *properties of fresh and hardened concrete.” Center for Transportation Research, University of Texas at Austin,* Texas, USA.

Zhang, X., and Han, J. (2000). “The effect of ultra-fine admixture on the rheological property of cement paste.” *Cement and Concrete Research, Elsevier,* 30(5), 827-830.

Zsigovics, I. (2005). “Effect of limestone powder on the consistency and compressive strength of SCC.” *Proc., SCC. ACBM,* Chicago, USA.

CHAPTER 5

INFLUENCE OF GLASS POWDER ON LONG-TERM MECHANICAL PROPERTIES OF SELF-COMPACTING CONCRETE

ACRONYMS USED

GP	GP cement control mix
FAF30%	Mix containing class F fly ash replaced by 30% of GP cement
FAC30%	Mix containing class C fly ash replaced by 30% of GP cement
LP30%	Mix containing limestone powder replaced by 30% of GP cement
20UG30%	Mix containing 20 microns unwashed glass powder replaced by 30% of GP cement
10G30%	Mix containing 10 microns washed glass powder replaced by 30% of GP cement
20G20%	Mix containing 20 microns washed glass powder replaced by 20% of GP cement
20G30%	Mix containing 20 microns washed glass powder replaced by 30% of GP cement
20G40%	Mix containing 20 microns washed glass powder replaced by 30% of GP cement
40G30%	Mix containing 20 microns washed glass powder replaced by 30% of GP cement
CTR	All materials class: GP, class F and C fly ashes and glass powder/Control materials class: GP, class F and C fly ashes
GL-FN	Washed glass powder classified according to fineness: having fineness of 10 µm, 20 µm and 40 µm; added at 30%
GL-CN	Washed glass powder classified according to content: added at 20%, 30% and 40%; having fineness of 20 µm

HIGHLIGHTS

- Discussion on water demand and strength activity indexes of mortars containing different glass sizes and contents as cement replacements.
- Analysis of the effects of various size ranges and quantities of glass powder on compressive strength and splitting tensile strength of SCC.
- Investigation of the influence on elastic modulus of SCC incorporating glass powder of different finenesses and replacement levels.
- Evaluation of the performance of various glass sizes and dosages included in mortar and SCC, compared to the behaviour exhibited by GP cement, fly ashes and limestone powder.
- Correlations between different mechanical properties.

5.1 Introduction

Self-compacting concrete (SCC) has been employed in the construction industry for more than 20 years. During the period of 90s, a number of studies were performed regarding the applicability, mix design, pumpability, and rheology of SCC but an insufficient attention was devoted to its mechanical properties and structural performance. However, the number of researches dedicated to the mechanical properties of SCC have been increased recently (Sonebi et al., 2005). Although these research projects include data on compressive strength, tensile strength, and Young's modulus, their main focus remains on other aspects of concrete as mentioned above. Some authors, such as Holschmacher (2002) and Domone (2007), have presented surveys on mechanical properties of SCC based on the available literature. Due to a limited amount of available test results, these studies are based on an inadequate set of data and only on the short-term mechanical performance of SCC. The influence of some major evolutionary measures on the mechanical performance of SCC, such as curing age, is not widely available. This lack of information motivated the researcher to develop results on the mechanical properties of different SCC mixes, tested up to 545-days of curing, in the scope of the research program.

The main objective of this study was to test long-term fundamental mechanical properties of SCC that utilised glass contents of 20%, 30% and 40% and glass finenesses of 10 µm, 20 µm and 40 µm as partial replacements for cement. The results of these tests on SCC, produced with increasing levels and finenesses of glass powder and their comparison with other CTR mixes, are presented and discussed in this chapter. To start with, compressive strength tests on mortar cubes were performed at curing ages of 7 to 180 days to evaluate strength activity index of each glass type. The SCC mixes were then cast to assess the effects of various glass contents and sizes on mechanical properties. The dosages of superplasticizer (SP) and stabilizer (SB) were adjusted so that predefined target fresh properties (slump flow ≈ 650 - 750 mm, T_{500} ≈ 2-7 sec and visual stability index value, VSIV ≈ 0) were achieved in each SCC mix. As outlined in Chapter 3, glass size ranges of 10-40 µm and replacement levels of 20-40% of cement by weight were selected, whereas the aggregate proportions and water to binder (w/b) ratio were established as constants. The types of SP and SB used in all SCC mixes were also kept the same. The mixes produced with these materials were then tested for compressive strength at curing ages of 1 to 545 days and splitting tensile strength and elastic modulus at curing ages of 7 to 545 days. All mixing and casting were done in Civil Engineering Laboratories on the campus of University of Canterbury, New Zealand. Prior to mix, all materials were stored in the laboratory at ambient temperature. The mixing and testing were carried out at room temperature, normally between 18^{o}C and 23^{o}C. All the materials, tests, mixing and experimental procedures have

Table 5.1: Tests on Mortar and SCC and references to their results

TESTS	AIMS	CTR[1]	GL-FN[2]	GL-CN[3]	UG[4]
Water demand of fresh mortar	To assess the influence of binders on flowability and water demand of mortar	Fig. 5.1	Fig. 5.2	Fig. 5.3	Fig. 5.4
Compressive strength tests on hardened mortar	To assess the influence of binders on strength activity index of mortar	Fig. 5.5	Fig. 5.6	Fig. 5.7	Fig. 5.8
Slump flow and T_{500} on fresh SCC	To assess the influence of binders on flowability, unconfined flow rate and VSIV of SCC	Tab. 5.2	Tab. 5.3 Fig. 5.9 (a)	Tab. 5.4 Fig. 5.9 (b)	-
Compressive strength, splitting tensile strength and elastic modulus tests	To assess the influence of binders on long-term mechanical properties of SCC	Figs. 5.10, 5.12, 5.14, 5.16, 5.17, 5.19, 5.21, 5.23, 5.24, 5.25, 5.27, 5.29, 5.31, 5.32	Figs. 5.11, 5.18, 5.26	Figs. 5.13, 5.20, 5.28	Figs. 5.15, 5.22, 5.30
Microstructure Examination	To assess the nature of the hydrated binder	Figs. 5.33 (a) (b)	Figs. 5.33 (c) (e) (g)	Figs. 5.33 (d) (e) (f)	Fig. 5.33 (h)

[1] Control materials class: GP cement, class F and C fly ashes and limestone powder.
[2] Glass powder classified according to fineness: having fineness of 10 µm, 20 µm and 40 µm; added at 30%
[3] Glass powder classified according to content: added at 20%, 30% and 40%; having fineness of 20 µm
[4] Glass powder classified according to quality: unwashed glass powder; added at 30%; having fineness of 20 µm

already been described in Chapter 3. Before undertaking tests, the specimens were prepared by grinding and levelling their uneven top surfaces. For each set of data, two to three specimens were tested and the average value was reported. In the case of variability in results, an additional specimen was also tested and the average value was recorded. The data range indicating no statistically significant difference between test results was selected only. The complete set of tests carried out and references for their results in this chapter are summarized in Table 5.1.

5.2 Strength activity indexes of mortars incorporating glass powder

In this section, the influence of glass fineness on water demand of glass incorporated mortars for a specific workability has been discussed. In addition, water requirements of various glass contents to maintain constant consistency of mortar have also been determined. In parallel to this, the effects of fineness and substitution level on strength activity index of ground glass mortar have been investigated. Overall, this section presents an assessment of the pozzolanic activity of waste glass, which is ground to different finenesses and incorporated as various partial replacements of cement, in mortars as well as its behaviour, in terms of strength activity index compared to GP cement (GP), class F and C fly ashes (FAF and FAC) and limestone powder (LP).

5.2.1 Evaluation of water demand

Figure 5.1 illustrates the water demand of GP, FAF, FAC and LP to achieve the predefined flow range of 110+/-5 mm in compliance with ASTM C109. In general, the incorporation of FA reduces the water demand of mortar and consequently, permits the mortar to be produced at a lower water content when compared to GP mortar of the same workability. FA starts to flow with the least water required and is very sensitive to the variation of w/b ratio (Liu, 2009). In this study, the reduction of 4.5%-6.8% was observed in water demand of FA mixes compared to GP. This finding can be related to the spherical particle shape of FA, which leads to the reduction in water requirement or increase in the consistency of the paste. Dietz and Ma (2000) similarly reported that inclusion of 10-50% FA reduces water demand due to better particle packing. In particular, water demand of FAC30% was found to be lower by 2.4% than FAF30%, which can be linked to the fact that coarser FAs or those with high levels of carbon generally produce a smaller reduction in water demand (Thomas, 2007).

Similar to FA, LP also affects the performance of the concrete (Livesy, 1991) and helps to reduce water demand (Allahverdi and Salem, 2010; Kopanitsa et al., 2002). Replacing cement with LP leads to an increase in the sensitivity to the change of w/b ratio (Domone and Chai, 1997); however, LP is lesser sensitive to this variation in comparison to FA (Liu, 2009). This fact is also evident in this study as LP30% demonstrated higher water demand than both FAF30% and FAC30% by 1.9% and 4.4% respectively. However, there was a reduction of 2.7% in water demand of LP30% compared to GP, which can be related to suitable texture fineness and particle size distribution of mortar containing LP (Gudissa and Dinku, 2010). This finding is compatible with that reported by Sakai et al. (2009) that the particle size distribution and the particle shape of LP lead to the increased fluidity of the paste compared to the standard GP mix, resulting in reduced water demand.

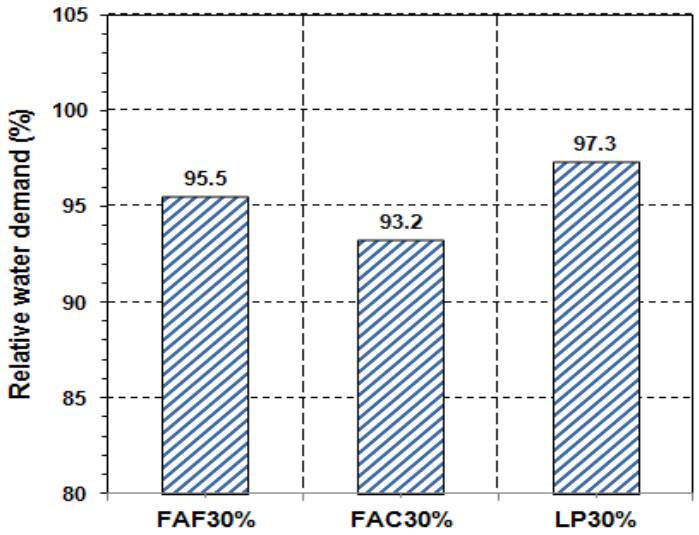

Figure 5.1: Water demand of FAF30%, FAC30% and LP30% relative to GP

(a) Effects of glass fineness on water demand

Figure 5.2 demonstrates the water demand of GL-FN mixes to achieve the predefined flow range of 110+/-5 mm in relation to GP. The results clearly indicate that the water requirement of glass incorporated mortars, to maintain the target flow as that of control mortar, varies depending on the inner structure and fineness range of glass particles. As a first estimation, the water demand increases with grinding due to the increased particle number and surface area. However, depending on the initial particle shape and surface characteristics, grinding may also decrease the water requirement (Kiattikomol et al., 2001). In the present case, the water requirement slightly reduced at lower grinding rates (40G30%). This could be related to the crumbling of coarse glass particles, which might absorbed most of the mixing water at the beginning of the mixing. However, as the grinding continued, water requirement to maintain the same consistency started to increase due to a rapid increase in the surface area of glass particles (Ferraris et al., 2001). The water demand reduced by 4.4% and 2.3% from 10 µm to 20 µm and from 20 µm to 40 µm glass mortars respectively. These findings are consistent to those reported by Shao et al. (2000) and Khmiri et al. (2012), who declared that the water demand of the mix decreases with the reduction in the glass fineness present in the mix.

In comparison to GP mortar, the relative water demands of 10G30%, 20G30% and 40G30% were found to be 102.3%, 97.7% and 95.5% respectively. Shao et al. (2000) consistently noticed that the water demands for glass sizes, ranging from 38 µm to 150 µm, were found to be lower than GP. It can also be seen that the water demand of 10G30% exceeded GP by 2.3%, which might be due to the significant variation in the finenesses of both materials. Comparing with other control mineral admixtures, the water required to produce a flow of

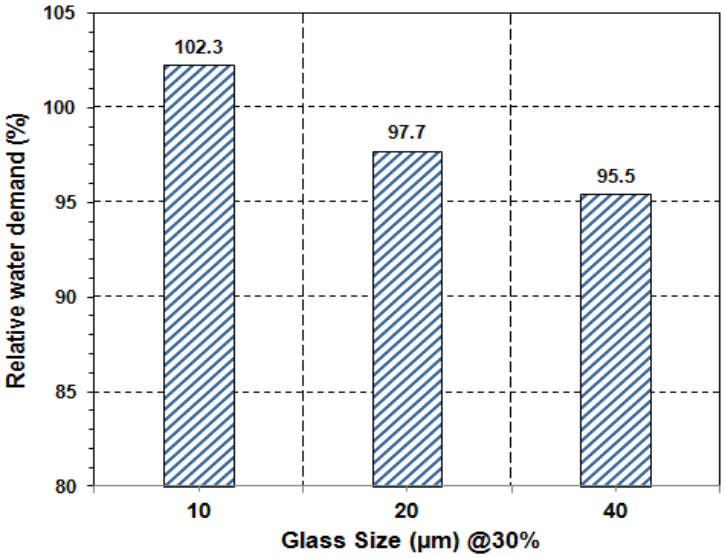

Figure 5.2: Effects of glass fineness on water demand relative to GP

110+/-5 mm for both 40G30% and FAF30% was 95.5% of the GP mortar, which is approximate to that reported by Schwarz and Neithalath (2008) for almost similar material sizes. Furthermore, 20G30% showed relatively similar water demand as that of LP30%, which might be due to the same softness level of 20 µm glass achieved by grinding as that of LP.

(b) Effects of glass content on water demand

Figure 5.3 illustrates the water demand of GL-CN mixes, to achieve the predefined flow range of 110+/-5 mm in relation to GP. The results clearly indicate that the water requirement of glass mortars, to maintain the target flow as that of control GP mortar, varies depending on their replacement level as a cement substitute in mortar. There was a noticeable reduction in water demand at the 20% glass replacement level compared to the GP control. The water demand, however, increased above the 20% replacement level resulting in an increase of 2.4% and 3.5% from 20% to 30% and 30% to 40% respectively. The requirement of water to lubricate the mortar increased with the higher replacement levels due to the increased surface area of glass particles and the number of angular-shaped glass particles in the mix (Shekhawat and Aggarwal, 2014) resulting in lesser fluidity. These results are in consistence with the findings of Metwally (2007) and Vandhiyan et al. (2013) that there is a great reduction in slump (loss in workability) when increasing the amount of waste glass in the mix; however, these studies were limited up to 20% glass replacement and further addition of waste glass beyond 20% was not investigated. Conversely, Khatib et al. (2012) and Kumarappan (2013) proved in their studies that there was an increase in the slump with the increase in the glass powder content in the mix, which is inconsistent to the present research.

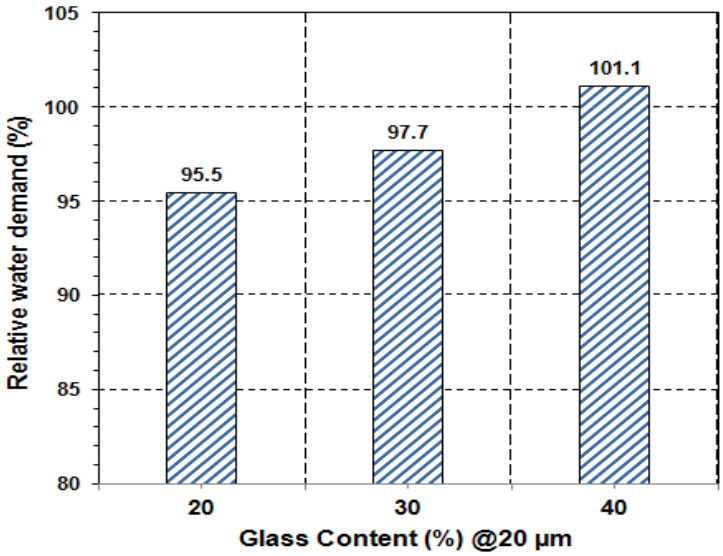

Figure 5.3: Effect of glass content on water demand relative to GP

Compared to GP mortar, the water demand of 20G20%, 20G30% and 20G40% were found to be 95.5%, 97.7% and 101.1% respectively. The particle size distribution of 20 µm glass powder, particularly in the finer range of particles, compared to GP cement might be the reason for the difference between the water demands of these two materials. As the glass content increased, the proportion of finer portions of glass powder also increased in the mix, leading to an increase in the relative water demand. 20% glass content, which means around 10% slightly finer material than GP, might be too low for the mortar to show higher relative water demand and hence, water absorption capacity of glass powder might be dominant in 20G20% reducing the water demand compared to GP. However, it is difficult to identify which of these reasons was the dominant factor responsible for the water requirement of each mix. The results also imply that 20G40% demonstrated reduced water demand than GP, which might be related to the significant reduction of cement content in the mix, which reduced the requirement of water to achieve the constant flow range. Additionally, 20G30% and LP30% demonstrated minor difference in water demand whereas, 20G20% and FAF30%, though having different finenesses, required similar quantity of water to achieve the same flow potentially due to the difference in their replacement levels. It is also interesting to note that 40G30% performed similarly to 20G20% in terms of water demand to achieve the constant flow as that of all other mortar types.

(c) Effects of glass quality on water demand

Figure 5.4 illustrates the comparison between the water demand of unwashed glass incorporated mix and washed glass modified mix, both having glass powders of similar fineness and replacement level, to achieve the predefined flow range of 110+/-5 mm in relation to GP. It was observed that 20UG30% required considerably higher water content to

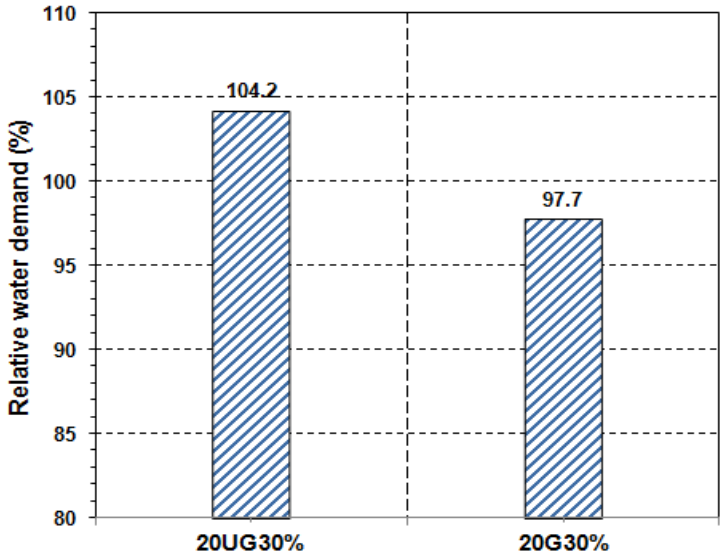

Figure 5.4: Comparison between water demand of 20UG30% and 20G30%

achieve the specified flow as that of GP mortar. This could be related to the presence of impurities and organic content in the unwashed glass that changed the material properties. In addition, the difference between water demands of unwashed glass mix and washed glass mix was further increased, where 20UG30% required higher water content than 20G30%.

5.2.2 Evaluation of pozzolanic behaviour from strength activity indexes

A pozzolan is defined as a siliceous or siliceous and aluminous material which in itself possesses little or no cementitious value but will, in finely divided form and in the presence of moisture, chemically react with the calcium hydroxide at ordinary temperatures to form compounds possessing cementitious properties (ASTM C125-15b). Compressive strength of mortar containing pozzolanic material is a function of both the pozzolanic reaction and particle packing. Hydration and pozzolanic reactions are the chemical reactions between GP cement and water and GP cement plus pozzolan and water respectively, but packing effect is a proper arrangement of small particles, which fills the voids and contributes to the compressive strength without undergoing any chemical reaction (Goldman and Bentur, 1993; Kiattikomol et al., 2000; Isaia et al., 2003). ASTM C 618 specifies that mortar incorporating a natural pozzolan should have strength activity index of at least 75% of the standard mortar at the curing ages of 7 or 28-days, when it is used at the rate of 20% by weight of cementitious materials. Strength activity index with GP cement is a measure of reactivity with a given cement and is subject to variation depending on the source of both the natural pozzolan and the cement (ASTM C618-15). It is calculated as the ratio (%) between the compressive strength of mortar containing substituting materials by weight of binder and that of control mortar at the same curing ages. The compressive strength development in CTR mortars have been presented in Figure 5.5. These tests were carried out at 7, 28, 90 and 180 days of standard water curing. The measurement of each batch at a particular age reported in this section is an average of three tests, having the maximum standard deviation of 10%. It was found that compressive strengths of standard GP mortar at the ages of 7, 28, 90 and 180-days were 44.8, 58.4, 67.0 and 70.8 MPa respectively. This implies that GP achieved about 75% of its 28-days strength at 7-days.

At an early age of 7-days, the compressive strengths of FA mortars were less than that of the standard GP mortar. It is already known that though FA shows pozzolanic activity, it does not fully react with $Ca(OH)_2$ at early ages of hydration (Wang et al., 2004). In addition, the rate of pozzolanic reaction compared to that of GP leads to lower strength at early ages (Liu, 2009). Therefore, compressive strengths of the mortars FAF30% and FAC30% were

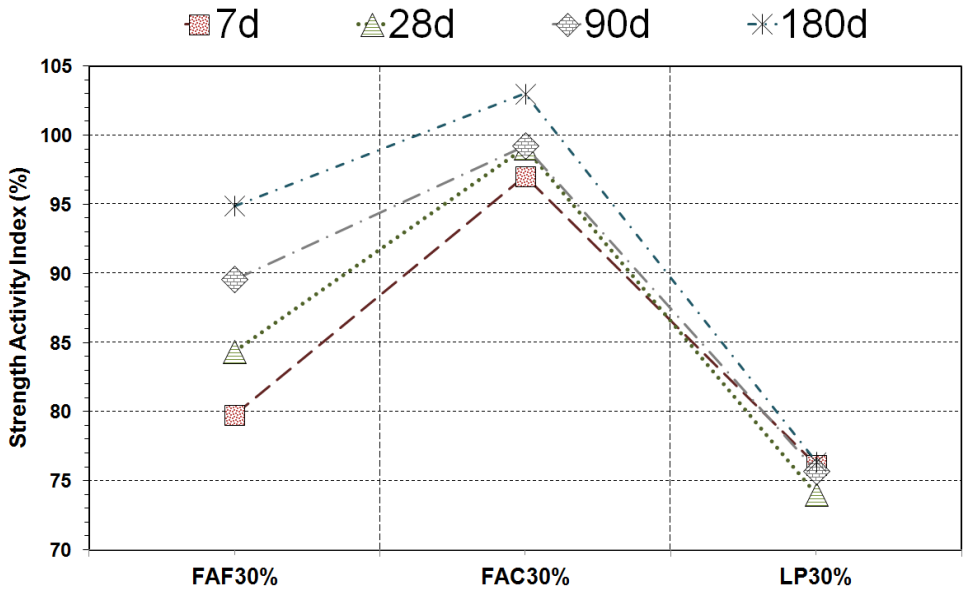

Figure 5.5: Strength activity indexes of FAF30%, FAC30% and LP30%

20.2% and 3.0% lower respectively, in comparison to GP at 7-days in the present study. This finding is consistent to that reported by Islam and Islam (2013) that at early ages of curing, the GP mix achieves relatively higher compressive strength as compared to FA mix. As the curing time progressed, FA mortars demonstrated their pozzolanic nature at 28-days. In particular, compressive strengths of the GP mortar and the mortar incorporating 30% FAC were nearly the same, which agrees to the finding by Felekoğlu et al. (2007). In addition, the rate of strength loss in FAF30% reduced from 20.2% at 7-days to 15.6% at 28-days than GP, which indicates the increase in degree of pozzolanic reaction, agreeing to Liu (2009). These results also reveal that both FAs fulfilled the criteria for being pozzolanic in accordance to ASTM C618, even when used at 30% replacement rate in mortar. FAC30% exhibited only 0.8% lower strength than GP mortar at 90-days. This is consistent to Thomas (2007) that long-term strength development is improved when FA is used and at some age, the strength of the FA mix will be equal to that of the GP mix. By 180-days, the compressive strength of FAC30% exceeded GP mortar by 2.1 MPa. Yamoto and Sugita (1983) also found that later age strength of fly ash mix is higher than that of control.

The early strength gained by LP30% was 4%-24% lower than the other CTR mixes. This might be due to the fact that LP does not participate in cement hydration as it is only a filler in mortar or concrete (Ye et al., 2007). However, these findings contradict those of Newman et al. (2003) who reported that the blending of GP cement with 10%-40% ground LP improves the early strength and also with Felekoğlu et al. (2007) who reported that LP fillers are more effective than FA in terms of early strength gain. The rate of strength gain did not increase in LP30% mortar even at 28-days and hence, it revealed 26.0% lower strength compared to GP. It has been established that LP filler does not have pozzolanic properties

but the continuous hydration of GP cement present in the mix can still contribute to strength development. This fact also became evident in this study by the continuous strength gain with curing age, though the rate of strength gain remained almost constant. At 90-days, LP showed 24.3% lower strength than GP mortar, which agrees to the findings by Nehdi et al. (1996) and Celik et al (2014) that higher levels of LP beyond 15% replacements cause significant strength loss in mortar. In addition, LP30% showed 15.5%-23.8% lower strength in comparison to FA mixes at 90-days. With the progress in curing time up to 180-days, LP30% did not show much strength improvement and gained 23.6% lower strength than GP. Menendez et al. (2003) also reported that LP addition reduces the later strength due to the dilution effect. However, it is also clear from the results that FA showed significant gain in pozzolanacity with curing time up to 180-days while LP did not, which agrees to Liu (2009).

(a) Effects of glass fineness on strength activity index

It has been established that grinding the glass powder improves the strength gain related with pozzolanic activity due to the increased surface area. However, the pozzolanic reaction takes place when the amorphous silica of glass is exposed to water molecules in order to react with $Ca(OH)_2$ obtained from hydrated cement. The extent to which individual glass particles are exposed depends on the surface of the individual grains relative to the surface of particles in which they are contained. This slow reaction can be accelerated by grinding process because the entrapped amorphous silica in the inner domains of coarse glass particles can be released with grinding and get itself involved in pozzolanic reaction. Glass powder with higher fineness can produce higher compressive strength due to the faster pozzolanic reaction of glass and contributes extra compressive strength to mortar by the packing effect. However, the compressive strength of mortar due to the pozzolanic reaction or the packing effect cannot be distinguished. Conversely, the inner core of coarse glass may carry less reactive compounds, which may decrease the efficiency of grinding in terms of pozzolanic activation.

Figure 5.6 demonstrates the strength activity indexes of GL-FN mixes. The results clearly indicate that the strength activity indexes of glass incorporated mortars, produced to maintain the target flow as that of control mortar, varied depending on the inner structure and fineness level of glass particles. Mortars with the smaller particle size of glass had higher strength activity indexes than those with larger particle size, which confirms the packing effect of the material, similarly reported by Neithalath (2008). Shao et al. (2000) suggested that relatively higher early strength index of 10 µm glass can be attributed to the high content of Na_2O in glass. The strength activity indexes of mortar containing 20 µm glass powder at the ages of 7, 28, 90, and 180 days were also calculated, which were recorded to

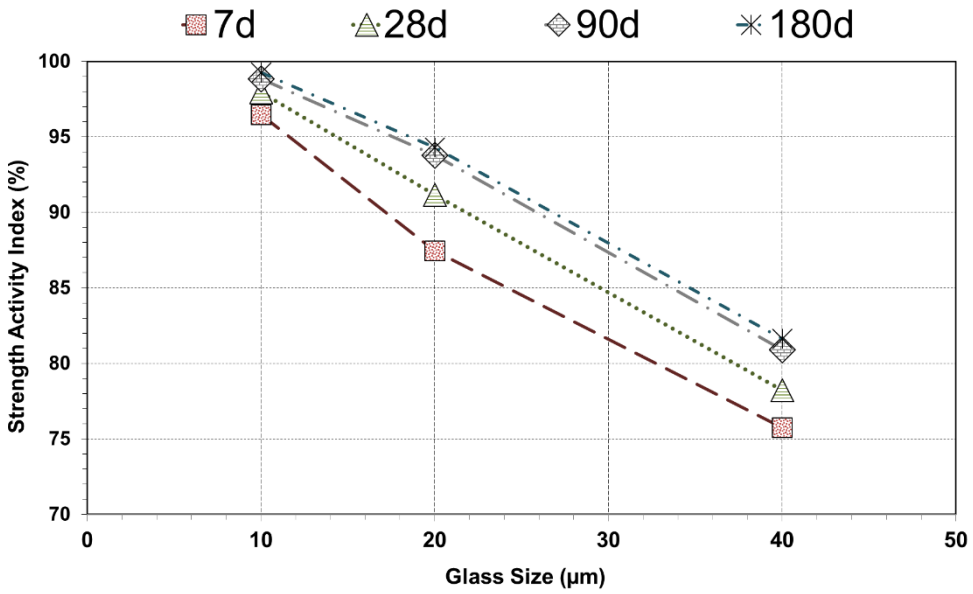

Figure 5.6: Strength activity indexes of GL-FN (added at 30% replacement rate)

be 87.5%, 91.2%, 93.8% and 94.3% of compressive strengths of standard GP mortar respectively. Idir et al. (2011) similarly noticed that significant pozzolanic activity develops over time with finer glass powder, highlighted by an increase in relative strength with hydration time. In addition, 40 µm glass modified mortar showed strength activity index that was high enough to satisfy the requirement for being pozzolanic, though it was marginally above the threshold. These results agree to the findings disclosed by Khmiri et al. (2012) that glass of 40 µm has strength activity index range of 75%-82% for white/coloured glasses.

The strength activity index results also reveal that the finer glass powder modified mixtures can develop strengths at a rate similar to or higher than that of the class F fly ash at the higher ages, which is consistent to Neithalath (2008). To elaborate, 10 µm and 20 µm glass incorporated mortars were found to exhibit pozzolanacity levels greater than that of the FAF30% at almost all the ages studied. The mortar containing 10 µm glass achieved higher strength activity indexes compared to FAF30% and lower strength activity indexes than FAC30%. Similarly, mortar incorporating 20 µm glass achieved higher strength activity indexes compared to FAF30% and lower strength activity indexes than FAC30%. It can be seen that the compressive strength of 20 µm glass mortar was closer to FAF30% by 180-days. However, the coarser glass mix containing 40 µm glass demonstrated lower strength indexes in comparison to FAF30% and FAC30%, which contradicts Shao et al. (2000) who reported that the 38 µm glass mix exhibits strength activity indexes higher than the class F fly ash mix by 90-days. Instead, strength activity index exhibited by 40 µm glass modified mortar was comparable to LP30% at 7-days. However, since 40 µm glass was initially ground to improve its fineness, therefore, the pozzolanic reaction accelerated and improved the later-age strength of 40 µm glass modified mortar in comparison to LP30%.

(b) Effects of glass content on strength activity index

It has been recognized that high brittleness of glass causes cracks, which leads to an incomplete adhesion between glass and cement paste interface. The poor geometry of waste glass prevents homogeneous distribution within the mix. Accordingly, higher amounts of glass powder contribute towards greater strength loss (Bhandari and Tajne, 2013). In addition, pozzolan reacts with available CH producing CSH similar to that produced in cement hydration reactions. The amount of hydration product CH is governed by cement content. Hence, there is an upper limit for cement replacement level, beyond which no further pozzolanic reaction of glass can occur (Du and Tan, 2014). In a mix where glass is present in higher proportions, there is insufficient cement paste available within the mix to assist bonding with all particles, resulting in the formation of microscopic voids, which adversely affect strength (Adaway and Wang, 2015). Therefore, when a higher percentage of glass is utilized, it can only play the role of an inert filler without being activated (Du and Tan, 2014) and will potentially decrease strength (Adaway and Wang, 2015). Conversely, lower replacement levels of glass powder leave higher amounts of cement particles available to undergo bonding within the mix and hence, promote higher compressive strength.

In the present study, strength activity indexes of various replacement levels of glass powder were investigated in order to reveal its pozzolanic behavior with variations in its contents, as illustrated in Figure 5.7. It can be observed that mortars with higher contents of glass powder have lower strength activity indexes in comparison with the lower contents; however, the difference becomes less evident with prolonged curing time, similarly reported by Nwaubani and Poutos (2013). The strength activity indexes of mortar containing 20% GL at the ages of

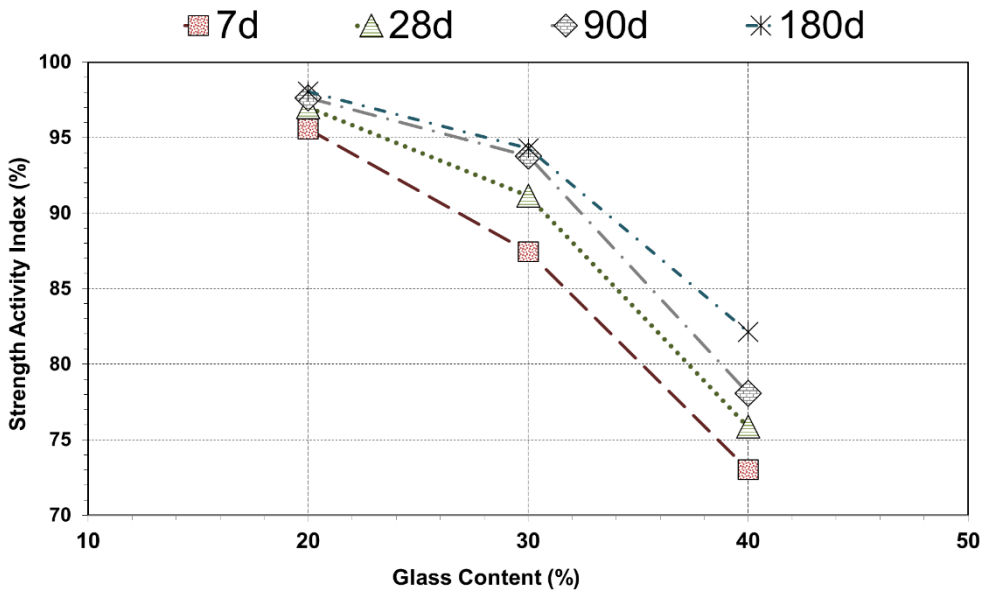

Figure 5.7: Strength activity indexes of GL-CN (having fineness of 20 µm)

7, 28, 90, and 180-days were found to be 95.6%, 97.0%, 97.6% and 98.0% respectively. These results are consistent with Taha and Nounu (2008) who observed reduction in compressive strength of a mix that utilized 20% glass powder replacing cement, simply due to change in the nature of the hydration products and CSH gel. Similarly, Metwally (2007) also found that using up to 20% glass to replace cement causes reduction in compressive strength. Moreover, strength activity indexes of the mortar incorporating 30% glass reduced than that of the mortar containing 20% glass. These findings are similar to Ozkan and Yuksel (2008) who reported that compressive strength generally decreases as the replacement value of cement with glass increases, mentioning that the early strength losses are relatively high. The strength improvement at early curing ages was slow, potentially due to the pore filling effect. Furthermore, 40% glass modified mortar showed the lowest activity index up to 7-days according to the requirement for being pozzolanic; however, it became active as the hydration time progressed. This investigation also reveals that glass powder, having fineness of 20 µm, exhibits pozzolanic reaction at least up to replacement level of 40%.

The strength activity index results indicate that the mortar incorporating glass powder, even at the low dosage of 20%, demonstrated worse pozzolanic behaviour in comparison to FAC30%. However, this mortar showed better results compared to FAF30%. The performance of 30% glass modified mortar lied somewhere between FAF30% and FAC30%. These results are compatible to those reported by Shao et al. (2000), Shi et al. (2005) and Schwarz and Neithalath (2008), Schwarz et al. (2008) and Federico (2013) that the compressive strength of mortar made with glass powder as a supplementary cementing material is higher than that made with an equivalent amount of class F fly ash. However, glass powder having the same fineness as 20% and 30% modified mortars but replaced at 40% acted worse than both FAs. Alternatively, 40% glass mortar performed better than LP30%, starting from 28-days to 180-days as it showed 2.4%, 3.2% and 7.5% higher strengths at 28, 90 and 180-days respectively.

(c) Effects of glass quality on strength activity index

Figure 5.8 illustrates the comparison between the strength activity indexes of unwashed glass incorporated mix and washed glass modified mix, both having glass powders of similar fineness and replacement level. The mortar produced with unwashed glass did not fulfil the criteria to be considered pozzolanic because it demonstrated 66.2%, 64.3%, 63.7% and 62.7% strength activity indexes at 7, 28, 90 and 180-days respectively. Its comparison with washed glass powder, having same fineness and added at similar replacement level, indicates the deficiency in strength development due to the presence of contaminants in the unwashed glass powder. Similar results have been reported by Cassar and Camilleri (2012).

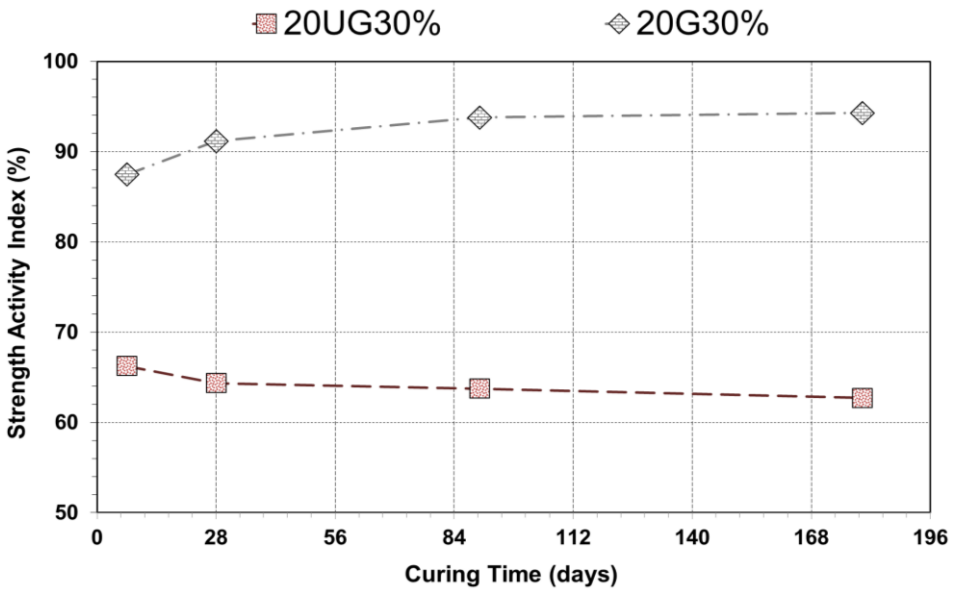

Figure 5.8: Comparison between strength activity indexes of 20UG30% and 20G30%

5.3 Influence of glass powder on mechanical properties of self-compacting concrete

The mechanical properties including compressive strength, splitting tensile strength and elastic modulus of all CTR and glass powder incorporated SCC mixes have been discussed in this section. Prior to this, SCC was produced with pre-defined fresh properties in order to perform these tests on hardened specimens. All these tests were undertaken at already designated curing ages. The materials used, test procedures, curing conditions and preparation of specimens before testing have already been explained in Chapter 3. All results are the average of three measurements. Complete individual data are reported in Appendix D.

5.3.1 Production of self-compacting concrete incorporating glass powder with target fresh properties

It is commonly reported that the addition of mineral admixtures improves concrete performance but reduces workability, provided that the volume concentration of the solid is maintained constant. The most accepted reasoning for poor workability is the increase in water demand owing to the increase in surface area after the addition of a mineral admixture (Ferraris et al., 2001). However, the use of good quality mineral admixture with higher fineness can also decrease the water demand of concrete, hence, allowing the production of concrete at lower water content in comparison to GP concrete of the same flow properties (Thomas, 2007).

In this study, all mixes were produced with the control value of 0.4 as a constant w/b ratio. The dosages of SP and SB were adjusted to produce SCC with pre-defined slump flow and flow time ranges as well as to counterbalance the water demand of all mixes. Hence, all SCC mixes were carefully cast having excellent flowability and good stability, with minimal segregation. Table 5.2 shows the fresh behaviour of CTR mixes in terms of SP dosage, T_{500} and VSIV. For the control GP mix without any mineral admixture, the SP dosage of 0.62% successfully produced the target SCC mix.

Generally, FA modified concrete has an improved workability when compared with GP concrete of the same slump, which implies that FA concrete flows and consolidates better than GP concrete. The incorporation of FA also improves the cohesiveness and reduces the segregation of concrete. In addition, FA reduces the rate and amount of bleeding, primarily due to the reduced water demand (Gebler, 1986). In this study, the mixes made with 30% FA replacements had lower SP demand than the GP, which might be due to the spherical shape and smooth surface of FA particles. Thomas (2007) indicated that the spherical particle shape of FA lubricates the mix, making it easier to pump and reducing wear on equipment. Bouzoubaa and Lachemi (2001) and Sukumar et al. (2008) similarly reported that inclusion of 17~60% FA in SCC helps to reduce SP usage to maintain the same slump flow as that of SCC made with GP cement only. Nevertheless, inclusion of FA did not significantly affect segregation and decreased flow time indicating reduction in viscosity. This is in agreement with Ferraris et al (2001), Newman and Choo (2003), and Tattersall and Banfill (1983) but in disagreement with Poon and Ho (2004) and Xie et al (2002). These dissimilar conclusions might be due to different types and sources of SP and fineness ranges of FA used in the studies. In addition, the incorporation of 30% LP replaced by GP in the SCC mix demonstrated better workability in comparison to GP hence, lower amount of SP was required to achieve similar slump flow as that of GP mix.

Table 5.2: Fresh behaviour of CTR mixes

CTR	w/b	SP by wt. of binder (%)	Flow (mm)	T_{500} (sec)	VSIV	Segregate/ Bleed
GP	0.4	0.62	700	5.5	0	None
FAF30%	0.4	0.53	680	3.1	0	None
FAC30%	0.4	0.60	690	4.0	0	None
LP30%	0.4	0.53	690	5.3	0	None

(a) Effects of glass fineness on superplasticizer demand

Table 5.3 demonstrates the influence of glass fineness on the fresh behaviour of SCC in terms of slump flow, T_{500}, VSIV, segregation and bleeding. It can be seen that the workability

of SCC reduced by using finer glass powder as cement replacement, resulting in an increased requirement of SP dosage to achieve target flow. There was decrease of 8.6% and 32.0% in SP demand from 10 µm to 20 µm and 20 µm to 40 µm glass powder incorporated mixes respectively, which might be related to the fact that finer particles increase the water demand due to an increase in the surface area. These results are consistent to those reported by Metwally (2007) that the addition of finer glass powder results in a higher surface area, which requires more water to achieve the same workability. However, Taha and Nonnu (2008) demonstrated conflicting conclusion which might be due to the fact that they used coarser range of glass powder than Metwally (2007). In addition, T_{500} increased as the maximum glass particle size increased, which is partly due to the increased interparticle contact and surface interlocking leading to increase in viscosity.

Table 5.3: Fresh behaviour of GL-FN

GL-FN (@30%)	w/b	SP by wt. of binder (%)	Flow (mm)	T_{500} (sec)	VSIV	Segregate/ Bleed
10 µm	0.4	0.58	700	4.0	0	None
20 µm	0.4	0.53	690	4.2	0	None
40 µm	0.4	0.36	690	4.8	0	Bleeding

(b) Effects of glass content on superplasticizer demand

Table 5.4 shows the influence of glass content on the fresh behaviour of SCC. It is evident from the results that inclusion of higher contents of glass led to a decrease in the SP demand to achieve constant flow but an increase in flow time. The reductions of 5.4% and 24.5% were observed in SP demand from 20% to 30% and 30% to 40% glass contents. The lower SP demand at higher glass replacement ratios could be due to higher compactness of concrete granular skeleton. Identical results have been reported by Ali and Al-Tersawy (2012) that same slump flows for recycled glass SCC mixes in comparison to control mix can be achieved at the reduced SP dosages and the slump flows of recycled glass SCC mixes increase with the increase in recycled glass content, indicating lower SP demand with the increase in glass replacement level. Additionally, 20UG30% that had the same fineness as that of glass powders used in GL-CN mixes, showed the maximum SP demand of 0.71% by

Table 5.4: Fresh behaviour of GL-CN

GL-CN (@20µm)	w/b	SP by wt. of binder (%)	Flow (mm)	T_{500} (sec)	VSIV	Segregate/ Bleed
20%	0.4	0.56	710	3.8	0	None
30%	0.4	0.53	690	4.2	0	None
40%	0.4	0.40	690	4.9	0	Bleeding

weight of binder. This finding might be related to the presence of impurities and organic content in the unwashed glass that increased its SP demand to achieve an optimum flow range. T_{500} increased with the increase in glass content, which is related to the increase in viscosity of the corresponding mixes.

(c) Discussion on bleeding observed in some glass modified mixes

From Tables 5.1 and 5.2, it can be seen that the replacement of GP cement by coarser ground glass and inclusion of higher glass content as cement substitute resulted in the increased bleeding of SCC, as if excess water could not be held by these glass particles. Figures 5.9 (a) and (b) show the bleeding observed in two glass incorporating mixes 20G40% and 40G30% respectively. After the mixer was stopped, thin layers of water appeared on the surface of these mixes and aggregates settled at the bottom. The concrete mix containing 40 µm glass powder was the worst of all because its aggregates rapidly settled during the slump flow test. This glass powder was coarser than GP cement and hence, the total surface area significantly decreased when it was replaced with GP cement. The water retained by particles was, therefore, less and more bleeding appeared. The halo of bleeding water at the edges of the SCC, during the slump flow tests, increased from 0 mm to 10 mm, when grain size of the glass powder increased from 10 µm to 40 µm and replacement level increased from 20% to 40%. This shows that the mixes containing coarser glass and including higher replacement glass levels were not homogeneous. This confirmed Paulou's discussion (2003) that the use of glass powder in concrete can have the problems of segregation and bleeding. This finding also correlates to Mackechnie and Munn (2012) that bleed of concrete is increased with increase in glass input. However, all these issues were resolved by the addition of SB, hence the mixes with VSIV equal to 0 were achieved, as mentioned in Table 5.1 and 5.2.

(a) 40G30% **(b) 20G40%**

Figure 5.9: Bleeding demonstrated by glass incorporated SCC mixes

5.3.2 Compressive Strength

The compressive strength measurements were taken at 1, 3, 7; 28, 90; 180, 365 and 545 days for early, normal and long-term strengths respectively. The data for CTR mixes have been illustrated in Figure 5.10. The compressive strength demonstrated by GP mix surpassed all other CTR mixes and continued to demonstrate strength increase until the last testing schedule. The early compressive strength development achieved by GP mix was the highest, which demonstrates its better pozzolanacity compared to other binders. It had the highest compressive strength of 18.5 MPa at the day it was removed from mould and exceeded its design strength at 7-days. The 50 MPa GP mix reached 65 MPa at 28-days of curing age. The percent compressive strength increase in GP from 28 to 90-days was found to be 14.7%, which reduced to 13.1% from 90 to 180-days. As the curing time prolonged to 545-days, the rate of strength increase in GP concrete was found to be 5.6% compared to 365-days.

The early compressive strength development in FA modified mixes was significantly lower in comparison to GP, possibly because the pozzolanic reactions of FAs were not sufficient at the early ages, similarly reported by Ramanathan et al. (2013). It was observed that the FA mixes sustained lower compressive strengths ranging from 15%-38% than the GP at 7 days, which might be connected to its inherent slow hydration rate. Mackechnie and Kesha (2005) identically discussed that the FA concretes are known to have slower strength development within the early ages of curing. FA generally exhibits very little pozzolanic reaction at the early ages and rather, like a filler, mainly serves as nuclei for precipitation of $Ca(OH)_2$ and CSH from the cement hydration (Fraay et al., 1989; Ramanathan et al., 2013). Additionally,

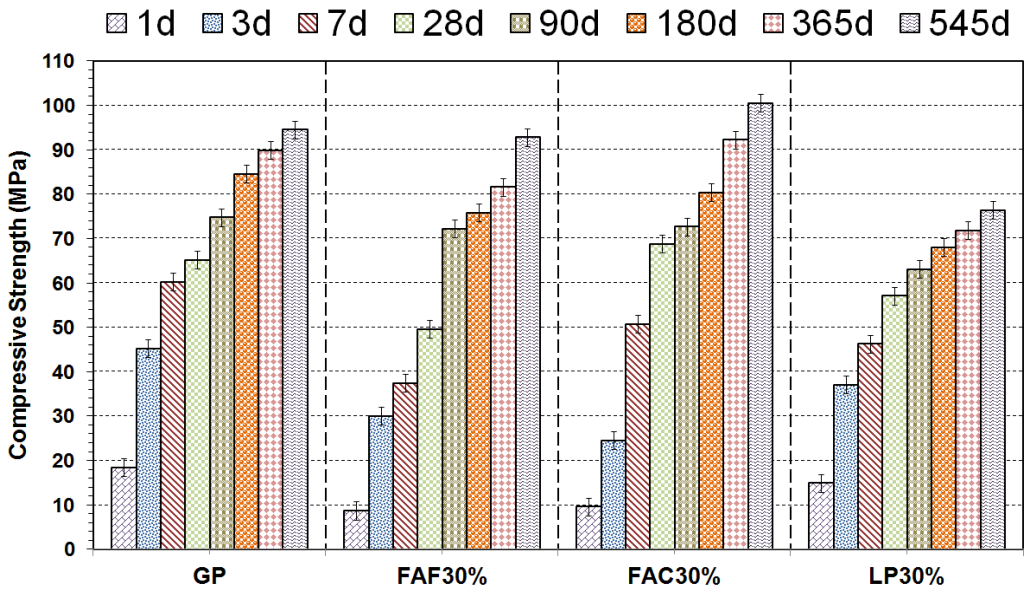

Figure 5.10: Compressive strength development in CTR mixes

class C fly ash concrete had higher compressive strength than class F at 7-days, similarly observed by Liu (2009). As the curing time advanced, FAC30% exceeded by 5.5% in compressive strength compared to GP at 28-days. This finding is consistent to Vengala et al. (2003) who also reported that the use of class C FA for producing SCC results in an increase of 28-days compressive strength. On the other hand, FAF30% demonstrated 23.9% lower strength than GP at 28-days, which might be due to its slower reaction rate compared to GP. However, the pozzolanic activity exhibited its presence clearly at 90-days and both FA mixes reached the compressive strengths closer to each other but still 2.8-3.5% lower in comparison to GP. Naik and Singh (1997) similarly reported that 90-days compressive strengths of concretes containing FA are not significantly influenced by the class of FA. Furthermore, the rates of strength increase from 180 to 365-days for FAF30% and FAC30% were 7.6% and 14.8% respectively, which were higher than GP found at 5.9%, indicating better pozzolanacity of FAs compared to GP. At 545-days, FAF30% exhibited 13.7% strength increase from 365-days, which is more advanced than GP. However, FAC30% outweighed both GP and FAF30% by showing 6.5% and 8.4% higher compressive strengths respectively. The improved long-term compressive strength might be due to the fact that in the case of FA, filling of the voids between the larger GP cement particles and increased production of secondary hydrates by pozzolanic reactions with the lime resulting from the primary hydration, enhances compressive strength (Yahia et al., 2005).

The early compressive strength development of LP30% was comparatively better than both FAF30% and FAC30%. At 1-day, LP30% showed 55%-71% higher strength than FA mixes but 19.5% lower strength than GP. This finding is consistent to Donme (2007) who reported that LP makes a contribution to strength gain, mainly in the beginning of hardening phase. LP causes better packing of cement granular skeleton and larger dispersion of cement grains (Opoczky, 1992). Furthermore, it acts as the crystallization nucleus for the precipitation of CH (Soroka and Stern, 1977). These simultaneous effects accelerate the hydration of cement grains and hence, improve early strength. At 7-days, LP30% mix demonstrated 23.1% and 8.7% lower compressive strength in comparison to GP and FAC30% respectively but 23.8% higher than FAF30%. As the curing time progressed to 28-days, the addition of LP decreased the compressive strength when compared to the GP control mix, suggesting its presence in SCC as only an inert material. Identical findings were noticed by Uysal and Yilmaz (2011). Likewise, the incorporation of LP led to 17.0% lower compressive strength compared to FAC at 28-days though equal cement content and a constant w/c ratio were employed in both mixes. Consistent results were reported by Siad et al. (2010). An improvement in compressive strength of LP30% from 7 to 28-days has been similarly observed by Boel (2010) who stated that LP helps realizing a more dense structure

by filling effect with positive influence on compressive strength with curing. At 90-days, the dilution effect became more prominent, leading to a relative strength reduction when LP was added as cement replacement, consistently noticed by Dhir et al. (2007), Ghrici et al. (2007), Ramezanianpour et al. (2009) and Guemmadi et al. (2009). Hence, all other CTR mixes had 14.5%-18.5% higher compressive strengths in comparison to LP30%. Finally, LP30% showed 6.4% strength increase from 365 to 545-days that was still lower than GP, FAF30% and FAC30% by 18%-24%. These overall results are in parallel with Uysal and Yilmaz (2011) and Diab et al. (2016) who also reported that LP acts like an inert mineral admixture, which reduces the long-term compressive strength when used as a partial replacement of cement.

(a) Effects of glass fineness on compressive strength

Figure 5.11 demonstrates the compressive strengths of GL-FN mixes up to 545-days of standard water curing. The compressive strengths of coarser to finer range of glass powders were investigated in order to highlight the changes in the strength behavior of the glass powder with variations in particle sizes. It was found that the glass activity was more related to fineness than the other factors such as particle shape and composition (Byars et al., 2004). Primarily, the compressive strength of SCC incorporating GL dropped as the glass particle size became coarser, which is compatible with the findings reported by Shao et al. (2000), Shayan and Xu (2006), Taha and Nounu (2008) and Idir et al. (2011).

The early-age compressive strength demonstrated by GL-FN series varied according to the fineness of glass particles. On the day of sample removal from the moulds, the finest glass containing mix (10G30%) showed the highest compressive strength of 11.3 MPa, which was

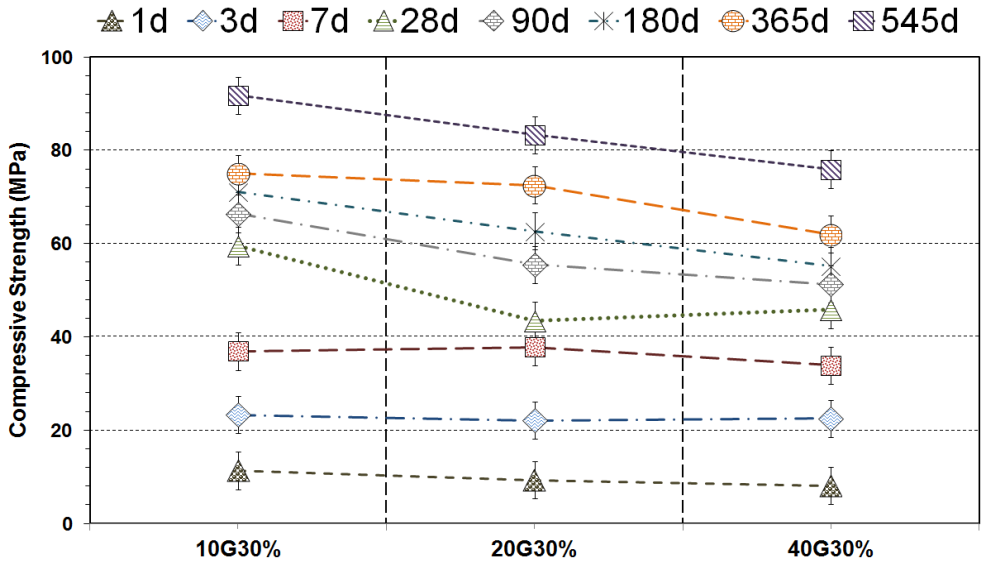

Figure 5.11: Compressive strength development of GL-FN (added at 30% replacement level) with curing age up to 545-days

17.7% and 28.3% higher than 20G30% and 40G30% respectively. The coarser glass modified mix 40G30% led to poorer performance that might be related to the retarding effect on the cement hydration caused by minor elements leached from coarser glass particles in the first hours after casting and hence, affecting the strength development at young age, consistently reported by Idir et al. (2011). Conversely, finer glass particles in 10G30% counteracted the delay in strength development, probably because of the germination effect of very fine glass particles, which acted as nuclei for cement hydrates and thus, enhanced short-term hydration. This physical effect has already been reported by several authors (Ogawa et al., 1980; Cook and Cao, 1987; Lawrence et al., 2003). The compressive strength exhibited by all GL-FN samples approached closer at 3-days, having variation in strengths up to 1.2 MPa. In addition, the pozzolanic behavior of 20G30% and 40G30% was also observed to start functioning at 3-days. The rate of compressive strengths increase from 3 to 7-days in case of 10G30%, 20G30% and 40G30% were observed to be 58.4%, 71.0% and 50.7% respectively. There were insignificant variations between compressive strengths achieved by all glass powder sizes at 3 and 7-days, similarly reported by Shao et al. (2000) who utilized 38 µm, 75 µm and 150 µm glass powders. This indicates that there was an identical level of activity undergoing in glass powders of all sizes, from finer to coarser ones, at these curing ages.

At 28-days of standard water curing, compressive strength reduced by 26.9% with the increase in glass size from 10 µm to 20 µm, potentially due to worse pozzolanic behaviour demonstrated by coarser glass as that of finer glass. An increase in the compressive strength was observed as glass size increased from 20 µm to 40 µm, which could only be related to an experimental error. However, 10G30% exhibited 16.4% and 22.7% higher compressive strength than 20G30% and 40G30% at 90-days respectively. Unlike the early-age compressive strengths, a definite improvement at normal-ages was observed in case of 10G30% as compared to 20G30% and 40G30%. Shao et al. (2000) similarly reported that compressive strength variations for different glass finenesses become more pronounced by 28 and 90 days of curing. The continuous strength development in all glass mixes indicate that there was at least a slight pozzolanic effect developed by even the coarsest glass used in this study, which was not over by 90-days of curing period and might have counteracted the negative effect of possible alkali-silica reaction (ASR). This finding confirms the previous results presented by Jin et al. (2000), Shi et al. (2004), Schwarz (2008) and Saccani and Bignozzi (2010) that the ground glass smaller than 0.3 mm does not contribute to ASR and hence, promotes strength development. Caijun et al. (2005) also mentioned that the finely ground glass powder exhibits high pozzolanic activity, and higher pozzolanic activity with increased fineness of the glass powder, which is also evident in this study.

The compressive strength increased throughout the long-term hydration time, especially for the finer glass sizes, which is a sign that there was still some pozzolanic activity occurring, similarly mentioned by Idir et al. (2011). The tests done at 180-days revealed that compressive strength reduced by 11.8% and 11.9% with the increase in glass size from 10 µm to 20 µm and from 20 µm to 40 µm respectively. These results are in agreement with those presented by Shao et al. (2000) and Shi et al. (2005). The strengths of all glass specimens further increased as the curing time progressed to 365-days. Taha and Nonnu (2008) similarly reported that the concrete containing 45 µm glass shows continuous strength gain, even until 365-days of curing. Finally, the mix 10G30% revealed marked improvement of 22.4% in strength from 365 to 545 days of testing, which is very high for this curing duration. It can be observed in Figure 5.12 and Figure 5.13 that a number of pozzolan containing mixes (FAF and glass for instance) showed an increasing trend between 365 and 545 days. The sudden increase might be due to environmental effects if the average curing temperature was somewhat lower for an extended period prior to the 365 days and then higher until 545 days. All the samples, however, were in the same climate control room so the temperature should not have changed significantly over the year but some variation is possible. A change in environmental conditions might explain why the slower hydrating pozzolanic samples displayed a sudden unexpected jump, while the GP samples did not. Some variation in results is also expected due to the limited number of samples (two) for each testing age. The best performance shown by 10G30% might be linked to the better packing since it was the finest material used. In addition, 20G30% and 40G30% exhibited lower strengths by 9.3% and 17.3% in comparison to 10G30%, which is consistent to Shayan and Xu (2006). Metwally (2007), Wright et al. (2014) and Du and Tan (2014a) equally reported that the use of finely milled glass in concrete mixes considerably improved the strength of concrete at later ages.

Figure 5.12 illustrates the comparison between the compressive strength development in some CTR mixes and the glass mixes categorized in GL-FN class. It is evident that GP surpassed these glass mixes in compressive strength development up to 545-days. Moreover, comparisons of glass when compared to FA indicate that FA at a similar particle size performed better than glass at all ages. To elaborate, 10G30% and 20G30% demonstrated almost similar compressive strengths to FAF30%, with an insignificant variation of 1% by the time of 7-days. These results are coherent to those reported by Neithalath (2008). The 28-days tests demonstrate that pozzolanic reactivity shown by 10G30% exceeded the reactivity demonstrated by FAF30%, which is noticeable as the higher strength increase of 61.2% from 7 to 28-days in 10G30% in comparison to 32.6% in FAF30%. Nevertheless, contradictory effect appeared in 20G30%, where the rate of strength

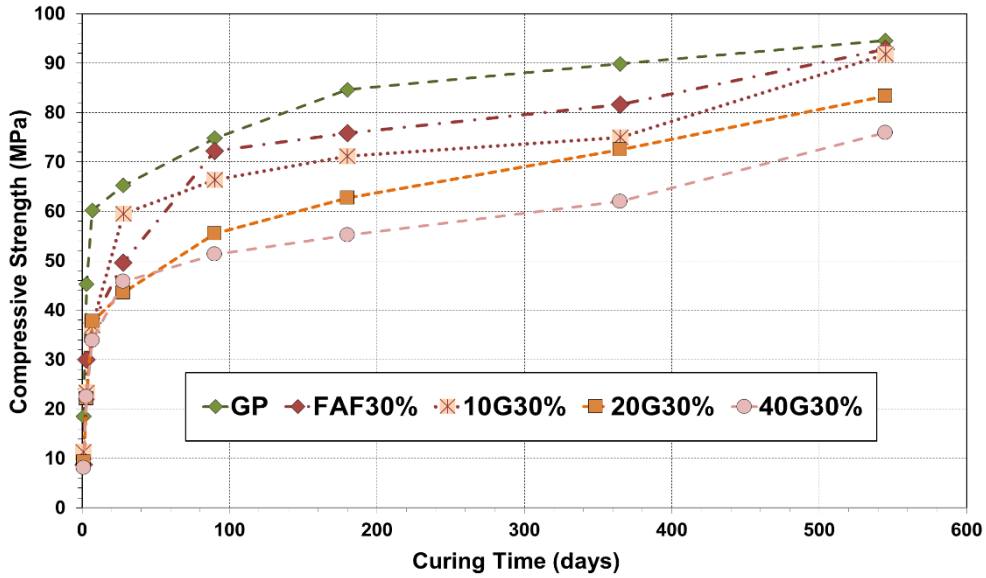

Figure 5.12: Comparison between compressive strength development in GL-FN and some CTR mixes

increase was lower than FAF30% and LP30% at 28-days. The similar pattern in the compressive strength development was observed up to 365-days. A large increase in compressive strength was observed in GL-FN mixes compared to CTR mixes, at the curing age of 545-days. Considering that the mixes containing glass had only 70% of the cement content, their long-term strength values are considered to be very good, which is consistently reported by Shayan and Xu (2006). 10G30% demonstrated 22.4%, 20G30% showed 14.9% and 40G30% exhibited 22.4% increase in the compressive strength from 365 to 545-days, which is relatively greater in comparison to 5.1%, 13.7%, 8.9% and 6.4% shown by GP, FAF30%, FAC30% and LP30% respectively. Idir et al. (2011) similarly noticed that significant pozzolanic activity develops over time with glass in comparison to GP mix, highlighted by an increase in the relative strength with the hydration time.

(b) Effects of glass content on compressive strength

The compressive strength development of GL-CN series up to 545-days of standard water curing has been illustrated in Figure 5.13. As anticipated, the compressive strength was affected by glass powder contents. It was observed that although the glass powder distribution within the composite was uniform but compressive strength varied inversely with the percentage of glass content, which is coherent with the findings reported by Dyer and Dhir (2001), Topcu and Canbaz (2004), Idir et al. (2011) and Vanjare and Mahure (2012).

The early-age compressive strength exhibited by GL-CN class varied according to the content of glass particles. At 1-day, the mix containing the lowest glass content 20G20% showed the highest compressive strength of 15.6 MPa, which was 40.4% and 53.8% higher than 20G30% and 20G40% respectively. The GL-FN mixes showed increase in compressive

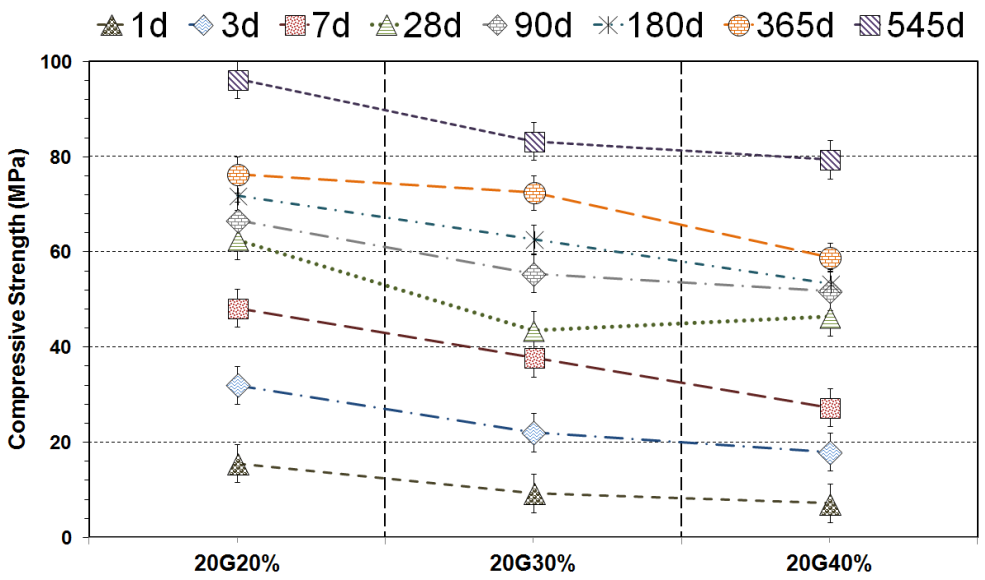

Figure 5.13: Compressive strength development of GL-CN (having fineness of 20 µm) with curing age up to 545-days

strengths at the curing age of 3-days, having strength variations of 31%-44% between each other. The mix having higher cement to powder ratio resulted in a higher strength. At 7-days, the pozzolanic behavior of 20G20%, 20G30% and 20G40% was found to begin working. The rate of strength increase in 20G20%, 20G30% and 20G40% was 50.6%, 25.8% and 51.7% respectively, from 3 to 7 days. These results are consistent with those reported by Ozkan and Yuksel (2008).

Being the highest at 28-days, 20G20% showed a positive value of compressive strength, equally reported by Vasudevan and Pillay (2013). The compressive strength reduced by 30.4% with the increase in glass content from 20% to 30% at 28-days. However, an increase of 6.7% in the compressive strength was observed as GL content increased from 30% to 40%, which could only be attributed to an experimental error. At 90-days of testing, all glass mixes improved in compressive strength; however, the mix 20G20% exhibited 20.0% and 28.6% higher compressive strength than 20G30% and 20G40% respectively, which could be related to its superior pozzolanacity. Identical observations were reported by Ismail and Al-Hashmi (2009) and Metwally (2007) that pozzolanic reactions help to improve the compressive strength in glass incorporated mixes after 28-days.

It is evident from the results that compressive strength increased throughout the long-term curing time, for all glass contents. At 180-days of curing, the compressive strength reduced by 12.6% and 15.0% with the increase in glass content from 20% to 30% and from 30% to 40% respectively. Similar results were also found by Zsigovics (2005). With the advancement in curing time up to 365-days, the mix 20G20% showed 5.2% and 29.5% higher compressive strengths than 20G30% and 20G40% respectively. The mineralogical

analysis of hydrating pastes containing glass (45 µm), undertaken by Dyer and Dhir (2001), confirmed that glass undergoes a pozzolanic reaction, which leads to enhanced strength development in mixes containing lower glass levels. Finally, the mix 20G20% exhibited improvement of 26.2% in compressive strength from 365 to 545-days of curing, possibly due to the same reason mentioned before. However, 20G30% and 20G40% demonstrated 13.5% and 17.4% lower compressive strengths in comparison to 20G20% after 545-days of hydration, due to variations in glass contents. The difference in compressive strength results, observed in mixes modified with various glass levels, has also been noticed by Taha and Nounu (2008).

Figure 5.14 shows the comparison between the compressive strength development in some CTR mixes and the glass mixes categorized in GL-CN class. It is clear from the results that the GP mix mostly exceeded all of these glass mixes in compressive strength development, which is consistent to the conclusion drawn by Khatib et al. (2012) that beyond 10% of glass addition, the compressive strength tends to decrease and is lower than that of GP control. The strength loss in glass modified mixes could be due to high brittleness of glass leading to cracks in glass particles, which then resulted in an incomplete adhesion between the waste glass and cement paste, while the poor geometry of crushed glass and reduced specific gravity resulted in heterogeneous distribution (Topcu and Canbaz, 2004). Furthermore, it has also been observed that FA at a similar replacement level performed better than glass in terms of strength development at all ages. To elaborate, LP30% showed 4.5% lower compressive strength compared to 20G20% and 60.2% and 106.9% higher compressive strength in comparison to 20G30% and 20G40% respectively, at 1-day. It appears that the

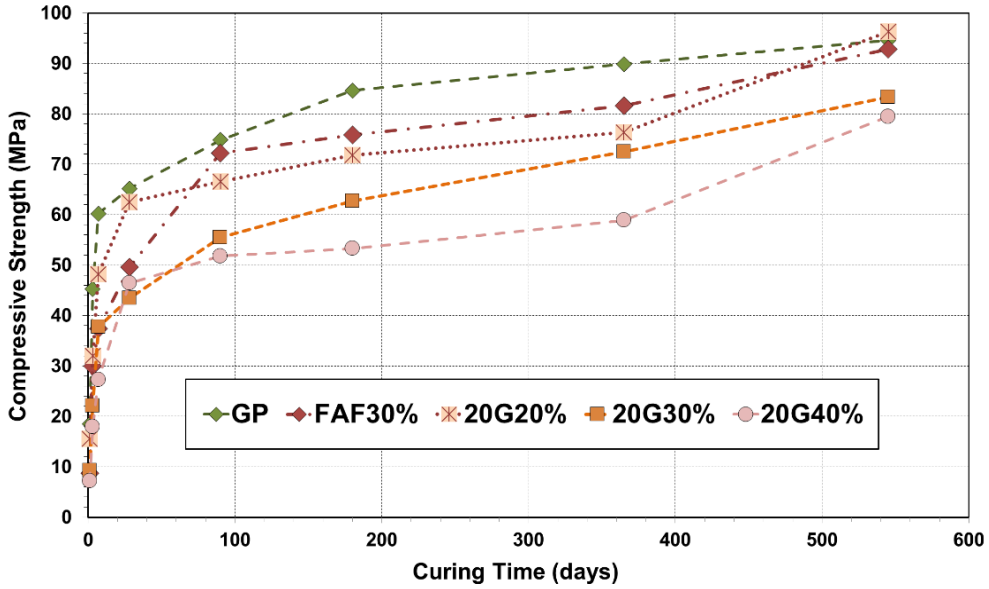

Figure 5.14: Comparison between compressive strength development in GL-CN and some CTR mixes

degree of hydration in LP30% at an early age could not function superior to the pozzolanacity of 20G20%; however, as the glass content increased, the pozzolanic reactivity of the glass mix reduced, giving LP a chance to perform better. At 7-days, 20G20% demonstrated compressive strength closer to FAC30%, within a variation of 5%; however, it achieved 4.1% higher compressive strength than LP30%. On the other hand, 20G30% showed almost similar compressive strength to FAF30% at 7-days. The compressive strength of 20G20% reduced by 4.1% compared to GP at 28-days, which is similar to Metwally (2007) and Taha and Nounu (2008) who noticed that the 28-day compressive strength decreases in concrete that utilizes 20% glass replacing GP cement, simply due to a change in the nature of the hydration products and CSH gel. The 28-days tests inform that the pozzolanic reactivity shown by 20G40% exceeded the pozzolanic reactivity demonstrated by FAF30%. The same trend in the compressive strength development was observed up to 365-days. Nevertheless, at the curing age of 545-days, much greater increase in compressive strength was observed in GL-CN mixes compared to CTR mixes. This might be linked to the same aforementioned reason discussed in 5.3.2 (a).

(c) Effects of glass quality on compressive strength

Figure 5.15 shows the comparison between the compressive strengths of unwashed glass incorporated mix and washed glass modified mix, both having glass powders of similar fineness and replacement level. 20UG30% achieved the least compressive strength of 5.1 MPa at 1-day, which might be related to the presence of impurities in the glass powder employed in 20UG30%. The unwashed glass mix (20UG30%) could only reach 21.7 MPa at 7-days, which was the lowest of all glass mixes, laying emphasis on the necessity of utilizing

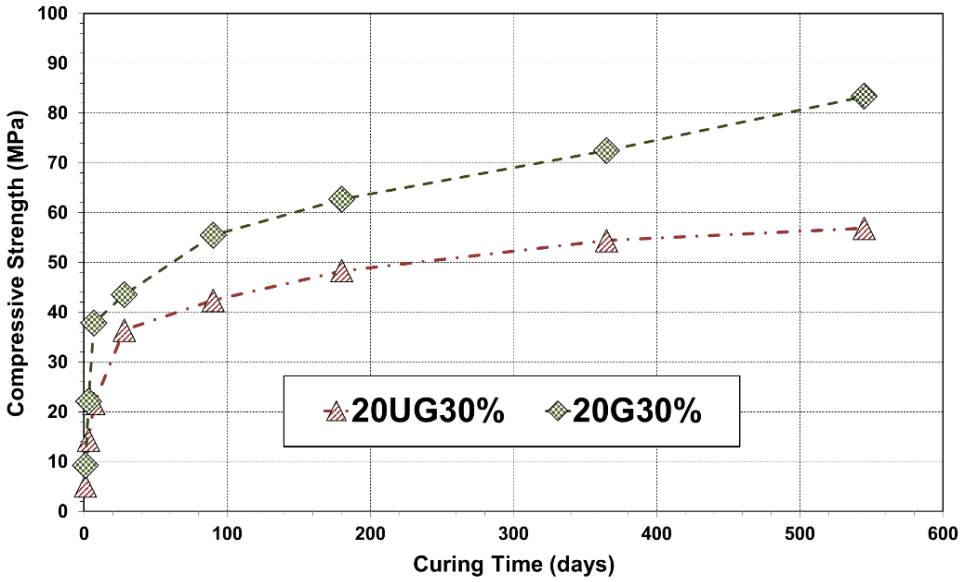

Figure 5.15: Comparison between compressive strength development in 20UG30% and 20G30%

clean glass powder in concrete. Phillips et al. (1972) also observed that the main challenges in utilizing waste glass would be the removal of contamination, processing, and cost. A reduction of 23.6% in compressive strength at 90-days was noticed in 20UG30% compared to 20G30%, although similar amounts of glass were added in both mixes. This might be due to the fact that the organic content present in the unwashed glass degrades with time, creates voids in the microstructure of concrete and hence, affects the concrete strength. Taha and Nounu (2008) similarly reported that the performance of hardened concrete incorporating waste glass is dependent on parameters including contamination and organic content in waste glass. Moreover, 20UG30% could only achieve the compressive strength almost equivalent to 7 to 28-days compressive strengths of CTR mixes even at 545-days of curing.

(d) Rate of compressive strength development in glass incorporated mixes

The ratio of the mean 545-days to the mean 28-days (545d/28d) compressive strengths for all concrete mixes is presented in Figure 5.16. It can be seen from the results that the ratio of 545-days compressive strength to 28-days compressive strength ranged from 145% for the control GP concrete to 187% for the high-volume class F fly ash concrete. Similar results have been reported by Langley et al. (1992) that the ratios of compressive strengths at a particular curing age to compressive strengths at 28-days are always higher in class F fly ash concrete compared to GP concrete. In addition, the results achieved for glass incorporated specimens clearly indicate the probability of long-term strength development from the use of glass, as concrete mixes with glass had higher 545d/28d ratio as compared

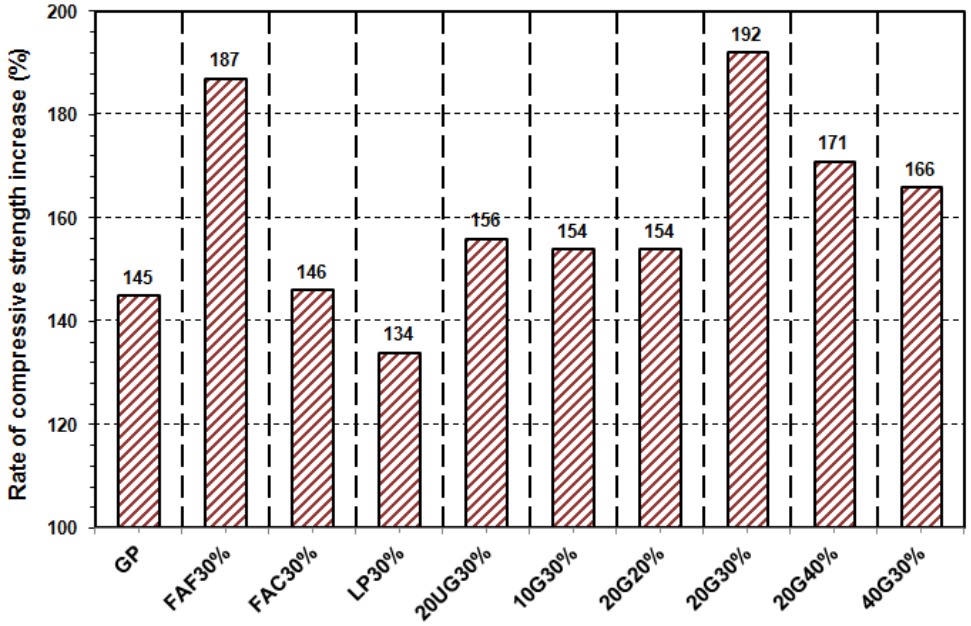

Figure 5.16: Rate of compressive strength development from 28 to 545 days in all SCC mixes

to most of the CTR mixes. This might be attributed to the pozzolanicity levels exhibited by glass powder that were comparable or better than the other types of binders employed in this study. The pozzolanicity levels improve the quality of paste in the presence of glass particles, especially at the interface transition zone (ITZ) between aggregate particles and paste. Therefore, it can be safely stated that the incorporation of GL can be useful for long-term compressive strength development in SCC mixes and its on-going performance is not less than the GP cement and other conventional supplementary cementing materials.

5.3.3 Splitting Tensile Strength

Concrete is considered a brittle material, primarily because of its low tensile strain capacity and poor fracture toughness. The tensile strength development of concrete is, therefore, important for the structural applications. In particular, findings related to the tension test are essential in predicting crack propagation patterns and quantifying the reliability of microstructure (Mimura et al. 2011, Yoshitake et al. 2012 and Swaddiwudiwudhipong et al. 2003). In the present study, splitting tensile strength measurements were taken at 7; 28, 90; 180, 365 and 545-days for early, normal and long-term strengths respectively. The data for CTR mixes have been illustrated in Figure 5.17. In general, the splitting tensile strengths showed a similar trend to the compressive strength results. The splitting tensile strength achieved by GP at 7-days was the highest of all other mixes (5.1 MPa). With curing up to 28-days, it reached 5.5 MPa, which is 7.8% higher than 7-days tensile strength. The rate of increase from 28 to 90-days was 3.6%; however, it raised to 12.2% from 90 to 180-days. Finally, from 365 to 545-days, the splitting tensile strength improvement in GP was 5.9%.

The long-term splitting tensile strengths shown by FAs were considerably lower than GP concrete, similarly noticed by Kou et al. (2007). It was observed that splitting tensile strength of FAF30% was 4.5% higher than FAC30% at 7-days; however, both FAs were 14%-17% lower than GP. These results are consistent with Naik et al. (1991) who reported that class F fly ashes in concrete cause reduction in splitting tensile strength at early ages. However, the study of early tensile strengths in FA modified mixes is complicated both in terms of the testing system and because the relevant material properties are time-dependent and change rapidly over the curing period. The results of 28-days tests support this explanation as FAF30% and FAC30% showed considerable improvements of 5.5% and 3.6% in splitting tensile strength compared to GP, with FAF30% being insignificantly higher than FAC30%. Similar results have been reported by Naik et al. (1991) and Kathirvel et al. (2013). With the progress in curing period up to 180-days, 4.7% and 1.6% lower strengths than GP were observed in the case of FAF30% and FAC30% respectively. These results validate the findings of Soni and Saini (2014) that concrete containing 30% FA as a cement replacement

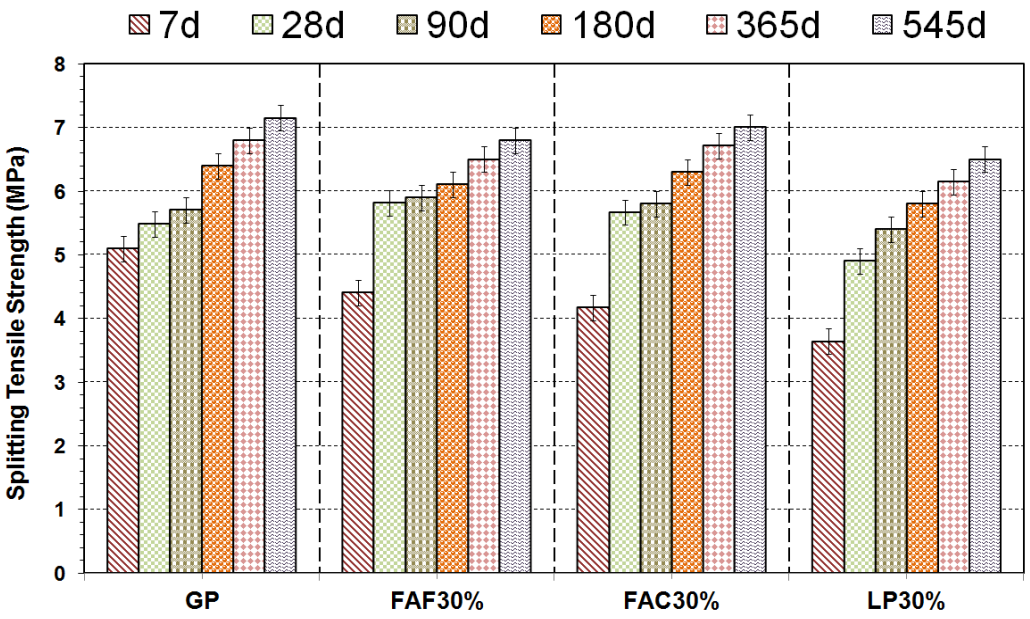

Figure 5.17: Splitting tensile strength development in CTR mixes

exhibits lower tensile strength than GP concrete. At 545-days, FAF30% and FAC30% showed 4.5%-4.6% increase from 365-days, which might be due to the continuous pozzolanic reaction strengthening the bond between paste and the aggregate, similarly indicated by Malhotra and Mehta (2005). The overall results coincide with the findings reported by Siddiqui (2004) that although the replacement of cement with FA reduces the tensile strength of concrete but there is continuous and significant improvement of strength properties beyond 28-days. This strength increase could be due to the formation of hydration products that strengthened the inner skeleton structure, which is clearly evident by comparing its tensile strength growth with GP concrete.

The behaviour shown by LP30% in terms of early splitting tensile strength was worse than the GP and FA mixes. Likewise, lower splitting tensile strength ranging from 10.9%-15.5% was obtained at 28-days with 30% LP compared to the other CTR mixes. Similar results of LP modified concrete in comparison to GP have been reported by Kathirvel et al. (2013). However, an improvement of 10.2% was observed in splitting tensile strength of LP30% at 90-days as that of 28-days, though this was still lower than GP, FAF30% and FAC30% by 5.3%, 8.5% and 6.9% respectively. The tendency of reduction in splitting tensile strength with the inclusion of LP is in accordance with Hesami et al. (2016) for the tests undertaken up to 90-days. The percentage of splitting tensile strength increase from 180 to 365-days for LP30% was 6.9%, which was slightly higher than FAF30% found at 6.6% and FAC30% at 6.4%. The filler effect and creation of nucleation centres for precipitation of hydrated products by LP particles assisted in its continuous strength gain (Lollini et al., 2013; Marzouki et al., 2013; and Avila-López et al., 2015). It is essential to note that the rate of

splitting tensile strength growth in LP30% was superior compared to FAF30% and FAC30%; nevertheless, at later ages, the differences between their growth rates reduced considerably. At 545-days of testing, LP30% exhibited 4.8% increase in splitting tensile strength from 365-days. This continuous and late age strength development in LP30% could be due to the its good ability of packing, formation of more CSH gel in the presence of lime and continuous hydration of GP, since LP has no pozzolanic properties that could contribute towards tensile strength gain.

(a) Effects of glass fineness on splitting tensile strength

Figure 5.18 demonstrates the splitting tensile strengths of GL-FN class of mixes up to 545-days of standard water curing. The splitting tensile strengths of coarser to finer range of glass powders were determined so as to focus on the variations in splitting tensile strength with changes in particle size of the glass powder. The splitting tensile strength of SCC incorporating GL generally reduced as the glass particle size became coarser, which is compatible with the findings reported by Shayan and Xu (2006) and Taha and Nounu (2008).

The early-age splitting tensile strength demonstrated by GL-FN class varied according to the fineness of glass particles. Tests undertaken at 7-days revealed that the finest glass modified mix 10G30% showed the highest splitting tensile strength of 4.2 MPa, which was 16.7% and 44.8% higher than 20G30% and 40G30% respectively. The coarser glass contributed towards the poor performance of concrete (40G30%) that could be due to the inherent smooth and plane surface of larger glass particles, weakening the bond between cement and glass and thereby, affecting the splitting tensile strength development at young

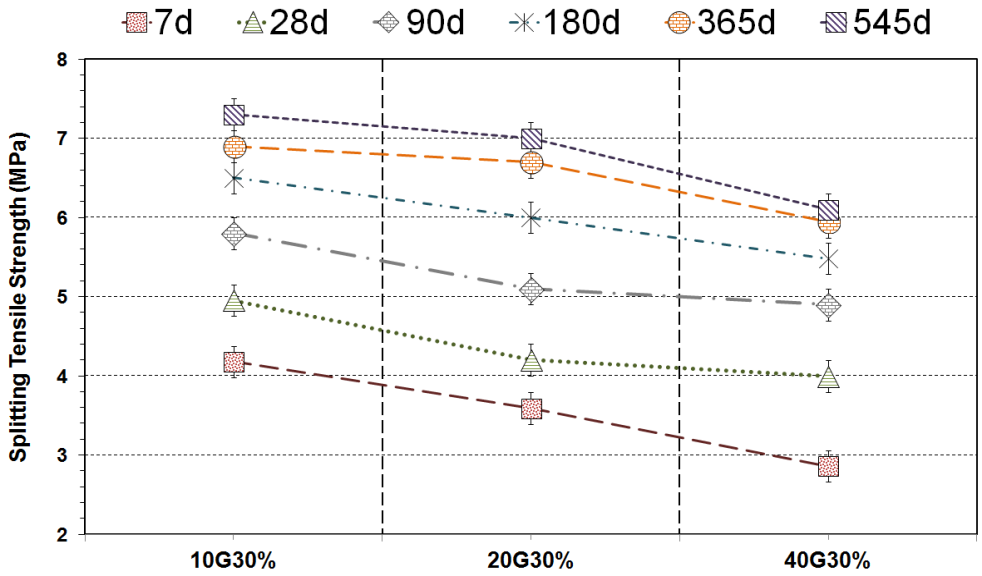

Figure 5.18: Splitting tensile strength development of GL-FN (added at 30% replacement level) with curing age up to 545-days

age, similarly discussed by Taha and Nonnu (2008). Conversely, the pozzolanic activity of the finer glass particles in 10G30% resulted in higher splitting tensile strength compared to the other glass mixes categorized in GL-FN.

The normal-age splitting tensile strength of GL-FN samples followed the same pattern as that of the early-age. At 28-days of testing, splitting tensile strength reduced by 16.0% with the increase in glass size from 10 µm to 20 µm. Furthermore, a decrease of 4.8% in splitting tensile strength was observed as glass size increased from 20 µm to 40 µm. As the curing time advanced, the mix 10G30% exhibited 13.7% and 18.4% higher splitting tensile strength than 20G30% and 40G30% at 90-days respectively. Another important finding is that a distinct development was observed in 10G30% compared to 20G30% and 40G30%, during any curing period. The continuous splitting tensile strength development in all glass modified mixes mention that there was a definite pozzolanic effect, working in all glass samples including coarsest to finest, contributing towards their strength growth.

At 180-days of curing, the splitting tensile strength was observed to reduce by 7.7% and 8.3% with the increase in glass size from 10 µm to 20 µm and from 20 µm to 40 µm respectively. As the curing time progressed to 365-days, 10G30% exhibited 3.0% and 17.0% higher splitting tensile strengths than 20G30% and 40G30% respectively, potentially due to less inherent cracks in the finest glass modified mix. These results are in agreement with those presented by Taha and Nonnu (2008). Finally, the mix 10G30% demonstrated unexpectedly high splitting tensile strength of 5.8% between 365 and 545-days of curing, which might be due to the same reason discussed before. Nevertheless, 20G30% and 40G30% showed lower splitting tensile strengths by 4.1% and 16.4% compared to 10G30%.

Figure 5.19 illustrates the comparison between the splitting tensile strength development in some CTR mixes and the glass mixes categorized in GL-FN class. It is evident from the results that GP performed better than the glass mixes in splitting tensile strength development up to 545-days. Vijayakumar et al. (2013) consistently revealed that glass powder concrete increases the tensile strength effectively when compared with GP concrete. In addition, comparisons of glass when compared to FA indicate that glass at a similar particle size performed better than FA in splitting tensile strength development by 545-days. To elaborate, the 7-days splitting tensile strength achieved by 10G30% was 4.5% lower than FAF30%, equal to FAC30% and 16.7% higher than LP30%. On the other hand, 20G30% achieved 18.2% and 14.3% lower splitting tensile strengths than FAF30% and FAC30% respectively but equal to LP30%. 40G30% exhibited lower splitting tensile strengths than all CTR mixes by 19-43%. The 28-days tests revealed that the splitting tensile strength shown by 10G30% fell behind by 12-14% than the strengths demonstrated by FA mixes. The similar

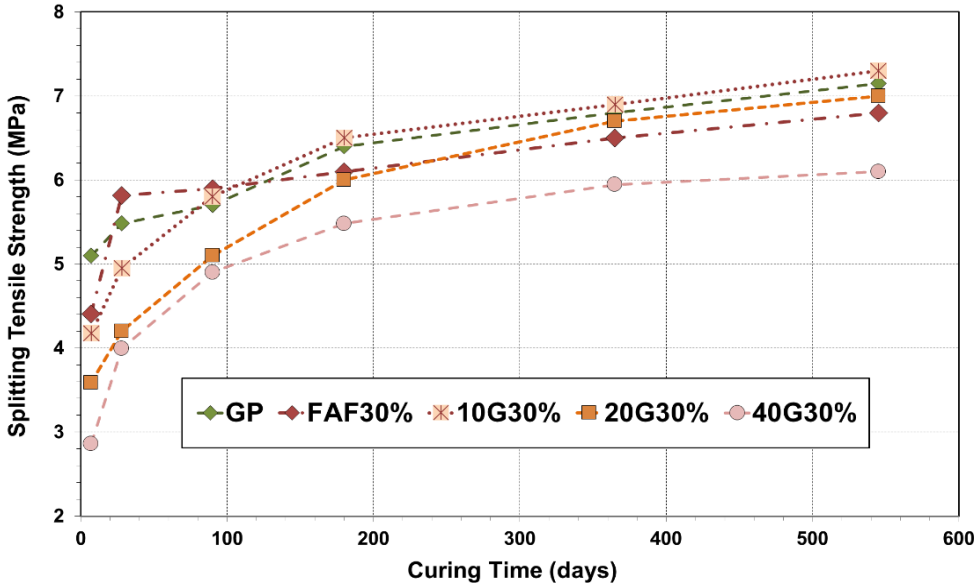

Figure 5.19: Comparison between splitting tensile strength development in GL-FN and some CTR mixes

reduction was observed in 20G30% and 40G30% compared to other CTR mixes. An interesting trend was noticed at 90-days, which declared the rate of tensile strength development much higher in glass mixes compared to CTR mixes. However, the differences in the rate of strength gain reduced for all mixes by 180-days. 10G30% showed 5.8%, 20G30% showed 4.4% and 40G30% exhibited 3.4% increase in tensile strength from 365 to 545-days, which is relatively within the same range of 4.5%-5.9% shown by CTR specimens.

(b) Effects of glass content on splitting tensile strength

The splitting tensile strength development of GL-CN mixes up to 545-days of standard water curing has been illustrated in Figure 5.20. The splitting tensile strengths of various replacement levels of glass powders were also studied to emphasize on the variations in splitting tensile strength of glass powder with differences in glass contents. Generally, the splitting tensile strength of SCC incorporating glass reduced with the addition of glass powder, which is consistent with the findings reported by Park et al. (2004), Topcu and Canbaz (2004), Liu (2011), Sharifi et al. (2013) and Hussain and Chandak (2015).

The early-age tensile strength exhibited by GL-CN class varied with the glass contents. At 7-days, splitting tensile strength of 20G20% was found to be 8.3% and 44.4% higher than 20G30% and 20G40% respectively. Chikhalikar and Tande (2012), in their study on steel fibre reinforced concrete, similarly presented that the tensile strength attains a peak value at 20% cement replacement by waste glass powder. Another related investigation also emphasized that as the amount of glass increases, so does the air content due to the awkward shape of glass and poor compactness and hence, tensile strength decreases since adhesion is not fully achieved in concrete containing glass (Park et al., 2004).

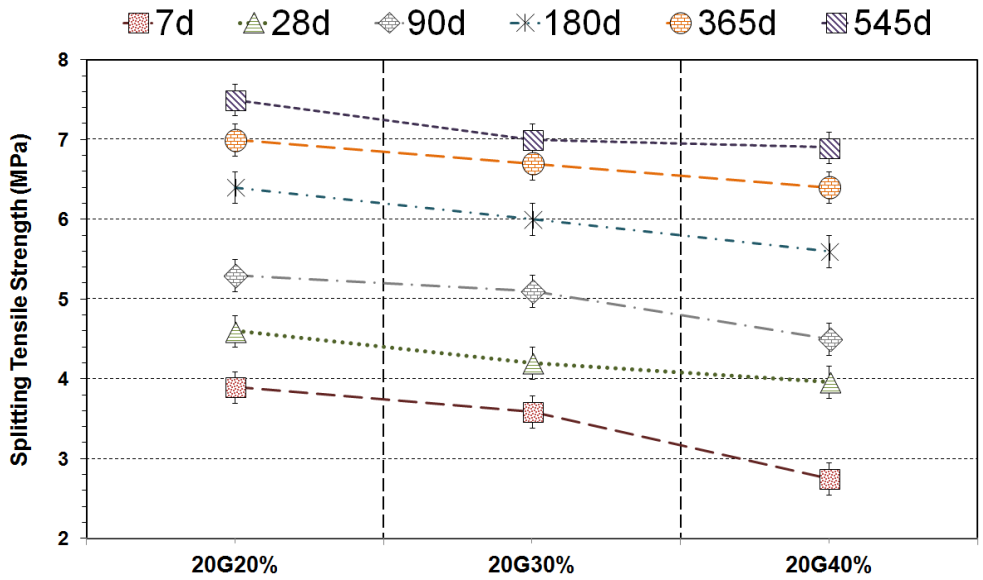

Figure 5.20: Splitting tensile strength development of GL-CN (having fineness of 20 µm) with curing age up to 545-days

The normal-age splitting tensile strength of GL-CN samples followed the same pattern of tensile strength development as that of early-age. As anticipated, 20G20% showed an increase in splitting tensile strength. The splitting tensile strength reduced by 7.7% with the increase in glass content from 20% to 30% at 28-days. However, a decrease of 25.0% in the splitting tensile strength was observed as glass content increased from 30% to 40%. At 90-days of testing, the mix 20G20% exhibited 3.9% and 17.8% higher splitting tensile strength than 20G30% and 20G40% respectively, equally mentioned by Wang (2009). This tendency towards decreasing splitting tensile strength with increasing mixing ratio might be due to the decrease in adhesive strength between the surfaces of the waste glass powder and cement paste, as discussed by Roberts (1989).

At 180-days of curing, tensile strength reduced by 6.3% and 6.7% with an increase in glass content from 20% to 30% and from 30% to 40% respectively. Vandhiyan et al, (2013) showed that there is marginal improvement in tensile strength up to 10% replacement level, after which it declines. Up to 365-days of curing, the mix 20G20% showed 4.5% and 9.4% higher splitting tensile strengths than 20G30% and 20G40% respectively, potentially due to higher pozzolanic reactivity in 20G20% even at this later stage of hardening. Finally, 20G20% exhibited improvement of 7.1% in tensile strength from 365 to 545 days of curing possibly due to the similar reason. However, 20G30% and 20G40% demonstrated lower splitting strengths by 6.7% and 8.0% in comparison to 20G20% after 545-days of hydration.

Figure 5.21 shows the comparison between splitting tensile strength development in control mixes and glass mixes categorized in GL-CN class. The GP mix mostly exceeded all glass mixes in splitting tensile strength development. Moreover, it can also be observed that FA at

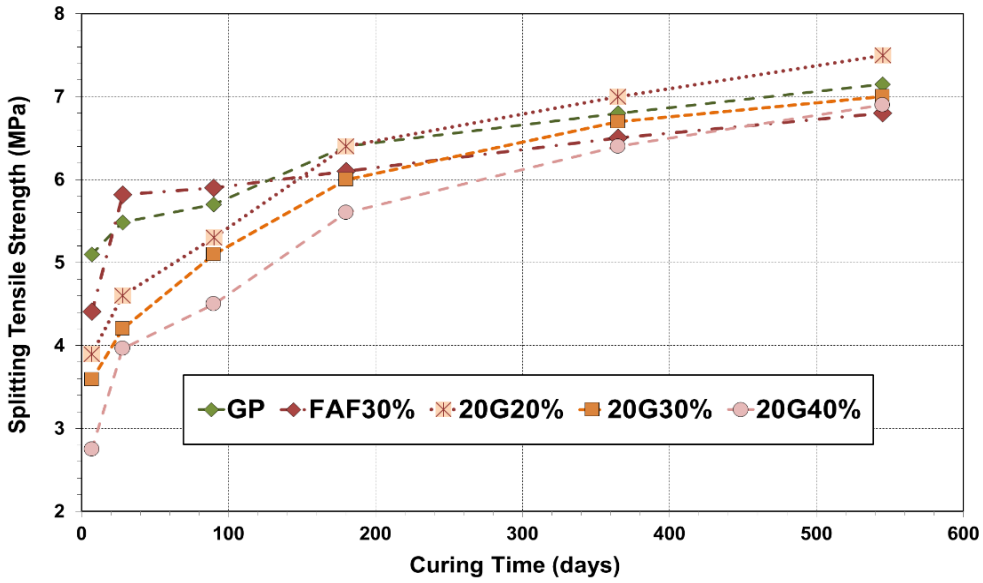

Figure 5.21: Comparison between splitting tensile strength development in GL-CN and some CTR mixes

a similar replacement rate performed better than glass in splitting tensile strength gain. To elaborate, 20G20% demonstrated splitting tensile strength lower than GP and FAs by 7-23%; however, it achieved 8.3% higher compressive strength than LP30% at 7-days. The splitting tensile strength of 20G20% reduced by 16.4% compared to GP at 28-days, whereas 20G30% and 20G40% demonstrated even lower tensile strength gain from 7 to 28 days. A significant boost was observed in glass mixes at 90-days when the rate of increase in splitting tensile strength was much higher in comparison to CTR mixes; for instance, 20G30% showed 21.4% increase from 28 to 90-days, whereas GP only increased by 3.6% during this curing period. Compatible results were presented by Cassar and Camilleri (2012) that at 90-days of curing, the GP mix has no sufficient gains in tensile strength of concrete while all the glass replacement mixes has increase in tensile strength. By 365-days, 20G20% gained higher splitting tensile strength than all CTR mixes and 20G30% showed same splitting tensile strength as FAC30%. As the curing time reached 545-days, 20G20%, 20G30% and 20G40% showed 7.1%, 4.5% and 7.8% increase in tensile strengths from 365-days, in comparison to 5.9%, 4.6%, 4.5% and 4.8% shown by GP, FAF30%, FAC30% and LP30% respectively.

(c) Effects of glass quality on splitting tensile strength

Figure 5.22 shows the comparison between splitting tensile strengths of unwashed glass incorporated mix and washed glass modified mix, both having glass powders of similar fineness and replacement level. Unwashed glass incorporated mix (20UG30%) could only reach 2.5 MPa at 7-days, which is the lowest of all mixes. Taha and Nonnu (2008) described an appropriate reasoning for this poor performance that contamination, foreign materials and

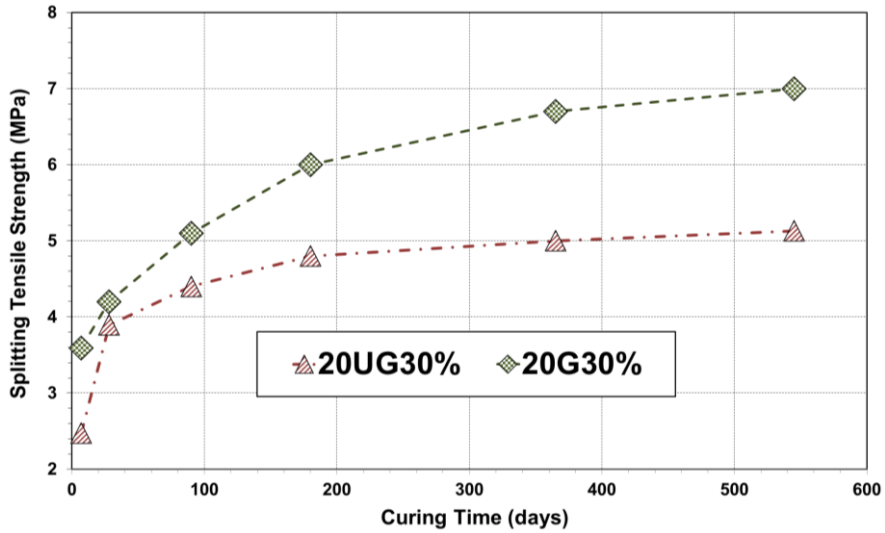

Figure 5.22: Comparison between splitting tensile strength development in 20UG30% and 20G30%

organic content may degrade with time and create voids in concrete microstructure leading to strength reduction. A reduction of 13.7% at 90-days was noticed in the unwashed glass mix (20UG30%) compared to the washed glass mix (20G30%). In addition, there was a reduction of 20.0% in tensile strength at 180-days when unwashed glass was used instead of washed glass, although it was substituted at the same level. At the curing age of 545-days, 20UG30% revealed 2.5% increase in splitting tensile strength than 365-days.

(d) Rate of splitting tensile strength development in glass incorporated mixes

The ratio of the mean 545-days to the mean 28-days (545d/28d) splitting tensile strengths for concrete mixes is presented in Figure 5.23. The results achieved for glass incorporated

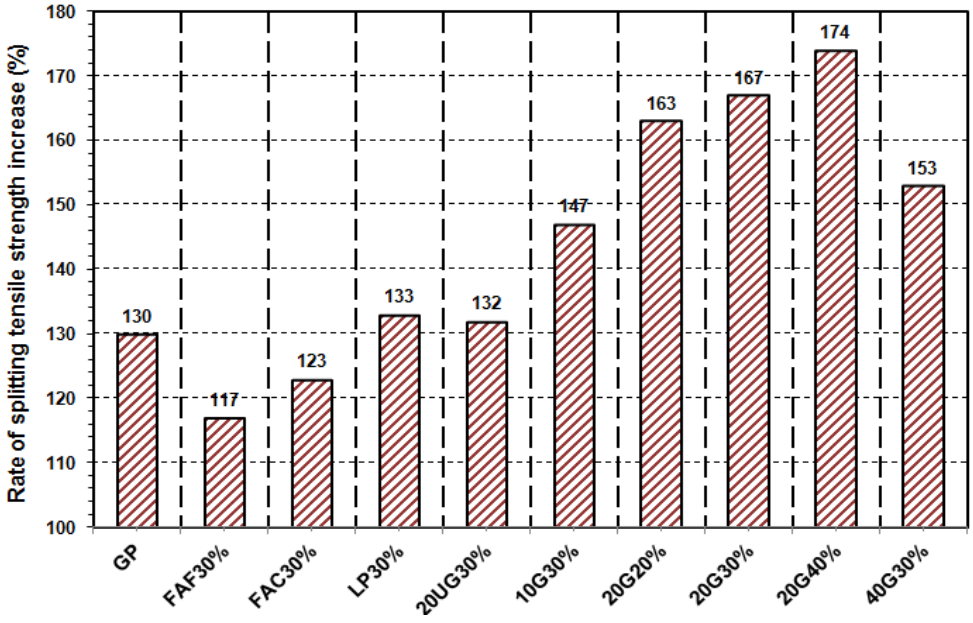

Figure 5.23: Rate of splitting tensile strength development from 28 to 545 days in SCC mixes

samples clearly indicate the probability of long-term splitting tensile strength development from the use of glass, as the concrete mixes with glass had a higher 545d/28d ratio compared to all CTR mixes. This can be associated with the pozzolanicity levels exhibited by glass powder that were comparable to the other types of binders used in this research program. These pozzolanicity levels improved the quality of paste in the presence of glass particles, especially at the ITZ between aggregate particles and paste. Therefore, it can be safely stated that the incorporation of GL can be useful for long-term splitting tensile strength development in SCC mixes and its on-going performance is not inferior to GP cement and other conventional supplementary cementing materials.

(e) Relationship between compressive strength and splitting tensile strength

For structural design purposes, mechanical parameters, such as splitting tensile strength are required. In general, there is a strong correlation between the compressive strength and splitting tensile strength of concrete. Since the addition of glass powder as cementitious material replacement would significantly alter the compressive strength, the variations in splitting tensile strength due to the addition of glass powder might be partly connected to the changes in compressive strength. To investigate these variations resulting from the changes in compressive strengths as well as the other effects of glass powder, the splitting tensile strength results have been correlated with the compressive strength data. Figure 5.24 demonstrates the relationship between compressive strengths and splitting tensile strengths

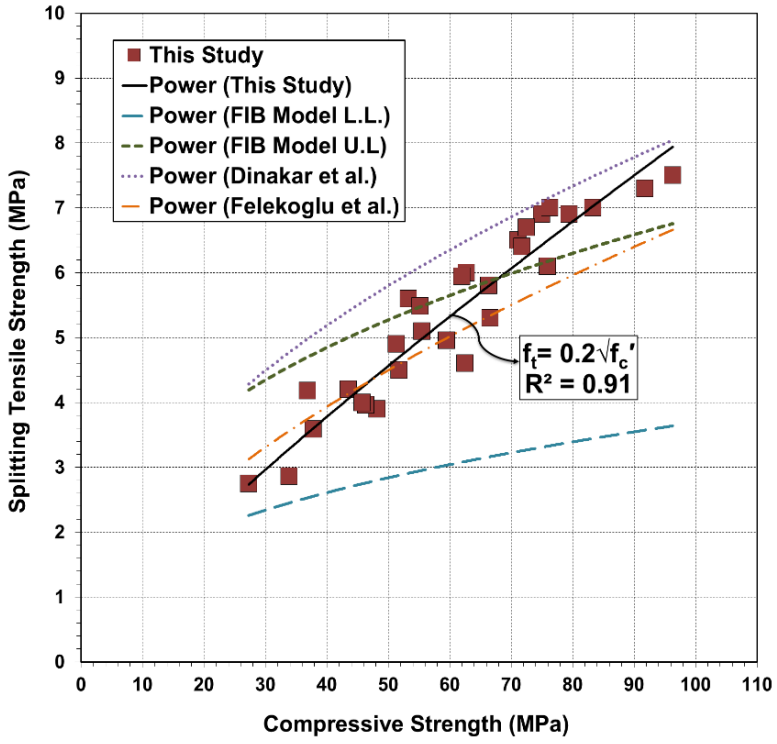

Figure 5.24: Relationship between splitting tensile strength and compressive strength of glass incorporated specimens

of all glass incorporated specimens. An increasing trend of splitting tensile strength has been noticed for increasing cylinder compressive strength. The results of the present study have also been correlated with the previous literature (Dinakar et al., 2008; Felekoglu et al., 2007) and the proposed upper limits (U.P.) and lower limits (L.L.) of relationships available in FIB model code 2010. It is essential to recognize that the proposed models by Felekoglu et al. (2007) and Dinakar et al. (2008) have not been developed using the data of SCC containing glass powder. The results have revealed that the glass powder considerably affects the relationship between the compressive strength and splitting tensile strength. The experimental data obtained in this study is within the range of the previous experimental results and FIB models. It can be seen that the model proposed by Dinakar et al. (2008) somewhat over-estimates the splitting tensile strength for concretes with compressive strengths over 60 MPa, most of which are from medium to long-term cured specimens. In addition, the model proposed by Felekoglu et al. (2007) provides reasonable estimate of the relationship between the compressive strength and splitting tensile strength for concrete with compressive strengths below 60 MPa. The data of the present study is much closer to the upper limit of FIB Model Code than the lower limit, which might be due to relatively high splitting tensile strengths obtained for glass specimens in this study. There are two possible reasons for the variation in the present data from the previous models. First the strength grade of tested specimens by researchers were not the same. Second the powder ingredients of the specimens prepared by researchers were all different. The overall results imply that the models already available for the relationship between splitting tensile strength and compressive strength can also be used for concrete incorporating glass powder with certain considerations.

5.3.4 Modulus of Elasticity

The elastic modulus measurements were taken at 7; 28, 90; 180, 365 and 545 days for early, normal and long-term modulus of elasticity respectively. The data for CTR mixes have been illustrated in Figure 5.25. Due to the non-destructive nature of elastic modulus test, the same three cylinders were repeatedly used throughout the testing schedule. The modulus of elasticity exhibited by GP mix exceeded all other reference mixes up to 545-days of experimental testing. At 7-days, elastic modulus of GP concrete was found to be 37.8 GPa, which increased by 7.7% at 28-days. The percent increase from 28-days to 90-days in elastic modulus of GP concrete was 6.9%, which reduced to 5.1% at 180-days in comparison to 90-days. Finally, the modulus of elasticity reached 48.9 GPa at 545-days of standard curing of GP mix, which is insignificantly higher by 2.3% compared to elastic modulus at 365-days.

The early-age elastic modulus results revealed that FAC30% demonstrated slightly higher modulus of elasticity in comparison to GP at 7-days. However, elastic modulus gained by FAF30% was found to be 17.4% and 15.6% lower than FAC30% and GP at 7-days. Diaz-Loya et al. (2011) consistently mentioned that the highest modulus of elasticity is achieved with class C fly ash compared to GP and class F fly ash. Furthermore, Naik et al. (1991) and Singh et al. (2014) also noticed that the replacement of GP cement by class F fly ash in concrete causes reduction in modulus of elasticity. In addition, elastic modulus of the mix FAF30% increased by 12.8% from 7 to 28 days; however, the rate of increase in FAC30% during this curing period was found to be inadequate. Nevertheless, mixes FAF30% and FAC30% were found to be 11.5% and 4.7% lower compared to GP at 28-days. At 90-days, FAC30% showed higher elastic modulus than FAF30% by 5.9%, both being lower than GP within the range of 2.8%-8.5%. Identical results related to class F fly ash were reported by Soni and Saini (2014). The percentages of elastic modulus increase from 180-days to 365-days for FAF30% and FAC30% were 1.4% and 3.8%, which is lower than the GP found at 4.6%. Sear (2001) consistently reported that elastic modulus of fly ash concrete is marginally less than for equivalent GP cement concrete at later ages. Moreover, FAF30% exhibited almost identical result to that reported by Sivasundaram et al. (1990) that the long-term elastic modulus of FAF modified concrete is about 44 GPa at the test age of 365-days. Similarly, on 545-days of testing, FAF30% and FAC30% were observed to increase in modulus of elasticity by 2.4%-3.2% from 365-days, which is higher than that of GP during this time of curing. The overall findings are consistent with the result reported by Siddiqui (2004) that there is a continuous improvement in elastic modulus with curing age when fly ash is incorporated in concrete.

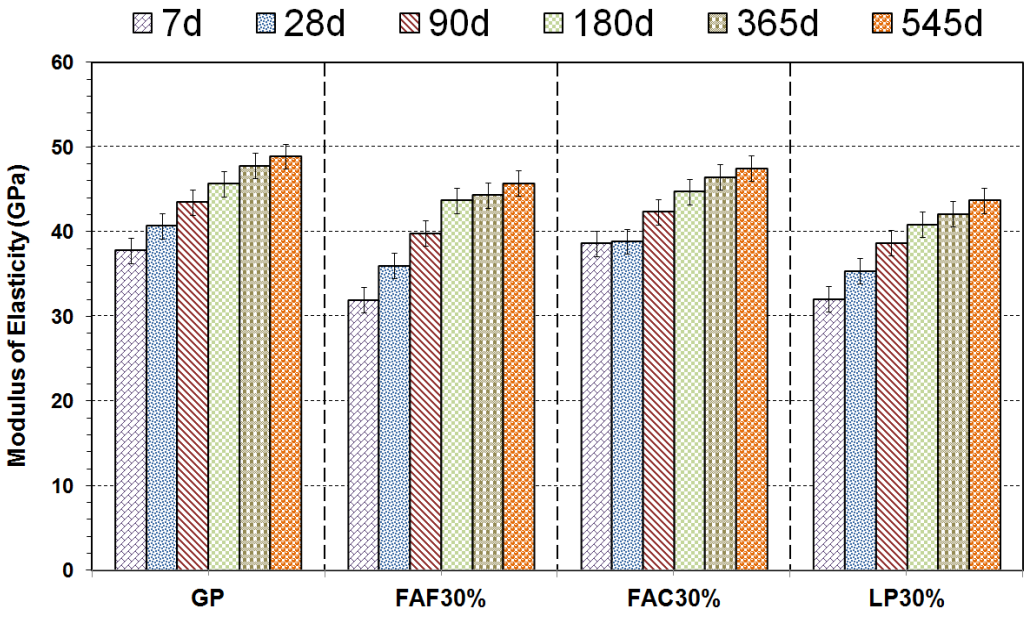

Figure 5.25: Elastic modulus development in CTR mixes

The modulus of elasticity demonstrated by LP30% was found to be lower than all other control mixes. This negative effect of limestone powder replacement might be due to cement content dilution effect, similarly discussed by Dhir et al. (2007), Ghrici et al. (2007), Ramezanianpour et al. (2009) and Guemmadi et al. (2009). At 7-days of curing period, LP30% mix showed 15.3% and 17.1% lower elastic modulus in comparison to GP and FAC30% respectively. However, 7-days elastic modulus of LP30% and FAF30% was nearly the same. Similarly, lower modulus of elasticity, ranging from 1.9%-13.3%, was obtained at 28-days in LP30% compared to other control mixes. Diab et al. (2016) presented almost identical results that modulus of elasticity reduced by 1%-12% at 28-days in concrete including 5%-25% limestone powder as cement replacement. Conversely, Li and Kwan (2015) mentioned that the addition of limestone powder as cementitious replacement significantly increases elastic modulus of concrete. One possible reason for this variation in findings can be the difference in water contents and addition of superplasticizer as these two are the governing factors in determining the mechanical behaviour of concrete. Furthermore, an improvement of 9.6% was found in elastic modulus of LP30% at 90-days as that of 28-days. This elastic modulus was, however, lower than GP, FAF30% and FAC30% by 11.0%, 2.8% and 8.5% respectively. The reduction in modulus of elasticity with the inclusion of limestone powder is similarly reported by Hesami et al. (2016) for the tests undertaken up to 90-days. The ratio of elastic modulus increase from 180-days to 365-days for LP30% was only 3.2%. This increase rate in LP30% was higher than FAF30% found at 1.4% but lower than FAC30% observed at 3.8%. Finally, LP30% exhibited only 3.8% increase in modulus of elasticity from 365 to 545-days but still 10.6%, 4.4% and 8.0% lower compared to GP, FAF30% and FAC30% respectively.

(a) Effects of glass fineness on elastic modulus

Figure 5.26 exhibits the modulus of elasticity in GL-FN mixes up to 545-days of standard water curing. The elastic modulus of a coarser to finer range of glass powders were tested in order to determine the variations in the elastic modulus with changes in particle size of the glass powder. The elastic modulus of SCC containing glass generally reduced as the glass particle size became coarser, which is compatible with the findings reported by Shayan and Xu (2006) and Wang et al. (2014).

The early-age elastic modulus demonstrated by GL-FN class varied according to the fineness of glass particles. Tests undertaken at 7-days revealed that the finest glass modified mix 10G30% showed the highest elastic modulus of 34.8 GPa, which was 9.1% and 5.1% higher than 20G30% and 40G30% respectively. It can be seen that 40G30% gained higher elastic modulus than 20G30%, which could be related to the variations in the

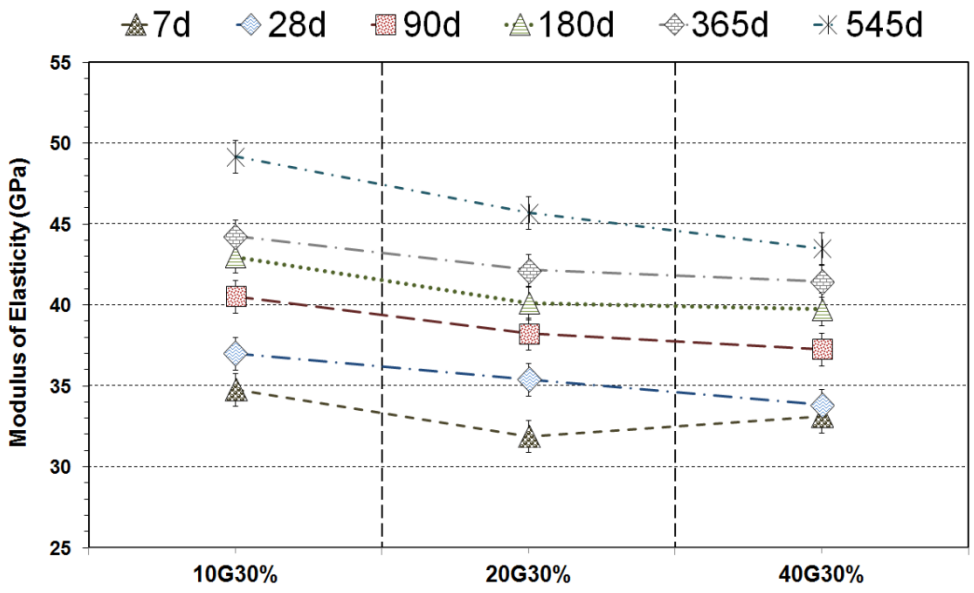

Figure 5.26: Elastic modulus development of GL-FN (added at 30% replacement level) with curing age up to 545 days

data achieved for individual cylinders. The coarser glass incorporated mix (40G30%) showed poor performance, probably due to a retarding effect on cement hydration caused by the coarser particles of glass, which is consistent with Idir et al. (2011). On the other hand, the finer glass particles in 10G30% expedited the process of hydration and resulted in better performance comparatively.

The normal-age elastic modulus of GL-FN samples demonstrated that 40G30% obtained lowest elastic modulus as anticipated. At 28-days of testing, the elastic modules reduced by 4.3% with an increase in glass size from 10 µm to 20 µm. Moreover, a decrease of 4.5% in elastic modulus was observed as glass size increased from 20 µm to 40 µm. The mix 10G30% exhibited 6.0% and 8.6% higher elastic modulus than 20G30% and 40G30% at 90-days respectively. There was a clear improvement in the elastic modulus in the case of 10G30% in comparison to 20G30% and 40G30%.

On 180-days of testing, the elastic modulus was observed to reduce by 7.2% and 8.3% with the increase in glass size from 10 µm to 20 µm and from 20 µm to 40 µm respectively. As the curing time progressed to 365-days, the mix 10G30% exhibited 4.8% and 6.7% higher modulus of elasticity than 20G30% and 40G30% respectively but it showed slight improvement from 180 to 365-days. Finally, 10G30% revealed very high elastic modulus, increased by 11.3% from 365 to 545-days of testing. However, 20G30% and 40G30% exhibited lower modulus of elasticity by 7.6% and 13.1% in comparison to 10G30%. Consistent results have been reported by Shayan and Xu (2006) that elastic modulus is reduced with the increase in glass fineness.

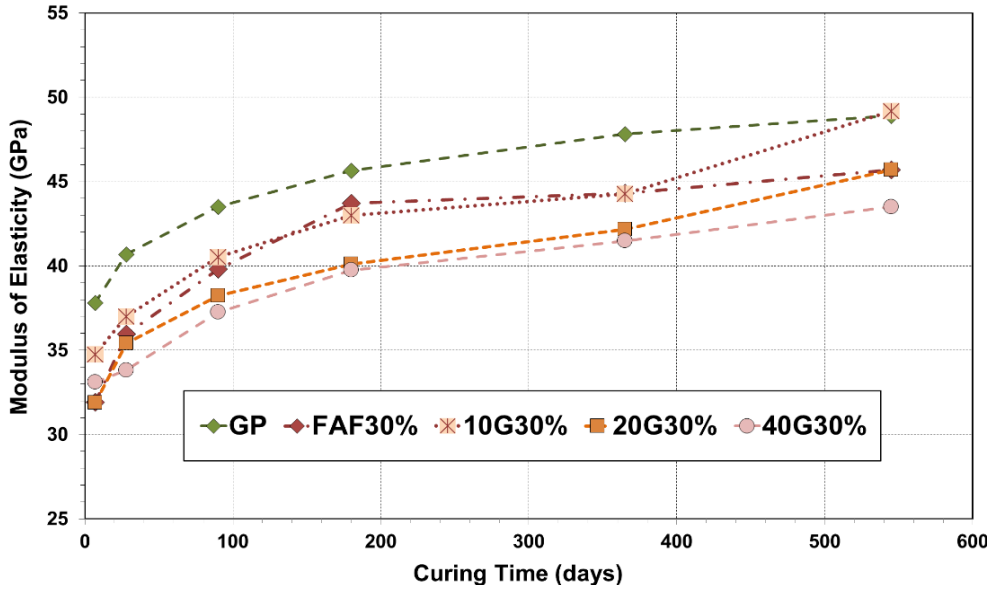

Figure 5.27: Comparison between elastic modulus development in GL-FN and some CTR mixes

Figure 5.27 illustrates the comparison between the elastic modulus development in some CTR mixes and the glass mixes categorized in GL-FN series. It is evident from the results that GP performed better than most of the glass mixes in elastic modulus development. The 7-days elastic modulus achieved by 10G30% was 9.8% lower than FAC30%, and up to 9% higher than FAF30% and LP30% respectively. On the other hand, 20G30% achieved 17.3% lower elastic modulus than FAC30% but equal to FAF30% and LP30%. 40G30% exhibited slightly higher elastic modulus than FAF30% by 4%. The 28-days tests revealed that elastic modulus shown by 20G30% remained close to the elastic modulus demonstrated by FAF30%. The similar reduction in elastic modulus was observed in 40G30% compared to other CTR mixes. The rates of strength increase from 28 to 90-days in 10G30%, 20G30% and 40G30% were 9.5%, 7.9% and 10.3%, which is relatively similar to CTR mixes ranging between 6.9%-10.5%. By 180-days, glass mixes continued to improve their performances as 10G30% showed insignificantly lower elastic modulus than FAF30% and became equal to this at 365-days. 20G30% and 20G40% exhibited approximately similar elastic modulus to LP30% from 180-days until 545-days. It can be seen from the results that 10G30% exceeded GP in elastic modulus at 545-days, though this increase was only 0.6%. In addition, 20G30% reached exactly similar elastic modulus as that of FAF30% at 545-days.

(b) Effects of glass content on elastic modulus

The elastic modulus development of GL-CN series up to 545-days of standard water curing has been illustrated in Figure 5.28. The elastic modulus of SCC containing various replacement levels of glass powders were also studied so as to investigate the variations in elastic modulus with the differences in glass contents. Generally, the elastic modulus of SCC

containing glass reduced with the addition of glass powder, which is in parallel with the findings given by Topcu and Canbaz (2004), Shayan and Xu (2006) and Kou and Poon (2009).

The early-age elastic modulus exhibited by GL-CN class varied according to the content of glass particles. At 7-days of testing, the elastic modulus of 20G20% was found to be 2.5% and 3.5% higher compared to 20G30% and 20G40% respectively. These results agree to those given by Kou and Poon (2009) that the elastic modulus decreases with the increase in the recycled glass content. However, these findings are inconsistent to those presented by Abdallah and Fan (2014) that elastic modulus of concrete containing waste glass as sand replacement increases as waste glass content in concrete increases, which was attributed to a higher elastic modulus of glass compared to that of natural sand by the researchers.

The normal-age elastic modulus of GL-CN samples followed the same pattern of elastic modulus development as that of early-age. 20G20% showed the highest elastic modulus. Parallel results were noticed by Shayan and Xu (2006) for lower glass contents. Elastic modulus reduced by 2.8% with an increase in glass content from 20% to 30% at 28-days. However, a reduction of 3.4% in elastic modulus was observed as glass content increased from 30% to 40%. These results are in accordance with the findings reported by Ali and Al-Tersawy (2012). At 90-days, 20G20% exhibited 2.6% and 1.3% higher modulus of elasticity than 20G30% and 20G40% respectively. It can be seen that 20G40% showed higher elastic modulus than 20G30%, which could only be linked to the variability between individual cylinders and averaging a wide range of data achieved from different methods of testing.

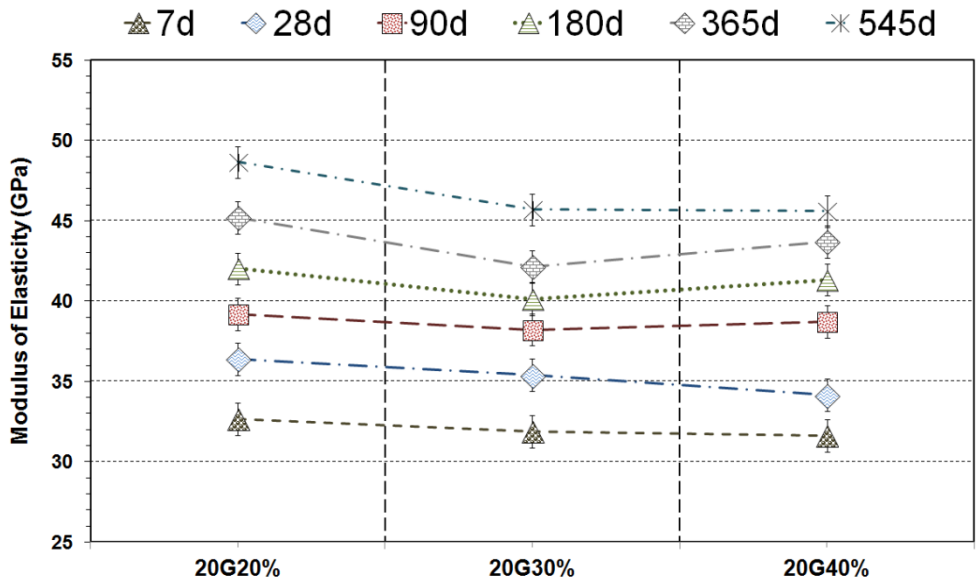

Figure 5.28: Elastic modulus development of GL-CN (having fineness of 20 μm) with curing age up to 545 days

Up to 365-days of curing, the mix 20G20% showed 7.1% and 3.4% higher elastic modulus than 20G30% and 20G40% respectively, might be due to the higher pozzolanic reactivity in 20G20%. Finally, the mix 20G20% exhibited improvement of 7.7% in elastic modulus from 365 to 545 days of curing, possibly due to the same reason previously mentioned. 20G30% and 20G40% showed lower elastic modulus by 6.6% and 6.8% in comparison to 20G20% after 545-days of hydration. An important observation from these results is that unexpected variations in elastic modulus were noticed at some instances, which is potentially due to the fact that the reported results are the average of 6 - 9 readings measured by different methods.

Figure 5.29 shows the comparison between the elastic modulus development in some CTR mixes and the glass mixes categorized in GL-CN. The GP exceeded all of these glass mixes in elastic modulus development. 20G20% demonstrated elastic modulus lower than GP and FAC30% by 13-15%; however, it achieved 2.5% and 2.2% higher elastic modulus than FAF30% and LP30% at 7-days. On the other hand, 20G30% showed similar elastic modulus to FAF30% at 7-days. The elastic modulus of 20G20% reduced by 10.6% compared to GP at 28-days, whereas 20G30% and 20G40% demonstrated even worse elastic modulus than GP. These results are in disagreement with the results reported by Taha and Nounu (2008), where the replacement of GP cement with 20% glass had a negligible effect on 28-days modulus of elasticity. The data achieved at 90-days tests shows that 20G20% gained lower elastic modulus than FAF30%, which is in contrast to the finding at 28-days. However, 180-days tests revealed that all glass samples remained lower in elastic modulus development in comparison to all GP and FA incorporating samples. In addition, 20G30% demonstrated

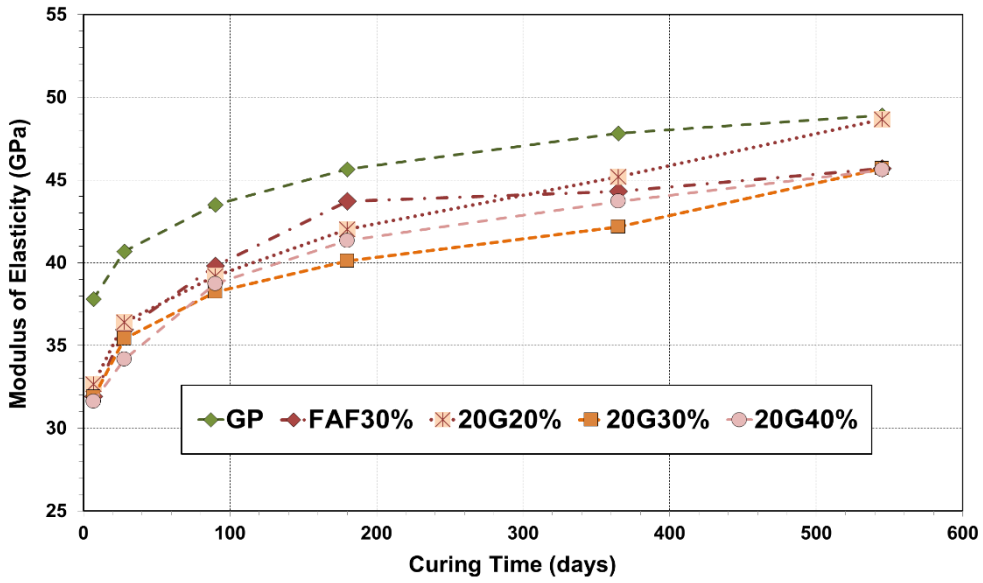

Figure 5.29: Comparison between elastic modulus development in GL-CN and some CTR mixes

insignificantly lower elastic modulus than LP30%. By 365-days, 20G40% approached higher elastic modulus than LP30% and 20G30% gained relatively similar elastic modulus as LP30%. As the curing time reached 545-days, 20G20% demonstrated 7.7%, 20G30% showed 8.3% and 20G40% exhibited 4.3% increase in elastic modulus from 365 to 545-days, in comparison to 2.3%, 3.2%, 2.4% and 3.8% shown by GP, FAF30%, FAC30% and LP30% respectively.

(c) Effects of glass quality on elastic modulus

Figure 5.30 shows the comparison between modulus of elasticity of unwashed glass incorporated mix and washed glass modified mix, both having glass powders of similar fineness and replacement level. The unwashed glass incorporated mix 20UG30% could only reach 28.5 GPa at 7-days that was the lowest of all mixes. A reduction of 15.5% in the modulus of elasticity at 90-days was noticed in the unwashed glass mix (20UG30%) compared to the washed glass mix (20G30%), although similar amount of glass was added as a cement replacement. In addition, there was a reduction of 15.9% in elastic modulus at 180-days when unwashed glass was used instead of washed glass, probably due to the presence of impurities in the unwashed glass present in 20UG30%. Moreover, as the curing time reached 545-days, 20UG30% revealed 2.0% increase in modulus of elasticity from 365-days.

(d) Rate of elastic modulus development in glass incorporated mixes

The ratio of the mean 545-days to mean 28-days (545d/28d) modulus of elasticity for all SCC mixes is presented in Figure 5.31. The results achieved for glass incorporated samples clearly indicate the probability of long-term development of elastic modulus from the use of

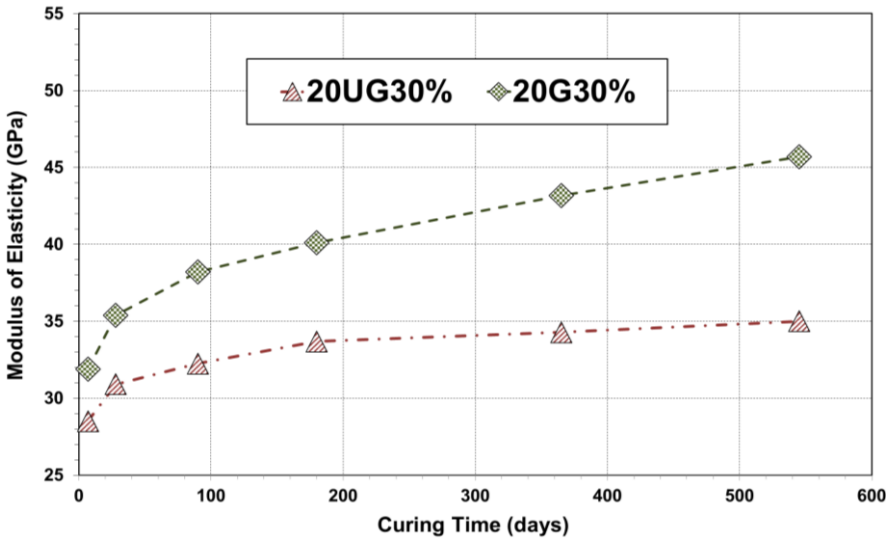

Figure 5.30: Comparison between modulus of elasticity in 20UG30% and 20G30%

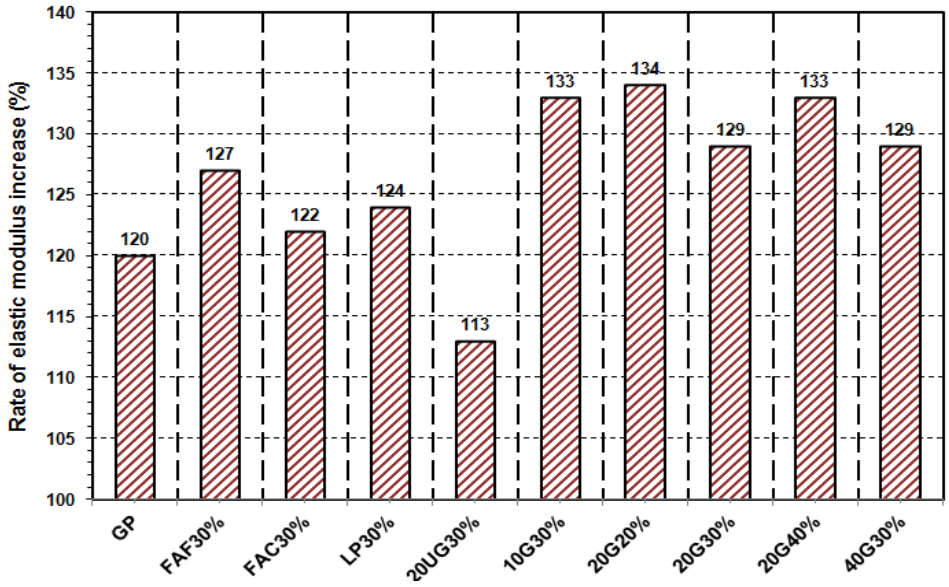

Figure 5.31: Rate of elastic modulus development from 28 to 545-days in all SCC mixes

glass, as the concrete mixes with glass had a higher 545d/28d ratio as compared to all of the CTR mixes. This could be related to the same reason mentioned in the previous sections. Hence, it can be safely established that the addition of glass powder can be useful for long-term elastic modulus development in SCC mixes and its continuous performance is not less than GP cement and other commonly used supplementary cementing materials.

(e) Relationship between compressive strength and elastic modulus

In general, there is a strong correlation between the compressive strength and modulus of elasticity of concrete. Zilch and Roos (2001) also suggested that the modulus of elasticity is dependent on the concrete's compressive strength and its density. Figure 5.32 demonstrates the relationship between elastic modulus and compressive strength based on the standard curing regime. Similar to splitting tensile strength, an increasing trend of elastic modulus is noticed for increasing cylinder compressive strength. A reasonably good R^2 value of 0.83 has been achieved for glass mixes, indicating that the elastic modulus is strongly related to the compressive strength of the mixes. It is evident that the modulus of elasticity is generally higher at a higher compressive strength, similar to the relationship between splitting tensile strength and compressive strength. The correlation between compressive strength and elastic modulus was compared with the previous studies undertaken by Persson (2001), Dinakar et al. (2008) and Felekoglu et al. (2007). It is essential to recognize that the proposed models by these authors have not been developed using the data of SCC containing glass powder. The experimental data obtained in this study generally fits within the previous experimental results for mature concretes though some modifications should be considered for SCC incorporating glass. It can be seen that the model proposed by Dinakar et al. (2008) estimates lower elastic modulus for the same range of compressive strengths

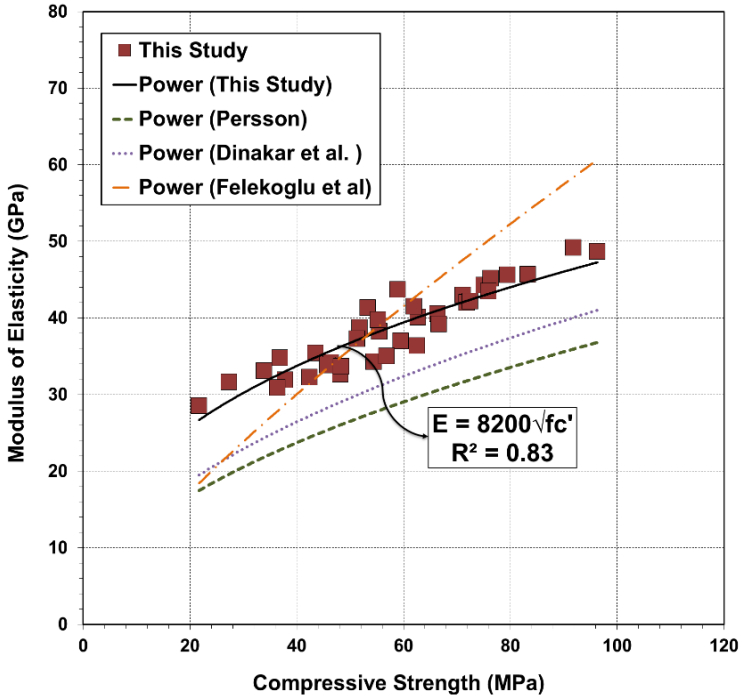

Figure 5.32: Relationship between elastic modulus and compressive strength of glass incorporated specimens

compared to that achieved in this study for glass mixes. This can be related to the higher elastic modulus achieved for glass mixes as previously mentioned. In addition, Felekoglu et al. (2007) model for concrete with compressive strength range between 40 MPa and 60 MPa provides reasonable estimate of the relationship between the compressive strength and elastic modulus. However, there are a few variations in the elastic modulus corresponding to compressive strength for different SCCs, which can be observed. First the strength grade of tested SCCs by researchers are not the same. Second the powder ingredients of SCCs prepared by researchers are all different. Most importantly, the reactivity or inert nature of binder changes the strength characteristics and stress strain relations of mixtures. Hence, the data points outside the boundary of the previously established models might be related to the increase in the elastic modulus of SCC specimens due to the presence of glass powder. The proposed relationship between compressive strength and elastic modulus for SCC containing glass powder therefore is $E = 8200\sqrt{fc'}$.

5.4 Scanning electron microscopic (SEM) examination

Scanning electron microscopic (SEM) analysis was used to examine the nature of the hydrated binders and the binder-aggregate interfacial zones in all the SCC mix types. Figures 5.33 (a) to (h) represent microscopic views (2000x) of all concrete specimens at the curing age of 365-days. The visual analysis of unwashed glass powder revealed the presence of wide cracks throughout the specimen representing deterioration of concrete, which can be related to the presence of impurities that reduced the quality of its

microstructure although continuous hydration was provided. 20G40% and 40G30% appeared to have voids and cracks, possibly due to the presence of coarser glass and glass at higher replacement levels in these mixes. In contrast, 10G30% seemed to have more refined microstructure compared to CTR mixes, which can be attributed to the combined effect of glass fineness and better dispersion of particles. It is important to recognize that these observations are based on the tests done on one specimen of each mix type, which might not be true representative of concrete being examined.

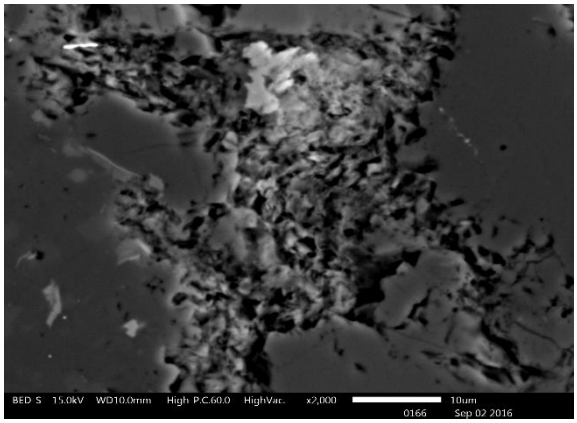

(a)

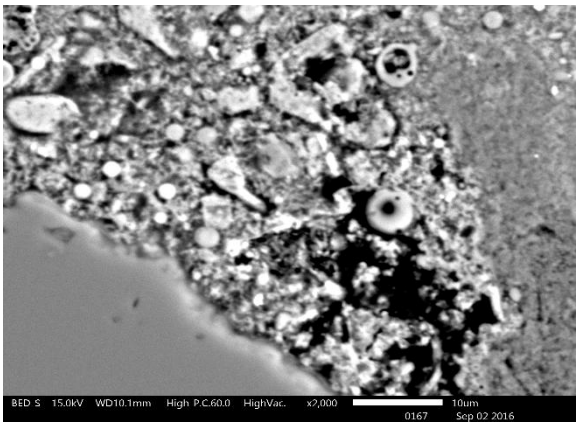

(b)

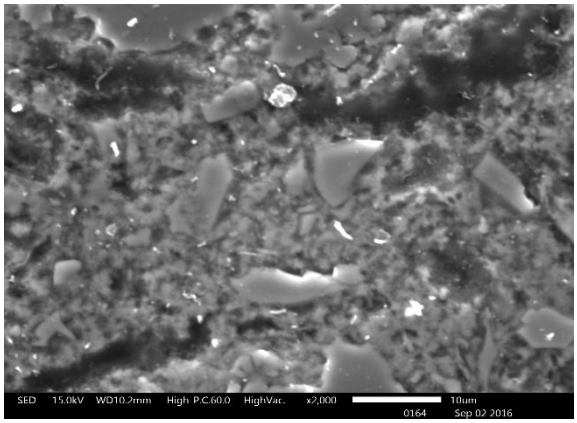

(c)

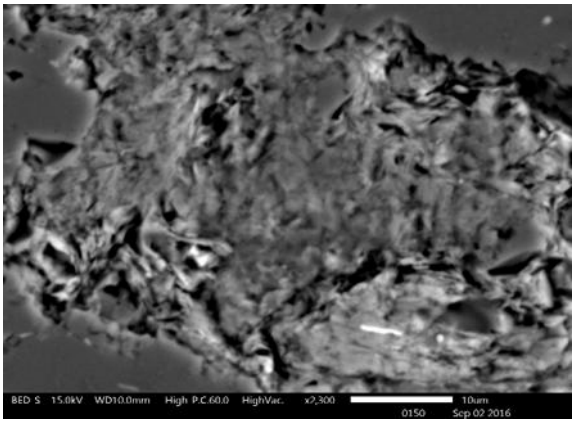

(d)

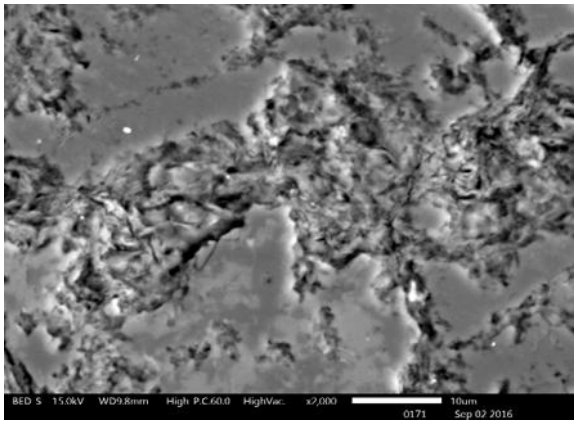

(e)

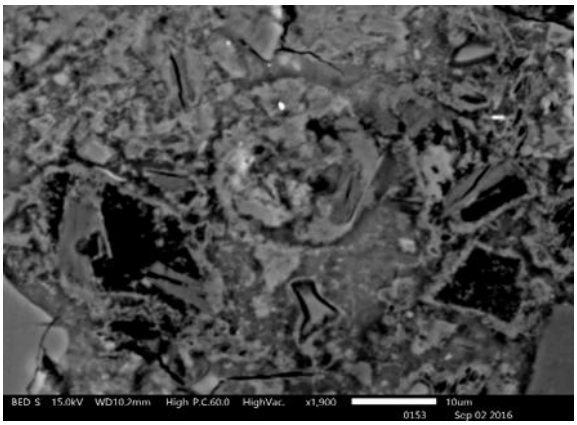

(f)

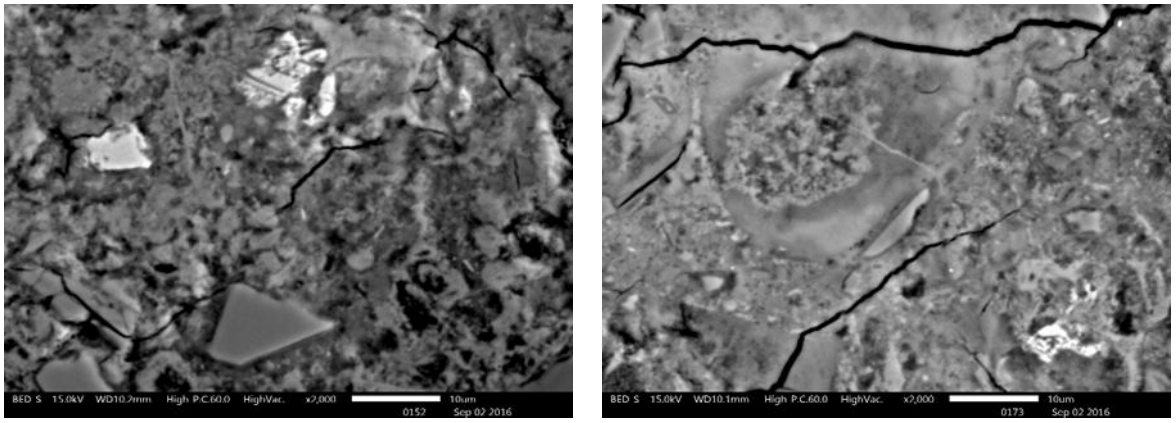

(g) **(h)**

Figure 5.33: Scanning electron microscopy (SEM) examination of (a) GP (b) FAF30% (c) 10G30% (d) 20G20% (e) 20G30% (f) 20G40% (g) 40G30% (h) 20UG30%

5.5 Conclusions

The findings presented in this chapter can be used to draw the following conclusions:

- The finer waste glass tested in this investigation was found to have higher strength activity index in comparison to the coarser waste glass when added in mortar. Similarly, the glass powder added at lower content in mortar had higher strength activity index compared with the glass powder incorporated at higher replacement level. For instance, the strength activity index of the 10 µm glass mix was approximately 98% at 28-days compared to the 40 µm glass mix at about 78% and the strength activity index of the 20% glass mix was approximately 97% at 28-days compared to the 40% glass mix at about 76%.

- Using glass led to some reduction in the compressive strength, splitting tensile strength and elastic modulus. The higher the replacement level, the higher the reduction. However, the reduction was higher at early stages and reduced with increasing curing age. In general, the use of the finer glass powder in SCC resulted in higher compressive strength, splitting tensile strength and elastic modulus than the coarser glass powder. This might be linked to the evidence that strength is a function of both pozzolanic reaction and particle packing, both of which are more evident in finer material. The small sized glass powder dispersed in the presence of superplasticizer to fill the voids between cement particles, accelerated the hydration of cement and resulted in better packed SCC mix. In addition, the improved particle distribution in finer glass led to the reduction of thickness of transition zone and therefore, densely packed stronger concrete. Hence, the final long-term (545-days) data demonstrated that 10 µm

glass replaced at 30% achieved compressive strength, splitting tensile strength and elastic modulus of about 92 MPa, 7 MPa, and 49 GPa whereas 40 µm glass replaced at 30% achieved about 76 MPa, 6 MPa, and 43 GPa respectively.

- The mechanical properties of concrete incorporating the unwashed glass powder as a partial replacement for the GP cement was also studied. It was observed that the unwashed glass powder reduced compressive strength, splitting tensile strength and elastic modulus compared to the washed glass of the similar fineness range and replacement level. This indicates the deficiency in strength gain due to the presence of contaminants in the unwashed glass powder. This finding revealed the importance of using washed or clean glass in concrete to gain maximum benefits.

- There was an increase in the splitting tensile strength and elastic modulus with the increase in compressive strength. However, the analysis of the experimental data showed that the relationships between splitting tensile strength and compressive strength and between elastic modulus and compressive strength were independent of the fineness or replacement level of the glass powder.

- Based on the data achieved on SCC incorporating glass powder in this study, it is concluded that SCC with the target fresh properties can be successfully produced with 20-40% of the GP cement replaced by the glass powder having fineness of 10-40 µm. The higher replacement level of 40% and coarser size range of 40 µm of glass powder had greater negative effects on the mechanical properties but not to an unacceptable extent. The long-term strengths of the mixes incorporating 10 µm glass at 30% and 20 µm glass at 20% and 30% were comparable to the GP cement and FAs and mixes containing 40 µm glass added at 30% and 20 µm glass added at 40% were equivalent to the LP. These results provide an indication of the suitability of 10 µm and 20 µm glass powder added at 30% and 20% respectively as pozzolan and 20 µm and 40 µm glass powder added at 40% and 30% respectively as filler in SCC.

References

Abdallah, S., and Fan, M. (2014). “Characteristics of concrete with waste glass as fine aggregate replacement.” *International Journal of Engineering and Technical Research (IJETR)*, 2(6), 11-17.

Adaway, M., and Wang, Y. (2015). “Recycled glass as a partial replacement for fine aggregate in structural concrete – Effects on compressive strength.” *Special Issue: Electronic Journal of Structural Engineering*, School of Engineering, Deakin University, Australia. 14(1), 116-122.

Ali, E. E., and Al-Tersawy, S. H. (2012). “Recycled glass as a partial replacement for fine aggregate in self-compacting concrete.” *Construction and Building Materials, Elsevier,* 35, 785-791.

Allahverdi, A., and Salem, S. (2010). “Simultaneous influences of micro-silica and limestone powder on properties of Portland cement paste.” *Journal of Ceramics – Silikáty,* 54(1), 65-71.

ASTM C 125-15B. *Standard Terminology Relating to Concrete and Concrete Aggregates*, ASTM International, United States.

ASTM C 618-15. *Standard Specification for Coal Fly Ash and Raw or Calcined Natural Pozzolan for Use in Concrete,* ASTM International, United States.

Avila-López, U., Almanza-Robles, J. M., and Escalante-García, J. I. (2015). “Investigation of novel waste glass and limestone binders using statistical methods.” *Construction and Building Materials,* Elsevier, 82, 296-303.

Bhandari, P. S., and Tajne, K. M. (2013). “Use of waste glass in cement mortar.” *International Journal of Civil and Structural Engineering,* 3(4), 704-711.

Boel, V. (2010). *Microstructure on Self-compacting concrete in relation to gas permeability and durability,* Ph.D. thesis, Ghent University, Belgium.

Bouzoubaa, N., Lachemi, M. (2001). “Self-compacting concrete incorporating high volumes of class F fly ash: Preliminary results.” *Cement and Concrete Research, Elsevier,* 31(3), 413-420.

Byars, E. A., Morales, B., and Zhu, H. Y. (2004). *ConGlassCrete II: Project Final Report.* Center of Cement and Concrete. University of Sheffield, UK.

Caijun, S., Yanzhong, W., Chris, R., and Hugh, W. (2005). “Characteristics and pozzolanic activity of glass powders.” *Cement and Concrete Research, Elsevier,* 35(5), 987-993.

Cassar, J., and Camilleri, J. (2012). “Utilization of imploded glass in structural concrete.” *Construction and Building Materials, Elsevier,* 29, 299-307.

Celik, K., Jackson, M. D., Mancio, M., Meral, C., Emwas, A. H., Mehta, P. K., and Monteiro, P. J. M. (2014). “High-volume natural volcanic pozzolan and limestone powder as partial replacements for Portland cement in self-compacting and sustainable concrete.” *Cement and Concrete Composites, Elsevier,* 45, 136-147.

Chikhalikar, S. M., Tande, S. N. (2012). “An Experimental Investigation On Characteristics Properties of Fibre Reinforced Concrete Containing Waste Glass Powder as Pozzolona.” *Proc., 37th Conference on Our World in Concrete and Structures,* Singapore. 9 pages.

Cook, D. J., Cao, H. T. (1987). “An investigation of the pore structure in fly ash/OPC blends.” *Proc., 1st international RILEM congress on pore structure and materials properties,* Versailles, France, 69-76.

Dhir, R. K., Limbachiya, M. C., McCarthy, M. J. and Chaipanich, A. (2007). “Evaluation of Portland limestone cements for use in concrete construction.” *Materials and Structures,* 40, 459–473.

Diab, A. M., Elmoaty, A. E. M. A., and Ayman, A. A. (2016). “Long term study of mechanical properties, durability and environmental impact of limestone cement concrete.” *Alexandria Engineering Journal, Elsevier,* 55(2), 1465-1482.

Diaz-Loya, E. I., Allouche, E. N., and Vaidya, S. (2011). “Mechanical Properties of Fly-Ash-Based Geopolymer Concrete.” *Materials Journal,* 108(3), 300-306.

Dietz, J., and Ma, J. (2000). “Preliminary examinations for the production of self-compacting concrete using lignite fly ash.” LACER 5, 125-130.

Dinakar, P., Babu, K. G., and Santhanam, M. (2008). “Mechanical properties of high-volume fly ash self-compacting concrete mixtures.” *Structural Concrete,* 9(2), 109-116.

Domone, P. L. (2007). “A review of the hardened mechanical properties of self-compacting concrete.” *Cement and Concrete Composites, Elsevier,* 29(1), 1-12.

Domone, P. L. J., and Chai, H. W. (1997). “Testing of binders for high performance concrete.” *Cement and Concrete Research, Elsevier,* 27(8), 1141-1147.

Du, H., and Tan, K. H. (2014). “Concrete with recycled glass as fine aggregates.” *ACI Materials Journal,* 111(1), 47-58.

Dyer, T. D., and Dhir, R. K. (2011). “Chemical reactions of glass cullet used as cement component.” Journal of Materials in Civil Engineering, 13(6), 412-417.

Federico, L. M. (2013). *Waste Glass - A Supplementary Cementing Material.* Ph.D. thesis, McMaster University Hamilton, Ontario, Canada.

Felekoglu, B., Turkel, S., and Baradan, B. (2007). “Effect of water/cement ratio on the fresh and hardened properties of self-compacting concrete.” *Building and Environment, Elsevier,* 42(4), 1795-1802.

Ferraris, C. F., Obla, K. H., Hill, R. (2001). “The influence of mineral admixtures on the rheology of cement paste and concrete.” *Cement and Concrete Research, Pergamon,* 31(2), 245-255.

FIB Model Code for Concrete Structures. (2010). Ernst and Sohn, Berlin, Germany.

Fraay, A. L. A., Bijen, J. M., de-Haan Y. M. (1989). “The reaction of fly ash in concrete. A critical examination.” *Cement and Concrete Research, Elsevier,* 19(2), 235-246.

Gebler, S. H., Klieger, P. (1986). “Effect of Fly Ash on the Durability of Air-Entrained Concrete.” *Proc., 2nd International Conference on Fly Ash, Silica Fume, Slag, and Natural Pozzolans in Concrete*, ACI SP-91, American Concrete Institute, MI, 1, 483-519.

Ghrici, M., Kenai, S., and Said-Mansour, M. (2007). “Mechanical properties and durability of mortar and concrete containing natural pozzolana and limestone blended cements”. *Cement and Concrete Composites, Elsevier,* 29(7), 542-549.

Goldman, A., and Bentur, A. (1993). "Influence of micro fillers on enhancement of concrete strength," *Cement and Concrete Research*, *Elsevier,* 23(4), 962-972.

Gudissa, W., and Dinku, A. (2010). “The use of limestone powder as an alternative cement replacement material: An experimental study.” *Journal of European Economic Association,* 27, 33-43.

Guemmadi, Z., Resheidat, M., Chabil, H., and Toumi, B. (2009). “Modelling the influence of limestone filler on concrete: a novel approach for strength and cost.” *Jordan Journal of Civil Engineering,* 3(2), 158-171.

Hesami, S., Modarres, A., Soltaninejad, M., and Madani, H. (2016). “Mechanical properties of roller compacted concrete pavement containing coal waste and limestone powder as partial replacements of cement.” *Construction and Building Materials,* Elsevier, 111, 625-636.

Holschmacher, K., and Klug, Y. (2002). “A Database for the evaluation of hardened properties of SCC.” LACER 7, 123-134.

Hussain, M. V., and Chandak, R. (2015). “Strength Properties of Concrete Containing Waste Glass Powder.” *International Journal of Engineering Research and Applications*, 5(4), 1-4.

Idir, R., Cyr, M., and Tagnit-Hamou, A. (2011). Pozzolanic properties of fine and coarse color-mixed glass cullet.” *Cement and Concrete Composites, Elsevier,* 33(1), 19-29.

Isaia, G. C., Gastaldini, A. L. G., and Moraes, R. (2003). “Physical and pozzolanic action of mineral additions on the mechanical strength of high-performance concrete.” *Cement and Concrete Composites, Elsevier,* 25, 69-76.

Islam, M. M., and Islam, M. S. (2013). “Strength and durability characteristics of concrete made with fly ash blended cement.” *Australian Journal of Civil Engineering,* 14(3), 303-319.

Ismail, Z. Z., and Al-Hashmi, E. A. (2009). “Recycling of waste glass as a partial replacement for fine aggregate in concrete.” *Waste Management, Elsevier,* 29(2), 655-659.

Jin, W., Meyer, C., and Baxter, S. (2000). “Glasscrete-Concrete with glass aggregate.” *ACI Materials Journal*, 27, 208-213

Kathirvel, P., Saraswathy, V., Karthik, S. P., Sekar A. S. S. (2013). “Strength and Durability Properties of Quaternary Cement Concrete Made with Fly Ash, Rice Husk Ash and Limestone Powder.” *Journal of Science and Engineering, ORIC Publications,* 38, 589-598.

Khatib, J. M., Negim, E. M., Sohl, H. S., and Chileshe, N. (2012) “Glass Powder Utilisation in Concrete Production.” *European Journal of Applied Sciences, IDOSI Publications* 4(4), 173-176.

Khmiri, A., Samet, B., and Chaabouni, M. (2012). “Assessment of the waste glass powder pozzolanic activity by different methods.” *International Journal of Research and Reviews in Applied Sciences,* 10(2), 322-328.

Kiattikomol, K., Jaturapitakkul, C., Songpiriyakij, S., and Chutubtim, S. (2001). “A study of ground coarse fly ashes with different fineness from various sources as pozzolanic materials.” *Cement and Concrete Composites,* 23, 335-343.

Kopanitsa, N. O., Anikanova, L. A., and Makarevich, M. S. (2002). “Fine additives filled with binders based on cement.” *Journal of Building Materials*, 9, 2-4.

Kou, S. C., and Poon, C. S. (2009). “Properties of self-compacting concrete prepared with recycled glass aggregate.” Cement and Concrete Composites, 31, 107-113.

Kou, S. C., Poon, C. S., and Chan, D. (2007). “Influence of Fly Ash as Cement Replacement on the Properties of Recycled Aggregate Concrete.” *Journal of Material and Civil Engineering,* 19(9), 709-717.

Kumarappan, N. (2013). “Partial Replacement Cement in Concrete Using Waste Glass.” *International Journal of Engineering Research and Technology (IJERT)*, 2(10), 1880-1883.

Langley, W. S., Carette, G. G., and Malhotra, V. M. (1992). “Strength development and temperature rise in large concrete blocks containing high volumes of low-calcium (ASTM Class F) fly ash.” *ACI Material Journal,* 89(2), 362–368.

Lawrence, P., Cyr. M., and Ringot, E. (2003). “Mineral admixtures in mortars – effect of inert materials on short-term hydration.” *Cement and Concrete Research, Elsevier,* 33(12), 1939-1947.

Li, G. L., and Kwan, A. K. H. (2015). “Adding limestone fines as cementitious paste replacement to improve tensile strength, stiffness and durability of concrete.” *Cement and Concrete Composites,* 60, 17-24.

Liu, M. (2009). *Wider application of additions in self-compacting concrete.* PhD Thesis, University College London, United Kingdom.

Liu, M. (2011). “Incorporating ground glass in self-compacting concrete.” *Construction and Building Materials, Elsevier,* 25(2), 919-925.

Livesy, P. (1991). “Performance of limestone-filled cements.” *Proc., International Conference on Blended Cements in Construction,* (Ed. Swamy, R. N.), Elsevier Science, Essex, UK, 1-15.

Lollini, F., Redaelli, E., and Bertolini, L. (2013). “Effects of Portland cement replacement with limestone on the properties of hardened concrete.” *Cement and Concrete Composites,* 46, 32-40.

Mackechnie, J. R., and Munn, C. (2012). “Characterising recycled aggregates for use in New Zealand ready-mix concrete production.” 8 pages.

Mackechnie, J. R., Kesha, B. (2005). “Mechanical properties of New Zealand self-compacting concretes.” *Proc., Developments in mechanics of Structures and Materials*, (Ed. Deeks and Hao), Taylor and Francis Group, London, 853-857.

Malhotra, V. M., and Mehta, P. K. (2005). “High performance, high-volume fly ash concrete: materials, mixture proportioning, properties, construction practice, and case histories.” *Supplementary Cementing Materials for Sustainable Development Inc.,* Ottawa Canada.

Marzouki, A., A., Lecomte, A., Beddey, A., Diliberto, C., and Ouezdou, M. B. (2013). “The effects of grinding on the properties of Portland-limestone cement.” *Construction and Building Materials, Elsevier,* 48, 1145-1155.

Menendez, G., Bonavetti, V., and Irassar, E. F. (2003). “Strength development of ternary blended cement with limestone filler and blast-furnace slag.” *Cement and Concrete Composites*, *Elsevier,* 25(1), 61-67.

Metwally, I. M. (2007). “Investigation on the performance of concrete made with blended finely milled waste glass.” *Advances in Structural Engineering,* 10(1), 47-53.

Mimura, Y., Yoshitake, I., and Zhang, W. (2011). “Uniaxial tension test of slender reinforced early age concrete members.” *Materials,* 4(8), 1345-1359.

Naik, T. R., and Singh, S. S. (1991). ‘‘Effects of inclusion of fly ash on abrasion resistance of concrete.’’ *Proc., 2nd CANMET/ACI Conf. on Durability of Concrete,* American Concrete Institute, Detroit, 683-707.

Naik, T. R., Sivasundaram, V., and Singh, S. S. (1991). *Use of high-volume class F fly ash for structural grade concrete,* Transportation Record No. 1301, Transportation Research Record, National Research Council, Washington, USA, 40-47

Nehdi, M., Mindess, S., and Aitcin, P. (1996). “Optimization of high strength limestone filler cement mortars,” *Cement and Concrete Research, Elsevier,* 26(6), 883-893.

Newman, J., and Choo, B. S. (2003). *Advanced Concrete Technology 1: Constituent materials,* Butterworth-Heinemann, Elsevier, Burlington, MA.

Nwaubani, S. O., and Poutos, K. I. (2013). “The Influence of Waste Glass Powder Fineness on the Properties of Cement Mortars.” *International Journal of Application or Innovation in Engineering and Management (IJAIEM),* 2(2), 110-116.

Ogawa K., Uchikawa H., Takemoto, K., and Yasui, I. (1980). “The mechanism of the hydration in the system C_3S pozzolana.” Cement and Concrete Research, Elsevier, 10(5), 683-696.

Opoczky, L. (1992). “Progress of the particle size distribution during the intergrinding of a clinker–limestone mixture.” *Zement.–Kalk–Gips,* 45(12), 648-651.

Ozkan, O., and Yuksel, I. (2008). “Studies on mortars containing waste bottle glass and industrial by-products.” *Construction and Building Materials, Elsevier,* 22(6): 1288-1298.

Park, S. B., Lee, B. C., and Kim, J. H. (2004). “Studies on mechanical properties of concrete containing waste glass aggregate.” *Cement and Concrete Research*, *Elsevier,* 34, 2181–2189.

Paulou, K. (2003). “Pre-testing of self-compacting concrete with various mineral additives and admixtures.” *Proc., 3rd International RILEM Symposium on Self- Compacting Concrete.* (Ed. Wallevik, O. H., Nielsson, I.), RILEM Publications S.A.R.L., Bagneux, France, 442-445.

Persson, B. (2001). “A comparison between mechanical properties of self-compacting concrete and the corresponding properties of normal concrete.” *Cement and Concrete Research, Elsevier,* 31, 193-198.

Phillips, J. C., Cahn, D. S., Keller, G. W. (1972). "Refuse Glass Aggregate in Portland Cement Concrete," *Proc., Third Mineral Waste Utilization Symposium,* U.S. Bureau of Mines, Chicago, Illinois, United States.

Poon, C. S., and Ho, D. W. S. (2004). “A feasibility study on the utilization of r-FA in SCC.” *Cement and Concrete Research, Elsevier,* 34(12), 2337-2339.

Ramanathan, P., Baskar, I., Muthupriya, P., and Venkatasubramani, R. (2013). “Performance of self-compacting concrete containing different mineral admixtures.” *KSCE Journal of Civil Engineering*, 17(2), 465-472.

Ramezanianpour, A. A., Ghiasvand, E., Nickseresht, I., Mahdikhani, M., and Moodi, F. (2009). “Influence of various amounts of limestone powder on performance of Portland limestone cement concretes.” *Cement and Concrete Composites, Elsevier,* 31(10), 715-720.

Roberts, L. R. (1989). “Microsilica in concrete I.” *Materials Science of Concrete, Vol. 1,* American Ceramic Society, Westerville, OH, 197-222.

Saccani, A., and Bignozzi, M. C. (2010). “ASR expansion behaviour of recycled glass fine aggregates in concrete.” *Cement and Concrete Research, Elsevier,* 40(4), 531-536.

Sakai, E., Masuda, K., Kakinuma, Y., Aikawa, Y. (2009). “Effects of Shape and Packing Density of Powder Particles on the Fluidity of Cement Pastes with Limestone Powder.” *Journal of Advanced Concrete Technology,* Japan Concrete Institute, 7(3), 347-354.

Schwarz, N., and Neithalath, N. (2008). “Influence of a fine glass powder on cement hydration: Comparison to fly ash and modeling the degree of hydration.” *Cement and Concrete Research, Elsevier,* 38(4), 429-436.

Schwarz, N., Cam, H., and Neithalath, N. (2008). “Influence of a fine glass powder on the durability characteristics of concrete and its comparison to fly ash.” *Cement and Concrete Composites, Elsevier,* 30(6), 486-496.

Sear, L. K. A. (2001). *The properties and use of coal fly-ash: A valuable industrial by-product.* Thomas Telford Publishing, Thomas Telford Ltd, UK.

Shao, Y., Lefort, T., Moras, S., and Rodriguez, D. (2000). “Studies on concrete containing ground waste glass.” *Cement and Concrete Research, Elsevier,* 30(1), 91-100.

Sharifi, Y., Houshiar, M., and Aghebati, B. (2013). “Recycled glass replacement as fine aggregate in self-compacting concrete.” *Frontiers of Structures and Civil Engineering,* 7(4), 419-428.

Shayan, A., and Xu, A. (2006). “Performance of glass powder as a pozzolanic material in concrete: A field trial on concrete slabs”. *Cement and Concrete Research, Elsevier,* 36(3), 457-468.

Shekhawat, B. S., and Aggarwal, V. (2014). “Investigation of Strength and Durability Parameters of Glass Powder Based Concrete.” *International Journal of Engineering Research & Technology (IJERT),* 3(7), 333-338.

Shi, C. J., Wu, Y. Z., Riefler, C., Wang, H. (2005). “Characteristics and pozzolanic reactivity of glass powders.” Cement Concrete Research, Elsevier, 35(5), 987-993.

Siad, H., Mesbah, H. A., Khelafi, H., Kmalai-Barnard, S., and Mouli, M. (2010). “Effects of Mineral Admixture on Resistance to Sulphuric and Hydrochloric Acid Attacks in Self-Compacting Concrete.” *Canadian Journal of Civil Engineering,* 37(3), 441-449.

Siddique, R. (2004). “Performance characteristics of high-volume Class F fly ash concrete.” *Cement and Concrete Research.* Elsevier, 34(3), 487-493.

Singh, K., Singh, S., and Singh, G. (2014). “Effect of Fly ash Addition on Mechanical and Gamma Radiation Shielding Properties of Concrete.” *Journal of Energy, Hindawi Publishing Corporation,* 2014, 7 pages.

Sivasundaram, V., Carette, G. G., and Malhotra, V. M. (1990). “Selected properties of high-volume fly ash concretes.” *Concrete International,* 12(10):47–50.

Sonebi, M., Bartos, P. J. M., Zhu, W., Gibbs, J., and Tamimi, A. (2005). *Task 4: Properties of Hardened Self-Compacting Concrete—Final Report.* Advanced Concrete Masonry Center, University of Paisley, Scotland. p. 73.

Soni, D. K. and Saini, J. (2014). “Mechanical properties of high volume fly ash (HVFA) and concrete subjected to evaluated 120°C temperature.” *International Journal of Civil Engineering Research,* 5(3), 241-248.

Soroka, I., and Stern, N. (1977). “The effect of fillers on strength of cement mortars,” *Cement and Concrete Research, Elsevier,* 7(4), 449-456.

Sukumar, B., Nagamani, K., and Raghavan, R. S. (2008). “Evaluation of strength at early ages of self-compacting concrete with high volume fly ash.” *Construction and Building Materials, Elsevier,* 22(7), 1394-1401.

Swaddiwudiwudhipong, S., Lu, H., and Wee, T. (2003). “Direct tension test and tensile strain capacity of concrete at early age.” *Cement Concrete Research, Elsevier,* 33(12), 2077-2284.

Taha, B., and Nounu, G. (2008). “Properties of concrete contains mixed colour waste recycled glass as sand and cement replacement.” *Construction and Building Materials, Elsevier,* 22(5), 713-720.

Tattersall, G. H., and Banfill, P. F. G. (1983). *The rheology of fresh concrete.* Pitman Advanced Publishing Program, The University of Michigan.

Thomas, M. (2007). *Optimizing the Use of Fly Ash in Concrete.* University of New Brunswick. Portland Cement Association, Illinois, USA.

Topcu, I. B., and Canbaz, M. (2004). “Properties of Concrete Containing Waste Glass.” *Cement and Concrete Research, Elsevier,* 34(2), 267-274.

Uysal, M., and Yilmaz, K. (2011). “Effect of mineral admixtures on properties of self-compacting concrete.” *Cement and Concrete Composites, Elsevier,* 33(7), 771-776.

Vandhiyan, R., Ramkumar, K., and Ramya, R. (2013). “Experimental study on replacement of cement by glass powder.” *International Journal of Engineering Research and Technology (IJERT)*, 2(5), 234-238.

Vanjare, M. B., and Mahure, S. H. (2012). “Experimental investigation on self-compacting concrete using glass powder.” *International Journal of Engineering Research and Applications*, 2(3), 1488-1492.

Vasudevan, G., and Pillay, S. G. K. (2013). “Performance of using waste glass powder in concrete as replacement of cement.” *American Journal of Engineering Research (AJER),* 2(12), 175-181.

Vengala, J., Sudarsan, M.S., and Ranganath, R. V. (2003). “Experimental study for obtaining self-compacting concrete”. *Indian Concrete Journal,* 1261-1266.

Vijayakumar, G., Vishaliny, H., and Govindarajulu, D. (2013). “Studies on glass powder as partial replacement of cement in concrete production.” *International Journal of Emerging Technology and Advanced Engineering*, 3(2), 153-157.

Wang, C. C., Wang, H. Y., Tang, C. W. and Huang, J. J. (2014). “A nonlinear-multivariate regression prediction of compressive strength of waste glass concrete.” *Springer International Publishing,* Switzerland, 561-567.

Wang, H. Y. (2009). “A study of the effects of LCD glass sand on the properties of concrete.” *Journal of Waste Management*, 29(1), 335-341.

Wright, J. R., Cartwright, C., Fura, D., and Rajabipour, F. (2014). “Fresh and hardened properties of concrete incorporating recycled glass as 100% sand replacement.” *Journal of Materials in Civil Engineering*, ASCE, 26(10), 04014073-1-04014073-11.

Xie, Y., Liu, B., Yin, J., and Zhou, S. (2002). “Optimum mix parameters of high-strength self-compacting concrete with ultra-pulverized fly ash.” *Cement and Concrete Research, Elsevier,* 32(3), 477-480.

Yahia, A., Tanimura, M., and Shimoyama, Y. (2005). “Rheological properties of highly flowable mortar containing limestone filler-effect of powder content and w/c ratio.” *Cement Concrete Research, Elsevier,* 35(3), 532-539.

Yamato, T., and Sugita, H. (1983). *SP 79: Fly ash, silica fume, slag, and other mineral by products in concrete.* American Concrete Institute, Detroit, 87-102.

Ye, G., Liu, X., De Schutter, G., Poppe, A. M., and Taerwe, L. (2007). “Influence of limestone powder used as filler in SCC on hydration and microstructure of cement pastes.” *Cement and Concrete Composites, Elsevier,* 29(2), 94-102.

Yoshitake, I., Rajabipour, F., Mimura, Y., and Scanlon, A. (2012). “A prediction method of tensile Young’s modulus of concrete at early age.” *Advances in Civil Engineering,* Hindawi Publishing Corporation, 2012, 10 pages.

Zilch, K. and Roos, F. (2001). “An equation to estimate the modulus of elasticity of concrete with recycled aggregates.” *Civil Engineering,* 76(4), 187-191.

Zsigovics, I. (2005). “Effect of limestone powder on the consistency and compressive strength of SCC.” *Proc., 4th International RILEM Symposium on Self-Compacting Concrete*, 173-180.

CHAPTER 6

INFLUENCE OF GLASS POWDER ON LONG-TERM DURABILITY OF SELF-COMPACTING CONCRETE

ACRONYMS USED

GP	GP cement control mix
FAF30%	Mix containing class F fly ash replaced by 30% of GP cement
FAC30%	Mix containing class C fly ash replaced by 30% of GP cement
LP30%	Mix containing limestone powder replaced by 30% of GP cement
20UG30%	Mix containing 20 microns unwashed glass powder replaced by 30% of GP cement
10G30%	Mix containing 10 microns washed glass powder replaced by 30% of GP cement
20G20%	Mix containing 20 microns washed glass powder replaced by 20% of GP cement
20G30%	Mix containing 20 microns washed glass powder replaced by 30% of GP cement
20G40%	Mix containing 20 microns washed glass powder replaced by 30% of GP cement
40G30%	Mix containing 20 microns washed glass powder replaced by 30% of GP cement
CTR	All materials class: GP, class F and C fly ashes and glass powder/Control materials class: GP, class F and C fly ashes
GL-FN	Washed glass powder classified according to fineness: having fineness of 10 µm, 20 µm and 40 µm; added at 30%
GL-CN	Washed glass powder classified according to content: added at 20%, 30% and 40%; having fineness of 20 µm

HIGHLIGHTS

- Investigation of the influence of different finenesses and replacement levels of glass powder on oxygen permeability, porosity, electrical resistivity, chloride diffusion and drying shrinkage of SCC.
- Evaluation of the durability characteristics of SCC consuming different glass sizes and contents compared to the behaviour demonstrated by GP cement, fly ashes and limestone powder.

6.1 Introduction

The durability of concrete is defined as its ability to resist weathering action, chemical attack, abrasion and any other mechanism of deterioration or its quality to perform for a certain time with required safety and corresponding characteristics, preserving its original form and quality, when exposed to an aggressive environment (Mehta and Monteiro, 2006). At the beginning, durability issues generally appear as the material deterioration. Although material deterioration does not present an immediate safety concern, it progressively leads to structural damage, which reduces its load carrying capacity or ductility. Physical deterioration mechanism in concrete material includes wetting/drying, freeze/thaw or heating/cooling cycles whereas, chemical damage consists of sulphate attack, acid attack, chloride attack and ASR in which water acts as a carrier. All these damages are strongly related to the resistance of the cover layer to transport mechanisms, such as permeation, absorption, and diffusion of gas and liquid (Alexander and Magee, 1999). Since many concrete structures are located in the marine environment, such as cross-ocean tunnels, long-span bridges and offshore drilling platforms, the main degradation process for durability of reinforced concrete structures in the marine environment is the corrosion of the concrete reinforcement. Out of the few methods to reduce the deterioration of concrete in the marine environment, one is the addition of mineral admixtures in the production of concrete. For concretes made by cement blended with certain kind of mineral additions, however, there can be a decrease in chloride threshold for corrosion, reduction in its binding ability, lower pH in concrete porous network solution as well as with its lower buffering effect (Meira et al., 2014).

Despite some of the possible limitations on using SCMs, they have generally resulted in significant improvements to the durability of concrete. Although the inadequate durability is by far the most common cause of premature degradation of concrete structures, yet little attention is often given to durability in the concrete design process. Most of the current design methods do not use rational or targeted durability design approach and/or the design is mostly covered by prescriptive specifications only. In general, the durability design is done by the use of prescriptive methods and putting limiting values in mix constituents, such as maximum w/c and minimum cement content. These limiting values are generally based on lab and field tests, empirical relations and past experience. Very often the issue of durability is overlooked since engineers make the assumption that strong concrete is also durable. This lack of attention led the researchers to investigate the durability of SCC, incorporating mineral admixtures, particularly waste glass powder, in the scope of this research program.

Many durability tests have been developed to measure the fluid or gas permeation through concrete by various mechanisms. The approach for durability index testing has been

proposed in order to provide practical ways to identify the durability potential of concrete (Alexander, 1997). The key aim of material indexing is to provide a reproducible engineering measure of microstructure and characteristics of concrete, essential for its durability, at a relatively early age. Hence, it becomes possible to produce concretes of similar durability by a number of different ways, including additional curing, lower w/c ratio, different binder types, etc. (Alexander and Beushausen, 2009). The material indexing approach is based on the principles including (1) durability of reinforced concrete structures mainly depends on the quality of the surface layer, which means its capability to protect the reinforcing steel (2) it is a way to identify the quality of concrete cover layer using parameters that affect the deterioration processes, which are linked with transport mechanisms. Therefore, each index test is linked to a transport mechanism, such as gaseous and ionic diffusion and water absorption, relevant to a particular deterioration process. Three durability index tests have been developed in order to investigate the extent of potential damage to concrete materials (Alexander et al., 2001; Ballim, 1991; Streicher and Alexander, 1995; Alexander and Magee, 1999; Streicher and Alexander, 1999); namely the oxygen permeability test, the water permeability test and the chloride resistivity test. These tests that have been developed and proved in the laboratories are increasingly being applied on site in actual construction works (Gouws et al., 2001; Preez and Alexander, 2004) and have also been undertaken in this study.

Out of the key objectives of this study was to investigate the long-term durability properties of SCC, utilizing glass contents of 20%, 30% and 40% and glass finenesses of 10 µm, 20 µm and 40 µm as partial replacements for GP cement. The results of these investigations have been presented and discussed in this chapter. As outlined in Chapter 3, the aggregate proportions and water to binder ratio (w/b) were maintained as constants while glass size ranges of 10-40 µm and replacement levels of 20-40% of GP cement by weight were selected for production of SCC. The concrete produced with these materials was then tested for oxygen permeability, porosity and electrical resistivity at the curing ages of 3 to 545 days, coefficient of chloride diffusion at the curing ages of 28 to 545 days and drying shrinkage at the curing ages of 7 to 180 days. All testing was done in Civil Engineering Laboratories on the campus of University of Canterbury, New Zealand, except few drying shrinkage tests that were undertaken at Allied Concrete, Christchurch Plant, New Zealand. Before performing the tests, all specimens were kept under the standard conditions according to the requirement of each test. The tests were carried out at room temperature, normally between 18°C and 23°C. All the materials, tests, and experimental procedure have already been described in Chapter 3. The complete list of performed tests and references for their results are summarized in Table 6.1.

Table 6.1: Tests on SCC and references to their results

TESTS	AIMS	CTR/AM [1]	GL-FN [2]	GL-CN [3]	UG [4]
Oxygen permeability tests	To assess the influence of binders on resistance to oxygen permeation through SCC	Figs. 6.1, 6.3, 6.5, 6.7	Fig. 6.2	Fig. 6.4	Fig. 6.6
Porosity tests	To assess the influence of binders on transport of water through porous SCC	Figs. 6.8, 6.10, 6.12, 6.14, 6.15	Fig. 6.9	Fig. 6.11	Fig. 6.13
Electrical resistivity tests	To assess the influence of binders on chloride ion penetration resistance of SCC	Figs. 6.16, 6.18, 6.20, 6.22	Fig. 6.17	Fig. 6.19	Fig. 6.21
Chloride diffusion tests	To assess the influence of binders on apparent chloride diffusion coefficient of SCC	Figs. 6.23, 6.25, 6.27, 6.29, 6.30, 6.31	Fig. 6.24	Fig. 6.26	Fig. 6.28
Drying shrinkage tests	To assess the influence of binders on drying shrinkage characteristics of SCC	Fig. 6.32	Fig. 6.33	Fig. 6.34	Fig. 6.35

[1] Control materials class: GP cement, class F and C fly ashes and limestone powder/All materials class: containing all materials
[2] Glass powder classified according to fineness: 10 µm, 20 µm, and 40 µm; added at 30%
[3] Glass powder classified according to content: 20%, 30%, and 40%; having fineness of 20 µm
[4] Glass powder classified according to its quality: unwashed glass; fineness of 20 µm; added at 30%

6.2 Oxygen permeability of self-compacting concrete incorporating glass powder

Theoretically, the key factors that control the permeation characteristics of concrete are the relative volume of paste matrix, pore structure of the bulk matrix and interfacial zone around the aggregate particles. It is believed that the enhanced stability of the fresh mix, use of additional fine powder and elimination of vibration allow more homogeneous microstructures and denser interfacial zones in SCC, as more efficient packing and less bleeding may improve its permeation resistance. Furthermore, the addition of mineral admixtures in SCC may also improve particle packing and decrease the permeability of concrete (Assie et al., 2007). Out of the permeation properties, oxygen permeability has widely been used to quantify durability characteristics of concrete (Zhu and Bartos, 2003). To determine oxygen permeability index (OPI), Ballim (1991) developed a falling-head permeameter that allows simple measurement of an oven-dried concrete. A pressure gradient is applied across the concrete specimen placed in the permeameter and the OPI is the measurement of the pressure decay of oxygen through the concrete specimen over time (Beushausen and Alexander, 2008). Concrete with OPI values above 10 indicate excellent impermeability, whereas values below 9 are considered to have poor impermeability (Mackechnie and

Alexander, 2002). The OPI obtained with this test is based on the coefficient of permeability (K-value) and is defined as the negative log of the K-value (Beushausen and Luco, 2016). Therefore, the K-values below 1E-10 represent excellent impermeability of concrete. This standard value (1E-10) has been marked as the red line in Figures 6.1, 6.2 and 6.4.

The present section consists of the findings from the experimental study on oxygen permeability of a range of SCC mixes, incorporating control binders as well as glass powders of varying finenesses, contents and quality. The test procedures, curing conditions and preparation of concrete cores prior to testing have already been explained in Chapter 3. All the tests were undertaken at predefined curing ages. The average K-values were obtained from four replicate specimens. Complete data are shown in Appendix E. Figure 6.1 illustrates the average K-values of the control (CTR) specimens at the curing ages of 3, 7, 28, 90, 180, 365 and 545 days. GP concrete exhibited the highest K-values compared to the other CTR mixes at almost all curing ages, with a significant reduction of 48% between 3-days and 7-days, followed by only a slight decrease up to 14% from 7-days to 545-days.

It has been established that the partial replacement of GP cement by FA leads to a significant reduction in permeability of both cement paste (Manmohan and Mehta, 1891; Marsh et al., 1985) and concrete (Thomas et al., 1989). This reduction can be linked to the combination of the reduction in water content for a given workability and the pore structure refinement due to the pozzolanic reaction. Due to long-term nature of the pozzolanic reaction, the advantages associated with it are more obvious in the long-cured concrete (Thomas and Matthews, 1992), similarly noticed in this study. In comparison to GP, both FA

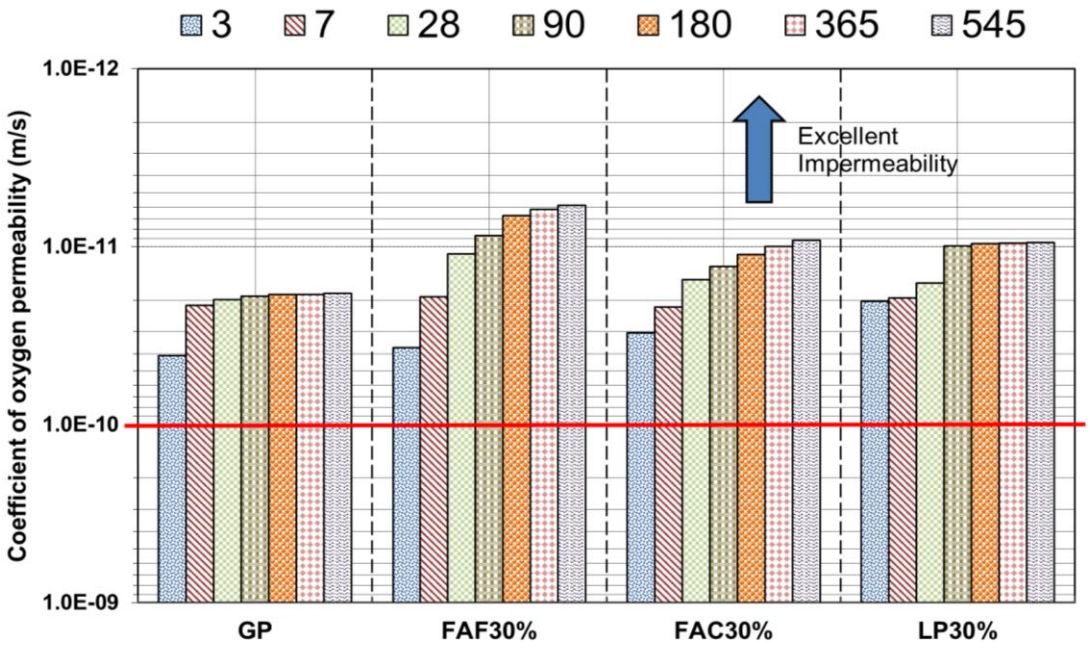

Figure 6.1: Coefficients of oxygen permeability of CTR mixes

types showed significant improvement in oxygen permeation resistance with the curing period. The 28-days K-values of SCCs with 30% class F and class C fly ashes on average decreased by 45% and 23% respectively, compared with the K-value of the SCC containing GP (no fly ash). The reduction in K-value due to FA became more marked as the curing period was extended; at 90-days of curing, SCC with FAF and FAC were 54% and 32% less permeable than SCC with GP cement. It is also apparent from the results that incorporation of FAs had a very significant influence on K-values up to 180-days of curing but after 180-days, minor reductions in K-values were recorded for FA levels at 30%. Hence, FAF30% and FAC30% demonstrated 68% and 49% lower K-values in comparison to GP by the end of 545-days curing, showing only 5%-7% reduction in K-values with respect to 365-days. The significantly higher resistance to oxygen penetration in SCC mixes produced with FAs might be attributed to their less porous interfacial zone and also the refined pore structure of the paste matrix, consistently mentioned by Zhu and Bartos (2003). Another important observation is the difference in oxygen permeability of both FA types throughout the study schedule. FAF30% demonstrated lower K-values relative to FAC30%, which can be related to the higher pozzolanic activity in class F FA in comparison to class C FA.

Several studies have shown that the nucleation effect of fine particles of $CaCO_3$ present in LP leads to the refinement of the pore structure of their pastes with cement, reduction in the connectivity of the pore structure and hence, the improvement in the pore structure (Ramezanianpour, 2014). The key to the lower permeability of LP incorporated SCC is related to its pore structure connectivity. The early-age K-value of LP30% was found to be the lowest of all CTR mixes, potentially due to the better packing of cement granular skeleton (Opoczky, 1992) and its performance as the crystallization nucleus for the precipitation of CH (Soroka and Stern, 1977), which accelerated the hydration of cement grains and thus, improved permeability at 3-days. Nevertheless, LP demonstrated 5%-31% higher K-values compared to FAF30% and FAC30% at 28-days. Bhuiyan (2012) similarly reported that LP replaced by cement at 30% shows higher K-values in comparison to FA substituted by GP at the same replacement level at 28-days. As the curing time progressed to 90-days, K-value obtained by LP30% was found to be 93% lower than GP, which is consistent to Moir and Kelham (1993) who also found that the presence of LP reduces the permeability to oxygen for concretes made with GP and 5%-25% LP. Tsivilis et al. (2002) similarly concluded that LP incorporated concretes have competitive concrete properties compared with GP concrete, as the inclusion of LP improves the oxygen permeability of concrete. Although long-term standard curing did not have a significant influence on its better performance, LP30% still showed a continuous reduction in K-values between 90-days and 545-days and achieved improved permeation resistance than GP and FAC30%. Hence, the findings from

oxygen permeability tests are consistent with the literature, which in general appears to approve the hypothesis that the use of LP as an SCM improves the durability of the concrete (Thomas and Hooton, 2010).

(a) Effects of glass fineness on coefficient of oxygen permeability

Finely ground glass powder as a replacement for cement is known to exhibit very high pozzolanic activity. The addition of fine glass powder also results in a denser structure and in the disconnection of existing pores forming an impermeable medium and limiting the transfer of gases or fluids inside concrete (Chaid et al., 2015). Similar behaviour of glass powder was also observed in this study, as SCC including recycled glass powder exhibited good permeation resistance to oxygen. Figure 6.2 demonstrates the coefficients of oxygen permeability of GL-FN class cured up to 545-days under standard curing conditions. The oxygen permeability of coarser to finer range of glass powders was investigated in order to highlight the changes in the oxygen permeation resistance with variations in particle sizes.

Primarily, coefficient of oxygen permeability of SCC incorporating glass increased as the glass particle size became coarser, indicating its lower resistance to gaseous permeation due to coarser particles. The K-value obtained at 3-days for 10G30% was observed to be the lowest in GL-FN class; more specifically, it was 25% and 94% lower compared with 20G30% and 40G30% respectively. However, as the curing time advanced to 7-days, 20G30% affected the permeation resistance to a considerable extent. Thus, 20G30% exhibited 84% and 232% lower K-values than 10G30% and 40G30% at 7-days respectively, followed by a similar behaviour until 90-days of standard curing. This discrepancy in result might be related

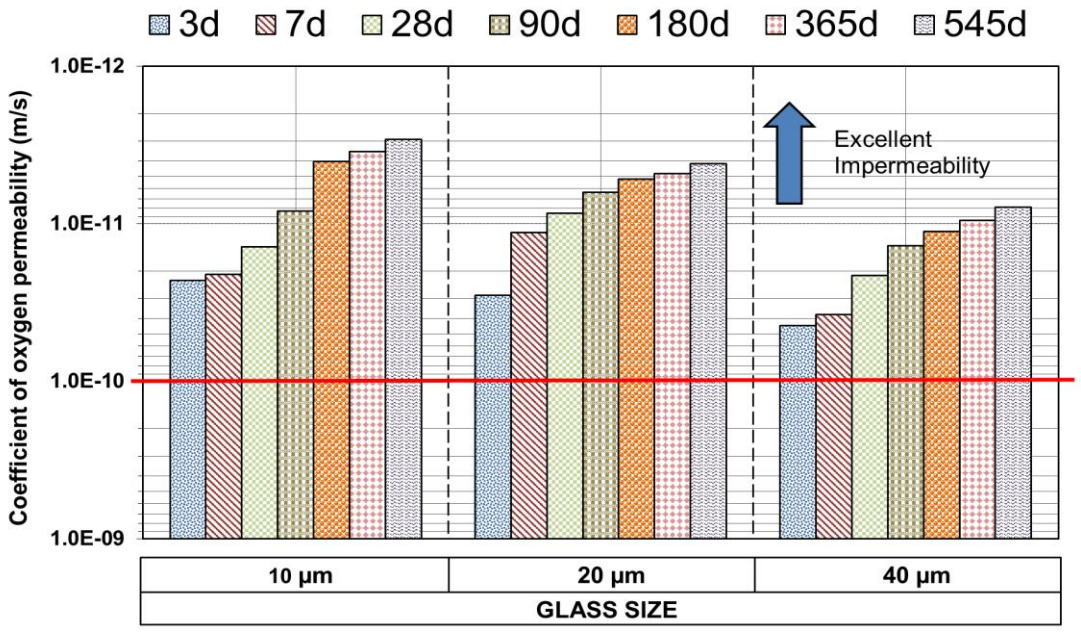

Figure 6.2: Coefficients of oxygen permeability of GL-FN with curing age up to 545-days

to the fact that concrete is a complex heterogeneous material and hence, perfect trends in the results cannot be expected. Subsequently, as the curing period advanced to 180-days, the test results informed that 10G30% exhibited 29% and 176% lower K-values in comparison to 20G30% and 40G30%. This might be ascribed to the addition of very fine glass powder, which resulted in substantial pore refinement and as the cement hydration period progressed, it transformed bigger pores into smaller ones due to the pozzolanic reaction, improved its transport properties and hence, the permeation resistance of concrete. However, from 180-days until 545-days of water curing, the lowest K-value in all GL-FN specimens was shown by the 10G30%, which was dropped by 42% and 168% than 20G30% and 40G30% respectively, at 545-days. In addition, the rate of improvement in oxygen penetration resistance in 10G30% was found to be higher in comparison to the other SCC types between 180-days and 365-days, which implies that water curing has more significant effect on the oxygen penetration resistance of the finer glass powder compared to the coarser glass powder. Hence, it can be concluded that particle size and prolonged curing of the glass powder have a considerable influence on a proper structure formation in concrete, also affecting its permeability.

Figure 6.3 shows the comparison between coefficients of oxygen permeability of few CTR mixes and glass mixes categorized in GL-FN class. It is evident that GP mix exhibited the highest coefficients of permeability in comparison to all of these glass mixes at most of the curing ages up to 545-days. Moreover, comparison of glass and FA as SCMs indicate that the glass at a similar particle size showed comparable oxygen permeability coefficients corresponding to the FA. To elaborate, 3-days K-values achieved by 10G30%, 20G30% and

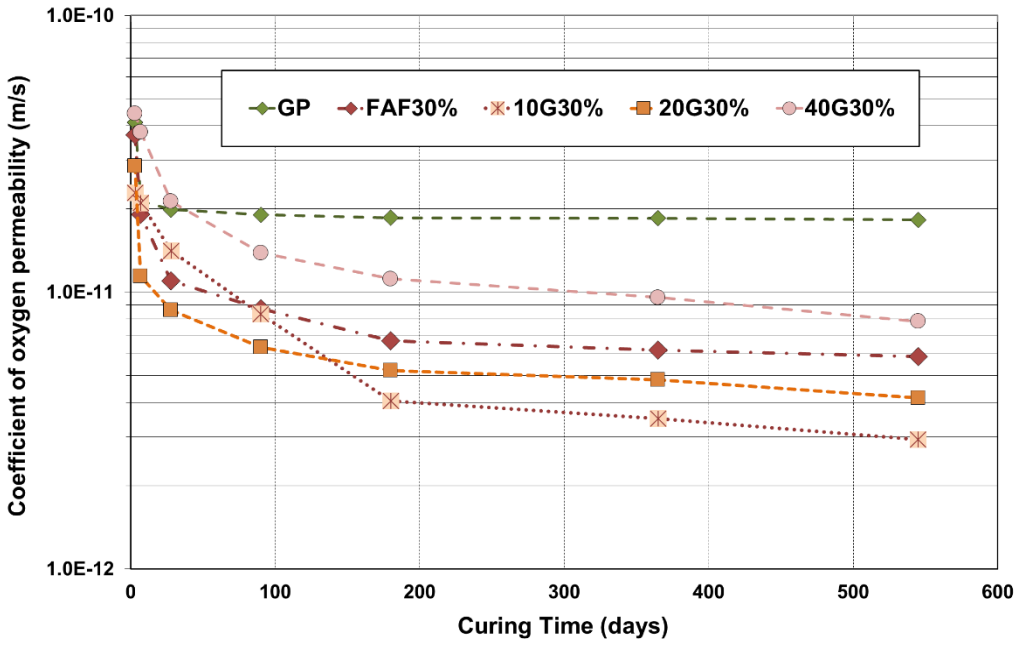

(a)

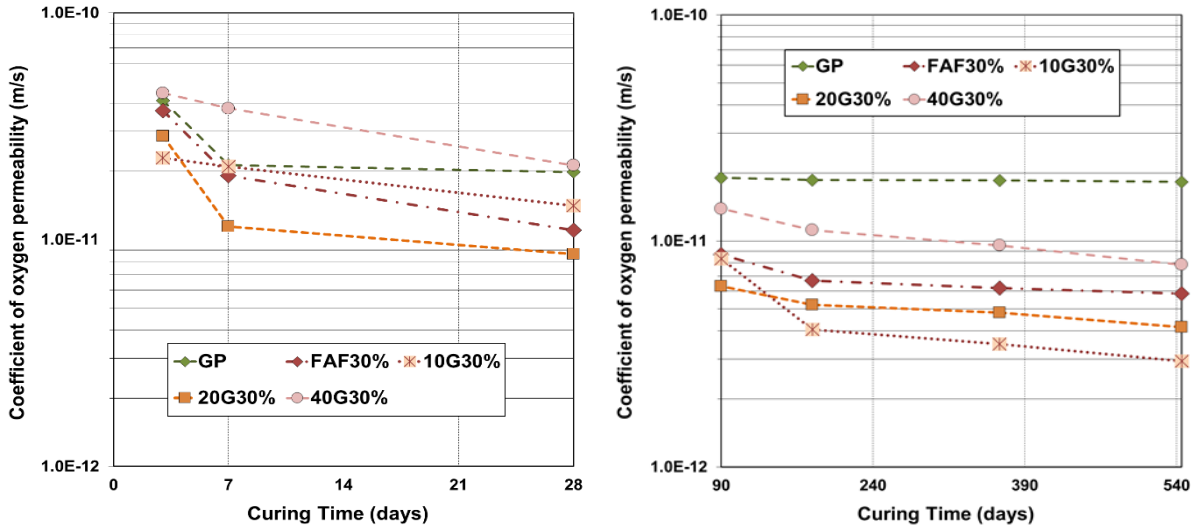

Figure 6.3: (a) Comparison between coefficients of permeability of GL-FN, GP and FAF30% up to 545-days; (b) Comparison between coefficients of permeability of GL-FN, GP and FAF30% from 3 to 28 days; (c) Comparison between coefficients of permeability of GL-FN, GP and FAF30% from 90 to 545 days

40G30% were 33%-62%, 6%-30% and 16%-31% lower than FAF30% and FAC30% respectively. In addition, 10G30%, 20G30%, and 40G30% showed 11%, 29% and 54% higher K-values compared to LP30% at 3-days respectively, which indicates that similar to better compressive strength development than GL-FN at 3-days, LP30% also showed better durability than GL-FN at 3-days. By 7-days, 10G30% demonstrated almost similar K-value to GP, with an insignificant variation of 2%. The 28-days tests demonstrate that the K-value shown by 10G30% was higher than FAF30% by 22% but lower than FAC30% by 8%. The K-value of 20G30% was found to be lower by 86% than LP30% at 28-days; however, 40G30% exhibited 25% higher K-value than LP30%. Moreover, 20G30% showed 29% lower K-value compared to FAF30% whereas, 40G30% showed almost similar permeability coefficient to FAC30% at 180-days. The progress in curing time enhanced the oxygen permeation resistance of all specimens. Hence, 10G30%, 20G30% and 40G30% demonstrated 99%-223%, 41%-128% and 17%-25% lower K-values than FAs and LP at 545-days. Another important observation is that GL-FN demonstrated a higher rate of reduction in K-values from 365-days to 545-days in comparison to CTR mixes. This can be related to more complete pozzolanic reactions and pore refinement of glass powder compared to GP, FAs, and LP, which lead to more improvement in their gas permeation resistance.

(b) Effects of glass content on coefficient of oxygen permeability

Several aspects account for the improvement of oxygen penetration resistance with the presence of glass powder content in concrete. Firstly, glass by nature is an impermeable

material thus the presence of glass particles in concrete reduces the permeability of the concrete mix and restricts the migration of gas inside the concrete. Secondly, the dense CSH gel hydrate is produced at the interfacial transition zone between the glass particles and the cement paste, which improves the structure of the interfacial transition zone (Pacheco-Torgal et al., 2013). These characteristics of glass powder improve the permeation resistance of concrete, depending on its replacement level in the mix. The coefficients of oxygen permeability of GL-CN class up to 545-days of standard water curing have been illustrated in Figure 6.4.

The oxygen permeability of various replacement levels of glass powders was studied so as to emphasize on the variations in the oxygen permeability with differences in glass contents. As anticipated, the oxygen permeability was strongly influenced by the addition of glass powder and hence, K-values varied directly with the increase in the glass powder content. The K-values obtained at 3-days for 20G20% was the lowest in GL-CN class and was found to be 28% and 104% lower compared with 20G30% and 20G40% respectively. The progress in curing time made a significant contribution towards the permeation resistance, which became apparent at 7-days. Hence, 20G20% exhibited 14% higher K-value than 20G30%; however, it still showed 97% lower K-value than the mix 20G40% at 7-days, followed by a continuously similar behaviour until 90-days of standard curing. The unexpected result shown by 20G30% can be related to the same reason mentioned before. Nevertheless, 180-days tests revealed that 20G20% exhibited 24% and 93% lower K-values than 20G30% and 20G40%, which might be related to the improvement in the pore structure of 20G20% affecting the permeation resistance with the advanced curing time. A consistent performance

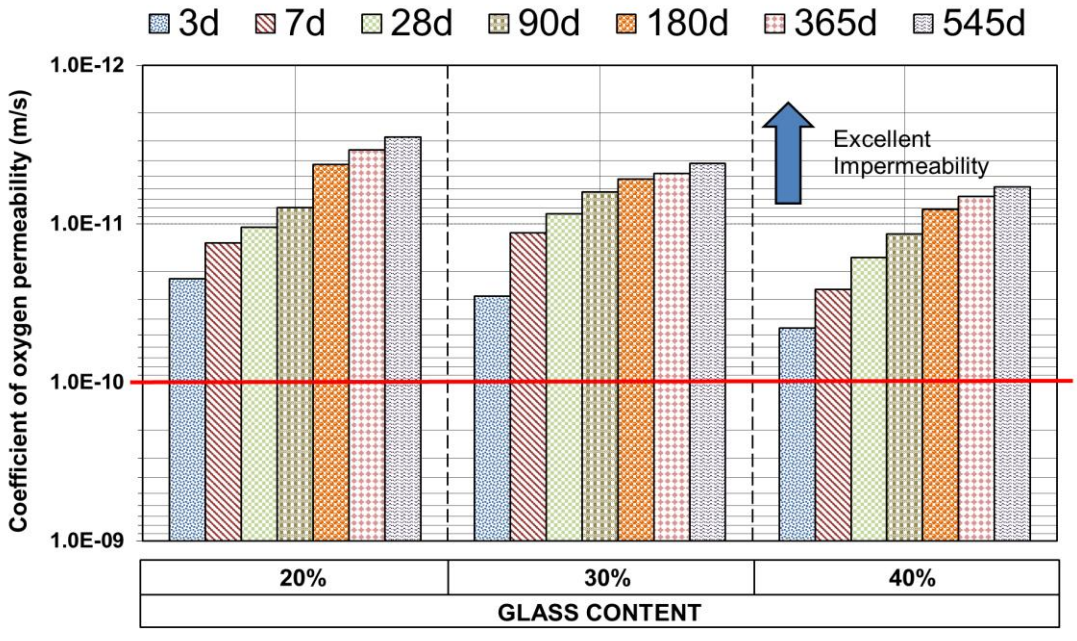

Figure 6.4: Coefficient of oxygen permeability of GL-CN with curing age up to 545-days

was observed in all GL-CN samples until 545-days of testing when 20G20% demonstrated 46% and 106% lower K-values than 20G30% and 20G40% respectively. Another significant finding is that the rate of improvement in oxygen penetration resistance in 20G20% was found to be higher as compared to the other SCC types between 180-days and 365-days, which implies that oxygen penetration resistance at lower glass levels progresses more with the curing time. These results, however, generally indicate that addition of glass powder has positive effects on concrete durability as glass replacement can fill in the internal pores of the concrete and reduce oxygen penetration, consistently noticed by Matos et al. (2016).

Figure 6.5 shows the comparison between coefficients of permeability achieved by CTR mixes and glass mixes categorized in GL-CN class. It is clear from the results that GP mix demonstrated lower resistance to oxygen permeation compared to all of these glass mixes at most of the curing ages up to 545-days. Furthermore, it has been observed that FAs at a similar replacement level performed worse than glass in terms of oxygen permeation resistance at all ages with an exception at 90-days. To elaborate, 3-days K-values achieved by 20G20% and 20G30% were 36%-66% and 6%-30% lower respectively and 20G40% was 18%- 33% higher than FAF30% and FAC30%. In addition, GL-CN was 9%-55% higher than LP30% at the curing age of 3-days, which can be related to the surface texture of LP30% that restricted the migration of gases within the specimen in comparison to GL-CN. At 28-days, 20G20% demonstrated K-value closer to FAC30%, within a variation of 5%; however, it achieved 53% lower K-value than LP30%. It seems that better pore structure of GL-CN series outweighed the performance of LP30% with advancement in the curing period. On the other hand, 20G40% showed K-value in a close range to FAF30% at 28-days. The 180-days

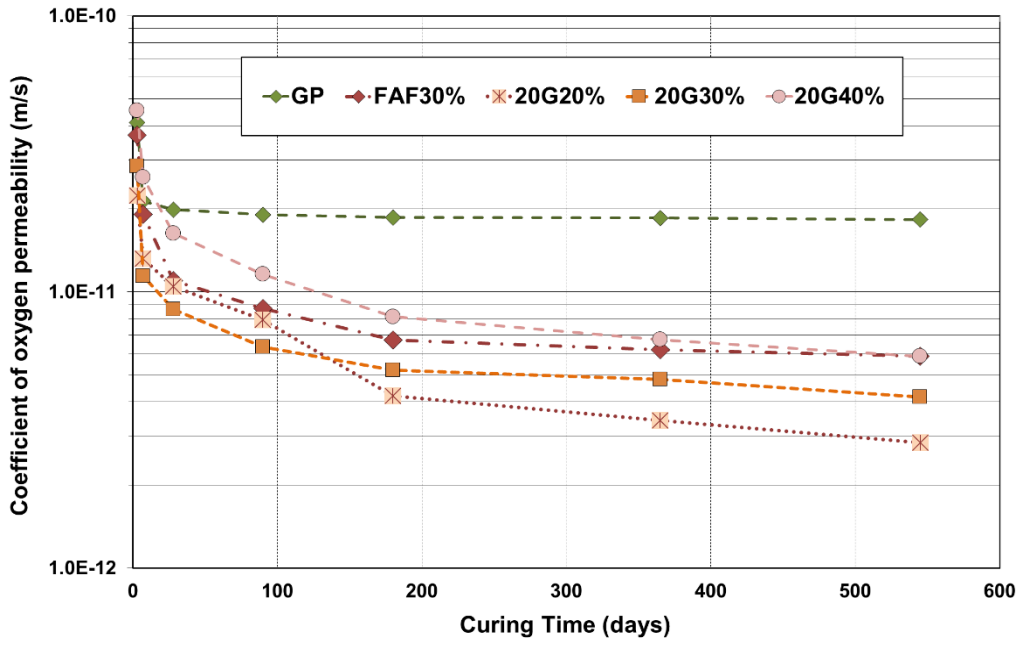

(a)

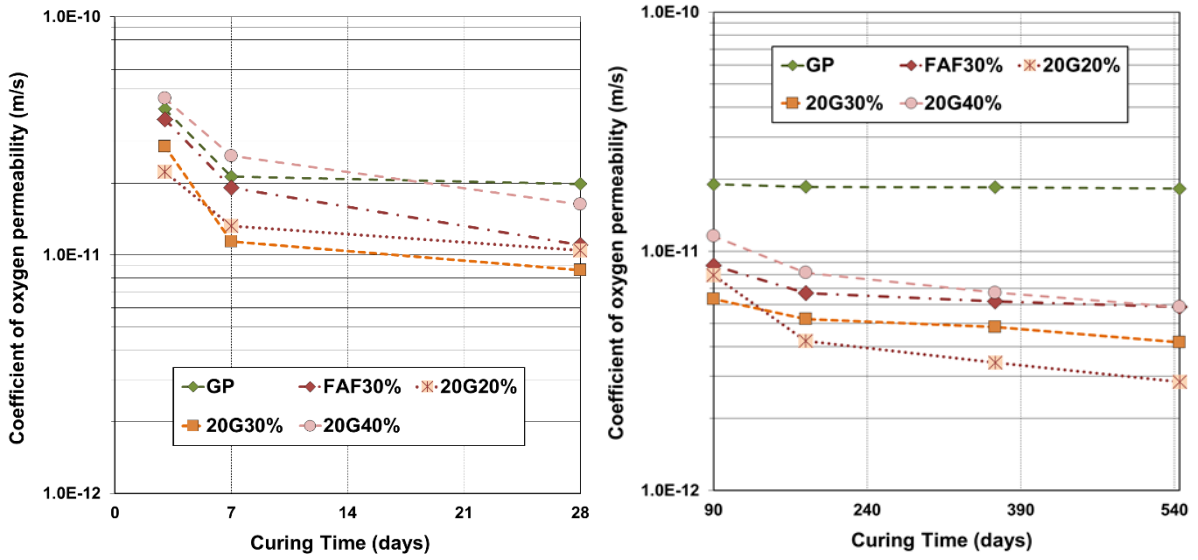

Figure 6.5: (a) Comparison between coefficients of permeability of GL-CN, GP and FAF30% up to 545-days; (b) Comparison between coefficients of permeability of GL-CN, GP and FAF30% from 3 to 28 days; (c) Comparison between coefficients of permeability of GL-CN, GP and FAF30% from 90 to 545 days

tests informed that K-value shown by 20G40% was lower than LP30% by 18%. Moreover, 20G20% and 20G40% showed 59%-163% and 18%-36% lower gas permeation resistances than FAs respectively. The similar trend in K-values was observed up to 545-days. At the curing age of 545-days, a greater decrease in K-values was observed in GL-CN mixes compared to CTR mixes. Hence, GL-CN series showed 15%-21% reduction in K-values between 365 and 545 days, which is greater in comparison to 1%-8% reduction shown by CTR mixes during this curing period. The overall results of oxygen permeability tests declare that glass powder affects the microstructure of the concrete favourably as it becomes denser and less permeable with the addition of glass compared to the addition of GP cement, fly ash and limestone powder. Chaid et al. (2015) similarly reported that coefficients of oxygen permeability of mixes with glass powder are lower than that of mixes without glass powder. In addition, it is worth mentioning here that although the optimum dosage to achieve the lowest K-value was found to be 20% in this study, the higher replacement levels of 30% and 40% were also able to provide better oxygen permeation resistance compared to GP cement and comparable oxygen permeation resistance to class F fly ash. Further testing between 0-30% glass replacements would be necessary to determine the optimal replacement level.

(c) Effects of glass quality on coefficient of oxygen permeability

The coefficients of oxygen permeability of 20UG30% up to 545-days of standard water curing are illustrated in Figure 6.6. The coefficients of oxygen permeability of GP and 20G30% up to 545-days are also included in the figure for comparative analysis. 20UG30%

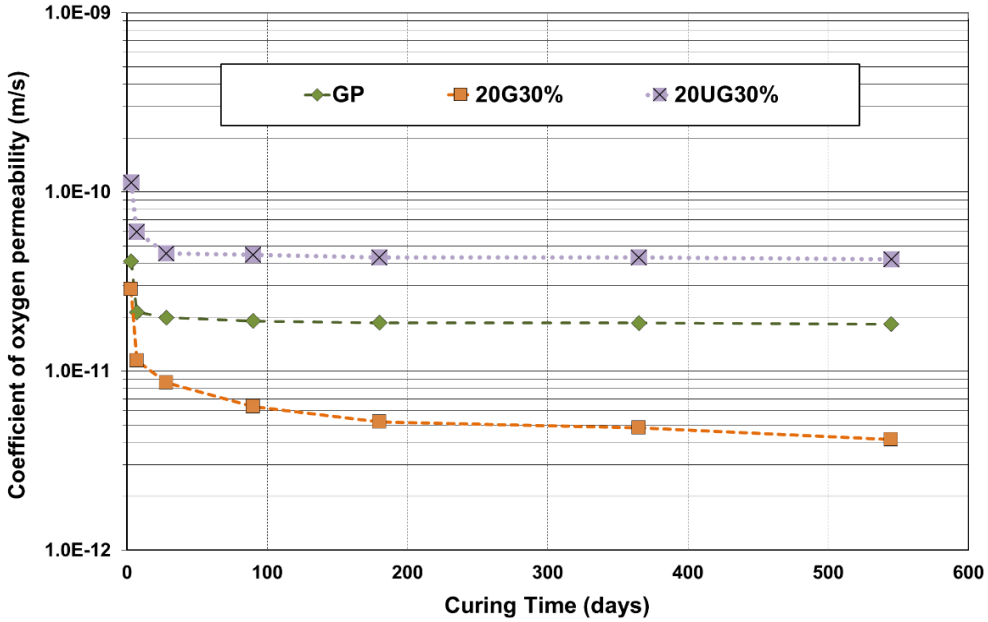

Figure 6.6: Coefficient of permeability of 20UG30% with curing age up to 545-days

showed the highest K-value of 1.1E-10 at 3-days, which was higher than GP by 64%. This depicts its poor durability characteristics due to the presence of impurities and high organic levels. Furthermore, 20UG30% demonstrated steady results up to 545-days of testing and hence, a decrease of only 7% was observed in permeability coefficients from 28-days to 545-days, in comparison to 52%-72% reduction in other glass types during the same curing period. The reduction in K-values of 20UG30% throughout the experimental programme was found to be four times lower in comparison to other glass types, which signifies the necessity of cleaning waste glass before utilization in concrete.

(d) Relationship between coefficient of oxygen permeability and compressive strength

Both strength and transport characteristics are linked to the pore structure of the concrete. Therefore, it is always desirable to be able to predict the long-term permeability of concrete from compressive strength. It has been shown in the past (Torrent and Jornet, 1991) that oxygen permeability and the compressive strength of concrete made of different types of binders can be related. A general relationship between coefficient of oxygen permeability and compressive strength of concrete has been found by Costa et al. (1992) as follows:

$$Y = AX^{-B} \qquad \text{Equation 6.1}$$

where; Y is the coefficient of permeability (K-value)

X is the compressive strength (fc')

A and B are constants

The results of oxygen permeability versus compressive strength for different mixtures made from glass powder, fly ashes and general Portland cement are shown in Figure 6.7. The power regression analysis gave the following correlation equation for glass mixes.

$$K = 6 \times 10^{-9} fc'^{-1.64}; R^2 = 0.87 \quad \text{Equation 6.2}$$

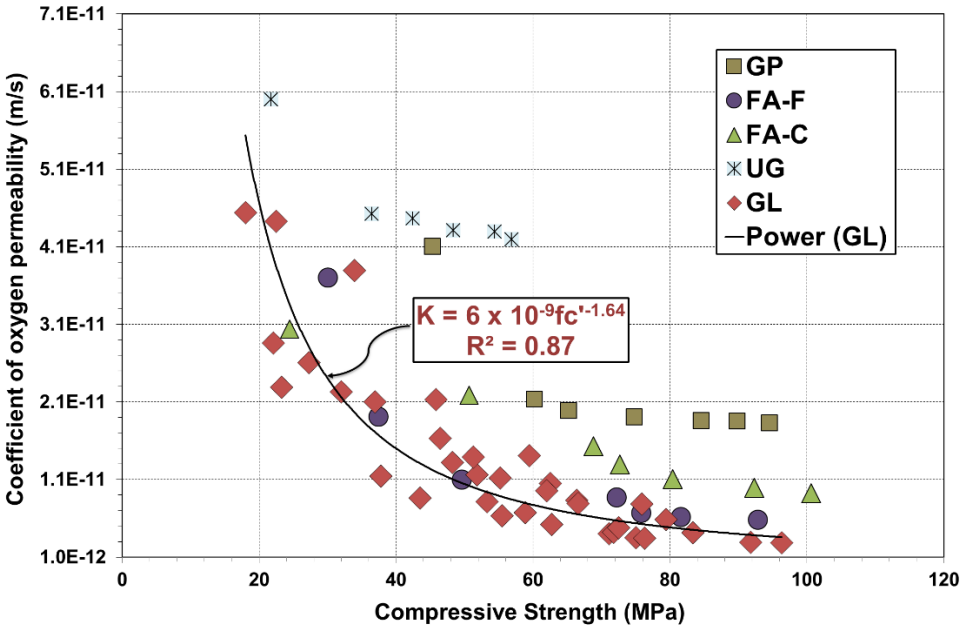

Figure 6.7: Relationship between compressive strengths and coefficients of permeability of GP, FAF, FAC, UG and GL (GL-FN and GL-CN) incorporating mixes tested up to 545-days

It can be seen that for the same compressive strengths, lower K-values were found for washed glass incorporating samples, regardless of their finenesses and replacement levels, compared to class C fly ash in particular. However, their performance corresponding to class F fly ash was much similar. On the other hand, although GP showed higher compressive strengths, its potential for long-term durability was observed to be worse as compared to FAs and glass specimens. Unwashed glass modified mix showed the similar trend as that of GP in terms of relatively consistent K-values after 28-days; however, its compressive strengths and K-values were lower and higher than GP, respectively. These findings disprove a general hypothesis that a strong concrete is also a durable concrete because durability is more related to its microstructure than simply the ability to withstand loads and a single relationship between strength and permeability, provided in Equation 6.2, is not appropriate.

6.3 Porosity of self-compacting concrete incorporating glass powder

Porosity is the bulk void content within concrete that can be filled with moisture and is also one of the common indicators of concrete durability. The reduction of water absorption in concrete can greatly enhance its long-term performance in aggressive environments (Nassar and Soroushian, 2012). However, the behaviour of concrete in porosity test is governed by

the characteristics of its pore structure. The pore structure of a cement-based composite concrete is dynamic and changes continuously. As cement hydration develops, it transforms previously unhydrated particles to a hydrated solid material (Diamond, 1999). During this process, a new pore structure is formed and meanwhile, the free available water is consumed to permit further progress of hydration (Chen and Odler, 1992). This physicochemical procedure results in the reduction of capillary and overall porosity since hydration products are being accumulated in the capillary pore space (Kanellopoulos et al., 2012). However, as the pore structure of SCC is somewhat different, the transport mechanisms taking place within the pore structure might vary as well. This indicates that segregation, bleeding and settlement may have an influence on the porosity of the interfacial transition zone (ITZ). Since these processes are influenced by the gravity, they may lead to an anisotropic ITZ with increased porosity at the bottom of aggregates and decreased porosity at the top (Hoshino, 1998). As a consequence, this anisotropy may cause variations in the transport properties of the concrete in either horizontal or vertical direction (Keller et al., 1992).

The present section contains the findings based on the average porosities of four replicate specimens being cut from the middle sections of a range of SCC samples, incorporating control binders as well as glass powders of varying finenesses, contents and quality. The test procedures, curing conditions and preparation of concrete cores prior to testing have already been explained in Chapter 3. All tests were undertaken at predefined curing ages. The average porosities were obtained from the same four specimens used for oxygen permeability tests. Complete data are shown in Appendix E. Figure 6.8 demonstrates the average porosities of CTR specimens at the curing ages of 3, 7, 28, 90, 180, 365 and 545 days. The porosity values below 10% represent excellent durability of concrete. This standard value (10%) has been marked as the red line in Figures 6.8, 6.9 and 6.11. It is evident from the results that porosity of SCC containing GP was dependent on the hydration period. In general, there was a significant reduction in porosity of GP concrete throughout the curing duration of the testing programme. The control GP mix demonstrated higher porosity values compared to the other CTR mixes at any particular curing age, showing a reduction of 11% between 3-days and 7-days, followed by a considerable decrease of approximately 20% from 7-days to 545-days, which is not very significant for this long period of hydration.

The incorporation of FA as an SCM in concrete contributes towards a significant reduction in water permeability of concrete and improves its long-term durability (Al-Amoudi et al., 2009). The reduction in its porosity can be related to a number of reasons. Firstly, the production of additional cementitious compounds reduces the pore interconnectivity due to the refinement

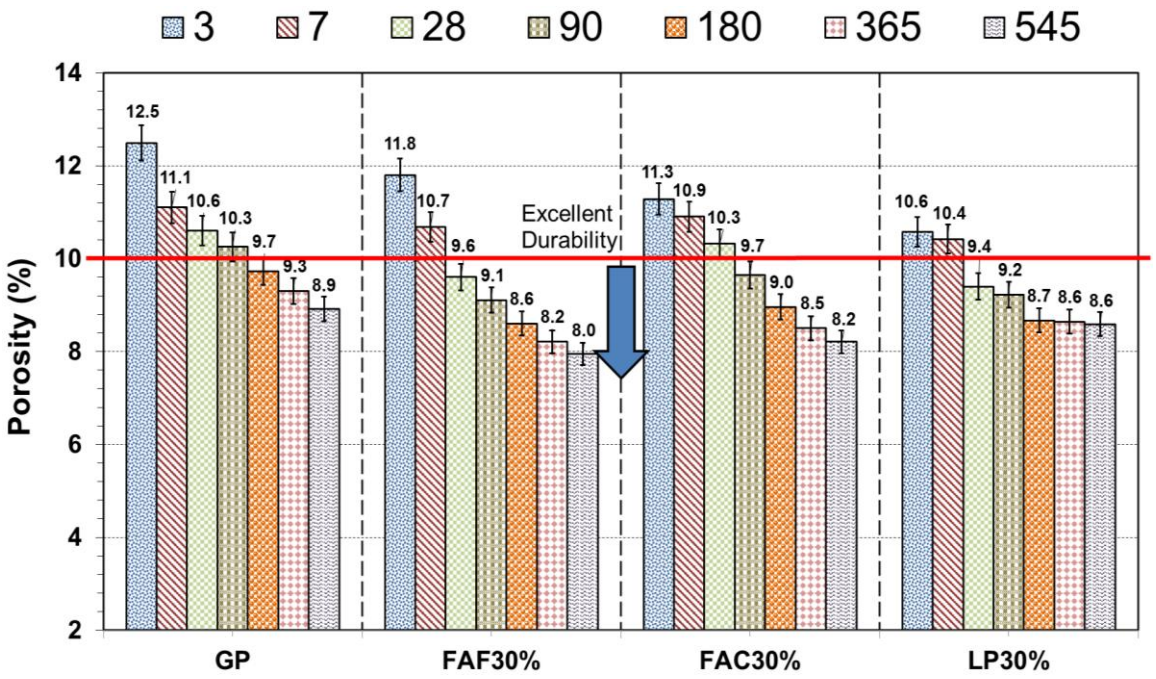

Figure 6.8: Porosity of CTR mixes with curing age up to 545-days

of the pore structure of concrete, resulting in reduced permeability (Siddiqui and Khan, 2011). Secondly, the reduced total water content is believed to have an effect, even if w/c is kept constant. The fraction of capillary water available in the mix is reduced because a larger fraction of the available water is consumed for hydration reactions, reducing the total capillary porosity (Bhuiyan, 2012). It can be noticed that with the addition of FA, the early-age concrete porosity reduced by 6%-10% compared to GP at 3-days. Moreover, FAF30% demonstrated 9% lower porosity than GP at 28-days, which can be related to better pore structure refinement in FAF30% in comparison to GP cement concrete. FAC30%, however, showed lower porosity by only about 3% in comparison to GP at 28-days. A continuous reduction in porosity was observed with progress in curing period up to 180-days and FAF30% exhibited approximately 12% lower porosity in comparison to GP whereas, FAC30% showed 8% lower porosity than GP. Khatib (2008) reported consistent results that there is a decrease in porosity with the increase in the curing period of concrete. Afterwards, the prolonged curing time continued to permit the free available water to be consumed and assisted in the reduction of overall porosity in FA mixes. Hence, the percent reduction in porosity of both FAs reached approximately 8%-11% compared to GP, as the curing period progressed to 545-days, implying that FA performs as a material that fills the pores and thereby, reduces water absorption. Similar results were reported by Al-Amoudi et al. (2009) that the addition of FA greatly decreases the water permeability of concrete. It can be concluded from the results that for 30% replacement of FA, there might be limited open porosity that could inhibit the high flow of water into concrete, consistently mentioned by Dhiyaneshwaran et al. (2013). Moreover, the reduced total water might also have resulted in

the reduction of porosity in FA mixes. All these factors might have played a role in reducing the total porosity of FA mixes but the individual effects of each are difficult to isolate, similarly concluded by Bhuiyan (2012).

The inclusion of LP generally dilutes the cement particle system, influencing both the average distance between cement particles and the water content available for cement hydration. However, when the w/c ratio is kept constant and the workability is adjusted with appropriate SP, the dilution effect of LP is limited. Hence, although the overall porosity is typically reduced due to its filler effect, higher porosities can still be obtained within the microstructure (Schutter, 2011). In addition, the improvement of pore structure, due to the nucleation effect of the fine particles of $CaCO_3$, also improves the porosity of concrete containing LP. However, it is important to recognize that this improvement may not be due to the reduction in total pore volume but due to the refinement of the pore structure, which reduces its connectivity (Sellevold et al., 1982). In this study, the tests done at early-age of 7-days exhibited that LP30% achieved about 6% lower porosity compared to GP and 2%-4% reduction in porosity when compared with FA mixes. This can be attributed to an optimum particle packing effect, a phenomenon known to occur with LP filler, as indicated in the literature (Ye and Breugel, 2009). The early-age physical pore-refining effects of LP on porosity are consistent with those of oxygen permeability. At 28-days, LP30% demonstrated 2%-11% lower porosity when compared with all other CTR mixes. Bhuiyan (2012) coherently reported that for the constant w/c mixes, LP mixes show lower porosities than FA mixes, which can be related to the formation of a denser and better-packed structure, superseding the pozzolanic effects of FA. Nevertheless, different behaviour in porosity was noticed at 90-days of testing since LP30% demonstrated slightly higher porosity measurement than FAF30%, although it still showed about 5% and 10% lower porosities than FAC30% and GP respectively. Another variation was noticed at 365-days tests when LP30% exhibited higher porosity than both FA mixes within the range of 2%-5%. This could possibly be due to the continuous pozzolanic reactions in FAs that ultimately outweighed the filler effects of LP30% with the progress the in curing period. However, LP30% continued to demonstrate lower porosity compared to GP until 545-days of standard curing. From the overall results, it can be safely stated that the higher amount of LP fillers (30%) in a concrete mix can result in satisfactory durability behaviour because the higher packing density of its solid particles is favourable for durability, similarly concluded by Courad and Michel (2014).

(a) Effects of glass fineness on porosity

The filling effect of very small sized glass particles leads to improvement in particle packing, which results in denser and hence, less permeable microstructure (Nassar and Soroushian,

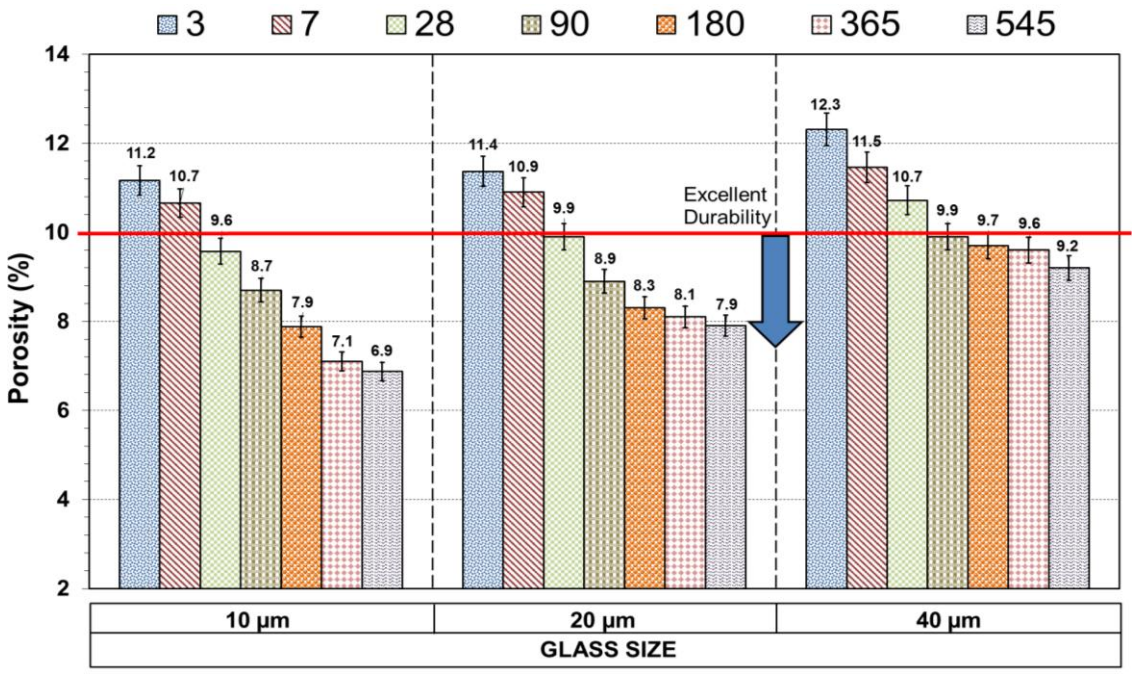

Figure 6.9: Porosities of GL-FN with curing age up to 545-days

2012). Figure 6.9 demonstrates the porosities of GL-FN class of specimens, cured up to 545-days under standard conditions. The porosity of coarser to finer range of glass powders was investigated in order to highlight the changes in the porosity with variations in particle sizes. In general, the porosities of SCC incorporating glass dropped as the glass particle size became finer, which can be related to better pore refinement of concrete due to the presence of finer glass, consistently reported by Ling et al. (2012). Use of finer waste glass as a partial replacement for cement also resulted in lowering the volume of voids in the concrete. The porosity obtained at 3-days for 10G30% was observed to be the lowest in GL-FN class and was 2% and 9% lower compared with 20G30% and 40G30%, respectively. This can be ascribed to the evidence that very fine glass undergoes pozzolanic reaction and improves the microstructure of concrete through improvement in the quality of the paste, consistently reported by Nassar and Soroushian (2012) who worked with 13 µm glass concrete produced with variable w/c of 0.38 to 0.5. Nevertheless, as the curing time advanced to 28-days, 10G30% demonstrated slightly lower porosity value than the mix 20G30% by 3% and approximately 10% lower porosity than 40G30%. Subsequently, with the progress in the curing time up to 180-days, 10G30% showed 5% and 19% lower porosities in comparison to 20G30% and 40G30%. Similar behaviour was noticed from 180-days to 545-days of water curing as 10G30% dropped by 13% and 25% than 20G30% and 40G30% respectively, at 545-days. In addition, the rate of improvement in porosity in 10G30% was found to be higher in comparison to the other GL-FN types between 3-days and 545-days. This implies that curing and particle size has a significant effect on the water penetration resistance of glass modified concrete. Dyer (2014) consistently mentioned that particle size plays an important

role in reducing porosity since larger particles have greater volumes of capillary porosity and pore diameters even when they are closely packed. These findings also signify the importance of particle size distribution as the presence of finer particles in the spaces between larger particles also acts to 'refine' the porosity. Analyzing the results, it can be stated that waste glass offers desired reactivity for use as an SCM for improving the pore refinement, pore filling, moisture resistance and durability of concrete but to achieve these benefits, waste glass needs to be milled to microscale particle size for accelerating its beneficial chemical reactions in concrete. A similar recommendation has been suggested by Nassar and Soroushian (2012).

Figure 6.10 shows the comparison between porosities of few CTR mixes and glass mixes categorized in GL-FN class. It is evident that GP mix exhibited higher porosities in comparison to glass mixes, with an exception of 40G30%, up to 545-days of standard curing. Moreover, comparisons of glass as an SCM compared to FA indicate that glass at a similar particle size showed higher porosities compared to FAs. However, it still obtained the benchmark for excellent porosity by the end of 545-days of curing. To elaborate, 3-days porosity achieved by 10G30% was 1%-5% lower and by 40G30% was 4%- 9% higher than FAF30% and FAC30%. In addition, 10G30%, 20G30% and 40G30% showed 6%, 8% and 16% higher porosities compared to LP30% at 3- days respectively. The 28-days tests demonstrate that the porosity shown by 10G30% was lower than FAF30% and FAC30% by 1% and 7% respectively. The porosity of 20G30% was found to be reduced by 2% than LP30% at 28-days; however, 40G30% exhibited 16% higher porosity than LP30%. Moreover, 20G30% demonstrated lower porosity by 3% compared to FAF30% whereas, 40G30% showed 8% higher porosity than FAC30% at 180-days. The progress in curing time

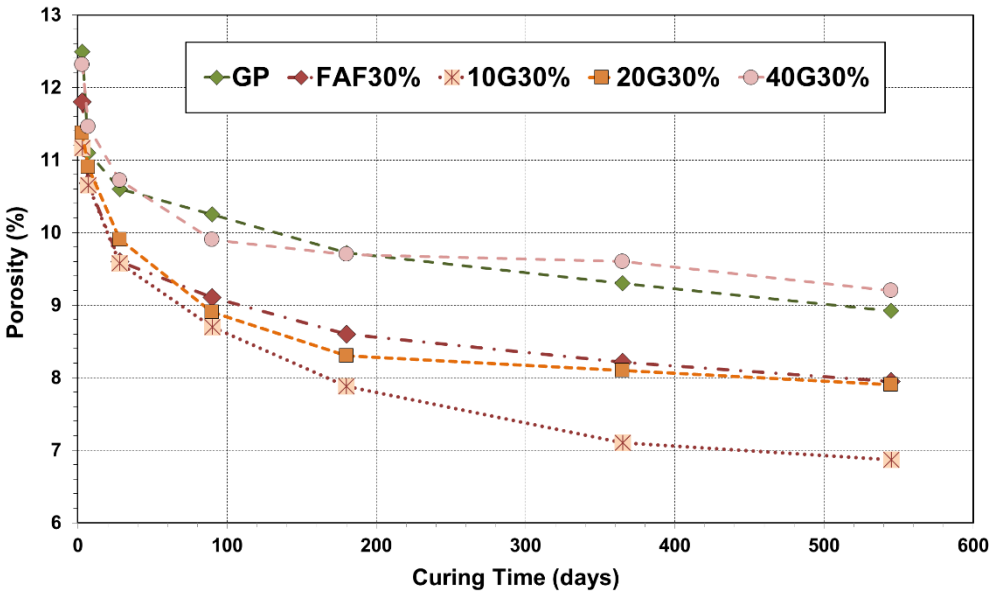

(a)

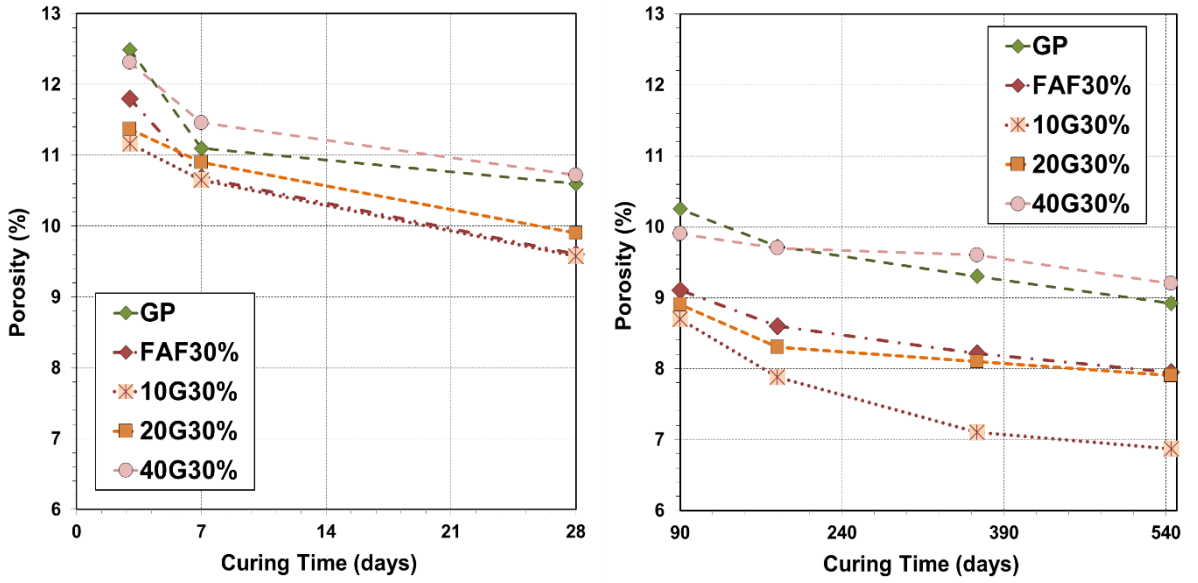

Figure 6.10: (a) Comparison between porosity of GL-FN, GP and FAF30% up to 545-days; (b) Comparison between porosity of GL-FN, GP and FAF30% from 3 to 28 days; (c) Comparison between porosity of GL-FN, GP and FAF30% from 90 to 545 days

reduced the porosity of all specimens. Hence, 10G30% and 20G30% demonstrated lower and 40G30% showed higher porosities than FAs and LP at 545-days. Another important observation was that 40G30% demonstrated worse porosity values throughout the testing programme, which might be related to the bleeding observed in this mix during its production, as discussed in Chapter 5. It seems that addition of SB in this mix to counterbalance bleeding could not effectively serve the purpose.

(b) Effects of glass content on porosity

Since glass by nature is an impermeable material as mentioned before, it can be safely assumed that the presence of glass particles in concrete can also reduce water permeability of the concrete mix (Taha et al., 2008). In addition, being a pozzolanic material, glass reacts with lime [$Ca(OH)_2$] to produce CSH, which is the main compound responsible for providing the gluing effect and strength of concrete. This effect is also responsible for improving its water permeability as it is related to the entry of external fluids, similarly discussed by Bhuiyan (2012). Considering this, the porosities of various replacement levels of glass powders were also studied so as to emphasize on the variations in the porosities with differences in glass contents. The porosities of GL-CN class of mixes up to 545-days of standard water curing have been illustrated in Figure 6.11. The increase in porosity directly with the percentage of glass powder content can be related to the variations in the amount of angular-shaped glass particles and number of pores within the microstructure of the specimens.

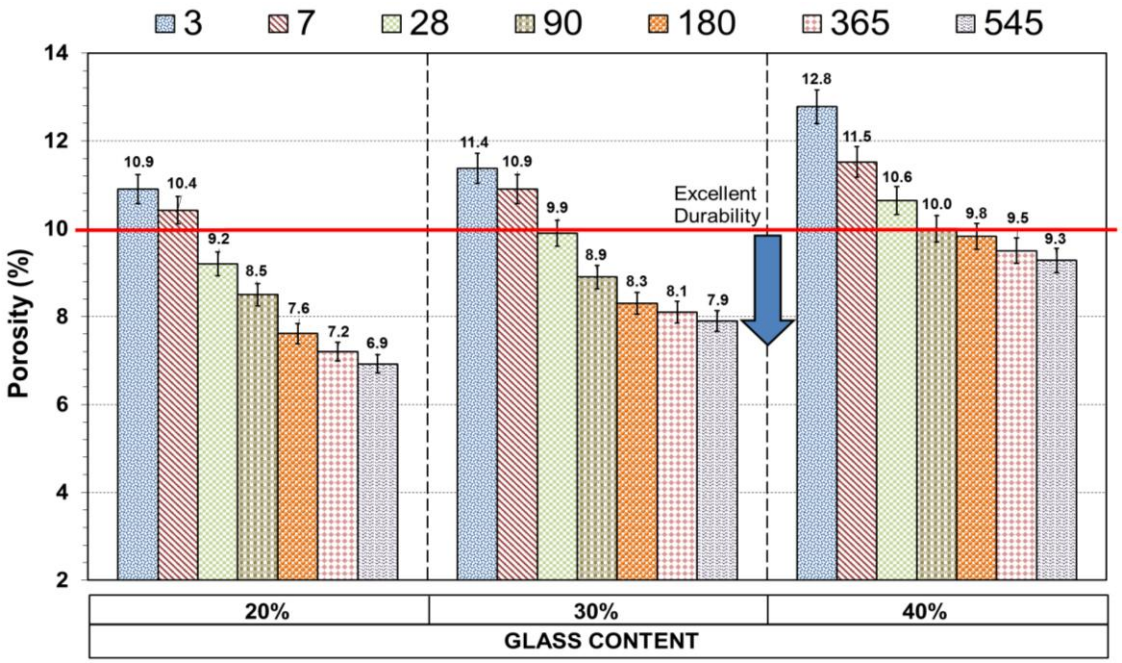

Figure 6.11: Porosities of GL-CN with curing age up to 545-days

The porosity obtained at 3-days for 20G20% was found to be the lowest in GL-CN class as it was 4% and 15% lower compared with 20G30% and 20G40% respectively. Further, 20G20% exhibited 5% lower porosity than 20G30% and 10% lower porosity than 20G40% at 7-days, which might be due to the change in pore size distribution (refined pore system) in the 20G20% glass mix, as mentioned by Du and Tan (2014). Nevertheless, 28-days tests revealed that 20G20% demonstrated 7% and 13% lower porosities in comparison to 20G30% and 20G40%, which can again be linked to better pore structure enhancement in 20G20% with curing that in turn improved its water permeation resistance more than other mixes. Consistent behaviour was observed in all GL-CN specimens until 545-days of testing when 20G20% demonstrated lower porosity by 13% and 26% than 20G30% and 20G40% respectively. Shayan and Xu (2006), who used glass powder of nominal 10 µm size, similarly reported that volume of permeable voids increases with an increase in glass powder content and the mixtures with higher glass contents are clearly more absorbent. Similar to the oxygen permeability, 20% glass replacement level also showed the best performance in terms of porosity among other glass mixes categorized in GL-CN. Overall, glass powder reduced concrete porosity, consistently noticed by Du and Tan (2014). This concludes that glass powder imparts technical benefits to the resulting concrete and enables it to achieve better durability characteristics, consistently confirmed by Bhuiyan (2012).

Figure 6.12 shows the comparison between porosities of some of the CTR mixes and the glass mixes categorized in GL-CN class. It is clear from the results that GP mix demonstrated higher porosity compared to glass mixes at curing ages up to 545-days, except 20G40%. Furthermore, it was also observed that FAs at a similar replacement level

performs worse than glass, starting from 28-days until 545-days. To elaborate, 3-days porosity value obtained by 20G20% was 4%-8% lower and by 20G40% was 8%-13% higher than FAF30% and FAC30%. In addition, 20G30% and 20G40% were 8%-21% higher than LP30% at the curing age of 3-days. 20G30% was also found to be 3% higher than LP30% at 3-days. At 28-days, 20G20% demonstrated lower porosity than FAC30%, within a variation of 4%-11%; however, it achieved only 2% lower porosity than LP30%. Moreover, porosity of 20G20% reduced by 17% compared to GP at 90-days. There was 14% reduction in 90-days

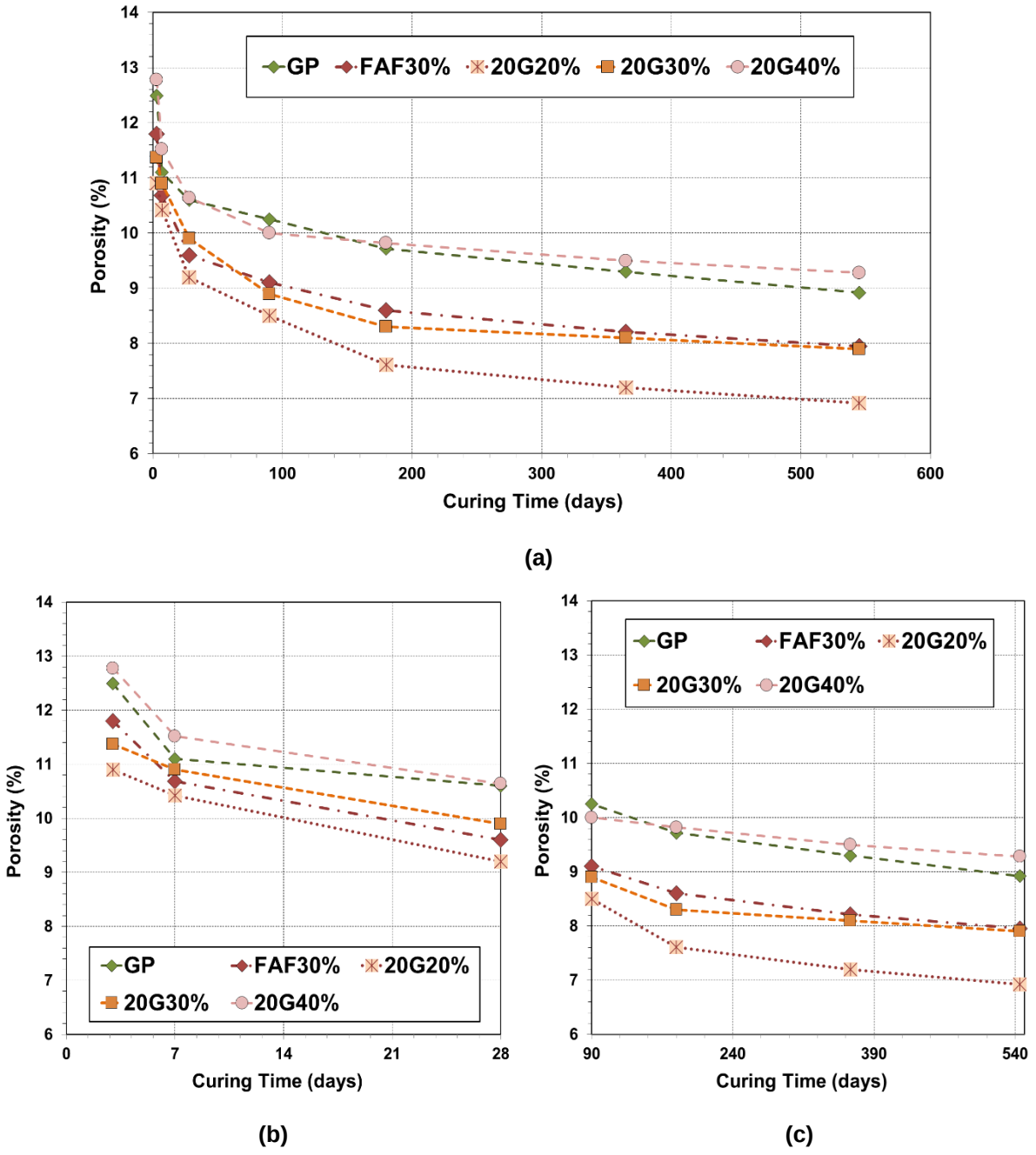

Figure 6.12: (a) Comparison between porosity of GL-CN, GP and FAF30% up to 545-days; (b) Comparison between porosity of GL-CN, GP and FAF30% from 3 to 28 days; (c) Comparison between porosity of GL-CN, GP and FAF30% from 90 to 545 days

porosity of 20G30% in comparison to GP. Schwarz et al. (2008) produced concrete with glass powder having a fineness of 10 µm and reported somewhat similar results that 10% glass powder modified concretes perform similar to or better than GP concrete and 10% fly ash modified concrete. The 180-days tests informed that porosity shown by 20G40% was higher in comparison to LP30% by 13%. Also, 20G20% and 20G40% showed 12%-16% lower and 9%-14% higher water permeation resistances than FAs respectively, at 180-days. A similar trend in the porosity reduction was observed up to 545-days. It seems that the refined pores structure, particularly the ITZ, was the main reason for the reduced porosity in most of the glass incorporating mixes relative to the CTR mixes. Hence, it can be concluded that glass powder, added at an optimum content, has the potential of being used as a pozzolan in concrete that can potentially replace traditional pozzolans, such as fly ash (Shayan and Xu, 2004) and enhance the durability of concrete.

(c) Effects of glass quality on porosity

The porosity of unwashed glass powder (20UG30%) was also investigated in order to comprehend the effects of the quality of glass material on porosity of SCC. The results of the porosity tests, undertaken on 20UG30% specimens, up to 545-days of standard water curing have been illustrated in Figure 6.13. The porosity measurements of 20G30% (having the same fineness and replacement level as unwashed glass) up to 545-days of standard water curing are also included in the figure for comparison. It is clear from the results that 20UG30% mix demonstrated higher porosity compared to all other glass mixes as well as CTR mixes at curing ages up to 545-days. In particular, 20UG30% showed the highest porosity value of 14.4% at 3-days, which implies that the presence of impurities and organic

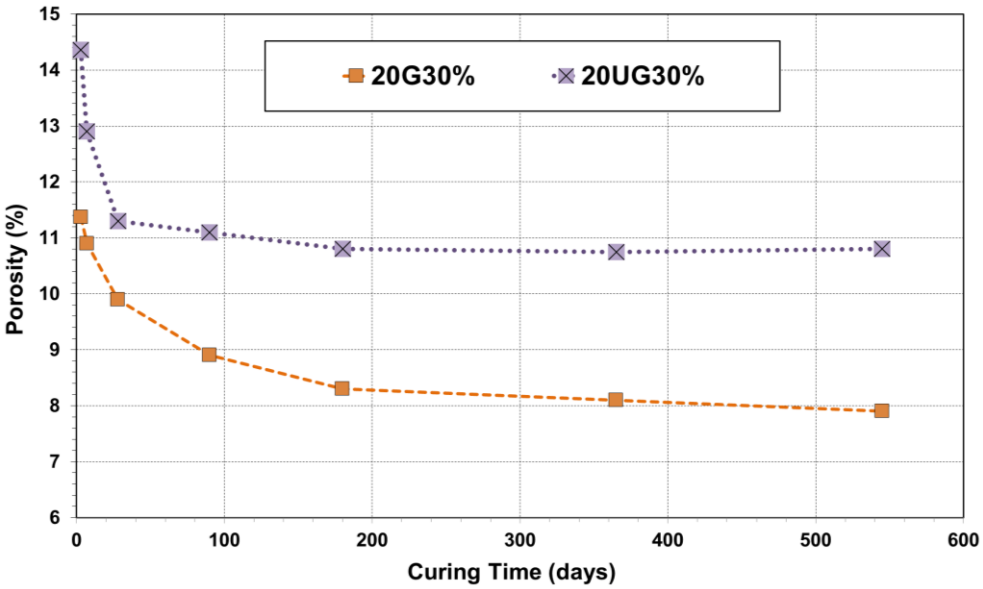

Figure 6.13: Porosity of 20UG30% with curing age up to 545-days

content deteriorated its durability performance in comparison to the washed glass and CTR specimens. In addition, it demonstrated 20%-34% higher porosity than the CTR mixes by the end of 545-days. A significant observation is that the reduction in porosity of 20UG30% between 3-days and 545-days was found to be the lowest in comparison to other glass types, which can be related to the differences in the composition of unwashed glass due to the presence of organic content. Vaitkevicius et al. (2014) consistently noticed that the impurities of the glass powder have the biggest effect on a proper structure formation in concrete, which also affects its durability properties.

(d) Relationship between porosity and compressive strength

Similar to the coefficient of permeability, a relationship between porosity and compressive strength was also developed through regression analysis. In general, there exists a fundamental inverse relationship between porosity and strength of concrete (Mehta and Monteiro, 2006). For simple homogeneous materials, it can be described by the expression given below:

$$fc' = fc_0 e^{-kp} \qquad \text{Equation 6.3}$$

where; fc' is the compressive strength of the material which has a given porosity (p)

fc_0 is the intrinsic strength at zero porosity

k is a constant

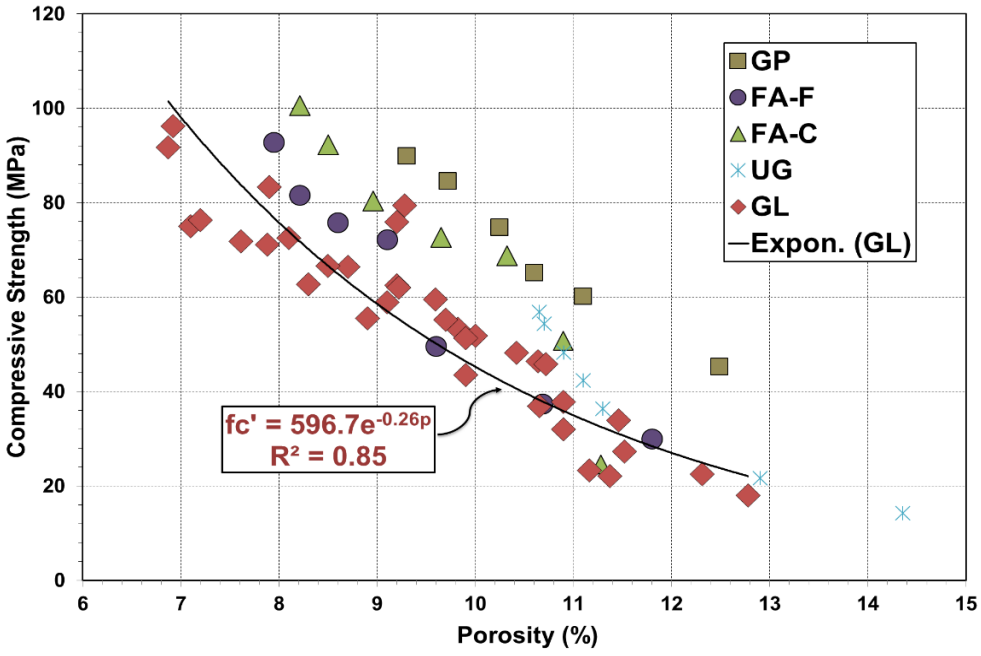

Figure 6.14: Relationship between porosities and compressive strengths of GP, FAF, FAC, UG and GL (GL-FN, and GL-CN) incorporating mixes tested up to 545-days

The results of porosity versus compressive strength for different mixtures made from glass powder, fly ashes and GP cement are illustrated in Figure 6.14. The exponential regression analysis gave the following correlation equation for glass incorporated mixes.

$$fc' = 596.7e^{-0.26p};\ R^2 = 0.85 \qquad \text{Equation 6.4}$$

A relatively worse relationship was observed between compressive strength and porosity in glass incorporated mixes compared to that between compressive strength and coefficient of permeability. However, it can be noticed that for similar compressive strengths, generally lower porosities were found for glass powder mixes compared to most of the control binder mixes, regardless of their finenesses, replacement levels, and quality. Similar to GP, FAC also demonstrated higher porosities, although their compressive strengths were higher than glass. On the whole, the analysis reveals that porosity test might be a worse indicator of durability compared to oxygen permeability test since a more reasonable relationship of K-value with compressive strength was developed in this study. Cement Concrete and Aggregates Australia (2009) similarly mentioned in the report on chloride resistance of concrete that the air permeability is found to be a more sensitive indicator of durability than the water permeability. Additionally, Zhao et al. (2014) reported that compressive strength and porosity are found to have discreteness, which makes simulating the relationship between strength and porosity difficult. Additionally, it is not always possible to achieve perfect relationships for concrete, since it is a highly complex heterogeneous material.

(e) Relationship between porosity and coefficient of oxygen permeability

Developments in concrete technology have indicated that durability of concrete should be assessed separately (Dali et al., 2012) instead of analyzing it with reference to compressive strength only. Cabrera et al. (1989) also found that concrete permeability is not only a function of strength but also of porosity and pore size distribution. Hence, a relationship between porosity and coefficient of oxygen permeability was also developed using regression analysis. The results of porosity versus coefficient of oxygen permeability for all mixtures made from glass powder, fly ashes and GP cement are illustrated in Figure 6.15. The power regression analysis gave the following correlation equation for washed glass incorporated mixes. It is important to recognize that the data points of unwashed glass are not included in the regression equation because they are outliers.

$$K = 4e^{-16}p^{4.52};\ R^2 = 0.93 \qquad \text{Equation 6.5}$$

A regression coefficient of above 0.90 represents a very strong relationship between any two parameters, which has also been achieved in this study. However, it can be noticed that all mixes including unwashed glass, washed glass of varying finenesses and contents, class F

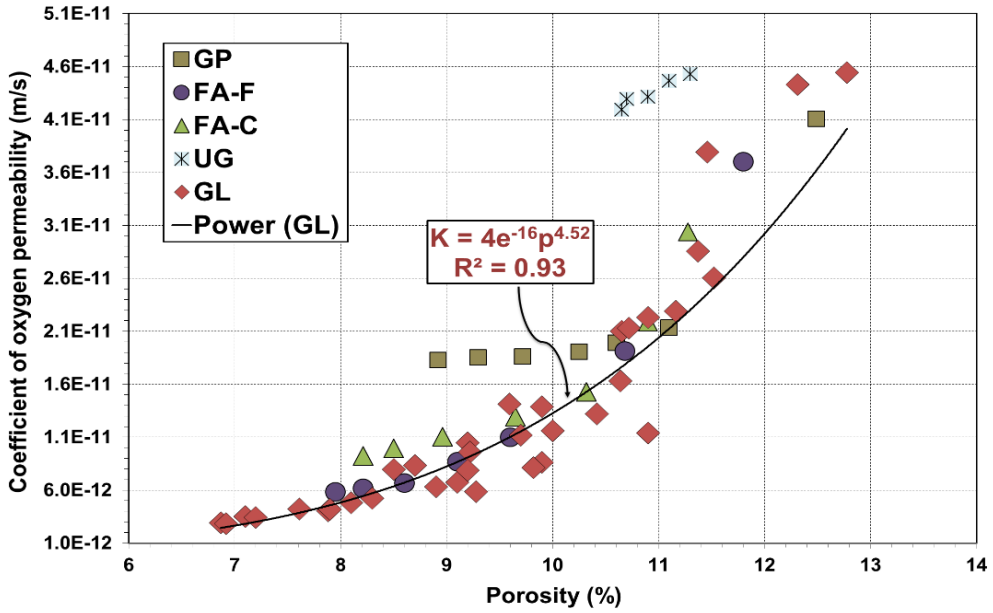

Figure 6.15: Relationship between compressive strengths and porosities of GP, FAF, FAC, UG and GL (GL-FN, and GL-CN) incorporating mixes tested up to 545-days

and class C fly ashes demonstrated similar relationship trend between porosity and K-value. Some discrepancies were noticed in the early-age relationships, which can be related to the fact that pozzolanic materials require time to demonstrate their characteristics. However, the relationship became stronger with the progress in a curing time when both durability properties started to improve at a comparable pace. Additionally, GP achieved higher K-value measurements than other mixes within a similar range of porosity. In general, the results indicate that bulk porosity are not a suitable replacement measurements for specific permeability testing, which is a better indication of refined pore system, particularly when comparing different binder systems.

6.4 Chloride penetration in self-compacting concrete incorporating glass powder

Most of the concrete used in the construction industry is intended to be used in the production of reinforced concrete structures. The presence of steel compensates for the weakness of tensile strength of concrete; however, steel is vulnerable to corrosion. Steel bars are naturally protected within concrete because a shielding outer layer (passive layer) is formed on the steel surface, restraining the corrosion rate to a negligible level. The passive layer refers to the high pH environment at the steel-concrete interface where the passivating iron oxide is formed on the surface of steel (Rosskopf and Vimelson, 1985). This passive layer is stable in alkali environments, such as the one provided by concrete under normal conditions (pH >13). However, the corrosion of steel in reinforced concrete is initiated when this passive layer is partially or totally damaged.

A principal phenomenon associated with concrete destruction is the penetration of chloride ions for concrete exposed to marine environments. Chloride ions can be present within or pass through the concrete microstructure as contaminants in the raw materials, seawater, and de-icing salts. The existence or entrance of chloride ions has extensively been documented in the literature as the cause of corrosion of metals in concrete. According to Liu (1996), the process of chloride-induced corrosion is recognized to be linked to chloride ions being integrated into the passive film, replacing some of the oxygen and increasing both its conductivity and solubility. Federal Highway Administration (FHWA) studies found that a threshold limit of 0.2% total (acid-soluble) chloride by weight of cement can induce corrosion of reinforcing steel in bridge decks (Clear, 1976). However, only water-soluble chlorides promote corrosion, whereas some acid-soluble chlorides may be bound within aggregates or cement paste and therefore, unable to promote corrosion. Work at FHWA found that the conversion factor from acid-soluble to water-soluble chlorides could range from 0.35 to 0.90, depending on the constituents and history of the concrete (Clear, 1973). Arbitrarily, 0.75 has been chosen, resulting in a water-soluble chloride limit of 0.15% by weight of cement.

The total chloride content of steel reinforced concrete, based on the measurements of chloride content arising from aggregate, mixing water and admixtures, has also been specified by NZS 3101, as listed in Table 6.2. In addition, the chloride threshold for black steel corrosion has a limit of 0.3%-0.5% on the mass of cementitious materials according to NZS 3101:2006. While considering the effect of chlorides on corrosion, it is very important to distinguish between ‘free’ chloride present in the pore water and chloride bound by the cement in the matrix. The ‘bound’ chlorides are unable to participate in corrosion directly while the ‘free’ chloride ions may damage the passive layer on the surface of the reinforcing bars. Free ions lead to increase in the electrical conductivity of the pore water and the rate of dissolution of metallic ions. However, the fraction of free to bound chlorides can change and bound chlorides can enter the solution. Hence, it is appropriate to specify total chloride content instead of just the free chloride content. Due to this, limits have been placed on the acid soluble chlorides also, which are closely linked to total chlorides (NZS 3101:2006).

Table 6.2: Maximum values of chloride ion content in concrete as placed (NZS 3101:2006)

Type of member	Maximum acid soluble chloride ion content (kg/m^3 of concrete)
Prestressed concrete	0.5
Reinforced concrete exposed to moisture or chloride in service	0.8
Reinforced concrete that will be dry or protected from moisture in service	1.6

The primary rate-controlling factors for corrosion are the availability of oxygen, the electrical resistivity, relative humidity of the concrete, and the pH and temperature (Portland Cement Association, 2002). Apart from these, corrosion activity is also affected by cement type, concrete cover, concrete carbonation, and the presence of corrosion inhibitors. Cement composition has a significant effect on the durability performance of concrete against corrosion of reinforcement where C_3A binds chloride ions to form calcium chloro-aluminate hydrate, causing it to be removed from the hazardous role of corrosion promotion (Al-Amoudi et al., 1994). The penetration of chloride ions also depends on the pore structure and permeability of the concrete. Thus, the type of attack on concrete structures, such as corrosion of reinforcement, is dependent on the permeability of the matrix. Generally, steel reinforced concrete structures are in continuous contact with oxygen and moisture from the atmosphere. When accessibility is significant, chloride induced corrosion can be sustained. The low permeability of concrete not only minimizes the permeability of corrosion inducing agents but also increases the electrical resistivity of concrete, which decreases the flow of current associated with electrochemical corrosion and in turn the corrosion rate.

Various test procedures have been developed to evaluate the chloride penetration resistance of concrete. These tests are classified into three categories: (Francisco et al., 2013)

- Diffusion tests: including AASHSTO T259 (salt ponding test), NT BUILT 433 (bulk diffusion test) and other natural long-term full-immersion tests.
- Migration tests: including ASTM C1202 (rapid chloride permeability test) and NT BUILT 492 (chloride migration test).
- Indirect tests: including electrical resistivity measurements.
- Chloride conductivity tests developed by Alexander et al. (1999a).

Out of these, electrical resistivity tests and bulk diffusion tests have been undertaken in this study to estimate the chloride penetration resistance of SCC incorporating glass powder.

6.4.1 Electrical resistivity of self-compacting concrete incorporating glass powder

Once corrosion is initiated by chloride ions, the corrosion rate is dependent on parameters, such as relative humidity, oxygen permeability and concrete resistivity as previously stated. The concrete electrical resistivity is a function of corrosion resistance of concrete where the increase of concrete resistivity constrains the flow of electrons and hence, the corrosion resistance increases. The determination of electrical resistivity of concrete has become an

established non-destructive measurement technique in the evaluation of the durability of concrete structures. It is affected by a number of factors, such as pore structure, pore solution composition, moisture content and temperature (Polder, 2001; Castellote et al., 2002; Butefuhr et al.; 2006; Langford, P. and Broomfield, 1987; Bertolini and Polder, 1997). Pore solution of concrete varies with w/c ratio, the degree of hydration, and use of mineral admixtures (Polder, 2001; McCarter, 2006). Nevertheless, it has been found that changes in pore structure have a greater effect on the measured electrical resistivity than changes in the pore solution composition and concentration (McCarter et al., 2000). The degree of hydration also affects resistivity since further hydration reduces the concrete porosity (McCarter, 2006) as mentioned in the previous section. In addition, moisture content plays a significant role in concrete resistivity because electrical resistivity in concrete is carried by the pore water (Elkey and Sellevold, 1995). The correlation between the corrosion rate of depassivated steel and concrete resistivity has been reported in various research works (Bertolini and Polder, 1997). Most of these investigations found a linear relationship between corrosion rate and concrete conductivity (inverse of resistivity). Langford and Broomfield (1987) proposed a relationship between corrosion rate of depassivated steel reinforcement and resistivity as shown in Table 6.3. Florida Department of Transportation (FDOT) has developed a correlation between resistivity and rapid chloride permeability test (RCPT) for specimens that were wet-cured in a controlled environment or cured in lime water. Based on this, the relationship between resistivity and chloride ion permeability was proposed as listed in Table 6.4.

Table 6.3: Relationship between electrical resistivity and corrosion rate of depassivated steel reinforcement in concrete (Castellote et al., 2002)

RESISTIVITY (kΩ.cm)	CORROSION RATE
< 5	Very high
5 – 10	High
10 - 20	Low/moderate
> 20	Low

Table 6.4: Relationship between surface resistivity and chloride ion permeability in concrete (NT Built 492, 1999)

RESISTIVITY (kΩ.cm)	RCPT CHARGE PASSED (coulombs)	CHLORIDE ION PERMEABILITY
< 9.5	> 4000	High
9.5 – 16.5	2000 - 4000	Moderate
16.5 - 29	1000 - 2000	Low
29 - 199	100 - 1000	Very Low
> 199	< 100	Negligible

The present section consists of the findings from the experimental study on determination of electrical resistivity of concrete, to obtain a rapid indication of the resistance to the penetration of chloride ions through SCC mixes, incorporating control binders as well as glass powders of varying finenesses, contents and quality. The test procedures, curing conditions and preparation of concrete cores for electrical resistivity measurements prior to testing have been explained in Chapter 3. All tests were undertaken at pre-defined curing ages. The average resistivity measurements were obtained from the same four replicate specimens that were previously used for oxygen permeability and porosity measurements. Complete data are shown in Appendix E. Figure 6.16 illustrates the average electrical resistivity measurements of CTR specimens at the curing ages of 3, 7, 28, 90, 180, 365 and 545 days. The results clearly mention that the response of SCC containing GP on electrical resistivity was dependent on the duration of curing, which means the maturity of concrete. GP concrete showed the lowest electrical resistivity compared to the other CTR mixes at all curing ages, with a significant increase of 50% between 3-days and 28-days, followed by only a nominal increase up to 8% from 28-days to 545-days.

FA is a complex combination of inorganic compounds that are similar in characteristics to some vitreous insulating materials, which in the pure state have high electrical resistivities of the order of 10^{14} to 10^{15} ohm-cm (White, 1953). It was observed in this study that the addition of FA as cement replacement increased the electrical resistivity, which reveals its properties with regards to chloride penetration resistance compared to GP. Similar observation has been reported by Polder and Peelen (2002). The class F FA (FAF30%) resulted in about 6%

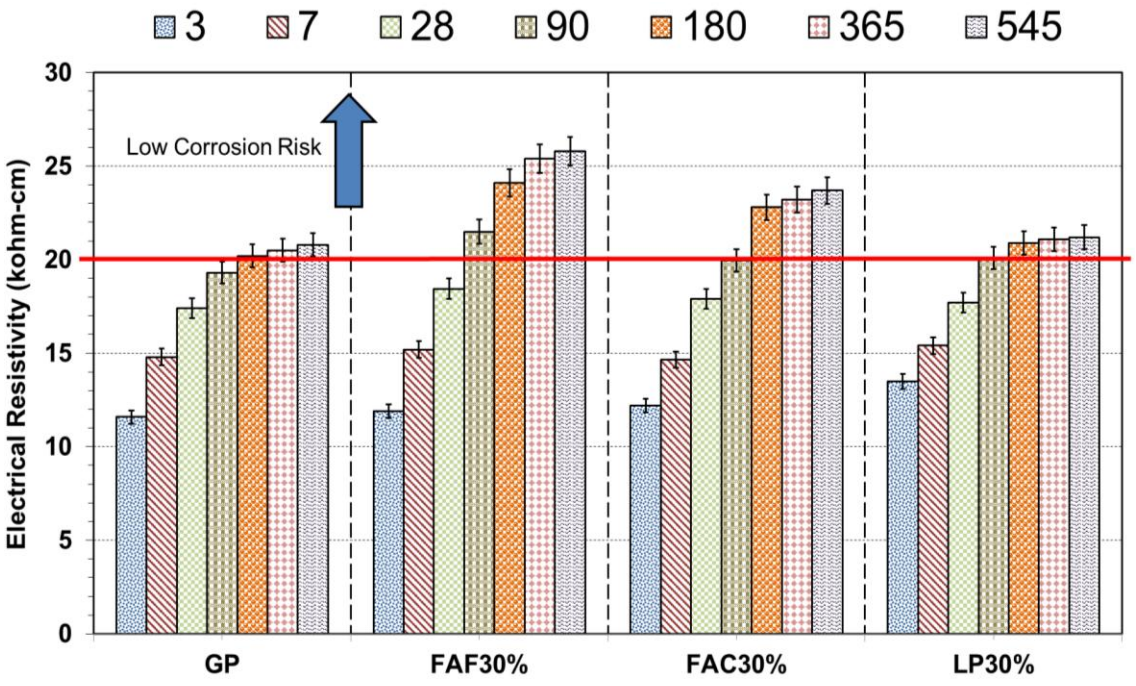

Figure 6.16: Electrical resistivity of CTR mixes with curing age up to 545-days

increased electrical resistivity compared to that of GP at 28-days, which further increased to more than 19% within 545-days of curing. On the other hand, although electrical resistivity of concrete with the inclusion of class C FA (FAC30%) was also increased compared to GP concrete, the rate of increase was lower than FAF30%. Moreover, FAC30% exhibited 3% higher electrical resistivity at 28-days, which further increased to 14% by 545-days. These results can mainly be attributed to some factors including (1) the reduction in the number of leachable ions during the hydration of GP since its proportion is decreased in the mixes (2) the refinement of the pore structures reduces the mobility of the ions that are present in the pore solution. Thus, the electrical resistivity of mixes with FA increased in comparison to mixes with GP only (Salem and Ragai, 2001; McCarter et al., 2000; Ferraris et al., 2001; Abo-El-Enein et al., 1996). The electrical resistivities of FA incorporated specimens increased more with the curing time, which was caused by the on-going hydration. However, they were higher than GP even at the early-ages of cuing. According to Polder et al. (2001), the hydration of FA only starts to contribute well after 28-days of age. So, in particular for GP-FA mixtures, the early increase could mainly be due to Portland clinker hydration and the later-age continuous increase could mainly be due to hydration of FA, which is supported by stronger resistivity increase after 28-days for mixes with 30% FAs. These results are in consistence with Topcu et al. (2016) who also reported that for any hydration span, the rate of the electrical resistivity of FA-cement paste increases having FA ratio from 0% to 30%. Thus, it is possible to produce an SCC of reduced chloride permeability by including 30% FA in the total binder, similarly concluded by Nath and Sarker (2011) and Camões et al. (2002).

The early-age 7-days tests showed that LP30% achieved up to 5% higher electrical resistivity compared to GP and FA mixes, possibly due to the reason mentioned in the previous sections. The electrical resistivity tests conducted on SCC, containing up to 30% LP, show that starting from 90-days curing, the mixes were likely to provide ‘low’ corrosion rate, as suggested by Dhanalaxmi and Nirmalkumar (2015). During 28 and 90 days, LP30% was found to be 4%-15% lower than FAF30%, which might be due to the activation of pozzolanicity in FAF30% that assisted in its improved durability compared to LP30%. However, a slight increase of about 3% was observed in LP30% at 180-days compared to GP mix. In a research undertaken by Silva and Brito (2013), it was similarly revealed that SCC containing up to 30% LP as cement replacement had an insignificant change in resistivity by 182-days of standard curing. The corrosion resistance of LP30% compared to FAF30% and FAC30% between 180 and 545 days was substantially lower since the rate of improvement in FAs at later-ages was much better due to their physical and chemical characteristics, leading to continued hydration. Some more previous researchers also indicated that when LP is included in concrete, the corrosion resistance of concrete

increases but extensive improvement depends on the content of LP (Dhir et al., 2007; Ramezanianpour et al., 2009; Lee et al., 2008; Pipilikaki et al., 2009; Gao et al., 2008; Tosun et al., 2009; Moon et al., 2004).

(a) Effects of glass fineness on electrical resistivity

Figure 6.17 demonstrates the electrical resistivities of GL-FN series, cured up to 545-days under standard conditions. The electrical resistivity of coarser to finer range of glass powders was investigated to highlight the changes in the chloride ion penetration resistance with variations in particle sizes. On the whole, the electrical resistivities of SCC containing glass increased as the glass particle size became finer. This can be related to the improvement in the behaviour of the concrete's pore structure and hindering ion mobility in the solution that fills the pores and consequently, increases the electrical resistivity. A consistent explanation has been reported by Hassan et al. (2009) and Lübeck et al. (2012). The electrical resistivity obtained at 3-days for 10G30% was observed to be the highest in GL-FN series and was observed to be 7% and 15% higher compared with 20G30% and 40G30% respectively. However, as the curing time proceeded to 28-days, 10G30% showed 6% and 15% higher electrical resistivities than 20G30% and 40G30% respectively. Afterwards, with the progress in the curing time up to 180-days, 10G30% exhibited 2% and 12% higher electrical resistivities in comparison to 20G30% and 40G30%. Similar behaviour was noticed from 180-days to 545-days of water curing as 10G30% increased by 4% and 11% than 20G30% and 40G30% respectively at 545-days. These results indicate that curing and particle size has a significant effect on the chloride ion penetration resistance of glass modified concrete.

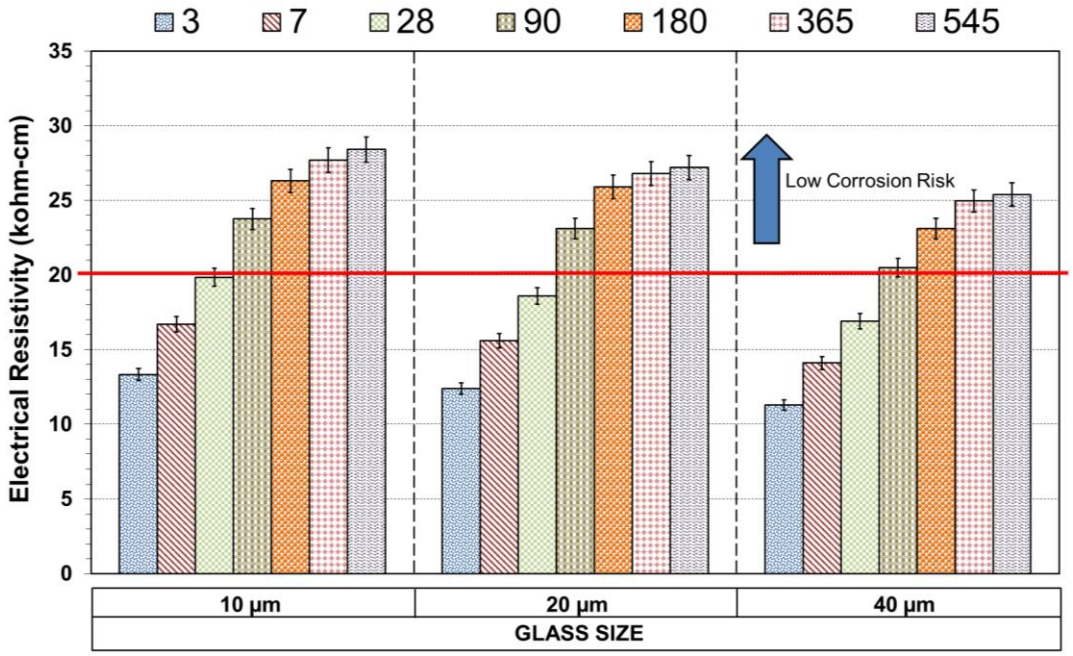

Figure 6.17: Electrical resistivities of GL-FN with curing age up to 545-days

Figure 6.18 shows the comparison between electrical resistivities of few CTR mixes and glass mixes categorized in GL-FN class. It is apparent that GP exhibited lower electrical resistivities compared to glass mixes, up to 545-days of standard curing. Moreover, comparisons of glass as an SCM compared to FA indicate that glass at a similar particle size showed lower electrical resistivity at 3-days compared to FAs but it demonstrated better electrical resistivities as the curing time progressed up to 545-days. To elaborate, 3-days electrical resistivities achieved by 10G30% was 9%-11% higher and by 40G30% was 5%-8%

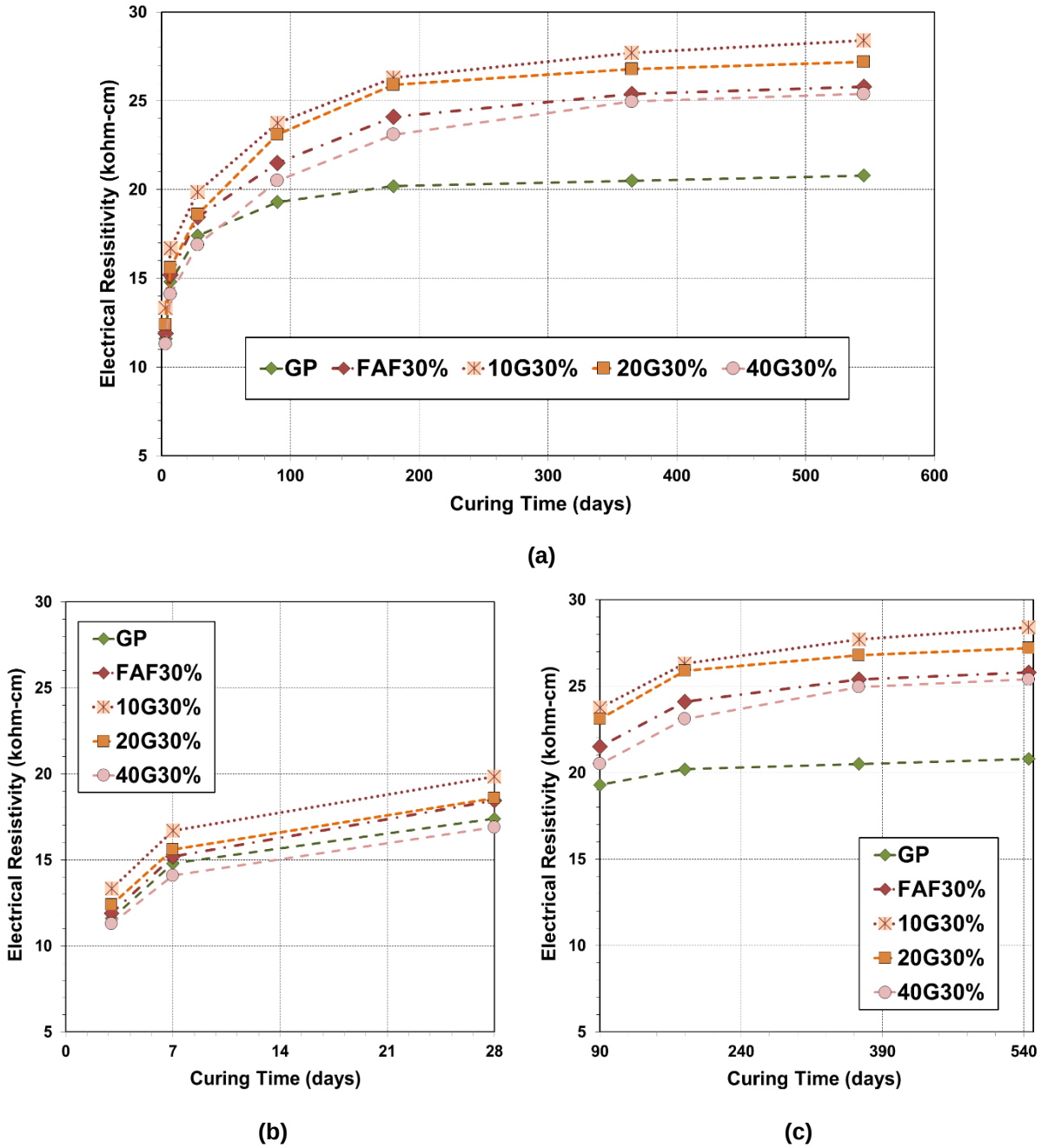

Figure 6.18: (a) Comparison between electrical resistivities of GL-FN, GP and FAF30% up to 545-days; (b) Comparison between electrical resistivities of GL-FN, GP and FAF30% from 3 to 28 days; (c) Comparison between electrical resistivities of GL-FN, GP and FAF30% from 90 to 545 days

lower than FAF30% and FAC30%. In addition, mixes 10G30%, 20G30%, and 40G30% showed 1%, 9% and 20% lower electrical resistivities compared to LP30% at 3- days respectively. By 7-days, 10G30% showed higher electrical resistivity than GP with a variation of 11%. The 28-days tests demonstrate that the electrical resistivity shown by 10G30% was higher than FAF30% and FAC30% by 7% and 10% respectively. The electrical resistivity of 20G30% was found to be higher by 5% than LP30% at 28-days; however, 40G30% exhibited 5% lower electrical resistivity than LP30%. Moreover, 20G30% showed higher electrical resistivity by 7% compared to FAF30% whereas, 40G30% showed only 1% higher electrical resistivity than FAC30% at 180-days. As anticipated, the progress in curing time enhanced the electrical resistivity of all specimens. Therefore, 10G30% and 20G30% demonstrated higher and 40G30% showed lower electrical resistivities than FAs at 545-days.

(b) Effects of glass content on electrical resistivity

The electrical resistivity of various replacement levels of glass powders was also studied to emphasize on the variations in the electrical resistivities with differences in glass contents. The electrical resistivities of GL-CN class of mixes up to 545-days of standard water curing have been illustrated in Figure 6.19. As anticipated, electrical resistivity was strongly influenced by the addition of glass powder in concrete. The decrease in electrical resistivity with the increase in the percentage of glass powder content can be connected to differences in the amounts of angular-shaped glass particles within the microstructure of the glass specimens. The electrical resistivity obtained at 3-days for 20G20% was observed to be the highest in GL-CN class as it was 7% and 14% higher compared with 20G30% and 20G40%

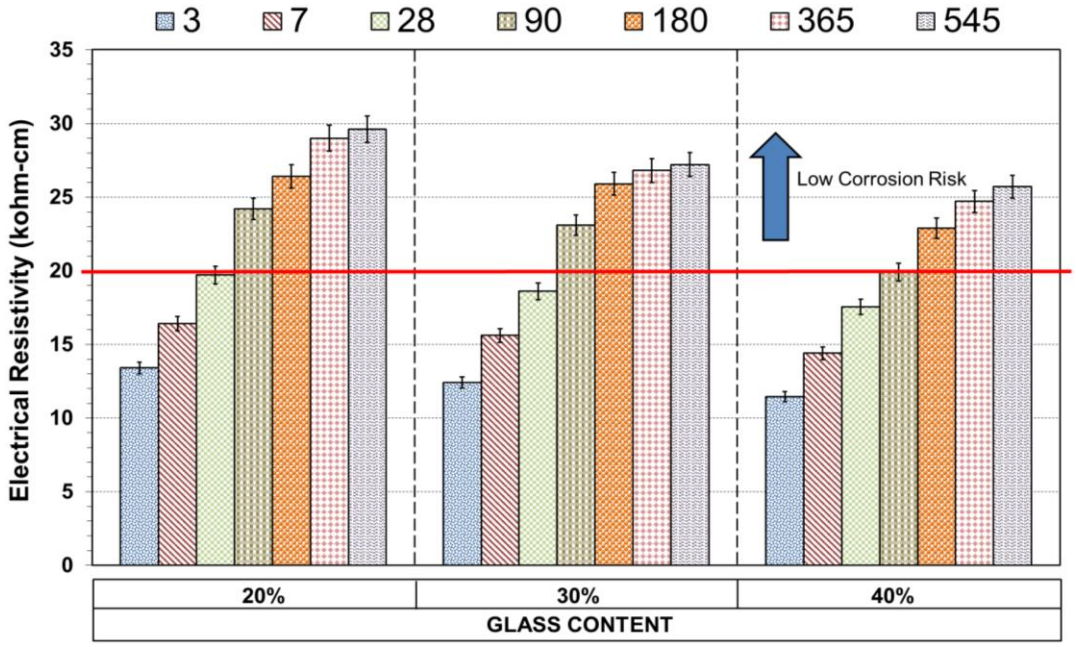

Figure 6.19: Electrical resistivities of GL-CN with curing age up to 545-days

respectively. Further, 20G20% showed 5% and 12% higher resistivities than 20G30% and 20G40% at 7- days, which might be linked to the better pore refinement and pore blocking in 20G20% glass mix, similarly mentioned by Nassar and Soroushian (2012). Nevertheless, 28-days tests revealed that 20G20% demonstrated 6% and 11% higher electrical resistivities in comparison to 20G30% and 20G40%, which can again be linked to better pore structure enhancement in 20G20% with curing. Consistent behaviour was observed in all GL-CN samples until 545-days of testing when 20G20% demonstrated 8% and 13% higher electrical resistivities than 20G30% and 20G40% respectively. These results are similar to a study undertaken by Nassar and Soroushian (2012) who reported that the addition of 20% milled waste glass (13 µm) resulted in 54% reduction of the number of coulombs passed through concrete compared to the concrete without waste glass, signifying better chloride ion resistance in glass incorporated concrete. However, glass replacement dosages above 20% were not investigated in that study. Cassar and Camilleri (2012) reported fairly similar results that the replacement of 10%-20% of cement by glass gives concrete a high resistance to chloride-ion penetration and the resistance reduces with an increase in the glass content. Moreover, up to 40% of the cement can be replaced by the glass and still obtain a concrete, suitable for use in the structure, similarly observed in the present study. The authors concluded that such concrete would be ideal for use in structures built close or in the sea.

Figure 6.20 shows the comparison between electrical resistivities of some of the CTR mixes and the glass mixes categorized in GL-CN class. It is evident from the results that GP mix demonstrated lower resistance to chloride ion permeation compared to GL-CN glass mixes at curing ages up to 545-days. Additionally, it was found that FAs at similar replacement level performed worse than glass in terms of resistance, starting from 7-days until 545-days.

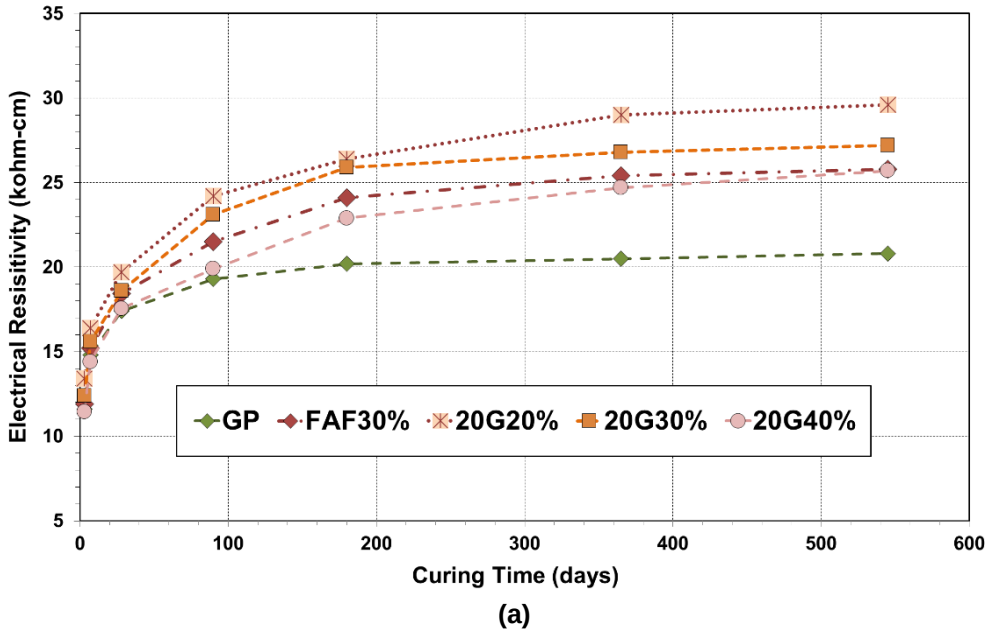

(a)

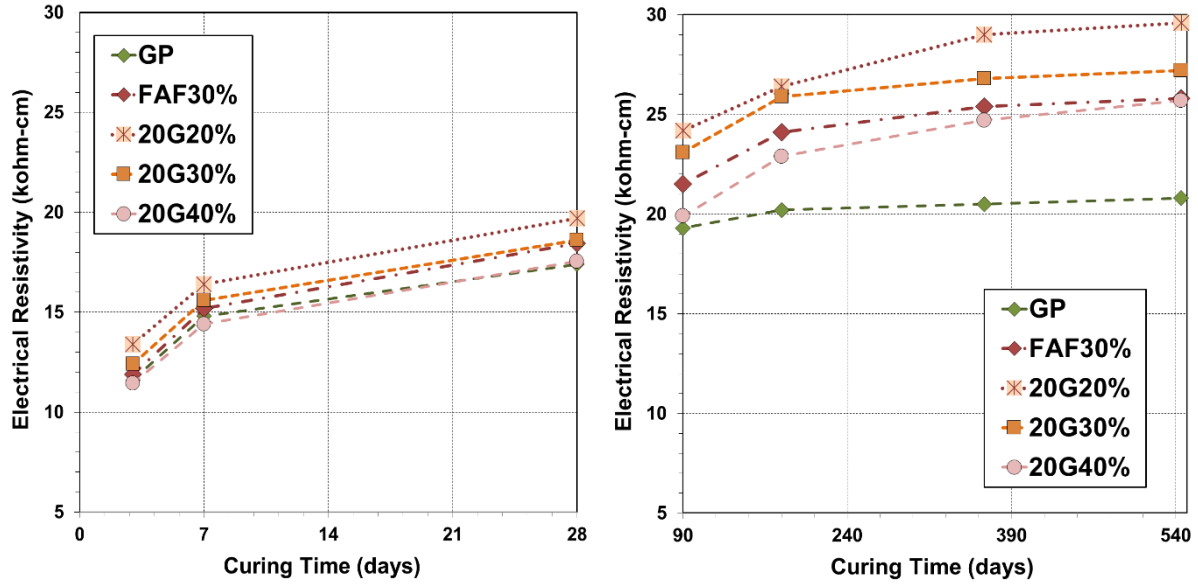

Figure 6.20: (a) Comparison between electrical resistivities of GL-CN, GP and FAF30% up to 545-days; (b) Comparison between electrical resistivities of GL-CN, GP and FAF30% from 3 to 28 days; (c) Comparison between electrical resistivities of GL-CN, GP and FAF30% from 90 to 545 days

To elaborate, 3-days electrical resistivities achieved by 20G20% was 9%-11% higher and by 20G40% was 4%-7% lower than FAF30% and FAC30%. In addition, 20G30% and 20G40% were 1%-18% lower than LP30% at the curing age of 3-days. 20G30% was also observed to be 9% lower than LP30% at 3-days. At 28-days, 20G20% showed higher electrical resistivity than FAF30%, within a variation of 6%; however, it achieved 10% higher electrical resistivity than LP30%. Furthermore, electrical resistivity of 20G20% reduced by 20% compared to GP at 90-days and there was about 16% reduction in 90-days electrical resistivity of 20G30% compared to GP. The 180-days tests informed that electrical resistivity shown by 20G40% was higher in comparison to LP30% by 9%. Also, 20G20% and 20G40% showed 13%-20% higher and 3%-12% lower chloride ion penetration resistances than FAs respectively, at 180-days. A similar trend in the increase was observed up to 545-days. Finally, GL-CN showed 2%-4% increase in electrical resistivity from 365-days to 545-days, which is somewhat higher than the increase shown by GP, FAC30%, and LP30%, during this curing period. Hence, it can be concluded that fine glass powder has the potential to improve durability of concrete compared to GP. Similar conclusion has been presented by Schwarz et al. (2008).

(c) Effects of glass quality on electrical resistivity

The results of the electrical resistivity tests, performed on 20UG30% specimens as well as on GP and 20G30% specimens, up to 545-days of standard water curing have been demonstrated in Figure 6.21. The results indicate that 20UG30% mix exhibited much lower

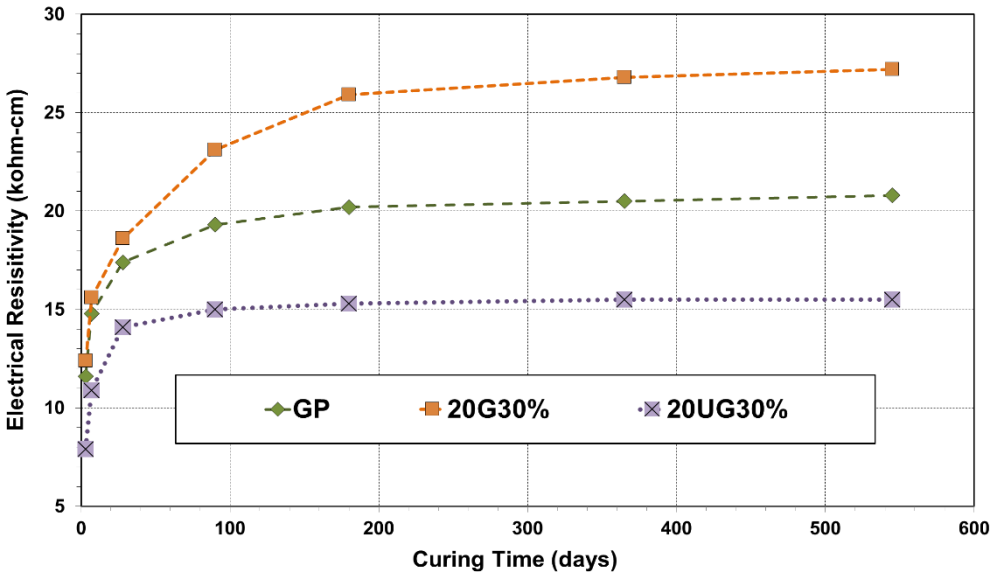

Figure 6.21: Electrical resistivity of 20UG30% with curing age up to 545-days

resistance to chloride ion penetration compared to all other glass mixes as well as CTR mixes at curing ages up to 545-days. Specifically, 20UG30% presented the lowest electrical resistivity value of 7.9 kohm.cm at 3-days, which implies that the presence of impurities and organic content deteriorated its durability performance in comparison to the washed glass as well as other CTR specimens. Furthermore, it established 34%-66% lower electrical resistivity than the other CTR mixes by the end of 545-days. Another noteworthy observation is that the rate of increase in resistivity of 20UG30% between 3-days and 545-days was found to be the lowest in comparison to other glass types, which can be linked to the same aforesaid reason.

(d) Relationship between electrical resistivity and porosity

A correlation between electrical resistivity and porosity was also developed using regression analysis. The results of electrical resistivity versus porosity for all mixtures made from glass powder, fly ashes and GP cement are illustrated in Figure 6.22. The exponential regression analysis gave the following correlation equation for glass incorporated mixes.

$$R_e = 109.1e^{-0.18p};\ R^2 = 0.92 \qquad \text{Equation 6.6}$$

The regression coefficient of 0.92 represents a very strong relationship between these two parameters. The results also show a decrease of porosity and increase in electrical resistivity with the exposure period. However, it can be noticed that all mixes including unwashed glass, washed glass of varying finenesses and contents, class F and class C fly ashes showed similar relationship trend between electrical resistivity and porosity. This indicates that the type of binder and curing age does not affect the correlation between resistivity and porosity.

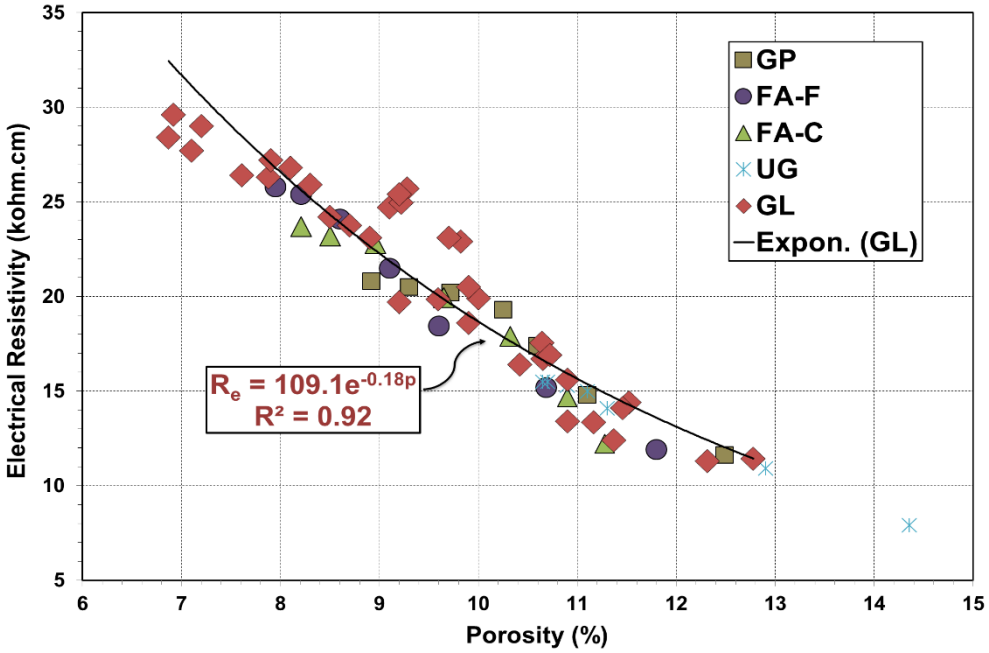

Figure 6.22: Relationship between porosities and electrical resistivities of GP, FAF, FAC and GL (UG, GL-FN, and GL-CN) incorporating mixes tested up to 545-days

6.4.2 Chloride diffusion coefficient of self-compacting concrete incorporating glass powder

The most dominant method of chloride ingress is by diffusion and a number of different service life models have been developed to elucidate this (Stanish and Thomas, 2003). These models require the diffusion value as an input parameter. A common experimental method of determining diffusion coefficients is through the bulk diffusion test, where saturated samples are exposed to a chloride containing the solution for a known period of time. The chloride profiles are then established and the diffusion coefficient is determined. However, concrete is not a static material as it continues to hydrate and hence, in reality, the situation for concrete is not simple because many substances of concern from a durability perspective interact with the concrete constituents. This variability may cause changes to porosity, which subsequently may cause changes in the concrete microstructure through cracking, precipitation of reaction products etc. This may also produce a change in the coefficient of diffusion with time with a higher rate of reduction occurring at early ages. At later ages, however, the effect of continuous chemical reactions on permeability appears to cause a change in the porosity of the concrete microstructure, resulting in the reduction of chloride permeability results. Similar to other properties, the resistance of concrete to chloride penetration increases as the concrete matures and this is more common in the case of concrete containing SCMs. Pozzolans reduce the chloride diffusion coefficient of concrete, however, the degree of reduction varies depending mainly on the nature of the pozzolan and the level of replacement. In addition, highly reactive pozzolans are expected to considerably

reduce the diffusion coefficient at early-ages compared to more slowly reacting pozzolans (Gruber et al., 2001). For this reason, comparative chloride diffusion measurements on immature concretes at early-ages may or may not essentially be an indicator of long-term performance.

The current section presents the results of the experimental study on apparent chloride diffusion coefficients of a range of SCC mixes, incorporating control binders as well as glass powders of varying finenesses, contents and quality. The test procedures, curing conditions, preparation of ground concrete for chloride diffusion measurements prior to testing and equations used for calculations have already been explained in Chapter 3. All tests were undertaken at predefined curing ages. The average chloride diffusion measurements were taken from two identical specimens that were ground to depths up to 20 mm. Complete data are shown in Appendix E. Figure 6.23 demonstrates the average chloride diffusion coefficients of CTR specimens at the curing ages of 28, 90, 180, 365 and 545 days. The results clearly mention that the response of SCC containing GP on chloride diffusion coefficient was dependent on the maturity of concrete, which means the duration of curing. GP concrete exhibited the highest chloride diffusion coefficients compared to the other CTR mixes at all curing ages, with a significant reduction of 29% between 28-days and 90-days, followed by a relatively lower decrease of about 21% from 7-days to 545-days.

The results indicate that FAF30% demonstrated reduction of about 46% in diffusion coefficient compared to GP concrete at 28-days. Additionally, class C FA concrete (FAC30%) resulted in approximately 39% reduced chloride diffusion coefficient than that of

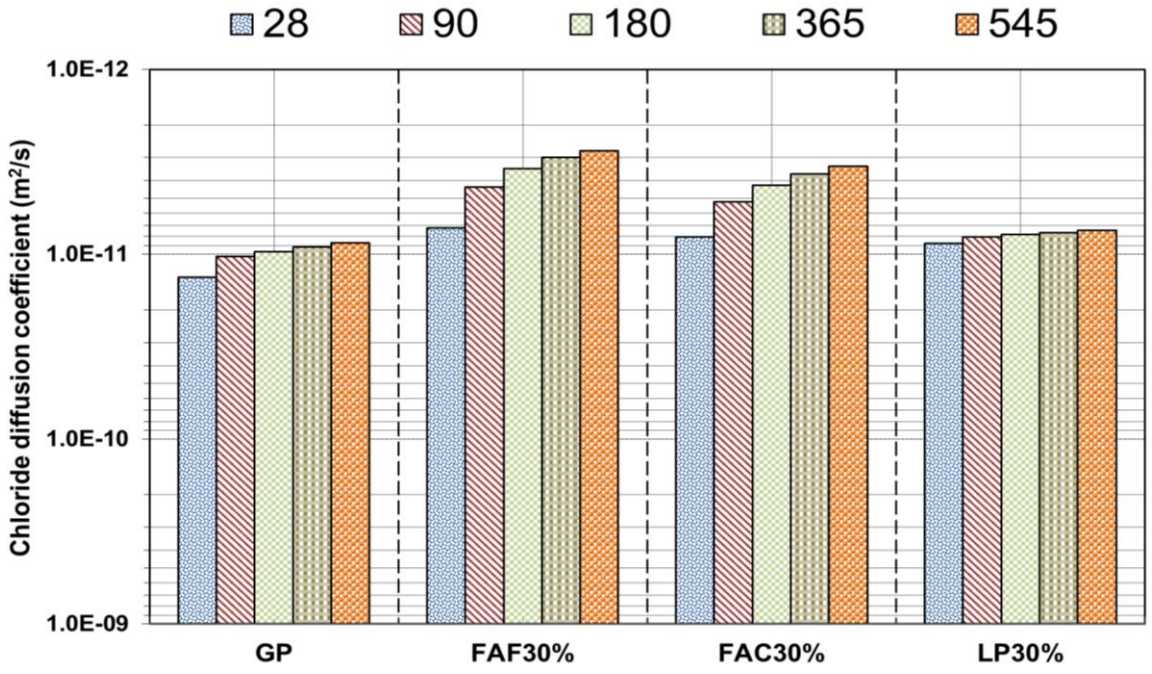

Figure 6.23: Chloride diffusion coefficients of CTR mixes with curing age up to 545-days

GP concrete at 28-days. The reduction in chloride diffusion coefficients of FAF30% and FAC30% reached 56%-64% within 180-days of curing. With the progress in the curing period, an improvement in the resistance to chloride diffusion was observed. Hence, FAF30% showed 68% reduced diffusion coefficient in comparison to GP, whereas FAC30% showed comparatively lower reduction of 61% to that of GP at 545-days. These findings can be related to the reaction of FA with $Ca(OH)_2$, which produces a denser concrete and thus, inhibits the ingress of chloride ions. Generally, both FA mixes were found to be adequately better resistant to chloride diffusion compared to GP, with FAF30% being further superior than FAC30%. These results are in accordance with Chisholm (1997) who similarly reported that chloride diffusion shows significant improvement for FA blended concrete compared with GP concrete. Siddique and Khan (2011) also mentioned that FA addition to concrete improves the long-term corrosion resistance of concrete. Bai et al. (2003) reported that 30% GP replacement by FA is effective in decreasing both the chloride concentration and penetration depth, especially at long exposure times. These authors attributed these results to the relative changes in intrinsic diffusivity and chloride binding capacity with curing age exhibited by the FA-GP compositions.

The 28-days tests revealed that LP30% achieved up to 34% lower chloride diffusion coefficient compared to GP and 9%-20% higher chloride diffusion coefficient compared to FA mixes. The 90-days curing further decreased chloride diffusion coefficient with an inclusion of LP in comparison to GP, similarly reported by Spitek (2014). However, very little change in diffusion coefficient was observed for LP30% beyond 90-days. Between 90 and 180 days, the chloride diffusion coefficients for FAF30% and FAC30% continued to decrease due to the pozzolanic reactions. From 180-days until the end of the study at 545-days, a slight reduction of 3% in coefficient of chloride diffusion was noted for LP30%. The resistance of LP30% to chloride diffusion compared to FAF30% and FAC30% between 180-days and 545-days was substantially lower because the rate of improvement in FAs at later-ages was much better due to the continued hydration and development of the pore structure, which did not occur with LP. In general, the effect of LP replacement on the long-term chloride resistance of SCC was that there was little change at 30% by weight as cement replacement compared with GP. Hooton et al. (2010) also performed chloride bulk diffusion tests and found that LP does not appreciably change diffusion coefficients. Similarly, Tennis et al. (2011) stated that concrete containing LP gives somewhat similar resistance to chloride ion penetration when it is proportioned to give the same compressive strength at 28-days. Conversely, Dhir et al. (2007) produced five series of concretes with 0%, 15%, 25%, 35% and 45% LP and reported that there is little difference in chloride diffusion coefficient between concrete produced with GP and 15% LP but at higher levels of LP, there is an

increase in chloride diffusion coefficient. The contradictory result obtained in the present study might be related to better dispersion of LP particles in SCC due to the addition of SP.

(a) Effects of glass fineness on chloride diffusion coefficient

Figure 6.24 shows the chloride diffusion coefficients of GL-FN specimens, cured up to 545-days under standard conditions. The chloride diffusion coefficients of coarser to finer range of glass powders were investigated to highlight the variations in the chloride diffusion with differences in particle sizes. In general, chloride diffusion coefficients of SCC containing glass reduced as the glass particle size became finer, which might be linked to the denser pore structure in finer glass incorporated SCC that modified the composition of cement hydrates and the ability to bind chloride ions. The 28-days chloride diffusion coefficient obtained for 10G30% was the lowest in GL-FN series and was found to be 16% and 41% lower compared with 20G30% and 40G30% respectively. As the curing time proceeded to 90-days, 10G30% demonstrated 23% lower apparent chloride diffusion coefficient value than 20G30% and 54% lower apparent chloride diffusion coefficient than 40G30%. Subsequently, with the progress in the curing up to 180-days, 10G30% exhibited 28% and 56% lower chloride diffusion coefficient compared to 20G30% and 40G30%. Identical behaviour was noticed in all GL-FN mixes from 180-days to 545-days of standard water curing.

Figure 6.25 shows the comparison between chloride diffusion coefficients of few CTR mixes and glass mixes categorized in GL-FN series. The data obtained through chloride profile analysis indicated that GP mix had higher chloride diffusion coefficients in comparison to glass mixes, up to 545-days of standard curing. In addition, the comparisons of glass as an

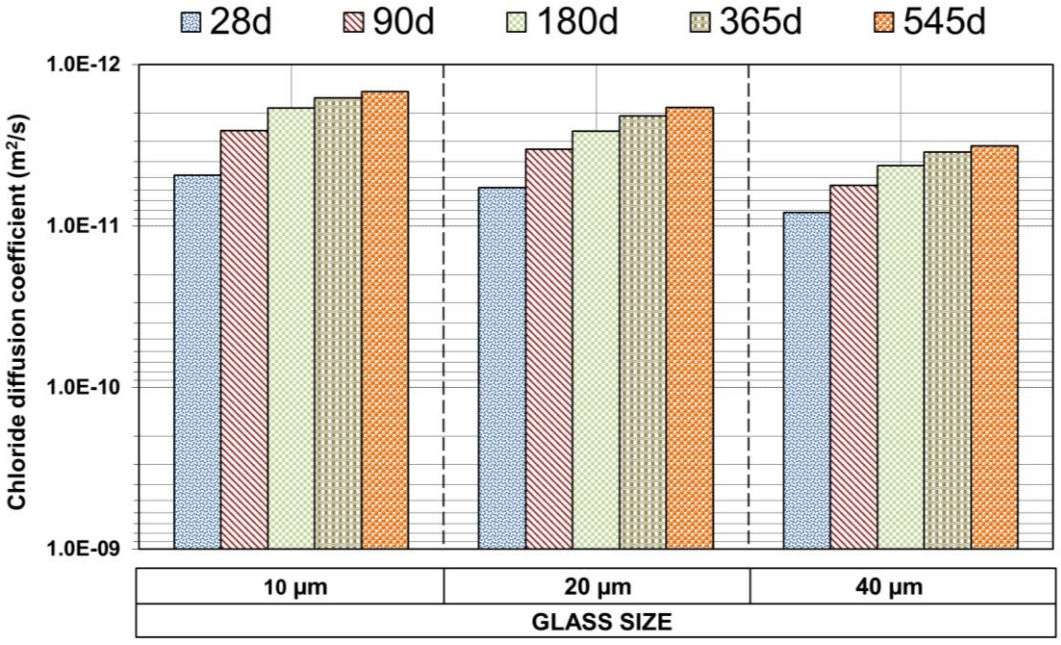

Figure 6.24: Chloride diffusion coefficients of GL-FN with curing age up to 545-days

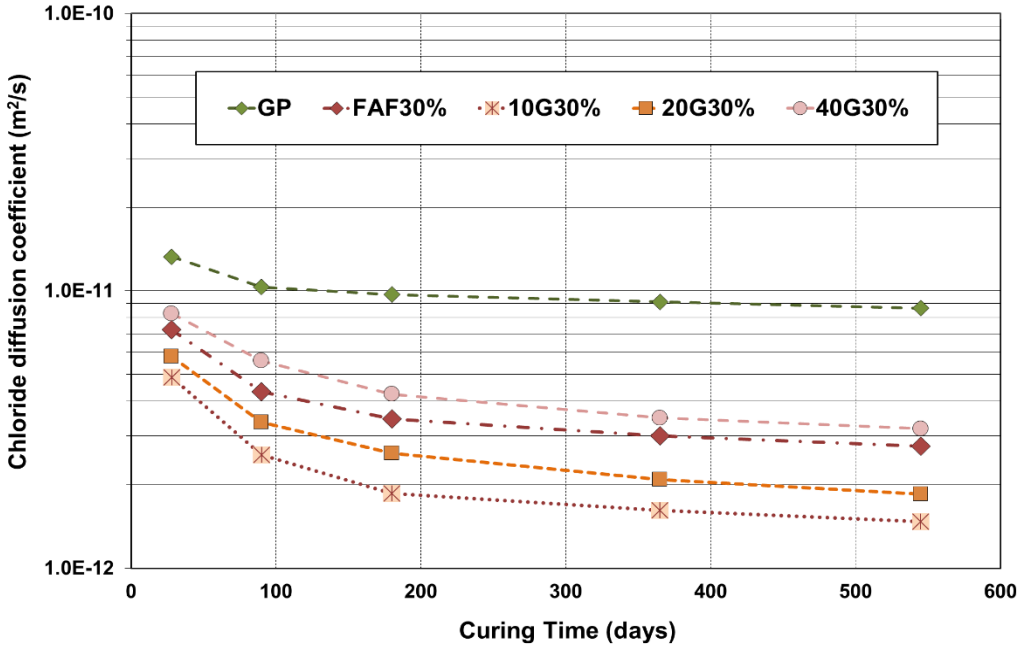

Figure 6.25: Comparison between chloride diffusion coefficients of GL-FN, GP and FAF30% up to 545-days

SCM compared to FA indicate that glass at a similar particle size showed higher chloride diffusion coefficients at 28-days compared to FAs but it demonstrated lower chloride diffusion coefficients as the curing time reached up to 545-days, lying somewhere between FAF30% and FAC30%. The chloride diffusion coefficient of 20G30% was found to be reduced by 33% than LP30% at 28-days and 40G30% exhibited insignificantly lower chloride diffusion coefficient than LP30%. As the curing time reached 90-days, 10G30% showed 41% lower coefficient of chloride diffusion than FAF30% and its behaviour in comparison to FAC30% was much better as it showed 51% lower coefficient of chloride diffusion than FAC30%. Moreover, 20G30% demonstrated 25% lower apparent chloride diffusion coefficient compared to FAF30% whereas 40G30% showed only 1% lower coefficient than FAC30% at 180-days. As anticipated, the progress in curing time enhanced the resistance to chloride ion penetration of all specimens. Therefore, 10G30% and 20G30% demonstrated lower and 40G30% showed higher chloride diffusion coefficients than FAF30% at 545-days. Nevertheless, all GL-FN mixes demonstrated higher resistance to chloride diffusion than GP mix. The overall results of the present study are consistent with those presented by Shayan and Xu (2006) who also discovered that chloride penetrability of mixes containing glass powder were significantly lower than that of the reference GP concrete.

(b) Effects of glass content on chloride diffusion coefficient

The chloride diffusion coefficients of various replacement levels of glass powders were also studied to emphasize on the variations in the resistance of chloride diffusion with differences in glass contents. The chloride diffusion coefficients of GL-CN class of mixes up to 545-days

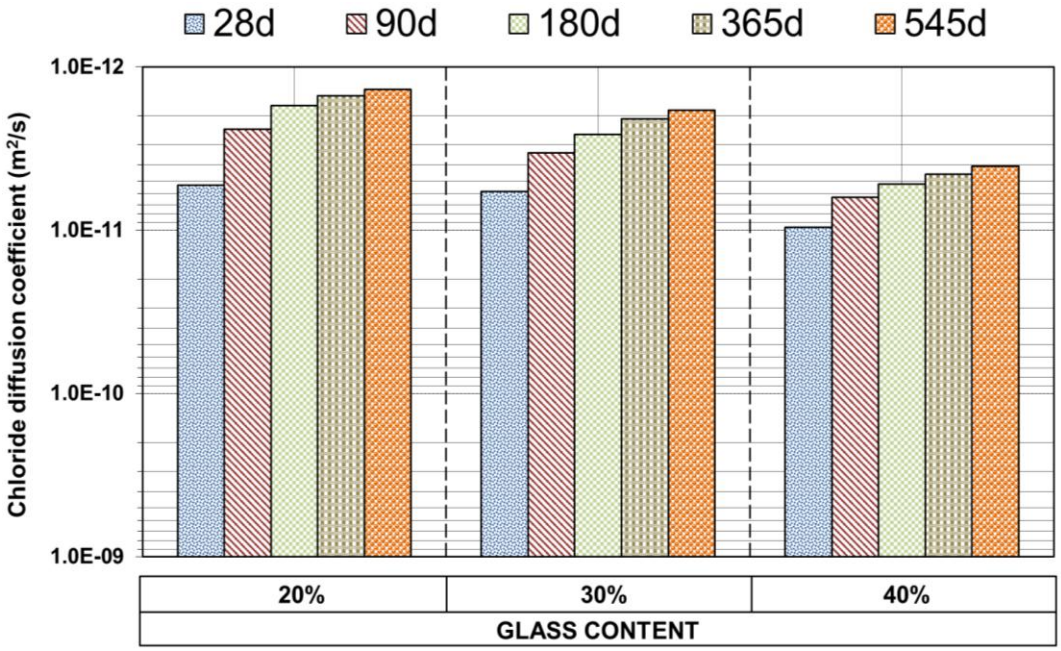

Figure 6.26: Chloride diffusion coefficients of GL-CN with curing age up to 545-days

of standard water curing have been illustrated in Figure 6.26. The resistance to chloride diffusion was strongly affected by the addition of glass powder in SCC. The reduction in chloride diffusion coefficients inversely with the percentage of glass powder content can be linked to the same reason mentioned in the previous section. The 28-days tests revealed that 20G20% demonstrated 9% and 45% lower chloride diffusion coefficients in comparison to 20G30% and 20G40%. With the progress in curing, reduction in chloride diffusion is evident and hence, consistent behaviour was observed in all GL-CN specimens until 545-days of testing when 20G20% revealed 26% and 66% lower chloride diffusion coefficient in comparison to 20G30% and 20G40% respectively. Shi and Wu (2006) also reported that the addition of glass powder to increase the flow ability and segregation resistance of SCC was also found to increase chloride migration resistance.

Figure 6.27 shows the comparison between chloride diffusion coefficients of some CTR mixes and the glass mixes categorized in GL-CN class. The data from the chloride profiles of all tested specimens revealed that GP mix demonstrated lower resistance to chloride diffusion compared to all GL-CN glass mixes at curing ages up to 545-days. Furthermore, it was also observed that FAs at a similar replacement level performed better than glass powder in terms of resistance to chloride diffusion, starting from 7-days until 545-days. At 28-days, 20G20% demonstrated lower chloride diffusion coefficient than FAF30% by 27%; however, it achieved 39% lower chloride diffusion coefficient than LP30%. Moreover, the chloride diffusion coefficient of 20G20% reduced by 77% compared to GP at 90-days and there was approximately 67% reduction in 90-days chloride diffusion coefficient of 20G30% in comparison to GP. The 180-days tests informed that chloride diffusion coefficient exhibited

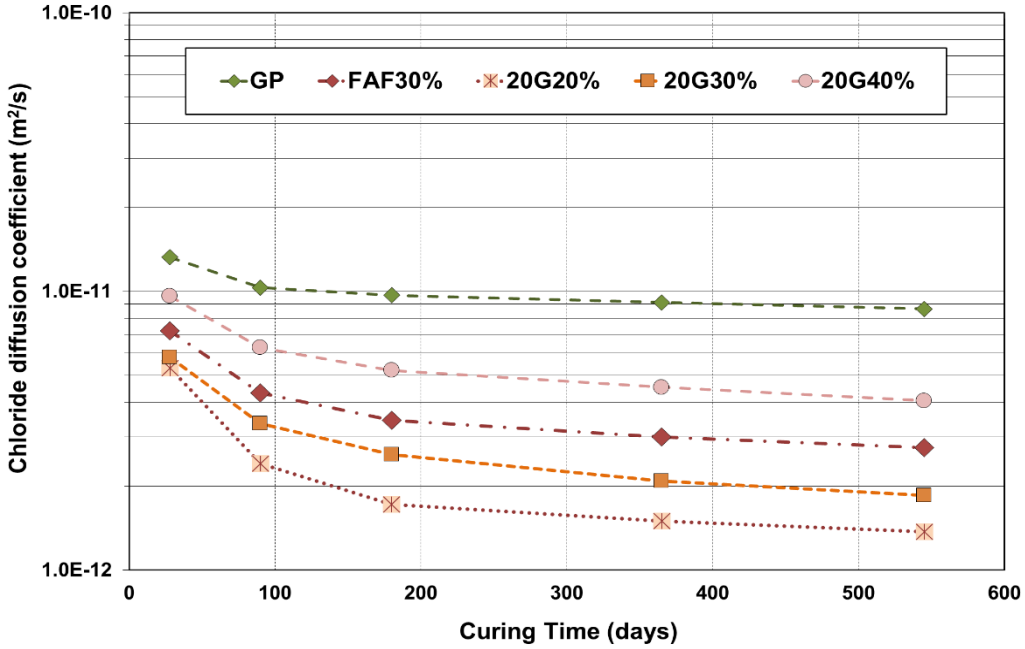

Figure 6.27: Comparison between chloride diffusion coefficients of GL-CN, GP and FAF30% up to 545-days

by 20G40% was considerably lower in comparison to LP30%. Likewise, 20G20% and 20G40% showed 50%-59% lower and 23%-51% higher diffusion coefficients than FAs respectively, at180-days. A similar trend of the reduction in chloride diffusion coefficient was observed up to 545-days. Finally, GL-CN demonstrated 9%-29% decrease in chloride diffusion coefficient from 365-days to 545-days, which is higher than the reduction shown by GP, FAC30%, and LP30%, during this curing period.

(c) Effects of glass quality on chloride diffusion coefficient

The resistance to chloride diffusion of unwashed glass powder (20UG30%) was also observed in order to understand the effects of the quality of glass material on chloride diffusion coefficient of SCC. The results of chloride diffusion tests, undertaken on 20UG30% specimens as well as on GP and 20G30% specimens, up to 545-days of standard water curing have been demonstrated in Figure 6.28. The results indicate that 20UG30% mix demonstrated much lower resistance to chloride diffusion compared to all other glass mixes as well as CTR mixes at curing ages up to 545-days. Precisely, 20UG30% presented the highest chloride diffusion coefficient value of 2.52E-11 m^2/s at 28-days, which suggests that the presence of impurities and organic content deteriorated its durability performance in comparison to the washed glass as well as CTR specimens. Furthermore, it demonstrated extremely high chloride diffusion coefficients than the CTR mixes by the end of 545-days. Another noteworthy observation is that the rate of increase in electrical resistivity of 20UG30% between 3-days and 545-days was found to be the lowest in comparison to other glass types, which can be linked to the same aforesaid reason.

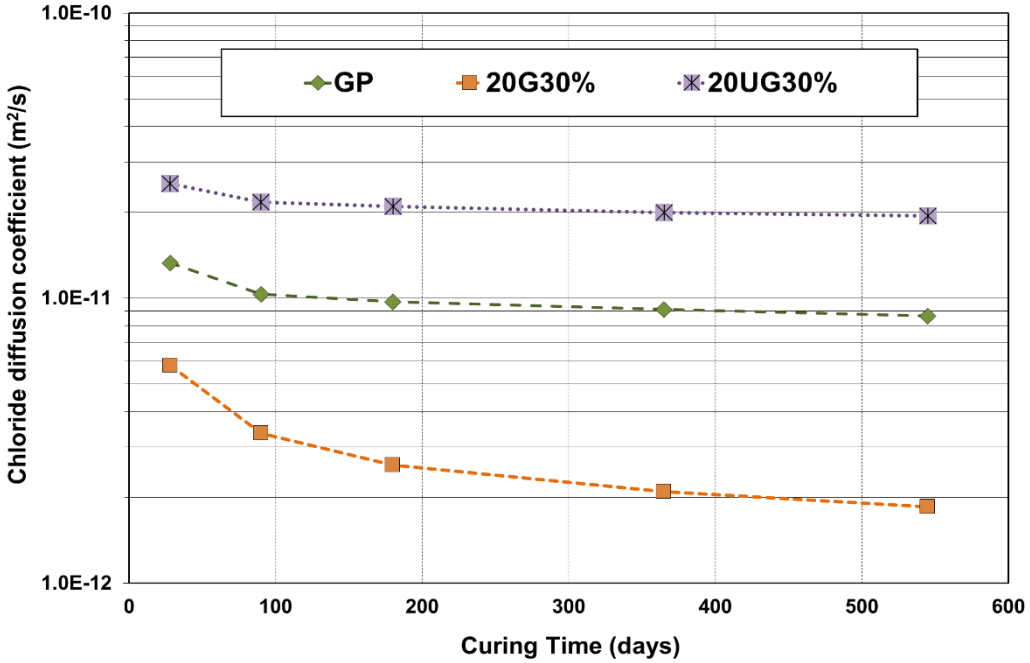

Figure 6.28: Chloride diffusion coefficients of 20UG30% with curing age up to 545-days

(d) Relationship between chloride diffusion coefficient and electrical resistivity

Generally, an increase in the electrical resistivity is accompanied by a decrease in the chloride diffusion values. An attempt has been made to derive a possible correlation between electrical resistivity and chloride diffusion coefficient. Figure 6.29 shows the relationship between the findings of electrical resistivity and chloride diffusion coefficient for

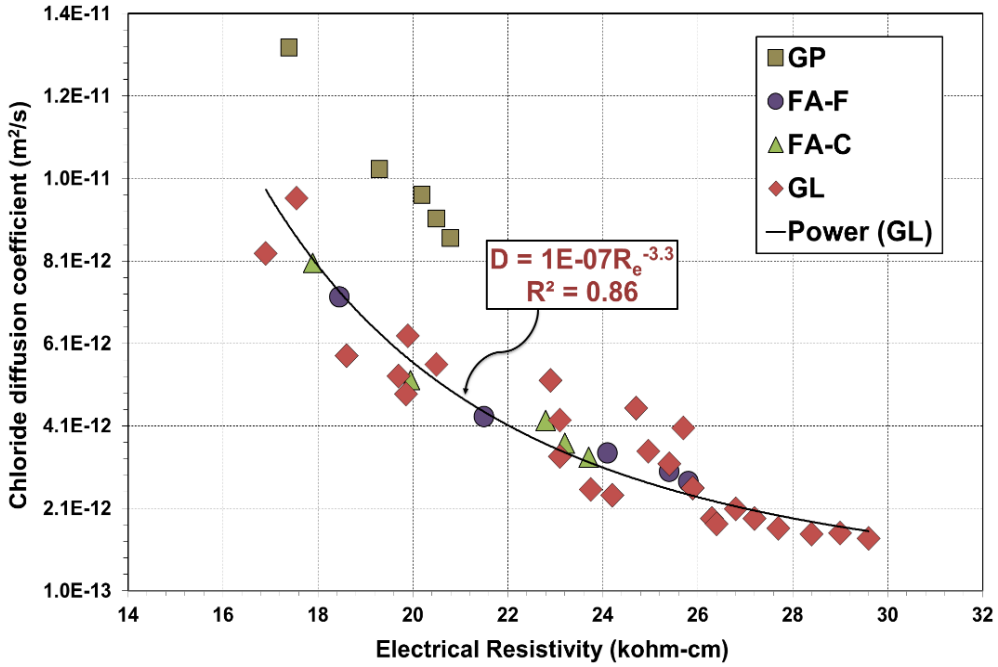

Figure 6.29: Relationship between chloride diffusion coefficients and electrical resistivities of GP, FAF, FAC and GL (GL-FN, and GL-CN) incorporating mixes tested up to 545-days

a wide range of SCC produced in this study. There is a broad correlation between the results of the tests. The regression analysis gave the following correlation equation for glass mixes.

$$R = 1E\text{-}7R_e^{-3.3};\ R^2 = 0.86 \qquad \text{Equation 6.7}$$

The regression coefficient of 0.86 achieved in this study represents a very strong relationship between these two parameters. The results also show a reduction of chloride diffusion coefficient and increase in electrical resistivity with the curing period. However, it can be noticed that all glass mixes of varying finenesses and contents, class F and class C fly ashes demonstrated similar relationship trend between electrical resistivity and chloride diffusion coefficients except GP.

(e) Relationship between chloride diffusion coefficient and coefficient of oxygen permeability

A correlation was observed between the chloride diffusion coefficient and coefficient of oxygen permeability. Figure 6.30 demonstrates the relationship between the results of the chloride diffusion coefficients and coefficients of oxygen permeability for a wide range of SCC produced in the present research program. Not only is there a strong correlation between the results of these tests, the regression analysis also identifies that the type of binder affects the correlation between the two properties with the GP series showing the highest chloride diffusion coefficients and oxygen permeability. The power regression analysis provided the following correlation equation for glass mixes.

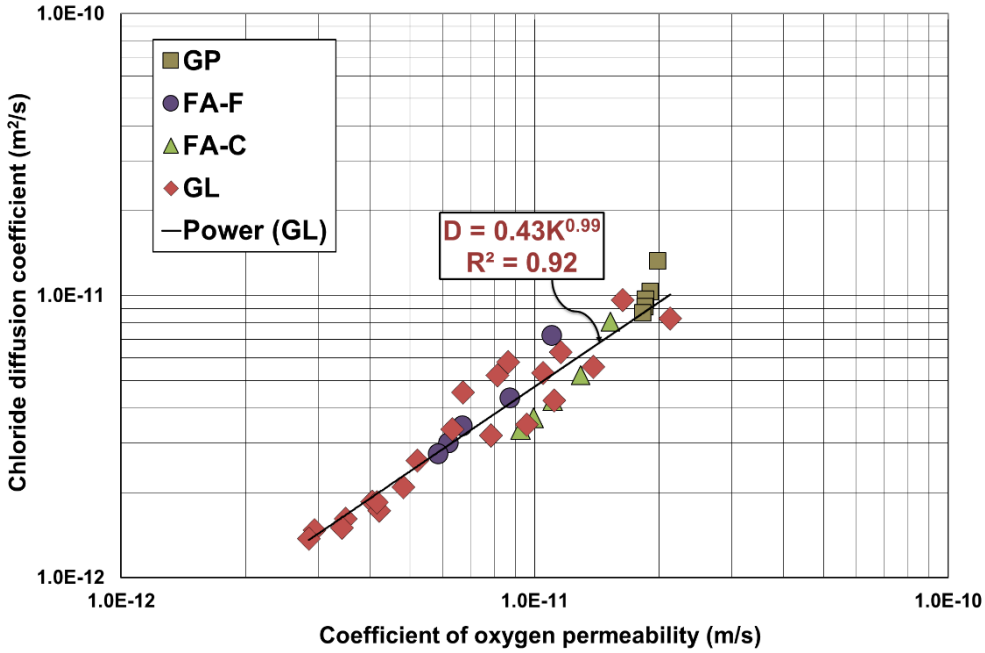

Figure 6.30: Relationship between chloride diffusion coefficients and coefficients of oxygen permeability of GP, FAF, FAC and GL (GL-FN, and GL-CN) mixes tested up to 545-days

$$D = 0.43K^{0.99};\ R^2 = 0.92$$ Equation 6.8

It can be noticed that all glass mixes of varying finenesses and contents, class F and class C fly ashes demonstrated similar relationship trend between oxygen permeability and chloride diffusion. Hence, the results show a reduction in both chloride diffusion coefficients and coefficients of oxygen permeability with the curing period, with relatively stronger correlation in mature concretes.

(f) Relationship between chloride diffusion coefficient and porosity

The results of chloride diffusion coefficient versus porosity for all mixtures made from glass powder, fly ashes and GP cement are illustrated in Figure 6.31. The power regression analysis gave the following correlation equation (Equation 6.9) for glass incorporated SCC mixes.

$$D = 4e^{-16}p^{4.18};\ R^2 = 0.95$$ Equation 6.9

The regression coefficient of 0.95 represents very strong relationship between these two parameters. The results also show a reduction in both porosity and chloride diffusion coefficient with the exposure period. However, it can be noticed that mixes including glass powder of varying finenesses and replacement levels, class F and class C fly ashes showed similar relationship trend between chloride diffusion coefficient and porosity, while the GP mixes showed higher chloride diffusion coefficients for similar range of porosity compared to the other mixes.

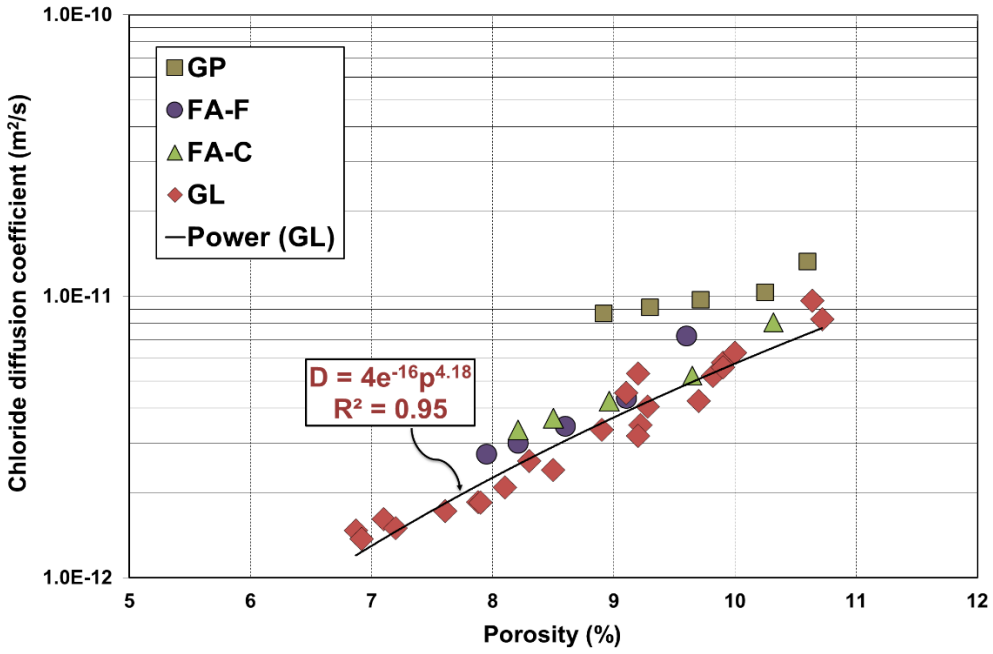

Figure 6.31: Relationship between chloride diffusion coefficients and porosities of GP, FAF, FAC and GL (GL-FN, and GL-CN) incorporating mixes tested up to 545-days

6.5 Drying shrinkage of self-compacting concrete incorporating glass powder

Drying shrinkage of concrete is characterized by the time-dependent volume decrease due to moisture migration and transfer when exposed to a relatively lower humidity environment than the initial one in its own pore system. The amount of water added to the mixture for workability purposes is much higher than that actually needed for hydration of concrete (Neville, 1995; Mehta and Monteiro, 2006). It has been recognized that almost half of the water added to the mixture does not take part of the hydration products and as a consequence, it does not chemically bound to the solid phase. Subsequently, when the curing period is completed and concrete is exposed to a low relative humidity (RH) environment, the resulting gradient acts as a driving force for moisture transfer out of the material, which leads to a volume reduction of the porous material (Acker, 2004). The volume change due to the shrinkage is of considerable significance. In practice, this movement is partly or completely restrained in the concrete slabs laid on the granular sub-bases, which provides high friction and may cause high tensile stresses (Neville, 1995). Drying shrinkage of concrete is responsible for a significant amount of cracking and will also open up existing cracking caused by other mechanisms. In many concrete applications where drying shrinkage cracking is certain, it is usually dealt with the placement of control joints in concrete. Thin structural elements, such as slabs, experience significant shrinkage and control joints are designed to allow some movement of the structure.

The key material properties that influence drying shrinkage are the aggregate type, aggregate/cement ratio, w/c ratio and cement type. There is generally a good correlation between the capability of aggregate to absorb water and the magnitude of drying shrinkage observed in concrete containing it. This is primarily due to the aggregates that are normally not prone to shrinkage and have a larger modulus of elasticity compared to cement paste. Consequently, their presence in concrete acts to internally restrain shrinkage. The reason for the correlation between water absorption and shrinkage is the outcome of the strong relationship between the porosity of aggregate and its stiffness. It is sometimes believed that shrinkage increases as water content increases, which actually means a change in the aggregate/cement ratio. In the case where w/c ratio is fixed, an increase in water content means an increase in the volume of cement paste and hence, a decrease in the volume of aggregate. As the w/c ratio reduces, the modulus of elasticity of the hardened cement paste increases, presenting a greater resistance to shrinkage (Dyer, 2014). Hence, drying shrinkage can be limited by keeping the water content of concrete as low as possible and maximizing the coarse aggregate content (Portland Cement Association, 2002). This leads

to the fact that concrete with less water in the pores and a higher hydrated product tend to exhibit lower shrinkage, similarly mentioned by Wattanapornprom and Stitmannaithum (2015).

SCC usually contains large quantities of mineral fillers, higher quantities of high-range water-reducing admixtures, and smaller maximum size of the coarse aggregate (Aslani and Nejadi, 2011a; 2012). These modifications in the composition of the mixture affect the behaviour of the concrete in its hardened state, including the shrinkage deformations. SCC, used in precast applications, also typically has a low w/c ratio. Since SCC has a higher paste volume (or higher sand to aggregate ratio) to achieve high workability and high early strength, several researchers have claimed larger shrinkage of the SCC for precast concrete, resulting in larger prestress losses (Issa et al., 2005; Naito et al., 2006; Suksawang et al., 2006; Schindler et al., 2007), although mechanical properties of the SCC are superior to those of the conventional concrete (Issa et al., 2005). Naito et al. (2006) also found that the SCC exhibits higher shrinkage than the conventional concrete, which is due to the higher fine aggregate volume in the SCC. Aslani and Nejadi (2011b; 2011c) observed the following conclusions by considering experimental results of drying shrinkage in the database: (1) increase in the w/b ratio causes increase in the drying shrinkage (2) the proper use of mineral admixture in SCC can reduce drying shrinkage remarkably (3) increase in the volume of coarse aggregate can reduce drying shrinkage significantly. Additionally, the change in the sand volume ratio has little effect on the drying shrinkage of the medium strength SCC (Aslani and Nejadi, 2011b; 2011c).

The present section contains the findings based on the average drying shrinkage measurements of three replicate specimens, incorporating control binders as well as glass powders of varying finenesses, contents and quality. The test procedures, curing conditions and preparation of concrete specimens prior to testing have already been explained in Chapter 3. Complete data are shown in Appendix E. Figure 6.32 demonstrates the average drying shrinkage measurements of CTR specimens at the curing ages of 7, 14, 28, 56, 90 and 180 days. It is evident from the results that drying shrinkage of SCC containing GP was dependent on the time period for which it was kept in the shrinkage chamber under controlled temperature and humidity. In general, there was an increase in the shrinkage strain measurement of GP throughout the curing duration but the rate of increase declined significantly with time. GP concrete mix mostly demonstrated higher shrinkage measurements compared to the other CTR mixes at a given curing age, showing a significant increase of 62% between 14-days and 28-days, followed by a nominal increase of approximately 6% from 90-days to 180-days.

It has been established that FA has the effect of reducing drying shrinkage, with the finer fractions producing the least amount of length change. However, Dyer (2014) has clearly mentioned that there must be other mechanisms effective also because even the coarsest FA, which is coarser than the GP and requires a higher w/c ratio, produces lower drying shrinkage than the control GP mix (Dyer, 2014). The reduction in drying shrinkage with the use of FA in concrete can, therefore, be explained by the dilution effect of FA. Similar results were evident in this study since both FAs used in this investigation were coarser than GP and still showed lower drying shrinkage measurements. More specifically, drying shrinkage measurements recorded for FAF30% were found to be lower compared to FAC30%. This might be due to the fact that class F fly ash is a superior material in terms of overall densification with slower and more complete pozzolanic reactions, which convert more $Ca(OH)_2$ to CSH and reduce lesser internal voids left after the initial cement hydration reactions. In contrast, class C fly ash might be competing for space to deposit its reaction products in the initial first few weeks and then, rapidly reduced in terms of reactivity leaving capillary voids. Moreover, class F and C fly ashes, added at the replacement level of 30%, mostly demonstrated lower shrinkage strain measurements than GP and LP30%. Xie et al. (2002) consistently reported that FA in SCC helps to reduce early-age cracking in SCC and low drying shrinkage is achieved by incorporating 30%-40% FA. Additionally, Cengiz Duran Atis (2003) studied concrete mixes produced with different percentage of replacements of GP with FA and reported a reduction in the drying shrinkage values. These results are also in agreement with the findings presented by Ghosh and Timusk (1981), Teorenau and Nicolescu (1982), Cripwell et al. (1984), Nelson et al. (1992), Chindaprasirt et al. (2004), Bouzoubaa et al. (2001), Khatib (2008) and Nayak et al. (2015).

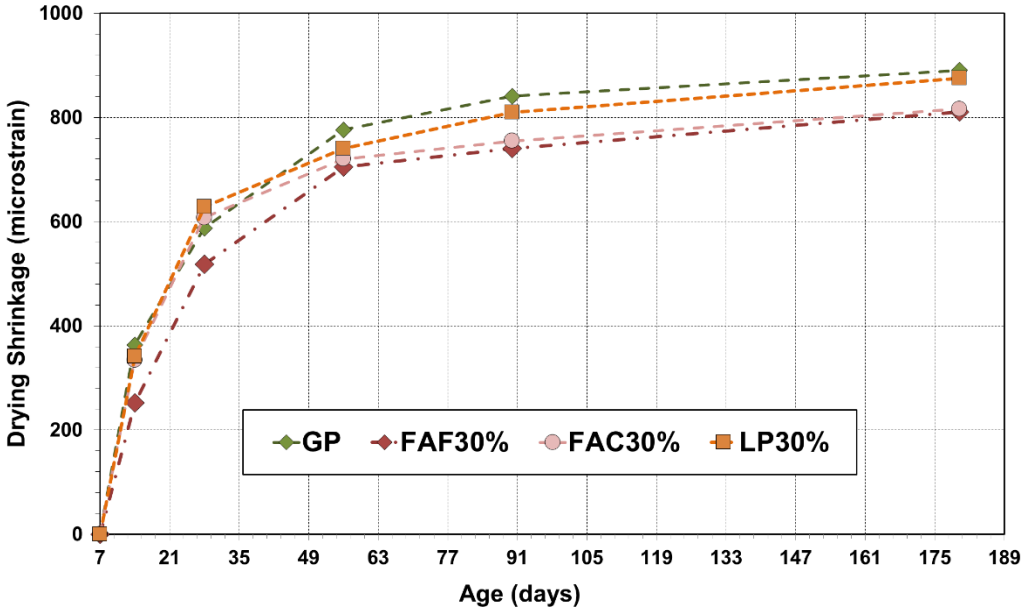

Figure 6.32: Drying shrinkage of CTR mixes with curing age up to 180-days

Incorporating LP in SCC also resulted in the reduction of drying shrinkage in comparison to GP mix, possibly due to a more efficient particle packing, which contributed to the reduction in shrinkage strain. Identical findings have been reported by Bui and Montgomery (1999a), Chopin et al. (2003) and Felekoglu (2008) that the application of LP in SCC has been found to reduce drying shrinkage. The increased drying shrinkage in LP30% compared to FA incorporated mixes can be related to lower elastic modulus observed in LP30% than those observed in FA mixes. However, the long-term drying shrinkage of FA and LP modified concretes could meet the criteria of allowable shrinkage limits outlined in AS 3600.

(a) Effects of glass fineness on drying shrinkage

Generally, the drying shrinkage of a cementitious system at a constant w/c ratio appears to be affected by the degree of hydration depending on material reactivity. The reactivity is determined by cementitious material particle size distribution and chemical composition, such as alkali content and crystalline compounds content. Ca/Si ratio of the cementitious material is another important influence factor that changes the volume of gel pores in CSH system and hence drying shrinkage in a blended mixture. Figure 6.33 demonstrates the drying shrinkage measurements of GL-FN class of specimens and some of the CTR mixes up to 180-days. The measurements of coarser to finer range of glass powders were recorded to highlight the changes in the drying shrinkage with variations in particle sizes. The drying shrinkage of glass mixes decreased as the glass particle size became finer, which can be related to the denser microstructure of concrete due to the presence of finer glass, which suppressed drying shrinkage (Concrete Society & BRE, 2005) and hence, lower

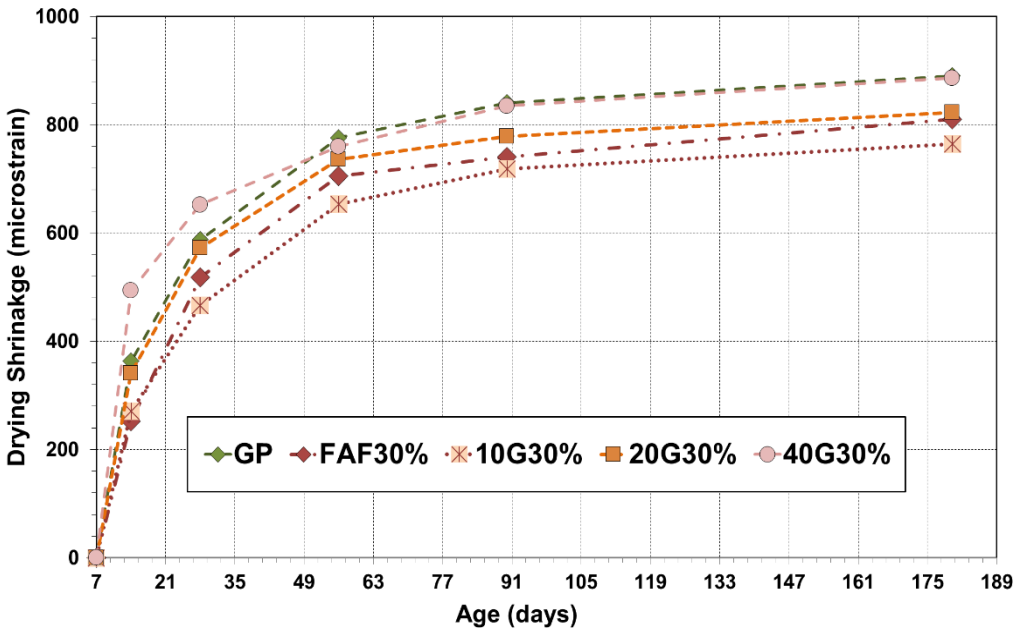

Figure 6.33: Comparison between drying shrinkage measurements of GL-FN, GP and FAF30% up to 180-days

shrinkage strain was observed (Bouzoubaa and Lachemi, 2001; Sonebi and Bartos, 2000). Liu (2009) consistently mentioned that drying shrinkage of concrete with glass powder decreases with an increase in the fineness of the glass since the near-zero water absorption of glass leads to no shrinkage and improvement in the mix rheology. Similar observation was reported by Shi and Wu (2005). In comparison to the CTR mixes, the drying shrinkage values recorded for 10G30% were found to be the lowest. This can be attributed to lower water absorption by very fine glass powder (much less than by FA); therefore, this glass powder could provide more water for cement hydration and consequently, hydrated product in concrete was increased and the water in capillary pores was reduced, leading to reduced drying shrinkage. In another study by Wattanapornprom and Stitmannaithum (2015), it was similarly revealed that concrete with average particle size 12-15 µm glass powder had lower drying shrinkage at 75-days than concrete containing FA at the same replacement level and the similar w/b of 0.44. Conversely, overall results indicate that 20G30% demonstrated higher drying shrinkage strain measurements compared to FA incorporating mixes, possibly due to the variance in elastic modulus in these mixes. Few others studies (Shi et al., 2005; Shi and Wu, 2005) also revealed that drying shrinkage of concrete with glass powder is higher than FA when it shows lower water demand. However, 20G30% showed lower drying shrinkage than GP, which can be related to the denser microstructure of 20G30% compared to GP in combination with differences in cement hydration and the pozzolanic reaction of both mixes. 40G30% demonstrated higher drying shrinkage measurements than all other CTR and GL-FN mixes, potentially due to the variations in the amounts of angular-shaped glass particles and the number of pores within the microstructure of the specimens. However, it showed comparable drying shrinkage measurements to GP, which can be linked to their closer final porosity as discussed in Section 6.3.

(b) Effects of glass content on drying shrinkage

Figure 6.34 illustrates the drying shrinkage measurements of GL-FN class of specimens and some of the CTR mixes up to 180-days. The drying shrinkage of the mixture with 20% of glass content was lower than in the case of 30% and 40% glass content. As the binder composition changed with glass content, it affected the paste shrinkage levels due to the differences in the hydration product and pozzolanic reaction and hence, water escaped more slowly within the matrix of 20G20%. Mix that contained 40% glass in the binder had the highest shrinkage deformation. This probably arose because total water was not utilized in the hydration of cement (20% less cement compared to 20G20%). This could also be due to the fact that drying shrinkage is also related to the elastic modulus of concrete and 20G40% had the lowest elastic modulus among GL-CN mixes. This also accords with the effect of alkali on cement, that is, shrinkage tends to increase with alkali contents, which was similarly

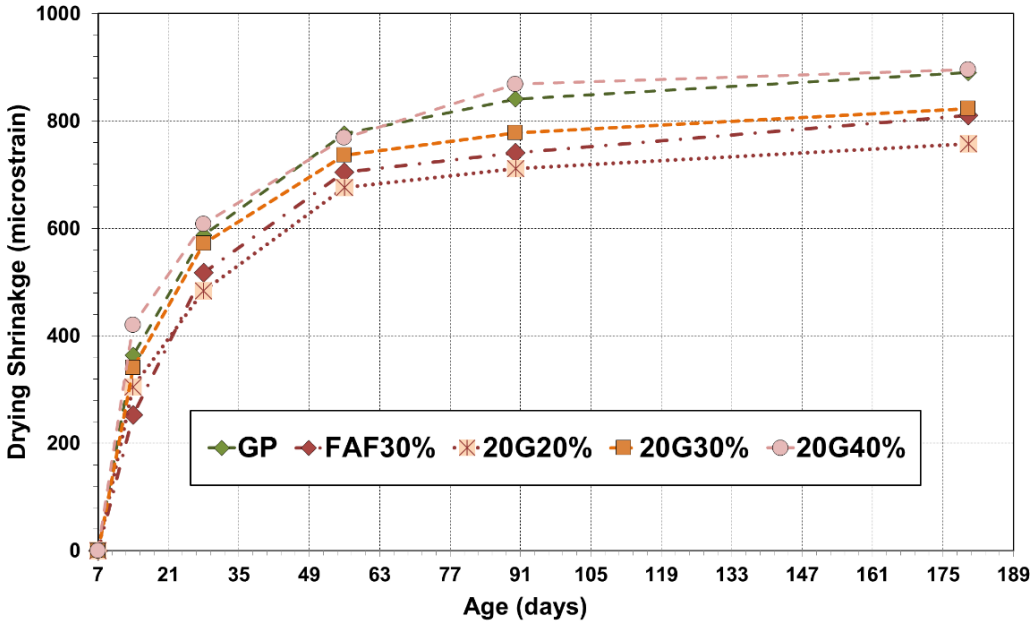

Figure 6.34: Comparison between drying shrinkage measurements of GL-CN, GP and FAF30% up to 180-days

concluded by Jawed and Skalny (1978). The findings of this study are consistent with Shayan and Xu (2006) and Patricija et al. (2014) who reported that drying shrinkage of concrete increases with increasing glass content. In addition, a good correlation was found between drying shrinkage and water absorption for concrete containing glass powder. The effects of glass powder on water absorption of concrete can be attributed to the factors already mentioned in the previous section. Reduction in water absorption of concrete with lower contents of the recycled glass, which means a relatively low water loss when concrete is exposed to drying, finally resulted in reduced drying shrinkage. Additionally, the increase in elastic modulus of concrete with lower replacement levels of recycled glass was also helpful to reduce their drying shrinkage. It can be also realized from the results that 20G30% and 20G30% showed lower drying shrinkage than the reference GP mixture (that was made without glass powder). Conversely, 20G40% demonstrated somewhat higher drying shrinkage values than GP but it should be noted that the difference between GP and the tested mixture 20G40% was not significant. Therefore, it can be concluded that glass increases drying shrinkage of concrete provided that it is replaced at more than 30% by cement. In addition, 20G20% demonstrated lower drying shrinkage than FA incorporating mixes, whereas the mixes containing higher replacement levels of glass powder showed opposite results due to the same reason mentioned before. Overall results indicate that all GL-CN mixes produced acceptable drying shrinkage values, as required by the Australian Standard AS 3600. Hence, being a hygrometrically stable material, the application of waste glass powder as cement substitute did not influence the drying shrinkage deformation of SCC negatively, during the period of 180-days.

(c) Effects of glass quality on drying shrinkage

The shrinkage strain measurements of unwashed glass powder (20UG30%) were also recorded in order to investigate the effects of the quality of glass material on drying shrinkage of SCC. The results of drying shrinkage measurements observed in 20UG30% up to 180-days have been illustrated in Figure 6.35. The drying shrinkage measurements observed in GP and 20G30% up to 180-days have also been included in the figure for comparison. It is clear from the results that 20UG30% mix demonstrated higher drying shrinkage measurements compared to all other glass mixes as well as CTR mixes. In particular, 20UG30% showed the highest drying shrinkage value of 507 microstrain at 14-days, which implies that the presence of irregular-shaped particles including organic content led to higher drying shrinkage in comparison to the washed glass as well as other CTR specimens. By the end of 180-days, the drying shrinkage value demonstrated by 20UG30% was found to be approximately 962 microstrain. The higher drying shrinkage recorded in 20UG30% compared to other mixes can also be related to its higher porosity measurements and lower elastic modulus. In addition, long-term drying shrinkage of unwashed glass incorporating concrete did not meet the criteria outlined in AS 3600 due to same reasons mentioned before.

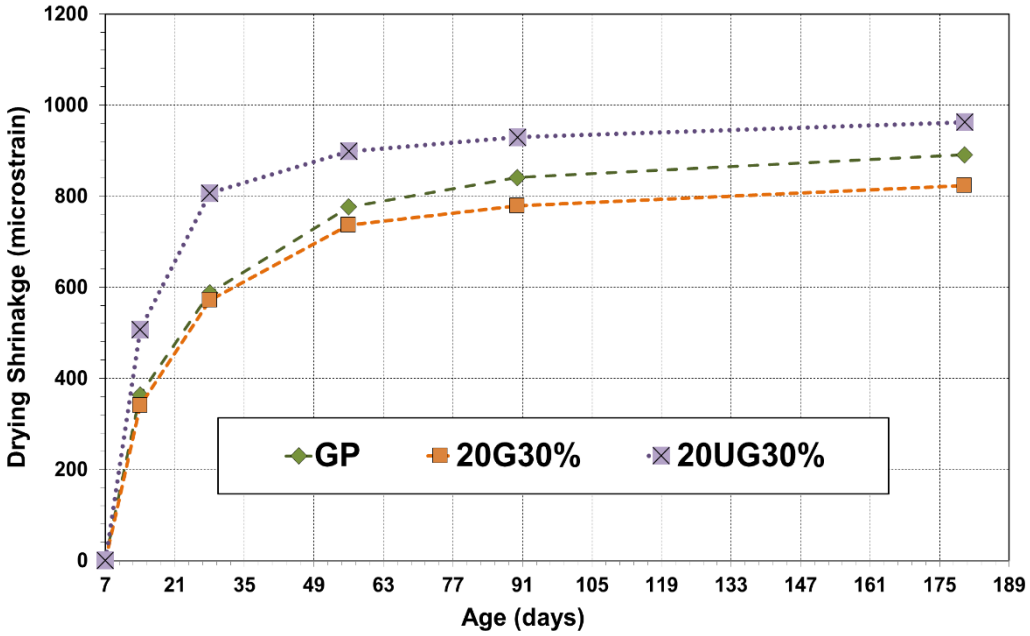

Figure 6.35: Drying shrinkage of 20UG30% with curing age up to 180-days

6.6 Conclusions

One of the measures of the success or failure in utilizing waste glass in concrete can be attributed to its observed durability. Results of the experiments on properties, including oxygen permeability, porosity, electrical resistivity, chloride diffusivity and drying shrinkage of

a range of glass modified SCC mixes have been presented in comparison with those of GP cement, fly ashes and limestone powder incorporated SCC mixes. The long-term data presented in this chapter show that there is great potential for the utilization of waste glass, in several fineness and content levels, as a cement replacement in SCC.

- The amount of incorporated waste glass largely influences durability properties of SCC. Porosity increases with an increase in glass powder contents above 20%, whereas the coefficient of permeability, electrical resistivity, and apparent chloride diffusion coefficients reduce. It is evident from the results that although ground glass enhances the durability properties of SCC, its improvement depends on the level of replacement. There is a relatively reduction on the improvement in the microstructure when a glass replacement level of more than 20% is used. However, mixtures with ground glass powder, even at higher replacement levels of 40%, seem to offer a better durability performance compared to GP cement, fly ashes and limestone powder. This implies that SCC with 20%-40% glass powder replacing the cement exhibits a high resistance to chloride ion penetration making such concrete ideal for marine structures.

- The filling effect of small-sized glass particles results in improved particle packing, forming a denser and hence, the less permeable microstructure of SCC. The pozzolanic reaction between the glass and calcium hydroxide leads to further refinement of the pore structure, which enhances durability characteristics, such as oxygen permeability, porosity, and chloride permeability. Compared with the other binders, glass powder of fineness 10 µm and 20 µm added at 30% replacement level provide greater durability than GP cement, fly ashes and limestone powder. Additionally, 40 µm glass powder, added in the similar proportion, also fulfills the criteria of achieving good durability.

- Replacement of GP cement with unwashed glass results in SCC with inadequate durability properties. The contaminants present in unwashed waste glass increases the porosity and reduces the oxygen and chloride ion penetration resistances of SCC compared to washed glass powder, GP cement, fly ashes and limestone powder.

- The correlation between the various durability tests was investigated in this study. Porosity, for instance, was found to provide a reasonable indication of the likely oxygen permeability for a particular binder type. The correlation, however, was not generally as strong when multiple types of binders were included. GP cement and glass powder

could have virtually identical resistivity values but very different diffusion coefficients even though individually there was a reasonable correlation between resistivity and chloride diffusion for GP cement and glass powder separately.

- The resistance of the concrete depends largely on the porosity and interconnectivity of the pore system in the concrete. The chloride resistance of concrete thus depends on the mix constituents, mix proportions, the degree of compaction and curing given to the fresh and hardened concrete. It should be noted that chloride binding capacity of the binder was not explicitly studied in this investigation.

- The drying shrinkage values of all washed glass incorporating mixes, irrespective of their fineness and content, were below 0.075% after 56-days drying and met the requirements of the Australian Standard AS 3600. Conversely, unwashed glass mix does not meet this above mentioned criterion, possibly due to the presence of impurities in the mix.

References

Abo-El-Enein, S. A., Abou-Gamra, Z. M., El-Hosiny, F. I., and El-Gamal, S. M. A. (1996). "Characteristics of $Ca(OH)_2^-$ silica fume mixtures." *Journal of Thermal Analysis,* 46, 275.

AL-Amoudi, O.S.B., Abduljauwad, S. N., Maslehuddin, M., Rasheeduzzafar. (1994). "Influence of chloride ions on sulphate deterioration in plain and blended cements.' *Magazine of Concrete Research,* 167, 113-123.

Alexander, M. G. (1997). "An indexing approach to achieving durability in concrete structures." *FIP '97 Symposium: The Concrete Way to Development,* Concrete Society of Southern Africa, Johannesburg, 571-576.

Alexander, M. G., Beushausen, H. (2009). "Performance-based durability testing, design and specification in South Africa: latest developments." *Excellence in Concrete Construction through Innovation,* (Eds. Limbachiya and Kew), Taylor & Francis Group, London, 429-434.

Alexander, M. G., Mackechnie, J. R., and Ballim, Y. (2001). "Use of durability indexes to achieve durable cover concrete in reinforced concrete structures." Chapter, Materials Science of Concrete, Vol. VI, (Ed. J. P. Skalny and S. Mindess), American Ceramic Society, Westerville, 2001, 483-511.

Alexander, M. G., Mackechnie, J.R., Ballim, Y. (1999a). Guide to the use of durability indexes for achieving durability in concrete structures, Research Monograph No. 2: Department of Civil Engineering University of Cape Town and University of the Witwatersrand.

AS 3600-2009. (2009). *Concrete Structures.* Standards Australia, Sydney, Australia.

Aslani, F., and Nejadi, S. (2011a). "Comparison of the analytical models to determine modulus of rupture of self-compacting concrete and conventional concrete." *From materials to structures: Advancement through Innovation,* Taylor and Francis Group, London, 1105-1112.

Aslani, F., and Nejadi, S. (2012). "Mechanical properties of conventional and self-compacting concrete: an analytical study." *Construction and Building Materials, Elsevier,* 36, 330-347.

Aslani, F., Nejadi, S. (2011c). "Evaluation and comparison of the analytical models to predict creep and shrinkage behaviour of self-compacting concrete." *Proc. Structural Engineers World Congress (SEWC),* Technical Committee, Italy, 1-10.

Aslani, F., Nejadi, S., (2011b). “Comparison of shrinkage prediction models for self-compacting and conventional concrete.” *Proc. 9th International Symposium on High Performance Concrete,* (Ed. Khrapko, M. and Wallevik, O.), New Zealand Concrete Society, New Zealand, 1-10.

Assie, S., Escadeillas, G., and Waller, V. (2007). “Estimates of self-compacting concrete ‘potential’ durability.” *Construction and Building Materials, Elsevier,* 21(10), 1909-1917.

Bai, J., Wild, S., and Sabir, B. B. (2003). “Chloride ingress and strength loss in concrete with different PC–PFA–MK binder compositions exposed to synthetic seawater.” *Cement and Concrete Research, Elsevier,* 33(3), 353-362.

Ballim, Y. (1991). “A low cost falling head permeameter for measuring concrete gas permeability.” *Concrete Beton,* 61, 13-18.

Bertolini, L., and Polder, R., (1997). *Concrete resistivity and reinforcement corrosion rate as a function of temperature and humidity of the environment.* Netherlands Organization for Applied Scientific Research, TNO Building and Construction Research, 97-BT-R0574.

Beushausen, H., and Alexander, M. G. (2008). “The South African Durability Index tests in an international comparison.” *Journal of the South African Institute of Civil Engineering,* 50(1), 25-31.

Beushausen, H., and Luco, L. F. (Eds.). (2016). *Performance-Based Specifications and Control of Concrete Durability - State-of-the-Art Reports,* 1st Ed., Springer Netherlands, 18, 373 pages.

Bhuiyan, S. (2012). “Permeability of Concrete Incorporating Limestone Filler and Pulverised Fuel Ash.” *Proc., Eighteenth Postgraduate Student Conference on MSc Dissertations 2011-12,* Department of Civil & Structural Engineering, University of Sheffield.

Bondar, D., Lynsdale, C. J., Milestone, N. B., and Hassani, N. (2012). “Oxygen and Chloride Permeability of Alkali-Activated Natural Pozzolan Concrete.” *ACI Materials Journal,* 109(1), 53-62.

Bouzoubaa, N., and Lachemi, M. (2001). “Self-compacting concrete incorporating high volumes of class F fly ash Preliminary results.” *Cement and Concrete Research, Elsevier,* 31, 413-420.

Bui, V. K., Montgomery, D. (1999a). “Drying shrinkage of self-compacting concrete containing milled limestone.” *Proc., 1st RILEM International Symposium on Self-*

compacting Concrete, (Ed. Skarendahl, A., and Petersson, O.), RILEM Publications S.A.R.L., France.

Butefuhr, M., Fischer, C., Gehlen, C., Menzel, K., and Nurnberger, U. (2006). “On-site investigations on concrete resistivity – a parameter of durability calculation of reinforced concrete structures.” *Materials and Corrosion,* 57(12), 932-939.

Cabrera, J. G., Cusens, A. R., and Lynsdale, C. J. (1989). *Porosity and Permeability as Indicators of Concrete Performance*, IABSE Report, 57(1), 249-254.

Camões, A., Ferreira, R. M., Aguiar, J. L. B., and Jalali, S. (2002). “Durability of high performance concrete with fly ash.” *Proc., International Conference Challenges of Concrete Construction on Concrete for Extreme Conditions,* Dundee, Scotland, United Kingdom, 357-366.

Castellote, M., Andrade, C., and Alonso, M. C. (2002). “Standardization, to a reference of 25°C, of electrical resistivity for mortars and concretes on saturated or isolated conditions.” ACI Materials Journal, 99(2), 119-127.

Cement Concrete and Aggregates Australia. (2009). *Chloride Resistance of Concrete,* Australia.

Cengiz Duran Atis. (2003). “High-volume fly ash concrete with high strength and low drying shrinkage.” *Journal of Materials in Civil Engineering,* 15(2), 153-156.

Chaid, R., Kenai, K., Zeroub, H., and Jauberthie, R. (2015). “Microstructure and permeability of concrete with glass powder addition conserved in the sulphatic environment.” *European Journal of Environmental and Civil Engineering*, 19(2), 219-237.

Chen, Y., and Odler, I. (1992). “On the origin of Portland cement setting.” *Cement and Concrete Research, Elsevier,* 22(6), 1130-1140.

Chindaprasirt, P., Homwuttiwong, S., and Sirivivatnanon, V. (2004). “Influence of fly ash fineness on strength, drying shrinkage and sulphate resistance of blended cement mortar.” *Cement and Concrete Research, Elsevier,* 34, 1087-1092.

Chisholm, D. H. (1997). “Factors influencing reinforced concrete durability design in New Zealand’s marine environment.” *Proc., Fourth CANMET/ACI International Conference,* Sydney, Australia, SP 170, 797-822.

Clear, K. C. (1976). *Time-to-corrosion of reinforcing steel in concrete slabs*. Federal Highway Administration, Washington, United States, FHWA-RD-76-70.

Clear, K. C., and Hay, R. E. (1973). *Time-to-corrosion of reinforcing steel in concrete slab, V.1: Effect of mix design and construction parameters*. Report No. FHWA-RD-73-32, Federal Highway Administration, Washington, United States, 103 pages.

Costa, U., Fucoetti, M., and Massazza, F. (1992). "Permeability and Diffusion of Gasses in Concrete." *Proc., 9th International Congress of Chemistry of Cement*, NCB, New Delhi, India, 5, 107-114.

Courad, L., and Michel, F. (2014). "Limestone fillers cement based composites: Effects of blast furnace slags on fresh ad hardened properties." *Construction and Building Materials, Elsevier,* 51, 439-445.

Cripwell, J. B., Brooks, J. J., and Wainwright, P. J. (1984). "Time dependent properties of concrete containing pulverised fuel ash and a superplasticizer." *Proc., 2nd International Conference on Ash Technology and Marketing,* Barbican Centre, London, Central Electricity Generating Board, London, UK, 313-320.

Dhanalaxmi, C., and Nirmalkumar, K. (2015). "Study on durability properties of limestone powder concrete incorporated with steel fibers." *International Journal of Advanced Technology in Engineering and Science.* 3(5), 92-101.

Dhir, R. K., Limbachiya, M. C., McCarthy, M. J., and Chaipanich, A. (2007). "Evaluation of Portland limestone cements for use in concrete construction," *Materials and Structures*, 40, 459-473.

Dhiyaneshwaran, S., Ramanathan, P., Baskar, I., and Venkatasubramani, R. (2013). "Study on durability characteristics of self-compacting concrete with fly ash." *Jordan Journal of Civil Engineering,* 7(3), 342-353.

Diamond, S. (2000). "Mercury porosimetry – an inappropriate method for the measurement of pore size distributions in cement-based materials." *Cement and Concrete Research, Elsevier,* 30(10), 1517-1525.

Du Preez, A. A. and Alexander, M. G. (2004). "A site based study of durability indexes for concrete in marine conditions'." *Materials and Structures.* 37(267), 146-154.

Du, H., and Tan, K. H. (2014). "Waste Glass Powder as Cement Replacement in Concrete." *Journal of Advanced Concrete Technology,* 12, 468-477.

Elkey, W., and Sellevold, E. J. (1995). "Electrical Resistivity of concrete." Norwegian Public Roads Administration Publication.

Felekoglu, B. (2008). “A comparative study on the performance of sands rich and poor in fines in self-compacting concrete.” *Construction and Building Materials*, *Elsevier,* 22(4), 646-654.

Ferraris, C. F., Obla, K. H., and Hill, R. (2001). “The influence of mineral admixtures on the rheology of cement paste and concrete.” *Cement and Concrete Research, Elsevier,* 31, 245-255.

Gao, X., Ma, B., Yang, Y., and Su, A. (2008). “Sulphate attack of cement-based material with limestone filler exposed to different environments.” *Journal of Material Engineering and Performance, Springer,* 17(4), 543-549.

Ghosh, R. S. and Timusk, J. (1981). “Creep of fly ash concrete.” *ACI Materials Journal,* 78(5), 351-357.

Gouws, S. M., Alexander, M. G., and Martiz, G. (2001). “Use of durability index tests for the assessment and control of concrete quality on site.” *Concrete Beton,* 98, 5-16.

Gruber, K. A., Ramlochan, T., Boddy, A., Hooton, R. D., and Thomas, M. D. A. (2001). “Increasing concrete durability with high-reactivity metakaolin.” *Cement and Concrete Composites, Elsevier,* 23(6), 479-484.

Hooton, D., Ramezanianpour, A., and Schutz, U. (2010). “Decreasing the Clinker Component in Cementing Materials: Performance of Portland-Limestone Cements in Concrete in Combination with SCMs,” *Proc., 2010 Concrete Sustainability Conference,* National Ready Mixed Concrete Association, Tempe, Arizona.

Hoshino, M. (1988). “Difference of the w/c ratio, porosity and microscopical aspect between the upper boundary paste and the lower boundary paste of the aggregate in concrete.” *Material and Structures,* 21(125), 336-340.

Issa,, M., Alhassan, M., Shabila, H., and Krozel, J. (2005). “Laboratory Performance Evaluation of Self-Consolidating Concrete.” *Proc., Second North American Conference on the Design and Use of Self-Consolidating Concrete and the Fourth International RILEM Symposium on Self-Consolidating Concrete,* Center for Advanced Cement-Based Materials (ACBM), Chicago, 857-862.

Kanellopoulos, A., Petrou, M. F., and Ioannou, I. (2012). “Durability performance of self-compacting concrete.” *Construction and Building Materials, Elsevier,* 37, 320-325.

Kara, P., Borosnyói, A., and Fenyvesi, O. (2014). “Performance of waste glass powder (WGP) supplementary cementitious material (SCM) – Drying shrinkage and early age shrinkage cracking.” *Journal of Silicate Based and Composite Materials*, 66(1), 18-22.

Keller, T. et al. (1992). “Dauerhaftigkeit Stahlbetontragwerken: Transportmechanismen-Auswirkungen von Rissen.” ETH Zürich Nr. 9605, Zürich.

Khatib, J. M. (2008). “Performance of self-compacting concrete containing fly ash.” *Construction and Building Materials, Elsevier,* 22(9), 1963-1971.

Langford, P., and Broomfield, J. (1987). “Monitoring the corrosion of reinforcing steel.” *Construction Repair,* 32-36.

Lee, S. T., Hooton, R. D., Jung, H. S., Park, D. H., and Choi, C. S. (2008). “Effect of limestone filler on the deterioration of mortars and pastes exposed to sulphate solutions at ambient temperature.” *Cement and Concrete Research, Elsevier,* 38(1), 68-76.

Ling, T. C., Poon, C. S., and Kou, S. C. (2012). “Influence of recycled glass content and curing conditions on the properties of self-compacting concrete after exposure to elevated temperatures.” *Cement and Concrete Composites, Elsevier,* 34(2), 265-272.

Liu, Y., (1996). “Modeling the Time-to-Corrosion Cracking of the Cover Concrete in Chloride Contaminated Reinforced Concrete Structures,” PhD thesis, Virginia Polytechnic Institute and State University, Vicksburg, VA.

Lübeck, A., Gastaldini, A.L., Barin, D.S. and Siqueira, H.C. (2012), “Compressive strength and electrical properties of concrete with white Portland cement and blast-furnace slag”, Cement Concrete Comp., 34(3), 392-399.

Mackechnie, J. R., Alexander, M. G. (2002). “Durability Predictions Using Early-Age Durability Index Testing.” *Proc., 9th International Conference on Durability of Building Materials and Components, Paper 241,* 9 pages.

Manmohan, D. and Mehta, P. K. (1981). “Influence of pozzolanic, slag and chemical admixtures on pore size distribution and permeability of hardened cement paste.” *Cement and Concrete Aggregates,* 3(1), 63-67.

Marsh, B. K., Day, R. L., and Bonner, D. G. (1985). “Pore structure characteristics affecting the permeability of cement paste containing fly ash.” *Cement and Concrete Research, Elsevier,* 15(6), 1027-1038.

Matos, A. M., Ramos, T., Nunesb, S., and Sousa-Coutinhoa, J. (2016). “Durability enhancement of SCC with waste glass powder.” *Materials Research,* 19(1), 67-74.

McCarter, W. J., (2006). “Monitoring the influence of water and ionic ingress on cover-zone concrete subjected to repeated absorption.” *Cement and Concrete Research, Elsevier,* 18(1), 55-63.

McCarter, W. J., Starrs, G., and Chrisp. T. M. (2000). “Electrical conductivity, diffusion, and permeability of Portland cement-based mortars.” *Cement and Concrete Research, Elsevier,* 30(9), 1395-1400.

Mehta, P. K. and Monteiro, P. J. M. (2006). *Concrete: Microstructure, Properties and Materials*, 3rd Ed., McGraw-Hill, New York.

Meira, G. R., Andrade, C., Vilar, E. O. and Nery, K. D. (2014). “Analysis of chloride threshold from laboratory and filed experiments in marine atmosphere zone.” *Construction and Building Materials, Elsevier,* 55, 289-298.

Moir, G. K., and Kelham, S., (1993). “Durability 1,” Performance of Limestone-Filled Cements: Report of Joint BRE/BCA/Cement Industry Working Party, 28 November 1989, Building Research Establishment, Garston, Watford, England.

Moon, H. Y., Jung, H. S., and Kim, J. P. (2004). “Diffusion of chloride ions in limestone powder.” *Journal of the Korean Concrete Institute,* 16(6), 859-865.

Naito, C. J., Parent, G., and Brunn, G. (2006). “Performance of bulb-tee girders made with self-consolidating concrete.” *PCI Journal,* 51(6), 72-85.

Nassar, R. D., and Parviz, S. (2012). “Strength and durability of recycled aggregate concrete containing milled glass as partial replacement for cement.” *Construction and Building Materials, Elsevier, 29*, 368-377.

Nath, P., and Sarker, P. (2011). “Effect of Fly Ash on the Durability Properties of High Strength Concrete.” *Proc., Engineering The Twelfth East Asia-Pacific Conference on Structural Engineering and Construction 14,* 1149-1156.

Nayak, G., Shetty, K. K., Kumara, K., Jnaneshwar, S. S., Karkera, D. and Khandagale, V. (2015). “Shrinkage properties of self-compacting concrete with high volumes of class F fly ash.” *Proc., International Journal of Earth Sciences and Engineering,* 8(2), 173-177.

Nelson, P, V., Srivivatnanon, V., and Khatri, R. (1992). “Development of high volume fly ash concrete for pavements.” *Proc., 16th ARRB Conference,* Perth, Australia, 37-47.

Neville, A. M. (1995). *Properties of concrete.* 4th Ed. Longman Group Limited, Harlow Essex, England.

NT Built 492. (1999). *Concrete, Mortar and Cement based Repair Materials: Chloride Migration Coefficients from Non-steady state migration experiments*, Nordtest Method.

Omar, S., Al-Amoudi, B., Al-Kutti, W., Ahmad, S., and Maslehuddin, M. (2009). "Correlation between compressive strength and certain durability indices of plain and blended cement concretes." *Cement and Concrete Composites, Elsevier,* 31(9), 672-676.

Pacheco-Torgal, F., Jalali, S., Labrincha, J., and John, V. M. (2013). *Eco-efficient Concrete.* 1st Ed., Woodhead Publishing.

Pipilikaki, P., Katsioti, M., and Gallias, J. L. (2009). "Performance of limestone cement mortars in a high sulphates environment." *Construction and Building Materials, Elsevier,* 23(2), 1042-1049.

Polder, R. B. (2001). "Test methods for onsite measurement of resistivity of concrete — a RILEM TC-154 technical recommendation." *Construction and Building Materials, Elsevier,* 15(2–3), 125-131.

Polder, R. B., Peelen, W. H. A., (2002). "Characterisation of chloride transport and reinforcement corrosion in concrete under cyclic wetting and drying by electrical resistivity." *Cement & Concrete Composites, Elsevier,* (24), 427-435.

Portland Cement Association. (2002). "Types and Causes of Concrete Deterioration." *Concrete Information,* <http://www.cement.org/docs/default-source/th-paving-pdfs/concrete/types-and-causes-of-concrete-deterioration-is536.pdf?sfvrsn=4> (June 5, 2016).

Presuel-Moreno, Francisco; Liu, Yanbo; Wu, Yu-You; Arias, Wendy. (2013). Analysis and Estimation of Service Life of Corrosion Prevention Materials Using Diffusion, Resistivity and Accelerated Curing for New Bridge Structures - Volume 2: Accelerated Curing of Concrete With High Volume Pozzolans (Resistivity, Diffusivity and Compressive Strength) Florida Atlantic University, Dania Beach Florida Department of Transportation, Tallahassee, FL.

Ramezanianpour, A. A. (2014). *Cement Replacement Materials – Properties, Durability, Sustainability*. Concrete Technology Centre, Amirkabir University of Technology, Iran.

Ramezanianpour, A. A., Ghiasvand, E., Nickseresht, I., Mahdikhani, M., and Moodi, F. (2009). "Influence of various amounts of limestone powder on performance of Portland limestone cement concretes." *Cement & Concrete Composites, Elsevier,* 31, 715-720.

Rosskopf, P. A., and Vimelson, R. C. (1985). *Laboratory Tests for Corrosion of Steel in Concrete.* Laboratory Corrosion Tests and Standards, ASTM STP 866, ASTM International, West Conshohocken, PA, 275-284.

Salem T. M., and Ragai S. M. (2001). "Electrical conductivity of granulated slag-cement kiln dust-silica fume pastes at different porosities." *Cement and Concrete Research, Elsevier,* 31, 781-787.

Schutter, G. D. (2011). "Effect of limestone filler as mineral addition in self-compacting concrete." *Proc., 36th Conference on Our World in Concrete & Structures,* Singapore, 7 pages.

Schwarz, N., Cam, H., and Neithalath, N. (2008). "Influence of a fine glass powder on the durability characteristics of concrete and its comparison to fly ash." *Cement and Concrete Composites, Elsevier,* 30, 486-496.

Sellevold, E. J.; Bager, D. H.; Klitgaard-Jensen, E.; and Knudsen, T. (1982). "Silica Fume-Cement Pastes: Hydration and Pore Structure." *Condensed Silica Fume in Concrete, Institutt for Bygningsmateriallære, Norges Tekniske Høgskole,* Universitetet i Trondheim, Trondheim, Norway, BML 82.610, 19-50.

Shayan, A., and Xu, A. (2004). "Value-added utilisation of waste glass in concrete." *Cement and Concrete Research, Elsevier,* 34, 81-89.

Shayan, A., and Xu, A. (2006). "Performance of glass powder as a pozzolanic material in concrete: A field trial on concrete slabs." *Cement and Concrete Research, Elsevier,* 36(3), 457-468.

Shi, C., Krivenko, P. V., and Roy, D. (2005). *Alkali-Activated Cement and Concretes.* Taylor and Francis, London and New York, 392 pages.

Siddiqui, R. and Khan, M. I. (2011). *Supplementary Cementing Materials.* Springer.

Silva, P., and Brito, J. D. (2013). "Electrical resistivity and capillarity of self-compacting concrete with incorporation of fly ash and limestone filler." *Advances in Concrete Construction,* 1(1), 65-84.

Spitek, R. K. (2014). *Influence of limestone powder content and size on transport properties of self-consolidating concrete.* UNLV Theses/Dissertations/Professional Papers/Capstones. Paper 2149.

Stanish, K., and Thomas, M. (2003). “The use of bulk diffusion tests to establish time-dependent concrete chloride diffusion coefficients.” *Cement and Concrete Research, Elsevier,* 33, 55-62.

Streicher, P. E., and Alexander, M. G. (1995). “A chloride conduction test for concrete.” *Cement and Concrete Research, Elsevier,* 25(6), 1284-1294.

Streicher, P. E., and Alexander, M. G. (1999). “Towards standardization of a rapid chloride conduction test for concrete.” *Cement, Concrete and Aggregates,* 21(1), 23-30.

Tennis, P. D., Thomas, M. D. A., and Weiss, W. J. (2011). *State-of-the-Art Report on Use of Limestone in Cements at Levels of up to 15%.* Portland Cement Association.

Teorenau, I., and Nicolescu, L. D. (1982). “The properties of power station fly-ash concrete.” *Proc., International Symposium on the Use of PFA in Concrete,* Leeds, England, Central Electricity Generating Board, London, UK, 231-241.

Thomas, M. D. A., and Matthews, J. D. (1992). *The permeability of fly ash concrete.* Building Research Establishment, Garston, Watford, Herts WD2 7JR, UK Materials and Structures, 25, 388-396.

Thomas, M. D. A., Matthews, J. D., and Haynes, C. A., (1989). “The effect of curing on the strength and permeability of PFA concrete.” *American Concrete Institute SP-114,* (Ed. Malhotra, V. M. (ACI, Detroit, 1989), 191-217.

Thomas, M. D., and Hooton, R. D. (2010). “The durability of concrete produced with Portland-limestone cement: Canadian Studies.” *SN 3142, Portland Cement Association,* Skokie, Illinois, USA.

Topcu, I. B., Tayfun, U., and Hocaoğlu, I. (2016). “Electrical resistivity of fly ash blended cement paste at hardening stage.” *Materials Science,* 22(3), 458-462.

Torrent, R. J., Jornet, A. (1991). “The quality of the covercrete of low-, medium- and high-strength concretes.” *Proc., Second CANMET/ACI International Conference Durability of Concrete,* Canada.

Tosun, K., Felekoglu, B., Baradan, B., and Altun, I. A. (2009). “Effects of limestone replacement ratio on the sulphate resistance of Portland limestone cement mortars exposed to extraordinary high sulphate concentrations.” *Construction and Building Materials, Elsevier,* 23(7), 2534-2544.

Tsivilis, S., Chaniotakis, E., Kakli, G., and Batis, G. (2002). “An analysis of the properties of Portland limestone cements and concrete.” *Cement and Concrete Composites, Elsevier,* 24, 371-378.

Vaitkevicius, V., Šerelis, E., and Hilbig, H. (2014). “The effect of glass powder on the microstructure of ultra high performance concrete.” *Construction and Building Materials, Elsevier,* 68, 102-109.

Wattanapornprom, R., and Stitmannaithum, B. (2015). “Comparison of properties of fresh and hardened concrete containing finely ground glass powder, Fly Ash, or Silica Fume.” *Engineering Journal,* 19(3), 14 pages.

White, H. J. (1953). “Electrical Resistivity of Fly Ash.” *Air Repair,* 3(2), 79-86.

Xie, Y., Liu, B., Yin, J., and Zhou, S. (2002). “Optimum mix parameters of high-strength self-compacting concrete with ultra-pulverized fly ash.” *Cement and Concrete Research, Elsevier,* 32(3), 477-480.

Ye, G., and Breugel, K. (2009). *Simulation of Connectivity of Capillary Porosity in Hardening Cement-Based Systems Made of Blended Materials,* Delft University of Technology, 178-182.

Zhao, H., Xiao, Q., Huang, D., and Shiping Zhang, S. (2014). “Influence of Pore Structure on Compressive Strength of Cement Mortar.” *The Scientific World Journal,* 2014, 12 pages.

Zhu, W., and Bartos, P. J. M. (2003). “Permeation properties of self-compacting concrete.” *Cement and Concrete Research, Elsevier,* 33(6), 921-926.

CHAPTER 7

INFLUENCE OF ACCELERATED CURING ON LONG-TERM MECHANICAL PROPERTIES AND DURABILITY OF SELF-COMPACTING CONCRETE INCORPORATING GLASS POWDER

Scott, A., Mackechnie, J., Matthews, J., Bull, D., Cook, D., and Ali, S. (2014). "Preliminary assessment of the influence of accelerated curing on concrete quality." *Proc., The New Zealand Concrete Industry Conference,* Taupo, New Zealand, 111-120.

ACRONYMS USED

GP	GP cement control concrete cured under standard conditions
GPE-W	GP cement control concrete kept at elevated temperature (50^{o}C) for 18 hours and subsequently water-cured until testing
GPE-D	GP cement control concrete kept at elevated temperature (50^{o}C) for 18 hours and subsequently dry-cured until testing
FA	Concrete containing 30% class F Fly Ash and cured under standard conditions
FAE-W	Concrete containing 30% class F Fly Ash, kept at elevated temperature (50^{o}C) for 18 hours and subsequently water-cured until testing
FAE-D	Concrete containing 30% class F Fly Ash, kept at elevated temperature (50^{o}C) for 18 hours and subsequently dry-cured until testing
WG	Concrete containing 30% washed glass and cured under standard conditions
WGE-W	Concrete containing 30% washed glass, kept at elevated temperature (50^{o}C) for 18 hours and subsequently water-cured until testing
WGE-D	Concrete containing 30% washed glass, kept at elevated temperature (50^{o}C) for 18 hours and subsequently dry-cured until testing
UG	Concrete containing 30% unwashed glass and cured under standard conditions
UGE-W	Concrete containing 30% unwashed glass, kept at elevated temperature (50^{o}C) for 18 hours and subsequently water-cured until testing
UGE-D	Concrete containing 30% unwashed glass, kept at elevated temperature (50^{o}C) for 18 hours and subsequently dry-cured until testing

HIGHLIGHTS

- Analysis of the effects of accelerated curing on compressive strength and elastic modulus of SCC incorporating glass powder.
- Investigation on the influence of accelerated curing on oxygen permeability and porosity of glass powder modified SCC.
- Study of the effects of accelerated curing on electrical resistivity and chloride diffusion coefficient of SCC containing glass powder.
- Evaluation of the performance of SCC cured at an elevated temperature, incorporating washed and unwashed glass powder, compared to the behaviour exhibited by elevated cured SCC containing GP cement and class F fly ash.

7.1 Introduction

Curing of concrete involves maintenance of appropriate moisture and temperature conditions in a freshly placed concrete, in order to allow hydraulic cement hydration and if applicable, pozzolanic reactions to occur and continue without interruption, so that the potential properties of concrete may develop (ACI 308R-01, 2001).

7.1.1. Requirement of curing

Since cement hydration is a chemical process that needs the presence of water for a long duration as well as a reasonable environment, curing is the process undertaken to encourage cement hydration. As cement hydrates, the internal relative humidity of concrete decreases, which dries out the paste in cases, where no external water is provided. Concrete, therefore, should not be exposed to excessive drying before curing initiates, as calcium hydroxide is accumulated at the entries of capillaries by evaporating pore water, which restricts further entrance of water during curing (Scott et al. 2014). When moist curing is interrupted, concrete produced with a very low water to cement (w/c) ratio can dry out to a level where hydration discontinues, hence the development of strength continues only for a short period and then stops after the concrete's internal relative humidity drops to about 80% within the first 7-days (Steven et al., 2003). Nevertheless, if moist curing is resumed, strength development is reactivated but the original potential strength may not be achieved. Loss of water also causes the concrete to shrink, and hence, develops tensile stresses within the concrete. If these stresses are created before the concrete has achieved sufficient tensile strength, surface cracking can also occur (Steven et al., 2003). Deficiency in curing leads to deteriorate the quality of concrete, specifically in the curing affected zone, which normally consists of outer 30-40 mm cover concrete and is used to protect reinforcement from ingress of corrosive agents. Maintaining a moist environment at the concrete surface

has been shown to reduce concrete permeability and improve its properties such as abrasion, carbonation and chloride resistance (Scott et al., 2014). Hence, using proper curing regime, concrete becomes stronger, more impermeable and resistant to stress, abrasion, freezing and thawing. This improvement is rapid at the early ages but continues slowly for an indefinite period afterwards (Steven et al., 2003). The level of required curing is dependent on the exposure conditions and types of concrete, as outlined in NZS 3101 curing requirements, shown in Table 7.1.

Table 7.1: Curing guidelines from NZS 3101:2006

Exposure Classification[1]	Typical Concrete	Cementitious Material	Minimum Curing Period Required
A1, A2 & B1	20 – 40 MPa	Portland Cement	3 days
B2	25 – 45 MPa	PC with SCM optional	7 days
C, XA2, XA3	40 – 50 MPa	PC & SCM's	7 days wet

[1] Exposure Classification Description:
A1, A2: Relatively benign environments, building interiors, inland sites
B1: Moderately aggressive, close to the coast, onshore wind exposure
B2: Aggressive environment in locations 100-500m from an open sea situation
C: The most aggressive environment, tidal/splash/spray zones
XA2: Moderately aggressive chemical environment
XA3: Highly aggressive chemical environment

The basis for increasing the level of curing duration with the severity of exposure is as follows:

- The severity of exposure increases the risk of concrete deterioration and hence, more effective curing is required to ensure adequate durability performance.
- Supplementary cementitious materials (SCMs) often react slower than GP cement and hence, longer curing is required to achieve complete durability benefit from these materials.
- Higher strength concrete, with w/b ratios below 0.45, may be prone to self-desiccation as all mix water is utilized in cementing reactions, requiring external wet curing.

7.1.2. Equivalent curing

It has been established that hydration proceeds much slower at lower temperatures of concrete. Temperatures below 10°C (50°F) are unfavourable for the development of early strength; below 4°C (40°F) the development of early strength is greatly retarded; and at or below freezing temperatures, down to -10°C (14°F), little or no strength develops (Steven et al., 2003). The slower cement hydration at the lower temperatures gives dissolved ions more time to diffuse before precipitation. This produces a denser cement paste with more uniformly-distributed hydration phases that lowers the coarse porosity, which in turn affects

both strength and durability. The hydration process speeds up when the temperature of concrete is relatively high. The increase in temperature causes rapid cement hydration through the formation of denser calcium silicate hydrate (CSH) shells around cement grains, less homogeneous distribution of hydration phases and coarser porosity (Liu, 2012). In order to promote rapid early strength, precast concrete producers provide accelerated curing to concrete. However, accelerated curing has some disastrous effects on the properties of concrete, which include reduction of ultimate strengths by up to 30% and increase in the coarse porosity depending upon the peak temperature reached. The reason for reduction in strength and increase in coarse porosity is generally associated with the hydration products forming close to the original cement grains and not spreading uniformly within the space between the cement grains (Newman and Choo, 2003) as mentioned before.

In general practice, precast concrete receives initial curing (40^{o}-60^{o}C for 16 hours) prior to de-moulding. During this time, concrete is not only cured at elevated temperature but also kept covered to restrict moisture and heat loss. However, most of the precast elements are not provided with additional curing after de-moulding, unless this is particularly requested in specifications. The key reason for providing only overnight curing is that the material is considerably more mature within 18 hours of curing when de-moulded and lifted than a comparable concrete that has not received heat curing. According to the Australian standard AS 3600:2009, the equivalent curing by accelerated means is believed to be achieved when concrete reaches a compressive strength of 32 MPa. The advanced maturity of precast concrete at the time of de-moulding diminishes the impact of successive drying in comparison to concrete cured at ambient conditions having slower strength and microstructural development. When concrete is exposed to excessive drying at an early-age, the damage can result in shrinkage or thermal cracking, which will reduce the durability even if subsequent curing is applied to concrete (Scott et al., 2014). However, casting and initial curing of precast concrete has some benefits over in-situ casting and curing because environmental conditions are maintained in the former without excessive drying and under optimum compaction.

7.1.3. Research motivation

The available information on heating of concrete is primarily directed towards achieving the target performance, which is based on strength and prevention of thermal shock through managing the initial heating rate and subsequent cooling. Nearly all industry guidelines either disregard the necessity of additional water curing or insufficient guidance available on the advantages of additional curing is contradictory. There are two questions associated with accelerated heat curing of concrete. The first is what impact accelerated heat curing has on

the long-term strength and durability of concrete. In order to deal with this issue, it is important to produce suitable mixes, which are representative of those generally used in industry and correlate them to cast in-situ mixes. Correlating a low w/c ratio mix with itself under standard curing environment is not a suitable or justified comparison. Since there are a number of differences between the two mixes, such as use of high early strength cement and accelerators in precast concrete, the second question is linked to the advantages of additional water curing subsequent to the heat treatment. As there is an ambiguity in the currently available research, it is logical to investigate the benefits of applying additional water curing after accelerated treatment. In an attempt to answer these questions, it is important to compare equivalent fit for purpose mixes and not identical mix designs, which has been undertaken in this study.

7.1.4. Experimental Investigations

Although the effectiveness of glass powder in SCC has already been investigated and discussed in the preceding chapters, glass powder may also be used in precast concrete and in that case, accelerated curing would be an issue, which needs detailed research. Therefore, the main objective of this study was to investigate the effects of accelerated curing on long-term compressive strength, modulus of elasticity and durability properties of SCC, utilizing unwashed and washed glass powders of 20 µm fineness added at 30% content as cement substitutes. The results of all these investigations have been presented and discussed in this chapter. As outlined in Chapter 3, the aggregate proportions and water to binder ratio (w/b) were maintained as constants for casting SCC mixes. The SCC mixes, subjected to initial curing at elevated temperature, were produced according to the standard procedure that was adopted for casting standard cured SCC mixes. However, after representative samples from each mix were poured in cylindrical moulds, the moulds were covered and were placed in an oven, whose temperature was increased to 50^{o}C for approximately 18 hours. Thermocouples were used to measure the internal temperature of elevated temperature cured specimens, the measurements of which are provided in Figure 7.1. Prior to de-moulding, the specimens were allowed to cool for another 4 hours. After the specimens were removed from the moulds, half of the specimens were placed in a standard curing tank at about 21^{o}C and the other half were kept under ambient laboratory conditions with no further curing until testing. These curing regimes have been graphically represented in Figure 7.2. Afterwards, the hardened wet-cured and dry-cured concrete specimens were tested for compressive strength at the curing ages of 1 to 365 days, modulus of elasticity at the curing ages of 7 to 365 days, oxygen permeability, porosity and electrical resistivity at the curing ages of 3 to 365 days and chloride diffusion at the curing ages of 28 to 365 days. All

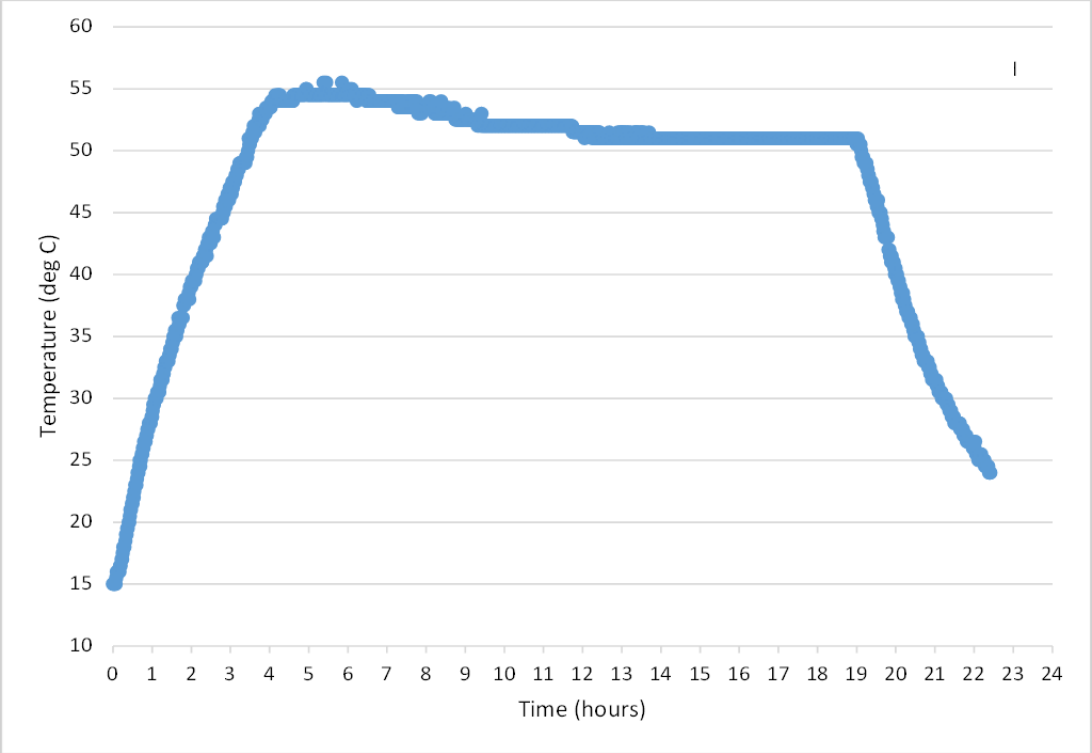

Figure 7.1: Internal temperature of SCC samples subject to curing at 50°C

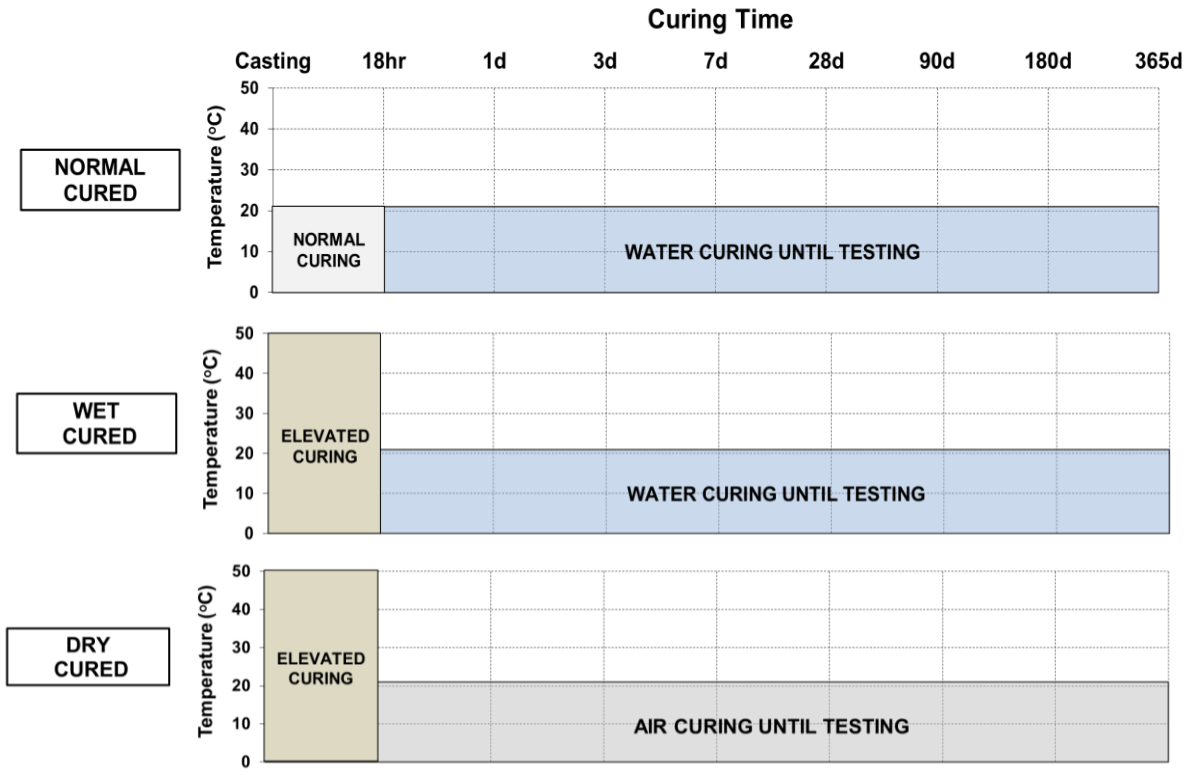

Figure 7.2: Different curing regimes for all SCC mixes

mixing and testing were done in Civil Engineering Laboratories on the campus of University of Canterbury, New Zealand. The tests were carried out at room temperature, normally between 18°C and 23°C. The materials, experimental procedures and tests have been

described in Chapter 3. The experimental results of standard cured mixes have already been explained in Chapter 5 and 6 but their discussion, again in this chapter, is solely for their comparisons with elevated temperature cured specimens. The complete list of tests and references for their results are summarized in Table 7.2.

Table 7.2: Tests on SCC and references to their results

TESTS	AIMS	GP[1]	FA[2]	WG[3]	UG[4]	AM[5]
Compressive strength tests	To assess the influence of binders on the crushing strength of SCC, initially cured at an elevated temperature	Fig. 7.3	Fig. 7.4	Fig. 7.5	Fig. 7.6	Fig. 7.7 Fig. 7.8 Fig. 7.9
Modulus of elasticity tests	To assess the influence of binders on the stiffness of SCC, initially cured at an elevated temperature	Fig. 7.10	Fig. 7.11	Fig. 7.12	Fig. 7.13	Fig. 7.14 Fig. 7.15 Fig. 7.16
Oxygen permeability tests	To assess the influence of binders on resistance to oxygen permeation through SCC, initially cured at an elevated temperature	Fig. 7.17	Fig. 7.18	Fig. 7.19	Fig. 7.20	Fig. 7.21 Fig. 7.22 Fig. 7.23
Porosity tests	To assess the influence of binders on transport of water through porous SCC, initially cured at an elevated temperature	Fig. 7.24	Fig. 7.25	Fig. 7.26	Fig. 7.27	Fig. 7.28 Fig. 7.29 Fig. 7.30 Fig. 7.31 Fig. 7.32
Electrical resistivity tests	To assess the influence of binders on electrical resistivity of SCC, initially cured at an elevated temperature	Fig. 7.33	Fig. 7.34	Fig. 7.35	Fig. 7.36	Fig. 7.37 Fig. 7.38 Fig. 7.39
Chloride diffusion coefficient tests	To assess the influence of binders on chloride diffusion coefficient of SCC, initially cured at an elevated temperature	Fig. 7.40	Fig. 7.41	Fig. 7.42	Fig. 7.43	Fig. 7.44 Fig. 7.45 Fig. 7.46

[1] General Portland cement class: GPE-W and GPE-D refer to GP kept at elevated temperature, subsequently dry-cured and water-cured respectively

[2] Class F Fly Ash class: FAE-W and FAE-D refer to FA kept at elevated temperature, subsequently dry-cured and water-cured respectively

[3] Washed Glass Powder class: WGE-W and WGE-D refer to GL kept at elevated temperature, subsequently dry-cured and water-cured respectively

[4] Unwashed Glass Powder class: UGE-W and UGE-D refer to GL kept at elevated temperature, subsequently dry-cured and water-cured respectively

[5] All materials class: All wet-cured and dry-cured specimens

7.2 Effects of accelerated curing on compressive strength of self-compacting concrete

In general, the concrete subjected to a higher temperature at an early age attains a greater early-age strength but eventually achieves a lower later-age strength, whereas the concrete subjected to a lower temperature at an early-age leads to lower early-age strength but approaches almost the same later-age strength as the isothermal cured one (Klieger, 1958; Alexander and Taplin, 1962; Kim et al., 1998). The explanation to this theory has been described by Neville and Brooks (1987) that accelerated initial hydration leads to a homogenous distribution of the cement gel with a worse physical structure, which is possibly more porous than the structure generated at ambient temperatures. When concrete is placed at a higher initial temperature, the time available for the hydration products to disperse away from the cement grains and for the consistent precipitation in the interstitial space is inadequate. Consequently, an assembly of these hydration products is developed within the area of hydrating cement grains. This process restricts further hydration and hence, affects the development of longer-term strength, similarly explained by Klieger (1958), Verbeck and Helmuth (1968), Detwiler et al. (1994) and Ozyildirim (1998). The reduction in the long-term compressive strength of concrete after elevated initial curing has been known as the "crossover" effect (Carino, 1994; Malhotra and Carino, 2003). Similar performance of SCC was observed in this study when it was initially treated with accelerated temperature.

The present section consists of the findings from the experimental study on compressive strength development in a range of SCC mixes, incorporating control binders as well as glass powders of different qualities but added at the constant replacement rate and subsequently treated with accelerated initial temperature. For the purpose of comparison of the curing temperature on the compressive strength development, the compressive strength of elevated-cured (50°C) specimen was correlated to the compressive strength value of each SCC type cured at 21°C. The compressive strength measurements were taken at 1, 3, 7; 28, 90; 180 and 365 days for early, normal and long-term strengths respectively and have been shown in Figures 7.3 - 7.6. The average compressive strength measurements were obtained from two replicate specimens at each curing age. Complete data are provided in Appendix F.

7.2.1 Effects of accelerated curing on compressive strength of control self-compacting concrete mixes incorporating GP cement and Fly Ash

The results from early-age (1-day) compressive strength measurements demonstrated an increase in the GP specimens subjected to an elevated curing compared to the normally-cured GP specimens as shown in Figure 7.3. Eliverly and Evans (1964) also reported that

the specimens mixed in normal temperature (17°C) and cured under high temperature (40˚C) have a higher initial crushing strength than those mixed and cured under normal temperature. Several other investigators (Escalante-Garcia and Sharp, 2001; Brooks and Kaisi, 2002; Ma et al., 1994) similarly noticed that high temperature improves strengths at an early-age. However, the compressive strength testing of the GP series showed virtually identical values for all the mixes at 3-days after casting. Further, GPE-W exhibited some development in compressive strength at 7-days though it was still lower than GP. Pointing out the importance of initial curing temperature, Price (1951) consistently reported that concrete cured at a high temperature shows higher strength at early-age and lower strength

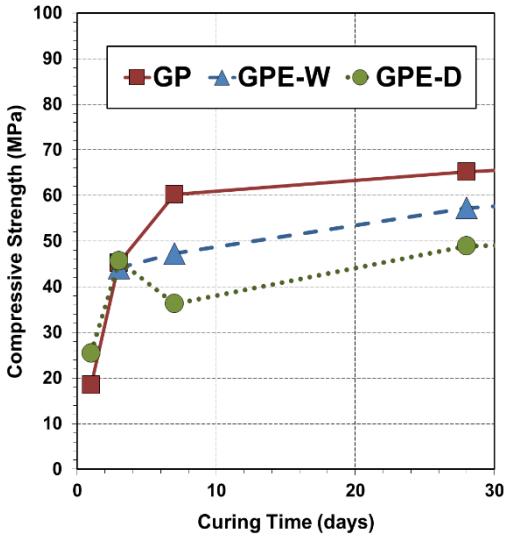

(a)

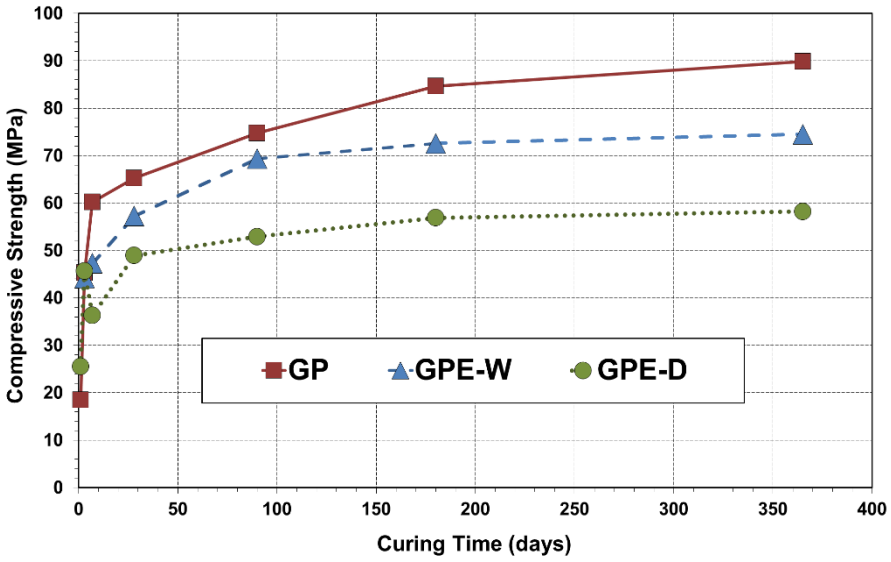

(b)

Figure 7.3: Compressive strength development in GP subjected to different curing conditions from curing age of (a) 1 to 28 days (b) 1 to 365 days

by 7-days compared to isothermally cured concrete at 20°C. The measured strength of GPE-W showed an increase of 10 MPa between 7 and 28 days, which is 50% higher than the increase found in the GP standard curing control mix during this period. At 90-days, however, the strength of GPE-W was 8% below than that of GP mix. Contrarily, Selman (2001) reported that the specimens cured at temperature of (60^{o}C) had increase of about 9%-22% in their 7, 28 and 90 days compressive strengths compared with those cured at normal temperature (25^{o}C), possibly due to a different mix design used in that study. As the curing time progressed, water curing subsequent to initial elevated temperature curing resulted in 17% lower 180-days strength than that of the standard curing. This difference in compressive strengths could be due to non-uniform hydration products for cement cured at high temperatures against the uniform distribution of hydration product for cement subjected to lower temperatures. Kjellsen et al. (1990) studied the microstructure of cement pastes hydrated at temperatures ranging from 5°C to 50°C and reached the similar conclusion. The final result noted at 365-days revealed the difference of approximately 15 MPa between GP and GPE-W, with the latter being lower. This strength loss can be attributed to the fact that at a later age, the important number of formed hydrates have no time to arrange suitably that influences the ultimate strength of elevated cured concrete. Cebeci (1987) similarly concluded that concrete cured within 37^{o}C has lower ultimate compressive strength (360-days) compared to concrete cured within 17^{o}C.

There seemed to be considerably lower compressive strength development in GPE-D specimens between 1 and 365 days after casting. The compressive strength of GP after 1-day was approximately 18 MPa compared to 25 MPa of GPE-D, which can be related to accelerated hydration in GPE-D, initially cured at higher temperature. Martínez-Ramírez and Frías (2009) also showed that curing temperature plays a fundamental role in the evolution of cement hydration and hence, significant changes occur in reaction kinetics, microstructure porosity and hydration degree of cement pastes when curing temperature increases (Frías, 2006a; Frias, 2006b). The reduction in measured strength of GPE-D at 7-days is possibly a function of variability between individual cylinders. At 28-days, however, the strength of GPE-D was found to be 17%-33% lower in comparison to GP and GPE-W. The effect of additional wet curing on strength development is evident with GPE-D specimens having 90-days strength approximately 16 MPa and 22 MPa lower than GPE-W and GP respectively. The 90-days results revealed the reduction in the rate of strength gain with the curing time, which is in agreement with the result of Al- Kafaji (2001) who reported that the percentage of increase in compressive strength slightly decreases from the age of 56-days. Overall, a significantly lower increase of 16% was observed in compressive strength of GPE-D between 28 and 365 days in comparison to approximately 23%-27% increase in

compressive strengths of GP and GPE-W during the same curing period. Comparing the water and air-cured specimens, in general, the compressive strength of the water-cured specimens remained higher than that of the air-cured specimens at all the tested curing ages, which is consistent with the findings reported by Ling et al. (2012). However, it is important to recognize that although the heat treated specimens had lower compressive strengths than the standard-cured specimens, both wet-cured and dry-cured concretes could ultimately reach their design strengths by 90-days.

The primary factors, determining the behaviour of concrete subjected to heat treatment, are fineness, composition, curing cycle parameters and type and quantity of mineral additions, used in blended cements. It has been established that temperature is an important parameter for the activation of the mineral admixture FA as the obstacle against its activation has to be overcome for the reaction to take place. The activation energy required for FA is higher than that is required for other SCMs, such as slag, and hence, heat treatment is more significant for the activation of FA (Jiang and Roy, 1990). However, initial rapid hydration in FA leads to the formation of hydration products with a less compact physical structure. This further leads to a lower strength in dry-cured concrete compared to less porous concrete hydrated slowly with continuous water-curing (Benammar et al., 2013). Similar behaviour was observed in FA incorporated mixes tested in this study. The compressive strengths in FA class of mixes from the curing period of 1-day to 365-days have been demonstrated in Figure 7.4.

The measured strength of FAE-W exhibited an increase of approximately 11 MPa between 3 and 7-days in comparison to approximately 7 MPa in FA mix during the same curing period. From 7-days to 28-days, however, compressive strength development in FAE-W was slightly higher than FA by a nominal rise of 3%. The relatively higher strength increase of FAE-W at 28-days can be related to the improved bond between the binder paste and the porous aggregate after treating with elevated temperature, as suggested by Lo and Cui (2004). Williams and Owens (1982) consistently reported that concrete with FA, cured between 30°C and 60°C, shows higher compressive strength at 28-days than those cured at 20°C. Since 28-days compressive strength of FAE-W was higher than that of FA, it can be seen that in case of GP, the situation was opposite. Similar findings have been reported in the literature that under normal curing with water, 28-days compressive strength with FA replacement mixes is generally lower than the strength of control GP mixes (Balendran and Martin-Buades, 2000) and at high temperature curing, compressive strength is reduced in GP concrete at 28-days (Thomas et al., 1989; Berhane, 1992) but increases in FA incorporated concrete compared to their normal-cured counterparts (Balendran and Martin-Buades, 2000; Alshamsi, 1994). These findings are also in an agreement with the conclusions presented by

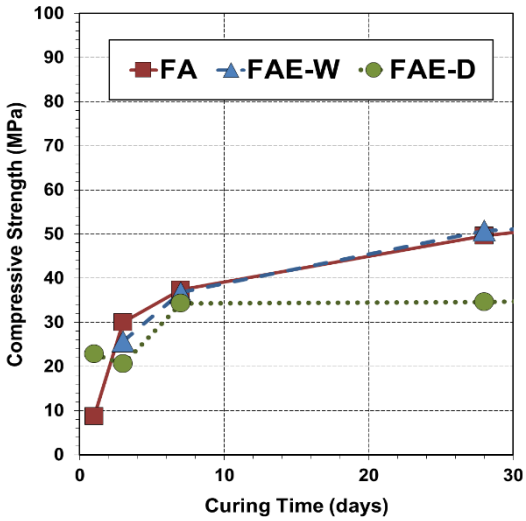

(a)

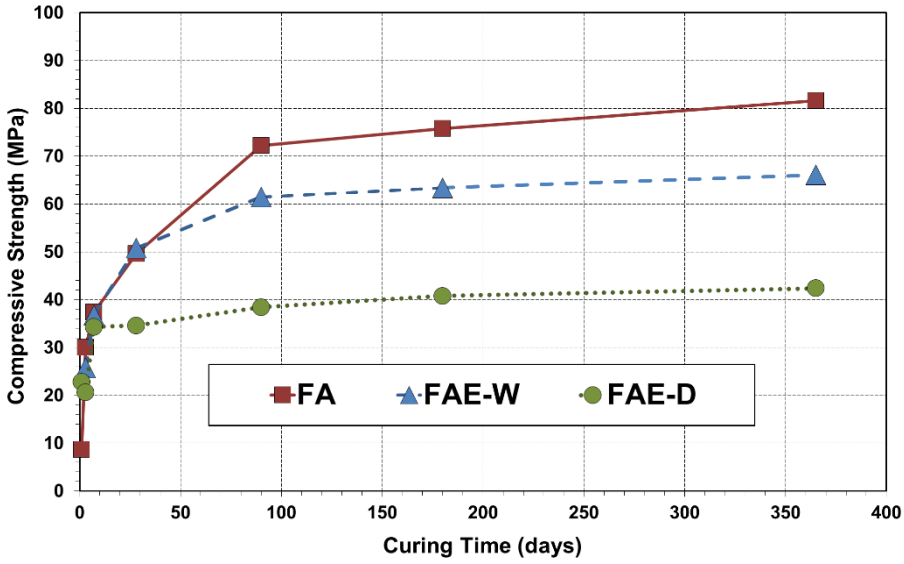

(b)

Figure 7.4: Compressive strength development in FA subjected to different curing conditions from curing age of (a) 1 to 28 days (b) 1 to 365 days

Turkel and Alabas (2005) that composite cements perform well under heat treatment and they do not exhibit considerable loss in compressive strength up to 56-days, however, longer-term effects of heat treatment after 56-days were not reported in that study. The present study revealed that FAE-W did not demonstrate much improvement in the long-term as there was considerably lower increase of about 15 MPa from 28 to 365-days of wet-curing in FAE-W compared to substantial increase of 32 MPa in FA within this curing time. The difference in compressive strengths between FA and FAE-W at 365-days was, however, found to be higher than the difference between GP and GPE-W. Consistent results were found by Kim et al. (2002) that although temperature rise at early-age increases the strength of a mix with FA but reduces long-term strength compared to cement without additions.

As opposed to FAE-W, the dry-cured specimen (FAE-D) subsequent to initial elevated temperature did not show considerable growth in compressive strength development after it gained its initial strength. The compressive strength for FA after 1-day was approximately 9 MPa compared to about 23 MPa for FAE-D. The drop in compressive strength of FAE-D at 3-days could only be related to an experimental error. However, FAE-D achieved substantial compressive strength development of approximately 14 MPa between 3-days and 7-days, which could be due to the presence of water in the specimen itself to aid the hydration process to continue. Nevertheless, the strength of FAE-D was found to be 43%-47% lower in comparison to FA and FAE-W at 28-days. This might be due to the loss of water already present in the specimens contributing to a reduced compressive strength, since no additional water was being applied for further hydration. Bingöl and Tohumcu (2013) also compared the compressive strengths of SCC mixtures including FA, cured in the standard situation, by air, and by exposure to steam and demonstrated that concrete cured in air had the lowest compressive strength. Moreover, Reinhardt and Stegmaier (2006) made clear that higher temperatures of 40°C and 60°C lead to lower compressive strengths in the absence of water-curing. There was an increase of 10% in strength of FAE-D from 28 to 90 days, which is about 1.8 times lower than FAE-W during these curing days. Nevertheless, the subsequent increase in compressive strength of FAE-D was observed to be only about 8 MPa, starting from 28-days up to 365-days of testing, whereas FA gained approximately 32 MPa and FAE-W achieved approximately 15 MPa during this curing period. These results conclude that for considerable strength development of concrete, not only the duration and temperature of curing are important parameters (Oztekin, 1984) but maintaining an appropriate curing environment is also very important.

7.2.2 Effects of accelerated curing on compressive strength of washed glass modified self-compacting concrete

The results from early-age compressive strength measurements done on the WG class of mixes exhibited an increase in WGE-W compared to WG, as shown in Figure 7.5. None of the other wet-cured mixes demonstrated such a high increase in initial compressive strength after elevated temperature curing. The reasons for higher compressive strength of WGE-W under accelerated curing are (1) increase of the pozzolanic reactions under an elevated temperature and (2) since the strength growth is usually slow under normal temperatures, accelerated curing promotes the late secondary strength of glass concrete. This early-age result exhibited that the combined effect of the pozzolanic and hydration reactions of the glass mixes was greater than that of the GP mix under an accelerated hydration reaction. Mirzahosseini and Riding (2014) similarly reported that glass specimens demonstrate slightly higher total hydration than control GP samples at high temperatures, including 50°C. The

compressive strength testing of WG class showed approximately identical values for all the mixes at 3-days after casting. With the progress in curing time, WGE-W exhibited an 18% increase in compressive strength at 7-days compared to 3-days; however, it was still considerably lower than WG concrete. The reason for the difference in compressive strengths at the elevated temperatures compared to the storage at 21°C lies in the difference in pore size distribution of the concretes. The measured compressive strength of WGE-W showed an increase of approximately 12 MPa between 7 and 28 days, which is two times more than the increase found in WG during this period. As the curing time progressed, water curing subsequent to initial elevated temperature curing resulted in approximately 11% lower 180-days strength to that of the standard curing of washed glass mix, which is less than the

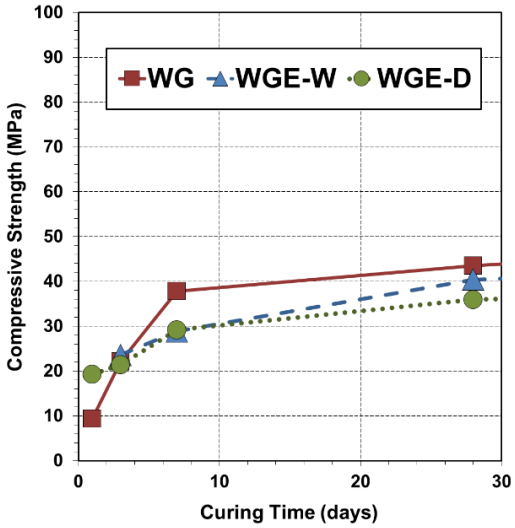

(a)

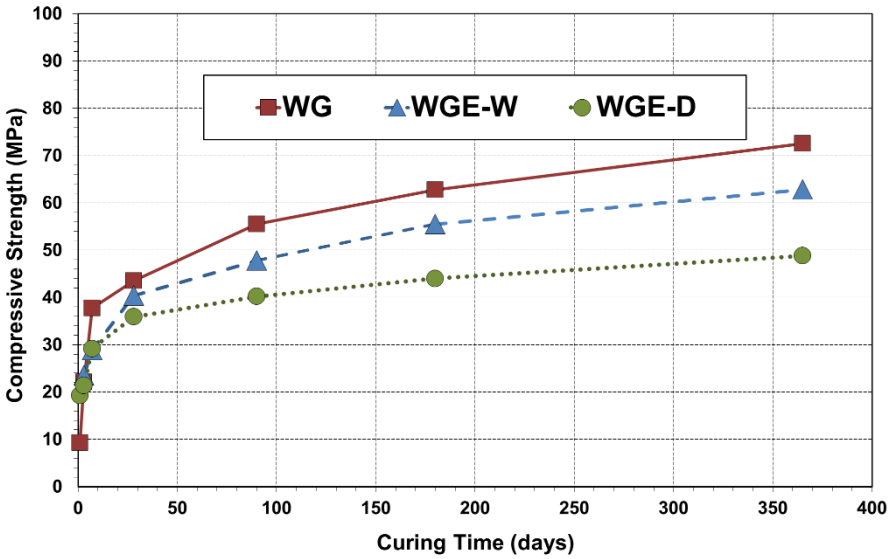

(b)

Figure 7.5: Compressive strength development in WG subjected to different curing conditions from curing age of (a) 1 to 28 days (b) 1 to 365 days

reduction observed in the GP series at 180-days. The difference in compressive strengths could be due to the same reason mentioned before. The final result recorded at 365-days revealed the difference of about 10 MPa between WG and WGE-W, where WGE-W exhibited the lower compressive strength. It can also be noted that there was about 13% decrease in 365-days compressive strength of GPE-W compared to WG mix, whereas this reduction in GP series was observed to be approximately 17%. This shows that with glass addition, compressive strengths are less negatively influenced by initial temperature rise and the glass reaction continues (or increases) at the later-ages compared to GP, similarly noticed by Mirzahosseini and Riding (2014).

There seemed to be a relatively larger compressive strength development in WGE-D specimens between 1 and 365-days after casting in comparison to FAE-D and UGE-D. The 1-day results showed an increase of 107% in WGE-D compared to WG. Moreover, at 28-days, the strength of WGE-D was found to be 11%-17% lower in comparison to WG and WGE-W. This can be related to the improvement in pore structure and lower porosity resulting from a greater degree of cement hydration and pozzolanic reaction in WGE-W compared to WGE-D as mentioned before. When exposed to elevated temperatures, the dry-cured samples had lower compressive strengths, which indicates that the positive effects of subsequent water-curing conditions remain present, even when the initial curing temperature is increased. The effects of additional wet-curing on strength development are evident with WGE-D having 90-days strength about 8 MPa and 15 MPa lower than WGE-W and WG mixes respectively. Overall, an increase of 21% was observed in strength of WGE-D between 90 and 365 days in comparison to about 31% increase in strengths of WG and WGE-W during the same curing period. In another study, using waste glass as fine aggregate in SCC, it was similarly shown that the strengths of water-cured samples are relatively higher than those of the corresponding air-cured samples due to the improved pore structure and lower porosity of water-cured specimens (Ling et al., 2012). These results are also consistent with previous results reported by Kou and Poon (2009) and Wang and Huang (2010). Moreover, the results from 90 to 365 days revealed that there was a reduction in the rate of strength gain with curing time in WGE-D. Another significant observation is that washed glass, either dry-cured or wet-cured, finally achieved its target strength for which it was cast, whereas unwashed glass failed to reach that even with subsequent water-curing.

7.2.3 Effects of accelerated curing on compressive strength of unwashed glass modified self-compacting concrete

It has been shown that rapid hydration due to elevated temperatures acts as a ‘shell’ that eventually hinders the diffusion of hydration products into the bulk cement paste matrix

(Kjellsen et al., 1990) and hence, the fast-formed hydrates cause a great porosity leading to a loss of ultimate strength. This phenomenon enhances further when a part of cement is substituted by the natural pozzolan (Ezziane et al. 2007). Kjellsen and Detwiler (1993), Verbeck and Helmuth (1968) and Carino (1981) explained this theory that when a pozzolan is added in concrete, porosity inside cement paste increases and micro-cracks develop due to the difference in thermal expansion coefficients of concrete constituents, which finally lead to lowering the strength at later time. The glass incorporated mixes produced in this study confirmed these previous observations. The performance of all unwashed glass mixes in terms of compressive strength development, throughout the curing time of 1 to 365 days, has been exhibited in Figure 7.6. It can be seen that even heated concrete containing unwashed glass powder as a cement replacement failed to gain appreciable compressive strength because organic content in the unwashed glass powder had a strong retarding effect on strength development of concrete.

The compressive strength of UGE-W showed that there was an increase of approximately 9 MPa between 3 and 7 days in comparison to approximately 7 MPa in the standard UG mix during the same curing period. As anticipated, increase in temperature, which means higher energy, led to higher immediate compressive strength. Liu et el. (2015) consistently reported that high curing temperature increases and promotes the cement hydration process (Stutzman and Clifton, 1992) and the glass pozzolanic reaction (Shi et al., 2005) simultaneously, both of which produce CSH and generate strength. According to the chemical equilibrium theory, the chemical reaction rate and reaction degree, including cement hydration reaction and glass pozzolanic reaction, increase directly with reaction temperature (Liu et al., 2015). The compressive strength development from 7 to 28 days in UGE-W was approximately half than in UG. An increase of about 27% was observed from 28

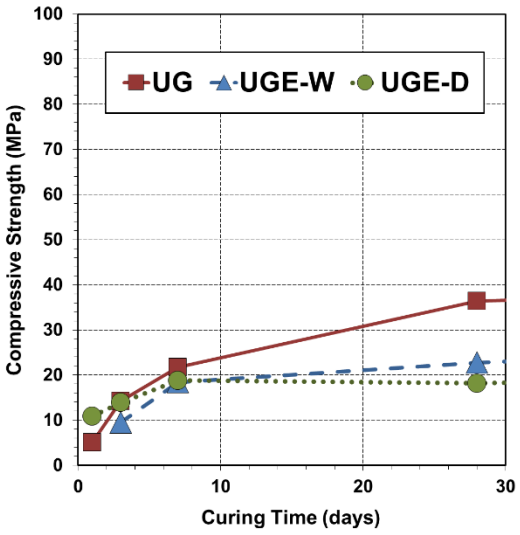

(a)

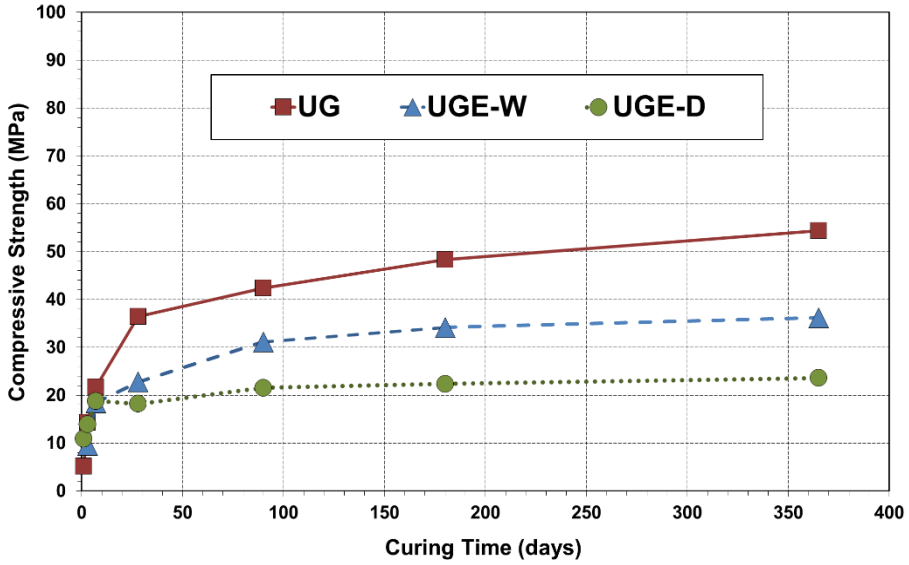

(b)

Figure 7.6: Compressive strength development in UG subjected to different curing conditions from curing age of (a) 1 to 28 days (b) 1 to 365 days

to 90 days in UGE-W, whereas UG only increased by 14% between these curing periods. This might be due to the rapid progress of hydration reaction after the heating treatment to UGE-W, which was considerably slower in the standard cured mix UG. Soroka (1993) also reported that when the temperature raises from 20°C to 40°C, the rate of hydration of cement increases by a factor of 2.45, and contributes towards strength gain. However, after 90-days, UGE-W did not demonstrate much improvement as there was a considerably lower increase of approximately 5 MPa from 90 to 365 days in UGE-W as compared to a significantly higher increase of 12 MPa in UG within this curing time. The lower rate of strength increase at late-ages might be due to the fact that activation energy reduces as hydration proceeds, consistently discussed by Kjellsen and Detwiler (1993). Wild et al. (1995) also reported that the long-term strength for 50°C cured concrete tends to be somewhat below those for 20°C cured concrete.

The compressive strength measurements revealed that the initial strength gained by UGE-D at 1-day was more than twice the initial strength achieved by UG specimens. This might be attributed to the early evolution of the heat of hydration (Swamy et al., 1975), as mentioned before. Another reasoning reported by Poutos et al., (2007) explains that glass absorbs less heat due to its low specific heat (Tipler, 1999) and consequently, water absorbs higher amount of heat produced during cement hydration. This makes concrete hotter and hence, the higher temperature promotes cement hydration. As the curing time progressed to 3-days, the compressive strength of UGE-D approached almost the same level to UG but became worse at the curing age of 7-days and demonstrated about 15% lower strength than UG. It is

well-documented in literature that although high temperatures during initial hydration accelerate the chemical reaction with beneficial effects on early strength development but they possibly have a detrimental impact on strength at or after 7-days (Kanda et al., 1992). The decrease in 28-days measured strength of UGE-D is possibly due to the variance between individual cylinders. However, UGE-D showed only 5.4 MPa increase in compressive strength from 28 to 365 days, which validates the importance of curing temperature and curing environment in the development of compressive strength. It can also be observed that the presence of impurities in UG mixes counteracted the development in compressive strength, even after the accelerated curing treatment that activated its pozzolanic and hydration reactions.

7.2.4 Consolidated summary of compressive strength results

The data achieved from the tests performed on elevated wet-cured and dry-cured FA, UG and WG specimens and elevated dry-cured GP specimens were correlated to the compressive strength data achieved for wet-cured GP. The consolidated results are demonstrated in Figure 7.7. The compressive strength factor was calculated by dividing each wet-cured and dry-cured compressive strength value by the compressive strength of wet-cured control GP mix. This means that data points of GPE-W were adjusted at the compressive strength factor of 1 to determine the compressive strength factors of remaining wet-cured and dry-cured specimens. On the whole, it was observed that although the negative influence of accelerated curing on compressive strength of WGE-W was less than that on GPE-W, its compressive strength was still lower than GPE-W but somewhat close to

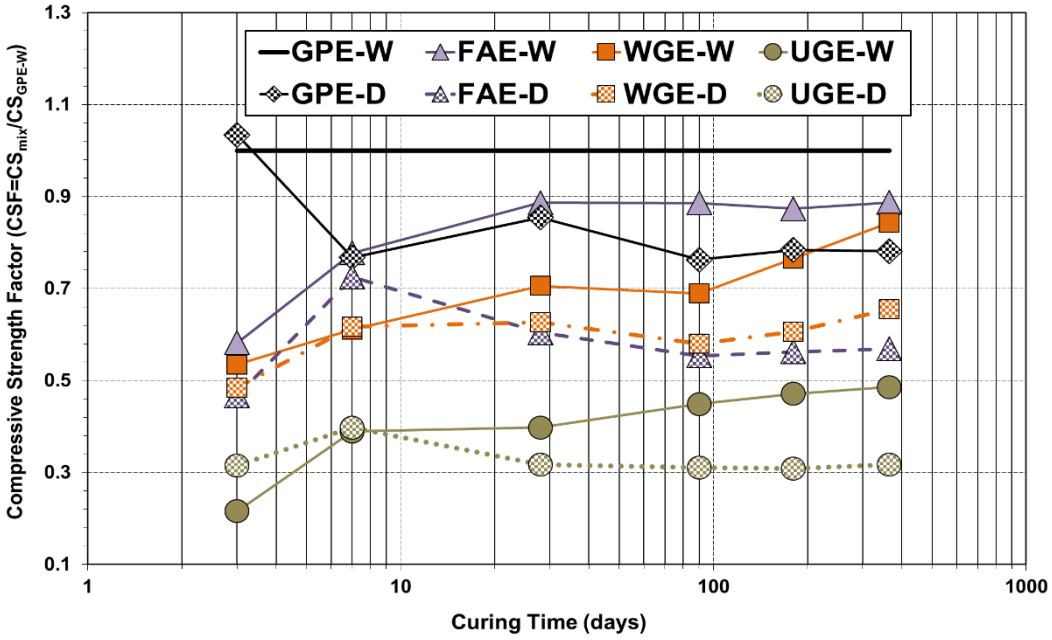

Figure 7.7: Consolidated summary of compressive strength data for elevated cured specimens

FAE-W. More specifically, dry-cured WG specimens showed closer performance to GPE-W and GPE-D in comparison to dry-cured FA mix. The better performance of WGE-W compared to GPE-D by 365-days suggests that proper water curing subsequent to elevated temperature treatment given to low cost and sustainable glass concrete can provide more benefit than no curing after elevated temperature treatment given to GP. Unwashed glass mixes, however, showed poor performance than all other dry-cured and wet-cured mixes.

7.2.5 Comparison between compressive strength development in standard cured specimens and elevated cured specimens

The effects of additional curing followed by accelerated heat treatment have been studied in the past. It has been documented in the literature that when curing is terminated, drying of the surface occurs and hydration stops as the moisture content decreases (Meeks and Carino, 1999). However, it takes time for this drying process to reach the interior of the concrete, meaning some compressive strength has already been gained by the time curing has stopped. Therefore, insufficient curing often has only a 'minor' effect on the strength development of thick concrete elements because the core has higher moisture content for a longer period of time compared to the outer layers (Meeks and Carino, 1999). In this study, however, somewhat incompatible results were found. Although some development in the compressive strength was observed after elevated curing but it still affected the overall strength gain in all dry-cured SCC types. Therefore, the results have been correlated with the previous literature (Persson, 2003) and the proposed relationships between elevated and standard concretes available in FIB model code 2010. Figure 7.8 and Figure 7.9 show comparison between compressive strength measurements done on all the standard class of specimens and the elevated cured specimens subjected to wet-curing and dry-curing respectively. It can be noted in Figure 7.8 and Figure 7.9 that the trends represented by the line composed of en dashes refers to FIB Model Lower Limit (2010), by the line made by hyphens refers to FIB Model Upper Limit (2010) and by the dotted line refers to model presented by Persson (2003). It should also be clear that continuous lines and dashed lines in both figures refer to relationships for normal strength and high strength normal weight and lightweight aggregate concretes respectively, as mentioned in FIB Model Code (2010). FIB code also indicates that these correlations have been derived for conventional concrete and no information is available for SCC so far. Hence, in the present study comparisons have been made using the relationships available in the code. From the figures (7.8 and 7.9), it has been observed that although the strengths in wet-cured specimens were found to be approximately close to the reference lines derived from the literature, the strengths of dry-cured specimens were much lower than they were observed in other instances. This result was more evident in the case of unwashed glass specimens.

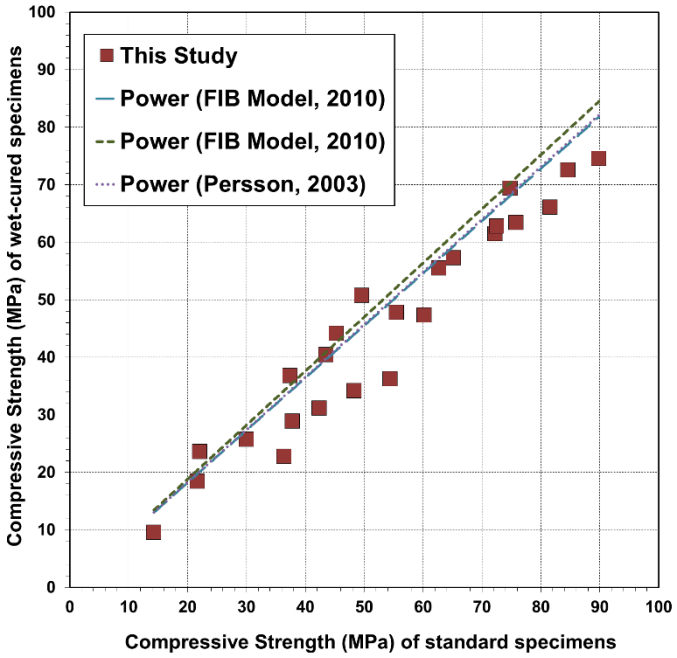

Figure 7.8: Comparison between compressive strength development in standard specimens and wet-cured specimens subjected to elevated curing

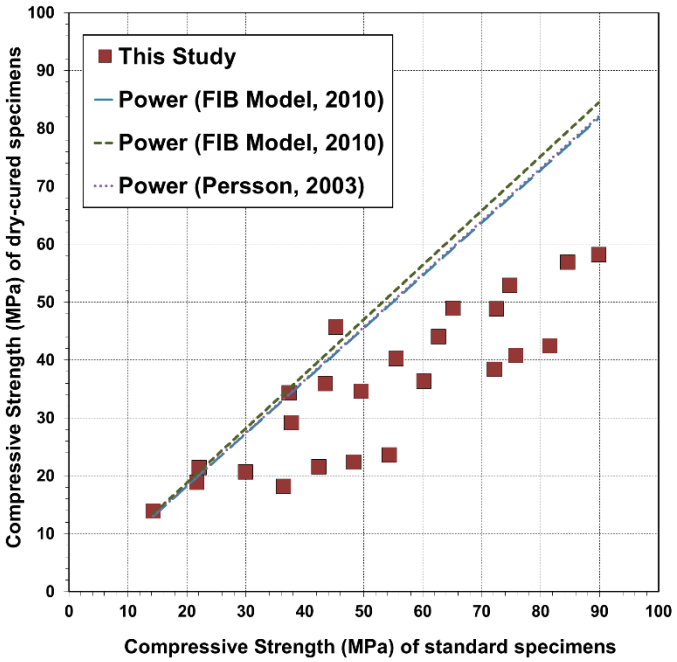

Figure 7.9: Comparison between compressive strength development in standard specimens and dry-cured specimens subjected to elevated curing

The rationale for the conflicting results has been discussed as follows:

- Since the strength of concrete is influenced by w/c ratio and rate of hydration, the lower the w/c ratio, the higher the initial strength. However, it is believed that a w/c ratio of 0.25 does not provide enough space for expanding hydration reaction to take place

and complete hydration rarely occurs when w/c ratio is below 0.38. Moreover, due to water being locked in the fine gel pores of the microstructure of concrete and unable to be used for hydration; a w/c ratio of approximately 0.42 is required for complete and unrestrained hydration. In addition, it has been well-documented in the literature (Newman and Choo, 2003; Scott et al., 2014) that a sealed concrete with a w/c ratio below 0.45-0.50 is susceptible to self-desiccation as all the free mixing water is utilized in cementing reactions and there is not enough water to cover the unhydrated particles. ACI 301-05 (2005) has reported that concrete mixtures, with a w/c ratio less than approximately 0.5 and are sealed also, cannot develop their full potential hydration due to lack of water; however, not all mixtures may need to reach their full hydration in order to develop adequate properties to achieve the specified design life. Hence, without additional moist curing, strength development may be limited due to an incomplete hydration. In the case where concrete has a lower w/c ratio, strength can be compromised if there is not enough water for hydration. This implies that some increase in strength with time may not be able to compensate for any loss of strength occurring due to drying and reduction in hydration. Similar is the case with dry-cured specimens in this study that although some of the dry-cured samples ultimately reached the design strength, they still had the lowest compressive strength values. Lee (2014) indicated that it is not clear if additional curing prevents self-desiccation of concrete with a low w/c ratio; the present study concludes that additional curing fails to counteract the strength loss occurred due to self-desiccation.

- The size and shape of the test cylinders, being used in tests, are also important considering that the impact of insufficient curing on strength depends on the thickness of the concrete element. In most laboratory tests, the concrete specimens are small, meaning that there is a large volume affected by the curing process in laboratory specimens (Taylor, 2013). In real circumstances, the concrete element being cured is considerably larger and thicker than the typical test cylinders. The effect of poor curing decreases as the specimen size increases since the concrete core is further away from the exposed surface.

- The use of admixtures is important when evaluating the required curing duration because blended cement hydrates at a different rate to GP cement, meaning that the optimum curing duration may be longer or shorter than expected (Reddy, 2013), depending on the type of mineral addition. The reactions that these admixtures undergo with the blended cement are also temperature sensitive; therefore, results may differ when such concrete is cured under accelerated temperatures. Therefore,

the conclusions made concerning GP concrete may not necessarily be true for concrete containing mineral admixtures at first and chemical admixtures on top of that. Hence, it is suggested that curing period for blended cement concrete containing glass powder should at least be long enough to ensure that 28-days strength at the depth of the first layer of reinforcement is equal to the design strength.

7.3 Effects of accelerated curing on elastic modulus of self-compacting concrete

Temperature variations, caused by heat of hydration in mass concrete or change of external environment, have a large influence on the mechanical properties of early-age concrete. It has already been discussed that the elevated temperature during early stage of hydration process has a negative effect on the final mechanical properties of specimens (Escalante-Garcia and Sharp, 2001; Lothenbach et al., 2007). Another property influenced by elevated curing is the modulus of elasticity of concrete, which changes as environmental conditions change (Alexander and Taplin, 1962; Hansen and Pedersen, 1977; Kjellsen and Detwiler, 1993; Naus and Graves, 2006; Yuan and Wan, 2002; Gardner et al. 2005; Zhou et al. 2008; Lee, 2008). At high temperature, decomposition of hydrated cement products and deterioration of bonds in the microstructure of cement paste reduce elastic modulus of concrete (Kodur, 2014). In fact, it is the poorly developed crystalline structure that prevents concrete from gaining its potential elastic modulus even when concrete is fully hardened. Literature indicates that the key factors influencing the elastic modulus at high temperature are the type of aggregate and the presence of sustained stress during heating, which result in the lower modulus of elasticity with increased temperature. The duration of temperature exposure, type of cement, w/c ratio and original concrete strength have little effect on elastic modulus (Naus, 2005).

The present section contains findings from the experimental study on elastic modulus of a range of SCC mixes, containing control binders as well as glass powders of different qualities but added at the constant replacement rate and subsequently treated with accelerated initial temperature. In order to easily understand the influence of the curing temperature on the modulus of elasticity, the elastic modulus of the specimens kept at 50°C was correlated to the elastic modulus value of each SCC type kept at 21°C for initial curing. The elastic modulus measurements were taken at 7; 28, 90; 180 and 365 days for early, normal and long-term elastic modulus respectively and have been demonstrated in Figures 7.10 - 7.13. The average elastic modulus measurements were obtained from three replicate specimens at each curing age. Complete data are shown in Appendix F.

7.3.1 Effects of accelerated curing on elastic modulus of control self-compacting concrete mixes incorporating GP cement and Fly Ash

The results from elastic modulus measurements revealed the reduction in GP specimens subjected to elevated curing compared to the normally-cured GP specimens as shown in Figure 7.10. GPE-W exhibited elastic modulus of approximately 34 GPa at 7-days, however, it was still lower than GP. The literature discusses that at elevated temperature curing and high temperature drying, shrinkage can result in micro-cracking. These micro-cracks appear during the heat treatment (Sylla, 1998) and deteriorate the material (Tepponen and Erickson, 1987), particularly in its thicker part (Bournazel and Moranville-Regourd, 1993). This damage creates mechanical stresses in concrete and modifies the elastic characteristics, specifically the elastic modulus, consistently observed in this study. Furthermore, the measured elastic modulus of GPE-W showed an increase of approximately 4 GPa between 7 and 28 days, which is about 1.5 times higher than the increase found in GP mix during this period. However, it still remained lower than GP, which might be due to the formation of weaker and more ductile hydration products in GPE-W with increased temperatures, similarly reported by Giannini and Zhu (2012). At 90-days, elastic modulus of GPE-W was 5% below that of GP mix. The final result noticed at 365- days revealed the difference of 4 GPa between GP and GPE-W, with the latter being lower. This might be due to the cross-over effect, which also appears in elastic modulus with increased initial curing temperature, similarly reported by Alexander and Taplin (1962). However, the crossover effect of elastic modulus was not as obvious as that of compressive strength, which could be due to the difference between the rates of increase in compressive strength and elastic modulus.

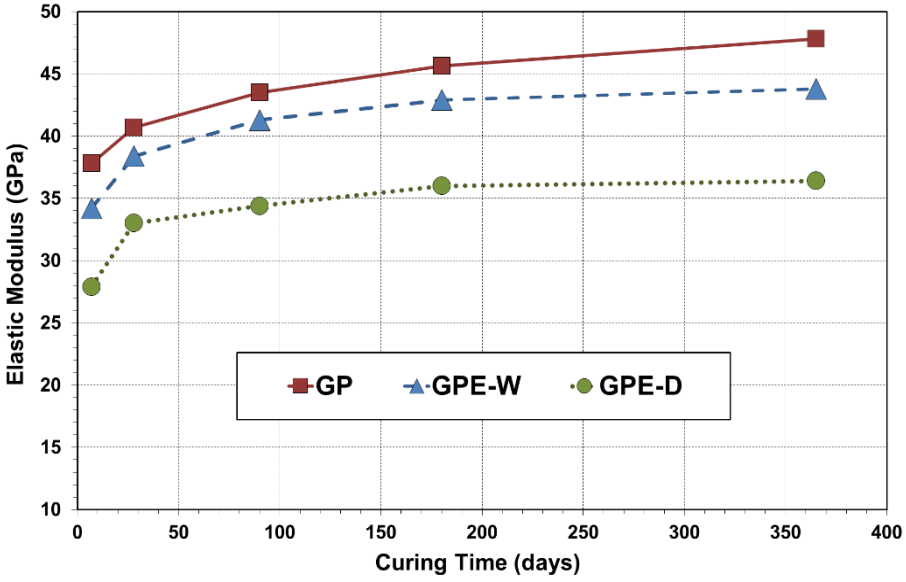

Figure 7.10: Elastic modulus development in GP subjected to different curing conditions

There seemed to be relatively small change in elastic modulus for GPE-D specimens between 7 and 365 days after casting. However, the variation of elastic modulus in dry-cured GP specimens with curing temperature was not as prominent as the variation of compressive strength. The elastic modulus for GP at 7-days was approximately 38 GPa compared to approximately 28 GPa for GPE-D. At 28-days, however, elastic modulus of GPE-D was found to be 14%-19% lower in comparison to GP and GPE-W. The effects of additional wet curing on elastic modulus development are evident with GPE-D having 90-days elastic modulus approximately 7 GPa and 9 GPa lower than GPE-W and GP mix respectively. It is recognized that water molecules reside in very small pores; thus, it takes several hours for the water molecules to work themselves out of the pores. Therefore, GP specimen's modulus of elasticity remained comparable to GP only until the specimen was completely dry, consistently reported by Shoukry (2009). From 180-days, it was observed that there was a significant reduction in the rate of elastic modulus development with the curing time. Comparing the water and dry-cured specimens, in general, elastic modulus of the water-cured specimens remained higher than that of the dry-cured specimens at all the tested ages. Naus (2005) consistently reported that elastic modulus decreases much more for concrete cured in air than for concrete cured in water and that the deterioration in elastic modulus of dry-cured concrete specimens is higher.

The elastic modulus development in FA series from the curing period of 7-days to 365-days has been demonstrated in Figure 7.11. The measured elastic modulus of FAE-W exhibited 28 GPa at 7-days in comparison to about 32 GPa in FA mix at the same curing period. At 28-days, nevertheless, the elastic modulus development in FAE-W was 12% lower than FA. These results are consistent to Kim et al. (2002) who reported that the rate of increase in 28-

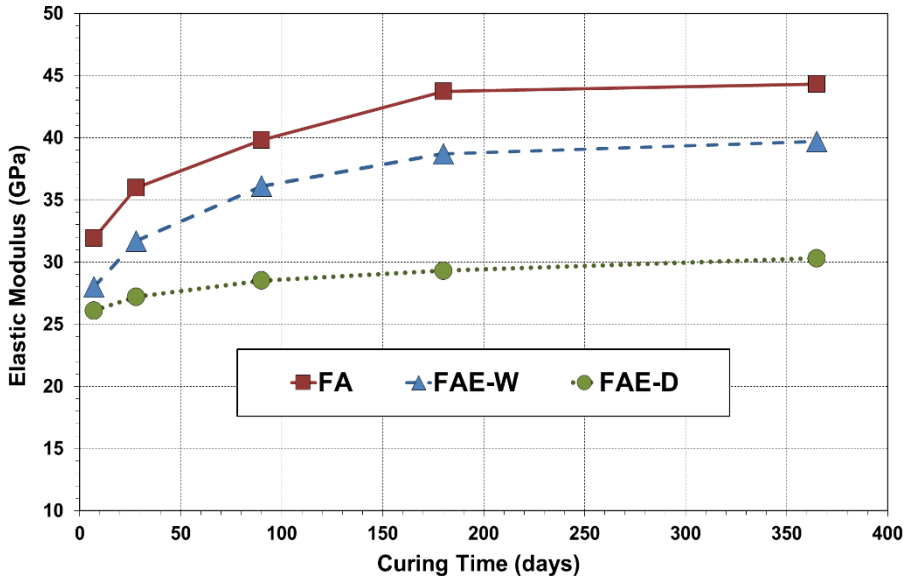

Figure 7.11: Elastic modulus development in FA subjected to different curing conditions

days elastic modulus of concrete cured at 23°C is greater than those cured at 35°C. With the progress in curing time, FAE-W showed an increase of 14% from 28 to 90 days though this elastic modulus was still lower than FA. Kou et al. (2004) similarly reported that the use of fly ash, replaced at 25% and 35% by cement in elevated cured concrete, reduced the modulus of elasticity of concrete at both 28-days and 90-days. In addition, Soni and Saini (2014) noticed reduction in elastic modulus in 30% FA modified concrete initially cured at 80°C. Furthermore, it was revealed that FAE-W and FA did not demonstrate similar improvement later as there was a considerably lower increase of 3.6 GPa from 90-days to 365-days in FAE-W specimens as compared to an increase of 4.5 GPa in FA mix within this curing time.

As opposed to FAE-W but in parallel to GPE-D, FAE-D did not show considerable growth in elastic modulus, once it achieved its initial modulus of elasticity. The increase in initial curing temperature also increased the development of elastic modulus at early-age of 7-days, but an insufficient increase in elastic modulus was noticed beyond 7-days. The elastic modulus for FA at 7-days was about 32 GPa compared to about 26 GPa for FAE-D. The elastic modulus of FAE-D was found to be approximately 14%-24% lower in comparison to FA and FAE-W at 28-days. Furthermore, there was an increase of 5% in elastic modulus of FAE-D from 28-days to 90-days in comparison to approximately 14% in FAE-W during similar curing period. The subsequent increase in elastic modulus of FAE-D was observed to be only about 1.8 GPa, starting from 90-days up to 365-days of testing, whereas FA gained 4.5 GPa and FAE-W achieved 3.6 GPa between these curing days. The results obtained from dry-curing of FA modified mix exhibit the significance of water-curing for the pozzolanicity of FA to remain active. In the absence of water, FA seems to have less potential for showing satisfactory performance, even if it is treated with accelerated initial curing.

7.3.2 Effects of accelerated curing on elastic modulus of washed glass modified self-compacting concrete

The results from elastic modulus measurements done on WG class of mixes exhibited reduction in the WGE-W specimens subjected to an elevated curing compared to the normally-cured WG specimens as shown in Figure 7.12. The elastic modulus of WGE-W showed an increase of approximately 7 GPa between 7 and 28 days, which is twice the increase found in WG during this period. At 90-days, the elastic modulus of WGE-W was 6% below that of WG mix. As the curing time progressed, the water-curing subsequent to initial elevated temperature curing again resulted in a 6% lower 180-days elastic modulus to that of the standard curing. It seems that the temperature rise had an adverse effect on inner and outer microstructure of the hydration product, particularly in the case of CSH, consequently affecting glass concrete performance. Regourd and Gautier (1980) similarly reported that the

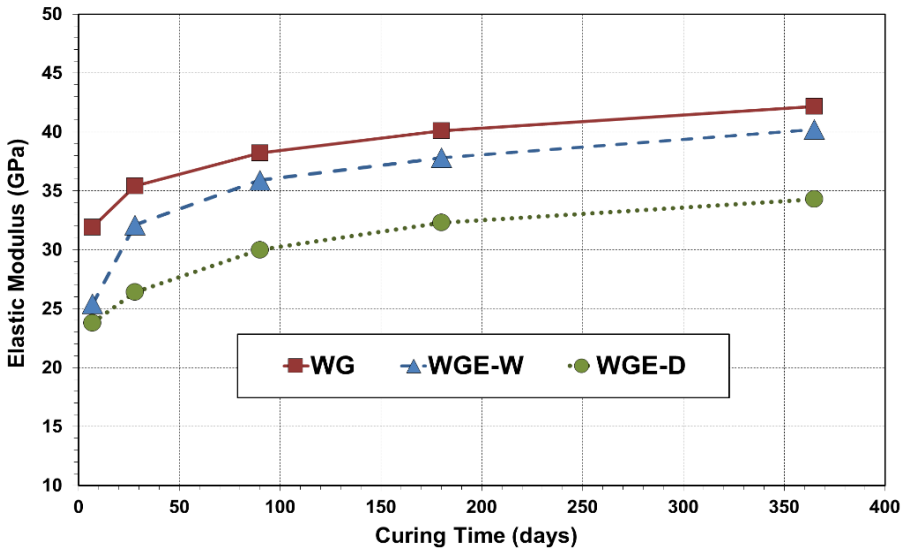

Figure 7.12: Elastic modulus development in WG subjected to different curing condition

outer CSH formed at 80°C is much more fibrous compared to normal curing temperature. In another study undertaken by Richardson (2004), a comparison of the size of CSH particles obtained at 20°C and 80°C showed that the size of CSH particles in high temperature system are about half the size of particles formed at lower temperatures. The final result recorded at 365-days revealed the difference of 2 GPa between WG and WGE-W, where WGE-W showed lower elastic modulus. It can also be noted that there was about 5% decrease in long-term elastic modulus of WGE-W at 365-days compared to WG mix, whereas this reduction in the GP class was found to be about 8%. Although WG series showed increase in both strength and elastic modulus with curing age, it is important to note that the difference between long-term compressive strengths of WG and WGE-W was found to be significant, whereas very small variation was noticed in their long-term elastic modulus.

The result from 7-days elastic modulus measurements demonstrated a reduction of 25% in WGE-D compared to WG. Nevertheless, at 28-days, the elastic modulus of dry-cured specimens (WGE-D) was found to be 18%-25% lower in comparison to standard-cured (WG) and wet-cured (WGE-W) specimens. The effects of additional wet curing on elastic modulus development are evident with the WGE-D specimens having 90-days elastic modulus approximately 5.9 GPa lower than the elevated cured samples with additional wet curing (WGE-W) and 8.2 GPa lower than standard cured WG mix. Overall, an increase of about 14% was observed in elastic modulus of WGE-D specimens between 90-days and 365-days. The data obtained from tests done on WGE-D specimens also demonstrated that there was a reduction in the rate of elastic modulus gain with the curing time. Generally, these results are comparable to Koibuchi et al. (1991), Frías (2006b) and Kjellsen et al. (1990) who showed that the exposure to high temperatures at early age, lead to a drop in the long-term mechanical properties due to the increase of the pores number in the cementitious matrix.

7.3.3 Effects of accelerated curing on elastic modulus of unwashed glass modified self-compacting concrete

The performance of unwashed glass (UG) class of mixes in terms of elastic modulus development, throughout the curing time of 7-days to 365-days, has been exhibited in Figure 7.13. It can be seen that heat treatment given to unwashed glass modified concrete could still not provide satisfactory results since organic content in UG had a strong retarding effect on the elastic modulus. The measured elastic modulus measurement showed that there was an increase of 2.3 GPa in UGE-W mix between 7 and 28 days, which is approximately similar to the standard UG mix during the same curing period. An increase of about 20% was observed from 28 to 90 days in UGE-W, whereas UG only increased by approximately 5% during these curing periods. However, after 90-days, UGE-W did not demonstrate much improvement as there was a small increase of approximately 3.1 GPa from 90-days to 365-days in UGE-W. The elastic modulus measurements done on UGE-D revealed that the initial elastic modulus gained by UGE-D at 7-days was approximately 42% lower than the initial elastic modulus achieved by the standard UG specimens. However, the performance of UGE-D became worse in comparison to UG at the curing age of 28-days as it demonstrated approximately 45% lower elastic modulus than UG. UGE-D showed only 1.4 GPa increase in elastic modulus from 90-days to 365-days, which indicates the importance of curing temperature and curing environment in the development of elastic modulus. It can also be observed that the impurities present in unwashed glass mixes reduced the development in elastic modulus, although treated with elevated curing temperature that triggered its pozzolanic as well as hydration reactions.

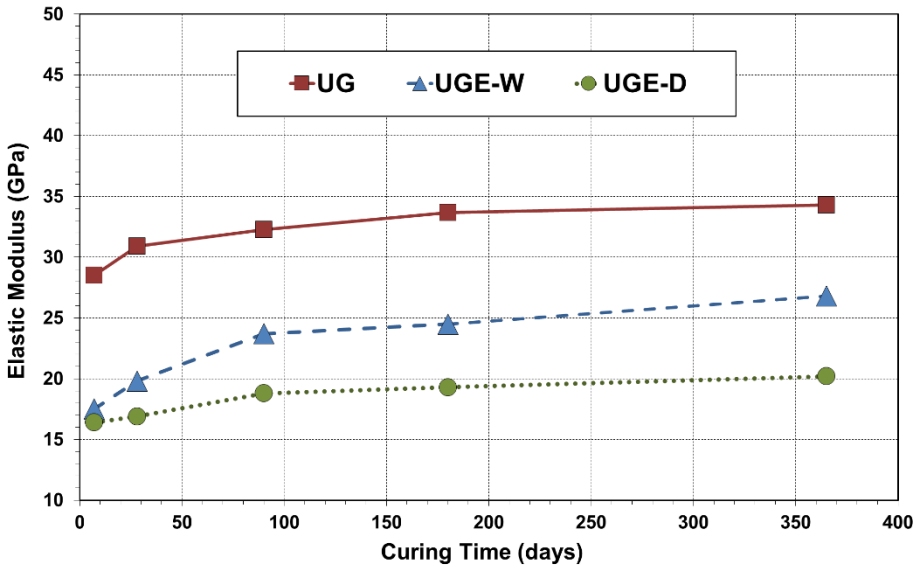

Figure 7.13: Elastic modulus development in UG subjected to different curing conditions

7.3.4 Consolidated summary of elastic modulus results

In order to obtain the clear view of the effects of elevated temperature treatment on SCC mixes, the data obtained from the elastic modulus tests undertaken on elevated wet-cured and dry-cured FA, UG and WG specimens and elevated dry-cured GP specimens were correlated to the elastic modulus achieved for elevated wet-cured GP mix. The consolidated results for elastic modulus are demonstrated in Figure 7.14. Elastic modulus factor was calculated by dividing each wet-cured and dry-cured elastic modulus value by the elastic modulus value of wet-cured control GP mix. Hence, the data points of GPE-W were adjusted at elastic modulus factors of 1 in order to determine the elastic modulus factors of the remaining wet-cured and dry-cured specimens. In general, it was observed that washed glass mixes, either wet-cured or dry-cured, demonstrated the most comparable behaviour to GP series. FAE-W was found to be slightly lower than WGE-W, whereas dry-cured FA specimens showed considerably worse performance than dry-cured WG specimens when correlated with GPE-D mix. In addition, similar correlation of unwashed glass in terms of elastic modulus was observed as that was noticed in the case of compressive strength.

7.3.5 Relationship between elastic modulus and compressive strength in elevated cured specimens

Most of the code relationships between compressive strength and elastic modulus have been developed based on experimental data for concrete cured at normal temperature and tested at 28-days. To apply the relationship to concretes cured at other curing temperatures or tested at different ages, it is necessary to examine validity of the relationships at different

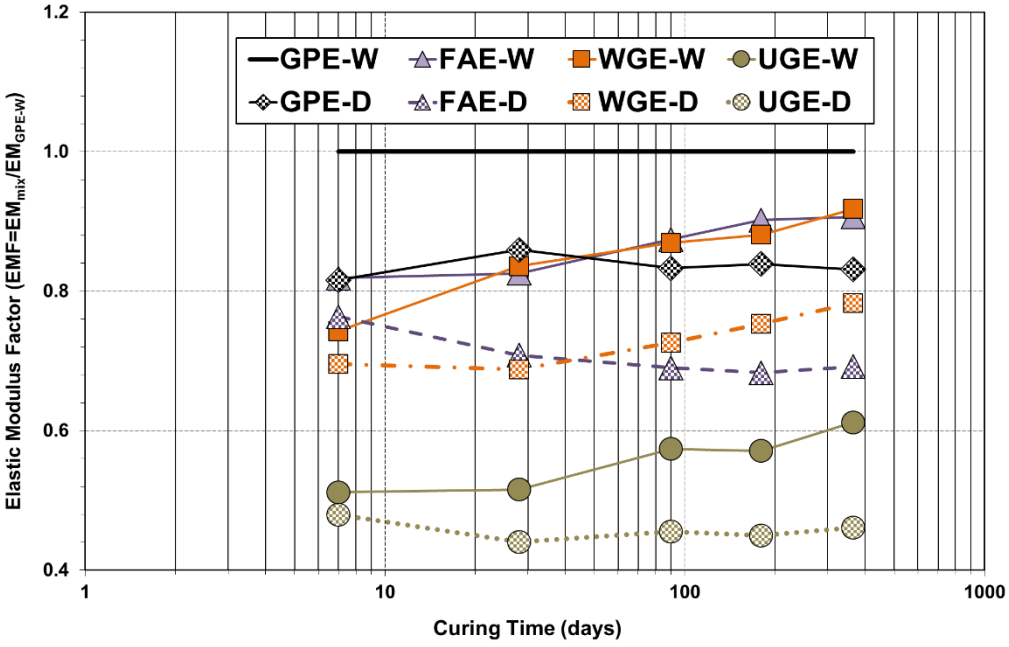

Figure 7.14: Consolidated summary of elastic modulus data for elevated cured specimens

temperatures and ages (CEB-FIP Model Code 1990, 1993; ACI 318-95, 1995; ACI Committee 363, 1992; Ahmad and Shah, 1985; Oluokun, 1991). However, very limited number of researchers have investigated their relationship when treated with higher curing temperatures. Figure 7.15 and Figure 7.16 demonstrate the relationships between elastic modulus and compressive strength based on the curing regime after initial accelerated curing. It can be observed that the difference in elastic modulus at the same compressive strength by binder typse is higher than ±5% in the interval considered. Moreover, regression

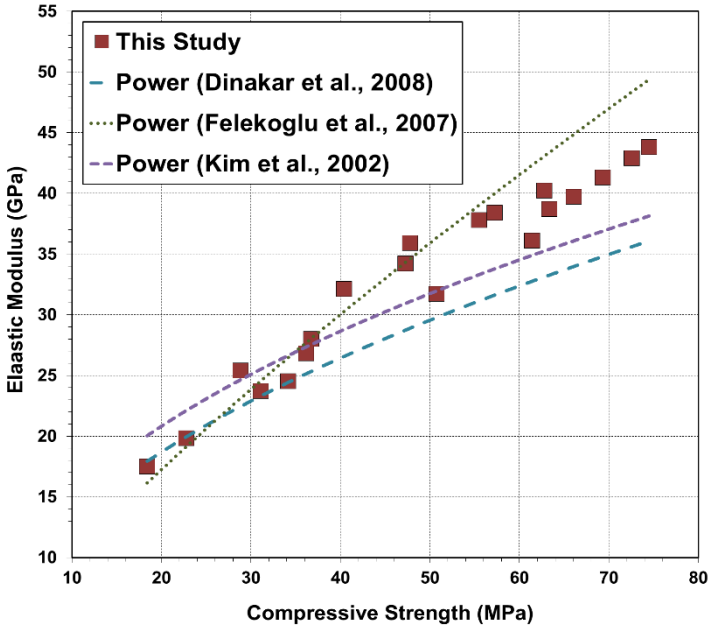

Figure 7.15: Relationship between compressive strength and elastic modulus in wet-cured specimens initially subjected to elevated curing

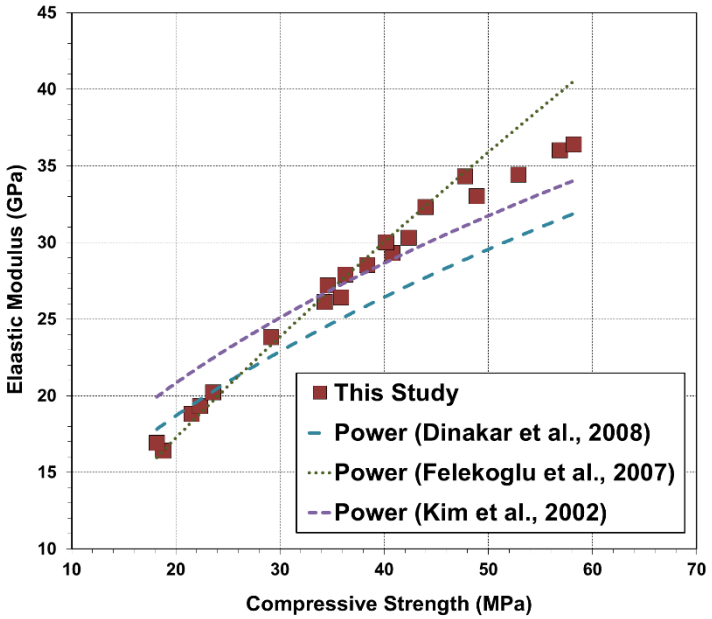

Figure 7.16: Relationship between compressive strength and elastic modulus in dry-cured specimens initially subjected to elevated curing

curves also consider concrete maturity. The results reveal that although the type of binder considerably affects the relationship between compressive strength and elastic modulus but the curing age does not substantially affect their relationship. The correlation between compressive strength and elastic modulus was compared with the previous studies undertaken by Dinakar et al. (2008), Felekoglu et al. (2007) and Kim et al. (2002). It is essential to recognize that the proposed models by Dinakar et al. (2008) [$E_c = 4180\sqrt{fc'}$] and Felekoglu et al. (2007) [$E_c = 1.57fc'^{0.8}$] have been based on standard-cured SCC specimens, whereas the model presented by Kim et al. (2002) [$E_c = 5250fc'^{0.46}$] has been established for higher curing temperatures. The experimental data obtained in this study fits within the previous experimental results rather well. It can be seen that the model proposed by Dinakar et al. (2008) almost accurately estimates the elastic modulus for concretes with compressive strengths under 30 MPa, most of which are from UGE specimens. In addition, Felekoglu et al. (2007) and Kim et al. (2002) models for concrete with compressive strengths over 30 MPa provides reasonable estimate of the relationship between the compressive strength and elastic modulus. This implies that the models produced for the relationship between elastic modulus and compressive strength can be used regardless of curing temperature and aging. Kim et al. (2002) similarly reported that the relationship between elastic modulus and compressive strength is independent of the initial curing temperature. However, few variations observed in elastic modulus corresponding to compressive strength with different SCC's can be attributed to two reasons. First the strength grade of tested SCCs by researchers are not the same. Second the powder ingredients of SCC's prepared by researchers are all different. Most importantly, the reactivity or inert nature of binder changes the strength characteristics and stress strain relations of mixtures. Hence, the data points outside the boundary of the previously established models might be related to the increase in the elastic modulus of SCC specimens due to the presence of glass powder.

7.4 Effects of accelerated curing on oxygen permeability of self-compacting concrete

Although initial curing at elevated temperature has already been established to result in a higher early-age strength but lower ultimate-strength in cement-based systems; however, in recent years, elevated temperature curing has been also applied to achieve higher early-age durability properties (ASTM C1202-12; Ozyildirim, 1998). At the microstructural level, the reduction in strength due to the elevated curing correlates with a higher capillary porosity (Scrivener and Young, 1995). To elaborate, elevated temperature treatment changes the microstructure of cement pastes, which affects the composition and structure of hydrates, ionic concentrations of pore solution, pore size distribution and micro-cracking. These

modifications can encourage the ingress of aggressive agents, such as gases, or the formation of expensive delayed ettringite and alkali-silica gels, and are function of the level of temperature and duration of the heat treatment. However, the products of cement hydration have low solubility and at high curing temperatures, the faster hydration does not allow sufficient time for the products to diffuse within the voids. This leads to a high concentration of hydration products in a zone immediately enclosing the grain, creating a relatively impermeable rim around the cement grain, hindering its further hydration (Verbeck and Helmuth, 1968) and leading to degradation. Oxygen permeability test is used to predict the resistance of concrete against carbonation, which is of critical significance (Beushausen and Burmeister, 2015) because it measures the pore network through which gaseous diffusion occurs in concrete. Carbonation process in concrete is both diffusion controlled and reaction controlled; relatively dry conditions are required for diffusion of CO_2, while higher moisture contents are needed for the carbonation reaction itself. Permeability of concrete increases as the quality of curing decreases. As strength increases, the effect of curing on microstructural quality tends to diminish due to refinement in the microstructure that limits the rate and extent of drying.

The present section contains the findings from the experimental study on oxygen permeability of a range of SCC mixes, including control binders as well as glass powders of different qualities but added at the constant replacement rate and subsequently treated with accelerated initial temperature. To comprehend the influence of curing temperature on the coefficient of permeability (K-value), the K-values of the specimens initially cured at 50°C were correlated to the K-values of its counterpart SCC type cured at 21°C. The oxygen permeability measurements were taken at 3, 7; 28, 90; 180 and 365 days for early, normal and long-term performance respectively and have been demonstrated in Figures 7.17 - 7.20. The average K-values were obtained from four replicate specimens taken out from two identical SCC samples at each curing age. Complete data are shown in Appendix F.

7.4.1 Effects of accelerated curing on oxygen permeability of control self-compacting concrete mixes incorporating GP cement and Fly Ash

The results from oxygen permeability testing demonstrated an increase in the early-age K-value of the GP specimens subjected to an elevated curing compared to the standard-cured GP specimens, as shown in Figure 7.17. GPE-W exhibited K-value of 5.59E-11 m/s at 3-days, which was higher than GP by 26%, possibly due to the immediate effect of higher initial curing temperature. Furthermore, the measured K-value of GPE-W showed the reduction of approximately 14% between 7 and 28 days, which is two times higher than the decrease found in GP during this period. Again at 28-days, there was difference of 43%

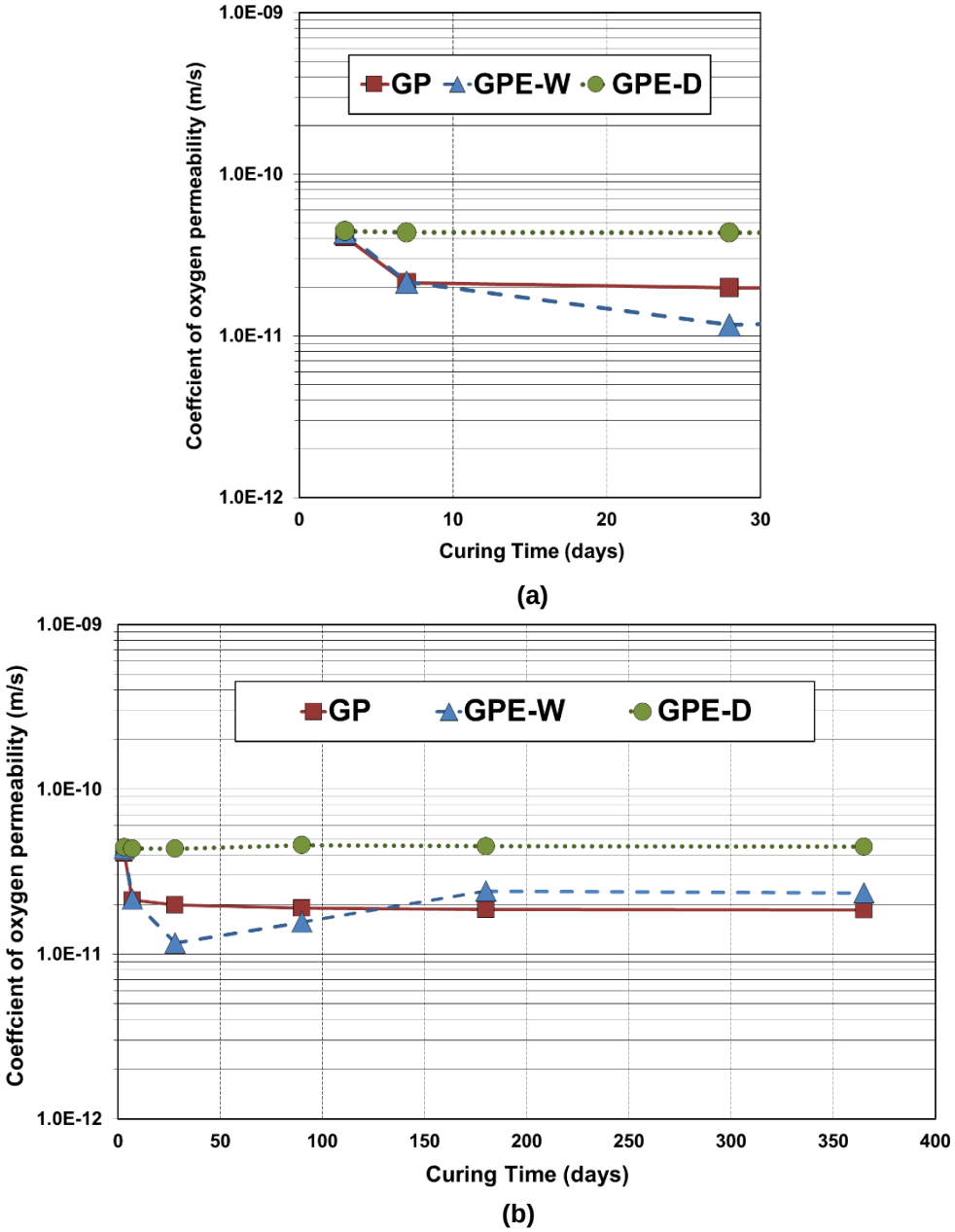

Figure 7.17: Coefficients of oxygen permeability in GP subjected to different curing conditions from curing age of (a) 3 to 28 days (b) 3 to 365 days

between K-values of GPE-W and GP with the latter being lower. With the progress in curing up to 90-days, the K-value of wet-cured elevated curing specimen (GPE-W) started to increase but still remained slightly lower that of the standard curing control (GP) mix. This might be linked to the fact that concrete is a complex heterogeneous material and hence, perfect trends in the results cannot be expected. There might be some variability in the testing for these results. There was some variability in the testing of different concrete cylinders since this test was repeated. The data achieved was variable and in thesis, average values of all tests have been reported. It has been established that when there is a development of dense hydration product, there is also a development of greater volume of

large pores and a coarser pore structure, which makes the concrete more susceptible to attack by harmful substances such as gases. Kjellsen et al. (1990) performed an investigation of the pore structure of plain cement pastes hydrated at 5°C, 20°C and 50°C and presented the similar information. Acquaye (2006) further clarified that the formation of large pores at high curing temperature occurs because low diffusivity of the hydration products does not permit uniform distribution due to the rapid rate of reaction. The final data recorded at 365-days revealed that the K-value of GPE-W was about 1.8 times higher than standard GP mix. These results are consistent to Gotto and Roy (1981) who reported that curing at 60°C results in a much higher volume of pores larger than 150 nm in diameter compared to curing at 27°C, which makes the concrete more permeable to harmful substances since they provide an easier pathway through the concrete. Few other studies (Cao and Detwiler, 1995; Lothenbach et al., 2007) also presented similar findings and explanations.

There seemed to be considerably small and inconsistent variations in K-values for GPE-D specimen between 3-days and 365-days after casting. The K-value of GPE-D at 3-days was 6.55E-11 m/s compared to 4.10E-11 m/s for GP. Dry-curing subsequent to elevated curing resulted in the difference of 61% between K-values of GP and GPE-D at 7-days, where GPE-D showed the higher K-value. Reduction of 15% in K-value was observed in GPE-D at 28-days compared to 7-days. The influence of additional wet-curing on oxygen permeability became clear with GPE-D specimens having 90-days K-value about 26% higher than GPE-W and approximately 58% higher than GP. A discrepancy in results was observed at 180-days when the K-value increased; however, it was found that there was again a reduction in K-values with the curing time from 180-days onwards. Overall, an insignificant decrease of 1% was observed in K-value of GPE-D specimens between 180-days and 365-days in comparison to approximately 2% decrease in GPE-W specimens during the same curing period. In general, K-values of water-cured specimens remained lower than dry-cured specimens at all the tested curing ages. This might be related to the termination of external moist curing in GPE-D, necessary for its hydration reaction to continue and drop in its internal relative humidity in the absence of ambient environment, which affected its permeation resistance.

According to Fraay et al. (1989), the reaction of FA requires an increase in alkalinity, which is achieved by the reaction of GP cement. The FA reaction takes place sooner at higher temperatures because of the increased hydration rate of GP cement. When the pH of the pore water becomes high enough, the products of reaction of FA are produced in the FA particles as well as in their proximity. As the time progresses, further products diffuse away and precipitate within the capillary pore system, which results in a decrease of the capillary

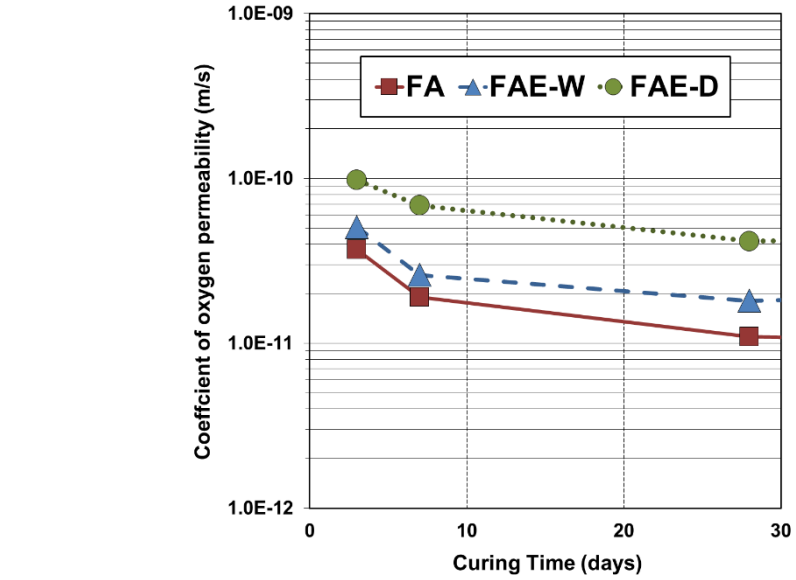

(a)

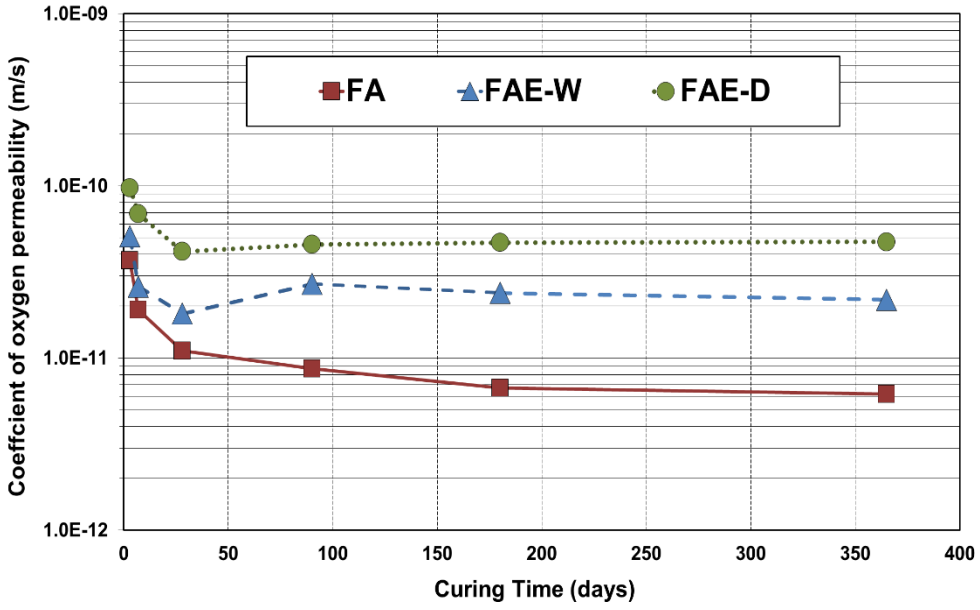

(b)

Figure 7.18: Coefficients of oxygen permeability in FA subjected to different curing conditions from curing age of (a) 3 to 28 days (b) 3 to 365 days

porosity and hence, a finer pore structure is achieved (Fraay et al, 1989). Consistent behaviour was observed in FA specimens tested in this study. The K-values in FA class of mixes from the curing period of 3-days to 365-days has been demonstrated in Figure 7.18. The measured K-value of FAE-W was found to be 5.05E-11 m/s at 3-days in comparison to 3.70E-11 m/s in the standard FA mix at the same curing period. The variation of 36% was observed at 7-daysbetween FA and FAE-W, with the former being lower. At 28-days, however, the K-value of FAE-W was 56% higher than FA. With the progress in curing time, FAE-W demonstrated a decrease of approximately 13% from 28 to 90 days, but its K-value

was still higher than FA by about 61%. Furthermore, it was revealed that FAE-W demonstrated 70% higher K-value than FA at 180-days. There was a considerably lower decrease of 2% from 180-days to 365-days of wet-curing in FAE-W as compared to a decrease of approximately 8% in the standard mix (FA) within this curing time, which confirms a significant change in the microstructure of FAE-W specimens with the elevated curing.

In general, an increase in the initial curing temperature did not significantly increase permeation resistance of FA incorporated dry-cured samples (FAE-D). FAE-D did not show considerable variation in K-values, once they reached their initial permeation resistance. At an early-age of 3-days, a significant increase in K-value (27%) was noticed in FAE-D in comparison to FA. The K-values of FA at 7-days was 1.91E-11 m/s compared to 4.26E-11 m/s in the case of FAE-D. Nevertheless, the K-value of FAE-D was found to be approximately 30%-70% higher in comparison to FA and FAE-W at 28-days. There was a decrease of 8% in K-value of FAE-D from 28-days to 90-days in comparison to approximately 27% loss in FA during similar curing period. However, a continuous but relatively small decrease in K-values of FAE-D was observed, starting from 90-days up to 365-days of testing, whereas FA reduced approximately 41% during this curing period. The overall results obtained from dry-curing of FA modified mixes demonstrate that FA appears to have lower capability of showing satisfactory durability performance in the absence of external water curing.

7.4.2 Effects of accelerated curing on oxygen permeability of washed glass modified self-compacting concrete

The oxygen permeability tests done on WG series showed an increase in K-values of WGE-W specimens subjected to an elevated curing compared to the normally-cured WG specimens as shown in Figure 7.19. At the early-age of 3-days, WGE-W showed 16% higher K-value in comparison to WG, exhibiting its lower resistance to oxygen permeation than WG. This result can be related to the presence of micro-cracks (Hakkinen, 1993) and increase of capillary porosity (Bentur et al., 1979) in WGE-W resulting from the accelerated curing. The measured K-value of the elevated temperature followed by wet curing (WGE-W) showed a substantial decrease of approximately 35% between 7 and 28 days, which is more than the decrease found in WG standard cured control mix during this period. However, at 90-days, the K-value of WGE-W was about 55% more than that of WG mix. The final result recorded at 365-days revealed the difference of approximately 62% between WG and WGE-W, where WGE-W was higher. The reduction in K-value over time for all specimens subjected to wet-curing indicates continuous hydration and refinement of the pore structure with water curing.

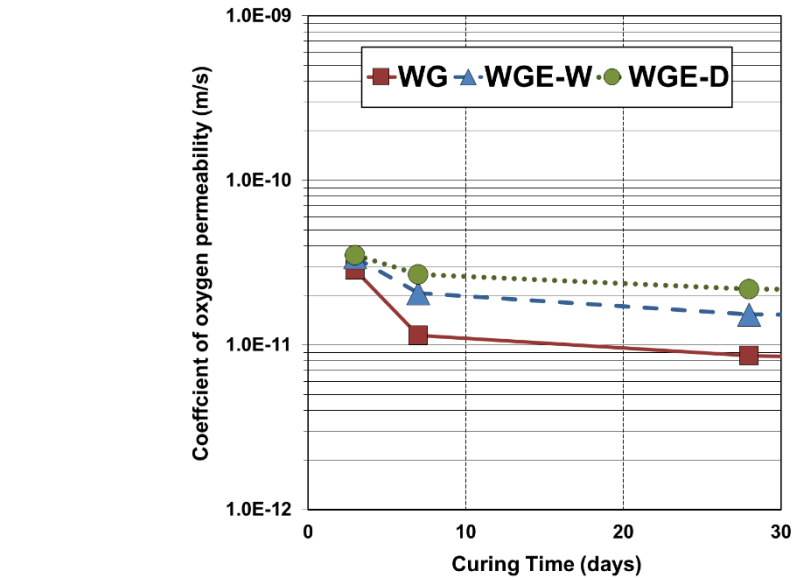

(a)

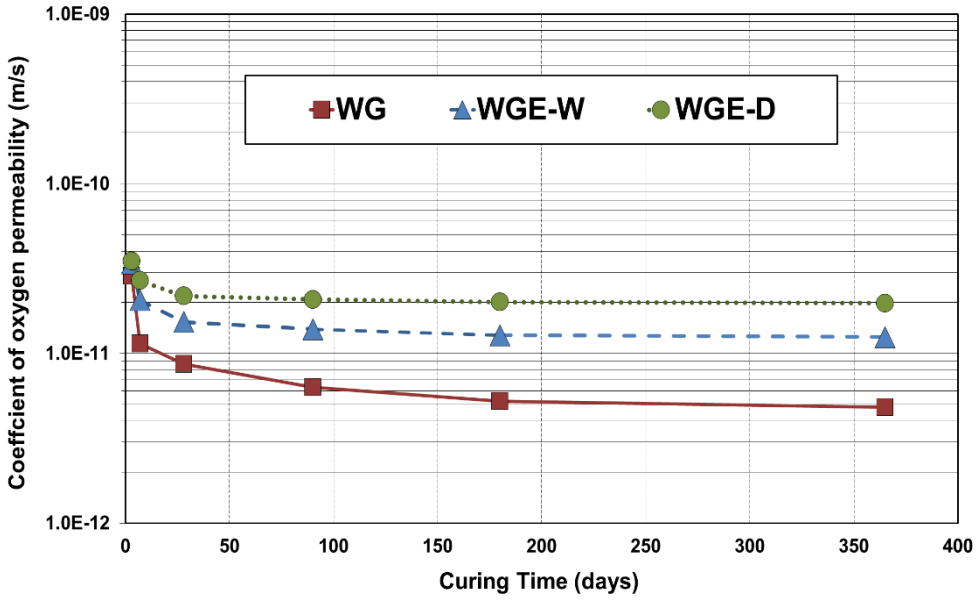

(b)

Figure 7.19: Coefficients of oxygen permeability in WG subjected to different curing conditions from curing age of (a) 3 to 28 days (b) 3 to 365 days

The results obtained in this study also suggest that due to the difference in thermal expansion coefficients of cement and glass powder, heating promotes the development of micro-cracks and porosity inside the concrete, which ultimately encourages the ingress to aggressive gases, similarly pointed out by Kjellsen and Detwiler (1993), Verbeck and Helmuth (1968) and Carino (1981).

A noticeable change in K-values was observed in WGE-D specimens between 3-days and 365-days after casting. The results from 3-days K-value measurements exhibited an increase of approximately 19% in WGE-D specimens subjected to an elevated curing

compared to the normally-cured WG specimens. From 3-days to 7-days, the decrease in K-value of WGE-D was about 31%, which is significantly lower than WGE-W observed at 65%. At 28-days, however, the K-value of WGE-D was found to be 30%-60% higher in comparison to WG and WGE-W. Overall, a small decrease of 5% was observed in K-values of WGE-D between 90-days and 365-days in comparison to approximately 11%-31% decrease in K-values of specimens WG and WGE-W during this curing period, possibly due to inhomogeneity in the microstructure of elevated cured specimens, which became worse with no subsequent water-curing. Regardless of its curing process, the K-values of WGE-D specimens indicate a concrete with low permeability. According to Alexander et al. (1999), such concrete would be considered to provide excellent durability protection. Overall, accelerated thermal curing without subsequent water-curing did not appear to compromise the resistance of the WG incorporated concrete to oxygen permeation, though additional water curing was observed to provide benefit for improving concrete's microstructure.

7.4.3 Effects of accelerated curing on oxygen permeability of unwashed glass modified self-compacting concrete

The performance of unwashed glass series in terms of oxygen permeation resistance, throughout the curing time of 3 to 365 days has been demonstrated in Figure 7.20. The K-values of UGE-W showed that there was decrease of approximately 35% between 3 and 7 days in comparison to 88% in UG during the same curing period. In addition, the reduction in K-value from 7-days to 28-days in UGE-W was approximately one fourth than UG incorporated SCC mix. An increase of about 48% was observed in UGE-W at 90-days in comparison to UG. At 180-days, the difference between K-values of UGE-W and UG samples was 47%, where the oxygen permeation resistance shown by UG was significantly

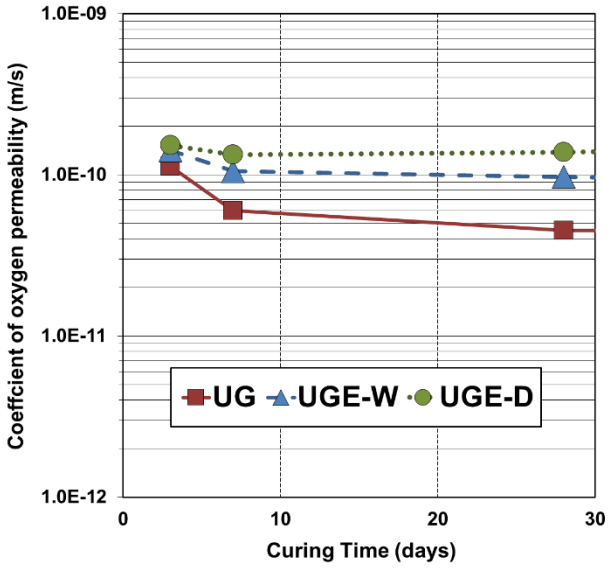

(a)

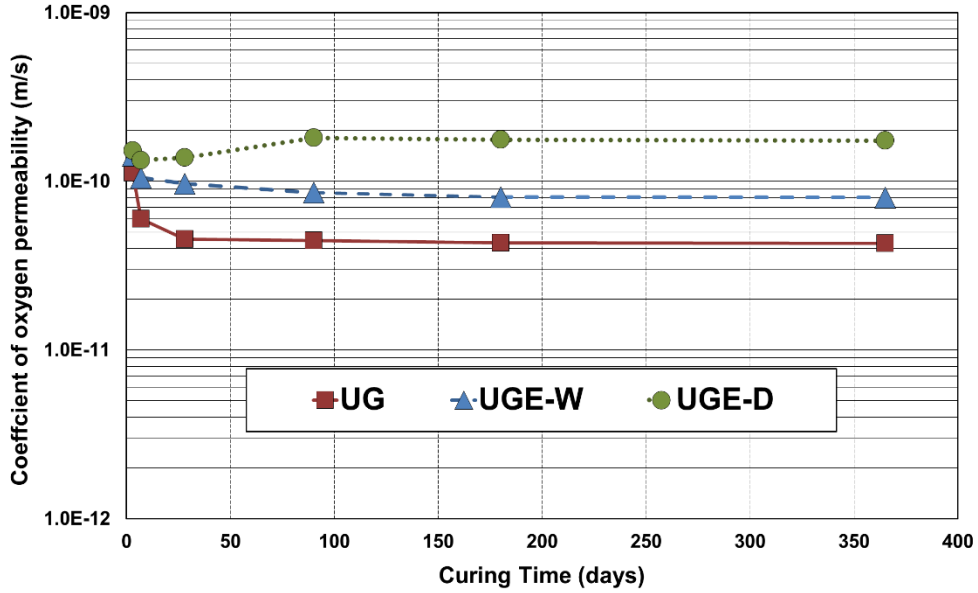

(b)

Figure 7.20: Coefficients of oxygen permeability in UG subjected to different curing conditions from curing age of (a) 3 to 28 days (b) 3 to 365 days

better than UGE-W. However, after 180-days, UGE-W and UG specimens did not show much reduction in K-values. There was almost similar reduction of 0.9% from 180 to 365 days in UGE-W compared to the reduction of about 0.6% in UG within this curing time.

The results from oxygen permeability tests informed that the K-value obtained by UGE-D at 3-days was approximately 43% higher than the K-value achieved by UG specimens. As the curing time progressed to 7-days, UGE-D approached the K-value of almost 2.6 times higher than UG. Subsequently, the performance of UGE-D became worse in comparison to UG as it continued to decrease and hence, at the curing age of 28-days, it demonstrated approximately 64% higher K-value than UG. Moreover, UGE-D showed only about 5% reduction in K-values from 90-days to 365-days compared to approximately 7% reduction in UGE-W, which demonstrates the importance of curing temperature and curing environment for improving permeation resistance of concrete. In general, this study conforms to the Clause C3.6 of NZS 3101:Part 2 that accelerated curing generally has a detrimental effect on durability, which is reasonably significant for SCM concretes, hence, 7-days water curing should be maintained after the completion of the accelerated curing cycle. Since these dry-cured specimens were not kept in the suggested curing environment for an appropriate time period, concrete could not reach satisfactory oxygen penetration resistance.

7.4.4 Consolidated summary of coefficient of permeability results

In addition to the compressive strength and elastic modulus, the data obtained from the oxygen permeability tests performed on elevated wet-cured and dry-cured FA, UG and WG

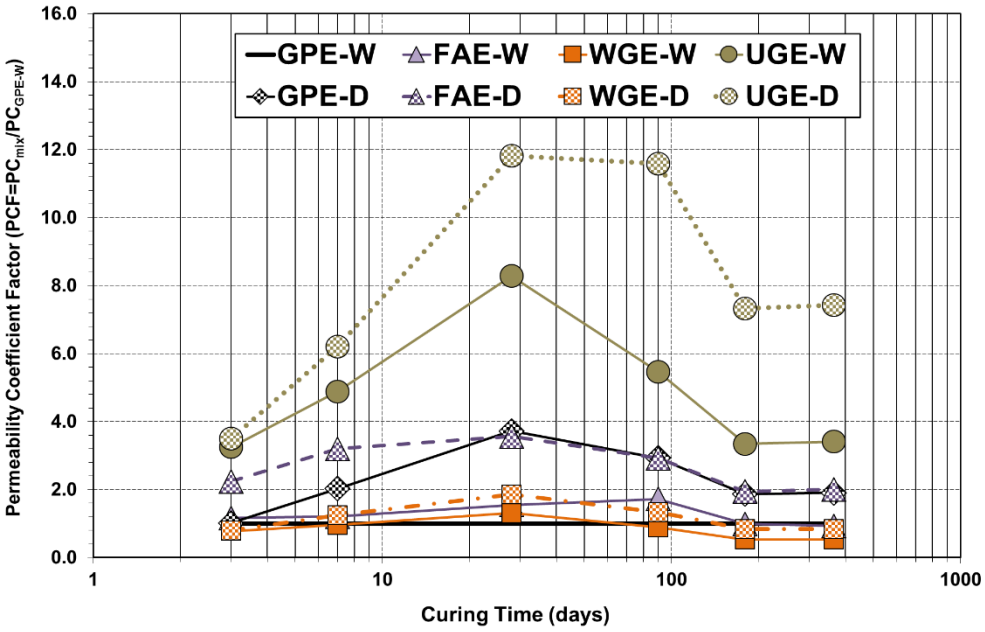

Figure 7.21: Consolidated summary of coefficient of permeability data for elevated cured specimens

specimens and elevated dry-cured GP specimens were correlated to the coefficient of permeability achieved for elevated wet-cured GP mix. The consolidated results for coefficient of permeability are illustrated in Figure 7.21. Coefficient of permeability factor was calculated by dividing each wet-cured and dry-cured coefficient of permeability value by the coefficient of permeability value of wet-cured GP mix. This means that the data points of GPE-W were fixed at the coefficient of permeability factor of 1 in order to determine the coefficient of permeability factors of the remaining specimens. It was observed that the wet-cured washed glass mix showed marginally better permeation resistance than the wet-cured GP mix. In addition, the dry-cured washed glass mix exceeded in the carbonation resistance than both the wet-cured and dry-cured GP mixes. However, FAE-W had almost similar correlation to GPE-W as that of WGE-D. The dry-cured unwashed glass mix exhibited poor performance in relation to the GP series as well as the other dry-cured and wet-cured SCC mixes; however, the wet-cured unwashed glass mix had significantly better correlation with GPE-W.

7.4.5 Relationship between coefficient of oxygen permeability and compressive strength in elevated cured specimens

Since both strength and transport characteristics are interrelated to the pore structure of concrete, it is desirable to predict the long-term permeability of concrete from compressive strength. Therefore, relationships between coefficient of oxygen permeability and compressive strength based on the curing regime after initial accelerated temperature treatment have been developed and are demonstrated in Figure 7.22 and Figure 7.23. The correlations revealed that binder type considerably affects the relationship between

compressive strength and coefficient of oxygen permeability. A number of variations were observed in the correlations between coefficient of permeability and compressive strength of GP and FA incorporated SCC mixes at early-ages of testing. On the other hand, both unwashed and washed glass mixes showed excellent correlations between these parameters in both cases of wet and dry curing. It is also evident that for same compressive

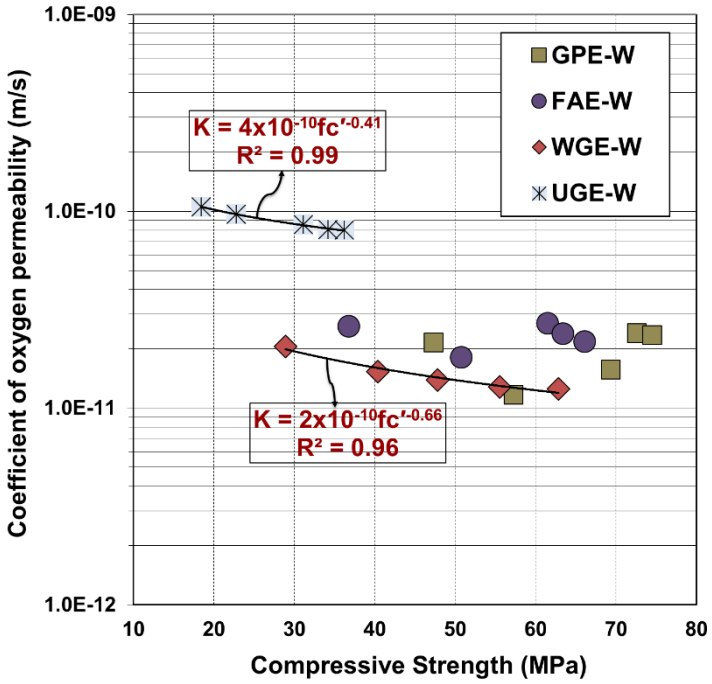

Figure 7.22: Relationship between compressive strength and coefficient of oxygen permeability in wet-cured specimens initially subjected to elevated curing

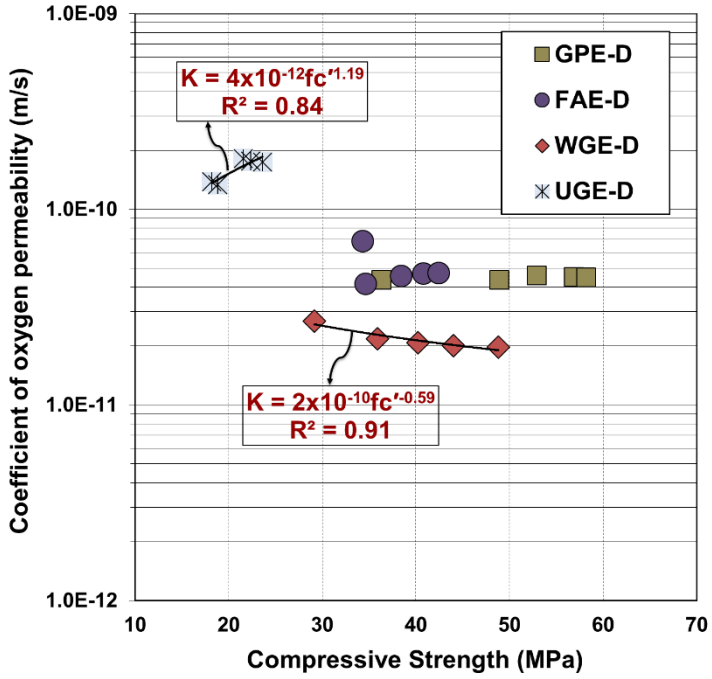

Figure 7.23: Relationship between compressive strength and coefficient of oxygen permeability in dry-cured specimens initially subjected to elevated curing

strengths,lower K-values were mostly achieved for washed glass incorporating samples, regardless of their subsequent curing regime after accelerated curing, compared to GP and FA mixes. Contrarily, unwashed glass mix showed lower compressive strengths and its potential for long-term durability was observed to be worse compared to all other specimens.

7.5 Effects of accelerated curing on porosity of self-compacting concrete

Concrete has a complex microstructure made up of aggregate, calcium hydroxide, calcium silicate hydrate, hydrated and unhydrated cement grains, and pores. Apart from this, water that is not consumed in the hydration reactions remains in the microstructure of the pore space (Lo and Cui, 2004). These pores weaken concrete because calcium silicate hydrate bonds are unable to form in sufficient quantity to provide strength development. Generally, hardened cement paste can have two types of pores: capillary and gel. The gel pores are the spaces between the solid products of hydration within the cement gel, whereas the capillary pores are the spaces between the cement gel formed during the hydration of the cement grains. When saturated, these pores are usually filled with water that is strongly held to the solids but when exposed to drying conditions, these pores are emptied due to evaporation (Milestone and Gorce, 2012). As discussed before, the rapid initial rate of hydration at higher temperatures hinders further hydration of cement, producing a non-uniform distribution of the products of hydration within the paste microstructure. This condition does not arise at normal temperature curing, when there is sufficient time for the hydration products to diffuse and precipitate relatively uniformly all over the interstitial space among the cement grains. The rapid hydration at initial higher temperature appears to form products of a poorer physical structure, possibly more porous, so that some of the pores always remain unfilled (Verbeck and Helmuth, 1968). This leads to an increase in total porosity of elevated cured concrete.

The present section includes the results from the experimental investigation on porosity of a range of SCC mixes, containing control binders as well as glass powders of different qualities but added at the constant replacement rate and treated with accelerated initial temperature afterwards. To understand the effects of curing temperature, the porosities of the specimens initially cured at 50°C were correlated to the porosities of its counterpart SCC types cured at 21°C. The porosity measurements were taken at 3, 7; 28, 90; 180 and 365 days for early, normal and long-term performance respectively and have been demonstrated in Figures 7.24 - 7.27. The average porosities were obtained from four replicate specimens taken out from two identical SCC samples at each curing age. The same specimens used for oxygen permeability were later tested for porosity. The procedure for testing and analyzing data have already been discussed in Chapter 3. Complete data are shown in Appendix F.

7.5.1 Effects of accelerated curing on porosity of control self-compacting concrete mixes incorporating GP cement and Fly Ash

The results from porosity testing demonstrated an increase in the early-age porosity measurements of GP specimens subjected to an elevated curing compared to the standard-cured GP specimens as shown in Figure 7.24. GPE-W exhibited porosity of 13.2% at 3-days, which was higher than GP by approximately 5%. Furthermore, the porosity of GPE-W showed a reduction of approximately 4% between 7 and 28-days, which is slightly lower than the increase found in GP during this curing period. Nevertheless, at 28 days, there was a difference of 7% between the porosity measurements of GPE-W and GP with the former being higher. With the progress in curing period up to 90-days, the porosity of GPE-W continued to decrease and remained approximately 8% below that of GP mix. Water curing subsequent to elevated temperature curing resulted in 11% higher 180-days porosity to that of the standard curing. The continuous water-curing up to 365-days revealed the difference of 12% between GP and GPE-W, where GPE-W was higher. This difference can be related to a relatively uneven distribution of the hydration products of GPE-W that led to the formation of large pores. Identical results were observed in a study of the microstructure of cement pastes, hydrated at temperatures ranging from 5°C-50°C (Kjellsen et al., 1990). The authors reported that low curing temperatures result in a uniform distribution of hydration products and fine self-contained pores. On the other hand, elevated temperatures lead to a non-uniform distribution of the hydration products within the microstructure and coarse, interconnected pores. These large, coarse and interconnected pores allow for an easy transportation of harmful materials into concrete with an increased likelihood for the concrete structure to deteriorate prematurely (Kjellsen et al., 1990).

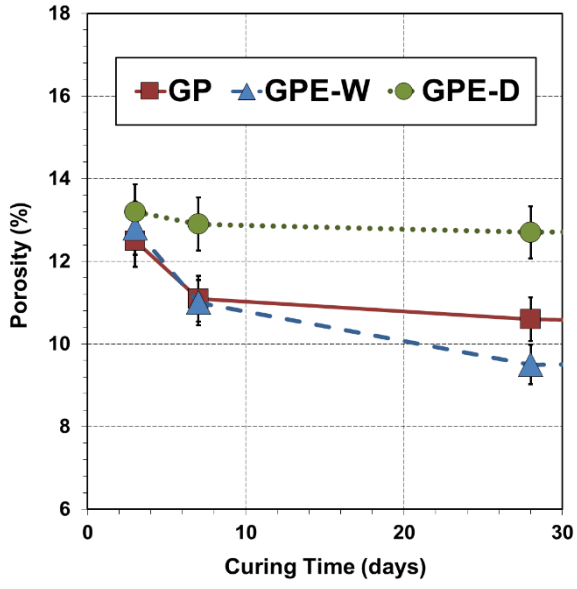

(a)

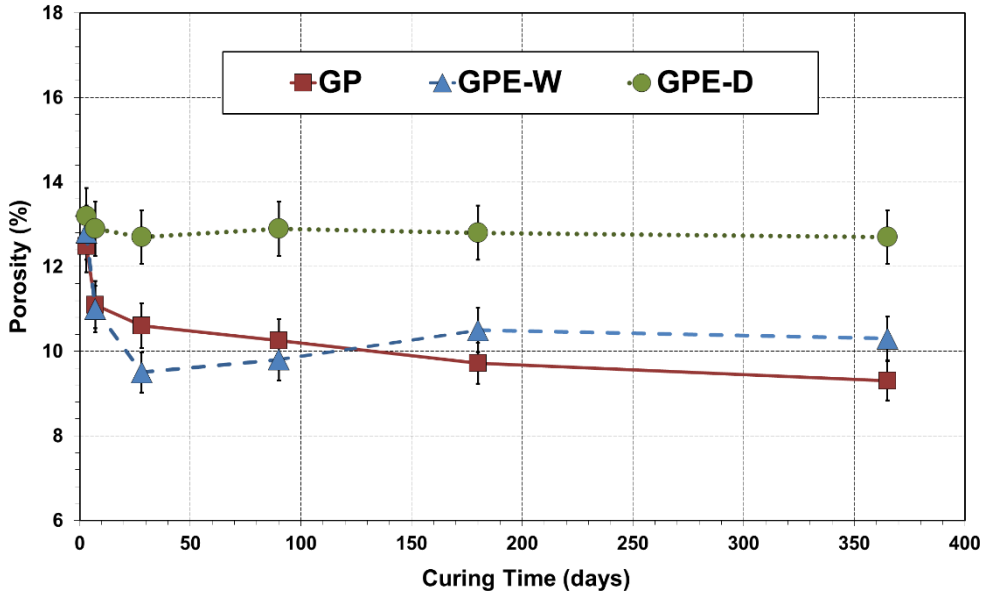

(b)

Figure 7.24: Porosity of GP subjected to different curing conditions from curing age of (a) 3 to 28 days (b) 3 to 365 days

Minor variations in porosity measurements of GPE-D specimens were noticed between 3 and 365 days. The porosity for GPE-D at 3-days was 13.2% compared to 12.5% for GP. Dry-curing subsequent to elevated curing resulted in the difference of 20% between the porosity of GP and GPE-D at 7-days, where GPE-D showed the higher value. A considerable reduction of 7% in porosity was observed in GPE-D at 28-days compared to 7-days. Moreover, GPE-D specimens achieved 90-days porosity approximately 13% higher than GPE-W and approximately 20% higher than GP specimens. A reduction of about 2% in porosity was observed at 90-days with respect to 28-days. From 90-days, it was found that the rate of porosity reduction with the curing time decreased to a considerable extent. No difference was observed in porosity of GPE-D specimens between 180 and 365 days in comparison to about 1% decrease in GPE-W specimens during the same curing period. This finding might be related to the retardation of subsequent cement hydration in the absence of external moist curing to GPE-D, after it lost its internal moisture for hydration process to continue. In an examination of the structure of the hydrated cement paste subjected to early high temperatures, similar findings were achieved by Goto and Roy (1981).

The porosity in FA mixes from the curing period of 3-days to 365-days has been demonstrated in Figure 7.25. The porosity of FAE-W was found to be 12.8% at 3-days in comparison to 11.8% in FA mix during the same curing period. The variation of approximately 5% was observed at 7-days between FA and FAE-W, when FAE-W was higher. At 28-days, however, the porosity in FAE-W was higher than FA, by an increase of about 10%. With the progress in curing time, it was revealed that FAE-W demonstrated 16%

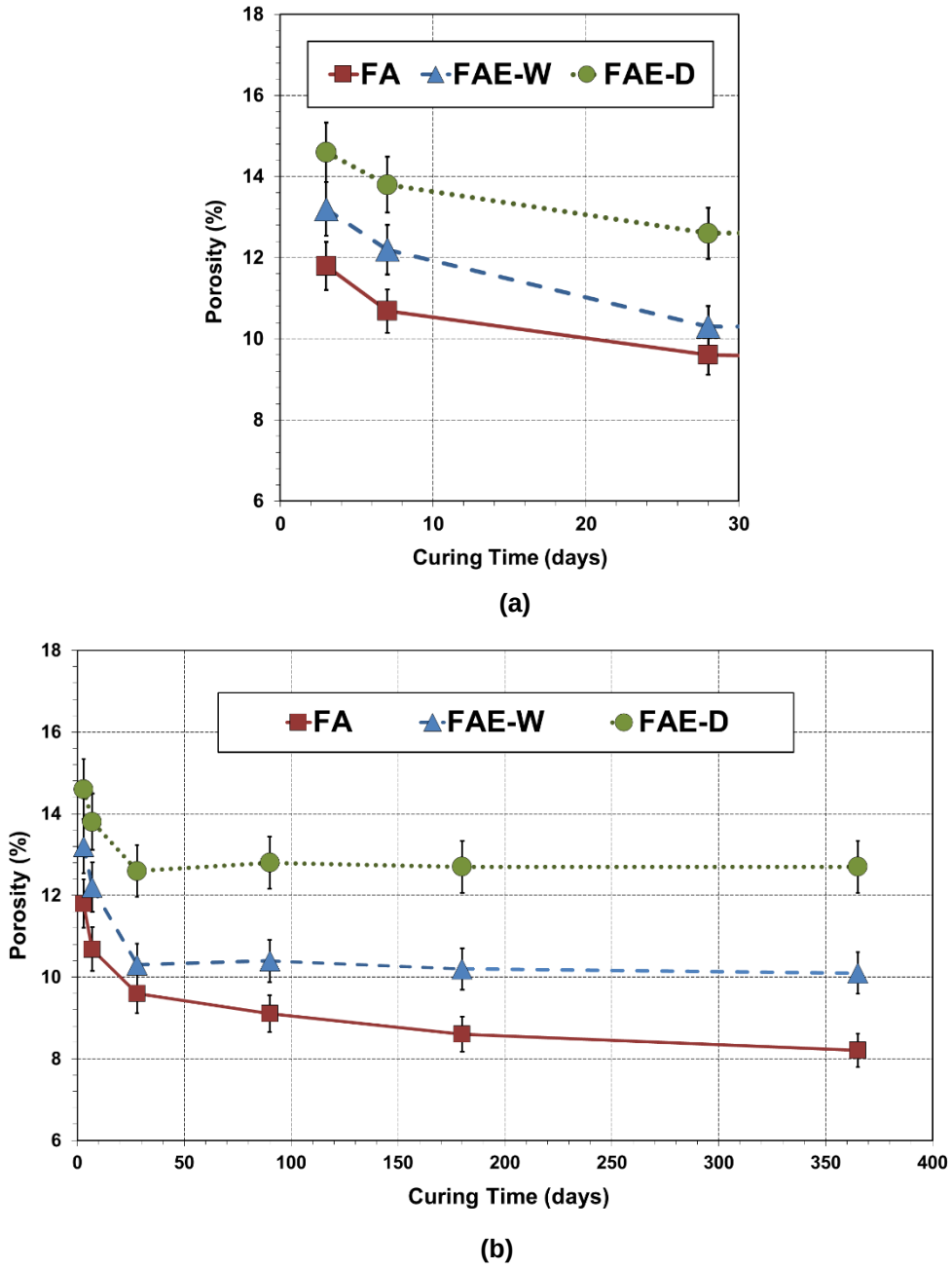

Figure 7.25: Porosity of FA subjected to different curing conditions from curing age of (a) 3 to 28 days (b) 3 to 365 days

higher porosity than FA at 180-days. There was a small decrease of 1% from 180-days to 365-days of wet-curing in FAE-W as compared to a two-fold decrease in FA within this curing time.

A significant increase of 10% in porosity was observed in FAE-D in comparison to FA at an early-age of 3-days. The porosity for FA at 7-days was 10.7% compared to 12.3% for FAE-D. However, the porosity of FAE-D was found to be approximately 10%-20% higher in comparison to FA and FAE-W at 28-days. Moreover, a further reduction in porosity was noticed in FAE-D at 90-days, similar to FAE-W specimens at this curing age. Nevertheless, a

minor decrease in porosity of FAE-D was observed, starting from 90-days up to 365-days of testing, whereas FA reduced approximately 8% during this curing period. The final data recorded at 365-days revealed that porosity measurement of FAE-D was approximately 13% higher than FAE-W. These results are consistent to the findings reported by Siddique and Khan (2011) that porosity of dry-cured concrete is higher than its corresponding wet-cured concrete with FA replacement; it is 9%-20% higher with 40% FA replacement level and 23%-40% higher at 50% FA replacement level.

7.5.2 Effects of accelerated curing on porosity of washed glass modified self-compacting concrete

The results from porosity tests done on washed glass series showed an increase in porosity of WGE-W specimens subjected to an elevated curing compared to WG specimens, as shown in Figure 7.26. At 3-days, WGE-W showed 8% higher porosity in comparison to WG, exhibiting its worse durability performance than WG. However, with the progress in curing time, WGE-W exhibited reduction of approximately 13% in porosity of 7 days in comparison to 3-days, though it was still somewhat higher than WG. The porosity of WGE-W showed a decrease of approximately 4% between 7-days and 28-days, which is 2.7 times less than the reduction found in WG during this period. At 90-days, however, the porosity of WGE-W was approximately 9% more than that of WG mix. As the curing time progressed, water curing subsequent to initial elevated temperature curing resulted in 13% higher 180-days porosity than that of the standard curing. The result noticed at 365-days showed the difference of approximately 13% between WG and WGE-W. The increase in porosity of WGE-W specimens could be a result of non-uniform diffusion of the hydration product in glass mix, as mentioned by Verbeck and Helmuth (1968). It could also be result of the formation of internal

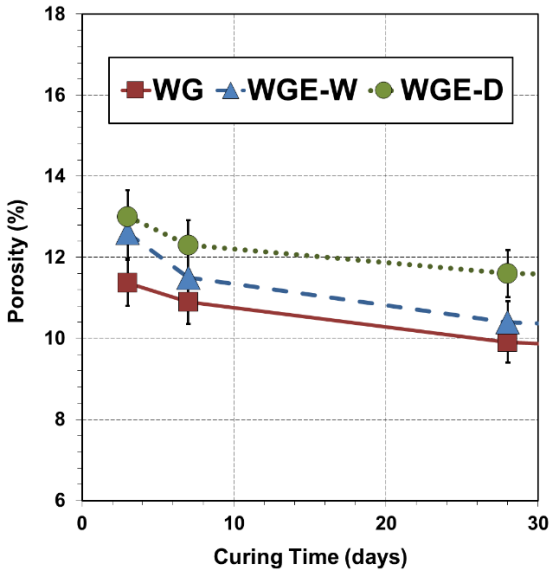

(a)

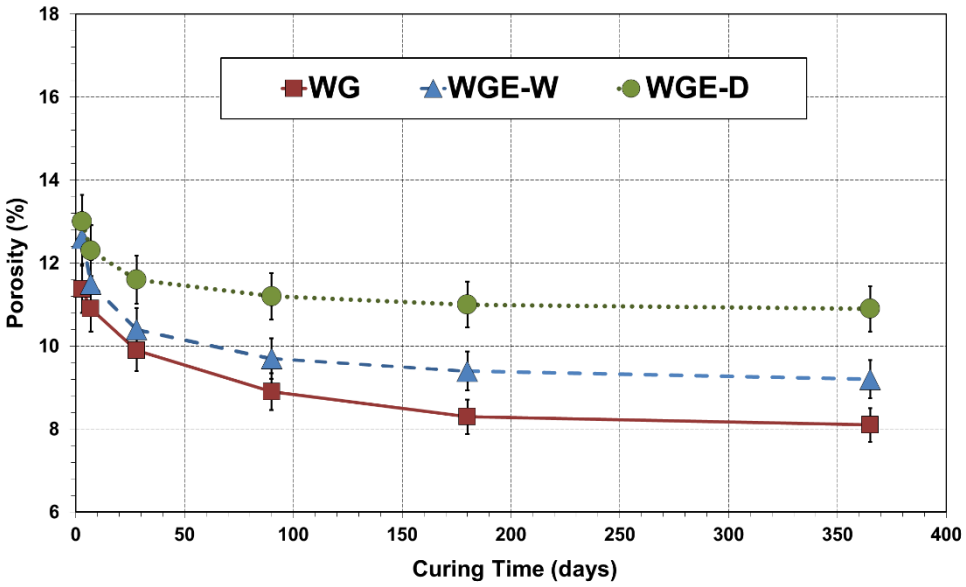

(b)

Figure 7.26: Porosity of WG subjected to different curing conditions from curing age of (a) 3 to 28 days (b) 3 to 365 days

stresses, exceeding the tensile strength of the immature glass concrete, which led to increased porosity and cracking, since the temperature was raised during early ages (Alexanderson, 1972). It can be noted that there was 11% increase in 365-days porosity of GPE-W compared to GP, while in case of WG class, this increase was found to be 13%.

A larger variation was observed in porosity measurements of WGE-D specimens between 3 and 365 days after casting. The results from 3-days measurements exhibited an increase of approximately 11% in WGE-D compared to WG. From 3 to 7 days, the decrease in porosity of WGE-D was about 6%, which is lower than the reduction of approximately 13% found in WGE-W. At 28-days, however, the porosity of WGE-D was found to be 9%-15% higher in comparison to WG and WGE-W. The WGE-D specimens had 90-days porosity approximately 13% and 21% higher than WGE-W and WG mixes. Overall, a small reduction of about 3% was observed in porosity of WGE-D specimens between 90 and 365 days in comparison to approximately 4%-9% decrease in porosity of specimens WG and WGE-W during the same curing period, possibly due to the inhomogeneity in the microstructure of WGE-D specimens as mentioned before. Incorporation of glass powder in concrete improved its behaviour, although it showed better durability performance with standard curing, it still lied within good durability range with subsequent dry and wet curing after elevated temperature treatment. Ling et al. (2012), however, presented partially conflicting results that there is a great increase in water porosity for both the water and air-cured specimens, in which water-cured specimens show the largest increase in porosity and the air-cured specimens have much lower porosity within the respective curing regime. The

variations in results can be related to differences in w/c as well as initial curing temperatures used as key parameters in these studies.

7.5.3 Effects of accelerated curing on porosity of unwashed glass modified self-compacting concrete

The performance of unwashed glass (UG) mixes in terms of porosity, throughout the curing time of 3-days to 365-days, has been demonstrated in Figure 7.27. The porosity of UGE-W showed that there was a decrease of about 11% between 3 and 7 days, which is almost similar to the reduction found in the standard UG mix during this curing period. In addition,

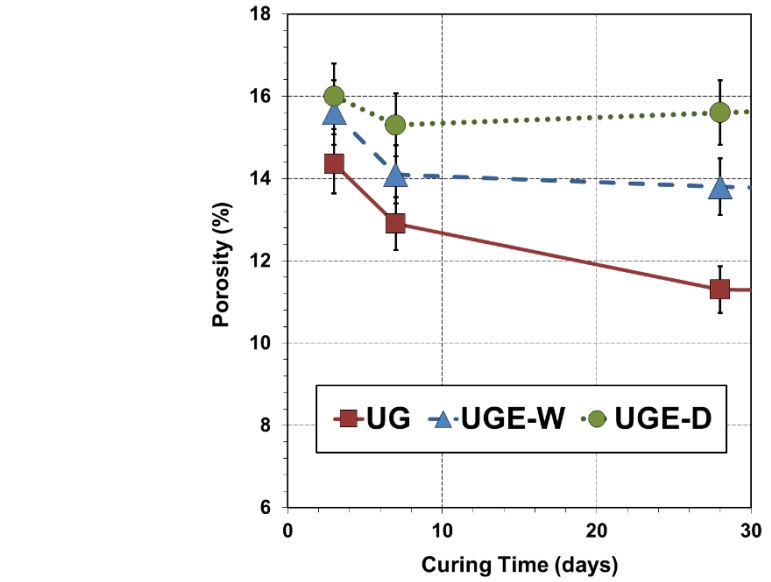

(a)

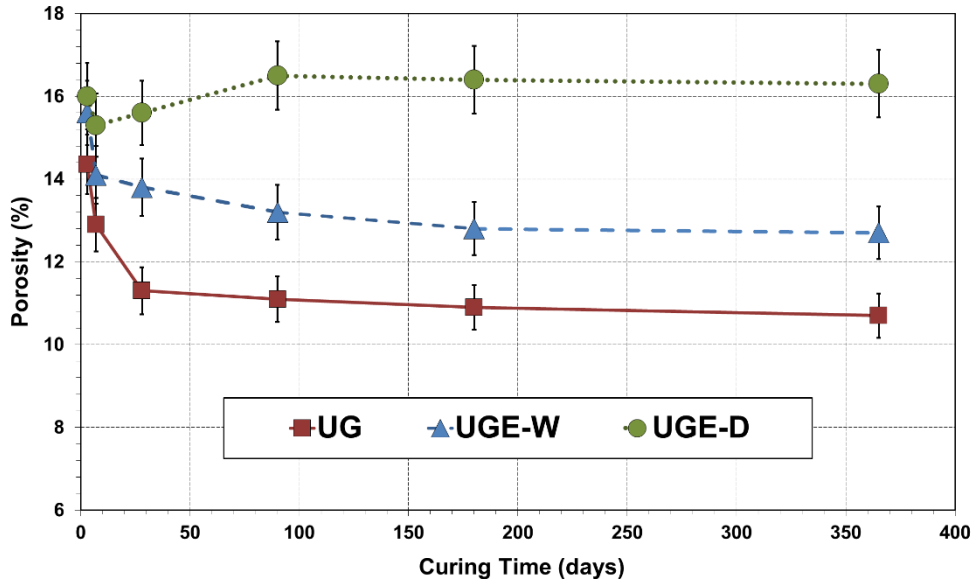

(b)

Figure 7.27: Porosity of UG subjected to different curing conditions from curing age of (a) 3 to 28-days (b) 3 to 365-days

the reduction in porosity from 7 to 28 days in UGE-W was about 4 times lower than the reduction observed in UG mix. An increase of approximately 17% was observed in UGE-W at 90-days in comparison to UG. At 180-days, the difference between porosity of UGE-W and UG samples was 17%, where the water permeation resistance shown by UG was considerably better than UGE-W. However, after 180-days, UGE-W and UG specimens did not exhibit much reduction in porosity. There was approximately similar reduction of 1% from 180-days to 365-days in UGE-W and UG.

The results from the experimental investigations showed that the porosity obtained by UGE-D at 3-days was approximately 15% higher than the porosity achieved by UG specimens. With the advancement in the curing time to 7-days, the porosity of UGE-D reached at the value almost 19% higher than UG. Subsequently, the performance of UGE-D became worse in comparison to UG as its porosity continued to decrease, thus, at the curing age of 28-days, it demonstrated approximately 27% higher porosity than UG. There was a small decrease of 2% in porosity of UGE-D from 28-days to 90-days. However, UGE-D showed porosity reduction of only 1.3% from 90 to 365 days compared to approximately 2.3% reduction in UGE-W, which demonstrates the importance of curing temperature and curing environment for improving durability performance of concrete. It should be noted that an increase in porosity does not necessarily indicate a similar level of increase in permeability. This is because permeability depends on many other factors including connectivity of pores, their sizes and how tortuous the path is for the permeating fluid (The Concrete Society, 1988).

7.5.4 Consolidated summary of porosity results

The data achieved from the porosity tests performed on elevated wet-cured and dry-cured FA, UG and WG specimens and elevated dry-cured GP specimens were correlated to the porosity measurements of wet-cured GP mix to obtain more information on the effects of elevated curing on the mixes. The consolidated results are shown in Figure 7.28. The porosity factor was calculated by dividing each porosity value by the porosity measurement of wet-cured control GP mix. This means that data points of GPE-W were fixed at the porosity factor of 1 to determine the porosity factors of remaining wet-cured and dry-cured specimens. It was found that wet-cured washed glass mix demonstrated much better performance than wet-cured GP mix whereas, dry-cured washed glass mix had much closer correlation to GPE-W than dry-cured GP mix. It is interesting to note that the data obtained at 365-days revealed almost the same correlation of GPE-D, FAE-D, and UGE-W to the wet-cured GP mix. This suggests the importance of water-curing after elevated temperature treatments because in the absence of proper curing environment, the advantages associated

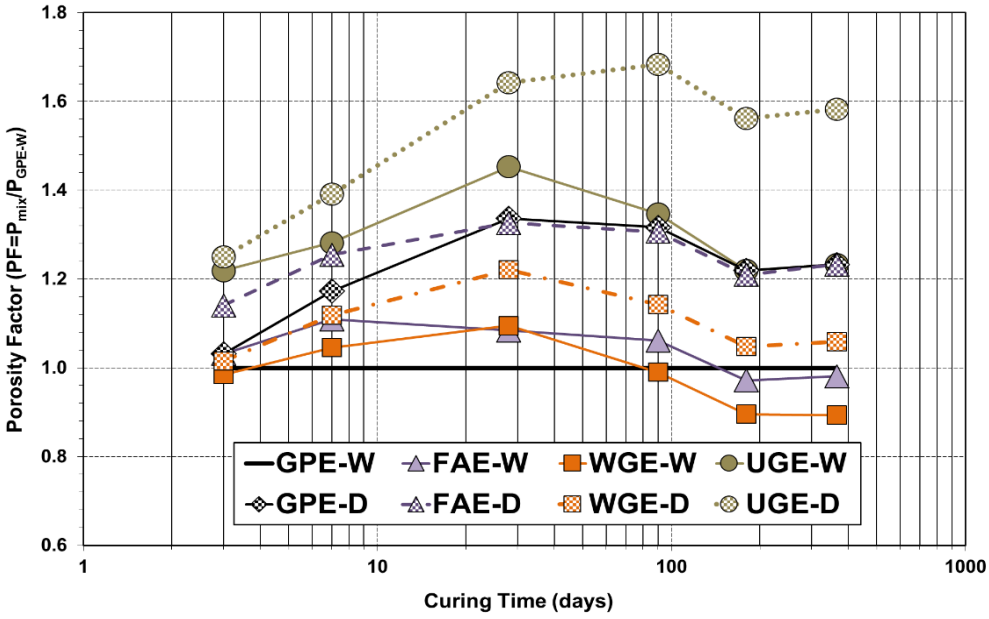

Figure 7.28: Consolidated summary of porosity data for elevated cured specimens

with using a high quality binder are likely to diminish. Dry-cured unwashed glass mix (UGE-W), however, exhibited poor performance in relation to GP series as well as the other dry-cured and wet-cured SCC mixes incorporating fly ash and washed glass powder.

7.5.5 Relationship between porosity and compressive strength in elevated cured specimens

The correlations between porosity and compressive strength based on the curing regime after initial accelerated temperature treatment are demonstrated in Figure 7.29 and Figure 7.30. Number of variations was observed in correlations between porosity and compressive

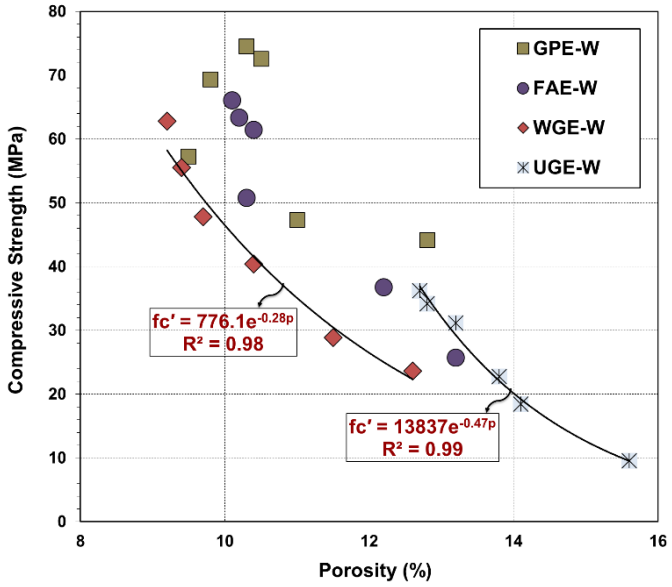

Figure 7.29: Relationship between compressive strength and porosity of wet-cured specimens initially subjected to elevated curing

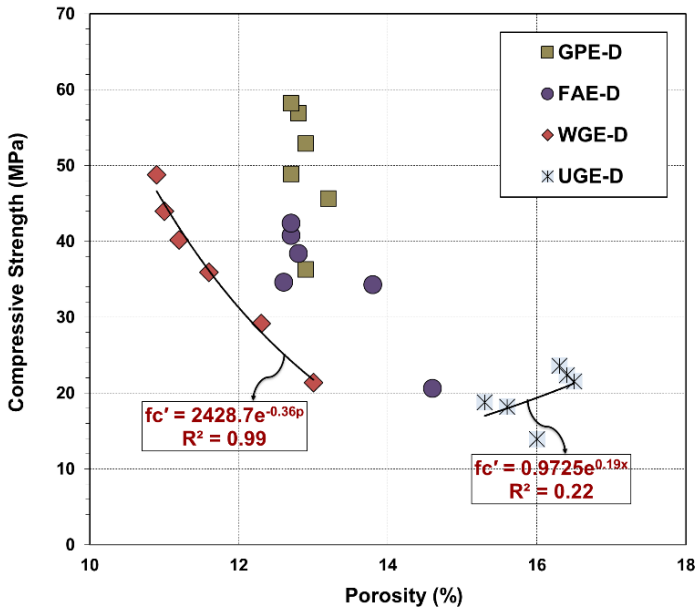

Figure 7.30: Relationship between compressive strength and porosity of dry-cured specimens initially subjected to elevated curing

strength of elevated cured wet-cured and dry-cured SCC mixes, particularly at the early-ages of testing. This might be related to the evidence that it cannot always be expected to achieve the perfect relationships between different parameters of concrete since it is a highly complex heterogeneous material. However, wet-cured and dry-cured washed glass and wet-cured unwashed glass mixes demonstrated strong correlations between these two parameters. This indicates that the correlation between compressive strength and porosity might work for some mixes with using similar materials.

7.5.6 Relationship between porosity and coefficient of oxygen permeability in elevated cured specimens

In addition to the relationships between compressive strength and elastic modulus, the relationships between porosity and coefficient of oxygen permeability were also developed using regression analysis, which are demonstrated in Figure 7.31 and Figure 7.32. It can be noticed that all wet-cured and dry-cured mixes exhibited similar relationship trend between porosity values and coefficients of oxygen permeability. This means that the decrease in porosity was mainly linked to the reduction in coefficient of oxygen permeability. The relationships between these two parameters became stronger with the progress in curing time. In addition, the specimens incorporating FA and GP showed higher coefficients of oxygen permeability and porosities compared to the specimens containing 20 microns washed glass powder. Opposite was true for their comparison with the mixes containing 20 microns unwashed glass powder. In general, porosity was found to be the most sensitive property to curing effects.

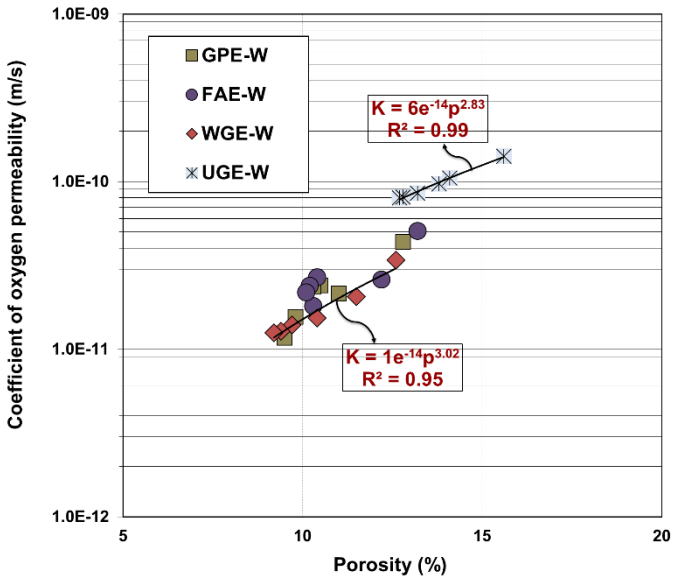

Figure 7.31: Relationship between porosity and coefficient of oxygen permeability of wet-cured specimens initially subjected to elevated curing

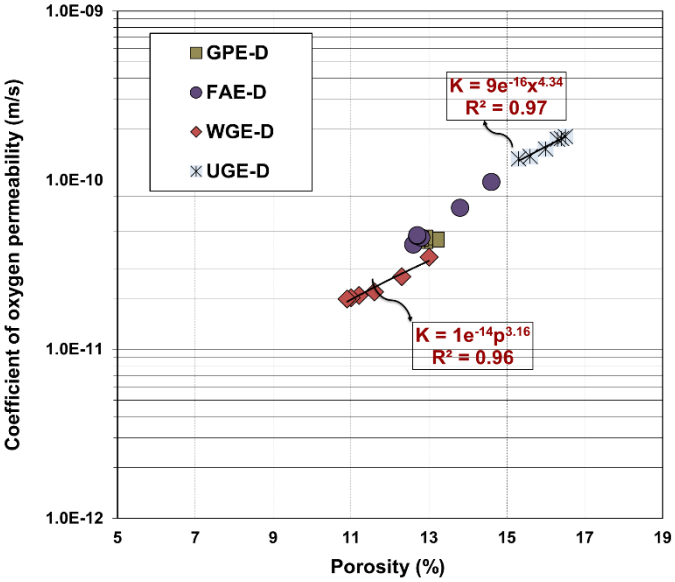

Figure 7.32: Relationship between porosity and coefficient of oxygen permeability of dry-cured specimens initially subjected to elevated curing

7.6 Effects of accelerated curing on electrical resistivity of glass modified self-compacting concrete

Electrical resistivity measurement is employed as an indirect method to estimate chloride ion permeability of concrete. The electrical resistivity depends on the same properties on which the concrete's pores microstructure depends. The changes in these properties, which result in changes in size and distribution of the concrete's pores, together with the variation of its humidity content and the curing conditions to which it is subjected, affect the concrete's electrical resistivity. In general, higher resistivity indicates lower corrosion rate (when active

corrosion is occurring) and higher resistance to chloride ion penetration. Concrete's electrical resistivity tends to increase with the hydration process, provided that it is subjected to an adequate curing, due to the influence of the curing process in the development of the pore structure, which can reduce its permeability and consequently, hinder ionic mobility (Whiting and Nagi 2003). The variation in initial curing temperature has been found to have a significant effect on electrical resistivity of concrete, and generally, an increase in temperature leads to a reduction in electrical resistivity. According to Francisco et al. (2013), temperature affects electrical resistivity by changing the ion-mobility, ion-ion and ion-solid interactions, as well as the ionic concentration in pore solution. Temperature effect is also significant when electrical resistivity is employed as a quality control method for estimating chloride ion permeability. Moreover, the subsequent curing conditions after accelerated temperature treatment have a considerable influence on resistivity since concrete is a poor electrical conductor, especially under dry conditions. Air-dried concrete has an electrical resistivity of the order of 10^6 ohm.cm (Neville, 1995). Conventional moist and oven-dried concrete can be classified as semiconductor and insulator respectively (Monfore, 1968). However, conductivity of moist concrete is influenced by the presence of salts in the electrolytic solution and the ambient temperature (Farrar, 1978; Monfore, 1968).

The present section consists of results from the experimental study on electrical resistivity of a range of SCC mixes, containing control binders as well as glass powders of different qualities but added at the constant replacement rate and followed by a treatment with accelerated initial temperature. To understand the effects of curing temperature on the electrical resistivity, the resistivity measurements of the specimens initially cured at 50°C were correlated to the resistivity measurements of its counterpart SCC types cured at 21°C. The electrical resistivity measurements were taken at 3, 7; 28, 90; 180 and 365 days for early, normal and long-term performance respectively and have been demonstrated in Figures 7.33 - 7.26. The average resistivity values were obtained from four replicate specimens taken out from two identical SCC samples at each curing age. The same specimens used for oxygen permeability and porosity were later tested for resistivity measurements. The procedure for testing and analyzing data have already been discussed in Chapter 3. Complete data are shown in Appendix F.

7.6.1 Effects of accelerated curing on electrical resistivity of control self-compacting concrete mixes incorporating GP cement and Fly Ash

The electrical resistivity measurements demonstrated that there was a significant drop in the electrical resistivity measurements of GP specimens subjected to an elevated curing compared to the standard-cured GP specimens as shown in Figure 7.33. GPE-W exhibited

electrical resistivity of approximately 11 kohm.cm at 3-days, which was higher than GP by about 9%. At 28-days, there was a difference of 13% between the electrical resistivity measurements of GPE-W and GP. By the time of 90-days in water for curing, electrical resistivity of GPE-W reduced further and reached about 12% lower resistivity value than that of GP mix. The continuous water-curing up to 365-days improved the electrical resistivity of all specimens, yet a difference of approximately 15% between the standard GP mix and GPE-W was observed, where GPE-W was lower. This finding can be related to comparatively non-uniform distribution of the hydration products in the specimens (GPE-W)

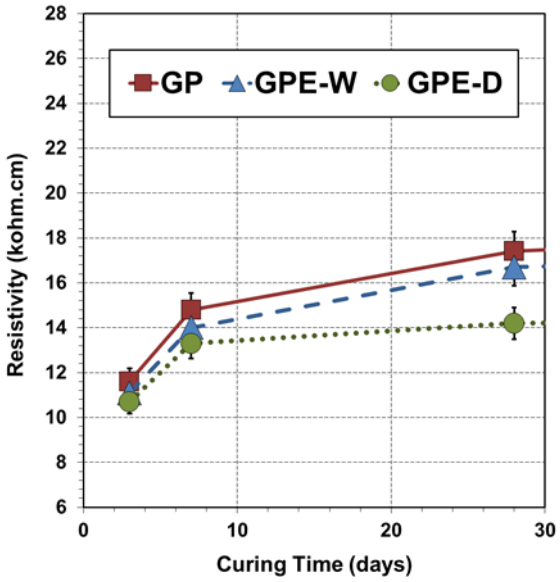

(a)

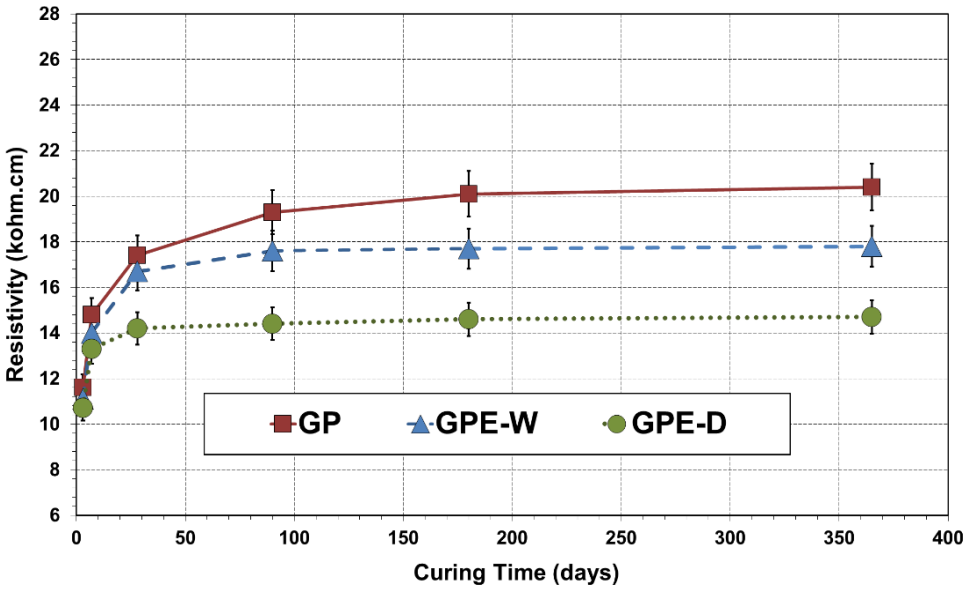

(b)

Figure 7.33: Electrical resistivity of GP subjected to different curing conditions from curing age of (a) 3 to 28 days (b) 3 to 365 days

that caused the formation of larger pores. The overall results reveal that even GP mix could only remain in the low/moderate resistivity zone until 180-days of curing, which indicates its moderate resistance against chloride ions. In addition, elevated thermal curing did not improve the chloride resistance of concrete containing GP cement. This implies that in situations where exposure to chloride ions is expected, a low w/c (in this case 0.4) with ideal curing conditions is still not sufficient and an appropriate SCM is needed as recognized in the NZS 3101 code.

The variations in electrical resistivity measurements of GPE-D specimens were recorded during 3 and 365 days after treating with accelerated curing. The electrical resistivity measurement of GPE-D at 3-days was found to be about 10 kohm.cm compared to about 12 kohm.cm for GP. A resistivity value within 9.5-16.5 kohm.cm corresponds to a rapid chloride permeability test (ASTM C1202) charge passed of 2000-4000 coulombs, which is considered to have a moderate penetrability to chloride ions, similarly attained by GP class up to 3-days. However, dry-curing subsequent to elevated curing resulted in an increase of electrical resistivity and a difference of 22% between measurements of GP and GPE-D was observed at 7-days, where the lower value was shown by GPE-D. An increase of 11% in electrical resistivity was observed in GPE-D at 28-days compared to 7-days. GPE-D specimens achieved 90-days electrical resistivity approximately 19% lower than GPE-W and approximately 33% higher than GP specimens. The rate of increase with the extended curing time decreased considerably from 180-days. Hence, an insignificant increase of 1% was observed in electrical resistivity of GPE-D specimens between 180 and 365 days in comparison to about 2% increase in GPE-W specimens during the same curing period.

The electrical resistivity achieved by FA mixes from the curing period of 3 to 365 days has been demonstrated in Figure 7.34. The measured electrical resistivity of FAE-W was found to be 11.6 kohm.cm at 3-days in comparison to 12.2 kohm.cm in the standard FA mix at the same curing time. However, the electrical resistivity in FAE-W was lower than FA, by about 13% at 28-days. With the further progress in curing time, it was noticed that FAE-W demonstrated 20% lower electrical resistivity than FA at 180-days. Moreover, there was a small increase of 1% from 180 to 365-days of wet-curing in FAE-W as compared to three times higher increase in FA within this curing time. The higher resistivity measurements achieved by the specimens incorporating FA compared to GP only, might be related to the pore connectivity of FA modified concrete specimens, which is the single most important parameter governing overall conductivity, similarly discussed by Rajabipour et al. (2007). The authors mentioned that replacing GP cement with FA has a significant effect on electrical conductivity of pore solution, depending on the replacement level and age, similarly evident in this study.

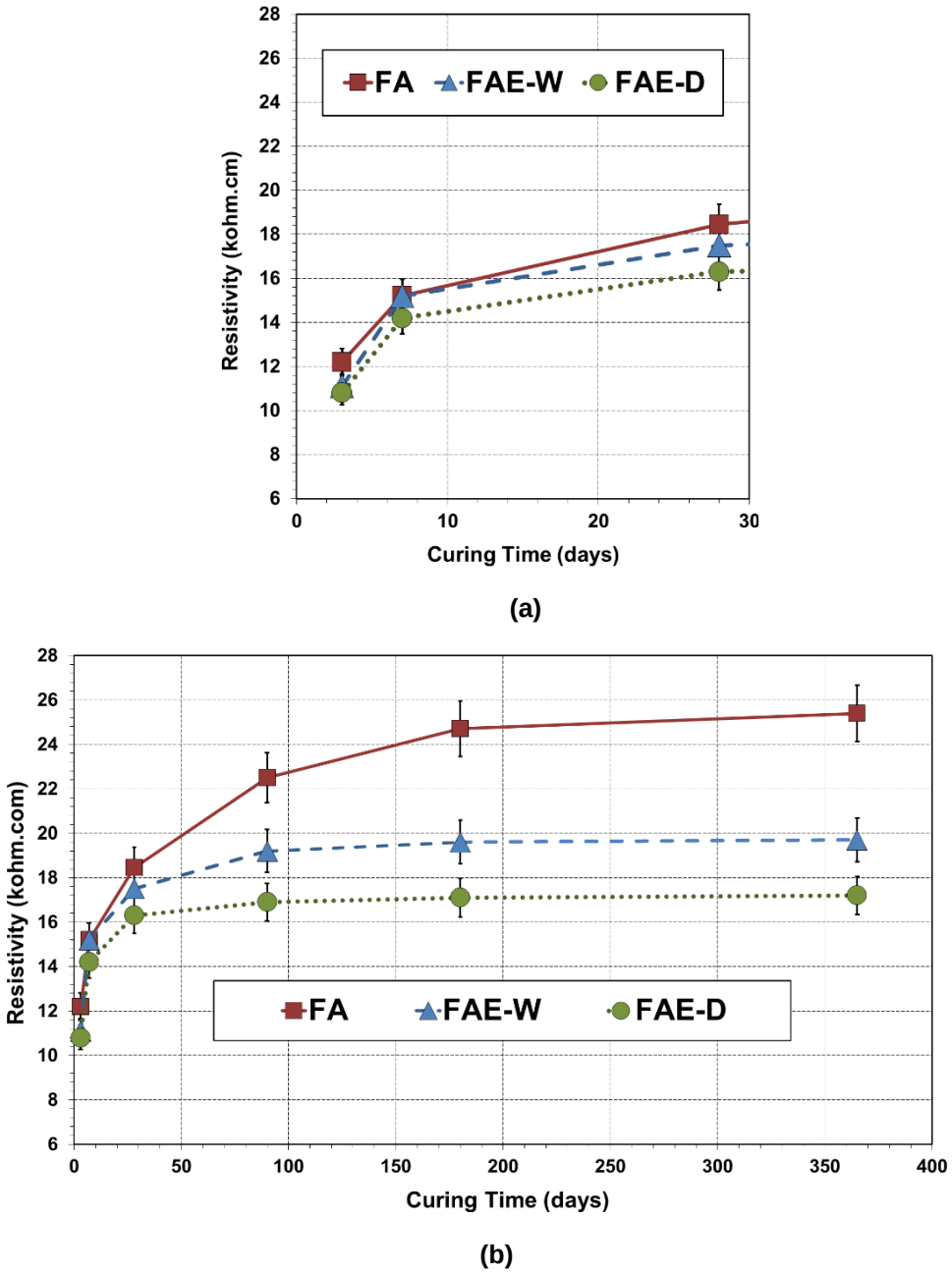

Figure 7.34: Electrical resistivity of FA subjected to different curing conditions from curing age of (a) 3 to 28 days (b) 3 to 365 days

At the early-age of 3-days, the reduction in electrical resistivity of 20% was observed in FAE-D compared to FA. The resistivity measurement of FA at 7-days was 15.2 kohm.cm compared to 12.5 kohm.cm for FAE-D specimens. The electrical resistivity of FAE-D was found to be approximately 12%-26% lower in comparison to FA and FAE-W at 28-days. Moreover, a further increase in electrical resistivity was noticed in FAE-D at 90-days, similar to FA and FAE-W specimens. There was an increase of 8% in electrical resistivity of FAE-D from 28 to 90 days in comparison to 18% increase in FA during the same curing period. Furthermore, only 0.6% increase in electrical resistivity of FAE-D was found during 90 and

365 days, while FA increased approximately 3% during this curing period. The final value found at 365-days showed resistivity measurement of FAE-D at 16.2 kohm.cm that was 57% lower than FA. Overall results revealed higher resistivity in FAE-D specimens than GPE-D specimens, potentially due to better microstructure of concrete containing FA even if not subjected to subsequent water-curing. Ozyildirim and Halstead (1994) studied concrete made with GP cement combined with class F fly ash and conversely reported that increasing the curing temperature from 23°C to 38°C reduced the chloride ion permeability in mixes incorporating both cement and fly ash as binders.

7.6.2 Effects of accelerated curing on electrical resistivity of washed glass modified self-compacting concrete

The data from electrical resistivity tests done on WG mixes demonstrated reduction in electrical resistivity of WGE-W specimens subjected to an elevated curing compared to the normally-cured WG specimens as shown in Figure 7.35. At 3-days, WGE-W showed 5% lower electrical resistivity in comparison to WG, which shows its lower resistance compared to WG. Although being lower than WG, WGE-W exhibited increase of approximately 20% at 7-days in comparison to 3-days. The electrical resistivity of WGE-W showed increase of about 17% between 7 and 28 days. At 90-days, however, the electrical resistivity of WGE-W was about 13% lower than that of WG mix. The final result recorded at 365-days revealed the difference of approximately 12% between WG and WGE-W. It can be seen from the results that cuing temperature had a more obvious accelerating effect on the electrical resistance of WG than on that of FA. Shi et al. (2005) similarly found that the cuing temperature influence the pozzolanic reactivity of glass powder more than that of the fly ash,

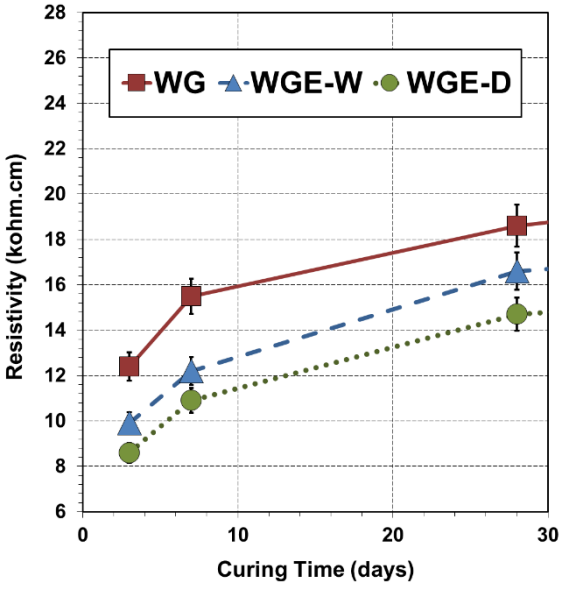

(a)

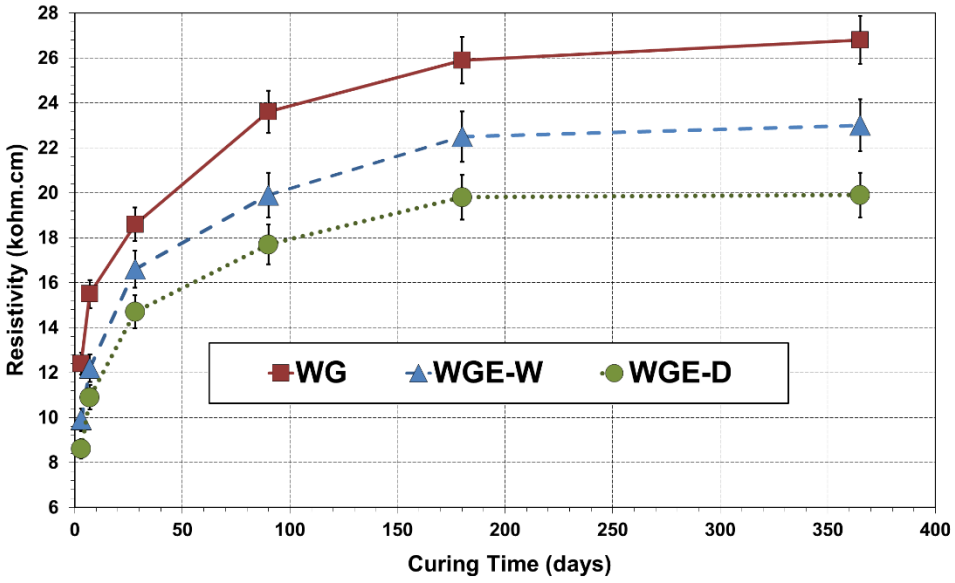

(b)

Figure 7.35: Electrical resistivity of WG subjected to different curing conditions from curing age of (a) 3 to 28 days (b) 3 to 365 days

which in turn significantly govern the structure formation and therefore, its durability. Matos et al. (2016) also revealed that the electrical resistivity is significantly enhanced in the presence of glass powder.

A very large increase of 47% was observed in electrical resistivity of WGE-D specimens between 3 and 365 days after casting. The results from 3-days electrical resistivity measurements exhibited a decrease of about 17% in WGE-D compared to WG specimens. From 3 to 7 days, the increase in electrical resistivity of WGE-D was about 18%, which is lower than the increase of approximately 20% found in WGE-W. At 28-days, the electrical resistivity of WGE-D was found to be 12%-19% lower in comparison to WG and WGE-W. The effects of additional wet curing on electrical resistance are significant with WGE-D having 90-days electrical resistivity approximately 18% and 33% lower than WGE-W and WG respectively. Finally, a small increase of about 0.5% was observed in WGE-D between 180 and 365-days in comparison to about 2%-4% increase in WG and WGE-W during the same curing period. These findings are in accordance with some other authors (Madandoust and Mousavi, 2012; Gesoğlua et al., 2009) who reported that the use of mineral additions increases electrical resistivity of SCC when compared to that of GP concrete.

7.6.3 Effects of accelerated curing on electrical resistivity of unwashed glass modified self-compacting concrete

Figure 7.36 demonstrates the electrical resistivity measurements of unwashed glass series for the curing period of 3 to 365 days. The measurement recorded at 7-days revealed the

difference of 12% in electrical resistivities of UG and UGE-W; however, the increase in resistivity from 3 to 7 days in UGE-W was somewhat lower than the increase observed in UG. A lower electrical resistivity value of UGE-W compared to UG was recorded at 28-days. Furthermore, a reduction of approximately 16% was observed in UGE-W at 90-days in comparison to UG. Following the similar trend, there was around 3.5% increase in electrical resistivity from 90 to 365 days in both UGE-W and UG. The tests undertaken for electrical resistivity measurements revealed that the resistivity obtained by UGE-D at 3-days was about 15% lower than the electrical resistivity achieved by the standard UG specimens. With

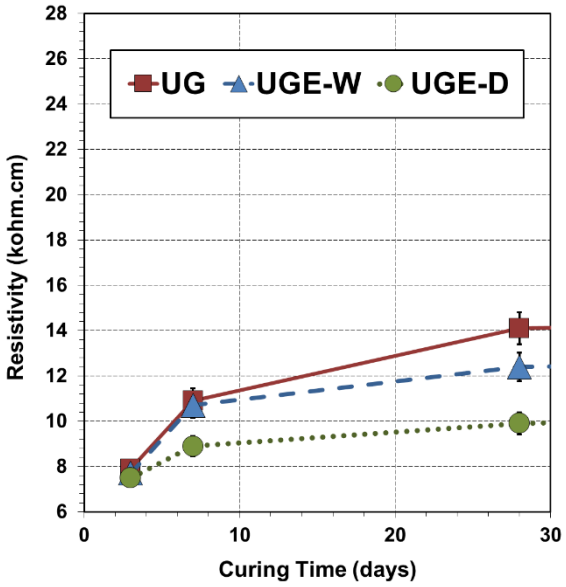

(a)

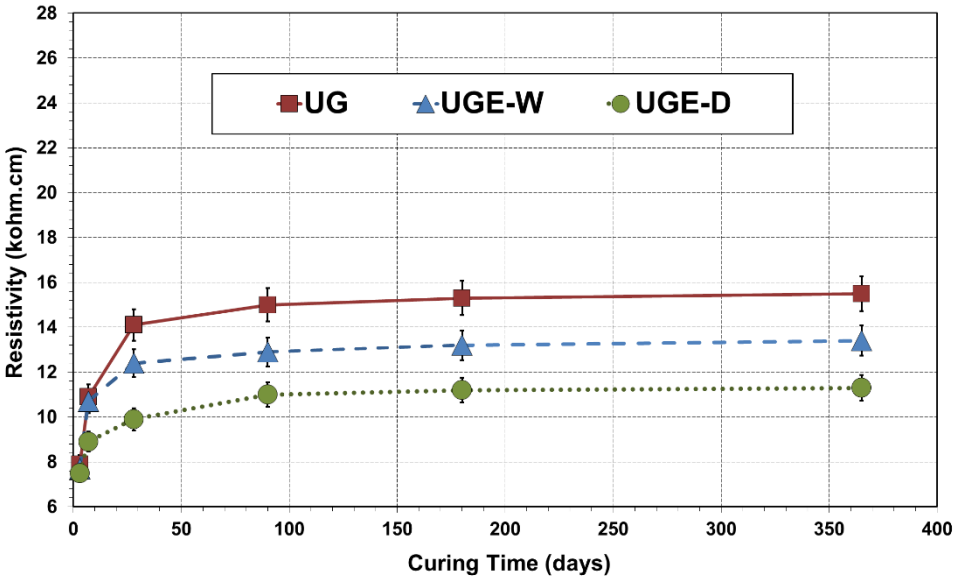

(b)

Figure 7.36: Electrical resistivity of UG subjected to different curing conditions from curing age of (a) 3 to 28 days (b) 3 to 365 days

the progress in curing time up to 7-days, the electrical resistivity of UGE-D approached the value that was almost 22% lower than the value achieved by UG. Subsequently, the performance of UGE-D became worse in comparison to UG as its resistivity was found to be 43% lower than UG at 28-days. Similar pattern was observed until 365-days of testing, when UGE-D showed decrease of 37% in electrical resistivity compared to UG and 19% compared to UGE-W.

7.6.4 Consolidated summary of electrical resistivity results

The data obtained from the electrical resistivity tests undertaken on elevated wet-cured and dry-cured FA, UG and WG specimens and elevated dry-cured GP specimens were also correlated to the elastic modulus achieved for elevated wet-cured GP mix. The consolidated results for elastic modulus are shown in Figure 7.37. Electrical resistivity factor was calculated by dividing each wet-cured and dry-cured electrical resistivity value by the electrical resistivity value of wet-cured control GP mix. Hence, the data points of GPE-W were adjusted at the electrical resistivity factors of 1 in order to determine the electrical resistivity factors of the remaining wet-cured and dry-cured specimens. In general, it was observed that the washed glass mixes, either wet-cured or dry-cured, demonstrated significantly better behaviour in relation to GP series. FAE-W was found to be slightly closer to GPE-W than WGE-D, whereas the dry-cured WG specimens showed considerably worse performance than the dry-cured FA specimens when correlated with GPE-W and GPE-D mixes. It is interesting to note that GPE-D specimens exhibited relatively poor correlation to GPE-W compared to all FA and WG mixes.

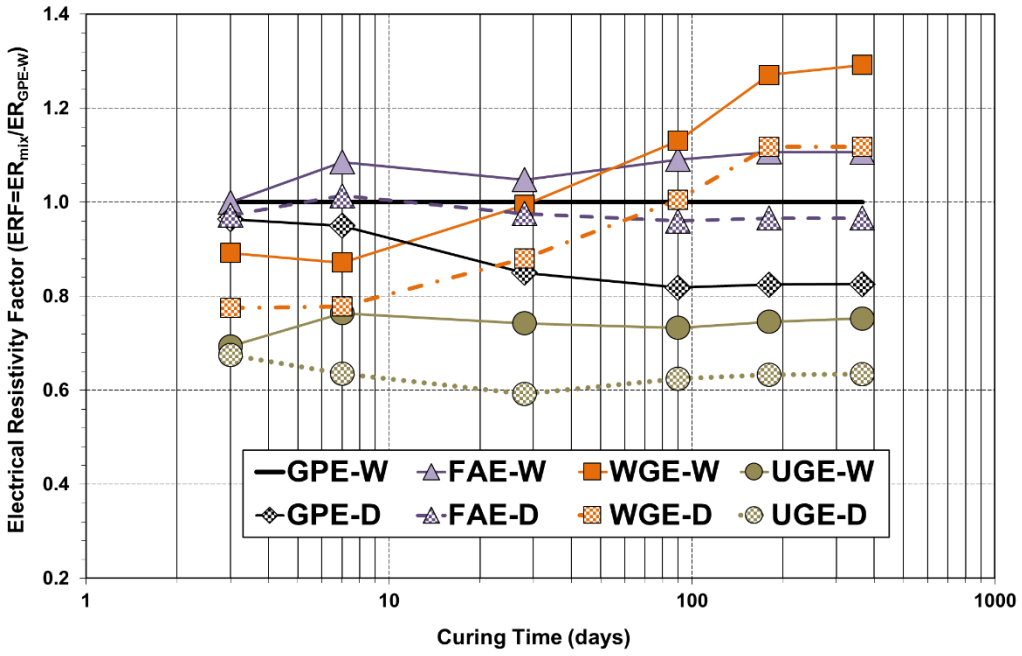

Figure 7.37: Consolidated summary of electrical resistivity data for elevated cured specimens

7.6.5 Relationship between porosity and electrical resistivity in elevated cured specimens

The correlations between porosity and electrical resistivity based on the curing regime after accelerated temperature treatment are demonstrated in Figure 7.38 and Figure 7.39. A number of variations were observed in the correlations between porosity and electrical resistivity of elevated wet-cured and dry-cured SCC mixes, particularly at higher porosity and lower electrical resistivity measurements. This might be related to the evidence that it cannot

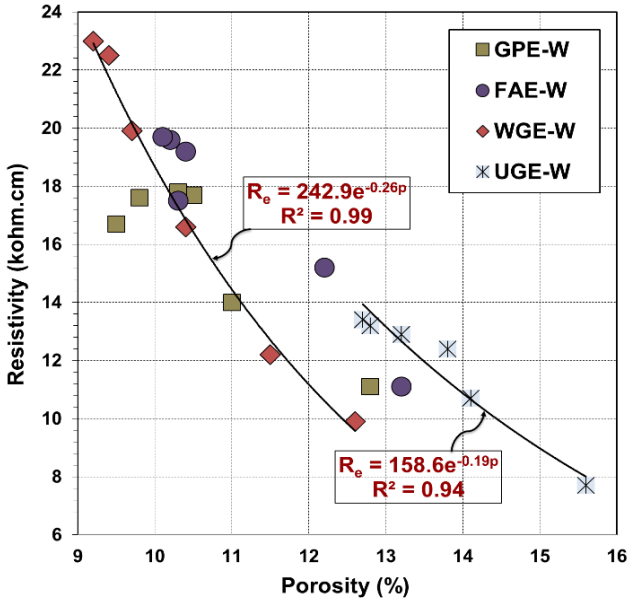

Figure 7.38: Relationship between porosity and electrical resistivity of wet-cured specimens initially subjected to elevated curing

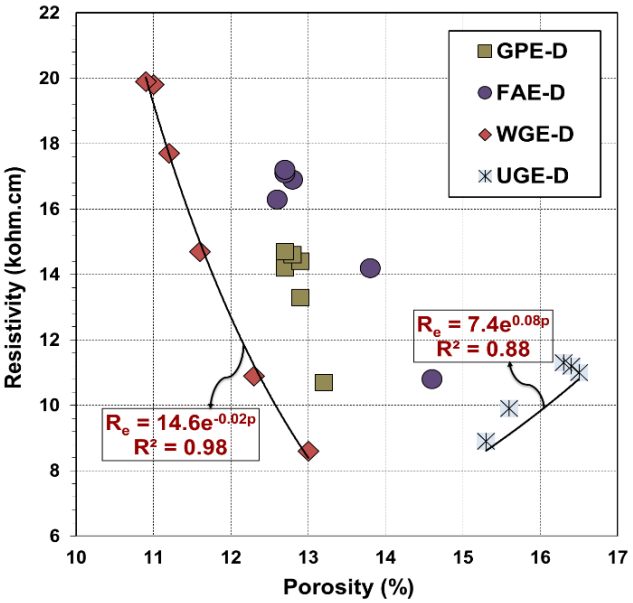

Figure 7.39: Relationship between porosity and electrical resistivity of dry-cured specimens initially subjected to elevated curing

always be expected to achieve perfect relationships for concrete because it is a complex heterogeneous material. However, wet-cured and dry-cured washed glass and wet-cured unwashed glass mixes demonstrated strong correlations between these two parameters. The dry-cured unwashed glass specimens were found to have opposite trend compared to the dry-cured washed glass specimens.

7.7 Effects of accelerated curing on chloride diffusion coefficient of glass modified self-compacting concrete

The effect of temperature is very important in predicting service life of reinforced concrete structures during both the initiation and propagation periods. Chloride diffusivity is an important parameter for service life of reinforced concrete structures and has been found to be dependent on temperature. Measuring changes in chloride diffusion has also been shown to be much more effective method of assessing curing efficiency of concrete, since the effectiveness of different curing systems can be more objectively compared if related to some estimate of chloride resistance of concrete (Hoppe, 1994). According to Francisco et al. (2013), higher temperatures increase both chloride ion penetration rates and corrosion rates of steel in concrete. Due to the significance of the effect of temperature on chloride diffusivity, it is necessary to consider the temperature effect while predicting the service life of reinforced concrete structures (Francisco et al., 2013). Therefore, similar investigations have been made in this study.

The present section consists of results from the experimental investigations on chloride diffusion coefficients of a range of SCC mixes, containing control binders as well as glass powders of different qualities (washed and unwashed) but added at the constant replacement rate (30%) and subsequently treated with accelerated temperature (50^0C) for 18 hours. The results of long-term chloride absorption, including the experimental Cl^- ion concentration determined at all test ages were adjusted to a particular solution of Fick's Second Law of diffusion to obtain the corresponding diffusion coefficients and total amount of diffusing chloride. To analyze the effects of elevated curing temperature on chloride diffusion coefficient, the chloride diffusion measurements of the specimens initially cured at 50°C were correlated to the measurements of its counterpart SCC types cured at 21°C. The chloride diffusion measurements were taken at 28, 90; 180 and 365 days for normal and long-term performance respectively and have been demonstrated in Figures 7.40 - 7.43. The average chloride diffusion coefficients were obtained from two replicate specimens, each taken out from two identical SCC samples at each curing age. The procedure for testing, measuring and analyzing data has already been discussed in Chapter 3. Complete data are shown in Appendix F.

7.7.1 Effects of accelerated curing on chloride diffusion coefficient of control self-compacting concrete mixes incorporating GP cement and Fly Ash

The chloride diffusion measurements showed that there was a considerable reduction in the chloride diffusion coefficients of GP specimens subjected to an elevated curing compared to the standard-cured GP specimens as shown in Figure 7.40. GPE-W exhibited chloride diffusion coefficient of approximately 1.9E-11 m^2/s at 28-days, which was higher than GP by about 30%. In addition, the measured chloride diffusion coefficient of GPE-W specimens kept at elevated temperature followed by wet-curing showed the reduction of approximately 21% between 7-days and 28-days, which was lower than the decrease found in GP standard curing control mix within this curing duration. At 90-days, there was a difference of 34% between the chloride diffusion measurements of GPE-W and GP, out of those GP had lower chloride diffusion coefficient. The continuous water-curing up to 365-days improved the chloride diffusivity of all specimens, however, a difference of about 37% between the standard GP mix and elevated wet cured mix (GPE-W) was observed, where GPE-W was lower.

The chloride diffusion coefficients of GPE-D specimens were recorded during 28 and 365 days after casting and accelerated curing. The chloride diffusion measurement of GPE-D at 28-days was found to be about 2.4E-11 m^2/s compared to about 1.3E-11 m^2/s for GP. Dry-curing subsequent to elevated curing resulted in the difference of 50% between chloride diffusion coefficients of GP and GPE-D at 90-days, where the higher value was shown by GPE-D. A reduction of 15% in chloride diffusion coefficient was observed in GPE-D at 180-days as compared to 90-days. The rate of decrease with the extended curing period reduced

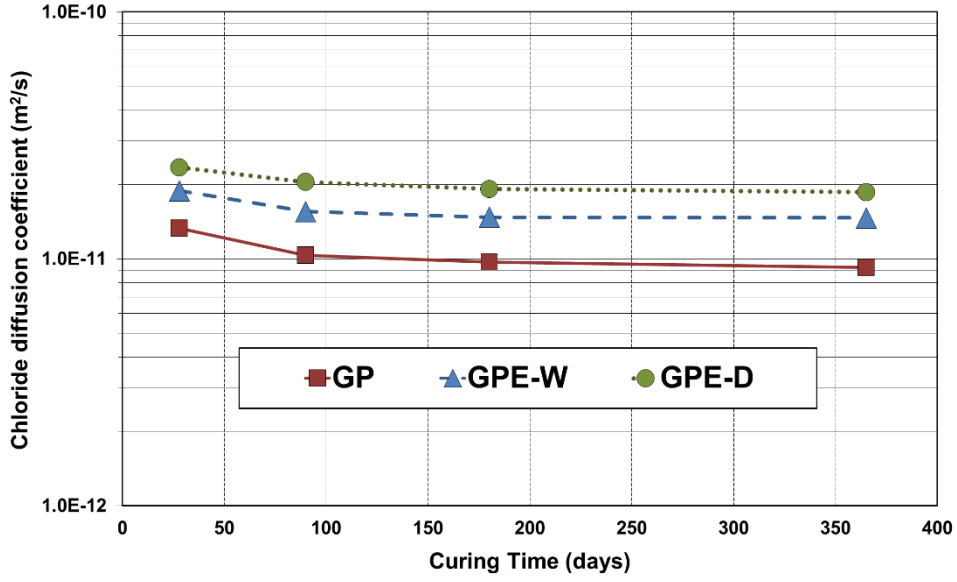

Figure 7.40: Chloride diffusion coefficients of GP subjected to different curing conditions

significantly from 180-days. Thus, a minor decrease of 3% was observed in chloride diffusion coefficient of GPE-D specimens between 180-days and 365-days in comparison to approximately 5% reduction in GPE-W specimens during the same curing period.

The chloride diffusion coefficient achieved by FA series from the curing period of 28 to 365 days has been demonstrated in Figure 7.41. The measured chloride diffusion coefficient of FAE-W was found to be 8.8E-12 m^2/s at 28-days in comparison to 7.2E-12 m^2/s in FA mix at the same curing time. A variation of approximately 32% was observed between FA and FAE-W at 90-days. However, the chloride diffusion coefficient of FAE-W was about 37% higher than the standard cured modified mix (FA) at 180-days. Finally, there was small decrease of 4% in chloride diffusion FAE-W from 180-days to 365-days as compared to 15% decrease in the standard mix (FA) within this curing time. An investigation by Lee (2014) also revealed that accelerated curing at 80°C had a detrimental effect on the absolute chloride- ion diffusivity of 400 kg/m^3 concrete, incorporating 30% class F FA and produced with w/c of 0.4, compared with concrete standard water-curing at ambient temperatures, complying with Clause C3.6 of NZS 3101: Part 2. Khatib and Mangat (2002) investigated the influence of high-temperature curing on chloride penetration in concrete containing FA and similarly observed higher chloride penetration resistance in FA modified concrete. At 28-days, the increase of 31% in chloride diffusion was observed in FAE-D compared to FA. Furthermore, there was a reduction of 7% in FAE-D from 90 to 180 days in comparison to 26% decrease in FA during the same curing period. Only 3% decrease in chloride diffusion coefficient of FAE-D was found between 180 and 365 days, while FA decreased approximately 13% during this curing period. The final measurement recorded at 365-days showed chloride diffusion measurement of FAE-D at 7.6E-12 m^2/s that was 61% lower than FA.

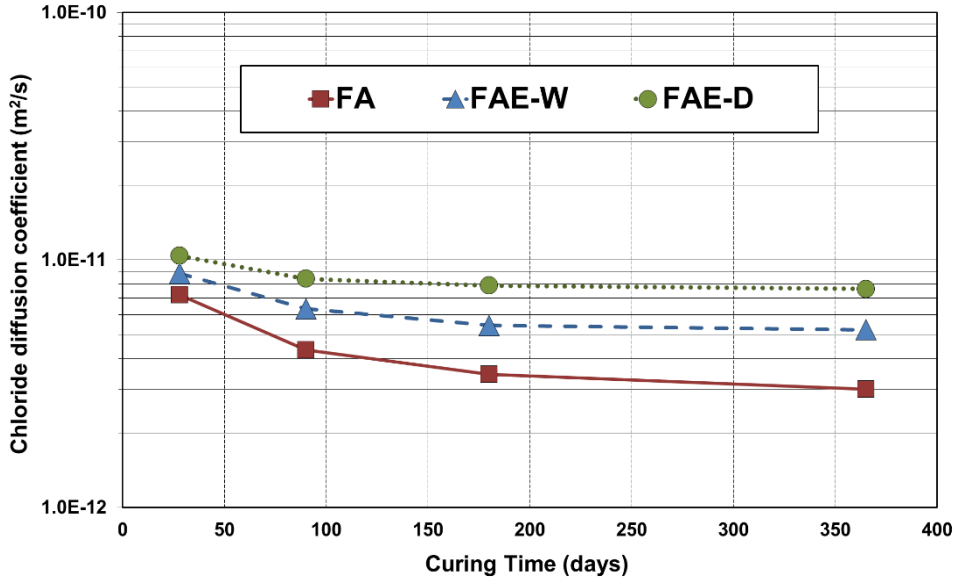

Figure 7.41: Chloride diffusion coefficients of FA subjected to different curing conditions

7.7.2 Effects of accelerated curing on chloride diffusion coefficient of washed glass modified self-compacting concrete

The results from chloride diffusion tests done on WG mixes exhibited an increase in diffusion coefficients of WGE-W specimens subjected to an elevated curing compared to the normally-cured WG specimens as shown in Figure 7.42. The measured chloride diffusion coefficients of the specimens treated with elevated temperature followed by wet curing (WGE-W) showed a decrease of approximately 34% between 28-days and 90-days. At 90-days, however, the chloride diffusion coefficient of wet-cured elevated curing specimens (WGE-W) was about 37% higher than that of the standard curing control (WG) mix. As the curing period progressed, water-curing subsequent to initial elevated temperature treatment resulted in lower 180-days chloride diffusion coefficient than that of the standard cured washed glass mix (WG). The result recorded at 365-days revealed the difference of about 41% between the standard WG mix and elevated wet cured mix (WGE-W), where WGE-W showed higher chloride diffusion coefficient. Overall results of this study are relevant to Matos et al. (2016) who similarly reported that the resistance to chloride ion penetration is greatly improved with the inclusion of glass powder in the mix. The reduction in chloride ion penetration might be due to the formation of a tighter pore structure, which is one of the main parameters that affect chloride penetration, similarly mentioned by Dali et al. (2012).

There was a significant decrease in chloride diffusion coefficients of WGE-D specimens between 28 and 365 days after casting. At 28-days, the chloride diffusion coefficient of WGE-D was found to be 24%-48% higher in comparison to WG and WGE-W. A minor decrease of about 3% was observed in chloride diffusion of WGE-D specimens between 180

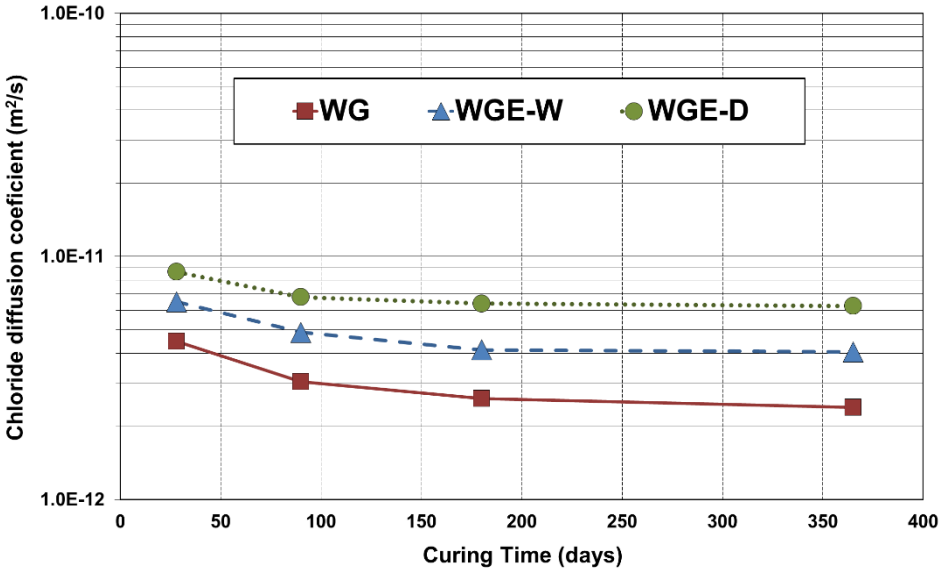

Figure 7.42: Chloride diffusion coefficients of WG subjected to different curing conditions

and 365 days in comparison to approximately 2%-8% reduction in diffusion coefficients of specimens WG and WGE-W during the same curing period. The obtained results are possibly because water is lost due to evaporation for mixtures cured at higher temperature and the cross linking is not as effective as it must occur in a restricted space and may well not be completed, which causes higher chloride ion penetration. The findings obtained in this study are consistent to those reported by Shayan and Xu (2006) that the moist-cured specimens exhibit lower chloride permeability than the specimens subjected to external exposure, indicating that glass powder might be beneficial under submerged marine exposure conditions against chloride-induced corrosion of reinforcement in concrete. The overall results are also in accordance to Clause C3.6 of NZS 3101: Part 2 that the accelerated curing generally has a detrimental effect on the measured chloride-ion diffusivity, compared with water-curing at ambient temperatures.

7.7.3 Effects of accelerated curing on chloride diffusion coefficient of unwashed glass modified self-compacting concrete

Figure 7.43 shows the chloride diffusion measurements of unwashed glass (UG) class of mixes throughout the curing time of 28-days to 365-days. The measurement recorded at 28-days revealed the difference of 27% in chloride diffusion coefficient of UG and UGE-W. From the tests done at 90-days, a higher chloride diffusion coefficient value in UGE-W compared to UG was recorded again. Furthermore, an increase of about 31% was observed in UGE-W at 180-days in comparison to the standard cured mix UG. The similar trend was observed until 365-days and an approximate decrease of 2% was observed from 180-days to 365-days in both UGE-W in comparison to 3% reduction found in the standard mix UG. The tests

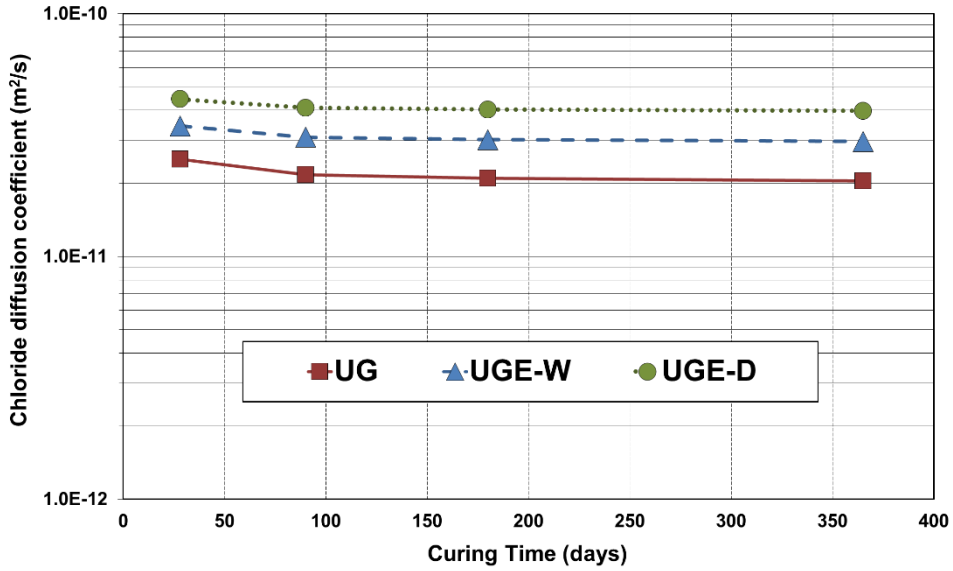

Figure 7.43: Chloride diffusion coefficients of UG subjected to different curing conditions

undertaken on UG dry-cured specimens informed that diffusion coefficient demonstrated by UGE-D at 28-days was approximately 44% higher than the diffusion coefficient achieved by the standard UG specimens. With the progress in curing time up to 90-days, the chloride diffusion coefficient of UGE-D approached the value that was almost 47% higher than the value achieved by UG. Subsequently, the performance of UGE-D became worse in comparison to UG as its diffusion coefficient was found to be 49% higher than UG at 365-days. These results indicate that the amount of Cl^- likely to be present in each concrete specimen depends on the nature of concrete. The more porous concrete is, the less absorbed less Cl^-, which is also reflected in the results of relatively more porous UGE-D compared to UGE-W in the present study.

7.7.4 Consolidated summary of chloride diffusion coefficient results

The findings from tests performed on elevated wet-cured and dry-cured FA, UG and WG specimens and elevated dry-cured GP specimens were related to the chloride diffusion coefficients of wet-cured GP mix to obtain more information on the effects of elevated curing on the mixes. The consolidated results are shown in Figure 7.44. Chloride diffusion coefficient factor was calculated by dividing each chloride diffusion coefficient value by the chloride diffusion coefficient of wet-cured control GP mix. It was observed that there was not a considerable difference between the correlations of WGE-W and FAE-W with GPE-W. Wet-cured washed glass mix demonstrated much better correlation factor with wet-cured GP mix compared to dry-cured GP mix; whereas, dry-cured unwashed glass mix demonstrated poor performance corresponding to all other mixes, either wet-cured or dry-cured.

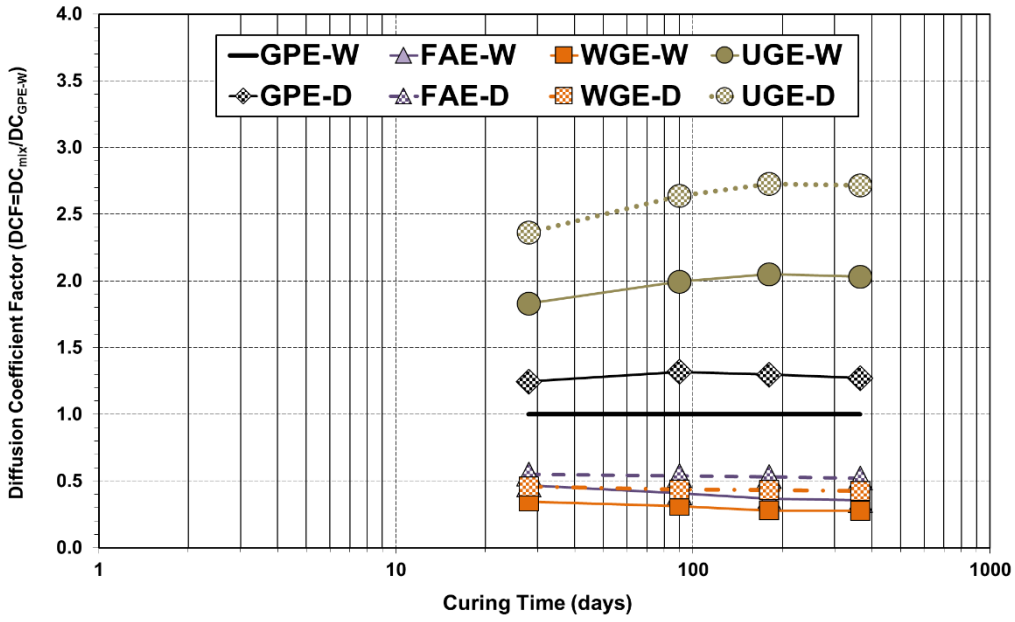

Figure 7.44: Consolidated summary of chloride diffusion coefficient data for elevated cured specimens

7.7.5 Relationship between electrical resistivity and chloride diffusion coefficient in elevated cured specimens

The correlations between electrical resistivity and chloride diffusion coefficient based on the curing regime after initial accelerated temperature treatment are shown in Figure 7.45 and Figure 7.46. Strong correlations between these two parameters were observed in all types of wet-cured and dry-cured mixes. However, the correlations were found to be dependent on the type of binder present in the mixes and therefore, the washed glass mixes had higher electrical resistivity and lower chloride diffusion coefficient compared to the unwashed glass mixes.

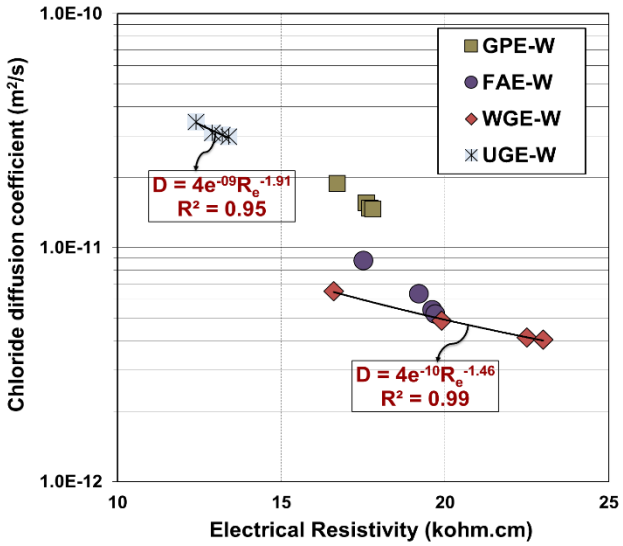

Figure 7.45: Relationship between compressive strength and porosity of wet-cured specimens initially subjected to elevated curing

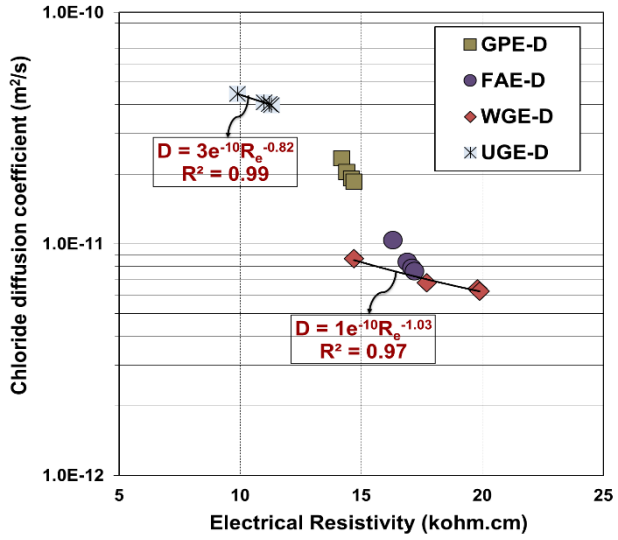

Figure 7.46: Relationship between compressive strength and porosity of dry-cured specimens initially subjected to elevated curing

7.8 Conclusions

The long-term performance of concrete materials is dependent upon a number of factors including the selection of appropriate curing methods. The findings presented in this chapter can be used to draw the following conclusions:

- Accelerated cured SCC, incorporating washed glass powder of fineness 20 μm and replaced at 30% by cement, has the potential to achieve its target strength, irrespective of the curing regime. Conversely, elevated cured SCC containing unwashed glass powder, having fineness of 20 μm and substituted by 30%, is unlikely to reach its design strength even with subsequent water-curing. This necessitates the utilization of clean glass powder in SCC to achieve satisfactory performance, particularly when the accelerated curing is the requirement for real concrete construction.

- The relationship between compressive strength and elastic modulus is not affected by the initial curing temperature. Their relationship available in the code for conventional standard cured concrete can be safely used for elevated cured SCC.

- In a marine application where durability is particularly important, an understanding of the effects and limitations of various curing conditions on SCM performance is critical. With washed glass addition, durability properties of SCC are less negatively influenced by initial temperature rise compared to GP concrete. The opposite is true for unwashed glass powder modified SCC, which shows worse durability behaviour compared to other binders such as washed glass powder, fly ash and GP cement, irrespective of the temperature rise and subsequent curing regime.

- Wet-curing followed by an accelerated heat treatment, given to washed glass modified SCC, can improve its microstructure and hence the durability, compared to heat treatment alone. However, accelerated thermal curing without subsequent water-curing does not appear to compromise the resistance of the washed glass incorporated SCC to permeation of aggressive agents and falls within good durability range. However, some debate still remains on the effectiveness of additional wet-curing of heat treated concrete and further detailed investigation, using more representative mix designs and heating conditions, is necessary before any final conclusion related to the effects of curing on precast concrete can be determined.

- The dry-cured unwashed glass SCC has the highest permeability to deteriorating agents in different curing conditions. This suggests that accelerated heat treatment given to unwashed glass powder further deteriorates its durability and is not a good alternative to standard curing regime.

- The standard curing conditions represent the ideal but unrealistic case of what can be achieved with laboratory concrete. The wet-cured washed glass case illustrates the potential for concrete, given initial accelerated thermal curing and subsequent continuous water-curing, which is also not a realistic option but does provide for a comparison with washed glass dry-cured case, which is more representative of what might be done in practice.

- When investigating the final quality of concrete, it is beneficial to compare the measured values from durability tests, such as gas permeability or resistivity, which have some correlation with real world deterioration processes. The efficiency of various curing methods should eventually be assessed on their measured in-situ performance.

- The findings of the present study indicate that the proper combinations of SCM type and cement may better tolerate curing at an elevated temperature, which may merit further investigation. In particular, it is suggested that the durability response as a function of increasing curing temperature should be examined.

References

ACI 308R-01. (2001). *Guide to curing concrete,* Reported by American Concrete Institute Committee 308, United States.

ACI 318-95. (1995). *Building Code Requirements for Reinforced Concrete and Commentary,* American Concrete Institute, United States.

ACI Committee 363, (1992). *State-of-the Art Report on High-Strength Concrete,* American Concrete Institute, United States.

ACl 301-05. (2005). *Specifications for Structural Concrete with Selected ACl Field Reference Manual,* American Concrete Institute, United States.

Acquaye, L. (2006). *Effect of high curing temperatures on the strength, durability and potential of delayed ettringite formation in mass concrete structures*, PhD Thesis, Graduate School of the University of Florida, Untied States.

Ahmad, S. H., and Shah, S. P. (1985). "Structural properties of high strength concrete and its implications for precast pre-stressed concrete." *Journal of Precast/Prestressed Concrete Institute,* 30(6), 92-119.

Alexander, K. M., and Taplin, J. H. (1962). "Concrete strength, cement hydration and the maturity rule." *Australian Journal of Applied Sciences,* 13, 277-284.

Alexander, M. G., Mackechnie, J. R., and Ballim, Y. (1999). *Guide to the use of durability indexes for achieving durability in concrete structures,* Research Monograph No. 2: University of Cape Town and University of the Witwatersrand.

Alexanderson, J. (1972). "Strength losses in heat cured concrete." Proc., Swedish Cement and Concrete Research Institute, Stockholm. 135 p.

Al-Khafaji, J. A. (2001). *Some Mechanical Properties of Accelerated Cured High Strength Concrete Cylinders*, Ph.D. Thesis, Al-Mustansiriyah University, Baghdad, Iraq.

Alshamsi, A. M. (1994). "Temperature rise inside paste during hydration in hot climates." *Cement and Concrete Research, Elsevier,* 24(22), 353–360.

AS 3600-2009. (2009). *Concrete Structures*. Standards Australia, Sydney, Australia.

ASTM C1202-12. (2010). *Standard Test Method for Electrical Indication of Concrete's Ability to Resist Chloride Ion Penetration.* ASTM International, United States.

Balendran, R. V., and Martin-Buades, W. H. (2000). “The influence of high temperature curing on the compressive, tensile and flexural strength of pulverized fuel ash concrete.” *Building and Environment, Elsevier,* 35(5), 415-423.

Benammar, B., Mezghiche, B., and Guettala, S. (2013). “Influence of atmospheric steam curing by solar energy on the compressive and flexural strength of concretes.” *Construction and Building Materials, Elsevier,* 49, 511-518.

Bentur, A., Berger, R. L., Kung, J. H., Milestone, N. B., and Young, J. F. (1979). “Structural Properties of Calcium Silicates Pastes.” *Journal of American Ceramic Society,* 62(7-8), 362-366.

Berhane, Z. (1992). “The behaviour of concrete in hot climates.” *Materials and Structures, RILEM,* 25(147), 157-162.

Beushausen, H., and Burmeister, N. (2015). “The use of surface coatings to increase the service life of reinforced concrete structures for durability class XC.” *Materials and Structures*, 48, 1243–1252.

Bingöl A.F., and Tohumcu, I. (2013). “Effects of different curing regimes on the compressive strength properties of self-compacting concrete incorporating fly ash and silica fume.” *Materials and Design, Elsevier,* 51, 12–18.

Bondar, D., Cyril, J., Lynsdale, Milestone, N. B., and Hassani, N. (2012). “Oxygen and Chloride Permeability of Alkali-Activated Natural Pozzolan Concrete.” *ACI Materials Journal,* 109(1), 53-62.

Bournazel, J. P., and Moranville-Regourd, M. (1993). “Concrete Technology, Past, Present and Future.” *American Concrete Institute,* 144, 233-250.

Bournazel, J.P., and Moranville-Regourd, M. (1995). “Microstructure of steam cured concretes deteriorated by alkali-silica reaction.” *Materials Research Society,* 370, 57-66.

Brooks, J. J., and Kaisi, A. F. (1990). “Early strength development of Portland and slag cement concretes cured at elevated temperature.” *ACI Materials Journal,* 87(5), 503-507.

Cao, Y., and Detwiler, R. J. (1995). “Backscattered electron imaging of cement pastes cured at elevated temperatures.” *Cement and Concrete Research, Elsevier,* 25(3), 627-638.

Carino, N. and Meeks, K. (1999). “Curing of High-Performance Concrete Strength: What is sufficient?” *American Concrete Institute*, 1-36.

Carino, N. J. (1981). *Temperature effects on the strength–maturity relation of mortar*. Report No. NBSIR81–2244, National Bureau of Standards, Washington, United States.

Carino, N. J., and Lew, H. S. (1994). “The maturity method: From theory to application.” *Cement Concrete Aggregate,* 6(2), 61-73.

Cebeci, O. Z. (1987). “Strength of Concrete in Warm and Dry Environment”, *Materials and Structures,* 20, 270-222.

CEB-FIP Model Code 1990, Thomas Telford, United Kingdom.

Detwiler, R. J., Fapohunda, C. A., and Natale, J. (1994). “Use of Supplementary Cementing Materials to Increase the Resistance to Chloride Ion Penetration of Concretes Cured at Elevated Temperatures.” *ACI Materials Journal,* 91(1), 4 pages.

Dinakar, P., Babu, K. G., and Santhanam, M. (2008). “Mechanical properties of high-volume fly ash self-compacting concrete mixtures.” *Structural Concrete,* 9(2), 109-116.

Eliverly, R. H., and Evans, E. P. (1964). “The effect of curing condition on physical properties of concrete.” *Magazine of Concrete Research,* 16(46), 11-20.

Escalante-Garcia, J. I., and Sharp, J. H. (2001). “The microstructure and mechanical properties of blended cements hydrated at various temperatures.” Cement and Concrete Research, Elsevier, 31(5), 695–702.

Ezziane, K., Bougara, A., Kadri, A., Khalafi, H., and Kadri, E. H. (2007). “Compressive strength of mortar containing natural pozzolan under various curing temperature.” *Cement and Concrete Composites, Elsevier,* 29(8), 587-593.

Farrar, J. R. (1978). "Electrically conductive concrete." *GEC Journal of Science and Technology,* 45(1), 45-48.

Felekoglu, B., Turkel, S., and Baradan, B. (2007). “Effect of water/cement ratio on the fresh and hardened properties of self-compacting concrete.” *Building and Environment, Elsevier,* 42(4), 1795-1802.

FIB Model Code for Concrete Structures. (2010). Ernst and Sohn, Berlin, Germany.

Fraay, A. L. A., Bijen, J. M., and de Haan, Y. M. (1989). “The reaction of fly ash in concrete.” *Cement and Concrete Research, Elsevier,* 19(2), 235-246.

Francisco, J. P. M., Liu, Y., Wu, Y. Y., and Wendy, A. (2013). *Analysis and Estimation of Service Life of Corrosion Prevention Materials Using Diffusion, Resistivity and Accelerated Curing for New Bridge Structures*, Vol. 2: Accelerated Curing of Concrete With High Volume Pozzolans (Resistivity, Diffusivity and Compressive Strength), Florida Department of Transportation Research Center, Florida, United States.

Frías, M. (2006a). “Study of hydrated phases present in a MK-lime system cured at 60°C and 60 months of reaction.” *Cement and Concrete Research, Elsevier,* 36(5), 827-831.

Frías, M. (2006b). “The effect of metakaolin on the reaction products and micro-porosity in blended pastes submitted to long hydration time and high curing temperature.” Advances in Cement Research, 18(1), 1-6.

Gardner, D. R., Lark, R. J., and Barr, B. (2005). “Effect of Conditioning Temperature on the Strength and Permeability of Normal- and High-Strength Concrete.” *Cement and Concrete Research, Elsevier,* 35(7), 1400-1406.

Gesoğlua, M., Güneyisi, E., and Özbay, E. “Properties of self-compacting concretes made with binary, ternary, and quaternary cementitious blends of fly ash, blast furnace slag, and silica fume.” *Construction and Building Materials. Elsevier,* 23(5), 1847-1854.

Giannini, E., and Zhu, J. (2012). “Effects of Elevated Curing Temperatures on the Mechanical Properties of Concrete Cylinders.” *Proc., 14th International Conference on Structural Faults and Repair*, Edinburgh, United Kingdom. 9 pages.

Goto, S., and Roy, D. M. (1981). “The effect of w/c ratio and curing temperature on the permeability of hardened cement paste.” *Cement and Concrete Research, Elsevier,* 11(4), 575-579.

Hakkinen, T. (1993). “The influence of slag content on the microstructure, permeability and mechanical properties of concrete.” *Cement and Concrete Research, Elsevier,* 23(2), 407-421.

Hansen, P. F., and Pedersen, E. J. (1977). “Maturity computer for controlled curing and hardening of concrete.” *Nordiska Betongfoerbundet,* 1, 21-25.

Hoppe, G. E., Mackechnie, J. R., and Alexander, M. G. (1994). *Measures to ensure concrete durability and effective curing during construction*. South African Department of Transport, South Africa.

Jiang, W., and Roy, D. (1992). “Hydrothermal processing of new fly ash cement.” *American Ceramic Society Bulletin,* 71(4), 642-647.

Kanda, T., Sakuramoto, F., Suzuki, K. (1992). “Compressive strength of silica fume concrete at high temperatures.” *Proc., Fourth International Conference on Fly ash, silica fume, slag and natural pozzolans in concrete,* (Ed. Malhotra, V. M.), Vol. 2, American Concrete Institute, SP-132, 1089-1103.

Khatib, J. M., and Mangat, P. S. (2002). “Influence of high-temperature and low-humidity curing on chloride penetration in blended cement concrete.” *Cement and Concrete Research, Elsevier,* 32(11), 1743-1753.

Kim, J. K., Moon, Y. H., and Eo, S. H. (1998). “Compressive strength development of concrete with different curing time and temperature.” *Cement and Concrete Research, Elsevier,* 28(12), 1761-1773.

Kim, J. K., Sang, H. H., and Young, C. S. (2002). “Effect of temperature and aging on the mechanical properties of concrete: Part I. Experimental results.” *Cement and Concrete Research, Elsevier,* 32(7), 1087-1094.

Kjellsen, K. O., and Detwiler, R. J. (1993). “Later-age strength prediction by a modified maturity model.” *ACI Material Journal,* 90(3), 220-227.

Kjellsen, K. O., and Detwiler, R. J. and Gjorv, O. E. (1990). “Pore structure of plain cement pastes hydrated at different temperatures.” *Cement and Concrete Research, Elsevier,* 20(6), 927-933.

Klieger, P. (1958). “Effect of Mixing and Curing Temperature on Concrete Strength.” *American Concrete Institute. Portland Cement Association, Research and Development Laboratories, Research Department,* 103, 1063-1081.

Kodur, V. (2014). “Review Article - Properties of Concrete at Elevated Temperatures.” *Hindawi Publishing Corporation,* 15 pages.

Koibuchi, K., Yamaguchi, H., Kabota, K., Ishikawa, Y. (1991). “Hydration and compressive strength development of high strength concrete heated to 60 or 80°C at the early age.” *Proc., Cement and Concrete*, Concrete Association of Japan, 45, 204-209.

Kosmatka, S. H., Kerkhoff, B., and Panarese, W. C. (2003). *Design and Control of Concrete Mixtures,* 14th Ed., Engineering Bulletin 001. Portland Cement Association, Illinois, United States.

Kou, S. C., and Poon, C. S. (2009). “Properties of self-compacting concrete prepared with recycled glass aggregate.” *Cement and Concrete Composites, Elsevier,* 31(2), 107-113.

Kou, S. C., Poon, C. S., and Chan, D. (2004). “Properties of steam cured recycled aggregate fly ash concrete.” *International RILEM Conference on the Use of Recycled Materials in Building and Structures Publisher,* RILEM Publications SARL, 10 pages.

Lee, J. (2008). “Properties of concrete after high-temperature heating and cooling.” *ACI Materials Journal,* 105(4), 334-341.

Lee, N. (2014). "Post-Demould Curing of Heat-Treated Concrete: Necessity or Complication?"<http://www.branz.co.nz/cms_show_download.php?id=4e3d2bff09ac0b16d183c2b407d30a964 d63bd87> (May 6, 2016).

Ling, T. C., Poon, C. S., and Shi-Cong Kou, S. C. (2012). "Influence of recycled glass content and curing conditions on the properties of self-compacting concrete after exposure to elevated temperatures." *Cement and Concrete Composites, Elsevier,* 34(2), 265-272.

Liu, S., Xie, G., and Wang, S. (2015). "Effect of curing temperature on hydration properties of waste glass powder in cement-based materials." *Journal of Thermal and Analysis and Calorimetry,* 119(1), 47-55.

Liu, Y. (2012). *Accelerated curing of concrete with high volume pozzolans – resistivity, diffusivity and compressive strength.* PhD Thesis, Florida Atlantic University, United States.

Lo, T. Y., and Cui, H. Z. (2004). "Effect of porous lightweight aggregate on strength of concrete." *Materials Letters, Elsevier,* 58(6), 916-919.

Lo, T. Y., Nadeem, A., Tang, W. C. P., and Yu, P. C. (2009). "The effect of high temperature curing on the strength and carbonation of pozzolanic structural lightweight concretes." *Construction and Building Materials, Elsevier,* 23(3), 1306-1310.

Lothenbach, B., Winnefeld, F., Alder, C., Wieland, E., and Lunk, P. (2007). "Effect of temperature on the pore solution, microstructure and hydration products of Portland cement pastes." *Cement and Concrete Research, Elsevier,* 37(4), 483-491.

Ma, W., Sample, D., Martin, R., and Brown, P. W. (1994). "Calorimetric study of cement blends containing fly ash, silica fume and slag at elevated temperatures." *Cement and Concrete and Aggregates,* 16(2), 93-99.

Madandoust, R., and Mousavi, S. Y. (2012). "Fresh and hardened properties of self-compacting concrete containing metakaolin." *Construction and Building Materials, Elsevier,* 35: 752-760.

Malhotra, V. M., and Carino, N. J. (2003). *Handbook on Non-destructive Testing of Concrete,* 2nd edition, CRC Press, Boca Raton, FL, 384 pages.

Martínez-Ramírez, S., and Frías, M. (2009). "The effect of curing temperature on white cement hydration." *Construction and Building Materials, Elsevier,* 23(3), 1344-1348.

Matos, A. M., Ramos, T., Sandra, N., and Sousa-Coutinho, J. (2016). “Durability enhancement of SCC with waste glass powder.” *Materials Research,* 19(1), 67-74.

Meeks, K. W., and Carino, N. J. (1999). *Curing of High-Performance Concrete: Report of the State-of-the Art.* Building and Fire Research Laboratory, National Institute of Standards and Technology, Maryland, United States.

Mehta, P. K., and Monteiro, P.J. M. (1993). *Concrete: Microstructure, Properties, and Materials*, 2nd Ed., United States.

Milestone, N. B., and Gorce, J. P. (2012). "Determining how water is held in composite cement binders," *Journal of the Australian Ceramic Society,* 48(2), 244-248.

Mirzahosseini, M., and Riding, K. A. (2014). “Effect of curing temperature and glass type on the pozzolanic reactivity of glass powder.” *Cement and Concrete Research, Elsevier,* 58, 103-111.

Monfore, G. E. (1968). "The electrical resistivity of concrete." *Journal of Portland Cement Association Research and Development Laboratories,* 10(2), 35-48.

Naus, D. J. (2005). *The Effect of Elevated Temperature on Concrete Materials and Structures - A Literature Review.* U.S. Nuclear Regulatory Commission, Office of Nuclear Regulatory Research, United States.

Naus, D. J., and Graves, H. L. (2006). “A Review of the Effects of Elevated Temperature on Concrete Materials and Structures.” *Proc., 14th International Conference on Nuclear Engineering,* ASME, Florida, USA, 10 pages.

Neville, A. M. (1995). *Properties of concrete.* 4th Ed. Longman Group Limited, Harlow Essex, England.

Neville, A. M., and Brooks, J. J. (1987). *Concrete Technology,* Longman Scientific & Technical, 438 pages.

Newman, J., and Choo, B. S. (2003). *Advanced Concrete Technology, 1: Concrete Properties,* Butterworth Heinemann, Elsevier, United Kingdom.

NZS 3101: 2006. The Design of Concrete Structures and Part 2 – Commentary. SNZ, Wellington, New Zealand.

Oluokun, F. A. (1991). “Prediction of concrete tensile strength from its compressive strength: Evaluation of existing relations for normal weight.” *American Concrete Institute,* 88(3) (1991) 302-309.

Oztekin, E. (1984). “Determination of heat treatment cycle for cements.” *Turkish Cement Manufacturers. Association Cement Bulletin,* 206(3), 24-26.

Ozyildirim, H. C. (1998). *Effects of Temperature on the Development of Low Permeability in Concretes.* Virginia Transportation Research Council, Charlottesville, United States, 26 pages.

Ozyildirim, H. C., and Halstead, W. J. (1994). “Improved Concrete Quality with Combinations Fly Ash and Slica Fume.” *ACI Materials Journal,* 91(6), 587-594.

Persson, B. (2003). “Self-consolidating concrete at fire temperatures.” *Division of Building Materials, Lund Institute of Technology,* 3110, 216 pages.

Poutos, K. H., Alani, A. M., Walden, P. J., and Sangha, C. M. (2007). *“Relative temperature changes within concrete made with recycled glass aggregate.” Construction and Building Materials, Elsevier,* 22(4), 557-565.

Price, W. H. (1951). “Factors influencing concrete strength.” *Journal of American Concrete Institute,* 47(2), 417-432.

Rajabipour, F., and Weiss, J. (2007). “Electrical conductivity of drying cement paste.” *Materials and Structures,* 40(10), 1143-1160.

Reddy, B. M. (2013). *Effect of water quality on the strength and durability characteristics of blended cement concrete silica fume concrete and fiber reinforced concrete.* Ph.D. thesis. Jawaharlal Nehru Technological University Anantapur, India.

Regourd, M., and Gauthier, E. (1980). “Comportement des ciments soumis au durcissement accélère.” *Durcissement accéléré des bétons, Ann. l'ITBTP 387,* Béton, 387, 83–96.

Reinhardt, H. W., and Stegmaier, M. (2006). “Influence of heat curing on the pore structure and compressive strength of self-compacting concrete (SCC).” *Cement and Concrete Research, Elsevier,* 36(5), 879–85.

Richardson, I. G. (2004). “Tobermorite/jennite – and tobermorite/calcium hydroxide based models for the structure of C–S–H: applicability to hardened pastes of tricalcium silicate, b-dicalcium silicate, Portland cement, and blends of Portland cement with blast furnace slag, metakaolin, or silica fume.” *Cement and Concrete Research, Elsevier,* 34(9), 1733–77.

Scott, A., Mackechnie, J., Matthews, J., Bull, D., Cook, D., Ali, S. (2014). “Preliminary assessment of the influence of accelerated curing on concrete quality.” *Proc., The New Zealand Concrete Industry Conference 2014,* Taupo, New Zealand.

Scrivener, K. L., Young, J. F. (1995). “Mechanisms of Chemical Degradation of Cement-based Systems.” *Proc., Materials Research Society’s Symposium*, Massachusetts, United States.

Selman, M. H. (2001). *Effect of Hot Weather on the Mechanical Properties of Concrete Produced using local Furnace Slag*. M.Sc. Thesis, Al-Mustansiriyah University, Baghdad, Iraq.

Shayan, A., and Xu, A. (2006). “Performance of glass powder as a pozzolanic material in concrete: A field trial on concrete slabs”. *Cement and Concrete Research, Elsevier,* 36(3), 457-468.

Shi, C. J., Wu, Y. Z., Riefler, C., Wang, H. (2005). “Characteristics and pozzolanic reactivity of glass powders.” Cement Concrete Research, Elsevier, 35(5), 987-993.

Shoukry, S. N., William, G. W., Downie, B., Riad, M. Y. (2009). “Effect of Moisture and Temperature on the Mechanical Properties of Concrete.” *Construction and Building Materials, Elsevier,* 25(2), 688-696.

Siddique, R. and Khan, M. I. (2011). *Supplementary Cementing Materials,* Springer, Berlin Heidelberg, Germany.

Soni, D. K., and Saini, J. (2014). “Mechanical Properties of High Volume Fly Ash (HVFA) and Concrete Subjected to Evaluated 120°C Temperature.” *International Journal of Civil Engineering Research,* 5(3), 241-248.

Soroka, I. (1993). *Concrete in hot environments.* E. & F. N. Spon, London, 251 pages.

Stutzman, P. E., and Clifton, J. R. (1992). *Microstructural features of some low water/solids, CSF mortars cured at different temperatures.* NISTER 4790, U.S. Department of Commerce. Virginia, United States.

Swamy, R. N., Ibrahim, A. B., and Anand, K. L. (1975). “The strength and deformation characteristics of high early strength structural concrete.” Matériaux et Construction, 8(48), 413-423.

Sylla, H. M. (1998). *Beton,* 38(2), 44-54.

Taylor, P. C. (2013). *Curing Concrete,* Taylor and Francis Group, New York, United States.

Tepponen, P. and Erickson, B. E. (1987). “Damages in Concrete Railway Sleepers in Finland," *Nordic Concrete Research,* 6, 199-209.

The Concrete Society. (1988). *Permeability testing of site concrete: A review of methods and experience.* Technical Report 31, The Concrete Society, London, 96 pages.

Thomas, M. D. A., Matthews, J. D., Haynes, C. A. (1989). “Effect of curing on the strength and permeability of PFA concrete.” *American Concrete Institute,* SP 114, 191-218.

Tipler, P. A. (1999). *Physics for scientists and engineers,* 4th edition. W. H. Freeman, New York, Unites States.

Turkel, S., and Alabas, V. (2005). “The effect of excessive steam curing on Portland composite cement concrete.” *Cement and Concrete Research, Elsevier,* 35(2), 405-411.

Verbeck, G. J., and Helmuth, R. A. (1968). “Structures and physical properties of cement paste.” *Proc., 5th International Conference on the Chemistry of Cement,* Tokyo, 1–32.

Wang, H. Y., and Huang, W. L. (2010). “Durability of self-consolidating concrete using waste LCD glass.” *Construction and Building Materials, Elsevier,* 24(6), 1008-1113.

Whiting, D. A., and Nagi, M. A. (2003). *Electrical resistivity of concrete: A literature review.* PCA R&D Serial No. 2457, Portland Cement Association, Skokie, Illinois, United States, 57 pages.

Wild, S., Sabir, B., and Khatib, J. M. (1995). “Factors influencing strength development of concrete containing silica fume.” *Cement and Concrete Research, Elsevier,* 25(7), 1567-1580.

Williams, J. T., Owens, P. L. (1982). “The Implications of a Selected Grade of United Kingdom Pulverized Fuel Ash on the Engineering Design and Use in Structural Concrete,” *Proc., International Symposium on the Use of PFA in Concrete,* Leeds, United Kingdom, 301-313.

Yanbo Liu, Y., and Francisco, P. M. (2014). “Effect of Elevated Temperature Curing on Compressive Strength and Electrical Resistivity of Concrete with Fly Ash and Ground-Granulated Blast-Furnace Slag.” *ACI Materials Journal,* 111(5), p 531.

Yuan, Y., and Wan, Z. L. (2002). “Prediction of Cracking within Early-Age Concrete due to Thermal, Drying and Creep Behaviour.” *Cement and Concrete Research, Elsevier,* 32(7), 1053-1059.

Zhou, W., Li, H., Nasser, H. (2008). “Study on Variability of Model Parameters of Concrete Structure: Humidity and Moisture Effect.” *Proc., SPIE 6934, Non-destructive Characterization for Composite Materials*, San Diego, United States.

CHAPTER 8

CONCLUSIONS AND RECOMMENDATIONS FOR FUTURE WORK

8.1 Context of the research

The principle objective of this research was to assess the viability of self-compacting concrete that utilized waste glass powder as a partial replacement for a traditional binder that is cement and as an alternative to conventional supplementary cementing materials, such as class F and class C fly ashes and limestone filler. This thesis includes findings on the practicability of using this self-compacting concrete, which was assessed by conducting various fundamental fresh and hardened concrete-related tests in the laboratory. Lab-based trials were undertaken to determine suitable glass finenesses and replacement levels in self-compacting concrete with the potential of being carried forward in commercial applications to achieve desired performance requirements. In a marine environment, the requirements for utilizing a supplementary cementing material in concrete are equally focused on both the strength and durability.

This research was motivated by the availability of waste resources in New Zealand and the goal of effective potential utilization of an existing resource of crushed waste glass, as its stockpiles are located throughout New Zealand, awaiting disposal or recycling. An extensive literature review indicated that currently there is a lack of research concerning the use of waste glass powder in concrete compared to the vast amount of research conducted on the use of fly ashes and limestone fillers in concrete. The available research is mostly based on the performance of concrete containing very coarse glass and there is inadequate information on the rheology of glass powder incorporated self-compacting concrete. From a review of previous studies, which were focused on the use of glass powder in concrete, it was found that concrete with glass powder has similar properties to few other supplementary

cementing materials, such as improved workability and durability. Concerning the use of crushed waste glass in concrete, prior literature generally indicated that the larger the size of the glass particles used in concrete, the more harmful the effects are on concrete properties, such as workability, air content, strength, and especially the alkali-silica reaction. The main hindrance of using waste glass in concrete was found to be the alkali-silica reaction, which is mainly dependent on the reactivity of glass powder and its particle size. Hence, the fineness of glass powder was given due importance in this study, in addition to its appropriate content, to achieve desired concrete properties.

The results presented and discussed in the previous chapters have been derived from the experimental investigations on the effects of replacing conventional binder (GP cement) by the ground waste glass in self-compacting concrete. Apart from a traditional control mix containing 100% GP cement, a number of other control mixes were also produced with 30% of the GP cement replaced by class F fly ash; 30% of the GP cement replaced by class C fly ash and 30% of the GP cement replaced by limestone powder. The glass was crushed to achieve various particle size distributions, which were either finer, comparable or coarser than that of the GP cement. The glass powders used for these investigations were produced by automatic crushing in a rod mill for different lengths of time. The shape and surface texture of the individual glass particles were generally different from those of the other binders used in this study. Self-compacting concrete mixes were produced with 20%, 30% and 40% of the GP cement replaced by 20 µm washed glass powder; 30% of the GP cement replaced by 20 µm unwashed glass powder and 30% of the GP cement replaced by 10 µm, 20 µm, and 40 µm washed glass powders. In general, the research work was focussed on the effects of glass powders on the rheological characteristics of fresh self-compacting concrete and the engineering/structural properties and time-related durability effects of hardened self-compacting concrete, and their comparison with GP cement, class F, and C fly ashes and limestone powder incorporated self-compacting concretes.

The conclusions reported in Section 8.2 must be viewed in the light that they relate to one specific self-compacting concrete mix, which was produced with 450 kg/m^3 binder content with a water-cement ratio of 0.4. This self-compacting concrete mix also contained admixtures, such as superplasticizer and stabilizer, which were varied according to the requirement of a particular investigation. There was no difference between the types of admixtures, cement, fine aggregates and coarse aggregates used in the control mixes and the glass modified mixes in any of the investigations. The variations observed between the results of the same mix type but produced again at a different time for a different investigation were attributed to the heterogeneous and somewhat variable nature of concrete. The properties of concrete depend on the environmental conditions, operator, and

equipment, handling and storing etc., which may complicate the analysis of concrete by producing somewhat inconsistent and misleading results. In general, however, there was a reasonable agreement between the various batches of the same mix design resulting in comparable results. Additionally, glass powders were ground in small batches and were collectively well-mixed before casting the large-scale mixes (discussed in Chapters 5, 6 and 7); however, they were ground separately for small-scale mixes (discussed in Chapter 4). Hence, there might be some small variations in the particle morphology of glass powders used in the preliminary and small-scale studies, though similar mean particle size was ultimately achieved.

8.2 Conclusions

The conclusions arising from this research into the assessment of concrete that utilizes waste glass powder are summarized below:

- The initial trials using glass powder in concrete were based on testing different dosages and sizes of glass powder in mortar, produced to determine the possibility of glass powder as a replacement for conventional binders. In the presence of very coarse (about 300 µm) unwashed glass powder, it was determined that 30%-50% glass powder replaced by weight of cement led to a large reduction in compressive strength, with a decrease in workability. Another trial with relatively finer unwashed glass powder of 50 µm also did not perform well in mortar due to the presence of impurities in the glass material. While washing the glass material before grinding offset many of the negative effects, grinding it to finer sizes of 10-40 µm after washing further ensured a uniform distribution of waste glass powder within the mortar mix, leading to more improved workability and compressive strength. These preliminary trials gave a valuable indication of the potential influence of particle size, content and quality of the glass powder on concrete.

- Self-compacting concrete mixes, with glass powder as cement replacements, were produced in large-scale trials, to assess the influence of fineness, content and quality control on the rheology. The incorporation of glass powder into self-compacting concrete, whether finer/coarser or in less/more proportions, influenced its rheological behaviour. The dosage of superplasticizer to achieve the same slump flow range varied directly with the fineness of glass powder and inversely with its substitution content. This means that a lower dosage of superplasticizer was needed to achieve the same slump flow range for the mix incorporating coarser glass powder and the mix including glass powder at higher replacement levels. For instance, superplasticizer

dosage of 0.58% was required to achieve an optimum flow of 660-750 mm for self-compacting concrete with 10 µm glass added at 30% in comparison to 0.36% for self-compacting concrete with 40 µm glass added at the same replacement level. Additionally, superplasticizer dosage of 0.53% was required to achieve the optimum flow for self-compacting concrete with 20% glass having the fineness of 20 µm in comparison to 0.40% for self-compacting concrete with 40% glass with similar fineness. However, better rheological performance in terms of yield stress and plastic viscosity was achieved by self-compacting concrete mixes, although with higher superplasticizer dosages, containing glass powders of finer sizes and added at lower contents. This concludes that the rheological parameters were dependent on the superplasticizer dosage as well as on the particle shape, size, and content of glass powder.

- The excessive use of superplasticizer beyond a certain limit resulted in the compressive strength loss due to the microstructural damage and increase in the pore area ratios of the glass modified mixes. The finer glass had generally a greater tendency to be affected by superplasticizer dosage compared with the coarser glass. Self-compacting concrete mixes with 10 µm and 20 µm glass powder added at 30% and 20% replacement level respectively, demonstrated the best performance in terms of rheology, compressive strength and durability compared with mixes incorporating coarser glass and glass at higher amounts. However, the durability behaviour of the 10 µm glass incorporated mix was found to be parallel to the 40 µm glass modified mix when there were minor variations in the superplasticizer dosage. This concludes that quality control during concrete production needs to be carefully monitored. While the workability of concrete is generally considered a fresh property, it strongly influences the durability of concrete.

- Experimental investigations were conducted on the mechanical properties of self-compacting concrete mixes containing glass powder. The mechanical properties of concrete containing glass powder were a function of both pozzolanic reaction and particle packing. Pozzolanic reaction is the chemical reaction between GP cement, glass powder and water whereas, packing effect is a proper arrangement of small glass particles, which fills the voids and contributes to the compressive strength without undergoing any chemical reaction. The use of finer glass powder at lower replacement levels in self-compacting concrete resulted in higher compressive strength, splitting tensile strength and elastic modulus than the coarser glass powder used at higher contents. Glass powder with higher fineness produced higher

compressive strength due to faster pozzolanic reaction of glass and extra compressive strength was contributed to finer glass concrete by the packing effect. The grinding of glass accelerated the pozzolanic reaction because the entrapped amorphous silica in the inner domains of coarse glass particles was released with grinding and involved itself in the faster pozzolanic reaction. Hence, grinding the glass powder improved the strength gain related with pozzolanic activity due to increased surface area.

- A significant increase in the later-age strengths and elastic modulus of 10 µm glass replaced at 30% and 20 µm glass replaced at 20% was achieved compared to those of 20 µm glass replaced at 40% and 40 µm glass replaced at 30%. The 545-days data revealed that 10 µm glass replaced at 30% achieved compressive strength, splitting tensile strength and elastic modulus of approximately 92 MPa, 7 MPa, and 49 GPa whereas 40 µm glass replaced at 30% achieved about 76 MPa, 6 MPa, and 43 GPa respectively. The mechanical properties of concrete incorporating the unwashed glass powder as a partial replacement for the GP cement was also studied, which essentially reduced compressive strength, splitting tensile strength and elastic modulus compared to the washed glass incorporated mixes. Further analysis of the experimental data showed that the relationships between splitting tensile strength and compressive strength and between elastic modulus and compressive strength were essentially independent of the fineness or replacement level of the glass powder.

- Additional testing and analysis were undertaken to further verify the satisfactory performance of glass powder in self-compacting concrete and understand its effects on the long-term durability. Durability properties of self-compacting concrete containing glass powder of various sizes and proportions were investigated. Fundamental durability properties including oxygen permeability, porosity, electrical resistivity, chloride diffusion and drying shrinkage were tested. Although the use of washed glass in self-compacting concrete was found to improve workability and did not significantly affect the mechanical properties, its long-term durability was considerably improved in comparison to the GP cement. Interfacial transition zone (ITZ), which is considered as the weakest link under mechanical loadings and also the most readily pathway for water and aggressive ions into concrete, was clearly more compacted in glass powder concrete. The pozzolanic reaction of glass powder further densified the bulk and ITZ paste, which had a positive effect on the microstructure and therefore, impermeability of glass modified concrete. Additionally, the fine glass powder dispersed in the presence of superplasticizer to fill the voids between the cement particles, by a physical mechanism called filler effect, also resulted in a well packed concrete mix.

These effects along with the improved particle distribution of glass powder resulted in the reduction of the thickness of ITZ and led to densely packed durable concrete.

- The durability characteristics were found to be enhanced with the addition of smaller sizes of glass powder and lower glass powder contents. Concretes with 20-40% glass powder of fineness 20-40 µm replacing the GP cement exhibited high resistance to chloride ion penetration making this concrete ideal for structures close to the shore. The negligible water absorption capacity of glass particles led to improved dimensional stability and hence, lower drying shrinkage of the washed glass modified mixes. On the other hand, the replacement of 30% of the GP cement with the unwashed glass powder resulted in concrete with inadequate durability properties.

- Accelerated cured self-compacting concrete, incorporating washed glass powder of fineness 20 µm and replaced at 30% by cement, achieved its target strength, irrespective of the following curing regime. Conversely, elevated cured self-compacting concrete containing unwashed glass powder, having fineness of 20 µm and substituted by 30%, could not reach its design strength even with subsequent water-curing. This concludes that the utilization of clean glass powder in self-compacting concrete is necessary to achieve satisfactory performance, particularly when the accelerated curing is the requirement for real concrete construction.

- Wet-curing followed by an accelerated heat treatment, given to the washed glass modified concrete, improved its microstructure and hence the durability, compared to heat treatment alone. Additionally, accelerated thermal curing without subsequent water curing did not compromise the resistance of the washed glass incorporated SCC to permeation of aggressive agents and fell within acceptable durability ranges particularly in the long term. Its coefficient of oxygen permeability was lower than 10^{-10} m/s, porosity below 11%, electrical resistivity around 20 kohm.cm and chloride diffusion coefficient below 10^{-11} m^2/s. Conversely, the accelerated heat treatment given to the unwashed glass powder led to further deterioration of its durability and was found to be an inappropriate alternative to the standard curing regime.

- In terms of the comparison with other binders (1) all glass incorporated mixes showed superior rheological performance compared to the GP cement and class C fly ash; however, 40 µm glass added at 30% and 20 µm glass added at 40% exhibited worse performance compared to the class F fly ash; (2) the long-term strengths of the mixes incorporating 10 µm glass at 30% and 20 µm glass at 20% and 30% were comparable to the GP cement and fly ashes and mixes containing 40 µm glass added at 30% and

20 µm glass added at 40% were equivalent to the limestone filler; (3) mixes containing 10 µm glass at 30% and 20 µm glass at 20% and 30% demonstrated definite improvement in durability compared to all the other control mixes; however, mixes containing 40 µm glass added at 30% and 20 µm glass added at 40% showed almost comparable durability performance to the class F and class C fly ash incorporated mixes but better than the GP cement and limestone filler mixes; (4) with washed 20 µm glass addition at 30%, long-term mechanical and durability properties of self-compacting concrete were less negatively influenced by initial temperature rise compared to GP cement and fly ash incorporation; however, the opposite was true for unwashed 20 µm glass powder added at 30% that showed worse durability behaviour compared to these binders, irrespective of the temperature rise and subsequent curing regime. To summarize, glass powder of fineness 10 µm added up to 30% and 20 µm added up to 20%-30%, can successfully replace GP cement, class F, and C fly ashes and limestone filler in a self-compacting concrete mix, particularly in concrete construction where both strength and durability are essential requirements. Moreover, glass powder of fineness 20 µm added up to 40% and 40 µm added up to 30% can replace limestone filler in a self-compacting concrete mix, in the sections where durability is of a greater concern than strength.

The results from this research have provided a good evidence for the application of an unconventional mineral admixture, the ground glass powder, in concrete industry; firstly by producing self-compacting concrete with pre-defined fresh properties and investigating the influence of glass powder on the rheological behaviour; secondly by assessing the influence of glass powder on the long-term mechanical and durability properties of the self-compacting concrete; thirdly by studying the effects of accelerated curing on the long-term mechanical and durability performance of self-compacting concrete containing glass powder and finally by evaluating the performance of glass powder in comparison to conventionally used binder and some other mineral admixtures. This research can lead to increasing economic and environmental advantages for the concrete industry by limiting the production of cement and utilizing the glass waste resources in New Zealand and around the globe. The environmental benefits must not be overlooked as waste glass addition into self-compacting concrete on an appropriate selective basis would provide a solution to problems encountered in waste management. When used as finely ground powder to substitute GP cement, this constitutes a positive response to global environmental problems, such as high CO_2 emissions generated by Portland cement production. In addition, it would reduce extraction of natural materials, such as limestone and improve the overall sustainability of the cement industry.

8.3 Future directions and recommendations

The utilization of higher volumes of supplementary cementing materials reduces waste disposal problems, saves natural resources, decreases CO_2 emissions and has positive economic effects. Glass powder also has the potential to be used as a mineral admixture in concrete applications and its use in optimum quantities can achieve more of these benefits. However, there remains considerable scope for further research to advance the understanding of the performance of concrete that utilizes waste glass powder. To facilitate future research direction, a set of recommendations is provided as follows:

- Based on the improved durability demonstrated by glass incorporated mixes, it can be predicted that glass powder of such small finenesses may be able to counterbalance the negative effects from the alkali-silica reaction. However, experimental investigations using the similar glass fineness ranges in self-compacting concrete are required to confirm this hypothesis. Comprehensive expansion tests, using direct measurement of dimensional changes (in three dimensions) of self-compacting concrete, containing glass powder are recommended, in addition to the detailed microscopic examination of sections to detect products of alkali-silica reaction.

- Most literature reports on accelerated laboratory based alkali-silica reaction test results, rather than long-term alkali-silica reaction test results from field trials. The alkali-silica reaction potential of waste glass also needs to be analyzed by conducting field trials on the self-compacting concrete incorporating waste glass. This method will give the most reliable results based on the exact concrete mix design used, rather than the modified concrete mixes used in accelerated laboratory alkali-silica reaction tests. In addition, the analysis needs to be conducted to understand the chemical effect that waste glass powder has on alkali-silica reaction, which is considered to be the negative effect in concrete containing waste glass powder.

- The dosage rate of waste glass powder in self-compacting concrete can possibly be modified with fine to coarse glass powders to optimize concrete properties, such as durability of concrete, which is one of the main advantages of using glass powder in self-compacting concrete. Hence, considering the energy consumption resulting from grinding, research into the effect of using a combination of low dosages of very fine waste powder coupled with higher dosages of coarse glass powder in concrete may lead to enhance durability with lower overall energy costs.

- Due to its specific mix design, self-compacting concrete behaves differently in comparison with conventional concrete. In general, design codes and mechanical properties for conventional concrete apply when using self-compacting concrete. However, in many cases, a considerable benefit can be achieved by considering the specific advantages of self-compacting concrete, such as the improvement of the interfacial transition zone with coarse aggregate and embedded reinforcement that can improve bond and structural behaviour. Unfortunately, these specific advantages are not yet covered in traditional design codes and further investigation is required towards the regulation of standards and code for self-compacting concrete.

APPENDIX A – LITERATURE ANALYSIS

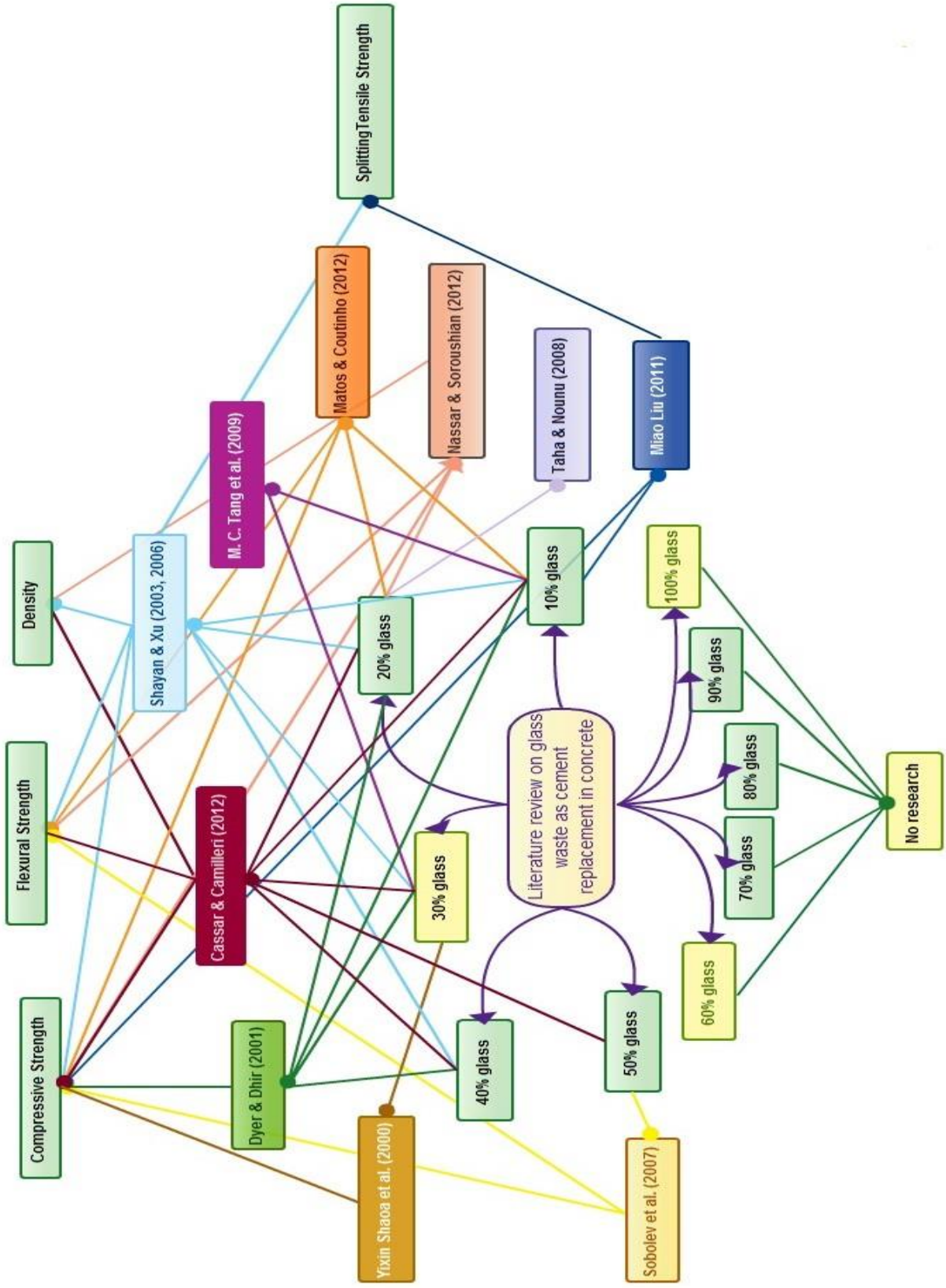

Figure A-1: A casual trial of compiling past research efforts

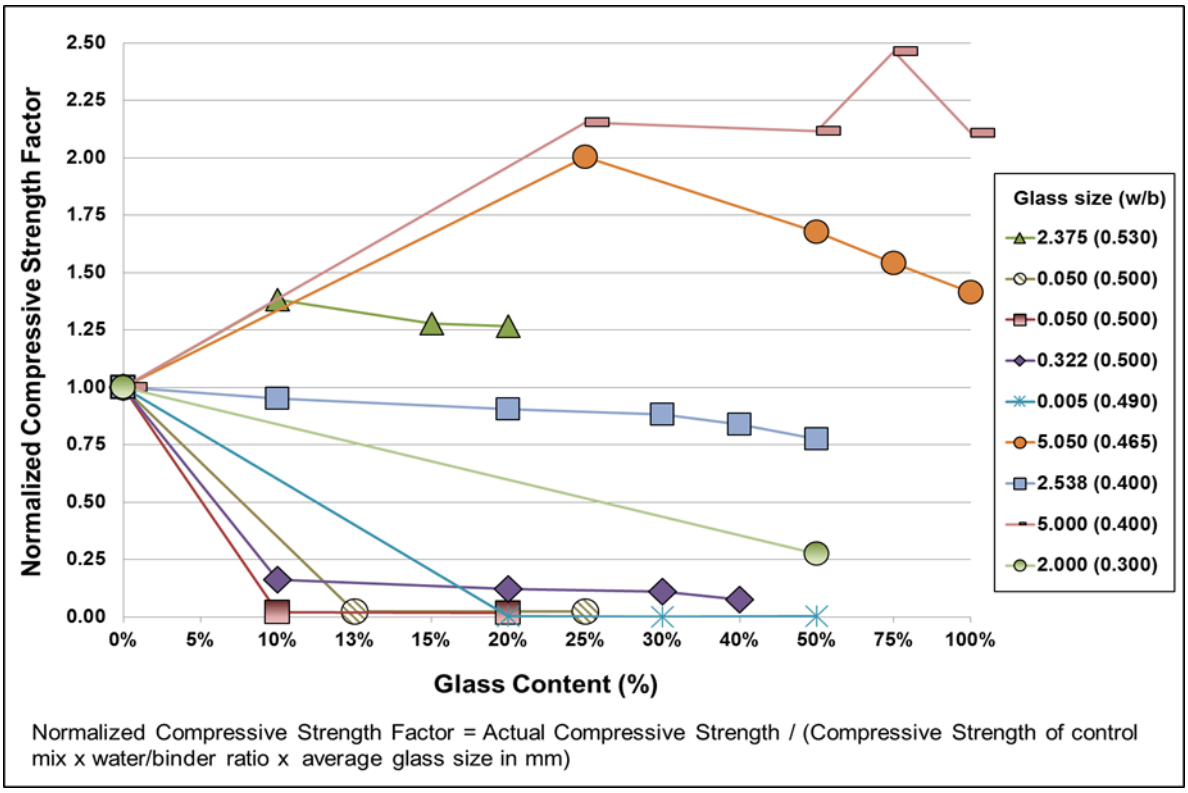

Figure A-2: Graph between glass proportions and normalized 7-days compressive strengths

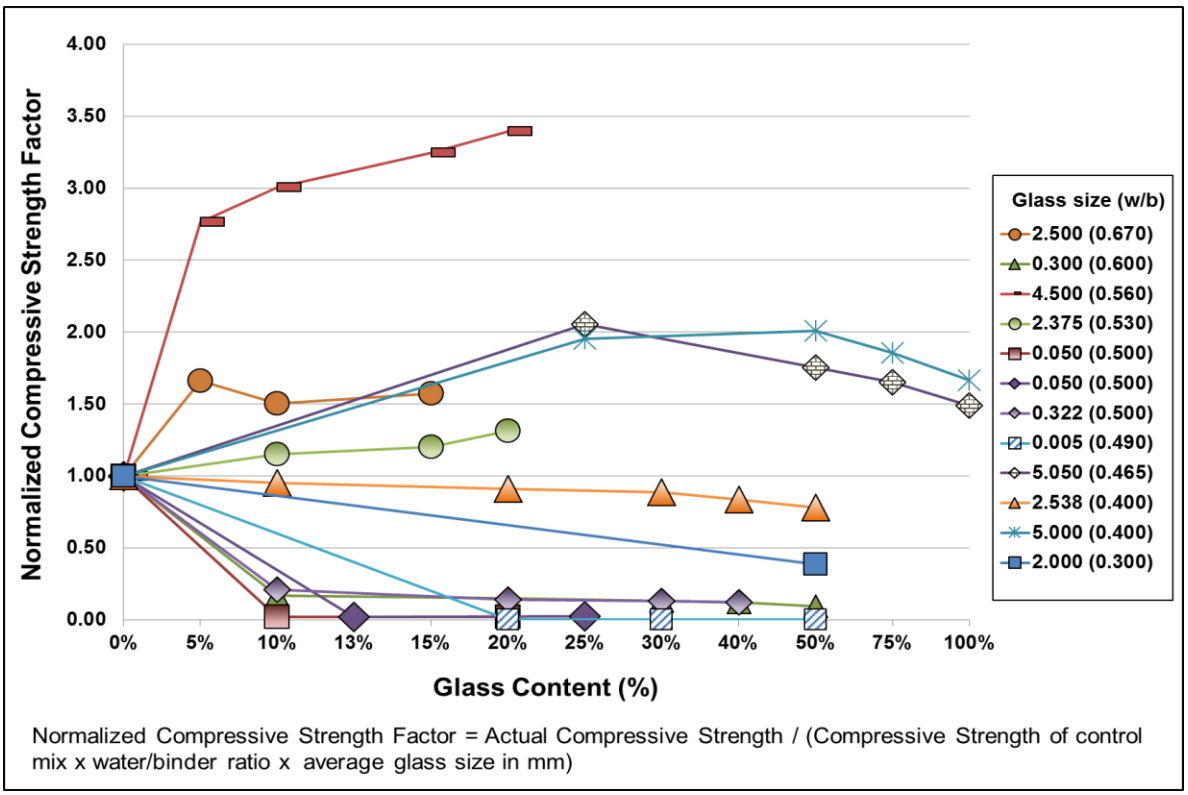

Figure A-3: Graph between glass proportions and normalized 28-days compressive strengths

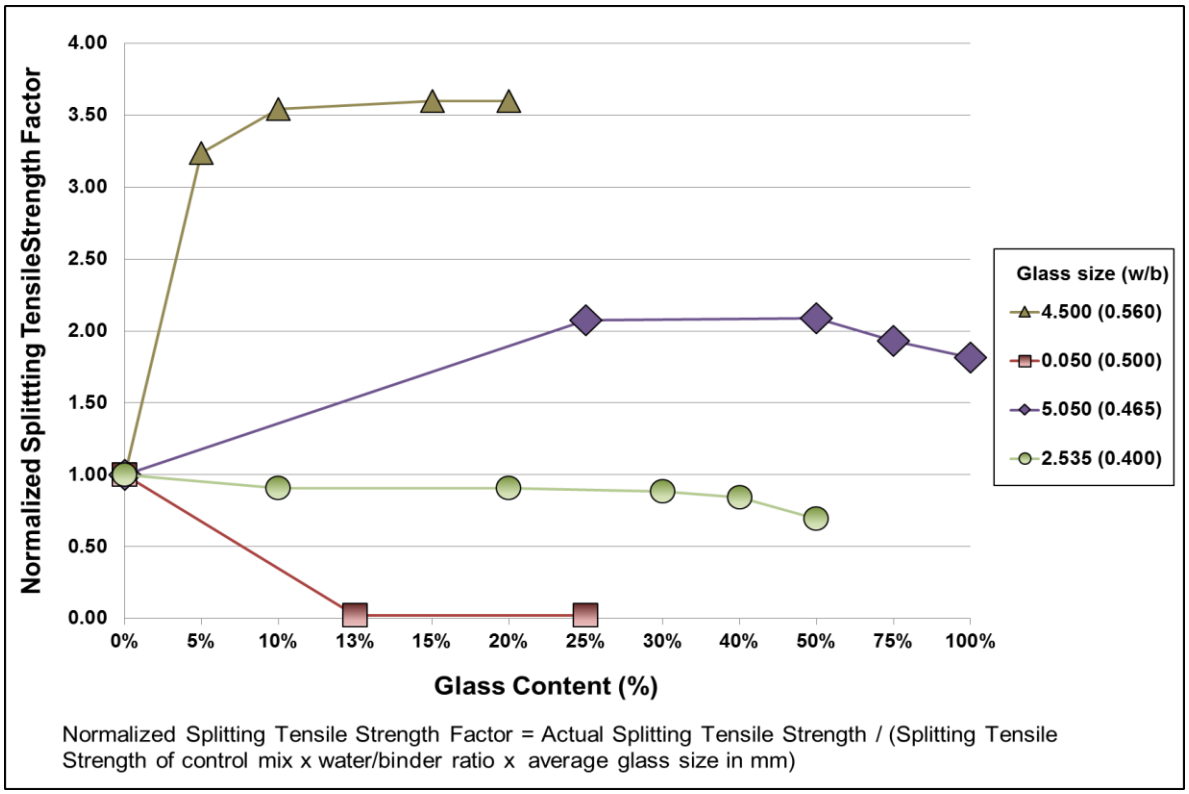

Figure A-4: Graph between glass proportions and normalized 28-days splitting tensile strengths

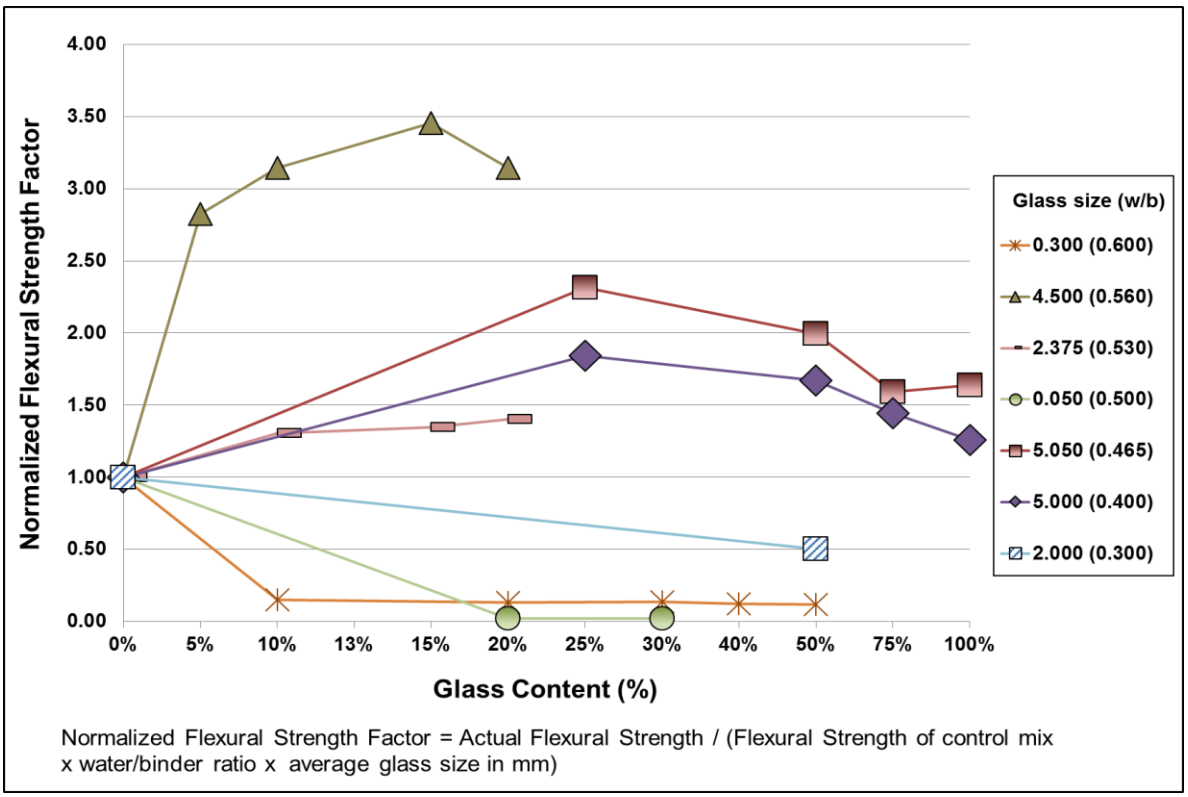

Figure A-5: Graph between glass proportions and normalized 28-days flexural strengths

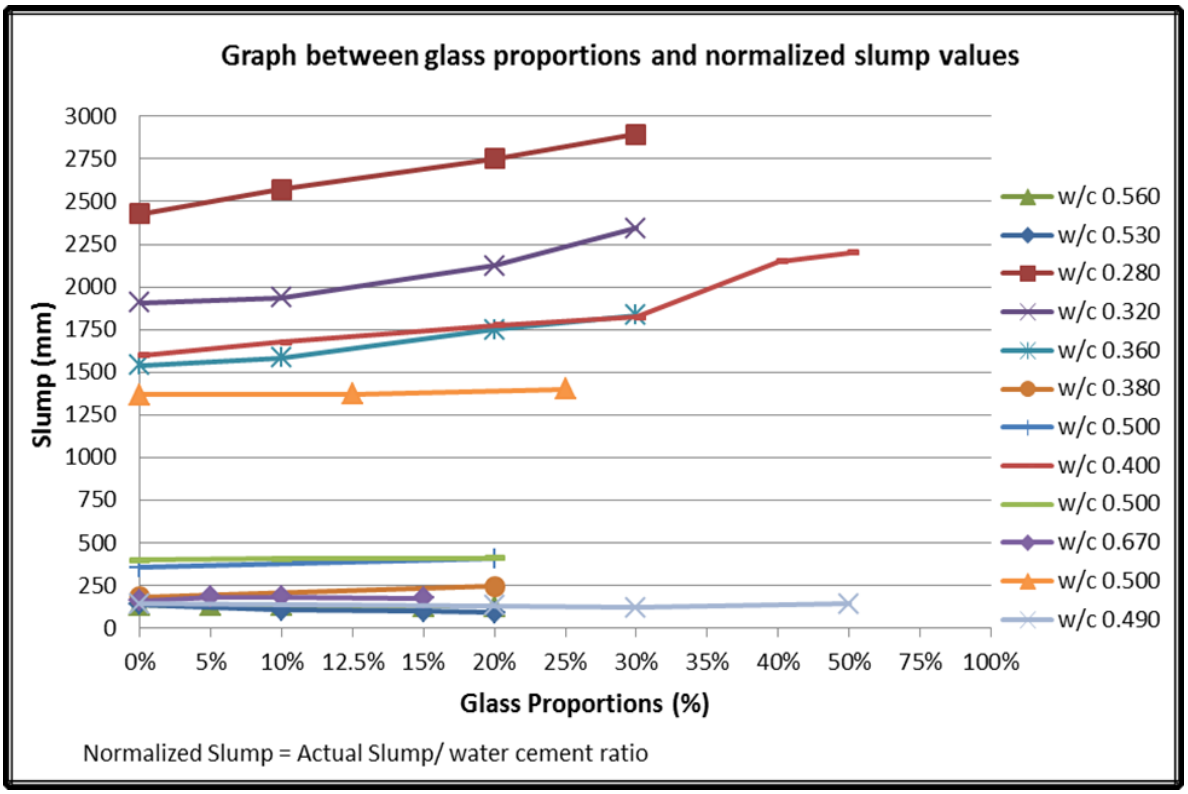

Figure A-6: Graph between glass proportions and normalized slump values considering w/c ratio

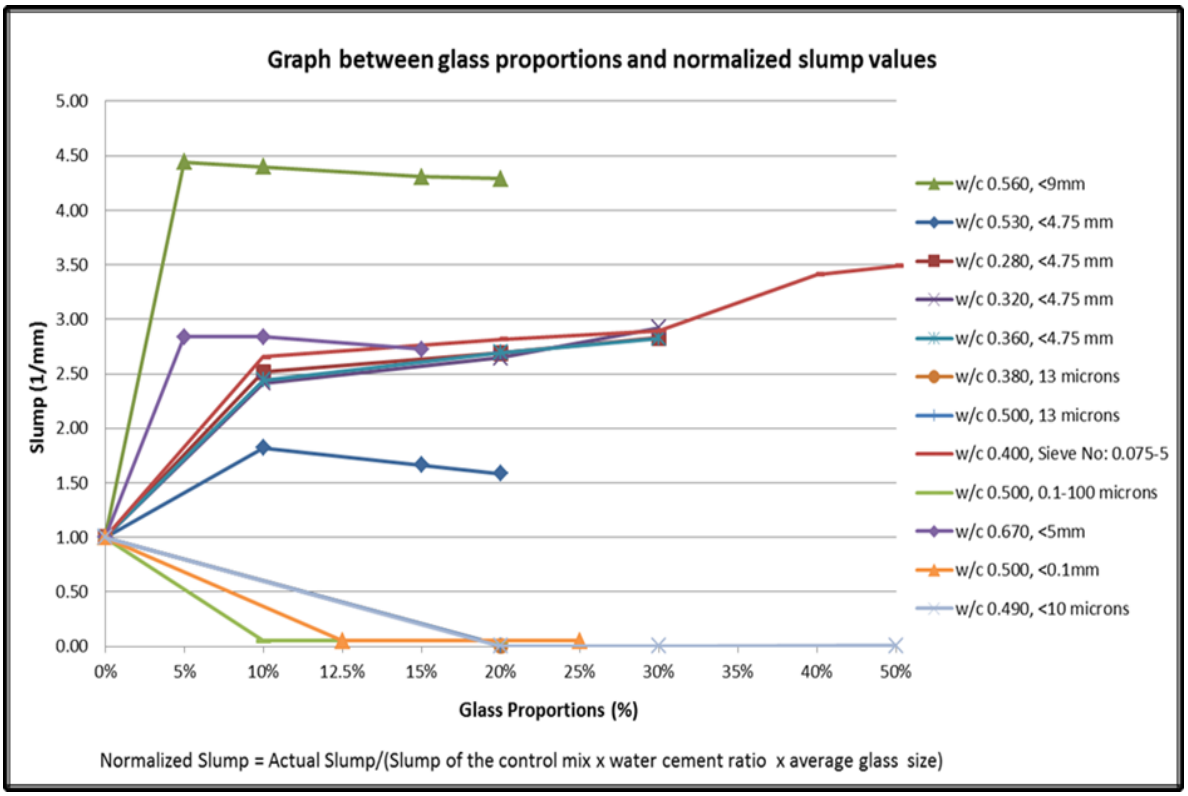

Figure A-7: Graph between glass proportions and normalized slump values considering slump of the control mix, w/c ratio, and average glass size

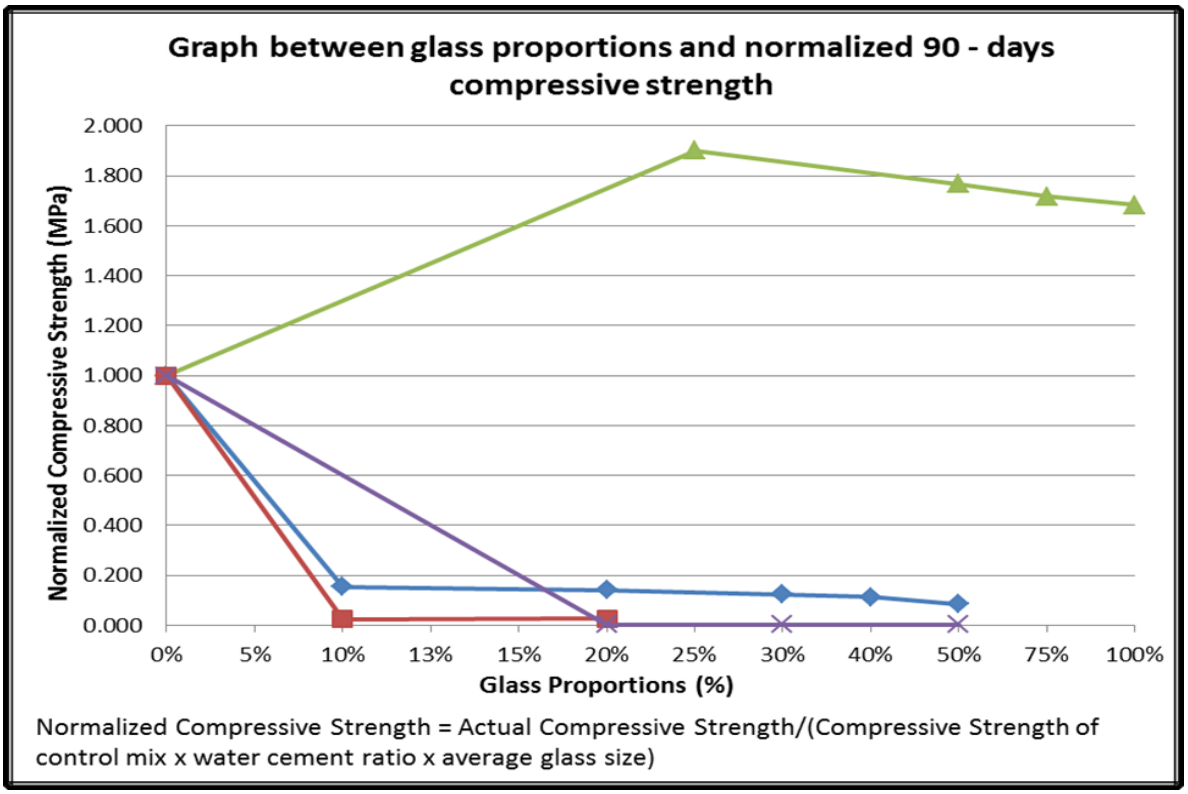

Figure A-8: Graph between glass proportions and normalized 90-days compressive strengths

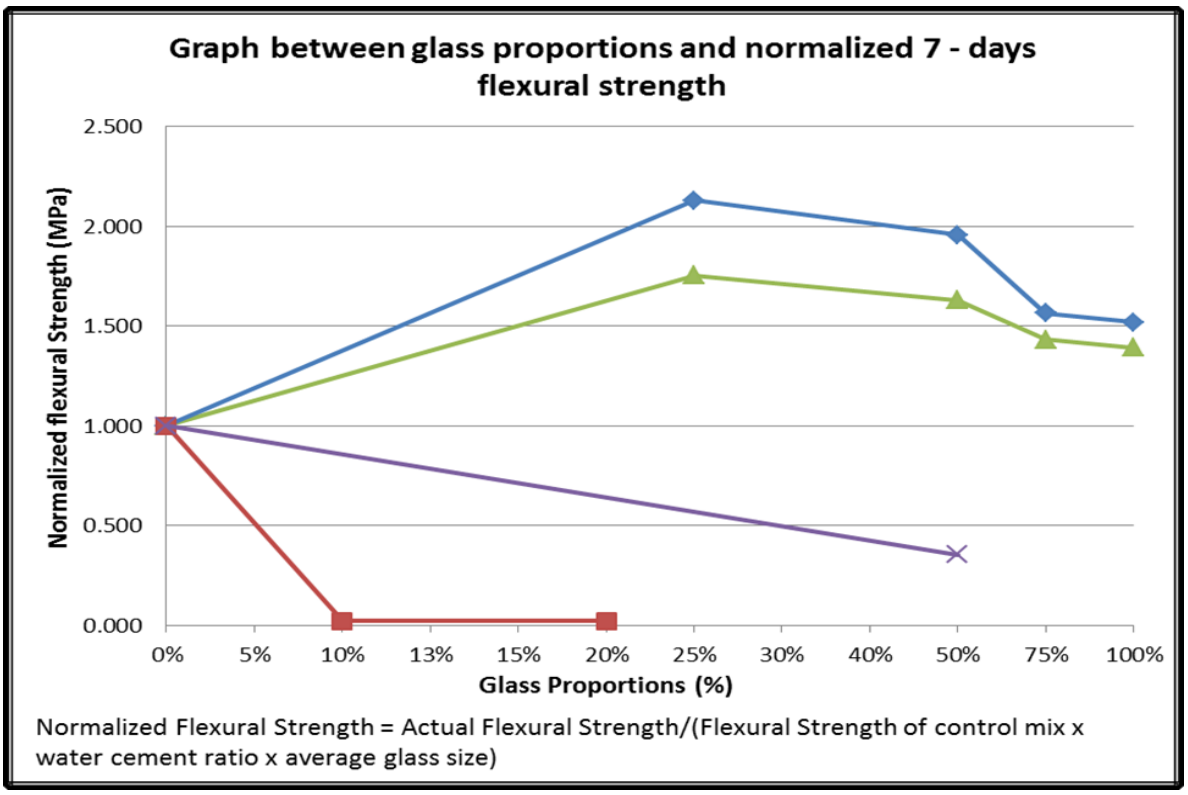

Figure A-9: Graph between glass proportions and normalized 7-days flexural strengths

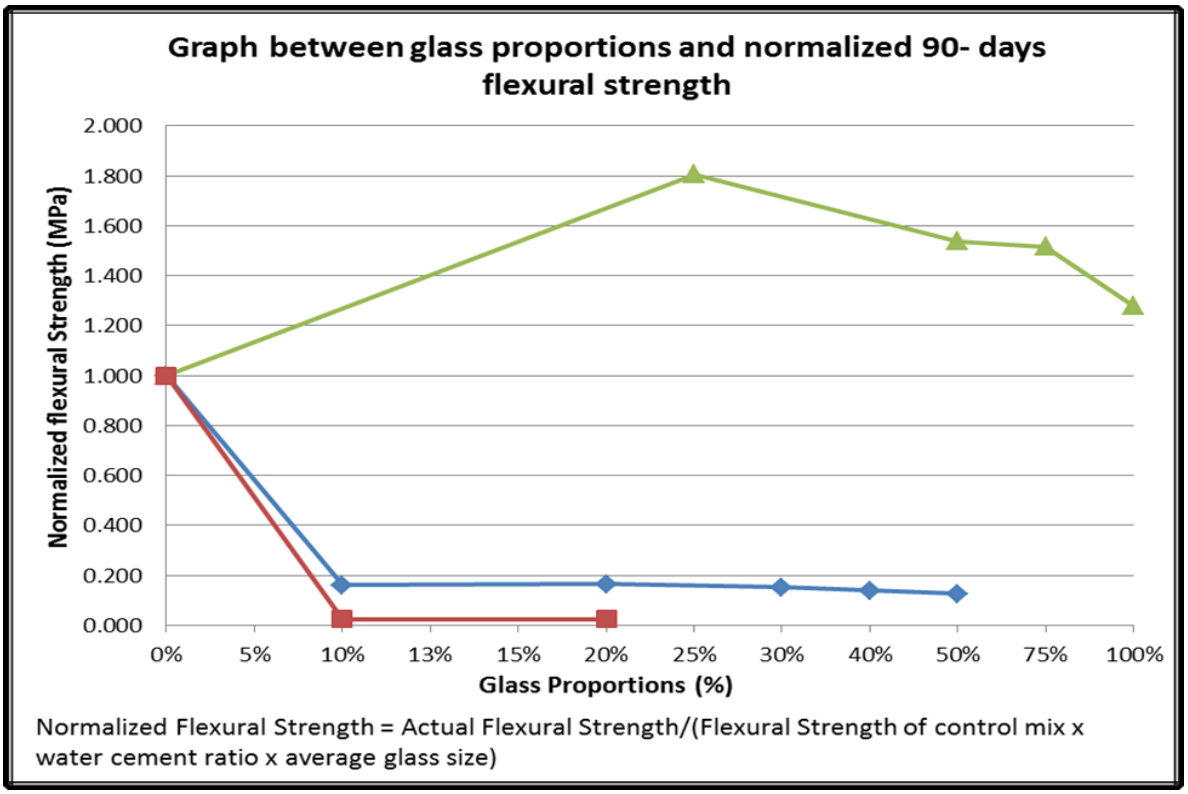

Figure A-10: Graph between glass proportions and normalized 90-days flexural strengths

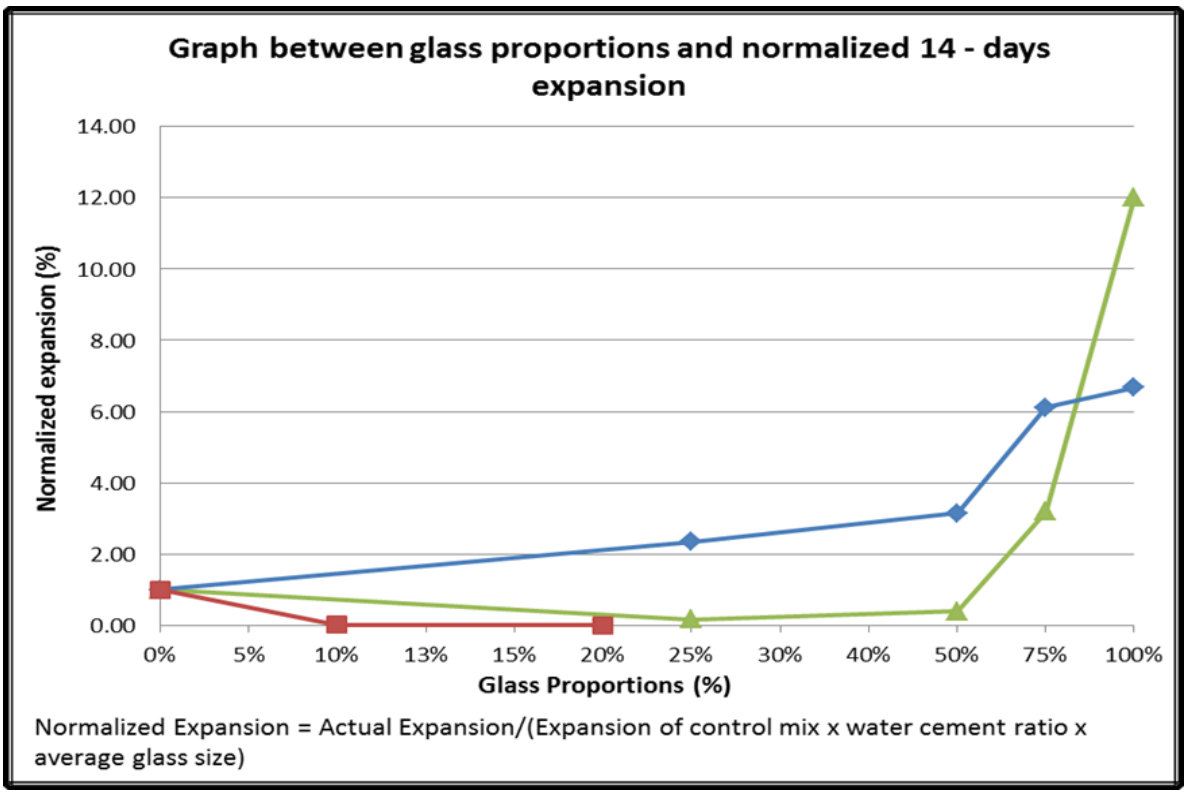

Figure A-11: Graph between glass proportions and normalized 14-days ASR expansion

APPENDIX B – MATERIAL CHARACTERIZATION

Table B-1: Particle size distribution of WG1 used in the preliminary trials

Size (µm)	Percent Passing (%)
	WG1
3000.00	100.0
2636.47	100.0
2301.84	100.0
2009.69	100.0
1754.61	100.0
1531.91	100.0
1337.48	100.0
1167.73	99.7
1019.52	99.1
890.12	98.2
777.14	96.4
678.50	93.3
592.39	88.3
517.20	81.1
451.56	72.1
394.24	62.0
344.21	52.0
300.52	43.0
262.38	34.9
229.08	28.0
200.00	22.3
174.62	17.7
152.45	14.1
133.10	11.2
116.21	8.9
101.46	6.9
88.58	5.1
77.34	3.6
67.52	2.4
58.95	1.6
51.47	1.0
44.94	0.6
39.23	0.3
34.26	0.1
29.91	0.0
26.11	0.0

Table B-2: Particle size distribution (PSD) of binders used in the large-scale trials

Size (µm)	Percent Passing (%)						
	GP	FAF	FAC	LP	10 µm GL	20 µm GL	40 µm GL
394.24	-	-	-	100.0	-	-	-
344.21	-	-	-	99.6	-	-	-
300.52	-	-	-	98.8	-	-	-
262.38	100.0	100.0	100.0	97.3	-	-	100.0
229.08	100.0	99.6	99.5	95.2	-	-	99.8
200.00	100.0	99.1	98.7	92.3	-	-	99.5
174.62	100.0	98.4	97.8	89.2	-	100.0	99.0
152.45	100.0	97.5	96.7	86.2	-	100.0	98.4
133.10	100.0	96.2	95.3	83.3	-	100.0	97.6
116.21	99.9	94.7	93.5	80.4	-	100.0	96.4
101.46	99.7	92.6	91.4	77.2	-	100.0	94.5
88.58	99.3	89.8	88.7	73.1	-	99.8	91.2
77.34	98.7	86.5	85.4	68.5	-	99.5	86.2
67.52	97.5	82.7	81.8	63.4	-	98.6	79.7
58.95	95.8	78.8	77.9	58.4	-	96.5	72.2
51.47	93.1	74.7	74.0	53.4	-	92.6	64.1
44.94	89.3	70.8	70.0	48.9	-	86.8	56.3
39.23	84.2	67.0	66.0	44.8	-	79.9	50.5
34.36	77.9	63.5	62.1	41.4	-	73.3	45.0
29.91	67.7	60.0	58.1	37.5	-	68.1	40.1
26.11	56.8	56.4	53.8	34.2	100.0	64.4	36.2
22.80	47.7	52.6	49.3	31.4	100.0	58.2	32.6
19.90	42.7	48.4	44.3	28.8	99.7	52.7	28.1
17.38	38.7	43.8	38.9	25.7	98.5	47.7	24.2
15.17	31.1	38.7	33.1	22.3	95.3	43.6	20.8
13.25	24.2	33.2	27.3	18.9	88.3	39.0	16.5
11.57	18.1	27.7	21.7	16.6	76.4	34.3	11.7
10.10	13.2	22.5	16.8	14.3	61.6	28.4	8.3
8.82	9.3	17.9	12.6	12.2	46.1	22.9	5.5
7.70	6.4	14.0	9.2	10.3	32.6	18.2	3.4
6.72	4.2	10.7	6.6	8.5	22.9	13.8	2.1
5.87	2.7	8.1	4.6	6.9	16.7	10.5	1.5
5.12	1.7	6.1	3.2	5.5	12.8	8.0	1.2
4.47	1.0	4.6	2.2	4.2	10.1	6.0	0.1
3.91	0.6	3.4	1.4	3.3	7.9	4.3	0.0
3.41	0.3	2.4	0.9	2.5	6.1	2.7	-
2.98	0.1	1.7	0.6	1.3	4.2	1.4	-
2.60	0.0	1.1	0.3	0.6	2.5	0.5	-
2.27	0.0	0.7	0.1	0.3	1.1	0.1	-
1.98	0.0	0.4	0.0	0.1	0.3	0.0	-
1.73	0.0	0.1	0.0	0	0.0	0.0	-

Table B-3: Effects of grinding time on mean diameter of glass powder used in the main SCC trials

Time (hrs)	Mean Diameter (μm)
0.5	110.3
1.0	94.7
2.0	68.0
3.5	41.9
5.0	32.3
6.0	23.4
6.5	21.9
8.0	18.2
9.5	15.6
12.5	12.2
15.0	9.9

The following results are symbolized as:

SAM1 – unwashed glass

SAM2 – 20 um glass

SAM3 – FA (C)

SAM4 – FA (F)

SAM5 – GP-GB

XRD Results

All values are estimates and given as percentage composition of the crystalline material present in the air dried sample.

The colours refer to the database lines on the XRD scan for each sample.

Sample Label	Quartz (blue)	Calcite (green)	Hematite (black)	Mullite (purple)	Gypsum (red)	Portlandite (yellow)
SAM 1	non crystalline					
SAM 2	non crystalline					
SAM 3	60	15	trace	5	10	10
SAM 4	60	15	5	10	10	

(a)

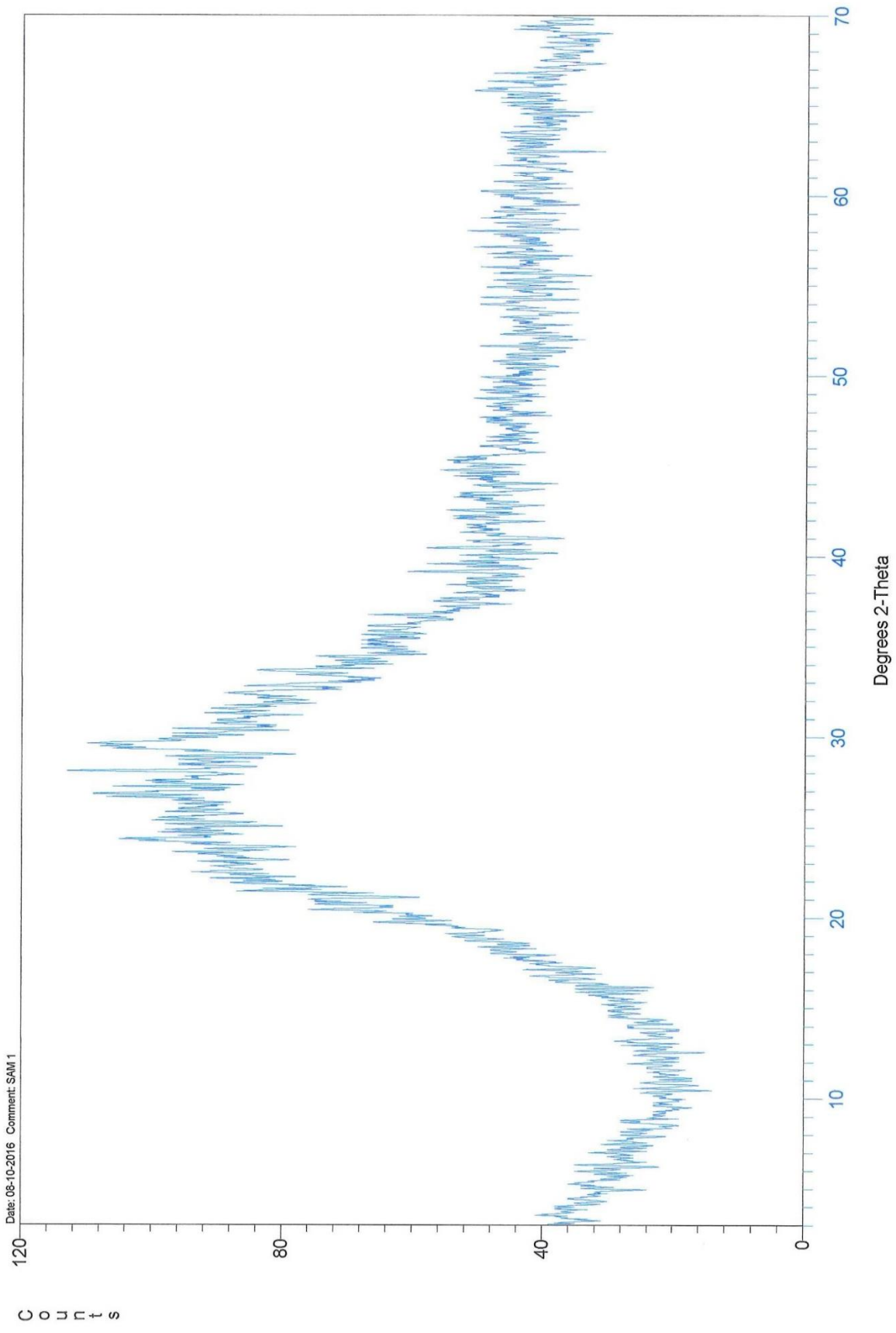
Date: 08-10-2016 Comment: SAM 1
Counts
120
80
40
0
10
20
30
40
50
60
70
Degrees 2-Theta

(b)

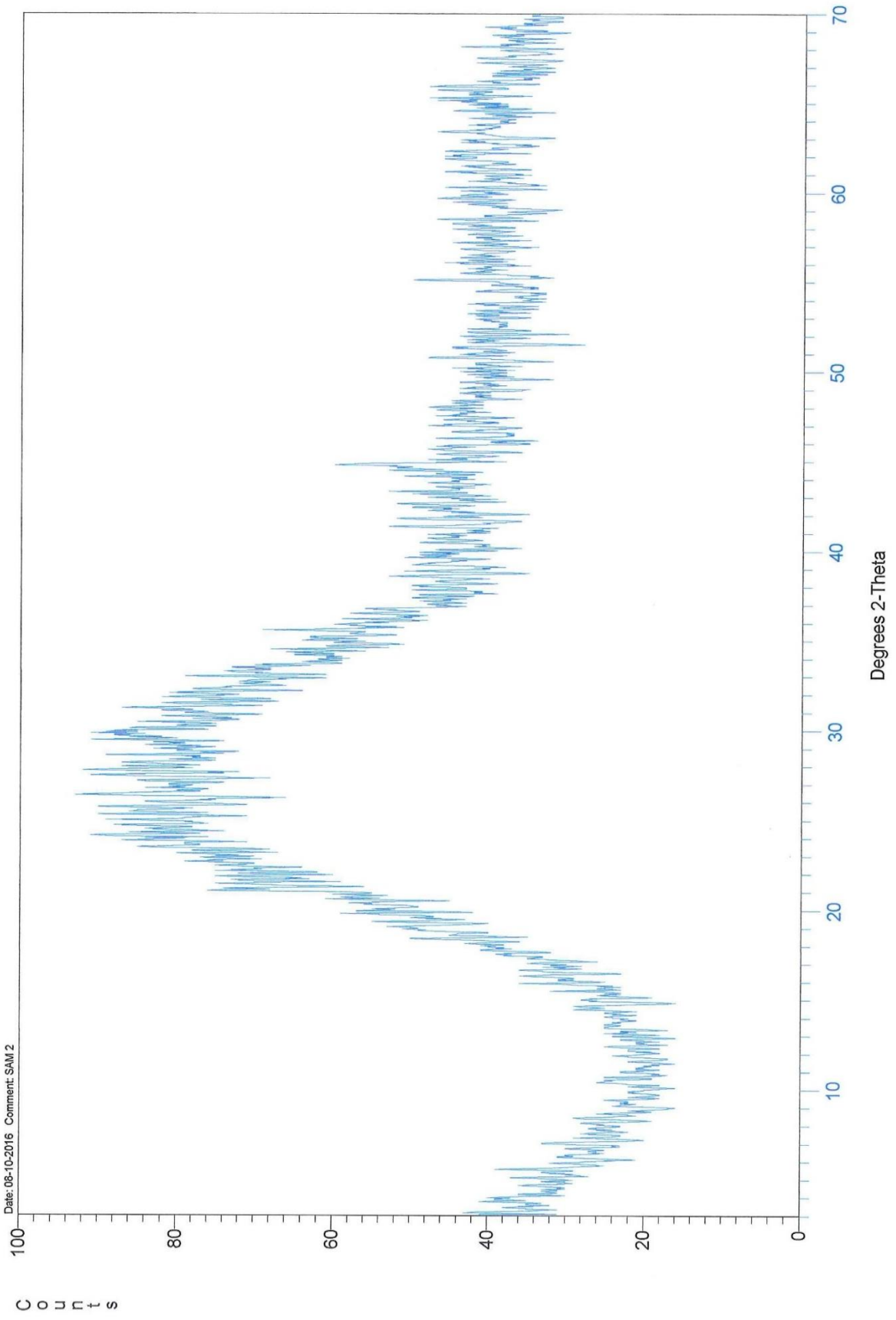
Date: 08-10-2016 Comment: SAM 2
Counts
100
80
60
40
20
0
10
20
30
40
50
60
70
Degrees 2-Theta

(c)

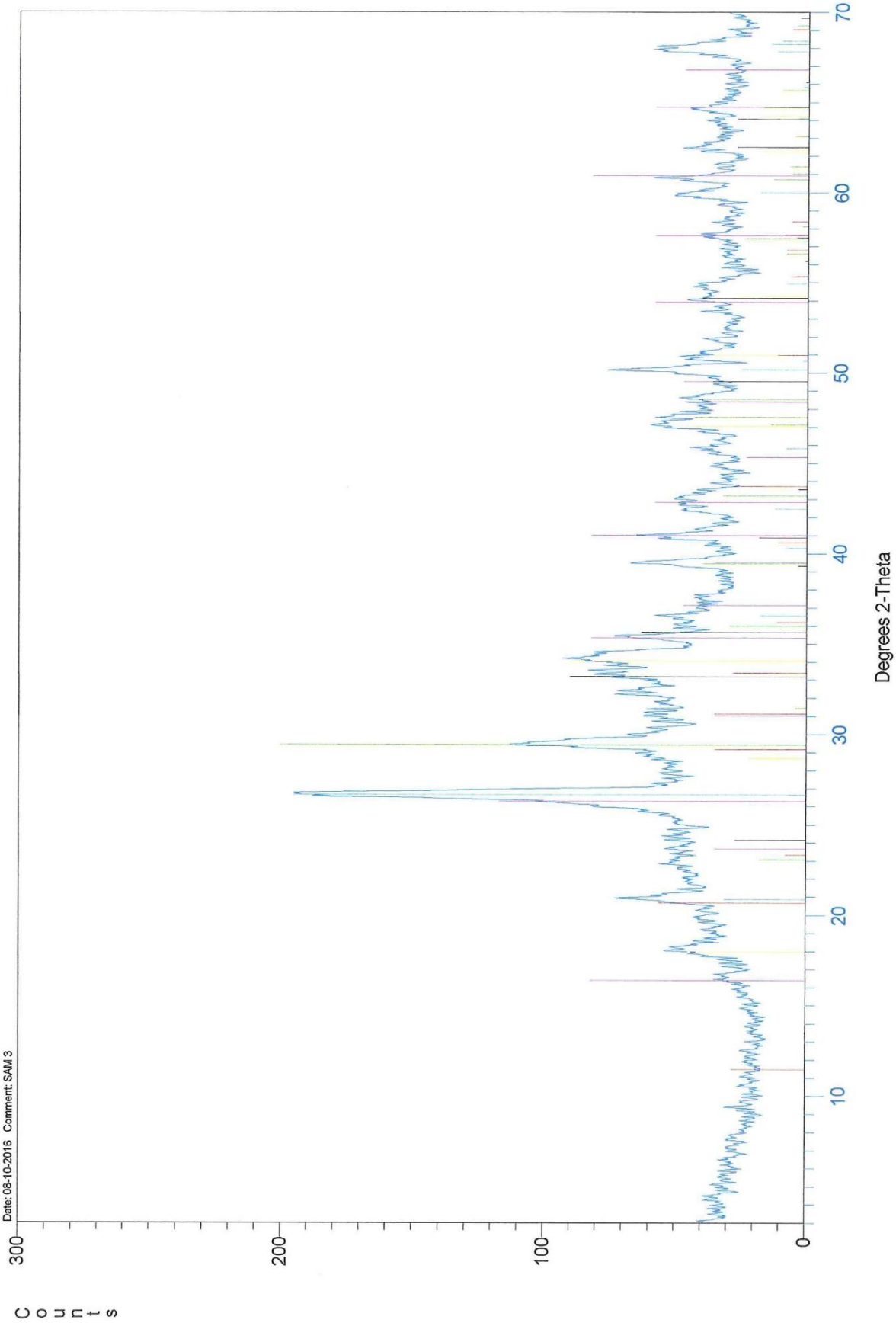
Date: 08-10-2016 Comment: SAM 3
Counts
300
200
100
0
10
20
30
40
50
60
70
Degrees 2-Theta

(d)

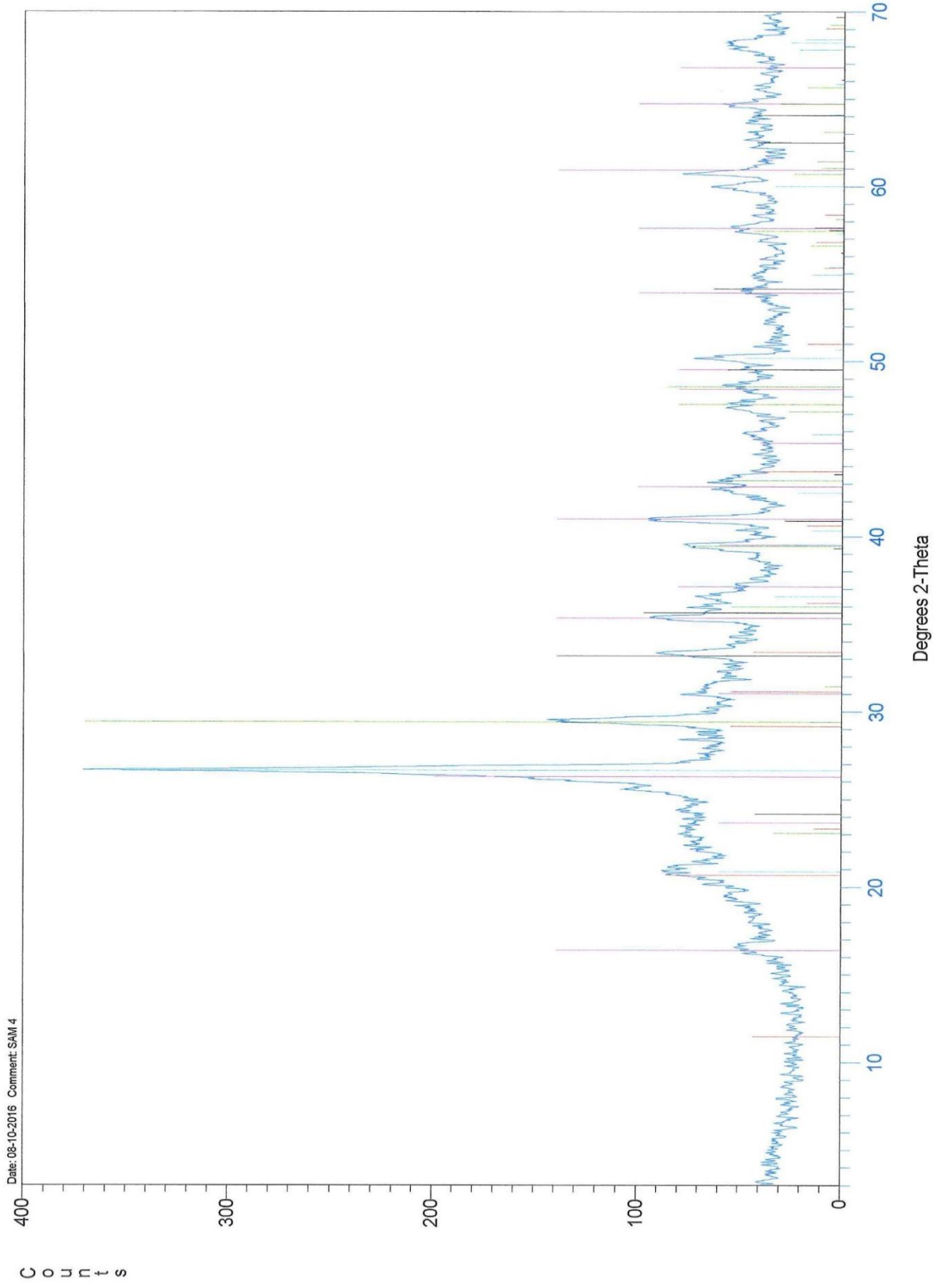
Date: 08-10-2016 Comment: SAM 4
Counts
400
300
200
100
0
10
20
30
40
50
60
70
Degrees 2-Theta

(e)

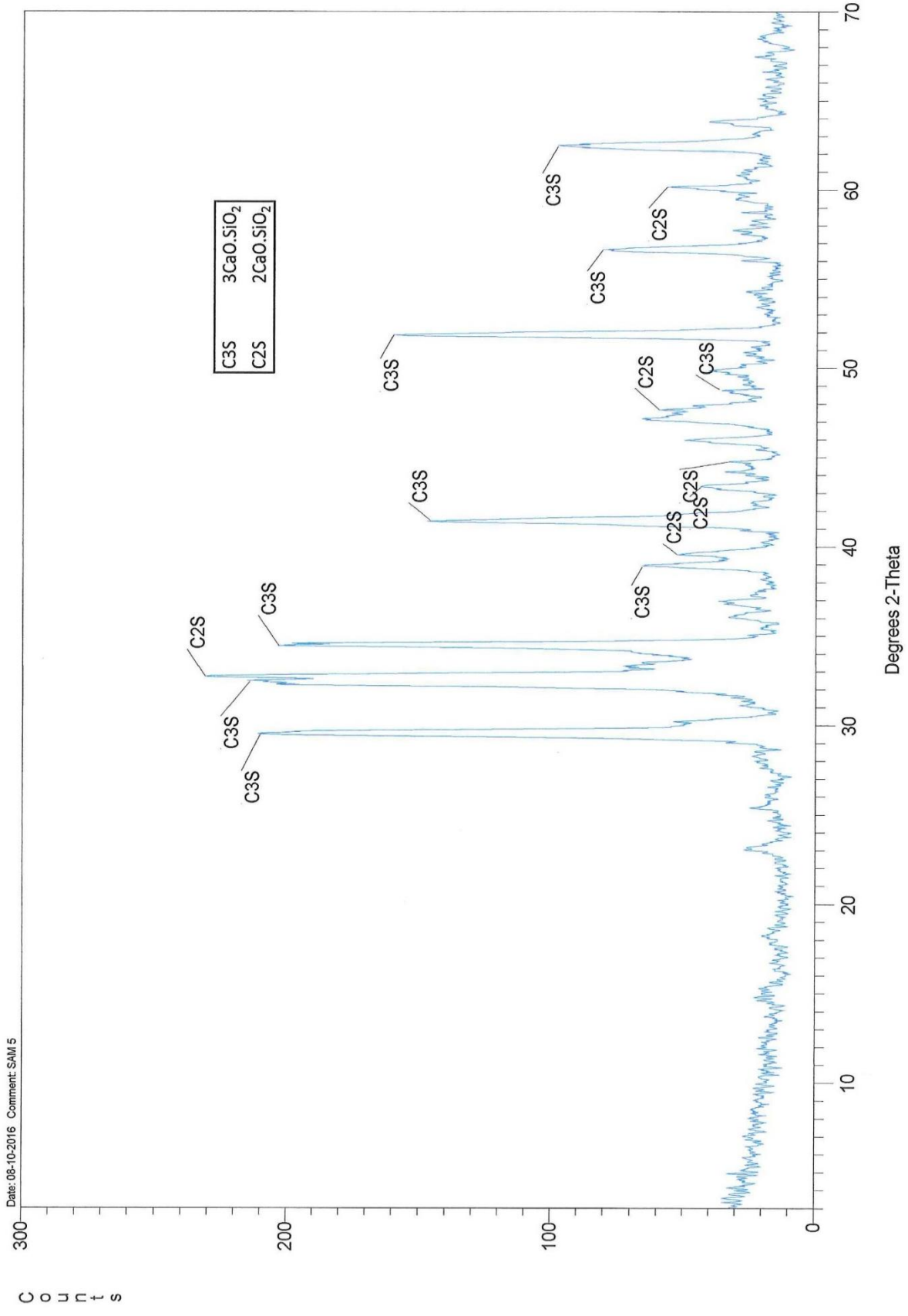

(f)

Figure B-1: (a) – (f) XRD Results

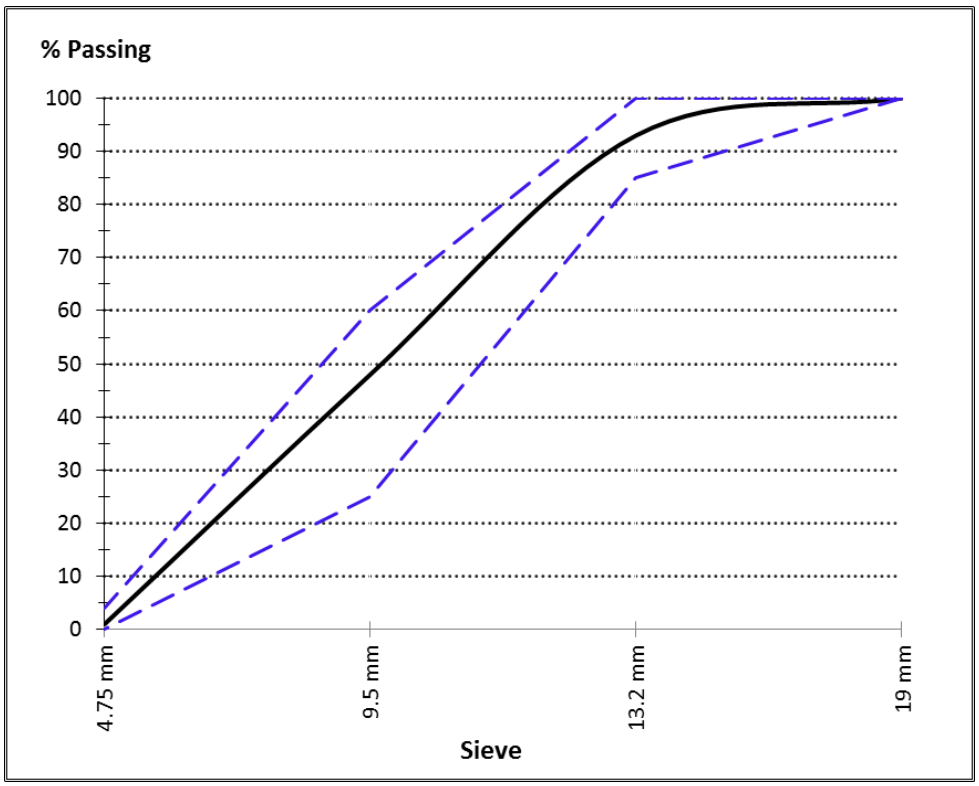

Figure B-2: Particle size distribution of coarse aggregate

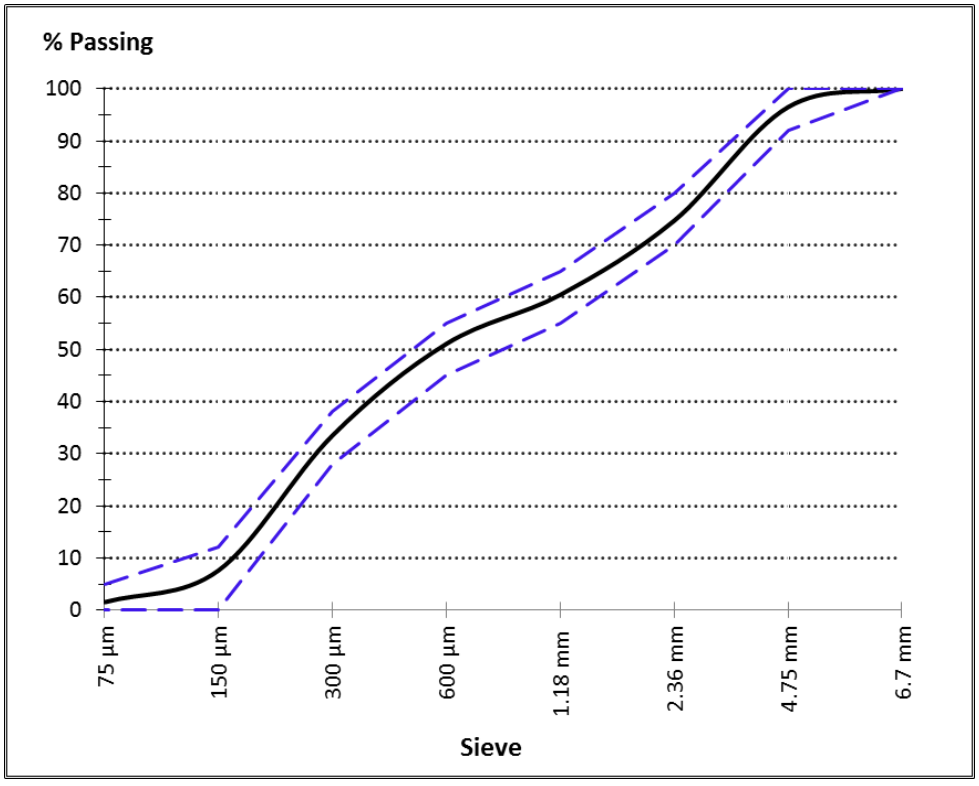

Figure B-3: Particle size distribution of fine aggregate

APPENDIX C – RHEOLOGY, STRENGTH AND DURABILITY OF SCC MIXES COMPOSED OF VARIOUS SUPERPLASTICIZER DOSAGES


Sika

Table C-1: The requirement of SP dosage and flow time achieved by each SCC mix type

Mix Type	SP dosage (%)			T_{500} (sec)	
	SF1	SF2	SF3	SF2	SF3
GP	0.36	0.62	0.80	5.5	2.3
FAF30%	0.31	0.53	0.71	3.1	2.8
FAC30%	0.34	0.60	0.76	4.0	2.9
20UG30%	0.51	0.71	0.84	6.5	4.5
10G30%	0.40	0.58	0.76	4.0	3.3
20G20%	0.36	0.53	0.71	3.4	3.2
20G30%	0.31	0.53	0.67	4.2	4.0
20G40%	0.28	0.40	0.58	4.9	3.7
40G30%	0.27	0.36	0.44	4.8	4.3

Table C-2: Yield stress and plastic viscosity of all SCC mixes for SF1 and SF3 flow types

Mix Type	Flow Type	Yield Stress (Pa)	Plastic Viscosity (Pas)
GP	SF1	277	65.9
	SF2	0	49.9
FAF30%	SF1	348	25.3
	SF2	27	20.2
FAC30%	SF1	583	34.2
	SF2	0	54.1
20UG30%	SF1	691	82.3
	SF2	275	65.8
10G30%	SF1	222	41.6
	SF2	55	34.8
20G20%	SF1	211	44.6
	SF2	85	34.5
20G30%	SF1	238	47.9
	SF2	103	37.4
20G40%	SF1	278	50.3
	SF2	111	41.3
40G30%	SF1	301	53.6
	SF2	115	43.9

Table C-3: Yield stress of GL-FN at different SP levels

Yield Stress (Pa)				
	SP (%)			
Glass Size (µm)	0.27%	0.31%	0.36%	0.40%
10	347	293	268	222
20	321	238	212	179
40	301	203	115	63

Table C-4: Yield stress of GL-CN at different SP levels

Yield Stress (Pa)				
	SP (%)			
Glass Content (%)	0.27%	0.31%	0.36%	0.40%
20	353	282	211	198
30	321	238	212	179
40	278	222	176	111

Table C-5: Plastic viscosity of GL-FN at different SP levels

Plastic Viscosity (Pas)				
	SP (%)			
Glass Size (µm)	0.27%	0.31%	0.36%	0.40%
10	58.7	50.2	46.3	41.6
20	55.2	47.9	44.8	40.0
40	53.6	46.2	43.9	38.8

Table C-6: Plastic viscosity of GL-CN at different SP levels

Plastic Viscosity (Pas)				
	SP (%)			
Glass Content (%)	0.27%	0.31%	0.36%	0.40%
20	58.7	50.3	44.6	43.2
30	55.2	47.9	44.8	40.0
40	50.3	46.5	43.1	41.3

Table C-7: Compressive strength development in all SCC mix types produced with different SP dosages

Type	Days	Compressive Strength (MPa)		
		SF1	SF2	SF3
GP	7	39.3	62.1	35.1
	28	45.7	67.5	40.2
	90	65.1	75.9	48.3
FAF30%	7	37.9	39.5	24.0
	28	53.4	51.8	39.1
	90	59.8	72.0	42.7
FAC30%	7	37.3	51.1	35.0
	28	41.2	68.9	55.3
	90	67.6	73.7	60.9
20UG30%	7	18.8	22.3	14.1
	28	26.8	37.3	21.5
	90	33.2	42.8	26.9
10G30%	7	29.5	37.6	27.4
	28	48.5	59.3	43.7
	90	55.5	67.3	48.1
20G20%	7	40.4	44.8	29.8
	28	55.5	58.3	43.5
	90	57.1	66.6	56.7
20G30%	7	35.4	37.8	30.9
	28	44.0	47.5	42.0
	90	54.4	57.1	55.3
20G40%	7	26.5	27.5	19.6
	28	41.0	46.8	39.1
	90	51.4	53.1	51.1
40G30%	7	32.4	32.1	30.6
	28	40.9	45.2	38.3
	90	50.6	51.7	50.3

Table C-8: Coefficient of oxygen permeability of all SCC mix types produced with different SP dosages

Type	Days	Coefficient of Oxygen Permeability (m/s)		
		SF1	SF2	SF3
GP	7	2.64E-11	2.13E-11	8.04E-11
	28	2.41E-11	1.99E-11	1.46E-10
	90	-	1.90E-11	-
FAF30%	7	3.60E-11	1.91E-11	1.17E-10
	28	5.63E-11	1.10E-11	7.67E-11
	90	-	8.70E-12	
FAC30%	7	1.76E-11	2.18E-11	9.19E-12
	28	9.02E-12	1.53E-11	1.27E-11
	90	-	1.29E-11	-
20UG30%	7	3.77E-11	6.00E-11	4.78E-10
	28	3.40E-11	4.53E-11	4.39E-10
	90	3.16E-11	4.46E-11	3.78E-10
10G30%	7	1.4E-11	2.10E-11	9.9E-11
	28	9.2E-12	1.41E-11	2.7E-10
	90	7.6E-12	8.34E-12	-
20G20%	7	1.9E-11	1.32E-11	4.8E-11
	28	1.1E-11	1.05E-11	7.9E-11
	90	-	7.94E-12	-
20G30%	7	2.0E-11	1.14E-11	1.6E-10
	28	1.3E-11	8.63E-12	3.3E-10
	90	-	6.32E-12	-
20G40%	7	3.1E-11	2.60E-11	1.6E-10
	28	1.7E-11	1.63E-11	6.0E-10
	90	-	1.16E-11	-
40G30%	7	2.2E-11	3.79E-11	6.9E-10
	28	1.7E-11	2.13E-11	2.9E-10
	90	9.2E-12	1.39E-11	2.2E-10

Table C-9: Porosity of all SCC mix types produced with different SP dosages

Type	Days	Porosity (%)		
		SF1	SF2	SF3
GP	7	12.8	11.2	12.7
	28	12.3	10.7	11.9
	90	11.9	10.4	11.6
FAF30%	7	11.8	10.8	11.7
	28	10.4	9.7	10.6
	90	8.6	9.2	10.1
FAC30%	7	11.9	11.0	12.0
	28	11.2	10.2	10.9
	90	10.4	9.5	10.1
20UG30%	7	15.7	13.4	15.2
	28	13.9	12.2	13.6
	90	13.5	12.0	13.3
10G30%	7	11.9	10.6	11.3
	28	10.4	9.4	9.9
	90	9.9	8.8	9.7
20G20%	7	11.4	10.2	11.1
	28	10.4	9.3	10.2
	90	9.6	8.6	9.2
20G30%	7	11.7	10.7	11.4
	28	10.8	9.8	10.3
	90	9.8	9.0	9.5
20G40%	7	12.2	11.4	12.1
	28	11.5	10.4	10.9
	90	10.6	9.8	10.1
40G30%	7	12.1	11.4	11.7
	28	11.7	10.6	11.1
	90	10.5	9.7	10.0

Table C-10: Electrical resistivity of all SCC mix types produced with different SP dosages

Type	Days	Electrical Resistivity (kohm.cm)		
		SF1	SF2	SF3
GP	7	11.1	13.0	12.1
	28	13.3	15.4	15.8
	90	15.1	18.1	18.1
FAF30%	7	10.5	14.3	11.1
	28	13.6	18.1	15.1
	90	15.7	20.4	16.8
FAC30%	7	16.0	13.7	17.2
	28	18.7	16.9	19.3
	90	20.6	19.9	21.8
20UG30%	7	8.2	9.6	10.9
	28	10.4	12.9	13.6
	90	12.4	15.3	16.0
10G30%	7	12.3	15.7	12.9
	28	16.0	19.1	17.8
	90	17.9	21.9	20.2
20G20%	7	11.7	16.4	13.7
	28	15.2	19.6	17.5
	90	19.6	22.4	20.3
20G30%	7	10.3	14.9	11.1
	28	13.4	18.4	15.1
	90	16.3	21.1	18.1
20G40%	7	10.0	12.4	10.3
	28	12.4	16.1	13.1
	90	14.7	18.8	15.8
40G30%	7	9.7	11.7	10.1
	28	10.7	14.7	12.9
	90	12.9	19.4	14.9

APPENDIX D – LONG-TERM MECHANICAL PROPERTIES OF SCC MIXES

Table D-1: Strength activity indexes of mortars

Curing Days	Strength Activity Index (%)								
	FAF30%	FAC30%	LP30%	20UG30%	10G30%	20G20%	20G30%	20G40%	40G30%
7	79.8	97.0	76.1	66.2	96.5	95.6	87.5	73.0	75.7
28	84.4	99.1	74.0	64.3	97.9	97.0	91.2	75.8	78.2
90	89.6	99.2	75.7	63.7	98.8	97.6	93.8	78.1	80.9
180	94.9	103.0	76.4	62.7	99.2	98.0	94.3	82.1	81.6

Table D-2: Compressive strength of all SCC mix types

Curing Days	Compressive Strength (MPa)									
	GP	FAF30%	FAC30%	LP30%	20UG30%	10G30%	20G20%	20G30%	20G40%	40G30%
1	18.5	8.7	9.6	14.9	5.1	11.3	15.6	9.3	7.2	8.1
3	45.3	30.0	24.5	37.1	14.3	23.3	32.0	22.1	18.0	22.5
7	60.2	37.4	50.7	46.3	21.7	36.9	48.2	37.8	27.3	33.9
28	65.2	49.6	68.8	57.1	36.4	59.5	62.5	43.5	46.4	45.8
90	74.8	72.2	72.7	63.1	42.4	66.4	66.6	55.5	51.8	51.3
180	84.6	75.8	80.4	68.1	48.3	71.1	71.8	62.7	53.3	55.2
365	89.9	81.6	92.3	71.8	54.4	75.0	76.3	72.5	58.9	62.0
545	94.5	92.8	100.6	76.4	56.8	91.8	96.3	83.3	79.5	75.9

Table D-3: Splitting tensile strength of all SCC mix types

Curing Days	Splitting Tensile Strength (MPa)									
	GP	FAF30%	FAC30%	LM30%	20UG30%	10G30%	20G20%	20G30%	20G40%	40G30%
7	5.1	4.4	4.2	3.6	2.5	4.2	3.9	3.6	2.7	2.9
28	5.5	5.8	5.7	4.9	3.9	5.0	4.6	4.2	4.0	4.0
90	5.7	5.9	5.8	5.4	4.4	5.8	5.3	5.1	4.5	4.9
180	6.4	6.1	6.3	5.8	4.8	6.5	6.4	6.0	5.6	5.5
365	6.8	6.5	6.7	6.2	5.0	6.9	7.0	6.7	6.4	5.9
545	7.2	6.8	7.0	6.5	5.1	7.3	7.5	7.0	6.9	6.1

Table D-4: Modulus of elasticity of all SCC mix types

Curing Days	Elastic Modulus (GPa)									
	GP	FAF30%	FAC30%	LP30%	20UG30%	10G30%	20G20%	20G30%	20G40%	40G30%
7	37.8	31.9	38.6	32.0	28.5	34.8	32.7	31.9	31.6	33.1
28	40.7	36.0	38.8	35.3	30.9	37.0	36.4	35.4	34.2	33.8
90	43.5	39.8	42.3	38.7	32.3	40.5	39.2	38.2	38.7	37.3
180	45.7	43.7	44.7	40.8	33.7	43.0	42.0	40.1	41.3	39.7
365	47.8	44.3	46.4	42.1	34.3	44.3	45.2	42.2	43.7	41.5
545	48.9	45.7	47.5	43.7	35.0	49.2	48.7	45.7	45.6	43.5

APPENDIX E – LONG-TERM DURABILITY OF SCC MIXES

Table E-1: Coefficient of oxygen permeability of all SCC mix types

Curing Days	Coefficient of Oxygen Permeability (m/s)									
	GP	FAF30%	FAC30%	LP30%	20UG30%	10G30%	20G20%	20G30%	20G40%	40G30%
3	4.1E-11	3.7E-11	3.0E-11	2.0E-11	1.1E-10	2.3E-11	2.2E-11	2.9E-11	4.5E-11	4.4E-11
7	2.1E-11	1.9E-11	2.2E-11	1.9E-11	6.0E-11	2.1E-11	1.3E-11	1.1E-11	2.6E-11	3.8E-11
28	2.0E-11	1.1E-11	1.5E-11	1.6E-11	4.5E-11	1.4E-11	1.0E-11	8.6E-12	1.6E-11	2.1E-11
90	1.9E-11	8.7E-12	1.3E-11	9.9E-12	4.5E-11	8.3E-12	7.9E-12	6.3E-12	1.2E-11	1.4E-11
180	1.9E-11	6.7E-12	1.1E-11	9.6E-12	4.3E-11	4.0E-12	4.2E-12	5.2E-12	8.1E-12	1.1E-11
365	1.9E-11	6.2E-12	1.0E-11	9.6E-12	4.3E-11	3.5E-12	3.4E-12	4.8E-12	6.7E-12	9.6E-12
545	1.8E-11	5.8E-12	9.2E-12	9.5E-12	4.2E-11	2.9E-12	2.8E-12	4.2E-12	5.9E-12	7.9E-12

Table E-2: Porosity of all SCC mix types

Curing Days	Porosity (%)									
	GP	FAF30%	FAC30%	LP30%	20UG30%	10G30%	20G20%	20G30%	20G40%	40G30%
3	12.5	11.8	11.3	10.6	14.4	11.2	10.9	11.4	12.8	12.3
7	11.1	10.7	10.9	10.4	12.9	10.7	10.42	10.9	11.5	11.5
28	10.6	9.6	10.3	9.4	11.3	9.6	9.2	9.9	10.6	10.7
90	10.3	9.1	9.7	9.2	11.1	8.7	8.5	8.9	10.0	9.9
180	9.7	8.6	9.0	8.7	10.8	7.9	7.61	8.3	9.8	9.7
365	9.3	8.2	8.5	8.6	10.8	7.1	7.2	8.1	9.5	9.6
545	8.9	8.0	8.2	8.6	10.8	6.9	6.92	7.9	9.3	9.2

Table E-3: Electrical resistivity of all SCC mix types

Curing Days	Electrical Resistivity (kohm.cm)									
	GP	FAF30%	FAC30%	LP30%	20UG30%	10G30%	20G20%	20G30%	20G40%	40G30%
3	11.6	11.9	12.2	13.5	7.9	13.3	13.4	12.4	11.4	11.3
7	14.8	15.2	14.7	15.4	10.9	16.7	16.4	15.6	14.4	14.1
28	17.4	18.5	17.9	17.7	14.1	19.9	19.7	18.6	17.6	16.9
90	19.3	21.5	20.0	20.1	15.0	23.8	24.2	23.1	19.9	20.5
180	20.2	24.1	22.8	20.9	15.3	26.3	26.4	25.9	22.9	23.1
365	20.5	25.4	23.2	21.1	15.5	27.7	29.0	26.8	24.7	25.0
545	20.8	25.8	23.7	21.2	15.5	28.4	29.6	27.2	25.7	25.4

Table E-4: Chloride diffusion coefficient of all SCC mix types

Curing Days	Chloride Diffusion Coefficient (m^2/s)									
	GP	FAF30%	FAC30%	LP30%	20UG30%	10G30%	20G20%	20G30%	20G40%	40G30%
28	1.3E-11	7.2E-12	8.1E-12	8.7E-12	2.5E-11	4.9E-12	5.3E-12	5.8E-12	9.6E-12	8.3E-12
90	1.0E-11	4.3E-12	5.2E-12	8.0E-12	2.2E-11	2.6E-12	2.4E-12	3.4E-12	6.3E-12	5.6E-12
180	9.7E-12	3.4E-12	4.2E-12	7.8E-12	2.1E-11	1.9E-12	1.7E-12	2.6E-12	5.2E-12	4.2E-12
365	9.1E-12	3.0E-12	3.7E-12	7.6E-12	2.0E-11	1.6E-12	1.5E-12	2.1E-12	4.5E-12	3.5E-12
545	8.7E-12	2.7E-12	3.3E-12	7.4E-12	1.9E-11	1.5E-12	1.4E-12	1.9E-12	4.1E-12	3.2E-12

Table E-5: Drying shrinkage of all SCC mix types

Curing Days	Drying Shrinkage (microstrain)									
	GP	FAF30%	FAC30%	LP30%	20UG30%	10G30%	20G20%	20G30%	20G40%	40G30%
7	0.0	0.0	0.0	0.0	0.0	0.0	0.0	0.0	0.0	0.0
14	363.6	252.4	334.4	341.2	507.1	271.1	304.7	340.8	419.7	493.3
28	587.6	517.8	607.6	628.4	806.4	465.8	484.0	572.0	608.3	652.0
56	776.2	705.1	720.1	740.4	898.4	653.3	676.0	736.0	768.7	759.7
90	840.9	740.7	754.8	810.0	929.4	718.7	712.0	778.2	868.8	834.7
180	890.5	810.2	816.4	875.2	962.4	764.7	757.3	823.2	895.6	886.1

APPENDIX F – LONG-TERM MECHANICAL PROPERTIES AND DURABILITY OF ACCELERATED CURED SCC MIXES

Table F-1: Compressive strength of all SCC mix types

Curing Days	Compressive Strength (MPa)							
	GPE-D	GPE-W	FAE-D	FAE-W	UGE-D	UGE-W	WGE-D	WGE-W
1	25.5	-	22.8	-	10.9	-	19.3	-
3	45.7	44.2	20.6	25.7	13.9	9.5	21.4	23.6
7	36.3	47.3	34.3	36.8	18.8	18.4	29.2	28.9
28	48.9	57.3	34.6	50.8	18.2	22.8	35.9	40.4
90	52.9	69.3	38.4	61.5	21.5	31.1	40.2	47.8
180	56.9	72.6	40.8	63.4	22.4	34.2	44.0	55.5
365	58.2	74.5	42.4	66.1	23.6	36.2	48.8	62.8

Table F-2: Modulus of elasticity of all SCC mix types

Curing Days	Elastic Modulus (GPa)							
	GPE-D	GPE-W	FAE-D	FAE-W	UGE-D	UGE-W	WGE-D	WGE-W
7	27.9	34.2	26.1	28.0	16.4	17.5	23.8	25.4
28	33.0	38.4	27.2	31.7	16.9	19.8	26.4	32.1
90	34.4	41.3	28.5	36.1	18.8	23.7	30.0	35.9
180	36.0	42.9	29.3	38.7	19.3	24.5	32.3	37.8
365	36.4	43.8	30.3	39.7	20.2	26.8	34.3	40.2

Table F-3: Coefficient of oxygen permeability of all SCC mix types

Curing Days	Coefficient of Oxygen Permeability (m/s)							
	GPE-D	GPE-W	FAE-D	FAE-W	UGE-D	UGE-W	WGE-D	WGE-W
3	4.45E-11	4.36E-11	9.77E-11	5.09E-11	1.52E-10	1.42E-10	3.51E-11	3.40E-11
7	4.36E-11	2.15E-11	6.88E-11	2.60E-11	1.34E-10	1.05E-10	2.68E-11	2.06E-11
28	4.35E-11	1.17E-11	4.16E-11	1.81E-11	1.38E-10	9.68E-11	2.18E-11	1.53E-11
90	4.58E-11	1.56E-11	4.57E-11	2.69E-11	1.81E-10	8.55E-11	2.08E-11	1.39E-11
180	4.51E-11	2.41E-11	4.69E-11	2.39E-11	1.77E-10	8.06E-11	2.01E-11	1.28E-11
365	4.48E-11	2.35E-11	4.73E-11	2.18E-11	1.75E-10	8.01E-11	1.98E-11	1.25E-11

Table F-4: Porosity of all SCC mix types

Curing Days	Porosity (%)							
	GPE-D	GPE-W	FAE-D	FAE-W	UGE-D	UGE-W	WGE-D	WGE-W
3	13.2	12.8	14.6	13.2	16.0	15.6	13.0	12.6
7	12.9	11.0	13.8	12.2	15.3	14.1	12.3	11.5
28	12.7	9.5	12.6	10.3	15.6	13.8	11.6	10.4
90	12.9	9.8	12.8	10.4	16.5	13.2	11.2	9.7
180	12.8	10.5	12.7	10.2	16.4	12.8	11.0	9.4
365	12.7	10.3	12.7	10.1	16.3	12.7	10.9	9.2

Table F-5:Electrical resistivity of all SCC mix types

Curing Days	Electrical Resistivity (kohm.cm)							
	GPE-D	GPE-W	FAE-D	FAE-W	UGE-D	UGE-W	WGE-D	WGE-W
3	10.7	11.1	10.8	11.1	7.5	7.7	8.6	9.9
7	13.3	14.0	14.2	15.2	8.9	10.7	10.9	12.2
28	14.2	16.7	16.3	17.5	9.9	12.4	14.7	16.6
90	14.4	17.6	16.9	19.2	11.0	12.9	17.7	19.9
180	14.6	17.7	17.1	19.6	11.2	13.2	19.8	22.5
365	14.7	17.8	17.2	19.7	11.3	13.4	19.9	23

Table F-6:Chloride diffusion coefficient of all SCC mix types

Curing Days	Chloride Diffusion Coefficient (m^2/s)							
	GPE-D	GPE-W	FAE-D	FAE-W	UGE-D	UGE-W	WGE-D	WGE-W
28	2.35E-11	1.88E-11	1.04E-11	8.83E-12	4.45E-11	3.45E-11	8.64E-12	6.51E-12
90	2.05E-11	1.55E-11	8.38E-12	6.35E-12	4.10E-11	3.10E-11	6.80E-12	4.87E-12
180	1.92E-11	1.48E-11	7.87E-12	5.44E-12	4.03E-11	3.03E-11	6.40E-12	4.13E-12
365	1.86E-11	1.46E-11	7.63E-12	5.22E-12	3.97E-11	2.97E-11	6.25E-12	4.05E-12